

BORNEO JOURNAL

OF RESOURCE SCIENCE
AND TECHNOLOGY



Volume 14 Number 2, December 2024
ISSN : 2229-9769
eISSN : 0128-2972


UNIMAS
UNIVERSITI MALAYSIA SARAWAK
PUBLISHER

Editorial Committee

Chief Editor

Prof. Dr. Edmund Sim Ui Hang, Universiti Malaysia Sarawak, Malaysia

Managing Editors

Dr. Teng Sing Tung, Universiti Malaysia Sarawak, Malaysia

Assoc. Prof. Dr. Showkat Ahmad Bhawani, Universiti Malaysia Sarawak, Malaysia

Associate Editors

Assoc. Prof. Dr. Tay Meng Guan, Universiti Malaysia Sarawak, Malaysia

Assoc. Prof. Dr. Faisal Ali Anwarali Khan, Universiti Malaysia Sarawak, Malaysia

Dr. Chong Yee Ling, The Education University of Hong Kong, Hong Kong

Dr. Freddy Kuok San Yeo, University Malaysia Sarawak, Malaysia

Assoc. Prof. Dr. Chung Hung Hui, Universiti Malaysia Sarawak, Malaysia

Dr. Nurashikin Suhaili, Universiti Malaysia Sarawak, Malaysia

Ratnawati Hazali, Universiti Malaysia Sarawak, Malaysia

Dr. Vu Thanh Tu Anh, Universiti Malaysia Sarawak, Malaysia

Dr. Maya Asyikin Mohamad Arif, Universiti Malaysia Sarawak, Malaysia

Dr. Wee Boon Siong, Universiti Malaysia Sarawak, Malaysia

Dr. Fatimah A'tirah binti Mohamad, Universiti Malaysia Sarawak, Malaysia

Dr. Muhammad Redza bin Mohd Radzi, Universiti Malaysia Sarawak, Malaysia

Dr. Lau Lik Ming, Universiti Malaysia Sarawak, Malaysia

Dr. Nor Hisam Binti Zamakshshari, Universiti Malaysia Sarawak, Malaysia

Dr. Voon Fui Ling, Universiti Malaysia Sarawak, Malaysia

Dr. Walfator bin Dumin, Universiti Malaysia Sarawak, Malaysia

Dr. Junidah binti Lamaming, Universiti Malaysia Sarawak, Malaysia

Dr. Mohd Ridwan bin Abd Rahman @ Tahir, Universiti Malaysia Sarawak, Malaysia

Cindy Peter, Universiti Malaysia Sarawak, Malaysia

Production Editorial assistants

Mr. Dunstan Goh Seng Chee, Universiti Malaysia Sarawak, Malaysia

Mr. Law Ing Kuo

Advisory Board

BJRST International Advisory Board Members:

Prof. Dr. Arvind Bhatt, Kuwait Institute for Scientific Research, Kuwait
Prof. Dr. Colin Llewellyn Raston, Flinders University, Australia
Prof. Dr. Flavio M Vichi, Universidade de São Paulo, Instituto de Química, Brazil
Prof. Dr. Kuangyu Yen, Southern Medical University, Guangzhou, China
Prof. Dr. Liu Chao, Lanzhou Institute of Chemical Physics, China
Prof. Dr. Marc Arlen Anderson, IMDEA Energy Institute, Spain
Prof. Dr. Muchlisin Zainal Abidin, Universitas Syiah Kuala, Indonesia
Prof. Dr. Motokawa Masaharu, Kyoto University, Japan
Prof. Dr. Koji Fukui, Shibaura Institute of Technology, Japan
Assoc. Prof. Dr. Tingga Kingston, Texas Tech University, USA
Assoc. Prof. Dr. Lien Luong, University of Alberta, Canada
Assoc. Prof. Dr. Tommy Tsan Yuk Lam, The University of Hong Kong, Hong Kong
Dr. Justin Jong-Leong Wong, University of Sydney, Australia
Dr. Nicolas Hubert, Institut de Recherche pour le Développement, UMR 226 ISEM (UM2-CNRS-IRD), France

BJRST National Advisory Board Members:

Prof. Emeritus Dato Dr. Latiff Mohamad, Universiti Kebangsaan Malaysia, Malaysia
Prof. Dato' Dr. Mohd Tajuddin bin Abdullah, Universiti Malaysia Terengganu, Malaysia
Prof. Dr. Latiffah Zakaria, Universiti Sains Malaysia, Malaysia
Prof. Dr. Kasing Apun, Universiti Malaysia Sarawak, Malaysia
Prof. Dr. Mustafa Ab Rahman, Universiti Malaysia Sarawak, Malaysia
Prof. Dr. Son Radu, University Putra Malaysia, Malaysia
Prof. Dr. Zainab Ngaini, Universiti Malaysia Sarawak, Malaysia
Prof. Dr. Indraneil Das, Universiti Malaysia Sarawak, Malaysia
Prof. Dr. Mhd Ikhwanuddin, Universiti Malaysia Terengganu, Malaysia
Assoc. Prof. Dr. Sin Yeng Wong, Universiti Malaysia Sarawak, Malaysia
Assoc. Prof. Dr. Syafiq Lee Nung Kion, Universiti Malaysia Sarawak, Malaysia
Dr. Hafizi Rosli, Universiti Sains Malaysia, Malaysia
Dr. Dzarifah Zulperi Universiti Putra Malaysia, Malaysia

Reviewers:

Dr. Farah Akmal bt. Idrus, Universiti Malaysia Sarawak
Associate Prof. Diqi Yang Hainan University
Dr. Mohd Zharif bin Ramli, Universiti Malaysia Kelantan
Dr. Hadi Hamli, Universiti Putra Malaysia
Associate Prof. Tay Meng Guan, Universiti Malaysia Sarawak
Associate Prof. Dr Abdul Hafidz Yusoff, Universiti Malaysia Kelantan
Dr. Tan Kian Ann, Beibu Gulf University
Associate Prof. Dr Siti Akmar Khadijah Ab Rahim, Universiti Malaysia Sarawak
Dr. Lee Yih Nin, Curtin University
Dr. Lau Lik Ming, Universiti Malaysia Sarawak
Assistant Prof. Dr. Preeda Phumee Rajamangala, University of Technology Srivijaya
Prof. Garry Benico Central Luzon State University
Dr. Lum Wai Mun, Assistant Professor, Mie University
Dr. Tuan Noorkorina Tuan Kub, Universiti Malaysia Sabah
Associate Prof. Dr. Zaima Azira Bt. Zainal Abidin, International Islamic University Malaysia
Dr. Hafisah binti Nahrawi, Universiti Malaysia Sarawak
Dr. Mogeret binti Sidi, Universiti Malaysia Sarawak
Associate Prof. Dr. Habibah Hj Jamil, Universiti Kebangsaan Malaysia
Dr. Lin Chin Yik, University of Malaya

Chm. Dr. Norsyafikah Asyilla Binti Nordin, Universiti Sultan Zainal Abidin
Dr. Nor Hisam Zamakshshari, Universiti Malaysia Sarawak
Dr. Ainaa Nadiyah binti Abd Halim, Universiti Malaysia Sarawak
Dr. Noorashikin Md Saleh, Universiti Kebangsaan Malaysia
Dr. Hanis Mohd Yusoff, Universiti Malaysia Terengganu
Dr. Nur Indah Ahmad, Universiti Putra Malaysia
Dr. Goh Soon Heng, Universiti Malaysia Kelantan
Dr. Jayaraj Vijaya Kumaran, Universiti Malaysia Kelantan
Dr. Mohd Ridwan Abd Rahman, Universiti Malaysia Sarawak
Dr. Hayder H. Abed, Al-Muthanna University
Dr. Yusralina binti Yusof, Universiti Malaysia Sarawak
Dr. Nur Aainnaa Hasbullah, Universiti Malaysia Sabah
Dr. Nurul Faziha Ibrahim, Universiti Malaysia Terengganu
Chen Yi Shang, Malaysian Pepper Board
Dr. Mohamad Hilmi bin Ibrahim, Universiti Malaysia Sarawak

BORNEO JOURNAL OF RESOURCE SCIENCE AND TECHNOLOGY

Borneo Journal of Resource Science and Technology (BJRST) publishes scientific articles in all fields of resource sciences. The journal welcomes the submission of manuscripts that meet the general criteria of significance and scientific excellence from but not limited to Borneo. Acceptance for publication is based on contributions to scientific knowledge, original data, ideas or interpretations and on their conciseness, scientific accuracy and clarity.

BJRST publishes scientific articles in all fields of resource sciences including land and forest resources, aquatic science, biodiversity and ecology, biotechnology and molecular biology, chemistry, microbiology, bioinformatics, plant science and zoology. It offers a forum for the discussion of local issues that are of global concern. It is a double-blind refereed online journal published bi-annually. Currently it is indexed by Scopus, MyCITE (Malaysian Citation Index), UDL edge Beta, DOAJ Directory of Open Access Journals, Index Copernicus, MyJurnal and Google Scholar.

When submitting the work, contributors are requested to make a declaration that the submitted work has not been published, or is being considered for publication elsewhere. Contributors have to declare that the submitted work is their own and that copyright has not been breached in seeking the publication of the work.

Views expressed by the author(s) in the article do(es) not necessarily reflect the views of the Editorial Committee.

Manuscripts can be submitted via <https://publisher.unimas.my/ojs/index.php/BJRST>

Correspondence on editorial matters should be addressed to: Prof

Dr Edmund Sim Ui Hang

Chief Editor

Borneo Journal of Resource Science and Technology

Faculty of Resource Science and Technology, Universiti

Malaysia Sarawak

94300 Kota Samarahan

Sarawak

Malaysia

uhsim@unimas.my

Contents

Title	Page
Assessment of Microplastics in the Surface Water of Mengkabong and Salut Rivers of Sabah, Malaysia Kalwant-Singh <i>et al.</i> 2024	1-18
Evaluation of Euphrates River Water Quality on Phytoplankton Biodiversity in Ramadi, Iraq Mohammed <i>et al.</i> 2024	19-30
Characterizing Fatty Acid Profiles and Evaluating Antibacterial Activity of Edible Yellow Puffer Fish, <i>Xenopterus naritus</i> Mohamad <i>et al.</i> 2024	31-40
Strategies for Enhancing Grow-Out Culture Technique of Community-Based Sea Cucumber (<i>Holothuria scabra</i>): A Case Study in Malawali Island, Sabah Mohamad <i>et al.</i> 2024	41-53
Effects of Salinity Changes on Hematological Blood Parameters and Stress Responses in Red Tilapia (<i>Oreochromis</i> spp.) Infected with <i>Vibrio harveyi</i> Ulkhay <i>et al.</i> 2024	54-67
Growth Performance, Digestive Enzymes Activities and Gut Microbiota of Malaysian Mahseer, <i>Tor tambroides</i> Fingerlings Affected by Various Probiotics Concentrations Chua <i>et al.</i> 2024	68-80
Morphology and Molecular Characterisation of <i>Karenia mikimotoi</i> (Dinophyceae) from Sabah Malaysian Borneo, with a Focus on the Second Internal Transcribed Spacer (ITS2) of Ribosomal RNA gene Andrew Chiba <i>et al.</i> 2024	81-97
Potential of Local Microorganisms Solution from Chicken Manure as a Bioactivator in Liquid Waste Treatment from the Fish Cracker Processing Industry Abdulgani <i>et al.</i> 2024	98-107
Antagonistic Potential of a Phosphate Solubilizing Bacteria (<i>B. cereus</i> PS1.1, <i>B. cereus</i> PS1.2, <i>B. cereus</i> PS1.4) Against the Patogent Fungus <i>Ganoderma</i> sp. Isolated from Basal Stem of Oil Palm (<i>Elaeis guineensis</i> Jacq.) with Rot Disease Khotimah <i>et al.</i> 2024	108-117
Physico-Chemical Properties and Mineral Identification of Salt Licks Soil in Segaliud Lokan Forest Reserve Mohamad Maidin <i>et al.</i> 2024	118-134
Synthesis, Antibacterial Properties and Molecular Docking of Nitrobenzoylthiourea Compounds and their Copper(II) Complex Mohd Yunus <i>et al.</i> 2024	135-155
Red Seaweed Carrageenan: A Comprehensive Review of Preparation in Cosmetics - An In Depth Analysis Mingu <i>et al.</i> 2024	156-172

The Danger of Foot and Mouth Disease in Livestock – A Review Khairullah <i>et al.</i> 2024	173-187
The Gut Microbiomes of Wild Rodents within Forested Environments in Sarawak, Borneo Azmi <i>et. al.</i> , 2024	188-200
Chemistry Profile and Biological Activity of <i>Camptosperma auriculatum</i> Extracts Muharini <i>et al.</i> , 2024	201-209
Farmers' Perception Towards Agroforestry Practices in Siburan Mathew <i>et al.</i> 2024	210-216
Optimizing Silicon Application for Enhancing Growth and Chlorophyll Concentration in Pepper Plants (<i>Piper nigrum</i> L.) Cultivar Kuching Rabae <i>et al.</i> 2024	217-225

Assessment of Microplastics in the Surface Water of Mengkabong and Salut Rivers of Sabah, Malaysia

RAVEENA-KAUR KALWANT-SINGH, CHEN-LIN SOO* & CHENG-ANN CHEN

Institute for Tropical Biology and Conservation, Universiti Malaysia Sabah, Jalan UMS, 88400, Kota Kinabalu, Sabah, Malaysia

*Corresponding author: soo@ums.edu.my

Received: 3 February 2024

Accepted: 21 August 2024

Published: 31 December 2024

ABSTRACT

Microplastics in river water are a global risk to aquatic ecosystems due to their longevity in the environment, causing toxicity, ingestion by organisms, and bioaccumulation. However, knowledge and research on microplastic pollution are still scarce in Sabah, Malaysia, as no studies have been carried out before. Hence, this study aimed (1) to determine the occurrence of microplastics in the surface water of the Mengkabong and Salut Rivers in Sabah and (2) to assess the spatial variability in the concentration and characteristics of microplastics within these rivers. Microplastics were extracted, counted, and characterized for their shape, colour, size, and polymer. An independent t-test was used to compare microplastic abundance and characteristics between the two rivers, whereas Hierarchical cluster analysis was used to group the eight stations based on similarities in microplastics. This study detected microplastics at all stations, with a significantly higher concentration ($p < 0.05$) of microplastic in the Salut River (4.78 ± 2.43 items/L) compared to those in the Mengkabong River (1.63 ± 0.87 items/L). Fibre was the most abundant microplastic shape in both Mengkabong (78%) and Salut (57%), likely sourced from textile washing, fishing, and aquaculture activities in the vicinity. Transparent microplastics were prevalent in Mengkabong (30%), while black microplastics dominated in Salut (42%). Size distribution exhibited the opposite trend, with 74% larger-sized microplastics in Mengkabong but 63% smaller-sized microplastics in Salut. Polymer analysis revealed rayon (68%) dominance in Mengkabong, while polyethylene (34%) and rayon (33%) in Salut. Spatial heterogeneity of microplastics was evident through cluster analysis, categorizing stations into clean, moderately polluted, and polluted. Stations adjacent to areas with fewer land-based activities were clean with a low microplastics count, while areas with intense developments, residential, and fishing activities were polluted with high microplastic counts. This study underscores the presence of microplastics in Sabah's rivers, serving as a foundational reference for future research. It is also imperative to conduct regular monitoring of microplastics in the rivers of Sabah since it is anticipated that microplastics contamination will escalate in the coming years globally.

Keywords: Fibre, microplastics, rayon, Sabah, tidal rivers

Copyright: This is an open access article distributed under the terms of the CC-BY-NC-SA (Creative Commons Attribution-NonCommercial-ShareAlike 4.0 International License) which permits unrestricted use, distribution, and reproduction in any medium, for non-commercial purposes, provided the original work of the author(s) is properly cited.

INTRODUCTION

Increasing plastic pollution particularly microplastics has been a serious worrying issue since the past decade (Henderson & Green, 2020; Issac & Kandasubramanian, 2021; Li *et al.*, 2023). Pittura *et al.* (2022) defined microplastics as microscopic sized of plastic particles smaller than 5 mm in sizes from two manufacturing origins; primary and secondary. Primary microplastics refer to plastic particles that are intentionally manufactured to be microscopic in size, such as microbeads found in skincare products. On the other hand, secondary microplastics are plastic particles that are formed through the degradation and fragmentation

processes of larger plastic materials (Hocking, 2022). The surge of demand in usage of plastics products results in their excessive production, if are not managed properly leads to indiscriminate disposal into the environment (Fauziah *et al.*, 2015). Additionally, the characteristics of plastics such as slow degradation period along with intense fragmentations of plastics into microscopic size rendered them as the most problematic persistent pollutant in the environment (Multisanti *et al.*, 2022).

Approximately 6,000 to 1.5 million tons of microplastics are transported to the ocean annually via rivers (D'Avignon *et al.*, 2022). It highlights the importance of rivers as primary

channels for the transportation of plastic debris from terrestrial environments to the marine ecosystem. Anthropogenic activities, including aquaculture and fishing activities, the direct disposal of plastic trash, and industrial discharges into rivers, were identified as significant contributors to the escalation of microplastics pollution in river ecosystems (Choong *et al.*, 2021; Primus & Azman, 2022). The transportation and deposition of microplastics in river ecosystems are influenced by various factors, including the presence of nearby sources, land use patterns, river flow dynamics, hydraulic conditions, and the terrain of the surrounding area. Additionally, the characteristics of the microplastic particles play a role in their movement and distribution within rivers (Lin *et al.*, 2018; Idrus *et al.*, 2022).

The rapid pace of new constructions and infrastructural changes in Sabah have greatly affected the general lifestyle of its residents, leading to the mismanagement of plastic garbage (Dusim, 2021). Despite having awareness of increasing plastic and microplastic pollution, the knowledge and research of microplastic pollution in Sabah however is still scarce. The majority of microplastic study conducted in Malaysian river waters has been concentrated on the regions of Peninsular and Sarawak. Seven studies were conducted in Peninsular Malaysia; Skudai River and Tebrau River in Johor (Sarijan *et al.*, 2018), Cherating River in Pahang (Pariatamby *et al.*, 2020), Dungun River in Terengganu (Hwi *et al.*, 2020), Klang River Estuary (Zaki *et al.*, 2021), Langat Rivers (Suardy *et al.*, 2020) in Selangor, Melayu River in Johor (Primus & Azman, 2022), and three rivers in East Malaysia; Kuching Rivers (Johnson *et al.*, 2020), Miri River Estuary (Liong *et al.*, 2021), and Baram River Estuary (Choong *et al.*, 2021) in Sarawak. The lack of documented works pertaining to research on microplastics in the river waters of Sabah accelerates the need of conducting this study.

Recognizing the substantial reliance of local communities on rivers and coastal areas for vital resources such as water, sustenance, and other basic necessities in their daily lives and endeavours, it becomes imperative to assess the rising issue of microplastic pollution as a key indicator of river water quality in Sabah. The rivers in the Tuaran District, which originate from the headwaters of the Crocker Range

Mountain and flow westward towards the South China Sea in Sabah, have played an important part in supplying fish and water for industrial, agricultural, and residential purposes in both the Tuaran and Kota Kinabalu Districts (Montoi *et al.*, 2017). On the other hand, these river systems are important conduits for transporting pollutants such as microplastics from nearby inland sources into the marine environment (Liu *et al.*, 2021). The distribution and fate of microplastics in these rivers could be influenced by velocity changes and tidal influx (Choong *et al.*, 2021; Jendanklang *et al.*, 2023).

Conducting a study into the occurrence of microplastic within the rivers of Tuaran is a preliminary endeavour aimed at expanding our knowledge of microplastic pollution in the region of Sabah. Knowing the microplastic status of these rivers allows further mitigation efforts by relevant agencies to monitor and reduce their presence in the environment along with promoting more further extensive research on this research area. Therefore, the objectives of this study were primarily to determine the occurrence of microplastics in the waters of Mengkabong and Salut Rivers in Tuaran, Sabah, and to assess the spatial variability in the concentration and characteristics of microplastics within these rivers.

MATERIALS AND METHODS

Study Area and Sampling Stations

Tuaran District is located in the west coast division of Sabah, having a tropical humid climate with an average rainfall of 2,800 mm. The annual average population growth rate for Tuaran is 2.8%, with a current total population of 135.7 thousand people recorded residing latest in 2020 by the Department of Statistics of Malaysia (2022). Rivers from the Tuaran District were selected in this study as they are one of the most important rivers in Sabah for fishing and aquaculture activities. Moreover, the expansion of adjacent Kota Kinabalu and Sepanggar Towns pressurised the urbanisation of the Tuaran District from its increasing developments. Two tidal rivers were selected for this study namely Mengkabong River, situated adjacent to Tanjung Badak, and Salut River, located close to Kuala Karambunai. A total of eight sampling stations were selected, with each river having four sampling stations with approximately 2 km

apart. Samplings were conducted during the period of high tide on 16th of February 2023 at Mengkabong River and on 15th of March 2023 at Salut River. Figure 1 shows the map of study area with sampling stations while Table 1 shows their sampling details.

Water Sample Collection

Bulk sample of 30 L of surface water was collected using a stainless-steel bucket and sieved using a 10 μm stainless sieve on field in a boat (Huang *et al.*, 2020). Retained materials were transferred into capped glass bottles using distilled water. All water samples were taken in triplicates for each station. All collected samples were taken to the Institute of Tropical Biology and Conservation (ITBC), Universiti Malaysia Sabah (UMS) for further laboratory analysis.

Sample Analysis

Microplastics Extraction

Microplastics were extracted from water samples by density separation method following Lin *et al.* (2018). Prior to microplastics extraction, organic matter in water samples were first digested using wet peroxide oxidation. Approximately 150 ml of 35% hydrogen peroxide (H_2O_2) were added to the glass bottles and incubated in incubator at 65 °C for 24 hours to aid in complete breakdown of organic matter. Digested samples were then sieved and rinsed with distilled water before pouring the residuals into 100 ml glass beakers using salt solution, 5 M of sodium chloride (NaCl). The salt solution was further added until the beaker's mouth and covered loosely with aluminium foil.

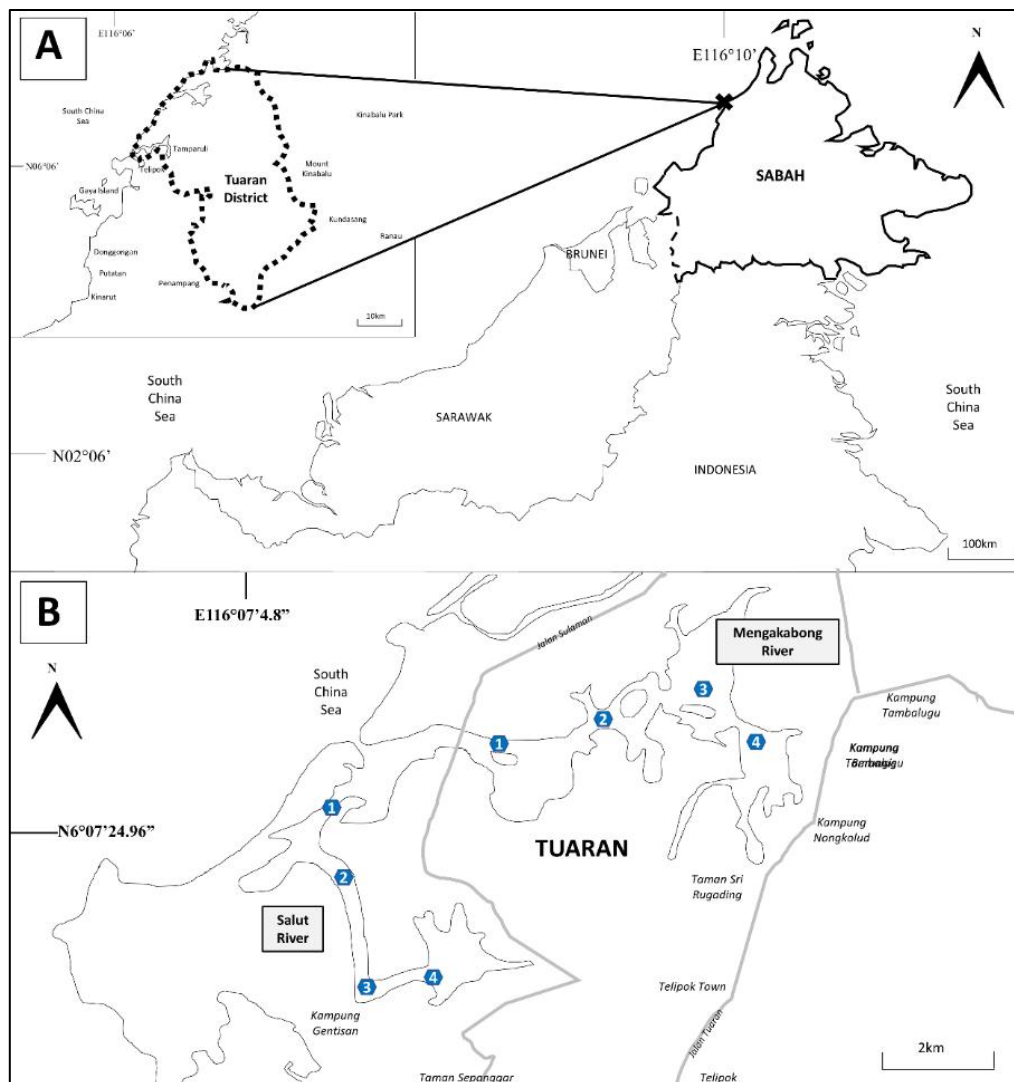


Figure 1. Map A: The map of study area of Mengkabong and Salut Rivers at Tuaran District of Sabah. Map B: Detailed sampling stations were indicated with blue circle and number for the stations

Table 1. Description of sampling stations and sampling regime

River	Station	Depth (m)	Coordinates	Time	Observation
Mengkabong River (16-02-2023)	Station 1 (S1)	6.5	06°08'27.2"N 116°09'42.0" E	9.20 am	Downstream near Mengkabong Bridge
	Station 2 (S2)	15	06°08'41.2"N 116°10'43"E	1.00 pm	Clear, surrounded by mangroves
	Station 3 (S3)	3	06°08'52.1"N 116°11'46.1" E	11.58 am	Below village houses
	Station 4 (S4)	2	06°08'32.2"N 116°12'18.9" E	10.50 am	Upstream near to village houses, aquaculture and fishing activities. Observed waste dump near shore and floating plastic wrappers and bottles
Salut River (15-3-2023)	Station 1 (S1)	3.17	06°04.037' N 116°09.025'E	10.10 am	Located downstream at Kampung Batangan, nearby to Trombong bay
	Station 2 (S2)	3	06°7'04.2"N 116°08'07.4"E	1.30 pm	Located near to a fishing jetty and a construction area
	Station 3 (S3)	2.6	06°5'59.5"N 116°8'19.3"E	12.21 pm	Located near to residential flats
	Station 4 (S4)	2	06°06'0.4"N 116°8'59.9"E	11.28 am	Located at the upstream boundary of the mangroves

The solution was allowed to settle overnight where the supernatant of the solution was then pump filtered through a 1.2 µm pore size glass microfiber filter (Whatman GF/C) the following day. The filter paper was placed in a clean glass petri dish and allowed to air dry before microscope examination. This process was repeated three times. Blank samples were prepared with distilled water and allowed to go through similar process as samples for quality control. To minimise external microplastics contamination from surrounding, only glass and stainless-steel equipment were used throughout microplastics extraction and examination in laboratory. Additionally, all equipment was rinsed with distilled water prior any microplastics analysis.

Microplastics Examination and Identification

In this study, microplastics were classified as plastic particles ranging from 10 µm to 5 mm in size. The size was further classified into two categories: small microplastics (SMP) that ranged from 10 µm to 1 mm, and large microplastics (LMP), which ranged from 1 mm to 5 mm. Microplastics were examined for visual identification, sorting, and counting process under a stereo microscope (Leica EZ24). Microplastics observed were sorted and classified according to shapes (fibre, filament, foam, fragment, pellet, and film) following

Singh *et al.* (2022) and colours (black, blue, red, white, yellow, transparent) following Peng *et al.* (2017) as described in Table 2. All colours were noted based on the surface colour dominancy, with the exception of transparent, which was noted based on the colour of the patches (if any) to minimize overestimation of transparent microplastic due to discolouration. Polymer types were identified by using micro-FTIR (Nicolet iN10 MX) scanned with a spectral range of 4000-1200 cm⁻¹ in the ALS Technichem Laboratory, Malaysia. The spectrum obtained were compared with available libraries on established database on polymers type with quality matching more than 80%. Only one replicate at each station was conducted for polymer type analysis.

Data Analysis

All data obtained during microplastics examination were recorded in concentration units of items/L. Prior to statistical analysis, all parameters were checked for outliers using boxplots, tested for normality using the Shapiro-Wilk's test, and examined for equality of variances using Levene's test. Normality and Levene's tests showed that the data was normally distributed and had equal variances (p>0.05). Therefore, a parametric test, the independent t-test, was used. Independent t-test was carried out to compare if there was any significant

difference in microplastics concentration and characteristics between Mengkabong and Salut Rivers at p value < 0.05 . Next, Hierarchical cluster analysis was used to investigate the grouping of sampling stations based on the similarities of microplastics concentration and characteristics of shape, colour and size of microplastics. Ward's method using Euclidean

distances as a measure of similarity and Z-score standardization of variables was used in this analysis. Output of the analysis was presented in a dendrogram with the cluster's number and linkage distances less than 60% was considered statistically significant. All statistical analysis was carried out using Statistical Software for Social Sciences (SPSS Version 25).

Table 2. Categories used in description and identification of microplastics

Characteristic	Categories	Description	References
Shape	Fibre	A very thin threadlike straight structure	Singh <i>et al.</i> (2022)
	Filament	A thicker and harder straight structure	
	Foam	A sponge-like lightweight structure	
	Fragment	An irregular edge of hard structures	
	Pellet	A round spherical hard structure	
	Film	A thin layer plan of flimsy structure	
Colour	Black	Black, transparent black, grey and white-striped black	Peng <i>et al.</i> (2017)
	Blue	Deep blue, light blue, deep green, light green	
	Red	Red, purple, pink	
	White	Opaque white, silver	
	Yellow	Yellow, brown, orange	
	Transparent	Colourless	

RESULTS

Microplastics Occurrence and Characteristics

Microplastics were present in all Mengkabong and Salut Rivers stations (Figure 2). The abundance of microplastics in Salut River water (4.78 ± 2.43 items/L) were three times higher than in Mengkabong River water (1.63 ± 0.87 items/L). Station 4 of Mengkabong River and Station 1 of Salut River waters recorded the highest number of microplastics, accounting 2.7 items/L and 6.5 items/L, respectively. The concentration of microplastics in the waters of the Mengkabong River displayed a decreasing pattern as it moved from the upstream station (Station 4) to the downstream station (Station 1). Conversely, the concentration of microplastics in the waters of the Salut River exhibited an opposite trend, increasing as it moved from upstream to downstream.

Both large size microplastics (LMP) and small size microplastics (SMP) were found in this study (Figure 3). Mengkabong River recorded 74% of LMP and the Salut River recorded 63% of SMP from their total counts. This pattern was similarly found in each respective individual station of the rivers, as depicted in Figure 4. Microplastics shapes

observed in both rivers were fibre, film, fragment, and foam, as shown in Figure 5. There were no pellet or filament observed in any stations. Fibre was the most abundant shape in both Mengkabong River (78%) and Salut River (57%) (Figure 6). Microplastics colours in Mengkabong and Salut Rivers waters were black, blue, red, yellow, white and transparent (Figure 7). In Mengkabong, transparent (30%), blue (26%) and black (24%) microplastics were dominant. Meanwhile in Salut, black (42%) and yellow (30%) microplastics were dominant (Figure 8). Microplastics polymers detected in Mengkabong River were rayon (68%) and polytetrafluoroethylene (PTFE) (25%). Meanwhile Salut River recorded high percentages of polyethylene (PE) (34%), rayon (33%), ethylene propylene diene monomer (EPDM) (21%) and polyethylene terephthalate (PET) (9%) as shown in Figure 9.

Spatial Variation of Microplastic Composition in Rivers

The results of independent t-test show that Salut River had significantly higher total microplastics (3.16 items/L, p value ≤ 0.05), foam (0.02 mg/L, p value = 0.04) and SMP (2.58 items/L, p value = 0.02) than in Mengkabong River (Table 3). Microplastics showed spatial heterogeneity in the Mengkabong and Salut Rivers where the

Hierarchical cluster analysis test grouped the eight stations into four different clusters according to the abundance and characteristic of microplastics (Figure 10). In general, the river stations were clustered based on three categories where it goes from clean, moderate to most microplastic polluted rivers as it goes down from Clusters 1 to 4. Stations 1, 2, and 3 of Mengkabong River and Station 4 of Salut River were clustered together as Cluster 1. This cluster was the indicative of minimal microplastic pollution, with microplastics counts less than 1.9 items/L. These stations were also grouped together as they are shared the same similarities of clean surroundings. Cluster 2 indicates a

moderate level of microplastic pollution, as evidenced at Station 2 of Mengkabong River, which documented high fibres (84%). Clusters 3 and 4 encompassed the remaining stations along the Salut River, that exhibit high microplastics counts (> 5.3 items/L) but distinct microplastics compositions. Both of these two stations were situated in close proximity to residential areas along the Salut River. Lastly, Station 2 of Salut River stands alone in cluster 4 because it had the highest percentage of fibre (80%), and large sized microplastics (51%). Additionally, the percentage of black colour (68%) microplastics were also higher than other stations.

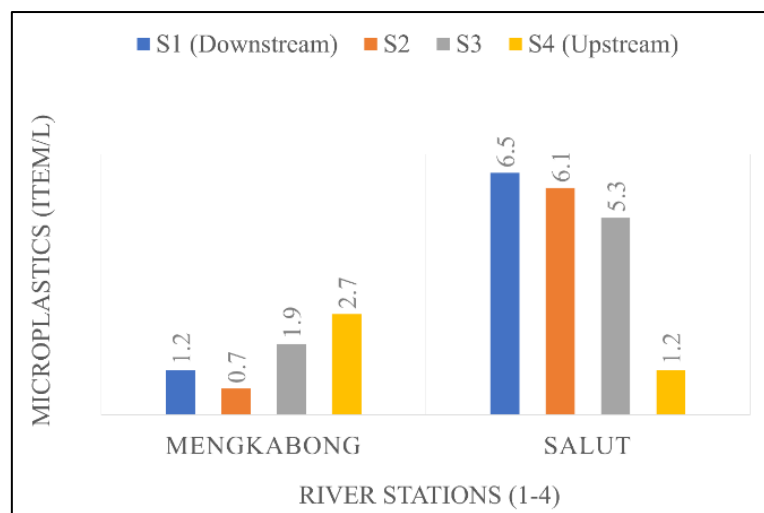


Figure 2. Microplastic concentration (items/L) in Mengkabong and Salut Rivers from downstream (S1) to upstream (S4) direction

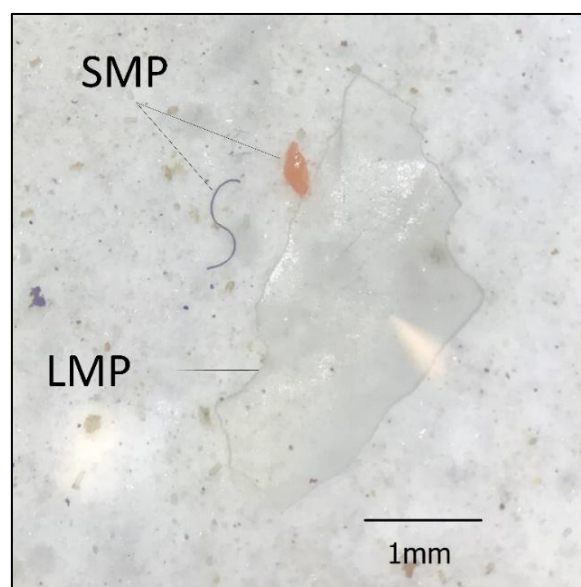


Figure 3. The difference between small sized microplastics (SMP) and large sized microplastics (LMP) observed in Mengkabong and Salut Rivers

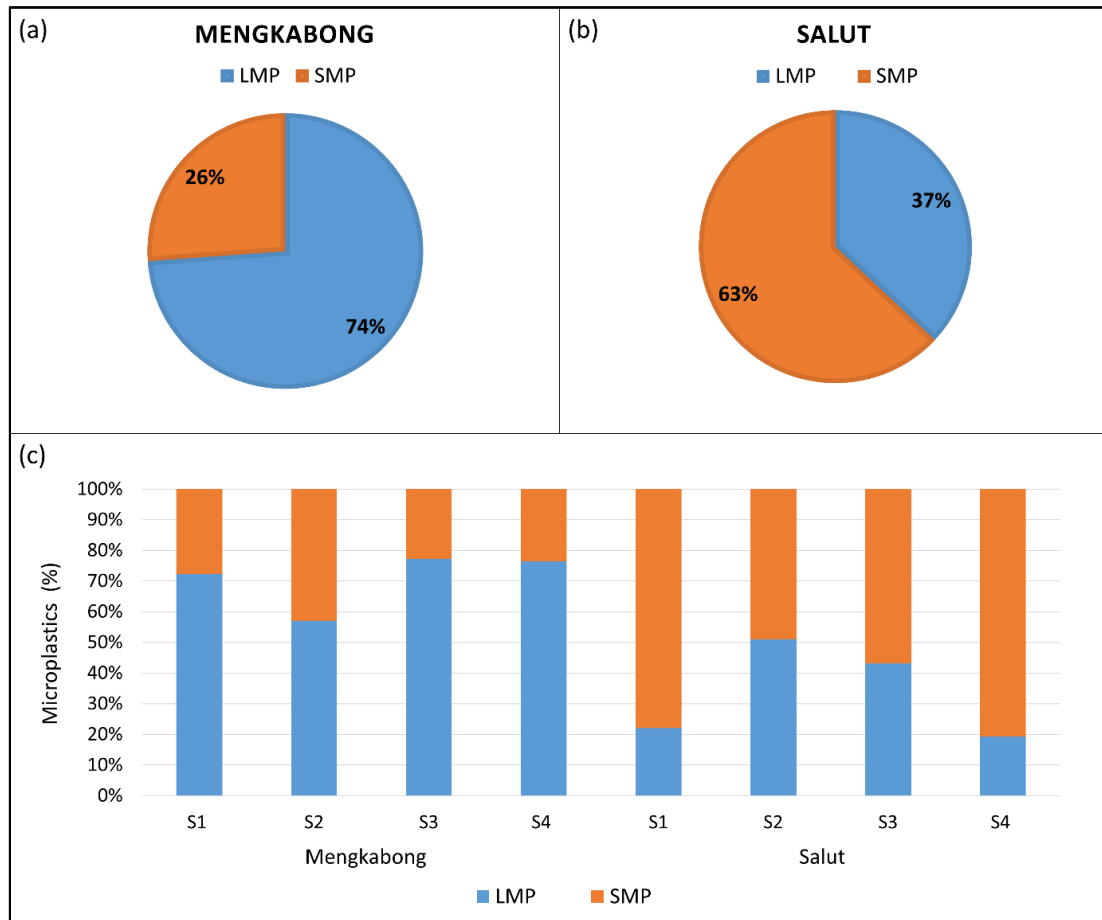


Figure 4. Composition of microplastics size observed in (a) Mengkabong River, (b) Salut River, and (c) individual stations of Mengkabong and Salut Rivers

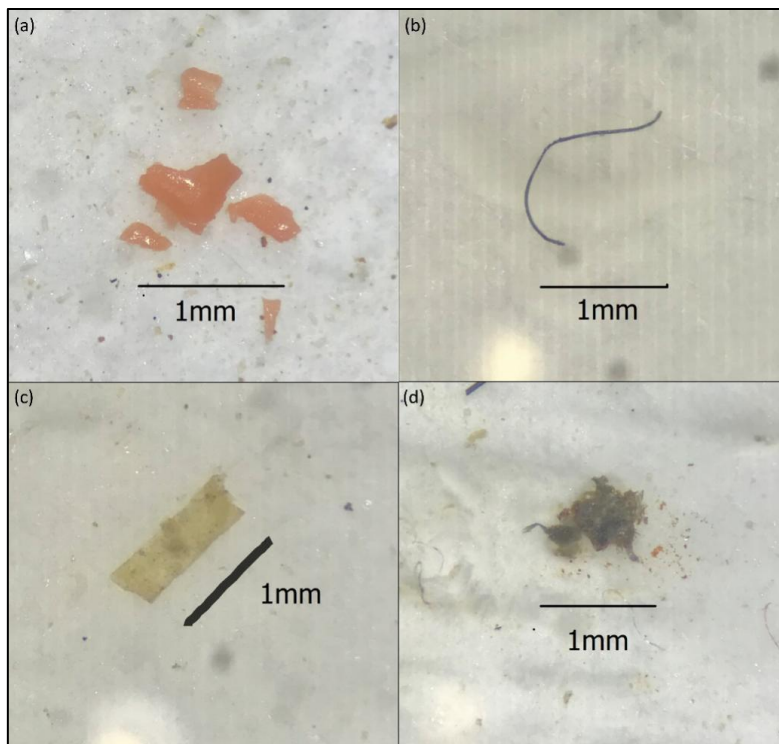


Figure 5. Examples of microplastics shape observed in Mengkabong and Salut Rivers waters, namely (a) fragment, (b) fibre, (c) film, and (d) foam

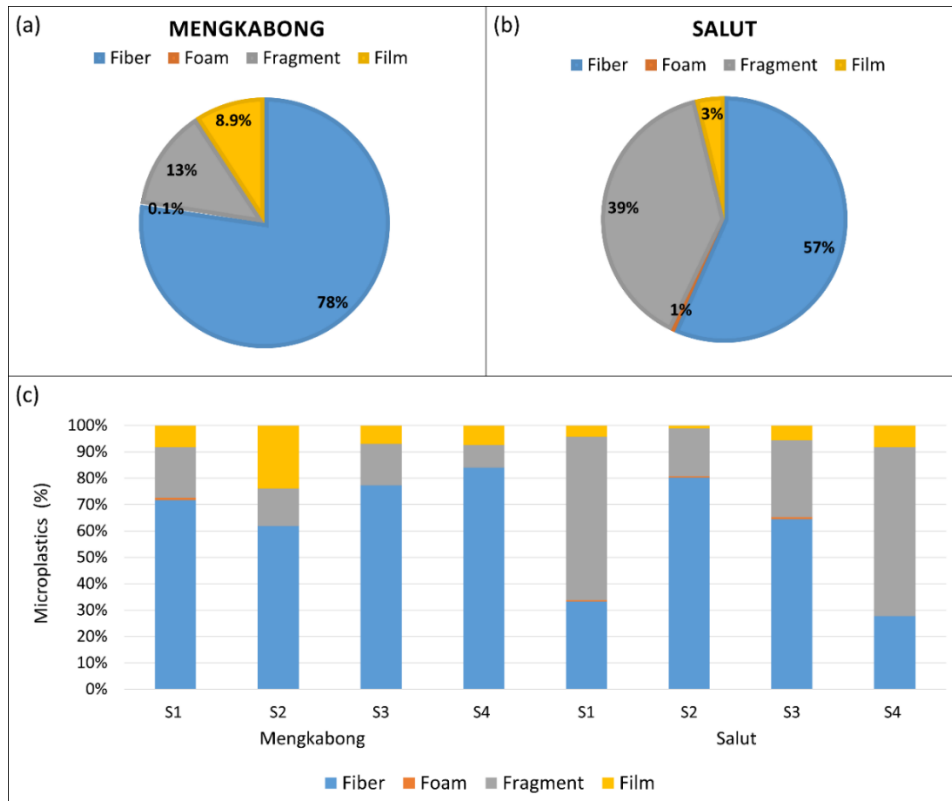


Figure 6. Composition of microplastics shapes observed in (a) Mengkabong River, (b) Salut River, and (c) individual stations of Mengkabong and Salut Rivers

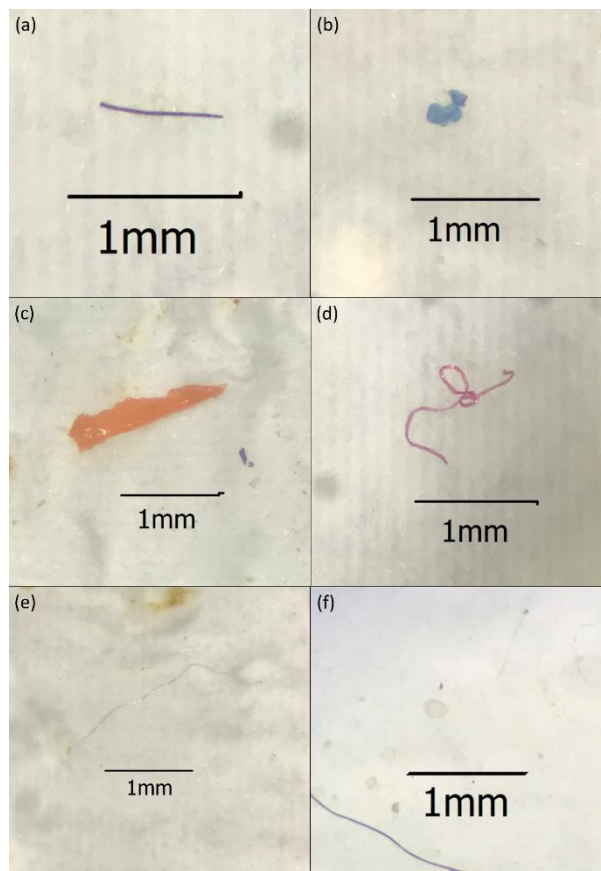


Figure 7. Examples of microplastics colour observed in Mengkabong and Salut River based on dominant colour categories; (a) black, (b) blue, (c) yellow, (d) red, (e) transparent, and (f) white

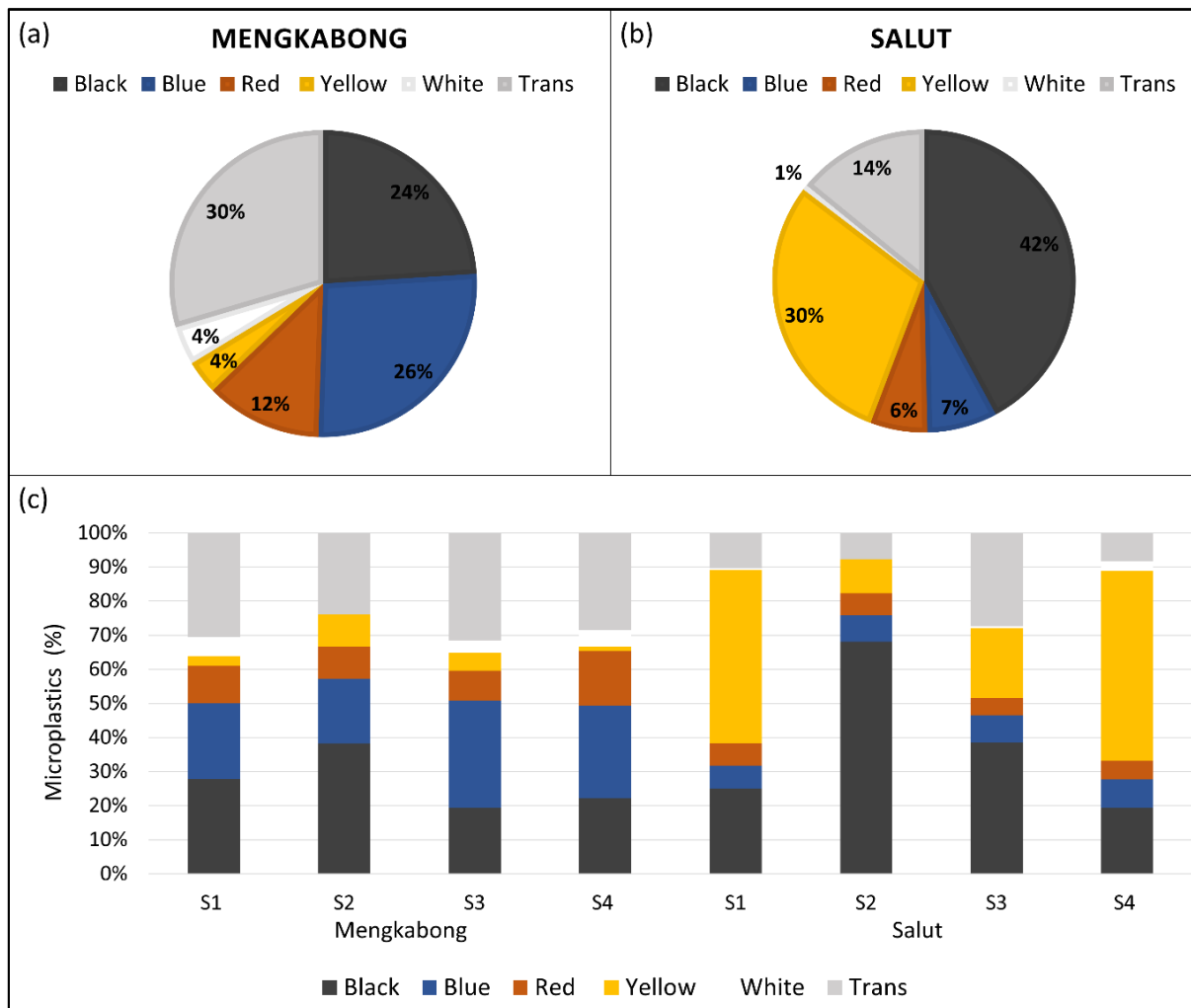


Figure 8. Composition of microplastics colours observed in (a) Mengkabong River, (b) Salut River, and (c) individual stations of Mengkabong and Salut Rivers

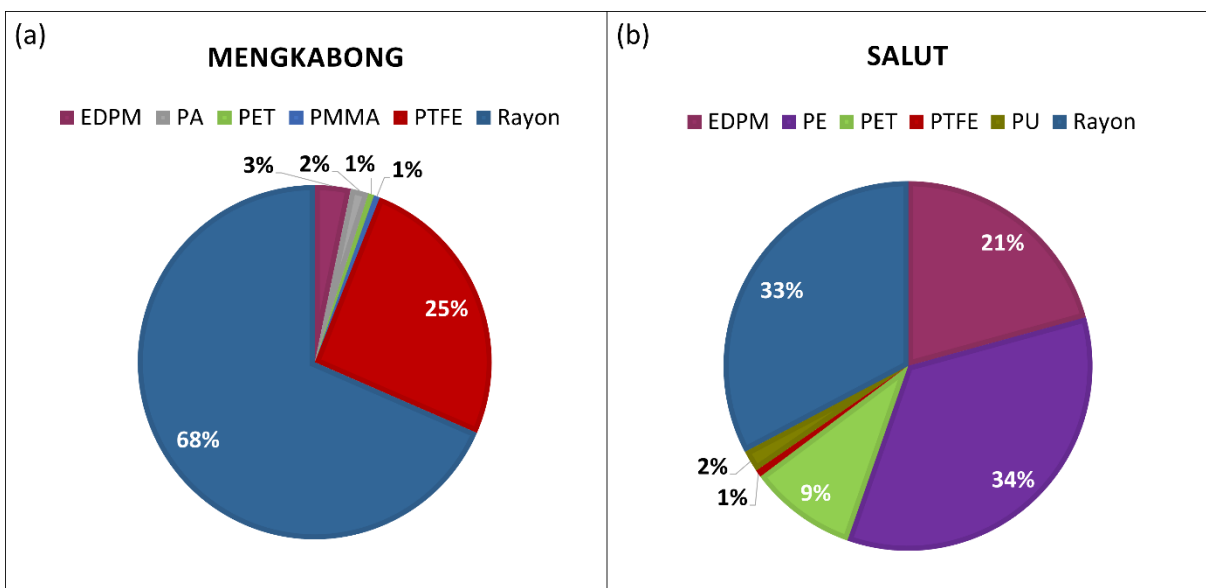
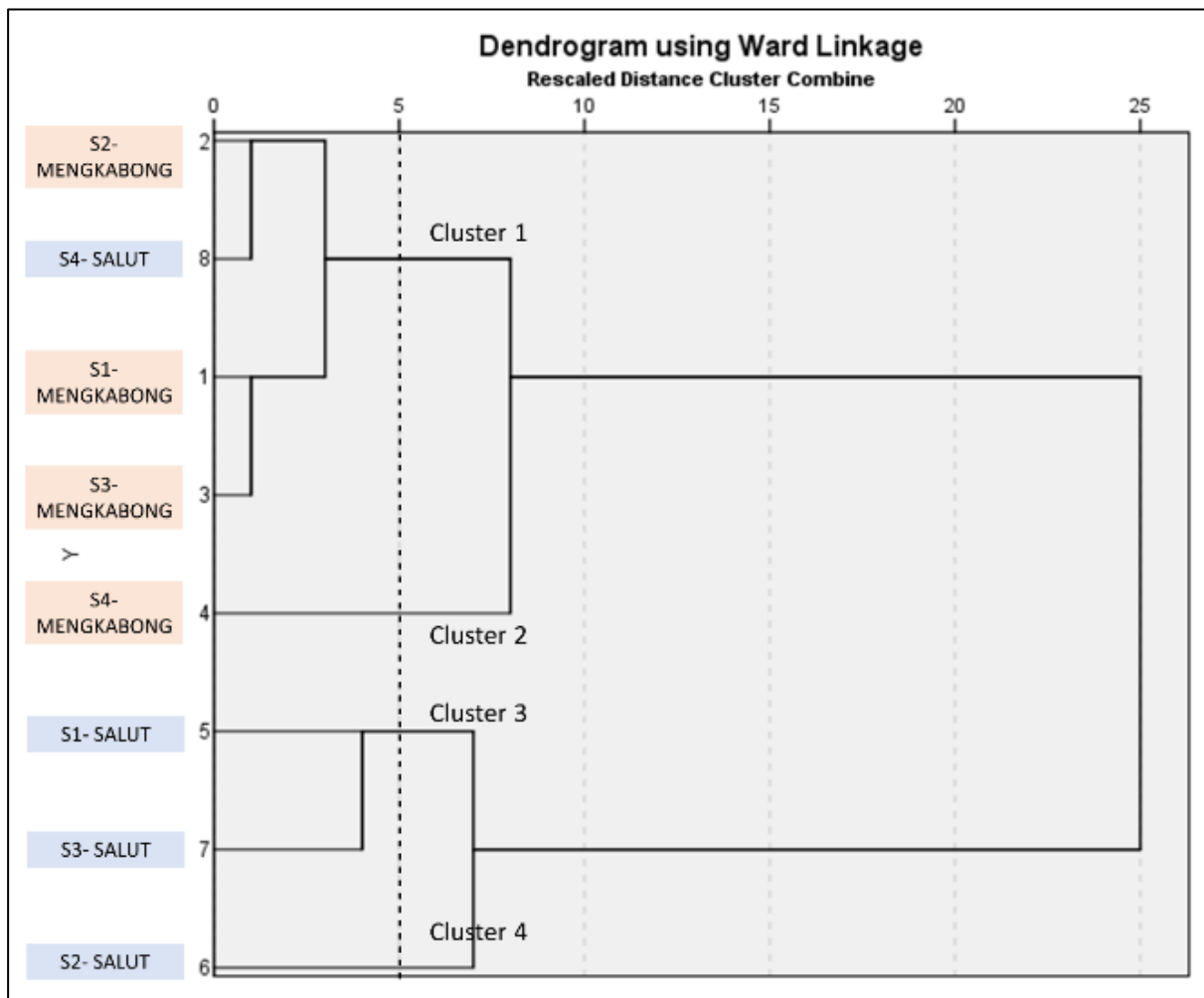


Figure 9. Composition of microplastics polymer type analysed by micro-FTIR in (a) Mengkabong River (b) and Salut River

Table 3. Mean difference of microplastics concentration and characteristics between the Mengkabong and Salut Rivers

Parameters		Mengkabong	Salut	Mean difference	<i>p</i> value
Total microplastics (items/L)		1.63 ± 0.87	4.78 ± 2.43	-3.16	0.05
Shape	Fibre	1.26 ± 0.78	2.71 ± 1.93	-1.45	0.21
	Foam	0.003 ± 0.01	0.03 ± 0.02	-0.02	0.04
	Fragment	0.22 ± 0.08	1.87 ± 1.48	-1.65	0.11
	Film	0.15 ± 0.04	0.18 ± 0.12	-0.03	0.62
Colour	Black	0.39 ± 0.14	2.01 ± 1.61	-1.63	0.09
	Blue	0.43 ± 0.28	0.36 ± 0.17	0.08	0.67
	Red	0.20 ± 0.16	0.29 ± 0.16	-0.09	0.46
	Yellow	0.06 ± 0.03	1.42 ± 1.27	-1.36	0.12
	White	0.07 ± 0.05	0.03 ± 0.02	0.04	0.19
	Transparent	0.48 ± 0.26	0.68 ± 0.58	-0.19	0.57
Size	LMP	1.20 ± 1.0.72	1.77 ± 1.22	-0.57	0.46
	SMP	0.43 ± 0.15	3.01 ± 1.67	-2.58	0.02

Positive value of mean difference indicates parameter studied was higher in the Mengkabong River whereas negative value indicates parameter studied was higher in Salut River. The significant difference in mean was indicated in bold, *p* value ≤ 0.05.

**Figure 10.** Clustering of the eight sampling stations of Mengkabong and Salut Rivers based on the similarities of microplastics concentration and characteristics. Red box on the left indicates stations in Mengkabong River and blue box for stations in Salut River.

DISCUSSION

Microplastic Pollution Status in Mengkabong and Salut Rivers

Microplastics have been documented to contaminate aquatic ecosystems worldwide, and the present study reveals that Sabah is no exception. Microplastics were found in both Mengkabong and Salut Rivers in the present study but in different level of pollution status. Microplastic in Salut River was significantly higher (p value ≤ 0.05) compared to Mengkabong River. In addition, cluster analysis demonstrated that most stations in the Mengkabong River were grouped in the Cluster 1 indicative of minimal microplastic pollution whereas stations in Salut River were grouped into clusters indicative of moderate and high counts of microplastics. One of the main factors that affecting the pollution level is the adjacent land use. Salut River is more urbanised with developments compared to Mengkabong River leading to higher microplastics counts coming possibly from land-based activities such as increased residential, more notable industrial presence, and recreational developments compared to Mengkabong River. Salut River is also smaller and shallower than Mengkabong River thus, contributing to more concentrated microplastics influx per chance due to a reduced dilution (De Arbeloa & Marzadri, 2024). The observed trend of decreasing microplastic concentrations downstream in the Mengkabong River, contrasted with increasing counts downstream in the Salut River, can be attributed to the intensity of the land uses adjacent to the sampling stations. The substantial land utilization in the vicinity of the stations could serve as a notable origin of microplastics entering the nearby river waters. The closer the river with area of intense activities, the more pronounced the occurrence of microplastic in that specific waterway (Idrus *et al.*, 2022).

Given the lack of international or national regulations pertaining to microplastics pollution standards, this study undertook a comparison of microplastic in relation to similar studies conducted in tidal rivers or estuaries (Table 4). Overall, Mengkabong River in the present study recorded as the least polluted with microplastics while the microplastics count in Salut River waters were comparatively higher than rivers in Selangor (Zaki *et al.*, 2021) and Johor (Primus

and Azman, 2022) but less polluted than rivers in Sarawak (Choong *et al.*, 2021; Liong *et al.*, 2021), Vietnam and Thailand (Babel *et al.*, 2022). The relatively lower levels of microplastics in the current study can be ascribed to the existence of mangrove forests in the Salut and Mengkabong Rivers. Similarly, Zaki *et al.* (2021) demonstrated that lower microplastic count was observed at area covered with forests and mangroves with less anthropogenic activities at that vicinity. Primus and Azman (2022) also attributed the lower microplastics count at Melayu River, Johor, as that particular area was preserved for eco-tourism activities and surrounded by mangroves forest. Mangrove forest could act as a natural physical barrier that traps, captures and retains microplastics by filtration process of mangrove sediment and roots system and thus, prevents microplastics entry into the river waters from plastic waste released from adjacent land.

The low microplastics counts in the present study also attributable to a lower intensity of anthropogenic activity as compared to a more urbanised river. The Saigon River in Thailand and the Miri River Estuary in Sarawak, for instance, were loaded with high microplastics due to their urban setting and the extensive land utilization for residential purposes, commercial activities, aquaculture and fishing operations that contributes to source of microplastics (Liong *et al.*, 2021; Babel *et al.*, 2022). High microplastics presence in river waters in these urbanised areas were reported to be sourced from intense residential activities through everyday plastic use and disposal practices (Hwi *et al.*, 2020), industrial processes through manufacturing and wastewater discharge (Choong *et al.*, 2021), while fishing activities contributed through the degradation and fragmentations of plastic-based fishing equipment (Johnson *et al.*, 2020).

Microplastics Characteristics and Their Potential Entry Sources

All microplastics in both present rivers were of secondary microplastics from the fragmentations of larger plastics as no pellets were recorded. It was observed that domestic wastes consisting plastics were piled up nearby the village houses while plastic bottles, wrappers and large fragments were seen floating in those river waters during sampling. Long exposure to direct

sunlight and sufficient oxygen could lead to microcracking and embrittlement of surface plastic leads to fragmentations of these larger plastics into small sized microplastics following physical, chemical and biological processes (Qaisrani *et al.*, 2020). The initiated UV-induced photo-oxidation then continues with autocatalytic degradation, which reduces the

polymer's molecular weight and weakens its structural integrity to more smaller fragmentations easily (Andrady, 2011). The elevated concentrations of SMP across all stations in the Salut River also may indicate a pronounced fragmentation process, leading to an increased abundance in the smaller size microplastics range (He *et al.*, 2020).

Table 4. Comparison of the microplastics concentration (Items/L) in river waters

Location	Concentration (items/L)	Remarks	Reference
Mengkabong River, Sabah	1.63 ± 0.87	Surrounded mainly with mangrove forests with less anthropogenic activities except at village houses that has fishing activities.	Present study
Klang River Estuary, Selangor	2.5 ± 2.00	Urban areas of industrial, residential and fishing and ecosystem of mangrove forests.	Zaki <i>et al.</i> (2021)
Melayu River, Johor	3.0 ± 0.00	Reserved river for eco-tourism activities. Residential and fishing area surrounded by mangrove forests.	Primus and Azman (2022)
Salut River, Sabah	4.78 ± 2.43	Surrounded by anthropogenic activities along river such as villages, residential and fishing.	Present study
Miri River Estuary, Sarawak	12.34 ± 1.54	Upstream surface water runoff end point while residential, agricultural and industrial activities at river banks. Improper waste disposal: Vast plastic wastes of bags, bottles, containers reported in terrestrial environment.	Liong <i>et al.</i> (2021)
Baram River Estuary, Sarawak	13.65 ± 4.65	Illegal waste disposal with anthropogenic activities of fishing. Lower estuary comprises of large wood production industries and interisland ports and shipyards.	Choong <i>et al.</i> (2021)
Saigon River, Vietnam	42.00 ± 5.00	Low population density of new residential area and agriculture activities but has canal water influence that carries sewages.	Babel <i>et al.</i> (2022)
Chao Phraya River, Thailand	48.00 ± 8.00	Extensive urban area for industrial, aquaculture, fishing and residential activities.	Babel <i>et al.</i> (2022)

The diverse and distinct characteristics of microplastics found in different stations are inherently linked to their respective sources, from which these pollutants originated. The highest abundance of fibres observed in both Mengkabong and Salut Rivers were hypothesized to originate from the fishing and aquaculture activities. Aquaculture activities of mussels and oysters were carried out in river waters at upstream (Station 4) of Mengkabong River while there was a fishing jetty at Station 2 of Salut River. Fishing equipment, such as fishing ropes, lines, and nets, are composed of fibres that could be released into rivers as a result of their breakdown during fishing operations (Zaki *et al.*, 2021). Besides, the prevalence of fibres may also be contributed from the release of synthetic fibres from the domestic wastewater

discharge that sips through filtration into watercourses (Chen *et al.*, 2021).

The occurrence of a substantial quantity of fibre has also been documented in previous studies such as the Melayu River in Johor (Primus & Azaman, 2022) and Cherating River in Pahang (Pariatamby *et al.*, 2020). The lower density and high surface area to volume area of fibres compared to other microplastics shapes allows them to remain floating on surface water. Therefore, fibres tend to accumulate and become more prevalent in aquatic environments (Choong *et al.*, 2021). Contradictorily, the percentage of fragment was greater than fibre at Stations 1 and 4 in Salut River, due to the substantial fragmentation of plastics derived from domestic garbage coming from nearby housing villages (Zaki *et al.*, 2021). Additionally, the elevated

presence of foam in the waters of the Salut River may be traced back to the foam shape plastic used for furniture and mattresses, shoe soles and car seats from these domestic households, as supported by the polyurethane (PU) that found in the Salut River (Liong *et al.*, 2021).

Microplastics in river waters display a diverse array of colours, providing valuable insights into their transportation and sources. The observed colours of microplastics play a crucial role in deciphering their origin and subsequent transport mechanisms within aquatic ecosystems. The prevalence of transparent, blue and black colours in this study may stem from fishing activities, as fibres from fishing nets and lines exhibit the same colours. Corroboratively, there was a notable abundance of fibre in this study potentially sourced from the similar fishing activities. This emphasizes that the colours observed can serve as a secondary confirmation of the microplastics' origin after initially discerning the source based on microplastic shapes. Likewise, other research studies have recorded that colour assisted in determining the origin of microplastics whereby in their investigations, the transparent (Wang *et al.*, 2017; Hwi *et al.*, 2020), blue (Primus & Azman, 2022) and black (Liu *et al.*, 2021) colours were also identified as fibres sourced from fishing activities.

The present study revealed that rayon was the most abundant polymer type in the Mengkabong River, accounting for 68% of the total polymer types, and the second most abundant polymer type in the Salut River (33%). Rayon is semi-synthetic cellulose-based polymer fibres from artificial clothing, textiles manufacturing, bedding, linens and fishing nets supports those fibres possibly released from household clothing washing and fishing activities. Hwi *et al.* (2020) mentioned that if the particular rayon was material from the natural fibre, there would be an assignment band at $1,735\text{ cm}^{-1}$ corresponding to C=O stretching of an ester. Notably, this peak was absent in the rayon spectrum (Figure 11) therefore verified that they were not natural fibre and were an actual plastic derived polymer. Natural rayon is from animal and plants and is not considered as plastic. Man-made fibres chemically synthesised through the polymerization of plastic materials unlike the non-natural fibre rayon. A high percentage of PTFE microplastics (25%) was also found in the

Mengkabong River. This polymer type of microplastics is commonly used in non-stick coatings for cookware and labware, implying that microplastics are sourced from the domestic waste. Also, the fact that polyamide (PA) microplastics, which are commonly used in textiles, fishing lines, and nets, were found in the Mengkabong River lends credence to the idea that the fibres came from fishing or textiles (Zaki *et al.*, 2021).

In contrast, PE (32%) was the most abundant in the Salut River, and when combined with PET (9%) yields the highest percentage (41%) of plastic polymer type found in Salut River waters. PE are often used in manufacturing products such as packaging like plastic bags and films, containers for plastic bottles, pipes and plumbing components, toys and household items (Ezeudu *et al.*, 2024). Similarly, PET is commonly utilized for more rigid packaging and containers, in addition to the application as polyester fibres used for clothing and textiles (Choong *et al.*, 2021). Additionally, EPDM, which is commonly used for automotive parts such as seals, roofing materials, and construction manufacturing (Liong *et al.*, 2021) was also abundant (21%) in Salut River. The presence of these polymer type microplastics suggests a possible origin from household appliances and construction materials from residential flats and a construction site spotted in Salut River.

The Potential Ecological Impacts of Microplastic to Aquatic Ecosystems

The occurrence of microplastics in the Mengkabong and Salut Rivers can pose an environmental hazard and health risk to the aquatic organisms inhabiting the rivers' ecosystem. The widespread dispersion of these microplastics makes their removal from the rivers challenging due to their small size properties. The microplastics in river waters can be transported to the ocean by currents (D'Avignon *et al.*, 2022) or deposited into river bottom (He *et al.*, 2019). The transportation of microplastics in river waters varies among rivers as it is greatly influenced by the hydrological features such as the overall topography, water flow and velocity as well as hydraulic parameters like depth and width of that particular river (Choong *et al.*, 2021). The present study is a preliminary endeavour with a one-time sampling in these rivers, hence, further studies

on temporal and tidal variations of microplastics abundance in rivers should be conducted to better understanding the dynamic of microplastics in the rivers for better management plan.

The next alarming issue is that aquatic organisms such as fish (Primus & Azaman, 2022), zooplanktons (Amin *et al.*, 2020) and invertebrates (Fachruddin *et al.*, 2020) can inadvertently ingest microplastics and mistake them for food. Both Mengkabong and Salut Rivers had the highest fibre which can be mistakenly ingested by these organisms that

favours fibres shape microplastics due to the resemblances to their diet. For instance, Yasaka *et al.* (2022) discovered ingestion of fibres by two fish species, *Barbonymus altus* and *Laloides longibarbis* were due to their threadlike resemblance of food to worms or zooplanktons. Numerous other studies have also shown that fibre is the highest microplastics shape extracted from fish (Lim *et al.*, 2023; Matupang *et al.*, 2023). Similarly, a study in the Bohai Sea, China, interestingly found microplastics being ingested by zooplankton were predominately blue fibres, likely due to the specific composition of microplastics in the area (Zheng *et al.*, 2020).

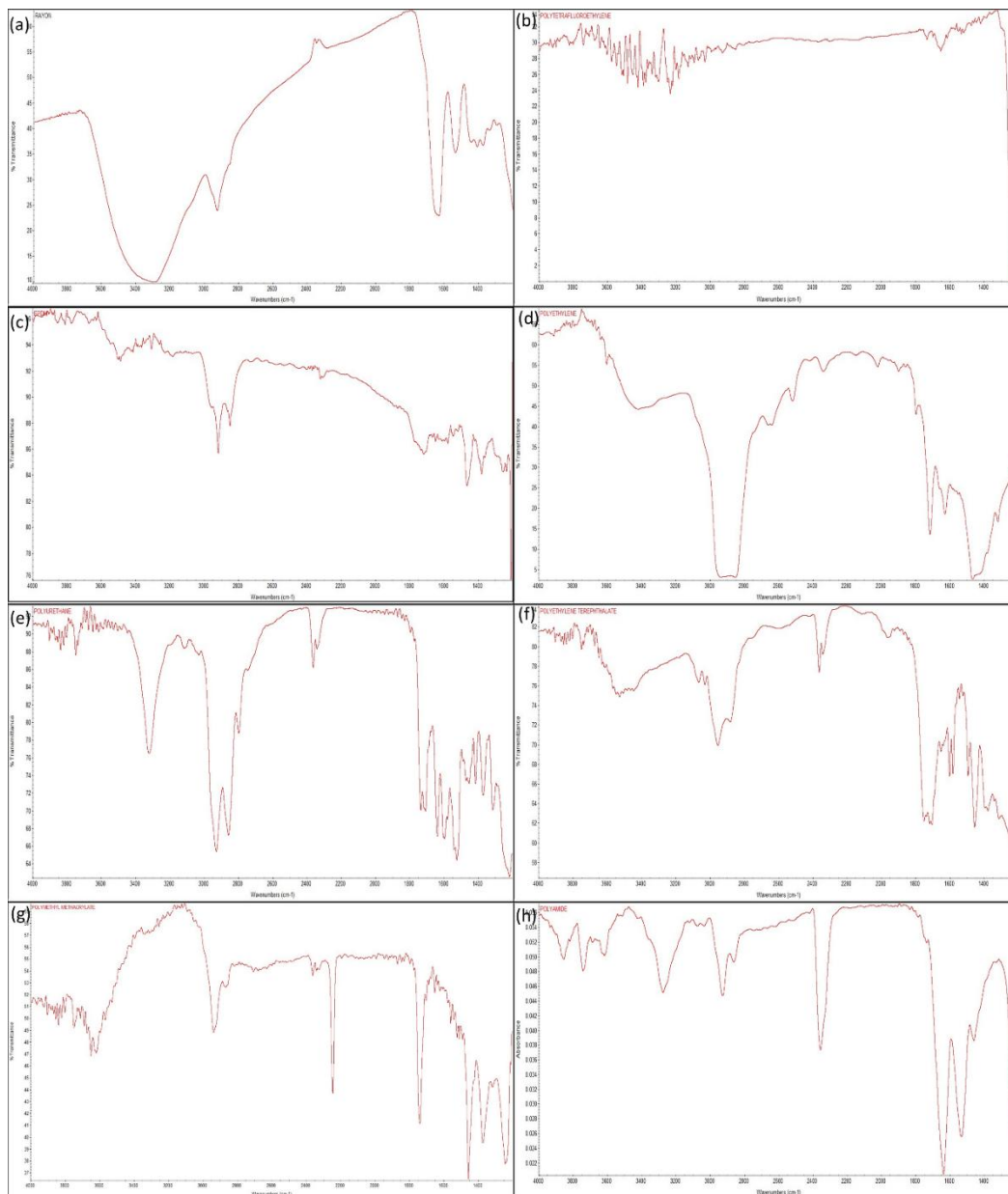


Figure 11. Micro-FTIR spectrum of polymer type (a) rayon, (b) polytetrafluoroethylene (PTFE), (c) ethylene propylene diene monomer (EPDM), (d) polyethylene (PE), (e) polyurethane (PU), (f) polyethylene terephthalate (PET), (g) polymethylmethacrylate (PMMA), and (h) polyamide (PA).

In addition to microplastic shape, studies have shown that microplastics smaller than 1 mm are frequently ingested by fish (Bianchi *et al.*, 2020; Primus & Azman, 2022; Arshad *et al.*, 2023), as well as by zooplanktons (Zheng *et al.*, 2020) and invertebrates like mussels (Li *et al.*, 2021). Consequently, the presence of a high number of small-sized microplastics in the water column of the Salut River may expose these organisms to a higher risk of ingestion. The presence of high numbers of transparent, blue and white microplastics in Mengkabong River waters and black and yellow microplastics in Salut River might be another risk factor to specific aquatic organisms that resembles their food preferences (Xiong *et al.*, 2019; Okamoto *et al.*, 2022).

The deposited microplastics in the benthic realm poses ingestion risk to benthic invertebrates too (Bertoli *et al.*, 2022). Microplastic contamination levels in grazers and filter-feeders were found to be three to five times greater than in predators and omnivores with highest microplastics count recorded in bivalves followed by gastropods, polychaete, amphipods, and actinia in Terra Nova Bay (Sfriso *et al.*, 2020). Although aquatic invertebrates capable of ingesting microplastics, invertebrate like mussel can expel 81-85% of the ingested microplastics through bio deposits (pseudofeces) within six days of depuration (Fernandez & Albentosa, 2019).

Lastly, both rivers in Sabah examined in this study showed a higher percentage of rayon in water. The rayon identified in this study was found to be synthetic fibres, and consequently, their effects on river waters are akin to those of fibre-shaped microplastics. Different polymer type of microplastics can pose different toxicity level to aquatic organisms based on their chemical structures and compositions (Laila *et al.*, 2020). Given all the potential risks of ingestion and toxicity, this study serves as a starting point to accelerate more research on the potential ecological impact of microplastic on native aquatic species in Sabah waters since microplastics were found in the present study.

CONCLUSION

The present study demonstrated that the Mengkabong and Salut Rivers, located in Sabah, exhibits a low level of microplastics pollution.

The microplastic concentrations in Salut River were significantly higher than Mengkabong River, which can be attributed to the greater level of development observed in the Salut River area. The microplastics found in both rivers were from the secondary microplastics and consisted primarily fibre, fragment, foam and film. The sources of microplastics in these rivers are mainly from domestic, fishing, and aquaculture activities. Microplastics showed spatial heterogeneity in the Mengkabong and Salut Rivers where the adjacent anthropogenic activities and land uses influence the abundance and characteristics of microplastics in rivers. Despite the low level of microplastic pollution, regular monitoring is necessary to evaluate the long-term pollution status of rivers and the potential ecological impacts of microplastics on aquatic organisms. This study can serve as a reference and a starting point to accelerate further research on microplastic pollution in Sabah rivers since there is confirmed presence of microplastics influx in the studied rivers.

ACKNOWLEDGEMENTS

The authors would like to thank the Universiti Malaysia Sabah (UMS) for funding this study through the Postgraduate Research Grant (UMSGreat) (GUG0589-1/2023). The authors gratefully acknowledge facilities provided by the Institute for Tropical Biology and Conservation (ITBC) and Borneo Marine Research Institute (BMRI), UMS. This study was conducted with the approval of the Sabah Biodiversity Council [Access License Ref. - JKM/MBS.1000-2/2 JLD.16 (53-55)].

REFERENCES

- Andrady, A. L. (2011). Microplastics in the marine environment. *Marine Pollution Bulletin*, 62(8): 1596-1605. DOI: 10.1016/j.marpolbul.2011.05.030
- Amin, R.M., Sohaimi, E.S., Anuar, S.T. & Bachok, Z. (2020). Microplastic ingestion by zooplankton in Terengganu coastal waters, southern South China Sea. *Marine Pollution Bulletin*, 150: 110616. DOI: 10.1016/j.marpolbul.2019.110616
- Arshad, N., Alam, M.M., Su'ud, M.B.M., Imran, S., Siddiqui, T., Saleem, K., Bashir, A. & Batool, A. (2023). Microplastic contamination from surface waters and commercially valuable fishes of Karachi Coast, Pakistan. *Regional Studies in*

- Marine Science*, 62: 102955. DOI: 10.1016/j.rsma.2023.102955
- Babel, S., Ta, A.T., Loan, N.T.P., Sembiring, E., Setiadi, T. & Sharp, A. (2022). Microplastics pollution in selected rivers from Southeast Asia. *APN Science Bulletin*, 12(1): 5-17 DOI: 10.30852/p.4589
- Banik, P., Anisuzzaman, M., Bhattacharjee, S., Marshall, D.J., Yu, J., Nur, A.A. U., Jolly, Y.N., Al-Mamun, M., Paray, B.A., Bappy, M.M.M. & Bhuiyan, T. (2024). Quantification, characterization and risk assessment of microplastics from five major estuaries along the northern Bay of Bengal coast. *Environmental Pollution*, 342: 123036. DOI: 10.1016/j.envpol.2023.123036
- Bertoli, M., Pastorino, P., Lesa, D., Renzi, M., Anselmi, S., Prearo, M. & Pizzul, E. (2022). Microplastics accumulation in functional feeding guilds and functional habit groups of freshwater macrobenthic invertebrates: Novel insights in a riverine ecosystem. *Science of The Total Environment*, 804: 150207. DOI: 10.1016/j.scitotenv.2021.150207
- Bianchi, J., Valente, T., Scacco, U., Cimmaruta, R., Sbrana, A., Silvestri, C. & Matiddi, M. (2020). Food preference determines the best suitable digestion protocol for analysing microplastic ingestion by fish. *Marine Pollution Bulletin*, 154: 111050. DOI: 10.1016/j.marpolbul.2020.111050
- Chen, H.L., Gibbins, C.N., Selvam, S.B. & Ting, K.N. (2021). Spatio-temporal variation of microplastic along a rural to urban transition in a tropical river. *Environmental Pollution*, 289: 117895. DOI: 10.1016/j.envpol.2021.117895
- Choong, W.S., Hadibarata, T. & Tang, D.K.H. (2021). Abundance and distribution of microplastics in the water and riverbank sediment in Malaysia—A review. *Biointerface Research in Applied Chemistry*, 11(4): 11700-11712. DOI: 10.33263/BRIAC114.1170011712
- De Arbeloa, N.P., & Marzadri, A. (2024). Modelling the transport of microplastics along river networks. *Science of The Total Environment*, 911: 168227. DOI: 10.1016/j.scitotenv.2023.168227
- Department of Statistics Malaysia. (2022). *Key findings population and housing census of Malaysia, 2020 Administrative district: Tuaran district, Sabah*, 11.
- Dusim, H.H. (2021). A study on the adequacy of Kota Kinabalu Sabah's solid waste management policy. *Journal of Administrative Science*, 18(1): 199-218.
- D'Avignon, G., Gregory-Eaves, I. & Ricciardi, A. (2022). Microplastics in lakes and rivers: an issue of emerging significance to limnology. *Environmental Reviews*, 30(2): 228-244. DOI: 10.1139/er-2021-0048
- Ezeudu, O.B., Tenebe, I.T. & Ujah, C.O. (2024). Status of production, consumption, and end-of-life waste management of plastic and plastic products in Nigeria: Prospects for circular plastics economy. *Sustainability*, 16(18): 7900. DOI: 10.3390/su16187900
- Fachrudin, L., Yaqin, K. & Iin, R. (2020). Comparison of two methods of analyzing microplastic concentrations of green mussels, *Perna viridis*, and their application in ecotoxicological studies. *Jurnal Pengelolaan Perairan*, 3(1): 1-13.
- Fauziah, S.H., Liyana, I.A. & Agamuthu, P. (2015). Plastic debris in the coastal environment: The invincible threat? Abundance of buried plastic debris on Malaysian beaches. *Waste Management and Research*, 33(9): 812–821. DOI: 10.1177/0734242X15588587
- Fernandez, B. & Albentosa, M. (2019). Insights into the uptake, elimination and accumulation of microplastics in mussel. *Environmental Pollution*, 249: 321-329. DOI: 10.1016/j.envpol.2019.03.037
- He, B., Goonetilleke, A., Ayoko, G.A. & Rintoul, L. (2020). Abundance, distribution patterns, and identification of microplastics in Brisbane River sediments, Australia. *Science of the Total Environment*, 700: 134467. DOI: 10.1016/j.scitotenv.2019.134467
- Henderson, L., & Green, C. (2020). Making sense of microplastics? Public understandings of plastic pollution. *Marine Pollution Bulletin*, 152: 110908. DOI: 10.1016/j.marpolbul.2020.110908
- Hocking, A. (2022). Microplastics in biosolids – definitions and implications. *Parliamentary Library & Information Service*. Melbourne: Parliament of Victoria. DOI: 10.25916/dp2h-aj97
- Huang, Y., Tian, M., Jin, F., Chen, M., Liu, Z., He, S., Li, F., Yang, L., Fang, C. & Mu, J. (2020). Coupled effects of urbanization level and dam on microplastics in surface waters in a coastal watershed of Southeast China. *Marine Pollution*

- Bulletin*, 154: 111089. DOI: 10.1016/j.marpolbul.2020.111089
- Hwi, T.Y., Ibrahim, Y.S. & Khalik, W. (2020). Microplastic abundance, distribution, and composition in Sungai Dungun, Terengganu, Malaysia. *Sains Malaysiana*, 49: 1479–1490. DOI: 10.17576/jsm-2020-4907-01
- Idrus, F. A., Fadhli, N.M. & Harith, M.N. (2022). Occurrence of microplastics in the asian freshwater environments: A review. *Applied Environmental Research*, 44(2): 1-17. DOI: 10.35762/AER.2022.44.2.1
- Issac, M.N. & Kandasubramanian, B. (2021). Effect of microplastics in water and aquatic systems. *Environmental Science and Pollution Research*, 28(16): 19544-19562. DOI: 10.1007/s11356-021-13184-2
- Jendanklang, P., Meksumpun, S., Pokavanich, T., Ruengsorn, C. & Kasamesiri, P. (2023). Distribution and flux assessment of microplastic debris in the middle and lower Chao Phraya River, Thailand. *Journal of Water and Health*, 21(6): 771-788. DOI: 10.2166/wh.2023.013
- Johnson, G., San Hii, W., Lihan, S. & Tay, M.G. (2020). Microplastics determination in the rivers with different urbanisation variances: A case study in Kuching City, Sarawak, Malaysia. *Borneo Journal of Resource Science and Technology*, 10(2): 116-125. DOI: 10.33736/bjrst.2475.2020
- Laila, Q.N., Purnomo, P.W. & Jati, O.E. (2020). Kelimpahan mikroplastik pada sedimen di Desa Mangunharjo, Kecamatan Tugu, Kota Semarang. *Jurnal Pasir Laut*, 4(1): 28-35. DOI: 10.14710/jpl.2020.30524
- Li, J., Wang, Z., Rotchell, J.M., Shen, X., Li, Q. & Zhu, J. (2021). Where are we? Towards an understanding of the selective accumulation of microplastics in mussels. *Environmental Pollution*, 286: 117543. DOI: 10.1016/j.envpol.2021.117543
- Li, X., Chen, Y., Zhang, S., Dong, Y., Pang, Q., Lynch, I., Xie, C., Guo, Z. & Zhang, P. (2023). From marine to freshwater environment: A review of the ecotoxicological effects of microplastics. *Ecotoxicology and Environmental Safety*, 251: 114564. DOI: 10.1016/j.ecoenv.2023.114564
- Lin, L., Zuo, L. Z., Peng, J.P., Cai, L. Q., Fok, L., Yan, Y., Li, H & Xu, X.R. (2018). Occurrence and distribution of microplastics in an urban river: a case study in the Pearl River along Guangzhou City, China. *Science of the Total Environment*, 644: 375-381. DOI: 10.1016/j.scitotenv.2018.06.327
- Lim, K.P., Ding, J., Loh, K.H., Sun, C., Yusoff, S., Chanthran, S.S.D., & Lim, P.E. (2023). First evidence of microplastic ingestion by crescent perch (*Terapon jarbua*) in Malaysia. *Regional Studies in Marine Science*, 67: 103202. DOI: 10.1016/j.rsma.2023.103202
- Liong, R.M.Y., Hadibarata, T., Yuniarto, A., Tang, K.H.D. & Khamidun, M.H. (2021). Microplastic Occurrence in the Water and Sediment of Miri River Estuary, Borneo Island. *Water, Air, & Soil Pollution*, 232(8): 1-12. DOI: 10.1007/s11270-021-05297-8
- Liu, Y., You, J., Li, Y., Zhang, J., He, Y., Breider, F., Tao, S. & Liu, W. (2021). Insights into the horizontal and vertical profiles of microplastics in a river emptying into the sea affected by intensive anthropogenic activities in Northern China. *Science of The Total Environment*, 779: 146589. DOI: 10.1016/j.scitotenv.2021.146589
- Matupang, D.M., Zulkifli, H.I., Arnold, J., Lazim, A.M., Ghaffar, M.A. & Musa, S.M. (2023). Tropical sharks feasting on and swimming through microplastics: First evidence from Malaysia. *Marine Pollution Bulletin*, 189: 114762. DOI: 10.1016/j.marpolbul.2023.114762
- Montoi, J., Hashim, S.R.M. & Tahir, S. (2017). A study on tuaran river channel planform and the effect of sand extraction on river bed sediments. *Transactions on Science and Technology*, 4(4): 442-448. DOI: 10.13140/RG.2.2.13437.61920
- Multisanti, C.R., Merola, C., Perugini, M., Aliko, V. & Faggio, C. (2022). Sentinel species selection for monitoring microplastic pollution: A review on one health approach. *Ecological Indicators*, 145: 109587. DOI: 10.1016/j.ecolind.2022.109587
- Okamoto, K., Nomura, M., Horie, Y. & Okamura, H. (2022). Color preferences and gastrointestinal-tract retention times of microplastics by freshwater and marine fishes. *Environmental Pollution*, 304: 119253. DOI: 10.1016/j.envpol.2022.119253
- Pariatamby, A., Hamid, F.S., Bhatti, M.S., Anuar, N. & Anuar, N. (2020). Status of microplastic pollution in aquatic ecosystem with a case study on Cherating River, Malaysia. *Journal of Engineering Science and Technology*, 52(2): 222-241. DOI: 10.5614/j.eng.technol.sci.2020.52.2.7

- Peng, G., Zhu, B., Yang, D., Su, L., Shi, H. & Li, D. (2017). Microplastics in sediments of the Changjiang Estuary, China. *Environmental Pollution*, 225: 283-290. DOI: 10.1016/j.envpol.2016.12.064
- Pittura, L., Gorbi, S., Mazzoli, C., Nardi, A., Benedetti, M. & Regoli, F. (2022). Microplastics and nanoplastics. In J. Blasco, A. Tovar-Sánchez, (eds.). *Marine Analytical Chemistry*, pp. 349-388. Cham, Switzerland: Springer. DOI: 10.1007/978-3-031-14486-8_8
- Primus, A. & Azman, S. (2022). Quantification and characterisation of microplastics in fish and surface water at Melayu River, Johor. In *IOP Conference Series: Materials Science and Engineering* (Vol. 1229, No. 1, p. 012014). IOP Publishing. DOI: 10.1088/1757-899X/1229/1/012014
- Qaisrani, Z., Shams, S., Guo, Z.R. & Mamun, A.A. (2020). Qualitative analysis of plastic debris on beaches of Brunei Darussalam. *Pollution*, 6(3): 569-580. DOI: 10.22059/poll.2020.297713.751
- Sarijan, S., Azman, S., Said, M.I.M., Andu, Y. & Zon, N. F. (2018). Microplastics in sediment from Skudai and Tebrau river, Malaysia: a preliminary study. In *MATEC Web of Conferences* (Vol. 250, p. 06012). EDP Sciences. DOI: 10.1051/mateconf/201825006012
- Singh, R., Kumar, R. & Sharma, P. (2022). Microplastic in the subsurface system: Extraction and characterization from sediments of River Ganga near Patna, Bihar. In P. K. Gupta, B. Yadav & S. Kumar (eds.) *Advances in Remediation Techniques for Polluted Soils and Groundwater*, pp. 191-217: Elsevier. DOI: 10.1016/B978-0-12-823830-1.00013-4
- Sfriso, A.A., Tomio, Y., Rosso, B., Gambaro, A., Sfriso, A., Corami, F., Rastelli, E., Corinaldesi, C., Mistri, M. & Munari, C. (2020). Microplastic accumulation in benthic invertebrates in Terra Nova Bay (Ross Sea, Antarctica). *Environment International*, 137: 105587. DOI: 10.1016/j.envint.2020.105587
- Suardy, N.H., Tahrin, N.A. & Ramli, S. (2020). Analysis and characterization of microplastic from personal care products and surface water in Bangi, Selangor. *Sains Malaysiana*, 49(9): 2237-2249. DOI: 10.17576/jsm-2020-4909-21
- Wang, T., Wang, J., Lei, Q., Zhao, Y., Wang, L., Wang, X. & Zhang, W. (2021). Microplastic pollution in sophisticated urban river systems: Combined influence of land-use types and physicochemical characteristics. *Environmental Pollution*, 287: 117604. DOI: 10.1016/j.envpol.2021.117604
- Xiong, X., Tu, Y., Chen, X., Jiang, X., Shi, H., Wu, C. & Elser, J. J. (2019). Ingestion and egestion of polyethylene microplastics by goldfish (*Carassius auratus*): influence of color and morphological features. *Heliyon*, 5(12). DOI: 10.1016/j.heliyon.2019.e03063
- Yasaka, S., Pitaksanurat, S., Laohasiriwong, W., Neeratanaphan, L., Jungoth, R., Donprajum, T. & Tawetanawanit, P. (2022). Bioaccumulation of microplastics in fish and snails in the Nam Pong River, Khon Kaen, Thailand. *Environment Asia*, 15(1). DOI: 10.14456/ea.2022.8
- Zaki, M.R.M., Ying, P.X., Zainuddin, A.H., Razak, M.R. & Aris, A.Z. (2021). Occurrence, abundance, and distribution of microplastics pollution: evidence in surface tropical water of Klang River estuary, Malaysia. *Environmental Geochemistry and Health*, 43(9): 3733-3748. DOI: 10.1007/s10653-021-00872-8
- Zheng, S., Zhao, Y., Liangwei, W., Liang, J., Liu, T., Zhu, M., Li, Q. & Sun, X. (2020). Characteristics of microplastics ingested by zooplankton from the Bohai Sea, China. *Science of the Total Environment*, 713: 136357. DOI: 10.1016/j.scitotenv.2019.136357

Evaluation of Euphrates River Water Quality on Phytoplankton Biodiversity in Ramadi, Iraq

MOHAMMED M. SHARQI¹, ABDUL-NASIR A. AL-TAMIMI¹ & OMAR M. HASSAN^{1*2}

¹Department of Biology, Education College for Women, University of Anbar, Ramadi, 31001, Iraq;

²Department of Biology, College for Science, University of Anbar, Ramadi, 31001, Iraq

Corresponding author: sc.omerhasan@uoanbar.edu.iq

Received: 28 March 2024

Accepted: 23 October 2024

Published: 31 December 2024

ABSTRACT

Water quality deterioration is a major global issue due to population growth and rapid economic development, making healthy water essential for human societies' and ecosystems' sustainable development. Therefore, the current study aims to evaluate the quality of Euphrates River water through its chemical and physical parameters, as well as the distribution of the phytoplankton community. An environmental comparison was conducted between three stations in Ramadi city to assess the Euphrates River's water quality. The comparison was based on physicochemical and biological variables. Fifteen environmental parameters were measured: temperature, pH, electrical conductivity, dissolved oxygen, biochemical oxygen demand, total turbidity, total dissolved solids, alkalinity, bicarbonate, nitrate, sulfate, phosphate, calcium, magnesium, and chloride. The occurrence of seasonal phytoplankton communities was also examined, and the Palmer diversity index, water quality index, and Pearson correlation were calculated. Significant differences were found in the physical and chemical variables of the Euphrates water between studied stations, and in the biological diversity of phytoplankton. The highest average temperature was 26.5 °C at station 1, the highest average pH was 7.575 at station 3, and the electrical conductivity was high at both stations 1 and 3, reaching 810 µS/cm. The Biochemical Oxygen Demand (BOD) ranged from 1.375 to 1.675 mg/L, the lowest average total hardness was 304.5 mg/L at station 3 and the highest average was 310.75 mg/L at station 1. In addition, the study revealed a high diversity in phytoplankton species and groups. 45 genera of green algae were found at all stations, while only 4 genera of Euglenophyceae and Dinophyceae were found. The study confirmed that the quality of the Euphrates River's water is medium and is characterized by high contamination with organic materials, according to the pollution index for water. It was concluded that phytoplankton groups are a sensitive and useful indicator of waterway health.

Keywords: Biodiversity, bioindicators, Euphrates River, phytoplankton, water quality

Copyright: This is an open access article distributed under the terms of the CC-BY-NC-SA (Creative Commons Attribution-NonCommercial-ShareAlike 4.0 International License) which permits unrestricted use, distribution, and reproduction in any medium, for non-commercial purposes, provided the original work of the author(s) is properly cited.

INTRODUCTION

Water quality is a critical factor in determining the health status of water bodies, which directly affects human health. Human activities can cause significant damage to water bodies, thereby depleting natural water resources. As a result of rapid economic progress and population expansion, water quality degradation has emerged as a major concern worldwide (Zhang *et al.*, 2021). Eutrophication, biodiversity extinction, and serious risks to public health are just a few of the negative impacts that this issue may have. Spatiotemporal variations and trends in water quality can be attributed to a variety of human activities, pollution sources, and geographic changes (Xu *et al.*, 2022).

Water quality in many bodies of water is subject to a variety of influences, such as climate change (Akhtar *et al.*, 2021), natural sources (Yousif *et al.*, 2024), human activities, specifically mining (Soleimani *et al.*, 2018), sewage discharge (Abbasnia *et al.*, 2018), agricultural and urban activities, and industrial pollution (Pereira *et al.*, 2023), while synergistic impacts have the potential to significantly alter water quality, leading to eutrophication, reduced dissolved oxygen levels, and other issues. Protecting and managing water quantity and quality is becoming more difficult due to the numerous threats to the aquatic environment (Weng *et al.*, 2023).

Phytoplankton are essential to freshwater ecosystems because they are the principal producers and a fundamental component of

aquatic ecosystems, and because of their short life cycle, extensive dispersion, and vital function in energy flow, material cycle, and information transmission (Li *et al.*, 2019; Aboim *et al.*, 2019; Huang *et al.*, 2023). Considered crucial markers of river health, phytoplankton composition, population size, and variety reveal a lot about water quality (Fathan *et al.*, 2020). Phytoplankton have varying levels of sensitivity to water contamination, making them an excellent early warning system for water quality deterioration. Therefore, phytoplankton are reliable environmental indicators for assessing the extent of pollution in different water bodies. The density of phytoplankton is influenced by various complex factors, which depend on the interactions and relationships between physicochemical parameters (Al-Anzy *et al.*, 2023). The ever-changing nature of water environmental quality can be fully and promptly understood by studying phytoplankton community traits (Sabater-Liesa *et al.*, 2018).

River health evaluation systems are now incorporating biological evaluation indices and water quality methodologies, which are crucial for assessing levels of water pollution and nutrition (Sabater-Liesa *et al.*, 2018; Noon *et al.*, 2021; Zhang *et al.*, 2021; Qu & Zhou, 2024). Thus, in order to effectively safeguard the environment and comprehend the effects of human activities on water quality and its variability of spatio-temporal features, aquatic biology-based water quality assessments are crucial (Edan & Sharqi, 2020).

The Euphrates River is one of the two major rivers that flow through Iraq. Its source is in Turkey, and it flows through Syria before entering Iraq from the western border. Finally, it discharges into the Shatt al-Arab. It is considered one of the longest rivers in West Asia, with forty percent of its water flowing into Turkey, twenty-5% into Syria, and 35% into Iraq. Unfortunately,

the most significant problem facing rivers and streams in Iraq is pollution (Sharqi *et al.*, 2021). The assessment of the ecological condition or potential of rivers generally relies on the evaluation of biological components, including phytoplankton, phytobenthos (mostly diatomaceous), macrophytes, zoobenthos, and ichthyofauna (Dembowska, 2021). Phytoplankton communities thrive in large, continuous-flow rivers that have extended water retention periods. Phytoplankton, as the primary component of the trophic hierarchy, show the highest degree of response to changes in the aquatic environment, making them a very reliable indicator of water quality (Chidiac *et al.*, 2023).

Limited studies have been conducted to assess the water quality of the Euphrates River using phytoplankton. It is crucial to comprehend the fluctuations in water quality over time and location, as well as the primary sources of influence. This understanding can aid in the developing effective methods for evaluating water quality, which is essential for environmental governance and public health. This study aimed to assess the water quality of the Euphrates River through its chemical and physical parameters, as well as the distribution of the phytoplankton community, by calculating pollution indices.

MATERIALS AND METHODS

Location of Study

The study was carried out in Ramadi, Anbar, Iraq. Three stations were chosen along the Euphrates River: the first station is situated at the eastern entrance to Ramadi, the second is in the city centre, and the third station is directly before the Al-Warar Canal Dam. Further details about the stations are included in Table 1 and Figure 1.

Table 1. Geographic location of study stations

Stations	Latitude (Northwards)	Longitude (Eastwards)
1	43° 15' 52"	25° 26' 23"
2	43° 17' 53"	27° 26' 33"
3	43° 19' 05"	36° 26' 33"

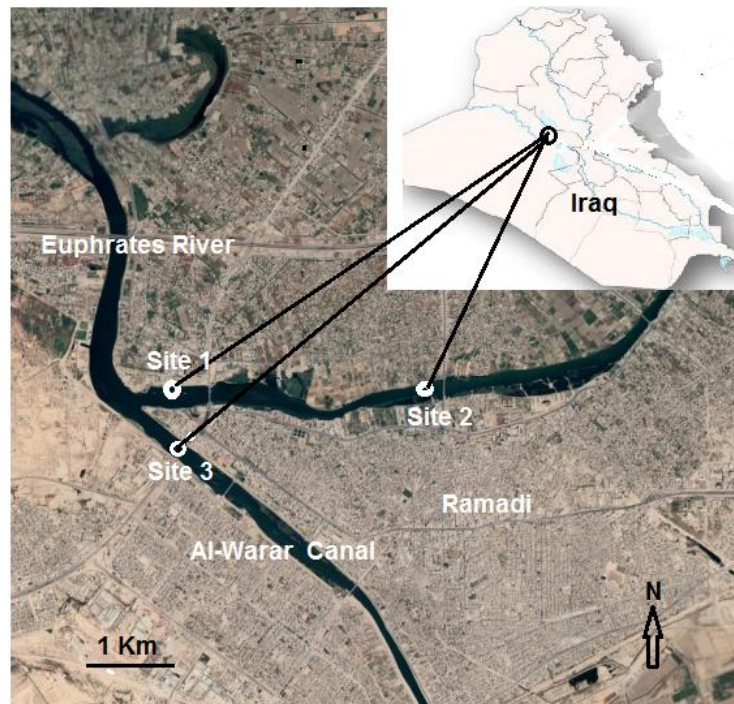


Figure 1. Sampling stations in the Euphrates River, Anbar, Iraq

Sample Collection

Physical and chemical parameters

Water samples were collected from the Euphrates River once a month during the period from July – October 2023 during the morning hours from 8:00 a.m. – 10:00 a.m. Water samples were collected in polypropylene bottles to measure turbidity and nutrients. Other water samples were collected in dark bottles for biochemical oxygen demand (BOD), immediately fixed with Winkler's reagent, and estimated in the lab using titration. A multi-sensor device (WTW 340i/set, Germany) was utilized for on-station measurement of water parameters, including temperature in Celsius, electrical conductivity (EC), pH, and dissolved oxygen (DO) concentration. Samples were analyzed in the lab using a spectrophotometer (PG T80+, England). Turbidity was measured by the nephelometric method using a HACH 2100P Portable turbidimeter, USEPA 180.1, EU. Analysis of essential nutrient parameters (nitrite, nitrate, ammonia, and phosphate) was performed in accordance with Standard Methods for the Examination of Water and Wastewater, 24th Edition (Lipps *et al.*, 2023). Each parameter was measured three times to ensure accuracy and consistency. The Water Quality Index (WQI) was calculated using Eq. (1) according to the

National Sanitation Foundation Water Quality Index (NSF-WQI) method, and the water quality was determined based on the classification given in Chidiac *et al.* (2023) as shown in Table 2.

$$NSF\ WQI = \sum_{i=1}^n Q_i W_i \quad \text{Eq.(1)}$$

Where NSF-WQI is the score of the water quality index; Q_i is the sub-index value of the water quality parameter; W_i is the weighted score; and n is the number of water quality parameters.

Phytoplankton Sampling and Identification

Phytoplankton samples were gathered from a depth of 1 m using a standard Towing-Henson plankton net (mouth diameter 0.35 m) constructed of threaded nylon fabric (mesh size 25 μm). The obtained phytoplankton biomass was immediately transferred to 100 ml sample tubes containing 5% neutralized formalin for microscopic examination. Taxonomic identification was done using a compound light microscope at 1000X magnification and taken with a Nikon 90i Eclipse trinocular microscope.

A sample of 1 ml was collected and transferred into the counting chamber of the Sedgwick Rafter in order to conduct a quantitative analysis of phytoplankton

communities. Once the substance had accumulated for a period of time, it was tallied. Each group was tallied a minimum of five times. Averaging was performed on the values. A calculation was performed to determine the overall count of phytoplankton in a 1 L water sample (Al-Obeidi & Al-Tamimi, 2024). The identification of phytoplankton species was conducted by consulting established guides and textbooks (Van Vuuren, 2006; Bellinger & Sigeo, 2015). Water quality characteristics (low or high organic pollution) were evaluated using the pollution index developed by Palmer (1969)

who created a list of 60 genera and 80 species of algae that are tolerant of organic pollution. He developed the Palmer algae genus index to assess the organic pollution of water bodies. This index is still used today and is calculated using a table listing the 20 algae genera that are most tolerant of organic pollution, each of which is assigned a number based on its relative tolerance. The total score obtained from the numbers assigned to each genus at each sampling station is used to assess organic pollution according to the classification given in Table 2.

Table 2. Water quality and pollution indices classification

NSF WQI		Palmer Index	
Index score	Quality Status	Index score	Quality Status
0–25	Very Bad	< 10	Very light organic pollution
26–50	Bad	10 to 15	Light organic pollution
51–70	Moderate	15 to 20	Moderate organic pollution
71–90	Good	> 20	High organic pollution
91–100	Very Good		

Statistical Analysis

Statistical analysis was performed using SPSS version 23. All data were expressed as mean and standard deviation. Analysis of variance (ANOVA) was used to examine multivariate spatial and temporal differences in physicochemical parameters and phytoplankton data. Tukey's test was used for post-hoc multiple comparisons between means of variables. Significance was attributed to values at $p < 0.05$.

RESULTS AND DISCUSSION

Physical and Chemical Parameters

Data from measurements of physicochemical parameters of temperature, pH, conductivity, turbidity, dissolved oxygen, BOD, and nutrients in the Euphrates at different sites are presented in Table 3. The highest temperature at Site 1 was recorded in August at 29 °C, while Site 2 recorded the highest temperature in July at 28 °C. The highest water temperature for site 3 was recorded in July at 29 °C. Water temperature changes depending on the change in air temperature (Saod *et al.*, 2019). As for the pH values, the highest value recorded in October was in Stations 1 and 3 (7.8), while it increased

slightly in Station 2 and reached 7.9 for the same month. The lowest pH value was recorded in Station 1 and Station 2 at 7.3 for August and July, while it decreased slightly in Station 3 to reach 7.2 for the month as a result of the scarcity of water from the Euphrates River in the summer season.

The Euphrates River's water is alkaline because of its highest carbonate and bicarbonate contents. The maximum values of electric conductivity noted in July were 1060, 1068, and 1071 $\mu\text{S}/\text{cm}$ respectively. The lowest ones were recorded in September reaching 627 $\mu\text{S}/\text{cm}$. This is caused by the fact that river levels during rainy months are lower than their normal levels which makes the wet months have a smaller conductivity value. On the other hand, resistivity values are generally higher for the arid period and this can be related to the phenomenon of lower water levels, which are intensified by the higher temperature and the inflow of salt from human activities (Hussein *et al.*, 2023). Regarding DO value, the highest value of DO was reported in October reaching up to 13 mg/L in station 2, whereas 12 and 13 mg/L in stations 1 and 3. The lowest value was 8 mg/L for July in stations 1 and 3 whereas 9 mg/L in station 2. Therefore, the Euphrates River water is well-

aerated (Muhammad & Ali, 2013; Hanjaniamin *et al.*, 2022). Furthermore, the highest value of BOD was 2 mg/L at stations 1 and 2 for October, while the highest was 1.9 in station 3 for July and October, but the lowest value was 1.2 and 1.4 mg/L in August and September, respectively. Based on these results, the Euphrates River water can be classified as clean water. The results of this study are consistent with the results indicated by (Khlaif & Al-Hassany, 2023). The highest total hardness (TH) value was recorded in July for all study stations and amounted to 353, 358, and 356 mg/L, respectively, while the lowest value was recorded in October in Stations 1 and 2, where it reached 226 mg/L, while Station 3 recorded It rose to 253 mg/L. Based on the findings of the present investigation of total hardness values, the Euphrates River is classified as having medium hardness (Khudair, 2023). As for calcium ions, the highest value for this element was recorded in July in all study stations and was 124, 129, and 128 mg/L, respectively, while the lowest value recorded in October and in all stations was 50, 52, and 56 mg/L, respectively.

High calcium values during dry seasons may be caused by lower water levels at higher temperatures (Dey *et al.*, 2021). As for magnesium (Mg), the highest value obtained was in August at all study stations; as it reached 49 mg/L for Stations (1 and 2) while Station (3) recorded a value of about 48 mg/L where October had the lowest values. It can occur in 24, 28, and 25 mg/L for all study stations to exist high Mg values of dry season may be caused by river water heat up accompanied by low river water levels (Wiranegara *et al.*, 2023), or the river may enter and pass-through agricultural land and precipitate, or it may be due to the decomposition of algae or other living organisms and their return to the river water (Han *et al.*, 2022). The greater influence of the calcium concentration over Mg values can be explained by sewage and irrigation wastewater that is poured into the river saturated with sulphate, resulting in magnesium precipitation as $MgSO_4$ (Potasznik *et al.*, 2015). The highest value of total dissolved solids in water was recorded during July for all study stations and amounted to 562, 569 and 560 mg/L, respectively, while the lowest value was recorded during October for all

study stations and was 331, 326, and 322 mg/L, respectively. The values recorded for TDS in the present study are within the permissible limits (Al-Heety *et al.*, 2011). The highest total alkalinity (TA) value was recorded in August, and for all study cases, it was 188, 185, and 180 mg/L of $CaCO_3$, respectively, while the lowest value was recorded during October and for all states of the study and was 115, 116, and 113 mg/L of $CaCO_3$, respectively. Higher TA values in the dry season may be attributed to lower phytoplankton densities, leading to lower carbonate and bicarbonate consumption from water (Rao & Rao, 2016).

The highest value recorded for the chloride ion (Cl) was at Station 1 of 168 mg/L during July, while the lowest value was recorded at Station 3 of 72 mg/L during September. The values recorded for Cl in the current study are within permissible limits (Saod *et al.*, 2019). In terms of sulfate values, the highest concentration was recorded at Station 3 during July, reaching 296 mg/L. On the other hand, the lowest concentration was recorded during October in the same location, reaching 164 mg/L. The high concentration of sulfates in the water is due to the decrease in water levels and the influence of agricultural lands adjacent to the Euphrates River (Jalal *et al.*, 2023). The phosphate PO_4 values monitored at Station 3 reached 0.31 mg/L in October, while the lowest value was at Station 2 and was 0.1 mg/L during August. The high phosphate values in the wet season may be attributed to the rains, which wash away (PO_4) from agricultural lands laden with phosphate fertilizers into the river water (Mekawey *et al.*, 2023). In the nitrate (NO_3), the highest value was recorded at Station 1, which was 4.2 mg/L in August; the lowest value was recorded at Station 1; it was 1.4 mg/L in October; the high NO_3 values during the dry season may be due to the effect of the river on sewage water and agricultural land water (Li *et al.*, 2023); and finally, the highest rate of turbidity (Tur.) was in the share of Station 1, and it was 18 NTU during September, while the lowest value for it was in Station 3, and it amounted to 6 NTU in October. The high turbidity values at Station 1 are due to the turbulence of the water, as it is located near the Ramadi Dam.

Table 3. Physicochemical parameters in the modeling stations of Euphrates River – Ramadi

Parameters	Station 1	Station 2	Station 3	p value
Temp. (°C)	26.5±4.04	25.25±3.30	26.25±3.10	0.800
pH	7.5±0.26	7.55±0.24	7.575±0.32	0.944
EC. (µs/cm)	810±202.98	804.75±199.95	810.25±210.64	0.989
DO (mg/L)	9.5±1.29	11±0.82	10.75±1.71	0.039
BOD (mg/L)	1.675±0.26	1.375±0.48	1.525±0.36	0.044
T.H. (mg/L)	310.75±45.98	305.5±59.44	304.5±57.69	0.598
Ca (mg/L)	91.25±32.26	89.75±28.62	91±30.17	0.986
Mg (mg/L)	39±10.49	37.75±12.66	38.75±8.88	0.690
T.D.S (mg/L)	425±102.30	428.25±99.69	429±104.89	0.998
AlK (mg/L)	148.75±33.75	154.25±34.94	152±33.67	0.489
Cl (mg/L)	106±37.17	111±42.97	108.5±0.29	0.052
SO ₄ (mg/L)	225.25±61.05	225.75±58.35	225.75±61.14	0.999
PO ₄ (mg/L)	0.2575±0.12	0.325±0.13	0.25±0.13	0.025
NO ₃ (mg/L)	2.625±0.99	2.875±1.26	0±0	0.019
Turb. (mg/L)	11.5±3.87	13.75±3.77	0±0	0.001

Phytoplankton Diversity

Table 4 shows the classification and density of phytoplankton for all the studied stations during the study period. Regarding the algal classes that were diagnosed, they were connected to many algal classes and genera. In Station 1, green algae were dominated Chlorophyceae with 45 genera, then Cyanophyceae with 17 genera, and so was Euglenophyceae. The Euglenophyceae, diagnosed with four genera, is considered evidence of organic pollution, and its absence indicates clean river water (Khudair, 2023). The Dinophyceae, with three genera, the Bacillariophyceae centrals, with six genera, and the pennales, with twenty genera, followed. Finally, the Crysophyceae, identified as a single genus, was found. As for Station 2, the Bacillariophyceae (pennales) were diagnosed with 44 genera and the Bacillartophyceae (certrales) with 6 genera, as well as the sentesns, and almost 11 sub-species were recorded. As for Station 3, the dominance was for the Chlorophyceae with 24 genera, then the Cyanophaceae with 17 genera, then the Euglenophyceae with 5 genera, the Dinophyceae with 2 genera, and finally the golden algae (Crysophyceae) with one genus.

The greater percentage of green algae density (52%) over blue-green algae (8%) confirms that the Euphrates River water in the current study stations is fresh and moderately polluted water (Khaleefa & Kamel, 2021). The highest total number of phytoplankton cells was recorded in Station 1 with limits of 1.272×10^7 cell/ml

(Table 4), which may be attributed to the station not being affected by human activities (Yousif *et al.*, 2024), while lower numbers were recorded in Station 2 and 3.

NSF-WQI and Palmer's Index

According to the NSF-WQI (Figure 2), most of the stations recorded values during the months of the study that exceeded 60. Therefore, the Euphrates River water in the current study area is considered to be of medium quality despite recording values that exceeded 20 according to Palmer's Pollution Index (Figure 3). This result indicates that the water in the studied area has high organic pollution, which may be due to the large numbers of species recorded in the study stations, which have a high classification according to the table prepared by this guide, Euglena and Oscillatoria (Al-Kanani & Al-Essa, 2018; Khalaf & Sharqi, 2023).

A group of blue-green algae and euglenoids, indicative of the eutrophication water condition, were classified as *Ocsillatoria limosa*, *O. tenuis*, *Euglena acus*, and *E. gracilis*. While the species of daitoms were classified for the condition of the eutrophication water, which is as follows: *Cocconeis placentula*, *Cyclotella meneghiniana*, *Diatoma vulgare*, and *Hantzschia amphioxys*, this confirms that the water in the Euphrates River at the current study stations suffers from high organic pollution. This result is consistent with the study conducted by Tamaki and Obedi (2023).

Table 4. Classification and density of phytoplankton (cell/ml) in during the study period

Taxa	Station 1	Station 2	Station 3
Cyanophyceae			
<i>Anabaena aequalis</i>	++	++	+
<i>Anabaena wisconsinensis</i>	++	-	+
<i>Chroococcus disperses</i>	++	++	+
<i>C. turgidus</i>	+	+	+
<i>Gomphosphaeria aponima</i>	+	+	+
<i>Merismopedia aponglauca</i>	++	++	+
<i>M. punctata</i>	+	-	++
<i>Nostoc linckia</i>	+	+	+
<i>Oscillatoria amoena</i>	+	+	+
<i>O. angusta</i> Koppe	+	+	+
<i>O. limosa</i> Roth	+	+	+
<i>O. tenuis</i>	+	++	+
<i>O. nigra</i>	+	++	+
<i>O. sancta</i>	+	+	+
<i>Rhabdoderm sigmoidea</i>	+	+	+
<i>R. linuaris</i>	++	-	+
<i>Spirulina laxa</i>	++	++	+
Euglenophyceae			
<i>Euglena proxima</i>	+	+	+
<i>E. convolute</i>	+	+	+
<i>E. acus</i>	+	-	+
<i>E. gracilis</i>	+	+	+
Crysophyceae			
<i>Mallomouas caudate</i>	+++	++	+
Dinophyceae			
<i>Peridinium cinctum</i>	+++	+++	+
<i>P. cinctum</i>	++	++	+
<i>P. puillum</i>	++	++	+
Chlorophyceae			
<i>Chlorella vulgaris</i>	+++	+++	+
<i>Closterium lanceolatum</i>	++	++	++
<i>C. setaceum</i>	+++	+++	++
<i>Cosmarium bioculatum</i>	+++	+++	+
<i>C. botrytis</i>	+++	+++	+
<i>C. depressum</i>	++	-	+
<i>C. granatum</i>	+++	+++	+
<i>C. quadrifarium</i>	++	++	+
<i>C. subtumidum</i>	+++	+++	+
<i>C. subcrenatum</i>	+++	+++	++
<i>Crucigenia rectangularis</i>	+++	+++	+
<i>Dictyosphaerium pulchellum</i>	+	++	+
<i>D. ehrenbergianum</i>	+++	-	+
<i>Golenkinia paucipina</i>	+++	-	+
<i>G. radiata</i>	+++	+++	++
<i>Kirchneriella obesa</i>	+++	+++	++
<i>Lagerheimia citrififormis</i>	++	++	+
<i>L. subsala</i>	+++	+++	++
<i>Microspora</i>	++	++	++
<i>M. floccose</i>	++	++	+
<i>Mougeotia elegantula</i>	+	+	+
<i>Oedogonium cardiacum</i>	++	++	+
<i>O. gallicum</i>	+	+	+
<i>O. gigas</i>	+	-	+
<i>O. elliptica</i>	++	++	++
<i>O. eremosphaeria</i>	++	++	++
<i>O. plusiosporum</i>	+	+	+

Table 4 (continued).

<i>O. undulatum</i>	++	++	+
<i>Pediastrum boryanum</i>	+	+	+
<i>P. simplex meyen</i>	++	++	+
<i>P. simplex</i>	++	++	++
<i>Scenedesmus aburdanus</i>	+++	+++	++
<i>S. aburdanus</i>	+++	++	+
<i>S. armatus</i>	+++	++	+
<i>S. arcuatus</i>	++	++	++
<i>S. quadricarda</i>	++	++	+
<i>Spirogyera collinsii</i>	++	++	+
<i>S. subsalsa</i>	++	++	+
<i>Staurastrum anatinum</i>	+++	+++	+++
<i>S. polymorphum</i>	++	++	++
<i>S. punctulatum</i>	++	+	+
<i>S. tetracerum</i>	+++	++	+
<i>Ulothrix subilissiuma</i>	++	++	+
Bacillaptophyceae - Centrates			
<i>Aulacoseira granulate</i>	+	+	+
<i>A. italic</i>	++	+	+
<i>A. varians</i>	+	+	++
<i>Cyclotella meneghiniana</i>	+++	+	++
<i>C. ocellata</i>	+++	++	+
<i>Stephanodiscus astera</i>	++	++	+
Bacillaptophyceae- Pennales			
<i>Amphora venta</i>	+++	++	+
<i>Asterionella bleakeleyi</i>	++	++	+
<i>Bacillaria paxillifer</i>	++	+	+
<i>Cocconeis pediculs</i>	+++	+++	+++
<i>C. placentula</i>	+++	+++	+++
<i>Cymbella affinis</i>	+++	+++	++
<i>Cymatopleura solea</i>	++	+	+
<i>C. tumida</i>	+	+	+
<i>Diploneis psudovalis</i>	+	+	+
<i>D. smuthii</i>	++	++	+
<i>Diatoma vulgare</i>	++	++	+
<i>Fragllaria covotonursis</i>	+	+	+
<i>F. pulchella</i>	++	+	+
<i>Gomphonema gracile</i>	++	+	+
<i>G. olivaceum</i>	++	+	+
<i>Hantzschia amphioxys</i>	++	++	+
<i>Mastogloia brauni</i>	+	+	+
<i>M. elliptica</i>	+	+	+
<i>M. smithi</i>	++	+	+
<i>M. smithi</i>	+	+	+
<i>Navicula anglica</i>	+	+	+
<i>N. laterostarata</i>	+	+	+
<i>N. parva</i>	++	+	+
<i>N. salinarum</i>	++	-	-
<i>N. subrhyncocephata</i>	++	++	+
<i>Nitzschia acicularia</i>	+	+	+
<i>N. amphibia</i>	++	+	+
<i>N. dissipata</i>	++	++	++
<i>N. fasciculata</i>	++	+	+
<i>N. elongatula</i>	+	+	+
<i>N. obtusa</i>	+	+	+
<i>N. palea</i>	+	+	+
<i>Pleurosigma angulatum</i>	+	+	+
<i>P. elongatum</i>	+	+	+

Table 4 (continued).

<i>Rhapalodia gibba</i>	+	+	+
<i>Rhaicosphenia abbreviate</i>	+	+	+
<i>Synedra fasciculata</i>	++	++	+
<i>S. pulchella</i>	+	+	+
<i>S. ulna</i>	+	+	+
<i>Surirella ovalis</i>	+	+	+
<i>Tryblionella hungarica</i>	+	+	+
<i>T. levidensis</i>	+	+	+
<i>T. littralis</i>	+	+	+
Total count	1272	927	510

+ (< 5 cell/ml), ++ (5- 10 cell/ ml), +++(> 10 cell/ ml)

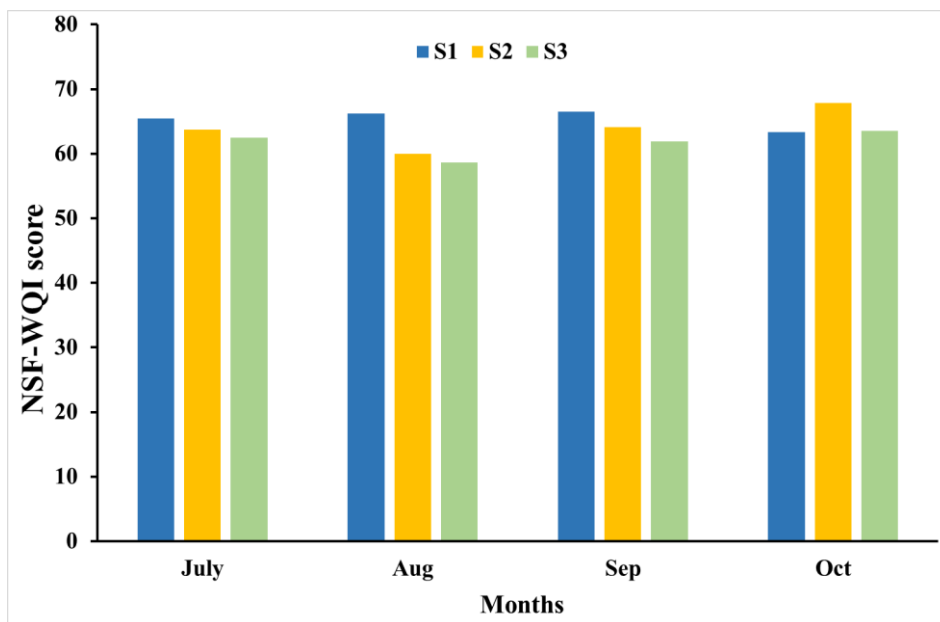


Figure 2. The values of the NSF-WQI in the study stations

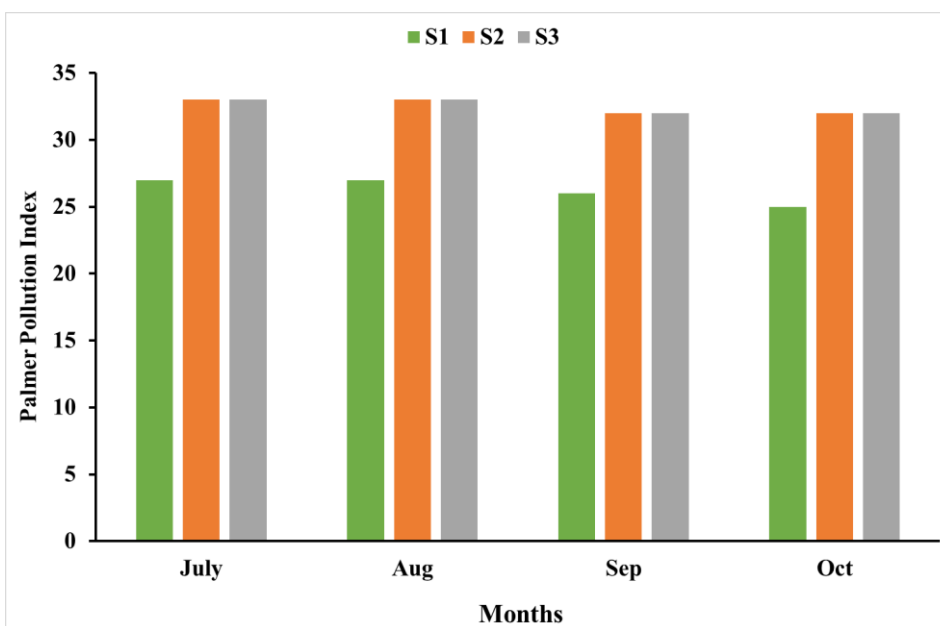


Figure 3. Spatial and temporal variations of Palmer pollution index in the Euphrates River

CONCLUSION

Many rivers around the world suffer from pollution problems. Therefore, the current study focused on evaluating the quality of Euphrates River water using chemical, physical, and biological criteria in the presence of phytoplankton. A spatial and temporal comparison was made for three stations in the Euphrates River in Ramadi city. The comparison was based on physical, chemical, and biological variables. The current study showed a variation in physical and chemical tests at all stations and in different months, and a large biological diversity was observed in algae categories and at all study stations. The Euphrates River water in the current study area is considered medium quality and has high organic pollution. We recommend conducting a comprehensive assessment of the Euphrates River in Iraq and the need to address its pollution problems, especially organic pollution.

ACKNOWLEDGMENT

The authors want to thank the Department of Environment in Anbar Governorate for providing assistance in completing this study.

Funding Information

Authors state no funding involved.

Conflict of interest

Authors state no conflict of interest.

REFERENCES

- Abbasnia, A., Radfard, M., Mahvi, A.H., Nabizadeh, R., Yousefi, M., Soleimani, H. & Alimohammadi, M. (2018). Groundwater quality assessment for irrigation purposes based on irrigation water quality index and its zoning with GIS in the villages of Chabahar, Sistan and Baluchistan, Iran. *Data in Brief*, 19: 623–631. DOI: 10.1016/j.dib.2018.05.061
- Aboim, I.L., Gomes, D.F. & Mafalda Junior, P. O. (2019). Phytoplankton response to water quality seasonality in a Brazilian neotropical river. *Environmental Monitoring and Assessment*, 192(1):70. DOI: 10.1007/s10661-019-7882-5
- Akhtar, N., Syakir Ishak, M.I., Bhawani, S.A. & Umar, K. (2021). Various natural and anthropogenic factors responsible for water quality degradation: A review. *Water*, 13(19): 2660. DOI: 10.3390/w13192660
- Al-Anzy, D.H.S., Al-Tamimi, A.N.A.M. & Sharqi, M.M. (2023). Biological and ecological monitoring using epiphytic diatoms on two aquatic plants to estimate the water quality of Habbaniyah Lake, Western Iraq. *IOP Conference Series: Earth and Environmental Science*, 1262(2): 022012. DOI: 10.1088/1755-1315/1262/2/022012
- Al-Heety, E.A., Turky, A.M. & Al-Othman, E. M. (2011). Physico-chemical assessment of Euphrates River between Heet and Ramadi Cities, Iraq. *Journal of Water Resource and Protection*, 03(11): 812–823. DOI: 10.4236/jwarp.2011.311091
- Al-Kanani, H.M. & Al-Essa, S.A. (2018). Assessment of Shatt Al-Arab River Water quality by using Palmer's Algal Index, Basrah, Iraq. *Basrah Journal of Agricultural Sciences*, 31(1): 70–77. DOI: 10.33762/bagsr.2018.160122
- Al-Obeidi, N.A.S. & Al-Tamimi, AN.A.M. (2024). Ecology and Biodiversity of Epiphytic Algae (Non-diatoms) on Typha Domingensis Pers. In the Upper Euphrates River Between Haditha Dam and Al Baghdadi in Western Iraq. In: Obaid, A.J., Al-Heety, E.A., Radwan, N., Polkowski, Z. (eds.) *Advanced Studies on Environmental Sustainability. ICES 2023*. Springer Proceedings in Earth and Environmental Sciences. Springer, Cham. pp. 41–58. https://doi.org/10.1007/978-3-031-57054-4_4
- Bellinger, E.G. & Sigeo, D.C. (2015). *Freshwater Algae: Identification, enumeration and use as bioindicators* (2nd ed.). John Wiley & Sons.
- Chidiac, S., El Najjar, P., Ouaini, N., El Rayess, Y. & El Azzi, D. (2023). A comprehensive review of water quality indices (WQIs): history, models, attempts and perspectives. *Reviews in Environmental Science and Bio/Technology*, 22(2): 349–395. DOI: 10.1007/s11157-023-09650-7
- Dembowska, E.A. (2021). The Use of Phytoplankton in the assessment of water quality in the lower section of Poland's largest river. *Water*, 13(23): 3471. DOI: 10.3390/w13233471
- Dey, S., Botta, S., Kallam, R., Angadala, R. & Andugala, J. (2021). Seasonal variation in water quality parameters of Gudlavalluru Engineering College Pond. *Current Research in Green and Sustainable Chemistry*, 4: 100058. DOI: 10.1016/j.crgsc.2021.100058
- Edan & Sharqi. (2020). A study some physico-chemical and bacterial properties of wastewater

- for Ramadi Teaching Hospital and its impact on the Euphrates River. *Indian Journal of Forensic Medicine & Toxicology*, 14(4): 2319-2325. DOI: 10.37506/ijfmt.v14i4.11903
- Fathan, M.R.R.N., Hasan, Z., Apriliani, I.M. & Herawati, H. (2020). Phytoplankton community structure as bioindicator of water quality in floating net cage area with different density at Cirata Reservoir. *Asian Journal of Fisheries and Aquatic Research*, 6(4): 19–30. DOI: 10.9734/ajfar/2020/v6i430103
- Han, C., Dai, Y., Sun, N., Wu, H., Tang, Y. & Dai, T. (2022). Algae bloom and decomposition changes the phosphorus cycle pattern in Taihu Lake. *Water*, 14(22): 3607. DOI: 10.3390/w14223607
- Hanjaniamin, A.E., Tabrizi, M.S. & Babazadeh, H. (2022). Dissolved oxygen concentration and eutrophication evaluation in Yamchi dam reservoir, Ardabil, Iran. *Applied Water Science*, 13(1):9. DOI: 10.1007/s13201-022-01786-1
- Huang, Z., Pan, B., Soininen, J., Liu, X., Hou, Y. & Liu, X. (2023). Seasonal variation of phytoplankton community assembly processes in Tibetan Plateau floodplain. *Frontiers in Microbiology*, 14: 1122838. DOI: 10.3389/fmicb.2023.1122838.
- Hussein, A.K., Muneam, R.R., Jafer, N.A., Ibrahimand, A.A. & Abojassim, A.A. (2023). Surface water assessment using water quality index: A case study of the Euphrates River, Najafi, Iraq, by using the GIS Technique. *IOP Conference Series: Earth and Environmental Science*, 1225(1): 012012. DOI: 10.1088/1755-1315/1225/1/012012.
- Jalal, A.D., Ani, Y.A., Thameel, S.S. & Ismael, Z.M. (2023). Study of the Euphrates River's water quality in front of and behind the Haditha Dam in Anbar Province, Iraq. *IOP Conference Series: Earth and Environmental Science*, 1222(1): 012042. DOI: 10.1088/1755-1315/1222/1/012042.
- Khalaf, H.K.A., & Sharqi, M.M. (2023). Identification of phytoplankton and its relationship to monthly changes and biological indexes in the water system of Warar Canal, Anbar Ramadi, Iraq. *Annals of Agri Bio Research*, 28(2): 386–392.
- Khaleefa, O., & Kamel, A.H. (2021). On the evaluation of water quality index: Case Study of Euphrates River, Iraq. *Knowledge-Based Engineering and Sciences*, 2(2): 35–43. DOI: 10.51526/kbes.2021.2.2.35-43.
- Khlaif, B.M., & Al-Hassany, J.S. (2023). Assessment of the Euphrates River's Water Quality at a some sites in the Iraqi governorates of Babylon and Karbala. *IOP Conference Series: Earth and Environmental Science*, 1262(2): 022021. DOI: 10.1088/1755-1315/1262/2/022021.
- Khudair, B.H. (2023). Assessment of water quality index and water suitability of the Tigris River for drinking water within Baghdad City, Iraq. *Journal of Engineering*, 19(6): 764–773. DOI: 10.31026/j.eng.2013.06.08.
- Li, X., Xu, Y.J., Ni, M., Wang, C. & Li, S. (2023). Riverine nitrate source and transformation as affected by land use and land cover. *Environmental Research*, 222: 115380. DOI: 10.1016/j.envres.2023.115380.
- Li, X., Yu, H., Wang, H. & Ma, C. (2019). Phytoplankton community structure in relation to environmental factors and ecological assessment of water quality in the upper reaches of the Genhe River in the Greater Hinggan Mountains. *Environmental Science and Pollution Research*, 26(17): 17512–17519. DOI: 10.1007/s11356-019-05200-3.
- Mekawey, M., Gamal, A. & Hussien, A. (2023). Assessment of water suitability to aquatic life using some water physicochemical variables and water quality index. *Egyptian Journal of Aquatic Biology and Fisheries*, 27(6): 739–757. DOI: 10.21608/ejabf.2023.330195.
- Muhammad, S.A. & Ali, A.F. (2013). Physiochemical properties and rotifera population density of Darbandikhan Lake, Kurdistan-Iraq. *Current Research Journal of Biological Sciences*, 5(2): 53–57. DOI: 10.19026/crjbs.5.5473.
- Noon, A.M., Ahmed, H.G.I. & Sulaiman, S.O. (2021). Assessment of water demand in Al-Anbar Province- Iraq. *Environment and Ecology Research*, 9(2): 64–75. DOI: 10.13189/eer.2021.090203.
- Palmer, C.M. (1969). A composite rating of algae tolerating organic pollution. *Journal of Phycology*, 5(1): 78–82. DOI: 10.1111/j.1529-8817.1969.tb02581.x.
- Pereira, L.C.C., Sousa, N.D.S.D.S., Silva, B.R.P.D., Costa, A.L.B.D., Cavalcante, F.R.B., Rodrigues, L.M.D.S., & Costa, R.M.D. (2023). Influence of Anthropogenic Activities on the Water Quality of an Urban River in an Unplanned Zone of the Amazonian Coast. *Limnological Review*, 23(2): 108–125. <https://doi.org/10.3390/limnolrev23020007>

- Potasznik, A., Szymczyk, S. & Potasznik, A. (2015). Magnesium and calcium concentrations in the surface water and bottom deposits of a river-lake system. *Journal of Elementology*, 20(3): 677-692. DOI: 10.5601/jelem.2014.19.4.788.
- Qu, S. & Zhou, J. (2024). Phytoplankton community structure and water quality assessment in Xuanwu Lake, China. *Frontiers in Environmental Science*, 11: 1303851. DOI: 10.3389/fenvs.2023.1303851.
- Rao, D. & Rao, G. (2016). Seasonal abundance of phytoplankton in relation to physico chemical features of Venkammacheruvu Veeraghattam, Sriakulam(Dist.)A.P, India. *IOSR Journal of Pharmacy and Biological Sciences*, 11(04): 91–98. DOI: 10.9790/3008-1104049198.
- Sabater-Liesa, L., Ginebreda, A. & Barceló, D. (2018). Shifts of environmental and phytoplankton variables in a regulated river: A spatial-driven analysis. *Science of the Total Environment*, 642: 968–978. DOI: 10.1016/j.scitotenv.2018.06.096.
- Saad, W.M., Mohammed, E. A. & Hussenc, A. H. (2019). Euphrates River water quality studies in Iraq: Critical Review. *Anbar Journal of Engineering Sciences*, 10(1): 61–66. DOI: 10.37649/aengs.2019.171364.
- Sharqi, M., M Hasan, O. & A Salih, T. (2021). Effect of Urban Sewage Water on Pollution of the Euphrates River, Iraq. *Indian Journal of Ecology*, 48: 296–298.
- Soleimani, H., Nasri, O., Ojaghi, B., Pasalari, H., Hosseini, M., Hashemzadeh, B., Kavosi, A., Masoumi, S., Radfard, M., Adibzadeh, A., & Feizabadi, G. K. (2018). Data on drinking water quality using water quality index (WQI) and assessment of groundwater quality for irrigation purposes in Qorveh & Dehgolan, Kurdistan, Iran. *Data in Brief*, 20: 375–386. <https://doi.org/10.1016/j.dib.2018.08.022>
- Tamaki, A.N.a.A. & Obeidi, N.a.A. (2023). Use of epiphytic diatoms in *Cyperus Papyrus* L. as bioindicators in the assessment of the health of the upper Euphrates River Between the Haditha Dam and Al-Baghdadi, Iraq. *IOP Conference Series Earth and Environmental Science*, 1222(1): 012020. DOI: 10.1088/1755-1315/1222/1/012020.
- Van Vuuren, S.J. (2006). *Easy identification of the most common freshwater algae: a guide for the identification of microscopic algae in South African freshwaters*. Resource Quality Services (RQS).
- Weng, X., Jiang, C., Yuan, M., Zeng, T. & Sheng, M. (2023). Assessment of a new nutrient management strategy to control harmful cyanobacterial blooms in Lake Taihu using a hydrodynamic-ecological model. *Environmental Research Communications*, 5(12): 125002. DOI: 10.1088/2515-7620/ad1063.
- Wiranegara, P., Sunardi, S., Sumiarsa, D. & Juahir, H. (2023). Characteristics and changes in water quality based on climate and hydrology effects in the Cirata Reservoir. *Water*, 15(17): 3132. DOI: 10.3390/w15173132.
- Xu, W., Duan, L., Wen, X., Li, H., Li, D., Zhang, Y. & Zhang, H. (2022). Effects of seasonal variation on water quality parameters and eutrophication in Lake Yangzong. *Water*, 14(17): 2732. DOI: 10.3390/w14172732.
- Yousif, Y. M., Hassan, O. M. & Ibraheem, I. J. (2024). Fabrication of nanocellulose membranes from freshwater green algae (*Chara corallina*) and their application in removing bacteria from water. *Environment and Ecology Research*, 12(2): 154–162. DOI: 10.13189/eer.2024.120206.
- Yousif, Y. M., Mutter, T. Y., & Hassan, O. M. (2024). Health risks and environmental assessments of heavy metals in road dust of Ramadi, Iraq. *Journal of Degraded and Mining Lands Management*, 11(2): 5301–5306. DOI: 10.15243/jdmlm.2024.112.5301.
- Zhang, Y., Gao, W., Li, Y., Jiang, Y., Chen, X., Yao, Y., Messyasz, B., Yin, K., He, W., & Chen, Y. (2021). Characteristics of the Phytoplankton Community Structure and Water Quality Evaluation in Autumn in the Huaihe River (China). *International Journal of Environmental Research and Public Health*, 18(22): 12092. <https://doi.org/10.3390/ijerph182212092>

Characterizing Fatty Acid Profiles and Evaluating Antibacterial Activity of Edible Yellow Puffer Fish, *Xenopterus naritus*

SAMSUR MOHAMAD*¹, NUR EQMAL DINIE NOR AZMI¹, ZAINI ASSIM¹, AHMAD SYAFIQ AHMAD NASIR¹, JULIAN RANSANGAN² & RABUYAH NI³

¹ Faculty of Resource Science and Technology, Universiti Malaysia Sarawak, 94300 Kota Samarahan, Sarawak, Malaysia; ² Borneo Marine Research Institute, Universiti Malaysia Sabah, Jalan UMS, 88400 Kota Kinabalu, Sabah, Malaysia; ³ Faculty of Applied Science, Universiti Teknologi Mara Sarawak, 94300 Kota Samarahan, Sarawak, Malaysia

*Corresponding author: msamsur@unimas.my

Received: 3 April 2024

Accepted: 5 July 2024

Published: 31 December 2024

ABSTRACT

Puffer fish oil extracted from *Xenopterus naritus* represents a beneficial source of bioactive compounds with health-promoting properties. Despite the known benefits of puffer fish oil, there is a lack of detailed information on its fatty acid composition. This study aimed to fill this gap by investigating the fatty acid profiles of puffer fish oil extracted from the liver and muscle tissues. The oil was extracted using the solvent Bligh & Dyer method, and the samples were derivatized into fatty acid methyl esters (FAME) before being analyzed via Shimadzu QP2010 Plus gas chromatography-mass spectrometry (GC-MS). This analysis highlighted the prevalence of omega-3 fatty acids, particularly Docosahexaenoic acid (DHA) ($8.28 \pm 0.08\%$ in liver, $6.15 \pm 0.33\%$ in muscle oil) and Eicosapentaenoic acid (EPA) ($3.29 \pm 0.12\%$ in liver and $2.16 \pm 0.06\%$ in muscle oil), along with the abundance of omega-6 and omega-9 fatty acids, including arachidonic and oleic acid. Additionally, the antimicrobial properties of these fish oils were assessed against Gram-negative and Gram-positive bacteria using the Minimum Inhibitory Concentration (MIC) method, revealing promising inhibitory effects, with liver oil demonstrating greater efficacy. These findings suggest that puffer fish oil is rich in beneficial fatty acids and possesses antimicrobial properties that could find applications in food preservation, medicine, and agriculture, thereby offering a fresh perspective on the functional and nutritional value of *Xenopterus naritus*.

Keywords: Antimicrobial activity, fish oil profiles, omega-3, *Xenopterus naritus*

Copyright: This is an open access article distributed under the terms of the CC-BY-NC-SA (Creative Commons Attribution-NonCommercial-ShareAlike 4.0 International License) which permits unrestricted use, distribution, and reproduction in any medium, for non-commercial purposes, provided the original work of the author(s) is properly cited.

INTRODUCTION

Omega-3 fatty acids are abundant in fish oil, which is well known for its many health advantages. Fish consumption offers numerous health benefits, including protection against atherosclerotic lesions, liver diseases, and cholestasis. These benefits are due to the presence of fish oil, peptides, hydrolysates, essential vitamins, and various fatty acids (Chen *et al.*, 2022). Additionally, fish consumption and omega-3 supplementation have been shown to reduce inflammation and improve outcomes in cognitive health, muscle mass decline, cancer treatment, and critical illness (Troesch *et al.*, 2020). Omega-3 and omega-6 fatty acids that obtained from both terrestrial and marine sources provide protection against diseases like osteoarthritis, cancer, and autoimmune disorders, and contribute to various cellular activities including cell signaling, structural

integrity, and regulation of blood pressure and glucose levels (Abbott *et al.*, 2020). Furthermore, EPA and DHA are omega-3 fatty acids which are rich in fish oil, and have been linked to improved brain structure and function, reduced mortality, lower risk of ischemic stroke, and better cognitive health (von Schacky, 2021). The quality of fish oil can be improved through the sustainable recovery of omega-3 fatty acids from fish waste, which enhances its nutritional value and environmental sustainability (Alfio *et al.*, 2021).

Fish oil, rich in polyunsaturated fatty acids (PUFA), has remarkable antibacterial properties (Noutsu *et al.*, 2022). These PUFAs disrupt bacterial communication, ATP production, and membrane properties, making them potent antimicrobial agents (Kannan *et al.*, 2021). Moreover, they have the potential to hinder bacterial colonization and the expression of

virulence factors. Recent research has highlighted specific omega-3 polyunsaturated fatty acids (ω -3 PUFAs), such as docosahexaenoic acid (DHA) and eicosapentaenoic acid (EPA), for their significant antimicrobial activity against various bacterial strains, including multi-drug resistant strains isolated from patients with periprosthetic joint infections (PJI) (Coraça-Huber *et al.*, 2021). These omega-3 PUFAs have been shown to disrupt bacterial communication, ATP production, and membrane properties, rendering them potent antimicrobial agents. Additionally, they possess the ability to hinder bacterial colonization and the expression of virulence factors, which are crucial for infection establishment. This underscores the importance of exploring marine species, such as fish, as valuable sources of these potent antibacterial compounds (Inguglia *et al.*, 2020).

Xenopterus naritus belongs to the family Tetraodontidae and is a marine fish that can inhabit both saltwater and freshwater environments, including Malaysian waters (Mohd Nor Azman *et al.*, 2014). In Malaysia, puffer fish including species such as *Lagocephalus lunaris*, *L. sceleratus* and *L. spadiceus* are caught and become a local delicacy (Mohd Nor Azman *et al.*, 2014). Among these, *X. naritus* stands out as a migratory species inhabiting the South China Sea's coastline waters off Sarawak (Ahmad Nasir *et al.*, 2017). In Sarawak, *X. naritus* also known as rebellious “Buntal Kuning” or yellow pufferfish, is celebrated as a culinary delight (Mohd Nor Azman *et al.*, 2014). The Yellow puffer fish exhibits a torpedo-shaped body with striking yellow or golden coloration, particularly on its lower body portion. These migratory fish return to rivers for spawning with juveniles found in coastal waters during the non-spawning season (Mohd Nor Azman & Wan Norhana, 2013).

However, puffer fish widely recognized for its toxicity attributed to the presence of tetrodotoxin (TTX) leading to lack essential nutritional information specifically regarding the fatty acid profile of *X. naritus*. This study aims to address the lack of knowledge regarding the nutritional value of *X. naritus* by comprehensively analyzing its fatty acid composition from liver and muscle tissues. The

findings highlight the significant presence of omega-3 fatty acids (DHA and EPA) alongside omega-6 and omega-9 fatty acids, emphasizing the potential nutritional benefits for human health. Additionally, this research promotes *X. naritus* fish oils as a promising supplement with antimicrobial properties against gram-positive and gram-negative bacteria, aiming to contribute to informed consumption and utilization of this species.

MATERIALS AND METHODS

Collection of Puffer Fish Samples and Extraction of Fish Oils

Puffer fish specimens (Figure 1) were purchased from Kubah Ria wet fish markets in Kuching, Sarawak. The fish were selected for their marketable size with an average weight of between 1 and 1.2 kilograms each. The fish samples were carefully brought to the lab and kept there at -20 °C. The fish samples were prepared to separate liver and muscle tissue. The liver and muscle tissue, each weighing 100 grams were then brought together separately. According to Iverson *et al.* (2001), oil extraction from the pooled samples was done using the procedure outlined in the method of Blich and Dyer (1959). The solvent mixture consisted of chloroform, methanol, and water in a 1:2:1 ratio (v/v/v). The homogenized samples were centrifuged at 3000 rpm for 10 minutes to separate the chloroform phase, which contained the fish oil. The chloroform phase was collected and subjected to solvent evaporation using a rotary evaporator to remove the chloroform. The concentrated fish oils were then blown with nitrogen gas to create an inert atmosphere and prevent oxidation. The oil refining process was following Nazir *et al.* (2017) with minor adjustments that involved three stages: degumming, neutralization, and bleaching. For degumming, the oil was heated and stirred at 70 °C, then centrifuged with hot water to separate oil, gum, and water layers, repeating until neutral pH was achieved. In neutralization, the degummed oil was heated and stirred at 80 °C, treated with a 20% KOH solution, and centrifuged to obtain oil, soap stock, and water layers, repeating until neutral pH. Finally, in bleaching, the neutralized oil was heated (80 – 100 °C), stirred with 1% activated charcoal, filtered, completing the process.



Figure 1. Yellow Puffer Fish, *Xenopterus naritus*

Fatty Acids Profiling in *Xenopterus naritus* by GC/MS Analysis

The extracted fish oil was derivatized following the procedure by Ichihara *et al.* (1996) with minor changes. In a centrifuge tube, a 20 mg oil sample was dissolved in 2 ml of n-heptane. The tube was then filled with 4 ml of 2 M methanolic potassium hydroxide, which was vortexed for 2 minutes at room temperature before being centrifuged for 10 minutes at 4000 rpm. After centrifugation and standing for 10 minutes, a clear solution of fatty acid methyl ester (FAME) separated on the cloudy aqueous layer. The top FAME layer, dissolved in n-heptane, was collected and analyzed directly using a Shimadzu gas chromatograph (GC-MS), model QP2010plus. The methylated oil samples were injected directly into the GC-MS column. The column used was a DB5 column measuring 30 m x 0.25 mm x 250 μ m with an autosampler. The test was started at 50 °C for 10 minutes, followed by a temperature increase to 350 °C at a rate of 4.5 °C/min to maintain final temperature for 10 minutes. The carrier gas was helium flowing at a rate of 1.0 ml/min. The retention times were compared to an external standard solution composed of a mixture of 37 FAME components, known as FAME 37, to determine the peaks.

Minimum Inhibitory Concentration (MIC) evaluation

According to the procedure outlined by Simplicite *et al.* (2018), the antibacterial effectiveness of fish oil was evaluated using a broth

microdilution technique in 96-well microtitre plates. Inoculum preparation was performed using the broth culture method, in which bacterial colonies were transferred to Mueller-Hinton broth (MHB) using a loop and then incubated at 35 – 37 °C for 24 h. To obtain turbidity corresponding to a McFarland standard of 0.5, the culture was adjusted with MHB. Turbidity adjustment was assessed photometrically at 625 nm (UV-VIS spectrophotometer, UV-1900i, SHIMADZU) in the desired absorbance range of 0.08 – 0.10 using EUCAST guidelines (2003). The fish oil stock solution was prepared by dissolving the oil in a 5% Tween 20 solution. This stock solution was then serially diluted to achieve concentrations ranging from 7.8 to 500 mg/ml, with each well containing a total volume of 100 μ l. Each well was then filled with 100 μ l of bacterial inoculum. The growth was then observed on the microtitre plates using P-iodotetrazolium chloride (INT; 0.2 mg/ml) and incubated at 35 °C for 18 hours. Iodonitrotetrazolium, a yellow dye, became pink in response to the living bacteria. The MIC was determined as the lowest oil concentration at which no obvious color change was observed. As a positive control, chloramphenicol was utilized at doses ranging from 3.9 to 250 g/ml.

RESULTS

Puffer Fish Oils Characterization

By using GC/MS, the fish oil fatty acid profiles (Figure 2) that were extracted from the liver and muscle of *X. naritus* were qualitatively

described. The analysis shows in Table 1 determines differences in the composition of saturated fatty acids (SFAs) and unsaturated fatty acids (UFAs) between liver and muscle tissues. In the liver, SFAs comprised 38.91% of the total fatty acids while UFAs made up 61.09%. This indicates a higher prevalence of UFAs in liver tissue. Conversely, muscle tissue showed a lower proportion of SFAs at 32.19% and a higher proportion of UFAs at 67.81% suggesting a greater abundance of UFAs in muscle tissue.

The study identified key fatty acids that were the primary contributors to each category in both liver and muscle tissues. Palmitic acid (C16:0) emerged as the most predominant SFA in both liver and muscle tissues which underscoring its significance in the fatty acid composition of these tissues. Oleic acid (C18:1n-9) was recognized as the primary monounsaturated fatty acid (MUFA) in both liver and muscle tissues highlighting its prominent role in these tissues. Docosahexaenoic acid or DHA (C22:6n-3) stood out as the dominant polyunsaturated fatty acid (PUFA) in both liver and muscle tissues.

In addition, liver tissue exhibited a higher concentration of specific MUFAs including

Vaccenic acid, Cis-10-heptadecenoic acid, Eruric acid and Gondoic acid as compared to muscle tissue. Conversely, liver tissue displayed a greater abundance of certain PUFAs, such as Adrenic acid, Arachidonic acid, Eicosapentaenoic acid and Docosapentaenoic acid when contrasted with muscle tissue.

Although the current study did not analysed toxicity, previous research has detected tetrodotoxin (TTX) in both muscle and liver tissues of *X. naritus*, with variations depending on individual specimens, seasons, and tissues (Mohd Nor Azman *et al.*, 2014). For instance, samples from Betong, Sarawak, showed TTX levels of 17.8 µg/g in liver tissue and 11.1 µg/g in muscle tissue (Mohd Nor Azman *et al.*, 2014). These concentrations are considered weakly toxic (Noguchi *et al.*, 2006) but still exceed the Japanese safety limit for human consumption (>2 µg/g), as Malaysia does not have specific regulations for TTX. Nevertheless, with proper preparation, the fish can be made safe to eat.

Overall, liver tissue contains a higher percentage of SFAs, while muscle tissue has a higher percentage of UFAs. Palmitic acid, oleic acid, and docosahexaenoic acid play pivotal roles as major constituents in these tissues.

Table 1. Fatty acid profile of *Xenopterus naritus* in liver and muscle oil

Name	IUPAC	Relative % ± D.S	
		Liver	Muscle
Myristic acid	C14:0	2.1 ± 0.07	2.46 ± 0.06
Pentadecanoic acid	C15:0	1.53 ± 0.38	2.29 ± 0.06
Palmitic acid	C16:0	17.37 ± 0.28	15.67 ± 0.51
Heptadecanoic acid	C17:0	2.86 ± 0.06	2.73 ± 0.05
Stearic acid	C18:0	9.62 ± 0.27	6.87 ± 0.53
Heneicosanoic acid	C21:0	2.24 ± 0.09	2.17 ± 0.14
Tricosanoic acid	C23:0	1.92 ± 0.29	0 ± 0
Lignoceric acid	C24:0	0.26 ± 0.05	0 ± 0
Palmitoleic acid	C16:1n-7	8.53 ± 0.28	9.19 ± 0.22
Cis-10-heptadecenoic acid	C17:1n-7	0.53 ± 0.22	2.62 ± 0.45
Vaccenic acid	C18:1n-7	0.95 ± 0.09	2.08 ± 0.43
Oleic acid	C18:1n-9	15.2 ± 0.19	20.05 ± 0.39
Paullinic acid	C20:1n-7	0.86 ± 0.11	0 ± 0
Gondoic acid	C20:1n-9	1.35 ± 0.44	5.05 ± 0.91
Eruric acid	C22:1n-9	0.79 ± 0.34	3.25 ± 0.64
Linoleic acid	C18:2n-6	2.46 ± 0.34	2.27 ± 0.07
Arachidonic acid	C20:4n-6	3.25 ± 0.47	2.02 ± 0.44
Adrenic acid	C22:4n-6	7.57 ± 0.43	5.97 ± 0.13
Docosapentaenoic acid	C22:5n-6	2.9 ± 0.35	1.91 ± 0.02
Eicosapentaenoic acid	C20:5n-3	3.29 ± 0.12	2.16 ± 0.06
Docosapentaenoic acid	C22:5n-3	5.84 ± 0.25	4.93 ± 0.14
Docosahexaenoic acid	C22:6n-3	8.28 ± 0.08	6.15 ± 0.33

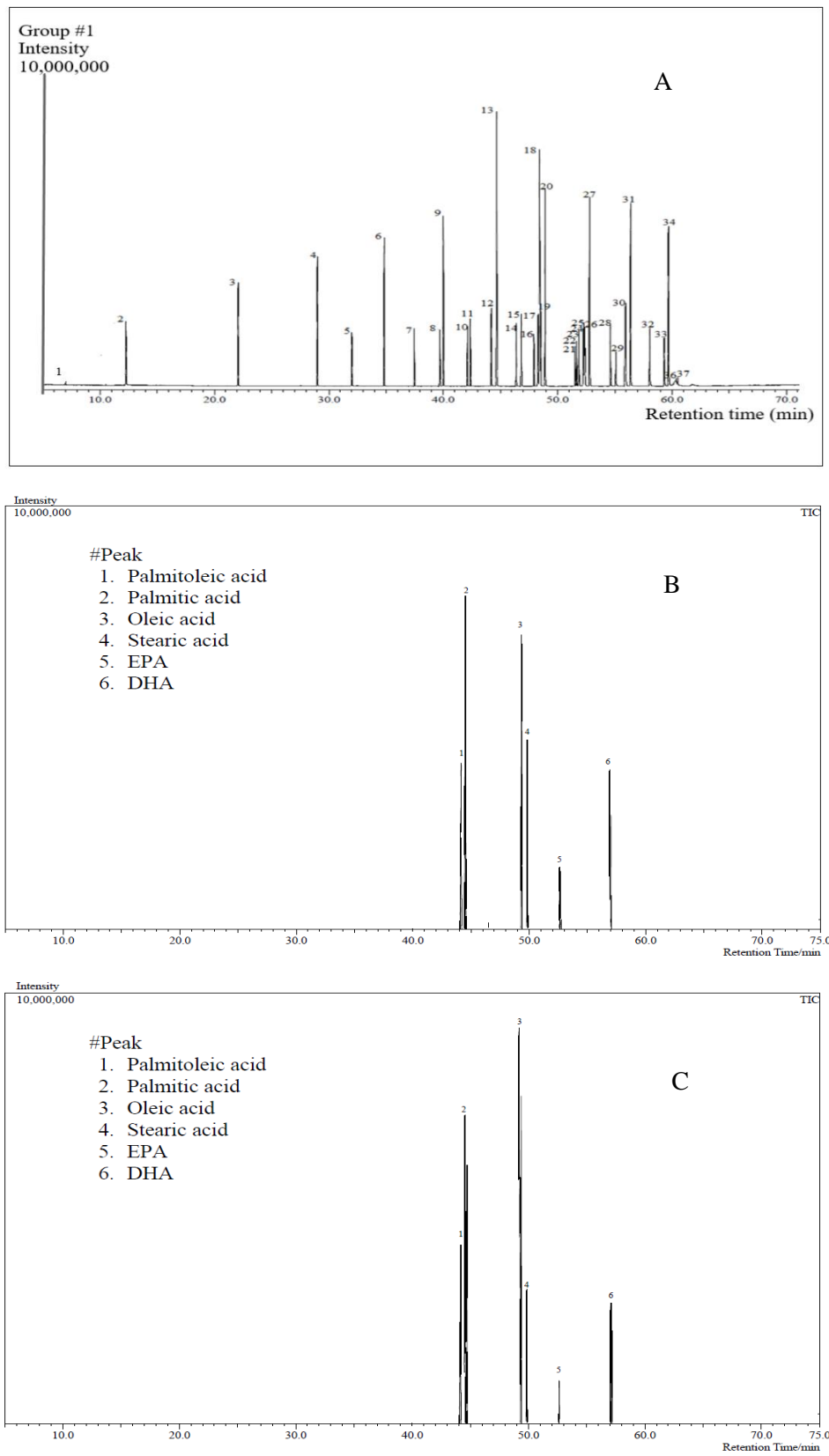


Figure 2. GC-MS Chromatogram of (A) standard solution containing 37 FAMES, (B) fatty acid profiles in *X. naritus* liver oil, and (C) muscle oil by Bligh & Dyer method

Antibacterial Activity of the *X. naritus* Fish Oils

The study assessed the antimicrobial effectiveness of oils extracted from both the liver and muscle tissue of puffer fish. In order to undertake this study, the MIC values against Gram-positive and Gram-negative reference strains of bacteria were evaluated. Table 2 provides an overview of the findings to present the antimicrobial activity of these fish oils. The liver oil displayed superior antimicrobial activity against several Gram-positive bacteria, including *S. aureus*, *B. cereus*, and *S. saprophyticus* with MIC values of 125 mg/ml as compared to the muscle oil with higher MICs (250-500% v/v). On the other hand, liver oil demonstrated increased potency against Gram-negative bacteria with *K. pneumonia* (MIC 62.5 mg/ml), while both oils were equally effective against *E. coli* and *E. cloacae* (MIC 125 mg/ml).

DISCUSSION

Due to its toxicity, puffer fish is always regarded as trash fish by trawlers. The huge mass of caught puffer fish may be a significant source of bioactive chemicals for supplementation in diet. *X. naritus* is a good protein resources and can be taken into account for human diet (Mohd Nor

Azman *et al.*, 2015) PUFAs is another significant source of high quality bioactive molecules that can be extracted from puffer fish oil.

The male *X. naritus* can represent up to 22.5 cm in total length and 274.05 g in body weight, while female *X. naritus* can up to 33.9 cm in total length and 711.00 g in body weight (Mohd Nor Azman & Wan Norhana, 2013).

This study has confirmed that PUFAs are present in the oil extracted from the *X. naritus* liver and muscle tissues and have demonstrated how these PUFAs are characterize by the presence of omega-3 fatty acids (Table 2). The most abundant omega-3 found in the fish oil was the DHA, which represent $8.28 \pm 0.08\%$ in liver oil and $6.15 \pm 0.33\%$ in muscle oil. Besides EPA represent $3.29 \pm 0.12\%$ in liver and $2.16 \pm 0.06\%$ in muscle also have health beneficial. The DHA and EPA is really important in the human diet such as proper fetal and infant development (Carver *et al.*, 2001; Ramakrishnan *et al.*, 2010), cardiovascular function (Kromhout *et al.*, 2010; Bernasconi *et al.*, 2021), Alzheimer's disease (Quinn *et al.*, 2010), immune response (Krauss-Etschmann *et al.*, 2008), cognitive function (Titova *et al.*, 2013) eye health (Cortina & Bazan, 2011) and prebiotics (Fu *et al.*, 2021).

Table 2. MIC of *Xenopterus naritus* from liver and muscle oil against gram-positive and gram-negative strains

	Bacteria strains	MIC (mg/ml)	
		Liver	Muscle
Gram-positive	<i>S. aureus</i>	125	250
	<i>B. cereus</i>	125	500
	<i>S. saprophyticus</i>	125	500
Gram-negative	<i>E. coli</i>	125	250
	<i>K. pneumonia</i>	62.5	500
	<i>E. cloacae</i>	125	250

The omega-6 linoleic acids are also the major precursor of the eicosanoids, including thromboxane, prostaglandins, prostacyclin, anandamides, and leukotrienes which regulate a wide range of physiological processes (Innes & Calder, 2018). Arachidonic acid (ARA) is a crucial component of cell structure and is required for growth and development as well as in the event of severe or pervasive cell injury (Tallima & Ridi, 2018). The liver ($15.20 \pm 19\%$)

and muscles ($20.050 \pm 39\%$) contained the highest concentrations of omega-9 oleic acid. This molecule is MUFA has shown to exert many biological function. Incorporating oleic acid into diets could be a valuable strategy in the context of high-lipid dietary trends with potential benefits for growth performance, feed utilization and overall health (Martins *et al.*, 2023).

Fatty acids play a significant role in the fight against microbial infections. Fatty acids may exert their antimicrobial effects by altering the hydrophobicity, charge, and integrity of cell membranes, which causes electron leakage and subsequent cell death (Inguglia *et al.*, 2020). A number of microorganisms have been shown to be resistant to omega-6, -7, and -9 fatty acids, such as arachidonic, linoleic, oleic, and palmitoleic acid, as well as their methyl esters and ethyl esters (Huang *et al.*, 2010). A number of microorganisms have been shown to be resistant to omega-6, -7, and -9 fatty acids, such as arachidonic, linoleic, oleic, and palmitoleic acid, as well as their methyl esters and ethyl esters (Huang *et al.*, 2010). Fatty acids are appealing for a variety of applications in medicine, agriculture, and food preservation, especially where convents are involved. This is because of their mechanism of antibacterial activity involves disruption of the bacterial cell membrane, interference with the electron transport chain and oxidative phosphorylation, impairment of nutrient uptake, inhibition of enzyme activity, auto-oxidation degradation, generation of peroxidation products and direct lysis of bacterial cells (Desbois & Smith, 2010).

In this study, the liver and muscle of puffers were tested for their antimicrobial abilities against Gram-positive and Gram-negative pathogens, and the results revealed a range of MIC values. Liver oil inhibit the growth of Gram-positive and Gram-negative bacteria with concentration at 125 mg/ml except, *K. pneumonia* (62.5 mg/ml). On the other hand, muscle oil inhibits the growth of bacteria with higher MIC than liver oil. This difference in effectiveness could be attributed to the fatty acid compositions of the oils.

Fish oil that contain PUFA inhibits bacterial growth by disrupting cell membrane hydrophobicity, charge, and integrity, leading to electron leakage and cell death (Calo *et al.*, 2015). Fatty acids play a crucial role in combating microorganism infections, as pathogens produce virulence factors and form biofilms (Schroeder *et al.*, 2017). Both omega-3 fatty acids, particularly linolenic acid, and omega-6, -7, -9 fatty acids, including γ -linolenic, linoleic, arachidonic, palmitoleic, and oleic acids, demonstrate antimicrobial properties (Chanda *et al.*, 2018). These fatty acids contribute to bacterial death through

mechanisms such as cell lysis, enzyme activity inhibition, and the production of lethal oxidation products (Desbois & Smith, 2010). Our findings suggest that fish oil from liver and muscle is effective against tested microorganisms regardless of the bacterial wall type, with liver oil showing greater efficacy, possibly due to differences in fatty acid compositions (Inguglia *et al.*, 2020). Hence, PUFA specifically accounts for the antibacterial activity, emphasizing the importance of preventing PUFA oxidation (Simplice *et al.*, 2018).

CONCLUSION

This study highlights the nutritional value of puffer fish oil from *X. naritus*, countering its negative reputation due to toxicity concerns. The fatty acid profile revealed high levels of beneficial omega-3, omega-6, and omega-9 fatty acids, important for fetal development, cardiovascular health, cognitive function, and immune response. Additionally, the antimicrobial properties of the oil, particularly from the liver, showed significant potency against both Gram-positive and Gram-negative bacteria. Although this study did not measure tetrodotoxin (TTX) levels, previous research indicates weakly toxic TTX concentrations in *X. naritus*, exceeding the safe limit for consumption. However, proper preparation can make the fish safe to eat. Overall, this study provides valuable insights into the nutritional and antimicrobial benefits of puffer fish oil, while also addressing safety considerations related to TTX.

ACKNOWLEDGMENT

The authors would like to acknowledge the valuable contributions of their colleagues, Mr. Rajuna Tahir and Mr. Benedict Samling, from the Faculty of Resource Science and Technology at Universiti Malaysia Sarawak. They also express gratitude to the Malaysia Comprehensive University Network-MCUN (UNIMAS, UiTM, and UMS) for the financial assistance provided through the grant program [GL/F07/MCUN/09/2020].

REFERENCES

- Abbott, K.A., Burrows, T.L., Acharya, S., Thota, R. N., & Garg, M.L. (2020). DHA-enriched fish oil reduces insulin resistance in overweight and obese adults. *Prostaglandins, Leukotrienes and*

- Essential Fatty Acids*, 159, 102154. DOI: 10.1016/j.plefa.2020.102154.
- Abedi, E., & Sahari, M.A. (2014). Long-chain polyunsaturated fatty acid sources and evaluation of their nutritional and functional properties. *Food Science and Nutrition*, 2(5): 443-463. DOI: 10.1002/fsn3.121.
- Ahmad Nasir, A.S., Mohamad, S., & Mohidin, M. (2017). The first reported artificial propagation of yellow puffer, *Xenopterus naritus* (Richardson, 1848) from Sarawak, Northwestern Borneo. *Aquaculture Research*, 48(8): 4582-4589. DOI: 10.1111/are.13103.
- Alfio, V.G., Manzo, C., & Micillo, R. (2021). From fish waste to value: an overview of the sustainable recovery of omega-3 for food supplements. *Molecules*, 26(4): 1002. DOI: 10.3390/molecules26041002.
- Bernasconi, A.A., Wiest, M.M., Lavie, C.J., Milani, R.V., & Laukkanen, J.A. (2021). Effect of Omega-3 dosage on cardiovascular outcomes: An updated meta-analysis and meta-regression of interventional trials. *Mayo Clinic Proceedings*, 96(2): 304-313. DOI: 10.1016/j.mayocp.2020.08.034.
- Calo, J.R., Crandall, P.G., O'Bryan, C.A., & Ricke, S.C. (2015). Essential oils as antimicrobials in food systems—A review. *Food Control*, 54: 111-119. DOI: 10.1016/j.foodcont.2014.12.040.
- Carver, J.D., Benford, V.J., Han, B., & Cantor, A.B. (2001). The relationship between age and the fatty acid composition of cerebral cortex and erythrocytes in human subjects. *Brain Research Bulletin*, 56(2): 79-85. DOI: 10.1016/s0361-9230(01)00551-2.
- Chanda, W., Joseph, T.P., Guo, X.F., Wang, W.D., Liu, M., Vuai, M. S., Padhiar, A.A., & Zhong, M.T. (2018). Effectiveness of omega-3 polyunsaturated fatty acids against microbial pathogens. *Journal of Zhejiang University-SCIENCE B*, 19(4), 253-262. DOI: 10.1631/jzus.B1700063.
- Chen, J., Jayachandran, M., Bai, W., & Xu, B. (2022). A critical review on the health benefits of fish consumption and its bioactive constituents. *Food Chemistry*, 369: 130874. DOI: 10.1016/j.foodchem.2021.130874.
- Coraça-Huber, D.C., Steixner, S., Wurm, A., & Nogler, M. (2021). Antibacterial and anti-biofilm activity of omega-3 polyunsaturated fatty acids against periprosthetic joint infections-isolated multi-drug resistant strains. *Biomedicines*, 9(4): 334. DOI: 10.3390/biomedicines9040334.
- Cortina, M.S., & Bazan, H.E. (2011). Docosahexaenoic acid, protectins and dry eye. *Current Opinion in Clinical Nutrition and Metabolic Care*, 14(2): 132-137. DOI: 10.1097/mco.0b013e328342bb1a.
- Desbois, A.P., & Smith, V.J. (2010). Antibacterial free fatty acids: activities, mechanisms of action and biotechnological potential. *Applied Microbiology and Biotechnology*, 85: 1629-1642. DOI: 10.1007/s00253-009-2355-3.
- European Committee for Antimicrobial Susceptibility Testing (EUCAST). (2003). EUCAST of the European Society of Clinical Microbiology and Infectious Diseases (ESCMID): Terminology relating to methods for the determination of susceptibility of bacteria to antimicrobial agents. *Clinical Microbiology and Infection*, 9: 1-7. DOI: 10.1046/j.1469-0691.2000.00149.x.
- Fu, Y.W., Wang, Y.D., Gao, H., Li, D.H., Jiang, R.R., Ge, L.R., Tong, C., & Xu, K. (2021). Associations among dietary omega-3 polyunsaturated fatty acids, the gut microbiota, and intestinal immunity. *Mediators of Inflammation*, 11. DOI: 10.1155/2021/8879227.
- Guil-Guerrero, J.L., & Belarbi, E.H. (2001). Purification process for cod liver oil polyunsaturated fatty acids. *Journal of the American Oil Chemists' Society*, 78: 477-484. DOI: 10.1007/s11746-001-0289-9.
- Holub, D.J., & Holub, B.J. (2004). Omega-3 fatty acids from fish oils and cardiovascular disease. *Molecular and Cellular Biochemistry*, 263: 217-225.
- Huang, C.B., George, B., & Ebersole, J.L. (2010). Antimicrobial activity of n-6, n-7 and n-9 fatty acids and their esters for oral microorganisms. *Archives of Oral Biology*, 55(8): 555-560. DOI: 10.1016/j.archoralbio.2010.05.009.
- Ichihara, K. I., Shibahara, A., Yamamoto, K., & Nakayama, T. (1996). An improved method for rapid analysis of the fatty acids of glycerolipids. *Lipids*, 31(5): 535-539. DOI: 10.1007/BF02522648.
- Inguglia, L., Chiaramonte, M., Di Stefano, V., Schillaci, D., Cammilleri, G., Pantano, L., Mauro, M., Vazzana, M., Ferrantelli, V., Nicolosi, R., & Arizza, V. (2020). *Salmo salar* fish waste oil:

- Fatty acids composition and antibacterial activity. *PeerJ*, 8, e9299. DOI: 10.7717/peerj.9299.
- Innes, J.K., & Calder, P.C. (2018). Omega-6 fatty acids and inflammation. *Prostaglandins, Leukotrienes and Essential Fatty Acids*, 132: 41-48. DOI: 10.1016/j.plefa.2018.03.004.
- Iverson, S.J., Lang, S.L.C., & Cooper, M.H. (2001). Comparison of the Bligh and Dyer and Folch methods for total lipid determination in a broad range of marine tissue. *Lipids*, 36(11): 1283-1287. DOI: 10.1007/s11745-001-0843-0.
- Kannan, N., Rao, A.S., & Nair, A. (2021). Microbial production of omega-3 fatty acids: an overview. *Journal of Applied Microbiology*, 131(5): 2114-2130. DOI: 10.1111/jam.15034.
- Krauss-Etschmann, S., Hartl, D., Rzehak, P., Heinrich, J., Shadid, R., del Carmen Ramírez-Tortosa, M., Campoy, C., Pardillo, S., Schendel, D.J., Decsi, T. and Demmelmair, H., 2008. Decreased cord blood IL-4, IL-13, and CCR4 and increased TGF- β levels after fish oil supplementation of pregnant women. *Journal of Allergy and Clinical Immunology*, 121(2): pp.464-470. DOI: 10.1016/j.jaci.2007.09.018.
- Kromhout, D., Giltay, E.J., & Geleijnse, J.M. (2010). n-3 Fatty acids and cardiovascular events after myocardial infarction. *New England Journal of Medicine*, 363(21): 2015-2026. DOI: 10.1056/NEJMoa1003603.
- Martins, N., Magalhães, R., Viera, L., Couto, A., Serra, C.R., Maia, M.R., Fonseca, A.J., Cabrita, A.R., Pousao-Ferreira, P., Castro, C., Peres, H., & Oliva-Teles, A. (2023). Dietary oleic acid supplementation improves feed efficiency and modulates fatty acid profile and cell signaling pathway in European sea bass (*Dicentrarchus labrax*) juveniles fed high-lipid diets. *Aquaculture*, 576: 739870. DOI: 10.1016/j.aquaculture.2023.739870.
- Mohd Nor Azman, A., Samsur, M., & Othman, M. (2014). Distribution of tetrodotoxin among tissues of puffer fish from Sabah and Sarawak waters. *Sains Malaysiana*, 43(7): 1003-1011.
- Mohd Nor Azman, A., Samsur, M., Mohammed, M., Shabdin, M.L., & Fasihuddin, B.A. (2015). Assessment of proximate composition and tetrodotoxin content in the muscle of Yellow puffer fish, *Xenopterus naritus* (Richardson 1848) from Sarawak, Malaysia. *International Food Research Journal*, 22(6).
- Mohd Nor Azman, A. & Wan Norhana, M.N. (2013). Detection of tetrodotoxin and saxitoxin in dried salted yellow puffer fish (*Xenopterus naritus*) eggs from Satok Market, Kuching, Sarawak. *International Food Research Journal*, 20(5): 2963-2966.
- Nazir, N., Diana, A. & Sayuti, K. (2017). Physicochemical and fatty acid profile of fish lipid from head of tuna (*Thunnus albacares*) extracted from various extraction method. *International Journal on Advanced Science, Engineering and Information Technology*, 7(2): 709-715. DOI: 10.18517/ijaseit.7.2.2339.
- Noguchi, T., Arakawa, O., & Takatani, T. (2006). TTX accumulation in puffer fish. *Comparative Biochemistry and Physiology, Part D* 1:145-152. DOI: 10.1016/j.cbd.2005.10.006.
- Noutsu, B.S., Tchabong, S.R., Djitieu, A.D.D., Dongmo, F.F.D., Ngamga, F.H.N., Zokou, R., Tamgue, O., Ngane, R.A.N., & Tchoumboungang, F. (2022). Chemical characterization and antibacterial properties of *Fontitrygon margarita* (Günther, 1870) liver oil. *Journal of Lipids*, 2022(1): 9369387. DOI: 10.1155/2022/9369387.
- Quinn, J. F., Raman, R., Thomas, R. G., Yurko-Mauro, K., Nelson, E. B., Van Dyck, C., ... & Aisen, P. S. (2010). Docosahexaenoic acid supplementation and cognitive decline in Alzheimer disease: a randomized trial. *Jama*, 304(17): 1903-1911. DOI: 10.1001/jama.2010.1510.
- Ramakrishnan, U., Stein, A.D., Parra-Cabrera, S., Wang, M., Imhoff-Kunsch, B., Juárez-Márquez, S., Rivera, J. and Martorell, R., 2010. Effects of docosahexaenoic acid supplementation during pregnancy on gestational age and size at birth: randomized, double-blind, placebo-controlled trial in Mexico. *Food and nutrition bulletin*, 31(2_suppl2): pp.S108-S116. DOI: 10.1177/15648265100312S203.
- Schroeder, M., Brooks, B.D., & Brooks, A.E. (2017). The complex relationship between virulence and antibiotic resistance. *Genes*, 8(1): 39. DOI: 10.3390/genes8010039.
- Simplice, M.R., Macaire, W.H., Hervé, N.N.F., Fabrice, T.D., Justin, D.D., François, T., & Jules-Roger, K. (2018). Chemical composition and antibacterial activity of oils from *Chrysiichthys nigrodigitatus* and *Hepsetus odoe*, two freshwater fishes from Yabassi, Cameroon. *Lipids in Health and Disease*, 17(1): 1-7. DOI:10.1186/s12944-018-0690-z.

- Tallima, H., & El Ridi, R. (2018). Arachidonic acid: physiological roles and potential health benefits—a review. *Journal of Advanced Research*, 11: 33-41. DOI: 10.1016/j.jare.2017.11.004.
- Titova, O.E., Sjögren, P., Brooks, S.J., Kullberg, J., Ax, E., Kilander, L., Riserus, U., Cederholm, T., Larsson, E. M., Johansson, L., Ahlström, H., Lind, L., Schiöth, H.B., & Benedict, C. (2013). Dietary intake of eicosapentaenoic and docosahexaenoic acids is linked to gray matter volume and cognitive function in elderly. *Age*, 35(4): 1495–1505. DOI: 10.1007/s11357-012-9453-3.
- Troesch, B., Eggersdorfer, M., Laviano, A., Rolland, Y., Smith, A.D., Warnke, I., Weimann, A., & Calder, P.C. (2020). Expert opinion on benefits of long-chain omega-3 fatty acids (DHA and EPA) in aging and clinical nutrition. *Nutrients*, 12(9): 2555. DOI: 10.3390/nu12092555.
- von Schacky, C. (2021). Importance of EPA and DHA blood levels in brain structure and function. *Nutrients*, 13(4): 1074. DOI: 10.3390/nu13041074.
- Zaidul, I.S.M., Norulaini, N.N., Omar, A.M., Sato, Y., & Smith Jr, R.L. (2007). Separation of palm kernel oil from palm kernel with supercritical carbon dioxide using pressure swing technique. *Journal of Food Engineering*, 81(2): 419-428. DOI: 10.1016/j.jfoodeng.2006.11.019

Strategies for Enhancing Grow-Out Culture Technique of Community-Based Sea Cucumber (*Holothuria scabra*): A Case Study in Malawali Island, Sabah

NURUL AIN JAIS¹, AUDREY DANING TUZAN*¹, NURZAFIRAH BINTI MASLAN¹, SOFIA JOHARI¹, BEN PARKER², WEI-KANG CHOR³

¹Borneo Marine Research Institute, Universiti Malaysia Sabah, 88400, Kota Kinabalu, Sabah, Malaysia;

²Attainable Sustainable Aquaculture, Mount Pleasant, 8081, Christchurch, New Zealand;

³WWF-Malaysia, 46150, Petaling Jaya, Selangor, Malaysia

* Corresponding author: audrey@ums.edu.my

Received: 23 May 2024

Accepted: 11 October 2024

Published: 31 December 2024

ABSTRACT

Initial efforts to cultivate *Holothuria scabra* in coastal communities on Malawali faced several challenges. Most notable were the high mortality rate and slow growth, especially after several harvests. In this study, an attempt was made to improve cultivation techniques to increase the growth and survival rate of hatchery-produced *H. scabra* on Malawali Island. A comparative analysis of growth and survival rates of 50 *H. scabra* juveniles (8.68 ± 3.88 g [mean \pm S.D.]) kept in 4 m² (stocking density: 12 ind. m⁻²) and 16 m² (3 ind. m⁻²) experimental pens with and without sediment enrichment with *Sargassum* spp. (enrichment ratio: 3% total biomass) for a period of 6 months was conducted. Several key biophysical parameters were recorded, including total organic matter (TOM) and chlorophyll-a (Chl-a). The results indicate that lower stocking density and sediment enrichment did not lead to a higher survival rate of juvenile *H. scabra*. However, stocking density had a noticeable effect on the growth of juvenile *H. scabra*. The average final total biomass of juveniles in enriched and non-enriched pens with low stocking density was significantly higher (1890.45 g and 1667.65 g, respectively), while juveniles in enriched and non-enriched pens with high stocking density had the lowest total biomass (889.7 g and 350.15 g, respectively). While there was no significant difference in TOM content between enriched and non-enriched pens on each observation day (one-way ANOVA; $p > 0.05$), the pooled data showed that enriched pens had significantly higher TOM content. Conversely, the enriched pens have a significantly higher Chl-a concentration than the non-enriched pens. Conclusively, the research findings indicate that a stocking density of 3 ind. m⁻² is a feasible approach to maximise the biomass of *H. scabra* in grow-out pens. On Malawali Island, it was also discovered that while a 3% sediment enrichment alters the properties of the sediment, it is insufficient to sustain *H. scabra*'s ideal development and survival. This study offers insights into sea cucumber farming in the region but highlights the need for further research. Future studies should determine optimal sediment enrichment ratios and use larger sample sizes with sufficient replicates for more conclusive results.

Keywords: Growth, grow-out sea pen, sandfish, sediment enrichment, survival

Copyright: This is an open access article distributed under the terms of the CC-BY-NC-SA (Creative Commons Attribution-NonCommercial-ShareAlike 4.0 International License) which permits unrestricted use, distribution, and reproduction in any medium, for non-commercial purposes, provided the original work of the author(s) is properly cited.

INTRODUCTION

The sea cucumber has a significant cultural value in Malaysia. About 80 out of 1200 sea cucumber species live in the marine and coastal waters of the country (Kamarudin *et al.*, 2017). These sea cucumbers are mainly exported to the Chinese market (Hair *et al.*, 2016; Conand, 2018) and are highly sought-after for their nutritional and medicinal properties (Conand, 2006). This has led to an increase in demand and subsequent overexploitation, resulting in some species being classified as vulnerable (*Holothuria fuscogilva*) or endangered (*H. scabra*, *H. nobilis*, *H. lessoni*,

H. whitmaei) on the IUCN Red List (IUCN, 2023).

Over the past decade, Sabah has emerged as the major center of sea cucumber production in Malaysia, with the highest production in the country, particularly in Tun Mustapha Park (TMP), Sabah (Chor *et al.*, 2016). Generally, the sea cucumber farms were constructed near sandy beaches, mangroves, coral reefs, and seagrass, such as Sibogo Island, Malawali Island, Tigabu Island, and Balambangan Island (Lim *et al.*, 2021). For coastal communities, sea cucumber farming has become a significant livelihood

option. Additionally, for many small-scale fishermen who have traditionally depended on declining wild fisheries, this sector offers a substitute source of income. These communities can lessen their economic vulnerability and improve food security through sea cucumber farming (Hair *et al.*, 2019). Furthermore, the grow-out culture of sea cucumbers, like *H. scabra*, is easy and accessible for low-income households (Juinio-Meñez *et al.*, 2017).

However, the initial attempts to farm *H. scabra* in the coastal regions, particularly in Malawali Island, Kudat faced numerous challenges that affected profitability. These challenges include the high mortality rate and slow growth of the farmed *H. scabra*. Farmers reported that the growth performance of their cultured *H. scabra* decreased significantly after two or three farming cycles. In addition, *H. scabra* farming practices in TMP are considered unsustainable as they rely too heavily on wild stocks, leading to the loss of marine habitats and inappropriate management practices.

Several developing countries, such as Fiji, Maldives, Papua New Guinea, Madagascar, Philippines, and Indonesia use the traditional sea ranching method of "place, grow and take" (Juinio-Meñez *et al.*, 2012; 2013; Robinson & Pascal, 2012; Hair *et al.*, 2016). Studies on sea cucumber farming have moved from monoculture to polyculture in the recent decade. According to Namukose *et al.* (2016) and Hamad *et al.* (2019), co-cultivating *H. scabra* with seaweed is one of the most effective methods for modern and successful sea cucumber farming. Additionally, Yu *et al.* (2014) and Cubillo *et al.* (2016) revealed that sea cucumbers farming in the IMTA (Integrated Multi-trophic Aquaculture) system aid in the bioturbation of sediments, improving nutrient cycling and lowering the buildup of organic matter, all of which can lessen the adverse effects of intense aquaculture system, which also indicated the ecological benefits of this farming. Small-scale fishermen in coastal communities utilise extensive sea pens to accelerate the growth of wild-caught *H. scabra* (Hair *et al.*, 2016). However, the feasibility of these culture systems depends on environmental variables that promote high growth and survival of hatchery-produced juveniles after release, as emphasised by Dumalan *et al.* (2019).

Stocking density is a crucial parameter that influences the growth and survival of sea cucumbers in aquaculture. Too low a stocking density can reduce productivity and wastes space, while too high a stocking density increases competition and limits available space (Serang *et al.*, 2016). A study by Lavitra *et al.* (2010) suggests that the optimal stocking density for sea cucumbers is 3 ind. m⁻² and achieves the highest growth rate (0.64 g day⁻¹). Sea cucumbers, including *H. scabra*, feed on sediments, with organic matter being an important component of their diet (Liu *et al.*, 2010). *Sargassum* spp. and compost fertilisers have been used to enrich the sediment in sea pen, promoting the growth of microalgae and directly supporting the growth of *H. scabra* due to increased food availability (Sinsona & Juinio-Meñez, 2018; Sabilu *et al.*, 2022).

Despite the extensive sea cucumber farming, there has been no formal assessment of the area under cultivation on Malawali Island. This study aims to refine the farming technique to improve the growth and survival rate of *H. scabra*, particularly on Malawali Island, focusing on a small-scale community-based *H. scabra* farm. The research will compare growth and survival rates at different stocking densities with and without sediment enrichment with *Sargassum* spp. This study hypothesized that low stocking density with the addition of sediment enrichment with *Sargassum* spp. will result in higher growth and survival rates of *H. scabra* juveniles in sea pens.

MATERIALS AND METHODS

Access License

This project was approved by the Sabah Biodiversity Centre (SABC) with access licence reference number JKM/MBS.1000-2/2 JLD. 13 (126) and gained ethical approval for animal research studies with file number AEC 0014 / 2022.

Experimental Site

The research site chosen for this study was located on the northern side of Malawali (Figure 1). The sea pens were constructed within the existing farm owned by the community. The selected research site is characterised by extensive intertidal and

shallow water areas characterised by a flat topography and sufficient sediment depth to allow for the installation of the pens. The sediment depth corresponds to the minimum requirement of at least 20 cm recommended by (Rougier *et al.*, 2013).

In addition, factors such as visibility and accessibility for both the community and the monitoring team were considered when

selecting the site to facilitate maintenance and monitoring of the enclosures. The rectangular sea pens of 16 m² and 4 m² were set up in a similar habitat to ensure that the habitat would not be a disturbance factor. The research sites consist of small patches of *Enhalus acoroides*, *Halodule* spp, *Cymdocea* sp. and *Thalassia hemprichii* seagrass species. However, the population density of each seagrass species was not quantified.

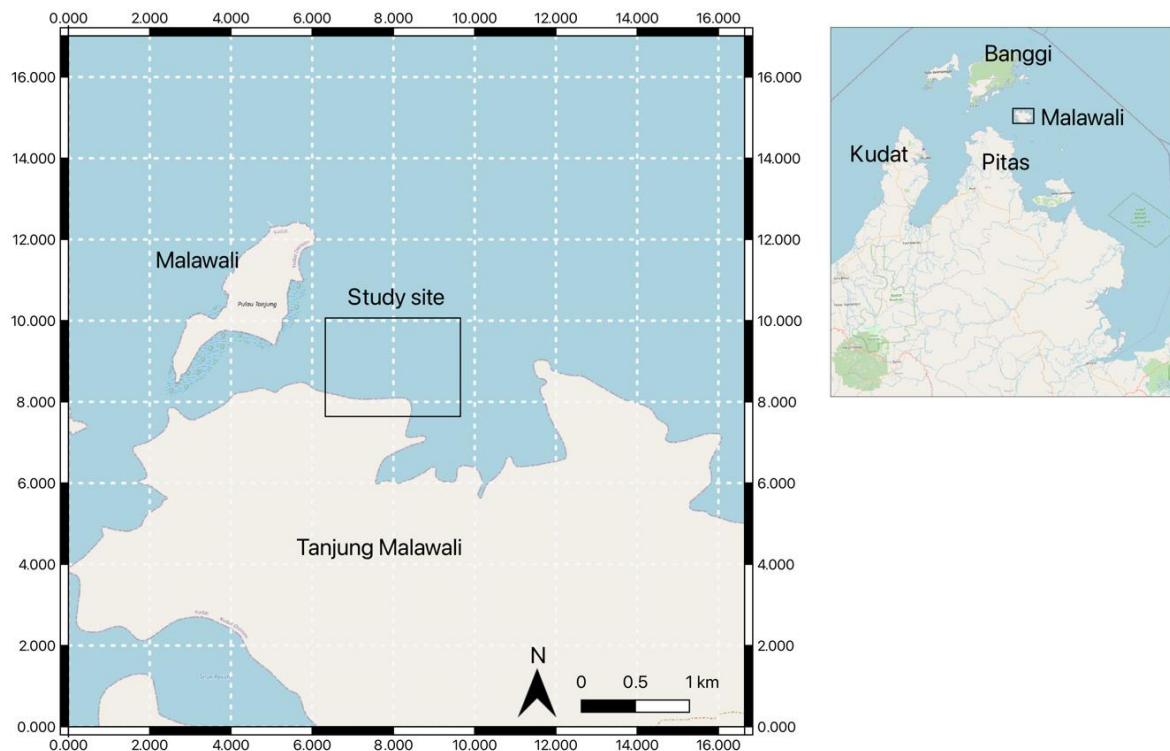


Figure 1. Location of the study site (Malawali)

Experimental Juveniles

The experimental animals used in this study were produced at the Borneo Scabra Hatchery in Tuaran, Sabah. A total of 600 *H. scabra* juveniles (8.68 ± 3.88 [S.D.] g body weight) from a single spawning were transported from the hatchery to the experimental sites in plastic bags filled with water (70%) and oxygen (30%) at a cool temperature.

Grow-Out Pen Trial and Sediment Enrichment

Sea pens measuring 2×2×1 m and 4×4×1 m (W×L×H) were constructed to maintain the natural habitat of the *H. scabra* juvenile while allowing a regular water supply and water

exchange. These sea pens were built with an 8 mm thick HDPE mesh net and stakes made from a rust-prone PVC pipe. The PVC pipes were reinforced by filling them with cement to create robust stakes. These stakes were buried 20–30 cm deep into the sediment together with the bottom net of the pen to prevent the juveniles from escaping by burrowing, as recommended by Purcell & Simutoga (2008) and Robinson & Pascal (2012).

In this experiment, a comparison of growth and survival rates was conducted with 50 *H. scabra* juveniles placed over a period of 188 days (6 months 4 days) in experimental pens of 4 m² (stocking density: 12 ind. m⁻²) and 16 m² (3 ind. m⁻²) with or without sediment enrichment with *Sargassum* spp. Four treatment pens were

used (16U (control) = 3 ind. m⁻² stocking density without enrichment; 16E = 3 ind. m⁻² stocking density with enrichment; 4U = 12 ind. m⁻² stocking density without enrichment; 4E = 12 ind. m⁻² stocking density with enrichment). The initial mean stocking weight of *H. scabra* juveniles in each treatment pens showed no significant difference (one-way ANOVA, $p = 0.488$).

The preparation and method of enrichment followed the approach described by Sinsona & Juinio-Meñez (2018). *Sargassum* spp. were collected, rinsed with freshwater to remove debris, and then sun-dried. After drying under natural sunlight, the *Sargassum* spp. was ground with an electronic grinder for about 25 seconds. Prior to enrichment, the *Sargassum* spp. was soaked overnight to increase its specific gravity and prevent it from floating during enrichment to ensure that it remained submerged in the sediment. The soaked *Sargassum* spp. was mixed directly into the top 2 cm layer of the sediment layer in pens 4E and 16E on day 1 and re-enriched every 30 days (Sinsona & Juinio-Meñez, 2018). During the 6-month experiment, the monthly enrichment amount was determined based on the body weight of the *H. scabra* juveniles in each treatment pen, using 3% of the body weight and adjusted every 30 days according to the weight of the juveniles. Ahmed *et al.* (2018) used an enrichment ratio of 3% total biomass for daily enrichment. However, since the enrichment in this study was only performed once a month during the monthly site visit, the 3% total biomass was multiplied by 30 days.

Data Collection and Calculation for Growth and Survival of Juveniles in Grow-out Pens

Before transporting and stocking juveniles into each pen, their weight was measured using digital scales with 1 decimal point, individually (Dumalan *et al.*, 2019). During the measurement, the *H. scabra* juveniles were manually removed from the pens and placed in a basin. To facilitate the expulsion of excess water from the body, the animals were allowed to remain out of the water for 2 minutes before weighing. Following the method described by Dumalan *et al.* (2019), the juveniles were carefully dried with a towel before being weighed using a digital scale accurate to one decimal place. Only the weight of *H. scabra* was used as their growth measurement because their

body length is inconsistent since it is influenced by stress (Lavitra *et al.*, 2010).

Monitoring of growth and survival was conducted monthly during the spring low tide to facilitate access to the experimental sites: day 0, 33, 63, 90, 119, 157, 188. The monitoring of the growth and survival of *H. scabra* juveniles involved the active participation of Malawali community members, who formed the monitoring team and supervisor of this community-based project. The field supervisor took responsibility for daily or weekly surveillance of the experimental pens to prevent poaching.

Survival rates in each pen were calculated monthly as a percentage of the remaining *H. scabra* juveniles. The absolute growth rate (AGR) was calculated as difference between the juvenile's average final weight and average initial weight over the number of rearing days (Yussuf & Yahya, 2021):

$$AGR \left(\frac{g}{day} \right) = \frac{\text{final weight} - \text{initial weight}}{\text{rearing days}}. \quad \text{Eq.(1)}$$

The total biomass was calculated by adding the individual weights per pen and expressing the result in grammes. Biomass increment was calculated to determine how much the total biomass in each experimental pens increased throughout the experimental period:

$$\text{Biomass increment (\%)} = \left[\frac{\text{final biomass} - \text{initial biomass}}{\text{initial biomass}} \right] \times 100. \quad \text{Eq.(2)}$$

Sediment Enrichment

To assess relative food abundance, sediment samples were collected from all treatment pens to analyse chlorophyll-a (Chl-a) and total organic matter (TOM). The sediment samples were collected prior to the next sediment enrichment. Analyses were performed on day 0, 33, 63, 90, 119, 157 and 188. Samples were collected from the top 2-3 cm of the surface at five random points within the pens using a 20 ml cut-off syringe as described in the method of Dumalan *et al.* (2019).

To ensure representative data, the samples from a single pen were combined in a zip-lock bag. As direct on-site analysis was impractical, all samples were stored in a cool box with ice to prevent oxidation and transported to the Borneo

Marine Research Institute. Upon arrival at the facility, the samples were frozen prior to analysis. To determine the TOM of the sediments, the loss on ignition method was used according to the procedure described by (Heiri *et al.*, 2001). For the determination of Chl-a in the sediment, the spectrophotometric method explained by Slater & Carton (2009) was used.

Water Quality

The water parameters such as temperature ($^{\circ}\text{C}$), salinity (ppt), pH, and dissolve oxygen (mg L^{-1}) of each site were measured in situ using a YSI multiparameter at every monitoring time (monthly).

Statistical Analysis

Normality and homogeneity of variance were tested using the Shapiro–Wilk test or Levene test, with the significance level set at $p < 0.05$. Logarithmic and square root transformation were conducted to normalize the data. A one-way ANOVA was used to assess significant differences in mean survival, total biomass, mean weight, and biomass increment in *H. scabra* juveniles between treatments on the same observation day. Post-hoc comparisons were performed using Duncan's multiple range test to identify specific differences between treatment groups. Similarly, a one-way ANOVA with Duncan's multiple range test was used to assess the difference in TOM and Chl-a content in the same monitoring day. Meanwhile, A Kruskal-wallis was used to assess significant differences of TOM and Chl-a, with pairwise comparison to identify the specific difference between treatment groups for the pooled data (combined from day 0 to day 188). The combined effect of stocking density and additional sediment enrichment on the survival rate, total biomass, mean weight, and biomass increment of *H. scabra* was analysed using a two-way ANOVA. A significance level of $p < 0.05$ was used for all statistical analyses, and SPSS Statistics version 28 was used for data processing.

RESULTS

Growth and Survival of Juveniles in Grow-Out Pen

Although there were no statistically significant differences in survival rates related to the addition of enrichment, stocking density, or the

interaction between these two factors (Two-way ANOVA; $p > 0.05$; Table 1), the pen with low stocking density and enrichment (16E) consistently showed higher survival throughout the experiment. Monthly data on survival percentage, total biomass, and mean weight during the grow-out trials are illustrated in Figure 2. The highest mortality occurred within the first two months after stocking across all pens. Notably, the pen with high stocking density and no enrichment (4U) experienced a significant decline in juvenile numbers from June to July, ending the experiment with the lowest survival rate ($7 \pm 5.66\%$) and total biomass ($350.15 \pm 213.6 \text{ g pen}^{-1}$).

Additionally, total biomass and mean weight of juveniles were not significantly different with respect to additional of enrichment and interaction between two main factors ($p > 0.05$; Table 1) but both total biomass and mean weight were significantly different with respect to stocking density (Two-way ANOVA; $p = 0.022$; Table 1). Maximum biomass (g pen^{-1}) was reached after 4 months of rearing at low stocking density (16U; $2422.25 \pm 169.25 \text{ g pen}^{-1}$ and 16E; $2727.25 \pm 444.25 \text{ g pen}^{-1}$) and after 3 months of rearing at high stocking density (4U; $709.4 \pm 97.8 \text{ g pen}^{-1}$ and 4E; $1172.5 \pm 74.05 \text{ g pen}^{-1}$). AGR is not significantly different with respect to additional of enrichment, stocking density and interaction between two main factors (Two-way ANOVA; $p > 0.05$; Table 1). AGR of juveniles reared in 16U was higher ($0.63 \pm 0.18 \text{ g day}^{-1}$) but not significantly different with 16E ($0.52 \pm 0.03 \text{ g day}^{-1}$), 4U ($0.49 \pm 0.08 \text{ g day}^{-1}$), and 4E ($0.41 \pm 0.11 \text{ g day}^{-1}$).

Based on the monthly survival rate (Figure 2) in grow-out sea pens, there was a dramatic decline of juvenile sandfish in almost all treatments after one month of stocking. Throughout the experimental period, 4U pens exhibit lowest survival although not significantly different from the other pens (One-way ANOVA; $p > 0.05$) Meanwhile, 16E consistently has slightly higher survival compared to the other treatments. At the end of the experiment, no treatment showed higher than 45% survival rate, with the highest is $35.00 \pm 12.73\%$, followed by $29.00 \pm 21.21\%$, $20.00 \pm 5.66\%$ and the lowest is $7.00 \pm 1.41\%$ for 16E, 16U, 4E and 4U respectively. On month 3 and 4 of the experiment, some of the juveniles in site A spotted with skin ulceration disease (SKUDs).

Despite the lack of proof, there is always a possibility that the disease contributed to the deaths of the juveniles. Monthly patterns indicate that continuous decline of juveniles occurred in all treatments. The inconsistent pattern of survival especially in 4U and 4E pens could be due to the difficulty in retrieving the juveniles during monitoring.

Sediment Characteristics: Total Organic Matter and Chlorophyll-A

The TOM and Chl-a content for each therapy are displayed monthly in Table 2. During the observation day, the TOM content in all treatments did not differ statistically significantly ($p > 0.05$), even though TOM was consistently slightly higher in the enriched pens (4E and 16E). However, the pooled data of TOM throughout the study showed that enriched pens (4E) and (16E) are significantly higher than those unenriched pens (4U) and (16U). (Kruskal-wallis with pairwise comparison; $p = 0.10$) (see Table 2). At the start of the experiment, chlorophyll-a content was significantly higher in the high stocking density and enrichment pens (4E) but was not significantly different from

16E. The Chl-a content in the pens with enrichment (4E and 16E) remained consistently higher than in the pens without enrichment ($p < 0.05$). Similarly, the pooled data of Chl-a throughout the experiment showed that enriched pens are significantly higher than those unenriched pens ($p < 0.01$). From these results, it can be concluded that *Sargassum* spp. has altered the sediment characteristics of the sea pens.

Water Quality

The monthly seawater temperatures in the experimental sea pens were relatively high during the study (28.3 – 32.9 °C) but still within the optimal range. The lowest temperature was recorded in June with a range of 28.8 – 29.1 °C and in November (28.3 – 29.5 °C) as it was cloudy during the monitoring. The highest temperature was in September (32.8 – 32.9 °C). Salinity ranged from 30.5 – 33.41 ppt, with the lowest salinity measured in November (28.2 – 31.2 ppt) which is still in optimal range for sea cucumber farming. Meanwhile, dissolved oxygen ranged from 3.65 to 6.08 mg L⁻¹.

Table 1. Two-way ANOVA (significant at $p < 0.05$) of survival (%), total biomass (g), mean weight (g) and AGR (g day⁻¹) of juveniles between each treatment for 7 months.

		DF	MS	F	p-value
Survival (%)	Enrichment	1	180.500	1.118	0.350
	Stocking density	1	684.500	4.238	0.109
	Enrichment x stocking density	1	24.500	0.152	0.717
	Error	4	161.500		
Total biomass (g)	Enrichment	1	0.098	2.689	0.176
	Stocking density	1	0.485	13.378	0.022*
	Enrichment x stocking density	1	0.048	1.325	0.314
	Error	4	0.036		
Mean weight (g)	Enrichment	1	1274.163	1.534	0.219
	Stocking density	1	4523.357	5.447	0.022*
	Enrichment x stocking density	1	65.310	.079	0.780
	Error	87	830.486		
AGR (g day ⁻¹)	Enrichment	1	0.018	1.452	0.295
	Stocking density	1	.031	2.509	0.188
	Enrichment x stocking density	1	.001	0.040	0.851
	Error	4	0.012		

Significant difference at $p < 0.05$. Asterisk (*) indicates significant difference.

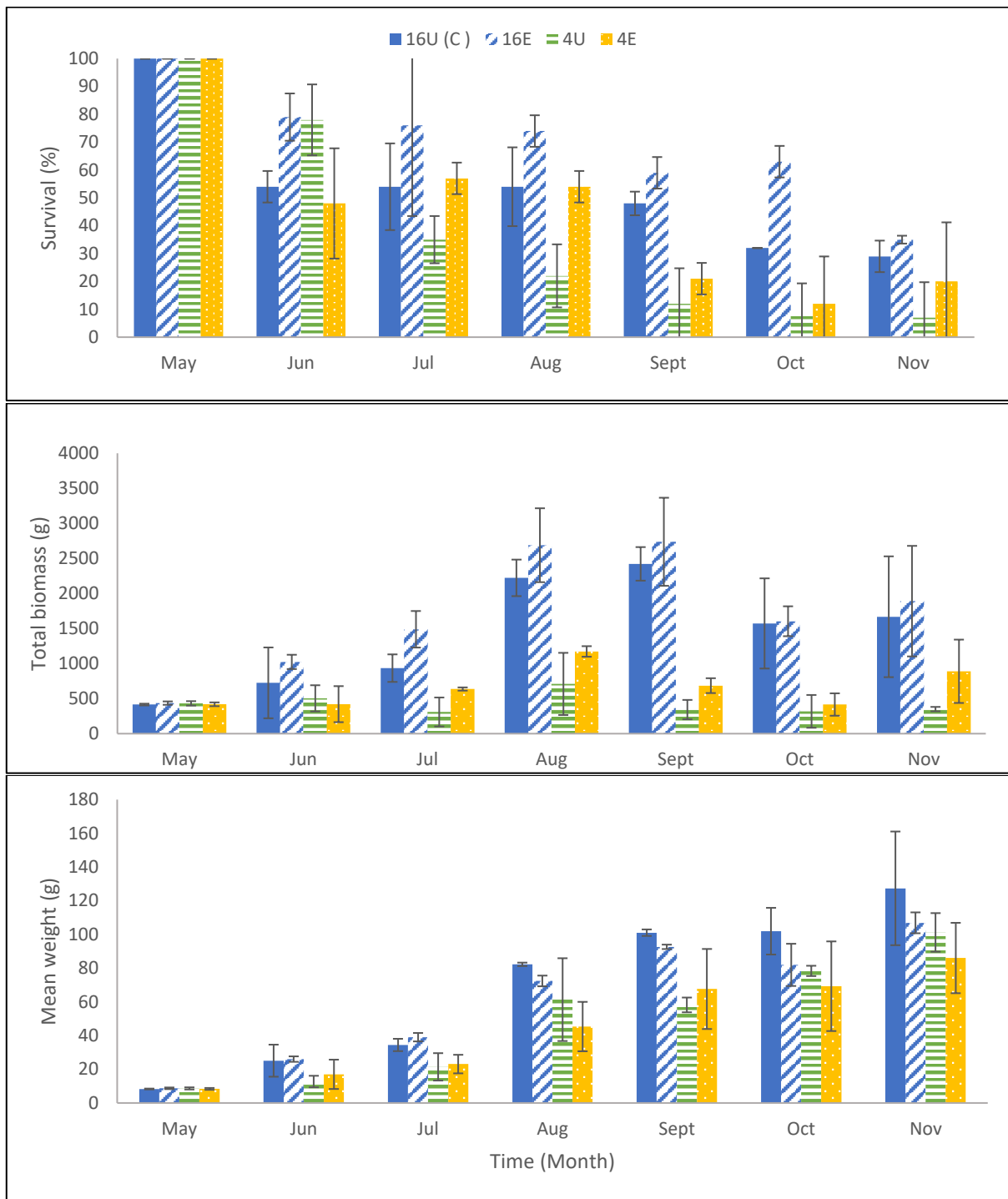


Figure 2. Monthly survival rate, total biomass and mean weight of juveniles. Error bars indicate standard deviation. 16U (3 ind.m⁻², non-enrich), 16E (3 ind.m⁻², enriched), 4U (12 ind.m⁻², non-enrich) and 4E (12 ind.m⁻², enriched).

Table 2. Monthly TOM and Chl-a \pm S.D in enriched and unenriched pens.

Day/Parameter/ Treatment	16U (Control)	4U	4E	16E	
0	TOM (%)	3.10 \pm 0.53 ^a	3.33 \pm 0.75 ^a	3.07 \pm 0.11 ^a	3.27 \pm 0.31 ^a
	Chl-a (ug/g)	1.04 \pm 0.13 ^b	0.88 \pm 0.35 ^b	2.60 \pm 0.27 ^a	1.74 \pm 0.29 ^{ab}
33	TOM (%)	3.06 \pm 0.33 ^a	3.05 \pm 0.21 ^a	3.21 \pm 0.23 ^a	3.64 \pm 0.74 ^a
	Chl-a (ug/g)	1.08 \pm 0.29 ^{ab}	1.14 \pm 0.42 ^b	2.32 \pm 0.8 ^{ab}	2.61 \pm 0.79 ^a
63	TOM (%)	3.24 \pm 0.12 ^a	3.07 \pm 0.24 ^a	3.07 \pm 0.26 ^a	3.31 \pm 0.29 ^a
	Chl-a (ug/g)	1.23 \pm 0.42 ^{ab}	0.71 \pm 0.08 ^b	1.34 \pm 0.31 ^a	1.78 \pm 0.31 ^a
90	TOM (%)	2.89 \pm 0.69 ^a	2.94 \pm 0.61 ^a	3.56 \pm 0.35 ^a	3.33 \pm 0.82 ^a
	Chl-a (ug/g)	1.29 \pm 0.42 ^a	0.71 \pm 0.25 ^a	1.82 \pm 1.30 ^a	1.42 \pm 0.48 ^a
119	TOM (%)	3.14 \pm 0.23 ^a	2.91 \pm 0.29 ^a	3.16 \pm 0.28 ^a	3.24 \pm 0.19 ^a
	Chl-a (ug/g)	0.87 \pm 0.29 ^a	0.74 \pm 0.12 ^a	1.05 \pm 0.25 ^a	1.13 \pm 0.19 ^a
157	TOM (%)	3.16 \pm 0.20 ^a	2.95 \pm 0.32 ^a	3.09 \pm 0.22 ^a	3.51 \pm 0.55 ^a
	Chl-a (ug/g)	1.34 \pm 0.81 ^a	1.36 \pm 0.65 ^a	2.45 \pm 0.20 ^a	2.42 \pm 0.72 ^a
188	TOM (%)	3.39 \pm 0.20 ^a	3.1 \pm 0.10 ^a	3.61 \pm 0.36 ^a	3.66 \pm 0.31 ^a
	Chl-a (ug/g)	0.79 \pm 0.42 ^b	1.05 \pm 0.15 ^b	2.08 \pm 0.52 ^a	2.18 \pm 0.90 ^a

Different letter superscripts indicate significance differences (One-way ANOVA; $p < 0.05$). 16U = Low stocking density with no enrichment, 4U = high stocking density with no enrichment, 16E = low stocking density with enrichment, 4E = high stocking density with enrichment.

DISCUSSION

The aim of this study was to evaluate the effects of stocking density and sediment enrichment with *Sargassum* spp. on the growth and survival rate of pen cultured *H. scabra*, commonly known as sandfish. Sea cucumber aquaculture is of significant interest due to its economic importance and ecological value. The main results of this study show that stocking density influences the total biomass and mean weight of farmed *H. scabra* (initial size at stocking: 8.68 \pm 3.88 [S.D.] g body weight). Although the stocking density of *H. scabra* has been studied in a number of studies, similar research is essential to verify results across a range of environmental conditions and methods of farming. Although no statistically significant difference ($p > 0.05$) was found between the growth and survival rate of *H. scabra* juveniles in enriched and unenriched sediment, it is still necessary to consider possible trends or patterns that could have practical implications for future studies.

Statistically, stocking density had no significant effect on *H. scabra* survival in this study ($p > 0.05$), although survival was slightly higher at low stocking densities (3 ind. m⁻²). Similar results were found in a previous study that suggested a stocking density of 3 ind. m⁻² to give sea cucumbers a better chance of finding sufficient food sources in an environment with limited supply and available area (Serang *et al.*, 2016).

Results of previous studies have shown that the growth of sea cucumbers is positively influenced by the enrichment of sediments with *Sargassum* spp. (Sinsona & Juinio-Meñez, 2018). Although the study found no significant differences in the survival and growth performance (total biomass and AGR) of *H. scabra* between the pens with enriched sediment and those without, it is important to note that the pens with lower stocking density with the sediment enriched with *Sargassum* spp. consistently showed better survival rates and

growth performance. The statistical insignificance of this result could be caused by the small sample size. However, this result is consistent with other studies by Sinsona & Juinio-Meñez (2018) which show that sediment enrichment has no significant effect on the survival of *H. scabra* juveniles in pen cultures.

In addition to TOM, Chl-a found in the sediment is an indicator of benthic microalgae, which are a food source for deposit feeders such as sea cucumbers (Hartati *et al.*, 2017). A previous study reported that Chl-a levels of $\sim 4 \mu\text{g g}^{-1}$ can increase by more than 17 g in just 30 days (Sinsona & Juinio-Meñez, 2018) and that an enrichment ratio of 0.9 kg m^{-2} increases Chl-a by $\sim 2.4 \mu\text{g g}^{-2}$. In the same study, the organic matter content in the enriched sediments was high (14.4 – 15.5%) compared to this study ($\sim 3\%$). Of note, Chl-a and TOM content is low at these sites, which was probably consumed by the cultured *H. scabra* in the existing farms owned by the community. Additionally, enriched pens consistently have a slightly higher TOM and Chl-a content than non-enriched pens, suggesting that powdered *Sargassum* spp. in sea pens support the development of microalgae in the sediment. Enrichment of the sediment provided more food resources. However, the enrichment ratio (3% of total biomass) is not sufficient to support the ideal development and survival of juvenile *H. scabra* at a high stocking density, suggesting that a higher enrichment ratio needs to be used in future studies.

In this study, juveniles of *H. scabra* raised in pen cultures showed poor survival rates (7 – 35% with initial weight: $8.68 \pm 3.88 \text{ g}$), similar to the reports of Dumalan *et al.* (2019). In a previous study, only 12% of the juveniles (initial weight: $6.7 \pm 0.7 \text{ g}$) survived after 8 months of grow out in seagrass bed areas while the mortality rate in the fish farm was 100%. In the same study, however, a survival rate of 65% was recorded for larger juvenile fish (initial weight: $57.4 \pm 4.3 \text{ g}$) after 8 months of rearing in the seagrass area and 49% in the fish farm. Since neither stocking density nor sediment enrichment had a significant effect on the survival rate of *H. scabra* ($p > 0.05$), escape was more likely the main cause of survival in this study. In addition, the highest mortality rate in all enclosures occurred in the 1st and 2nd month after stocking, suggesting that transport stress could be one of

the main reasons for the low survival rate. The transport of the juveniles from the hatchery to the experimental sea pen took about 4 hours by car and 1.5 hours by boat. According to Purcell *et al.* (2006), the issue in transporting live sea cucumber in water medium is the declining pH level when the water temperature is not maintained properly. The declines in pH at ambient water temperature would be stressful for the juveniles, as high-water temperature could lead to higher metabolic activity and ammonia excretion, thus increasing stress (Estudillo & Duray, 2003).

Although the top of the pens was covered with mesh net, the juveniles were able to slip through the gaps at the bottom of the pens more easily. A similar problem had previously been documented by Namukose *et al.* (2016). In addition, these openings attracted other marine animals, including potential predators such as crabs, which could enter the pens and prey on the sea cucumbers (Pitt *et al.*, 2004; Namukose *et al.*, 2016). In this study, crabs and fish were observed in the sea pens, which could pose a direct threat to the survival of *H. scabra*. Lavitra *et al.* (2009) and Altamirano *et al.* (2017) considered crabs such as *Thalamita crenata* as the most severe predator of juvenile sea cucumber.

The monthly water quality in this study is in the optimal range for temperature and salinity. Optimal temperature of *H. scabra* varies from 26-33°C (Agudo, 2006; Lavitra *et al.*, 2010; Kühnhold, 2017). Optimal salinity for *H. scabra* cultivation ranging from 27-35 ppt (Agudo, 2006) and 28-32 ppt (Serang *et al.*, 2016). However, the DO level in this study may be low ($< 5.0 \text{ mg L}^{-1}$), while the optimal DO level for sea cucumber culture according to Oh *et al.* (2015) is above 5.0 mg L^{-1} . Towards the end of the experiment (November), frequent rainfall occurred due to the onset of the northeast monsoon, which brings heavy rainfall to Peninsular Malaysia, west of Sarawak and east of Sabah (Malaysia Meteorological Department: <https://www.met.gov.my/>). The sharp decline in the survival rate of *H. scabra* in sea pens might coincides with this rainy season. Juinio-Meñez *et al.* (2013) previously found a sharp decrease in biomass in sea pens after a thypoon, which can be attributed to a change in sediment quality in the sea pen.

Based on this observation, the northeast monsoon in Malawali can occur from October to January, suggesting that the ideal grow-out period in Malawali is between February and September (8 months) to avoid high mortality or negative growth due to harsh weather. However, to reach a harvestable size in 8 months, which is typically > 300 g (Dumalan *et al.*, 2019), the growth rate should be at least 1.2 g day⁻¹. Comparing this growth rate with the current average absolute growth rate in Malawali, which is between 0.413 and 0.633 g day⁻¹, it becomes clear that reaching a harvestable size within 6 months is a challenge. However, the use of larger juveniles at release may be considered in a future study.

While sea pens are effective in many ways, they come with their own challenges in open environments. These challenges include high costs of construction, cleaning and maintenance (Robinson & Pascal, 2012). Sea pens are also susceptible to unfavourable weather conditions such as storms and rough seas, which can shorten their lifespan if they are not designed and maintained appropriately. In our case, heavy rain and storms led to the collapse of our experimental sea pens after 5 to 7 months of operation. This unfortunate event led to the escape of juvenile sea cucumbers and the interruption of data collection, so the experiment had to be cancelled prematurely and shortened from the originally planned 10 months to 6 months. For future studies, an improved construction of the enclosures that can withstand strong waves and heavy rain should be considered.

The presence of a clear trend in survival and growth of cultured *H. scabra* despite a lack of statistical significance is an intriguing aspect of our results. There are a number of possible causes for this scenario, all of which should be carefully considered. The sample size is limited due to a limited source of hatchery-produced *H. scabra* juveniles, replication is insufficient due to limited sea pens, and the variability within the data is large, so the statistical test is unable to detect a significant difference.

CONCLUSION

As a conclusion, lower stocking density led to a higher biomass, but did not significantly affect the survival rate. In pens with enriched sediment,

the results were slightly better, although not statistically significantly different. This study suggests that low stocking density (3 ind.m⁻²) with sediment enrichment by *Sargassum* spp. may promote higher biomass, but the optimal enrichment ratio remains to be determined. Several problems such as escape, and predation were observed. The study has also shown the importance of considering seasonal weather effects. This study provides valuable insights into sea cucumber farming in this region, but also acknowledges limitations and emphasises the need for future research and consideration of environmental aspects when optimising practises. Future studies ought to concentrate on figuring out the best ratios of sediment enrichment for large-scale, sustainable sea cucumber farming to increase biomass while preserving high survival rates. Increasing the length of the study might facilitate the capturing of seasonal fluctuations and long-term impacts. Additionally, further research with a larger sample size, and sufficient replicates of sea pen are required for conclusive findings.

ACKNOWLEDGEMENTS

The author would like to thank WWF-Malaysia for funding this research (Project no: 728/21247273), and to the community monitoring team in Malawali island and Borneo Marine Research Institute for their involvement and technical supports to all research activities during a field study in Malawali.

REFERENCES

- Agudo, N. (2006). *Sandfish hatchery techniques*. Nouméa, New Caledonia, Australian Centre for International Agricultural Research (ACIAR), Secretariat for the Pacific Community (SPC) and Worldfish Center. Nouméa, New Caledonia. pp. 43.
- Ahmed, H., Shakeel, H., Naeem, S. & Sano, K. (2018). Pilot study on grow-out culture of sandfish (*Holothuria scabra*) in bottom-set sea cages in lagoon. *Secretariat for the Pacific Community (SPC) Beche-de-mer Information Bulletin*, 38: 45-50.
- Altamirano, J.P., Recente, C.P., & Rodriguez, J. C. (2017). Substrate preference for burying and feeding of sandfish *Holothuria scabra* juveniles. *Fisheries Research*, 186: 514-523. DOI: 10.1016/j.fishres.2016.08.011.

- Chor, W.K., Ng, X.K., & Ramlee, S. (2016). *Profiling Study: Sea Cucumber Farming and Trading in Tun Mustapha Park*. Kota Kinabalu, WWF-Malaysia.
- Conand, C. (2006). *Sea Cucumber Biology, Taxonomy, Distribution and Conservation Status*. In Bruckner, A.W. (eds.). 2006. *Proceedings of the CITES workshop on the conservation of sea cucumbers in the families Holothuriidae and Stichopodidae*. NOAA Technical Memorandum NMFS-OPR-34, Silver Spring. pp. 33.
- Conand, C. (2018). Tropical sea cucumber fisheries: Changes during the last decade. *Marine Pollution Bulletin*, 133: 590–594. DOI: 10.1016/j.marpolbul.2018.05.014.
- Cubillo, A.M., Ferreira, J.G., Robinson, S.M., Pearce, C.M., Corner, R.A., & Johansen, J. (2016). Role of deposit feeders in integrated multi-trophic aquaculture—a model analysis. *Aquaculture*, 453: 54–66.
- Dumalan, R.J.P., Bondoc, K.G.V., & Juinio-Meñez, M.A. (2019). Grow-out culture trial of sandfish *Holothuria scabra* in pens near a mariculture-impacted area. *Aquaculture*, 507: 481–492. DOI: 10.1016/j.aquaculture.2019.04.045.
- Estudillo, C.B., & Duray, M.N. (2003). Transport of hatchery-reared and wild grouper larvae, *Epinephelus* sp. *Aquaculture*, 219(1): 279–290. DOI: 10.1016/S0044-8486(02)00413-1.
- Hair, C., Foale, S., Kinch, J., Frijlink, S., Lindsay, D., & Southgate, P. C. (2019). Socioeconomic impacts of a sea cucumber fishery in Papua New Guinea: Is there an opportunity for mariculture?. *Ocean and Coastal Management*, 179. DOI: 10.1016/j.aqrep.2016.03.004.
- Hair, C., Mills, D.J., McIntyre, R., & Southgate, P.C. (2016). Optimising methods for community-based sea cucumber ranching: Experimental releases of cultured juvenile *Holothuria scabra* into seagrass meadows in Papua New Guinea. *Aquaculture Reports*, 3: 198–208. DOI: 10.1016/j.aqrep.2016.03.004.
- Hamad, M.I., Mwandya, A.W., Munubi, R.S., Chenyambuga, S., & Lamtane, H.A. (2019). Comparative growth and survival performance of sea cucumber (*Holothuria scabra*) in co-cultured pen system with commercial macroalgae. *African Journal of Biological Sciences (South Africa)*, 1(4): 32–41. DOI: 10.33472/AFJBS.1.4.2019.32-41.
- Hartati, R., Widianingsih, Trianto, A., Zainuri, M., & Ambaryanto. (2017). The abundance of prospective natural food for sea cucumber *Holothuria atra* at karimunjawa island waters, Jepara, Indonesia. *Biodiversitas*, 18(3): 947–953. DOI: 10.13057/biodiv/d180311.
- Heiri, O., Lotter, A.F., & Lemcke, G. (2001). Loss on ignition as a method for estimating organic and carbonate content in sediments: reproducibility and comparability of results. *Journal of Paleolimnology*, 25: 101–110.
- IUCN. (2023). *Holothuria scabra*. The IUCN Red List of Threatened Species. <https://www.iucnredlist.org>. Downloaded on 20 May 2023.
- Juinio-Meñez, M.A., Evangelio, J.C., Olavides, R.D., Paña, M.A.S., De Peralta, G.M., Edullantes, C.M.A., Rodriguez, B.D.R., & Casilagan, I.L.N. (2013). Population Dynamics of Cultured *Holothuria scabra* in a Sea Ranch: Implications for Stock Restoration. *Reviews in Fisheries Science*, 21(3–4): 424–432. DOI: 10.1080/10641262.2013.837282.
- Juinio-Meñez, M.A., Paña, M.A., de Peralta, G.M., Catbagan, T.O., Olavides, R.D.D., Edullantes, C.M.A., & Rodriguez, B.D.D. (2012). Establishment and management of communal sandfish (*Holothuria scabra*) sea ranching in the Philippines. In Cathy, A. Hair, Timothy, D. Pickering, and David, J.M. (eds.). *Proceedings of an international symposium*, 15–17 February 2011, Noumea, New Caledonia. Australian Centre for International Agricultural Research. pp. 121–127.
- Juinio-Meñez, M.A., Tech, E.D., Ticao, I.P., Gorospe, J.R., Edullantes, C.M.A., & Rioja, R.A.V. (2017). Adaptive and integrated culture production systems for the tropical sea cucumber *Holothuria scabra*. *Fisheries Research*, 186: 502–513. DOI: 10.1016/j.fishres.2016.07.017.
- Kamarudin, K.R., Rehan, M.M., & Bahaman, N.A. (2017). Morphological and molecular identification of sea cucumber species *Holothuria scabra*, *Stichopus horrens* and *Stichopus ocellatus* from Kudat, Sabah, Malaysia. *Pertanika Journal of Tropical Agricultural Science*, 40(1): 161–171.
- Kühnhold, H. (2017). *Temperature tolerance of the sea cucumber *Holothuria scabra*: towards a systematic understanding of multi-level temperature effects*. (Doctoral dissertation), Universität Bremen.

- Lavitra, T., Rasolofonirina, R., & Eeckhaut, I. (2010). The Effect of Sediment Quality and Stocking Density on Survival and Growth of the Sea Cucumber *Holothuria scabra* Reared in Nursery Ponds and Sea Pens. *Western Indian Ocean J. Mar. Sci.*, 9(3): 153-164.
- Lavitra, T., Rasolofonirina, R., Jangoux, M., & Eeckhaut, I. (2009). Problems related to the farming of *Holothuria scabra* (Jaeger, 1833). *Secretariat for the Pacific Community (SPC) Beche-de-mer Information Bulletin*, 29: 20-30.
- Lim, V.C., Justine, E.V., Yusof, K., Mohamad Ariffin, W.N.S.W., Goh, H.C., & Fadzil, K.S. (2021). Eliciting local knowledge of ecosystem services using participatory mapping and Photovoice: A case study of Tun Mustapha Park, Malaysia. *PLoS ONE*, 16(7). DOI: 10.1371/journal.pone.0253740.
- Liu, Y., Dong, S., Tian, X., Wang, F., & Gao, Q. (2010). The effect of different macroalgae on the growth of sea cucumbers (*Apostichopus japonicus* Selenka). *Aquaculture Research*, 41(11): e881–e885. DOI: 10.1111/j.1365-2109.2010.02582.x.
- Namukose, M., Msuya, F.E., Ferse, S.C.A., Slater, M.J., & Kunzmann, A. (2016). Growth performance of the sea cucumber *Holothuria scabra* and the seaweed *Eucheuma denticulatum*: Integrated mariculture and effects on sediment organic characteristics. *Aquaculture Environment Interactions*, 8: 179–189. DOI: 10.3354/aei00172.
- Oh, Y.W., Kang, M.-S., Wi, J.H., & Lee, I.T. (2015). Development of Ecologically Suitable Habitat Model for the Sustainable Sea Cucumber Aquafarm. *Ecology and Resilient Infrastructure*, 2(1): 64–79. DOI: 10.17820/eri.2015.2.1.064.
- Pitt, R., Dinh, N., & Duy, Q. (2004). Breeding and rearing of the sea cucumber *Holothuria scabra* in Viet Nam. *Secretariat for the Pacific Community (SPC) Beche-de-mer Information Bulletin*, 32: 49-52.
- Purcell, S.W., Blockmans, B.F., & Agudo, N.N.S. (2006). Transportation methods for restocking of juvenile sea cucumber, *Holothuria scabra*. *Aquaculture*, 251(2–4): 238–244. DOI: 10.1016/j.aquaculture.2005.04.078.
- Purcell, S.W., & Simutoga, M. (2008). Spatio-temporal and size-dependent variation in the success of releasing cultured sea cucumbers in the wild. *Reviews in Fisheries Science*, 16(1–3): 204–214. DOI: 10.1080/10641260701686895.
- Robinson & Pascal. (2012). Sea cucumber farming experiences in south-western Madagascar. In Hair, C.A., Pickering, T.D., Mills, D.J. (eds.) *Asia-Pacific tropical sea cucumber aquaculture. Proceedings of an international symposium*, 15-17 February 2011, Noumea, New Caledonia. Australian Centre for International Agricultural Research. pp. 136.
- Rodrigues, T., Azevedo e Silva, F., Sousa, J., Félix, P.M., & Pombo, A. (2023). Effect of Enriched Substrate on the Growth of the Sea Cucumber *Holothuria arguinensis* Koehler and Vaney, 1906 Juveniles. *Diversity*, 15(3). DOI: 10.3390/d15030458.
- Rougier, A., Ateweberhan, M., & Harris, A. (2013). Strategies for improving survivorship of hatchery-reared juvenile *Holothuria scabra* in community-managed sea cucumber farms. *Secretariat for the Pacific Community (SPC) Beche-de-mer Information Bulletin*, 33: 14-22.
- Sabilu, K., Supriyono, E., Nirmala, K., Subhan, Ketjulan, R., Hamzah, M., Rahman, A., Patadjai, R.S., Alwi, L.O., & Sabilu, M. (2022). Application of compost in the different of pen culture substrates type for the intensification of sea cucumber, *Holothuria scabra* (Jaeger 1883) culture. *Earth and Environmental Science*, 1033(1): DOI: 10.1088/1755-1315/1033/1/012018.
- Serang, A.M., Tua Rahantoknam, S.P., & Tomatala, P. (2016). Effect of Different Stocking Densities on Growth and Survival Rates of Sea Cucumber *Holothuria scabra* Seedlings. *Aquacultura Indonesiana*, 17(1): 30. DOI: 10.21534/ai.v17i1.44.
- Sinsona, M.J., & Juinio-Meñez, M.A. (2018). Effects of sediment enrichment with macroalgae, *Sargassum* spp., on the behavior, growth, and survival of juvenile sandfish, *Holothuria scabra*. *Aquaculture Reports*, 12: 56–63. DOI: 10.1016/j.aqrep.2018.09.002.
- Slater, M.J., & Carton, A.G. (2009). Effect of sea cucumber (*Australostichopus mollis*) grazing on coastal sediments impacted by mussel farm deposition. *Marine Pollution Bulletin*, 58(8): 1123–1129. DOI: 10.1016/j.marpolbul.2009.04.008.
- Yu, Z., Zhou, Y., Yang, H., & Hu, C. (2014). Bottom culture of the sea cucumber *Apostichopus japonicus* Selenka (Echinodermata: Holothuroidea) in a fish farm, southern China. *Aquaculture Research*, 45(9): 1434–1441. DOI: 10.1111/are.12089.

Yussuf, Y.S., & Yahya, S.A. (2021). Stocking Density, Growth and Survival Rate of Post-Settled Juveniles of *Holothuria scabra* (Jaeger 1833)

Reared in an Ocean-Based Floating Hapa. *Tanzania Journal of Science*, 47(3): 1041–1054. DOI: 10.4314/tjs.v47i3.15.

Effects of Salinity Changes on Hematological Blood Parameters and Stress Responses in Red Tilapia (*Oreochromis* spp.) Infected with *Vibrio harveyi*

MOHAMMAD FAIZAL ULKHAQ*¹, KAVINA RENDA SAFITRI², DAIVA ILYANING ASRIN²,
LAKSMI SULMARTIWI³, JIUN-YAN LOH⁴

¹Department of Health and Life Sciences, Faculty of Health, Medicine and Life Sciences, Airlangga University, Banyuwangi, 68423 East Java, Indonesia; ²Aquaculture Study Program, School of Health and Natural Sciences, Airlangga University, Banyuwangi, 68423 East Java, Indonesia; ³Department of Marine, Faculty of Fisheries and Marine, Airlangga University, Surabaya, 60115 East Java, Indonesia; ⁴Tropical Futures Institute (TFI), James Cook University Singapore, 149 Sims Drive, 387380, Singapore

*Corresponding author: m-faizalulkhaq@fpk.unair.ac.id

Received: 3 June 2024

Accepted: 7 October 2024

Published: 31 December 2024

ABSTRACT

The effect of salinity manipulation on the blood parameters and stress responses of red tilapia, *Oreochromis* spp. During infection with *Vibrio harveyi* was investigated. The fish were reared in five different salinities (0, 5, 10, 15, and 20 ppt) with three replicates for 30 days and were injected with 10⁶ CFU/mL *V. harveyi* intramuscularly in all treatments except the negative control. After infection, the fish were observed for clinical signs for 14 days, collected blood samples, and measured stress responses in 0, 2, 3, 4, 5, 6, 7, and 14-days post-infection (dpi) with *V. harveyi*, meanwhile the cortisol plasma was taken on 0, 2, 3, 4, 5, and 6-dpi. The analysis of blood parameters consisted of total erythrocyte count (RBCs), total leucocyte count (WBCs), hemoglobin (Hb) level, percentage of monocytes (Mon), lymphocytes (Lym) and neutrophils (Neu). The stress response parameters included primary responses (cortisol plasma), secondary responses (blood glucose), and tertiary responses (ventilation rate). The results indicate that salinity manipulation influenced the resistance of red tilapia after infection with *V. harveyi*.

Keywords: Hematology, *Oreochromis* spp., salinity, stress responses, *Vibrio harveyi*

Copyright: This is an open access article distributed under the terms of the CC-BY-NC-SA (Creative Commons Attribution-NonCommercial-ShareAlike 4.0 International License) which permits unrestricted use, distribution, and reproduction in any medium, for non-commercial purposes, provided the original work of the author(s) is properly cited.

INTRODUCTION

Red tilapia (*Oreochromis* spp.) is one of the euryhaline commodities that have the highest production value in Indonesia compared to other fish species from 2015 – 2020 (Kementerian Kelautan dan Perikanan, 2022). This fish can be cultivated in a high salinity medium and is susceptible to bacterial pathogens (Vadhel *et al.*, 2017) including Aeromoniasis (Azzam-Sayuti *et al.*, 2021); Streptococcosis (Palang *et al.*, 2020) and Vibriosis (Eissa *et al.*, 2024). Luminous disease is one of the infectious diseases that cause mass mortality in brackish water and marine culture, including at the nursery and growth stages of fish (Zhang *et al.*, 2020). This disease causes high mortality and losses in aquaculture (up to 75%), including in marine teleosts (*Acanthurus sohal*) (Hashem & El-Barbary, 2013), shrimp (*Penaeus vannamei*) (Nurhafizah *et al.*, 2021), abalone (*Haliotis tuberculata*) (Cardinaud *et al.*, 2014), sea cucumber (*Holothuria scabra*) (Becker *et al.*, 2004), and seahorse (*Hippocampus kuda*) (Xie *et*

al., 2020). Furthermore, infection with *V. harveyi* also has an impact on human health (Brehm *et al.*, 2020).

This disease is caused by *Vibrio harveyi*, a curved rod (comma) shaped bacterium, measuring 1.4 – 5.0 µm in length, and 0.3 – 1.3 µm in width. It is a facultative anaerobe with polar flagella for movement (Montánchez & Kabardin, 2020). This opportunistic pathogen forms yellow colonies in Thiosulphate Citrate Bile Salt (TCBS) agar medium, exhibits bioluminescence, and requires sodium chloride to grow (Austin & Zhang, 2006). Several extracellular products (ECP) have been produced from *V. harveyi* including gelatinase, caseinase, lipase, phospholipase, and hemolysins (Zhang *et al.*, 2020). All of the ECPs produced from *V. harveyi* play as virulence factors in infecting the host. Infected fish show several alterations in behavior and lesions in external and internal organs. Behavioral changes seen in infected fish include passive swimming at the bottom of the pond, loss of balance, and abrupt darting

(Yanuhar *et al.*, 2022). The organ lesions accompanying with this disease consist of skin pigmentation and ulceration, ascites, inflammation in the heart, lesions in the dorsal body and fin, and necrosis and congestion in the liver and kidney (Atujona *et al.*, 2018).

Salinity manipulation can be used as an environmental tool to control opportunistic pathogens that cause mortality in cultured organisms. Salinity increased from 0.5 ppt to 3.5 – 4.5 ppt can reduce the rate of pathogen transmission from infected fish (Clulow *et al.*, 2018). Hauton *et al.* (2000) reported that high salinities show a significant effect on the immune system of the European flat oyster (*Ostrea edulis*) by increasing the number of large granulocytes. The effect of salinity in enhancing the immune system of aquatic organisms has been reported in other studies, including grass carp after being challenged with *Flavobacterium columnare* (Fang *et al.*, 2022); Pacific oyster (*Crastorea gigas*) after infection with *V. alginolyticus* (Li *et al.*, 2022) and coastal fish (*Scatophagus argus*) during infection with *Aeromonas hydrophila* (Lu *et al.*, 2022).

Stress responses can be used as indicators to evaluate the fish's condition after infection with pathogens (Shahjahan *et al.*, 2022). The stress responses that are shown include primary responses (increased the secretion of corticosteroid and catecholamine hormones) (Bonga, 1997); secondary responses (increased in glucose, lactate and heat-shock proteins) (Harper & Wolf, 2009), and tertiary responses consisting of changes in performance characteristics and behavioral patterns (Barton, 2002; Balasch & Tort, 2019). Furthermore, hematological analysis can be used to monitor the health status of fish, including erythrocyte count (RBC); hematocrit (Ht), hemoglobin concentration (Hb); leucocyte count (WBC); differential leucocyte count (DLC); and thrombocyte count (TC) (Witeska *et al.*, 2022).

Salinity is one of the major environmental factors affecting to the immune system. It is necessary to determine the effect of salinity changes on immune system of euryhaline fish infected with pathogens. However, the effect of salinity manipulation in reducing stress responses and increasing the immunity of red tilapia against infection has not been revealed before. Therefore, the objective of this study was

to analyze the hematological parameters and stress responses of red tilapia after being exposed to different salinity mediums and challenged with *V. harveyi*. The output of this study could be used in conjunction with the prevention of bacterial infection using environmental factor manipulation.

MATERIALS AND METHODS

Ethics Statement

This study was conducted from April to May 2022 at the Fish Anatomy Laboratory School of Health and Natural Sciences, Universitas Airlangga. The research was undertaken in accordance with the Law of the Republic of Indonesia No. 18 of 2002 on the National System of Research, Development, and Application of Science and Technology. The research was conducted with the approval of the School of Health and Life Sciences, Universitas Airlangga (ethical approval: 932/UN3.1.16/KP/2022).

Experimental Fish and Bacterial Isolates

Three hundred and sixty healthy red tilapia, *Oreochromis* spp. (10 ± 1.4 cm in mean length and 16.9 ± 0.5 g in mean weight) were collected from the Fish Hatchery Center of Kabat, Banyuwangi, East Java. They were divided into 18 glass aquariums (volume 36 L, 20 fish for each) and reared in freshwater with well aeration. The experimental fish were acclimatized for 7 days and fed with commercial pellets (30 % crude protein, 6 % lipid, and 3 % carbohydrate Matahari Sakti, Indonesia), three times a day (06.00 pm, 02.00 am and 10.00 am) and until satiation. The water quality parameters (temperature, pH, dissolved oxygen, and ammonia) were controlled to maintain optimum conditions. After 7 days, the fish were assigned to each salinity treatment with 5 ppt uplift every 3 days and reared for 30 days adaptation period.

Vibrio harveyi isolates were obtained from the Installation of Brackish Water Aquaculture, Jepara, Central Java inoculated and sub-cultured in TCBS agar medium (Merck, Germany). These isolates were then characterized using a biochemical test based on Barrow & Feltham, (1999).

Vibrio harveyi Pathogenicity Confirmation

The pure isolate of *V. harveyi* after biochemical confirmation was reintroduced to healthy red tilapia using Koch's Postulates procedures based on Mangunwardoyo *et al.* (2016). During the pathogenicity confirmation, fish were placed in an anesthetic tank (100 ppm eugenol) for 60 sec and injected with 0.1 ml of bacterial suspension in NaCl 0.9 % solution (density, 10^6 CFU ml⁻¹) intramuscularly, and 0.1 ml of NaCl 0.9 % solution for the negative control.

Experimental Design and *In-vivo* Challenge

This research was conducted with six experimental groups, each with triplicates. The experimental groups included rearing fish in 0 ppt for positive (PC) and negative control (NC); 5 ppt (T1), 10 ppt (T2), 15 ppt (T3), and 20 ppt (T4) for 30-day rearing period. After that, all fish being challenged with *V. harveyi* in NaCl 0.9% solution (density, 10^6 CFU ml⁻¹) to all treatments and PC except NC was injected with 0.1 mL of

NaCl 0.9% solution, the fish were kept for 14 days and fed with the same commercial feed (Matahari Sakti, Indonesia). After infection, the fish were returned to each aquarium and the survival rate was observed. All solid waste was removed from each aquarium once a day (every morning), and water quality parameters (temperature, pH, dissolved oxygen, and ammonia concentration) were measured every morning (06:00 – 06:30 am) and evening (04:00 – 04:30 pm) and maintained at optimum conditions (Table 1). The temperature and pH of the rearing water were measured by a water thermometer (Resun, Indonesia) and pH indicator paper (Merck, Germany), respectively. In the meanwhile, dissolved oxygen and ammonia concentration of the rearing water were obtained by a DO meter (Horiba, Poland) and SERA-ammonium/ammonia test kit (SERA, Germany), respectively. The research flow chart was represented in Figure 1.

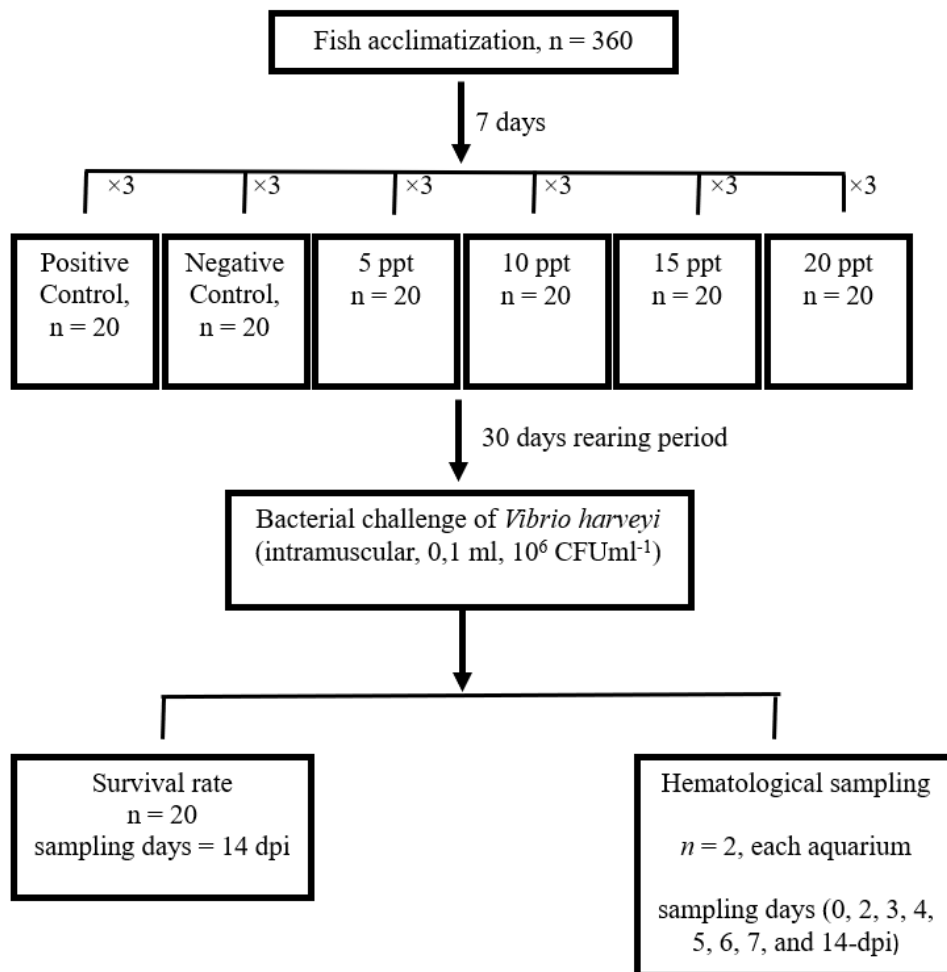


Figure 1. Research flow chart

Hematological Sampling

Sampling for blood examination was taken before (0 dpi) and after (2, 3, 4, 5, 6, 7, and 14-dpi) challenges with *V. harveyi* for stress responses (blood glucose) (Odhiambo *et al.*, 2020) and blood analyses, including total erythrocyte (RBCs), total leukocyte (WBCs), hemoglobin (Hb), percentage of monocyte (Mon), lymphocyte (Lym), and neutrophil (Neu), refers to Blaxhall & Daisley (1973), except cortisol plasma was taken on 2, 3, 4, 5, and 6-dpi with *V. harveyi*. Two fish were randomly sampled from each aquarium and moved to an anesthetic tank (100 ppm eugenol) for 60 sec. Blood was taken from two fish in each treatment from vena caudalis using a syringe and collected in an anticoagulant tube. Cortisol plasma and blood glucose were examined using the Enzyme-linked immunosorbent assay (ELISA) method according to Sadoul & Geffroy, (2019) and a glucometer (Easy Touch Glucose Test, Taiwan) refers to Bartoňková *et al.*, (2016), respectively. Analysis of ventilation rate as tertiary stress responses was conducted on 0, 2, 3, 4, 5, 6, 7, and 14-dpi with *V. harveyi* using a hand counter every 10 minutes for 1 hour in the evening. Ventilation rates were counted and averaged from all fish from each aquarium for analysis (Flint *et al.*, 2015). The survival rate of fish was counted based on Do Huu *et al.* (2016) [Eq.(1)].

$$\text{Survival rate (SR)} = \frac{N_t}{N_0} \times 100\% \quad \text{Eq.(1)}$$

Description:

N_t = fish number day-t (fish)

N_0 = fish number day-0 (fish)

Statistical Analyses

All parameters including blood profiles, stress response parameters, and water quality were analyzed descriptively and compared with normal values. Survival rate was analyzed by one-way Analysis of Variance (ANOVA) and followed by the Duncan Multiple Range Test (DMRT). Significance was determined at P values < 0.05 .

RESULTS

The results of the observation of blood parameters (Figure 2) showed a decrease in RBCs (Figure 2a) and Hb levels (Figure 2b) from 1-dpi to 14-dpi, especially in T4 (20 ppt)

compared to other treatments. The total WBCs (Figure 2c) showed an increasing trend in all treatments from 1-dpi until 6-dpi and remained stable until 14-dpi. There was a rise in the percentage of neutrophils (Figure 2d) to a peak at 4-dpi and 5-dpi in all treatments and then a decrease until 14-dpi. Meanwhile, the monocyte percentages (Figure 2e) increased to a maximum at 6-dpi in all treatments and decreased in the following days, except in the negative control (NC). The lymphocyte percentage (Figure 2f) showed a decline from 2-dpi to 5-dpi and then increased from 5-dpi until 14-dpi.

Observation of the stress response of red tilapia after infection with *V. harveyi* (Figure 3) presents a similar trend in all parameters (cortisol plasma, blood glucose, and ventilation rate). They all increased until reaching the maximum value in the middle of the observation and then slowly decreased until the end of the study, except for the negative control (NC). Cortisol plasma (Figure 3a), blood glucose (Figure 3b), and ventilation rate (Figure 3c) were peaked at 4-dpi, 5-dpi or 6-dpi, and 5-dpi, respectively.

The survival rate of *Oreochromis* spp. (Figure 4) varies significantly between treatments. The highest value in NC is not statistically different from T1, T2, or T3 ($P > 0.05$). However, its values are significantly different from PC and T4 ($P < 0.05$). Water quality parameters (Table 1) are optimum for *Oreochromis* spp. cultivation.

DISCUSSION

V. harveyi is a bacterial pathogen causing Vibriosis disease, leading to several changes in blood parameters and high fish mortality (Zhang *et al.*, 2020). Vibriosis in fish induces various modifications in total red blood cells (RBCs), white blood cells (WBCs), hemoglobin levels (Hb), and differential leucocytes (Qiao *et al.*, 2012). The hematological parameters and stress responses of red tilapia showed several changes after being treated in different salinity mediums and challenged with *V. harveyi*.

RBCs are the most numerous cell types essential to gas exchange in vertebrates (Shen *et al.*, 2018). In the present study, the RBC count of red tilapia after infection with *V. harveyi* decreased in all treatments (Figure 2a), with the highest decrease observed in T4 (salinity of 20

ppt) to 2.01×10^5 cells mL⁻¹. However, when compared to the normal value of RBCs in tilapia, the value still falls within the ranges of 2.08 to 2.93×10^5 cells mL⁻¹ (Vo *et al.*, 2022). Ruwandeepika *et al.* (2012) stated that *V. harveyi* can secrete the hemolysin toxin, which lyses the RBCs and causes hemorrhage and ulcers on the skin. Furthermore, Hernández-Cabanyero *et al.* (2022) reported that *Vibrio* infection can trigger an acute inflammatory response and a cytokine storm that leads to fish mortality. Previous studies have also reported similar results in sea bass (*Lates calcarifer*) (Pattah *et al.*, 2020) and yellowtail kingfish (*Seriola lalandi*) (Le & Fotedar, 2014).

Hb is a protein in vertebrate erythrocytes that used to transport and store oxygen (Wicher and Fries, 2006). The mean values of hemoglobin levels (Figure 2b) demonstrated a decline in all treatments from the beginning to the end of the observation, similar to the RBC count. The highest decline occurred in T4 (salinity of 20 ppt) compared to all groups, including the control. RBCs function to transfer hemoglobin to the body tissues, and therefore, there is a positive correlation between hemoglobin and RBCs, leading to anemia in fish (Witeska, 2015; Yuhana *et al.*, 2019). Jun & Woo (2003) stated that *Vibrio* bacteria secrete not only hemolysin but also siderophores, which can disrupt iron uptake, especially from hemoglobin. Studies in *Salmo salar* in Chile (Ruiz *et al.*, 2016) and European sea bass (*Dicentrarchus labrax*) (Abdel-Tawwab *et al.*, 2020) have reported a decrease in hemoglobin levels after infection with *Vibrio*. As a result, these data showed that infection of *Vibrio* can affect to the RBCs and hemoglobin from infected fish at high salinity.

Leucocytes have an important role in the fish's immune system to fight against pathogens. Based on the results, the WBCs value (Figure 2c) shows an increase from 1-dpi to 14-dpi in all treatments, including the control, and is higher than the normal value (range $7.5 - 8.2 \times 10^4$ cells mL⁻¹) (Mauel *et al.*, 2007). Group T4 (salinity 20 ppt) peaked at 6-dpi and dropped from 7-dpi to 14-dpi. This indicates that red tilapia responds to pathogen infection. The leukocytes will migrate and converge at the site of infection to defeat these pathogens (Ellis, 1977). The leukocyte levels dropped until the end of the observation. This happens because the leucocytes extravasate from the blood vessels and migrate to the

infected tissue (Nourshargh and Alon, 2014). Some reports also state similar results, such as in tilapia fish (*Oreochromis mossambicus*) after infection with *V. parahaemolyticus* (Fatima *et al.*, 2022) and *Aeromonas hydrophila* (Silviana *et al.*, 2022). Zhang *et al.* (2020) state that *V. harveyi* secretes biofilm compounds that can survive and spread throughout the fish's body and enhance the fish's immune system.

Neutrophils plays vital roles in wound healing, tissue regeneration, immune system signaling, and pathogen defense (Speirs *et al.*, 2024). The percentage of neutrophils (Figure 2d) shows an increasing number after infection with *V. harveyi* until the 4-dpi and then slowly decreases until 14-dpi. The increasing neutrophils indicate that red tilapia responds to *V. harveyi* infection, and it is higher than the normal value (less than 5%) (Havixbeck *et al.*, 2016). Neutrophil cells are the first leukocyte cells that migrate directly after infection and eliminate the pathogens through several mechanisms (Mortaz *et al.*, 2018). Furthermore, Zhao *et al.* (2017) state that chemotactic signals derived from pathogens and the host rapidly recruit neutrophils from the blood to infection sites. The decreasing number of neutrophils between 5-dpi and 14-dpi suggests that neutrophil cells can control and eliminate the pathogens. This is done through various mechanisms, such as producing reactive oxygen species (ROS) and releasing toxic intracellular granules (Havixbeck & Barreda, 2015). Buchmann (2022) stated that neutrophils can use Toll-like receptors (TLRs) and pattern recognition receptors (PRRs) to trap the pathogen and be easily engulfed by phagocytic cells. This result is similar to a previous study in hybrid sturgeon (Xiao *et al.*, 2022) and humpback grouper (*Cromileptes altivelis*) (Dangeubun and Metungun, 2017) after being infected with *Vibrio*.

During the inflammatory process, monocytes help to maintain tissue-resident macrophage populations (Witeska *et al.*, 2022). The mean values of monocyte percentages (Figure 2e) slowly uplifted to a peak at 6-dpi and dropped significantly until 14-dpi, but still within normal values. The normal value of monocytes in tilapia ranged from 11 – 24% (Corrêa *et al.*, 2017). The increasing monocyte count indicates that immune responses in red tilapia have been induced after infection with *V. harveyi*.

Monocytes are the largest type of leukocyte cells and have high phagocytosis activity. They can migrate and differentiate into macrophages in the tissues (Fischer *et al.*, 2006). The antipathogenic activities of monocytes include macrophage polarization, cytokine production, antigen presentation, and phagocytosis mechanisms (Lu and Chen, 2019). At 6-dpi, the percentage of monocytes decreased considerably. This is because monocytes have a short life span in the bloodstream (10 – 20 hours), leading to fluctuations in their numbers (Grayfer *et al.*, 2018). Several studies have reported similar results, such as in ayu (*Plecoglossus altivelis*) (Lu *et al.*, 2021) and sea bass (*Lates calcarifer*) (Pattah *et al.*, 2020) when facing *Vibrio* infection.

Lymphocytes play an important role in the innate immunity of teleosts (Van Muiswinkel, 1993). The percentage of lymphocytes (Figure 2f) in red tilapia after infection with *V. harveyi* slowly dropped until 5-dpi, then gradually increased until 14-dpi. Nevertheless, the values were within the range of normal conditions, ranging from 30.9 to 86.5% (Corrêa *et al.*, 2017). The decline in lymphocyte percentage after infection is caused by the dominance of neutrophils in WBCs at the beginning of the infection, replacing the number of lymphocytes (Scapigliati *et al.*, 2018). From 6-dpi to 14-dpi, the percentage of lymphocytes were steadily increased. This shows that the humoral immune response of red tilapia was activated to protect the fish from recurrent infections (Scapigliati, 2013). Activation of adaptive immunity in lymphocytes requires exposure to antigens presented by major histocompatibility complex (MHC) molecules (Zapata *et al.*, 2006). Previous studies have also supported this result, such as in pompano fish (*Trachinotus ovatus*) (Do Huu *et al.*, 2016) and gilthead seabream (Chaves-Pozo *et al.*, 2005) during *Vibrio* infections. Taken together, these findings suggest that *Vibrio* infection can enhance the immune response of red tilapia.

Stress responses in fish were divided into three groups, primarily, secondary, and tertiary. Secretion of cortisol in circulation was one of the primary stress responses that showed where fish in highly stressed (Peter, 2011). Releasing stress hormones affected the alterations of blood chemistry, such as blood glucose as secondary responses, and the escalation of ventilation rate

was a result of the fish adaptation process during stress conditions (Petitjean *et al.*, 2019). In the present study, all fish responses (Figure 3a, 3b, and 3c) showed the same result, starting from 1-dpi to the maximum at 5-dpi or 6-dpi and then slowing the falling until 14-dpi. This occurred because the red tilapia can adapt to external stressors (salinity) and internal stressors (infection of *V. harveyi*). *V. harveyi* released protease enzymes and several toxins (enterotoxin, cytotoxin, and endotoxin) that can damage fish tissue and act as biological stressors for the host (Austin and Zhang, 2006). According to Galhardo *et al.* (2011), secretion of the cortisol hormone affected the increase in blood glucose and ventilation rate in fish due to surviving under stress conditions. The optimum value of cortisol plasma, blood glucose, and ventilation rate in fish was 20-60 ng mL⁻¹ (Ellis *et al.*, 2012), 40-90 mg dL⁻¹ (Renitasari *et al.*, 2021), and 76-99 bpm (Iwama *et al.*, 1997), respectively. Previous studies also displayed similar results in Atlantic salmon (*Salmo salar*) (Wiik *et al.*, 1989), brown-marbled grouper (*Epinephelus fuscoguttatus*) juveniles (Amar *et al.*, 2018), juveniles of barramundi or Asian seabass (*Lates calcarifer*) (Talpur *et al.*, 2013; Siddik *et al.*, 2019), and Gilthead seabream (*Sparus aurata*) (Vargas *et al.*, 2018) during *Vibrio* infection. Taken together, these results indicate that several stress responses were expressed after *Vibrio* infection in red tilapia.

Environmental factors such as salinity can affect the increase in immune responses in fish after infection with pathogens and result in high survival rates (Figure 4). Exposure to high salinity can activate the immune responses and produce more active cells that fight against pathogen infections (Wen *et al.*, 2021). In euryhaline fish, environmental salinity can induce the alteration of indigenous hormones, especially growth hormone (Yada *et al.*, 1994). Furthermore, Evans and Kültz (2020) states that growth hormones can stimulate macrophage function and increase non-specific immunity. Modulation of the fish immune system after exposure to high salinity is also reported in several species, including Nile tilapia (*Oreochromis niloticus*) (Dominguez *et al.*, 2005), broad nose pipefish (*Syngnathus typhle*) (Birrer *et al.*, 2012), and sablefish (*Anoplopoma fimbria*) (Kim *et al.*, 2017). As a result, these data showed that salinity manipulation can stimulate the red tilapia immune system.

Table 1. Water quality parameters of rearing media during treatment

Parameters	Observing value
Temperature (°C)	27 – 28
pH	7 – 8
Dissolved oxygen (ppm)	5 – 7
Ammonia (ppm)	0 – 0.25

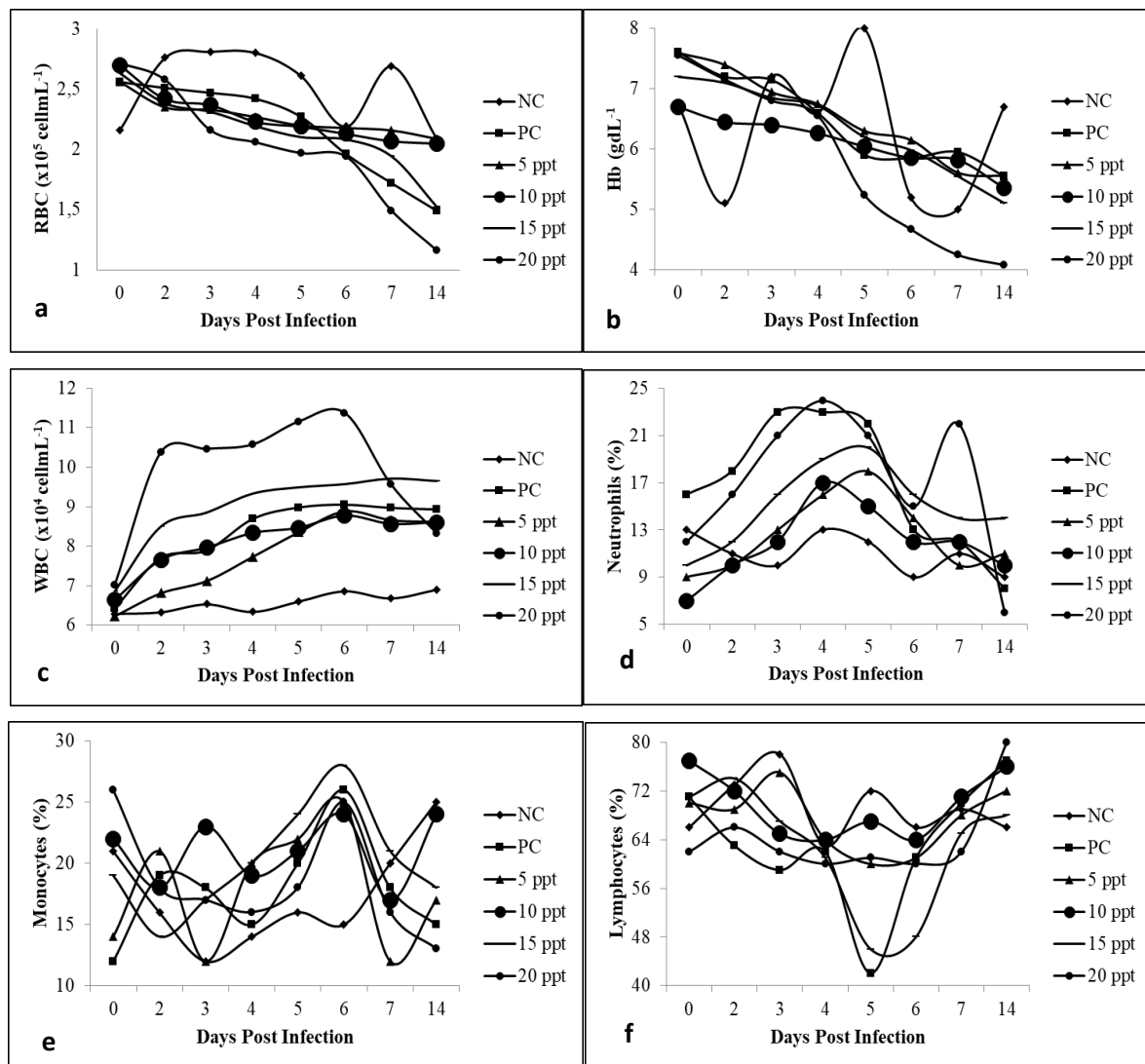


Figure 2. Variation of mean values for hematological parameters in red tilapia *Oreochromis* spp. reared in different salinity followed by challenges with *V. harveyi* at different sampling times. NC: negative control; PC: positive control

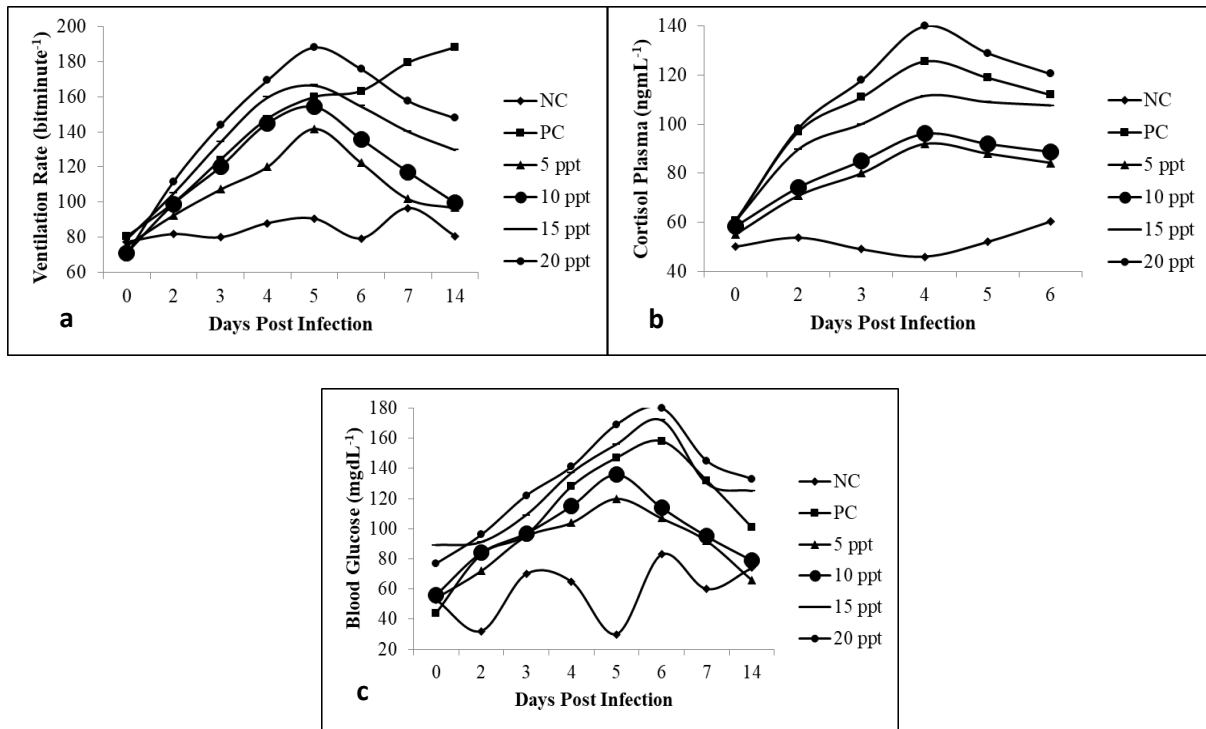


Figure 3. Mean values of stress responses in red tilapia *Oreochromis* spp. reared in different salinity followed by challenges with *V. harveyi* at different sampling times. NC: negative control; PC: positive control

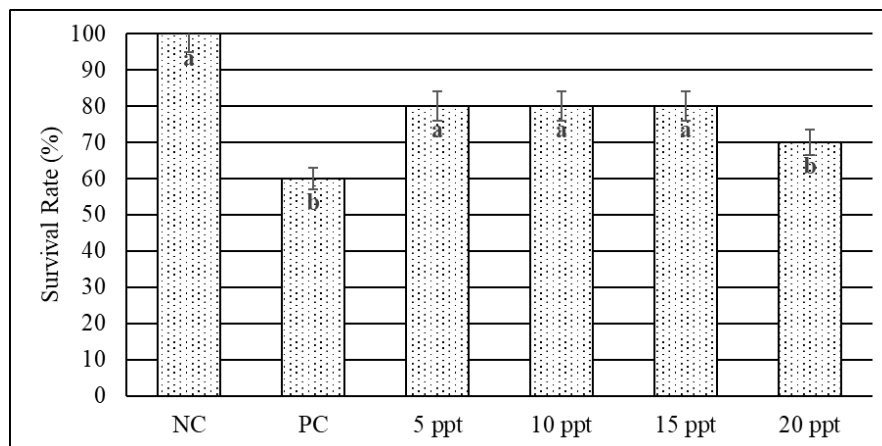


Figure 4. Survival rate of red tilapia *Oreochromis* spp. reared in different salinity followed by challenges with *V. harveyi*. NC: negative control; PC: positive control. Different letters indicate statistically significant between experimental groups ($p < 0.05$)

CONCLUSION

The findings of the current investigation indicated that salinity manipulation influenced the resistance of red tilapia after infection with *V. harveyi*. Low salinity (5 – 15 ppt) can increase the resistance of red tilapia infected with *V. harveyi* in terms of blood parameters and stress responses. However, further studies of co-infection with other pathogens would be needed

to detect histopathological alterations in red tilapia.

ACKNOWLEDGEMENTS

This study was supported by the Lecturer Research Grant (861/UN3.1.16/PT/2022), School of Health and Natural Sciences, Universitas Airlangga.

CONFLICT OF INTERESTS

The authors declare that they have no conflicts of interest.

REFERENCES

- Abdel-Tawwab, M. Khalifa, E.D, Amany M.K., Mohamed A.A., Nashwa K. & Riad H. (2020). Dietary garlic and chitosan alleviated zearalenone toxic effects on performance, immunity, and challenge of European sea bass, *Dicentrarchus labrax*, to *Vibrio alginolyticus* infection. *Aquaculture International*, 28(2): 493–510. DOI: 10.1007/s10499-019-00477-0.
- Amar, E.C., Apines-Amar, M.J.S. & Faisan, J.P. (2018). Dietary Onion or Ginger Modulates the Stress Response and Susceptibility to *Vibrio harveyi* JML1 Infection in Brown-marbled Grouper *Epinephelus fuscoguttatus* Juveniles. *Journal of Aquatic Animal Health*, 30(1): 39–49. DOI: 10.1002/aah.10005.
- Atujona, D., Cai, S. & Amenyoqbe, E. (2018). Mini review on *Vibrio* Infection-A Case Study on *Vibrio harveyi* Clade. *Fisheries and Aquaculture Journal*, 9(4): 9–12. DOI: 10.4172/2150-3508.1000258.
- Austin, B. & Zhang, X.H. (2006). *Vibrio harveyi*: A significant pathogen of marine vertebrates and invertebrates. *Letters in Applied Microbiology*, 43(2): 119–124. DOI: 10.1111/j.1472-765X.2006.01989.x.
- Azzam-Sayuti, M., Ina-Salwany, M., Zamri-Saad, M., Salleh A., Yusuf, M.T., Monir, Md.S., Aslah, M., Muhamad-Sofie, M.H.N., Lee, J.Y., Chin, Y.K., Amir-Danial, Z., Asyiqin, A., Lukman, B., Liles, M.R., & Amal, M.N.A. (2021). Comparative pathogenicity of *Aeromonas* spp. In cultured red hybrid tilapia (*Oreochromis niloticus* × *O. mossambicus*). *Biology*, 10(11): 1–14. DOI: 10.3390/biology10111192.
- Balasz, J.C. & Tort, L. (2019). Netting the stress responses in fish. *Frontiers in Endocrinology*, 10(FEB): 1–12. DOI: 10.3389/fendo.2019.00062.
- Barrow, G.I. & Feltham, R.K.. (1999). *Cowan and Steel's Manual for the Identification of Medical Bacteria*. Third edition. Cambridge: Cambridge University Press. pp. 95.
- Barton, B.A. (2002). Stress in fishes: A diversity of responses with particular reference to changes in circulating corticosteroids. *Integrative and Comparative Biology*, 42(3): 517–525. DOI: 10.1093/icb/42.3.517.
- Bartoňková, J., Hyršl, P. & Vojtek, L. (2016). Glucose determination in fish plasma by two different moderate methods. *Acta Veterinaria Brno*, 85(4): 349–353. DOI: 10.2754/avb201685040349.
- Becker, P., Gillan, D., Lanterbecq, D., Jangoux, M., Rasolofonirina, R., Rakotovao, J., & Eeckhaut, I. (2004). The skin ulceration disease in cultivated juveniles of *Holothuria scabra* (Holothuroidea, Echinodermata). *Aquaculture*, 242(1–4): 13–30. DOI: 10.1016/j.aquaculture.2003.11.018.
- Bonga, S.F. (1997). Degeneration and death, by apoptosis and necrosis, of the pavement and chloride cells in the gills of the teleost *Oreochromis mossambicus*. *Cell and Tissue Research*, 255: 235-243.
- Birrer, S.C., Reusch, T.B.H. & Roth, O. (2012). Salinity change impairs pipefish immune defence. *Fish and Shellfish Immunology*, 33(6): 1238–1248. DOI: 10.1016/j.fsi.2012.08.028.
- Blaxhall, P.C. & Daisley, K.W. (1973). Routine haematological methods for use with fish blood. *Journal of Fish Biology*, 5(6): 771–781. DOI: 10.1111/j.1095-8649.1973.tb04510.x.
- Brehm, T.T., Berneking, L., Rohde, H., Chistner, M., Schlickewei, C., Sena M.M., & Schmiedel, S. (2020). Wound infection with *Vibrio harveyi* following a traumatic leg amputation after a motorboat propeller injury in Mallorca, Spain: A case report and review of literature. *BMC Infectious Diseases*, 20(1): 1–7. DOI: 10.1186/s12879-020-4789-2.
- Buchmann, K. (2022). Neutrophils and aquatic pathogens. *Parasite Immunology*, 44(6): 1–11. DOI: 10.1111/pim.12915.
- Cardinaud, M., Barbou, A., Capitaine, C., Bidault, A., Dujon, A.M., Moraga, D., & Paillard, C. (2014). *Vibrio harveyi* adheres to and penetrates tissues of the European abalone *Haliotis tuberculata* within the first hours of contact. *Applied and Environmental Microbiology*, 80(20): 6328–6333. DOI: 10.1128/AEM.01036-14.
- Chaves-Pozo, E., Muñoz, P., López-Muñoz, A., Pelegrín, P., García Ayala, A., Mulero, V., & Meseguer, J. (2005). Early innate immune response and redistribution of inflammatory cells in the bony fish gilthead seabream experimentally infected with *Vibrio anguillarum*. *Cell and Tissue Research*, 320(1): 61–68. DOI: 10.1007/s00441-004-1063-7.

- Clulow, S., Gould, J., James, H., Stockwell, M., Clulow, J., & Mahony, M. (2018). Elevated salinity blocks pathogen transmission and improves host survival from the global amphibian chytrid pandemic: Implications for translocations. *Journal of Applied Ecology*, 55(2): 830–840. DOI: 10.1111/1365-2664.13030.
- Corrêa, S.A. da S., Abessa, D.M.S., Santos, L.G. dos da S., Edison, B., & Seriani, R. (2017). Differential blood counting in fish as a non-destructive biomarker of water contamination exposure. *Toxicological and Environmental Chemistry*, 99(3): 482–491. DOI: 10.1080/02772248.2016.1189554.
- Dangeubun, J.L. & Metungun, J. (2017). Hematology of *Vibrio alginolyticus*-infected humpback grouper *Cromileptes altivelis*, under treatment of *Alstonia acuminata* shoot extract. *AACL Bioflux*, 10(2): 274–284.
- Darshanee Ruwandepika, H.A., Sanjeeva Prasad Jayaweera, T., Paban Bhowmick, P., Karunasagar, I., Bossier, P., & Defoirdt, T. (2012). Pathogenesis, virulence factors and virulence regulation of vibrios belonging to the *Harveyi* clade. *Reviews in Aquaculture*, 4(2): 59–74. DOI: 10.1111/j.1753-5131.2012.01061.x.
- Do Huu, H., Sang, H.M. & Thanh Thuy, N.T. (2016). Dietary β -glucan improved growth performance, *Vibrio* counts, haematological parameters and stress resistance of pompano fish, *Trachinotus ovatus* Linnaeus, 1758. *Fish and Shellfish Immunology*, 54: 402–410. DOI: 10.1016/j.fsi.2016.03.161.
- Dominguez, M., Takemura, A. & Tsuchiya, M. (2005). Effects of changes in environmental factors on the non-specific immune response of Nile tilapia, *Oreochromis niloticus* L. *Aquaculture Research*, 36(4): 391–397. DOI: 10.1111/j.1365-2109.2005.01220.x.
- Eissa, E.S.H., Ahmed, R.A., Abd El-Aziz, Y.M., Hendam, B.M., Eissa, M.E.H., ElBanna, N.I. (2024). Impact of a varied combinatorial mixture of β -1, 3 glucan and fructooligosaccharides on growth performance, metabolism, intestinal morphometry, expression of antioxidant-related genes, immunity, and protection against *Vibrio alginolyticus* in Red tilapia. *Aquaculture International*, 32: 6575–6595. DOI: 10.1007/s10499-024-01479-3
- Ellis, A.E. (1977). The leucocytes of fish: A review. *Journal of Fish Biology*, 11(5): 453–491. DOI: 10.1111/j.1095-8649.1977.tb04140.x.
- Ellis, T., Yildiz, H.Y., López-Olmeda, J., Spedicato, M. T., Tort, L., Øverli, Ø., Martins, & C.I.M. (2012). Cortisol and finfish welfare. *Fish Physiology and Biochemistry*, 38(1): 163–188. DOI: 10.1007/s10695-011-9568-y.
- Evans, T.G. & Kültz, D. (2020). The cellular stress response in fish exposed to salinity fluctuations. *Journal of Experimental Zoology Part A: Ecological and Integrative Physiology*, 333(6): 421–435. DOI: 10.1002/jez.2350.
- Fang, H., Yang, Y.Y., Wu, X.M., Zheng, S.Y., Song, Y.J., Zhang, J., & Chang, M.X. (2022). Effects and Molecular Regulation Mechanisms of Salinity Stress on the Health and Disease Resistance of Grass Carp. *Frontiers in Immunology*, 13(June): 1–20. DOI: 10.3389/fimmu.2022.917497.
- Fatima, R., Nilofer, P.S., Karthikeyan, K., Vidya, R., Itami, T., & Sudhakaran, R. (2022). Enhancement of immune response and resistance to *Vibrio parahaemolyticus* in Tilapia fish (*Oreochromis mossambicus*) by dietary supplementation of *Portieria hornemannii*. *Aquaculture*, 547 (737448): 1-6. DOI: 10.1016/j.aquaculture.2021.737448.
- Fischer, U., Utke, K., Somamoto, T., Köllner, B., Ototake, M. & Nakanishi, T. (2006). Cytotoxic activities of fish leucocytes', *Fish and Shellfish Immunology*, 20(2): 209–226. DOI: 10.1016/j.fsi.2005.03.013.
- Flint, N., Crossland, M.R. & Pearson, R.G. (2015). Sublethal effects of fluctuating hypoxia on juvenile tropical Australian freshwater fish. *Marine and Freshwater Research*, 66(4): 293–304. DOI: 10.1071/MF14120.
- Galhardo, L., Vital, J. & Oliveira, R.F. (2011). The role of predictability in the stress response of a cichlid fish. *Physiology and Behavior*, 102(3–4): 367–372. DOI: 10.1016/j.physbeh.2010.11.035.
- Grayfer, L., Kerimoglu, B., Yaparla, A., Hodgkinson, J.W., Xie, J., & Belosevic, M. (2018). Mechanisms of fish macrophage antimicrobial immunity. *Frontiers in Immunology*, 9:1-22. DOI: 10.3389/fimmu.2018.01105.
- Harper, C. & Wolf, J.C. (2009). Morphologic effects of the stress response in fish. *ILAR Journal*, 50(4): 387–396. DOI: 10.1093/ilar.50.4.387.
- Hashem, M. & El-Barbary, M. (2013). *Vibrio harveyi* infection in Arabian Surgeon fish (*Acanthurus sohal*) of red sea at hurghada, Egypt. *Egyptian Journal of Aquatic Research*, 39(3): 199–203. DOI: 10.1016/j.ejar.2013.10.006.

- Hauton, C., Hawkins, L.E. & Hutchinson, S. (2000). The effects of salinity on the interaction between a pathogen (*Listonella anguillarum*) and components of a host (*Ostrea edulis*) immune system. *Comparative Biochemistry and Physiology - B Biochemistry and Molecular Biology*, 127(2): 203–212. DOI: 10.1016/S0305-0491(00)00251-0.
- Havixbeck, J.J., Rieger, A.M., Wong, M.E., Hodgkinson, J.W., & Barreda, D.R. (2016). Neutrophil contributions to the induction and regulation of the acute inflammatory response in teleost fish. *Journal of Leukocyte Biology*, 99(2): 241–252. DOI: 10.1189/jlb.3hi0215-064r.
- Havixbeck, J.J. & Barreda, D.R. (2015). Neutrophil development, migration, and function in teleost fish. *Biology*, 4(4): 715–734. DOI: 10.3390/biology4040715.
- Hernández-Cabanyero, C., Sanjuán, E.R.L., Felipe E., Vallejos-Vidal, E., Tort, & Lluís Amaro, C. (2022). A Transcriptomic Study Reveals That Fish Vibriosis Due to the Zoonotic Pathogen *Vibrio vulnificus* Is an Acute Inflammatory Disease in Which Erythrocytes May Play an Important Role. *Frontiers in Microbiology*, 13: 1-17. DOI: 10.3389/fmicb.2022.852677
- Iwama, G.K., Takemura, A. & Takano, K. (1997). Oxygen consumption rates of tilapia in fresh water, sea water, and hypersaline sea water. *Journal of Fish Biology*, 51(5): 886–894. DOI: 10.1006/jfbi.1997.0495.
- Jun, L. & Woo, N.Y.S. (2003). Pathogenicity of vibrios in fish: An overview. *Journal of Ocean University of China*, 2(2): 117–128. DOI: 10.1007/s11802-003-0039-7.
- Kementerian Kelautan dan Perikanan (2022) *Kelautan dan Perikanan dalam Angka, Pusat Data, Statistik dan Informasi Kementerian Kelautan dan Perikanan*. Kota Jakarta: Kementerian Kelautan dan Perikanan. 83 pp.
- Kim, J.H., Park, H.J., Kim, K.W., Hwang, I.K., Kim, D.H., Oh, C.W., Lee, J.S. & Kang, J.C. (2017). Growth performance, oxidative stress, and non-specific immune responses in juvenile sablefish, *Anoplopoma fimbria*, by changes of water temperature and salinity. *Fish Physiology and Biochemistry*, 43(5):1421–1431. DOI: 10.1007/s10695-017-0382-z.
- Le, K.T. & Fotedar, R. (2014). Immune Responses to *Vibrio anguillarum* in Yellowtail Kingfish, *Seriola lalandi*, Fed Selenium Supplementation. *Journal of the World Aquaculture Society*, 45(2):138–148. DOI: 10.1111/jwas.12104.
- Li, X., Yang, B., Shi, C., Wang, H., Yu, R., Li, Q. & Liu, S. (2022). Synergistic Interaction of Low Salinity Stress With *Vibrio* Infection Causes Mass Mortalities in the Oyster by Inducing Host Microflora Imbalance and Immune Dysregulation. *Frontiers in Immunology*, 13(May):1–13. DOI: 10.3389/fimmu.2022.859975.
- Lu, J.F., Luo, S., Jin, T.C., Wang, L.C., Yang, G.J., Lu, X.J. & Chen, J. (2021). Betaine protects ayu (*Plecoglossus altivelis*) against *Vibrio anguillarum* infection in salinity by regulating the immunomodulatory activity of monocytes/macrophages. *Aquaculture*, 536: 1-8. DOI: 10.1016/j.aquaculture.2021.736482
- Lu, M. Su, M., Liu, N. & Zhang, J. (2022). Effects of environmental salinity on the immune response of the coastal fish *Scatophagus argus* during bacterial infection', *Fish and Shellfish Immunology*, 124(January): 401–410. DOI: 10.1016/j.fsi.2022.04.029.
- Lu, X.J. & Chen, J. (2019). Specific function and modulation of teleost monocytes/ macrophages: polarization and phagocytosis. *Zoological research*, 40(3): 146–150. DOI: 10.24272/j.issn.2095-8137.2019.035.
- Mangunwardoyo, W., Ismayasari, R. & Riani, E. (2016). Uji Patogenisitas dan Virulensi *Aeromonas hydrophila* Stanier pada Ikan Nila (*Oreochromis niloticus* Lin.) melalui Postulat Koch. *Jurnal Riset Akuakultur*, 5(2): 245-255. DOI: 10.15578/jra.5.2.2010.145-255.
- Mauel, M.J., Miller, D.L. & Merrill, A.L. (2007). Hematologic and plasma biochemical values of healthy hybrid tilapia (*Oreochromis aureus* × *Oreochromis nilotica*) maintained in a recirculating system. *Journal of Zoo and Wildlife Medicine*, 38(3): 420–424. DOI: 10.1638/06-025.1.
- Montánchez, I. & Kaberdin, V.R. (2020). *Vibrio harveyi*: A brief survey of general characteristics and recent epidemiological traits associated with climate change. *Marine Environmental Research*, 154:1-15. DOI: 10.1016/j.marenvres.2019.104850.
- Mortaz, E., Alipoor, S.D., Adcock, I.M., Mumby, S. & Koenderman, L. (2018). Update on neutrophil function in severe inflammation. *Frontiers in Immunology*, 9(OCT): 1–14. DOI: 10.3389/fimmu.2018.02171.

- Nourshargh, S. & Alon, R. (2014). Leukocyte Migration into Inflamed Tissues. *Immunity*, 41(5): 694–707. DOI: 10.1016/j.immuni.2014.10.008.
- Nurhafizah, W.W.I., Lee, K.L., Laith A.A.R., Nadirah, M. Danish-Daniel, M., Zainathan, S.C. & Najiah, M. (2021). Virulence properties and pathogenicity of multidrug-resistant *Vibrio harveyi* associated with luminescent vibriosis in Pacific white shrimp, *Penaeus vannamei*. *Journal of Invertebrate Pathology*, 186: 1-12. DOI: 10.1016/j.jip.2021.107594.
- Odhiambo, E., Angienda, P.O., Okoth, P., & Onyango, D. (2020). Stocking Density Induced Stress on Plasma Cortisol and Whole Blood Glucose Concentration in Nile Tilapia Fish (*Oreochromis niloticus*) of Lake Victoria, Kenya. *International Journal of Zoology*, 2020: 1-8. DOI: 10.1155/2020/9395268.
- Palang, I., Withyachumnarnkul, B., Senapin, S., Sirimanapong, W., & Vanichviriyakit, R. (2020). Brain histopathology in red tilapia *Oreochromis* sp. experimentally infected with *Streptococcus agalactiae* serotype III. *Microscopy Research and Technique*, 83(8): 877–888. DOI: 10.1002/jemt.23481.
- Pattah, H., Wahjuningrum, D., Yuhana, M., & Widanarni W. (2020). Control of *Vibrio alginolyticus* infection in Asian sea bass *Lates calcarifer* using ambon banana plant powder *Musa paradisiacal* through the feed. *Indonesian Aquaculture Journal*, 15(2): 85–91. DOI: 10.15578/IAJ.15.2.2020.85-91.
- Peter, M.C.S. (2011). The role of thyroid hormones in stress response of fish. *General and Comparative Endocrinology*, 172(2): 198–210. DOI: 10.1016/j.ygcen.2011.02.023.
- Petitjean, Q., Jean, S., Gandar, A., Côte, J., Laffaille, P., & Jacquin, L. (2019). Stress responses in fish: From molecular to evolutionary processes. *Science of the Total Environment*, 684: 371–380. DOI: 10.1016/j.scitotenv.2019.05.357.
- Qiao, G., Park, S. II & Xu, D.H. (2012). Clinical, hematological, and biochemical alterations in olive flounder *Paralichthys olivaceus* following experimental infection by *Vibrio scophthalmi*. *Fisheries and Aquatic Sciences*, 15(3): 233–239. DOI: 10.5657/FAS.2012.0233.
- Renitasari, D.P., Kurniawan, A. & Kurniaji, A. (2021). Blood glucose of tilapia fish *Oreochromis mossambica* as a water bioindicator in the downstream of Brantas waters, East Java. *AACL Bioflux*, 14(4): 2040–2049.
- Ruiz, P., Balado, M., Toranzo, A.E., Poblete-Morales, M., Lemos, M.L., & Avendaño-Herrera, R. (2016). Iron assimilation and siderophore production by *Vibrio ordalii* strains isolated from diseased Atlantic salmon *Salmo salar* in Chile. *Diseases of Aquatic Organisms*, 118(3): 217–226. DOI: 10.3354/dao02976.
- Sadoul, B. & Geffroy, B. (2019). Measuring cortisol, the major stress hormone in fishes. *Journal of Fish Biology*, 94(4): 540–555. DOI: 10.1111/jfb.13904.
- Scapigliati, G. (2013). Functional aspects of fish lymphocytes. *Developmental and Comparative Immunology*, 41(2): 200–208. DOI: 10.1016/j.dci.2013.05.012.
- Scapigliati, G., Fausto, A.M. and Picchiatti, S., 2018. Fish lymphocytes: an evolutionary equivalent of mammalian innate-like lymphocytes?. *Frontiers in immunology*, 9:1-8. DOI: 10.3389/fimmu.2018.00971.
- Shahjahan, M., Islam, Md.J., Hossain, Md.T., Mishu, M.A., Hasan, J. & Brown, C. (2022). Blood biomarkers as diagnostic tools: An overview of climate-driven stress responses in fish. *Science of The Total Environment*, 843(June): 156910. DOI: 10.1016/j.scitotenv.2022.156910.
- Shen, Y., Wang, D., Zhao, J., & Chen, X. (2018). Fish red blood cells express immune genes and responses. *Aquaculture and Fisheries*, 3(1): 14–21. DOI: 10.1016/j.aaf.2018.01.001.
- Siddik, M.A.B., Howieson, J. & Fotedar, R. (2019). Beneficial effects of tuna hydrolysate in poultry by-product meal diets on growth, immune response, intestinal health and disease resistance to *Vibrio harveyi* in juvenile barramundi, *Lates calcarifer*. *Fish and Shellfish Immunology*, 89(November 2018): 61–70. DOI: 10.1016/j.fsi.2019.03.042.
- Silviana, N.R., Pamungkas, W. and Grandiosa, R., 2022. Utilizing of black cumin (*Nigella sativa*) flour to increase the immunity system of tilapia (*Oreochromis niloticus*) against *Aeromonas hydrophila* bacteria attack. *Jurnal Akuakultur Indonesia*, 21(2):161-177. DOI: 10.19027/jai.21.2.161-177.

- Speirs, Z.C., Loynes, C.A., Mathiessen, H., Elks, P.M., Renshaw, S.A. & Jørgensen, L.G. (2024). What can we learn about fish neutrophil and macrophage response to immune challenge from studies in zebrafish. *Fish and Shellfish Immunology*, 148:1-16 DOI: 10.1016/j.fsi.2024.109490.
- Talpur, A.D., Ikhwanuddin, M. & Ambok Bolong, A.M. (2013) 'Nutritional effects of ginger (*Zingiber officinale* Roscoe) on immune response of Asian sea bass, *Lates calcarifer* (Bloch) and disease resistance against *Vibrio harveyi*. *Aquaculture*, 400-401: 46-52. DOI: 10.1016/j.aquaculture.2013.02.043.
- Vadhel, N.P., Ng, A., Pathan, J., Tandel, J.T., Lende, S., & Shrivastava, V. (2017). Red Tilapia: A Candidate Euryhaline Species for Aqua Farming in Gujarat. *Journal of Fisheries Sciences.com*, 11(1): 48-50. DOI: 10.21767/1307-234x.1000107.
- van Muiswinkel, W.B. (1993). Fish immunology. *Veterinary Immunology and Immunopathology*, 35(SUPPL. 1): 169-175. DOI: 10.1016/0165-2427(93)90147-v.
- Vargas, R., Balasch, J.C., Brandts, I., Reyes-López, F., Tort, L., & Teles, M. (2018). Variations in the immune and metabolic response of proactive and reactive *Sparus aurata* under stimulation with *Vibrio anguillarum* vaccine', *Scientific Reports*, 8(1): 1-9. DOI: 10.1038/s41598-018-35863-w.
- Vo, V.-T., Tran, T., Nguyen, T., Truong, V., Pham, C., Pham, T. & Thuong, H.N.T. (2022). Hematological Parameters of Red Tilapia (*Oreochromis* sp.) Fed Essential Oils of *Mentha piperita* after Challenge with *Streptococcus agalactiae*. *Pakistan Journal of Zoology*, (May): 1-8. DOI: 10.17582/journal.pjz/20211106031127.
- Wen, X., Chu, P., Xu, J., Wei, X., Fu, D., Wang, T. & Yin, S. (2021). Combined effects of low temperature and salinity on the immune response, antioxidant capacity and lipid metabolism in the pufferfish (*Takifugu fasciatus*). *Aquaculture*, 531: 1-10. DOI: 10.1016/j.aquaculture.2020.735866.
- Wicher, K.B. & Fries, E. (2006). Haptoglobin, a hemoglobin-binding plasma protein, is present in bony fish and mammals but not in frog and chicken. *Proceedings of the National Academy of Sciences of the United States of America*, 103(11): 4168-4173. DOI: 10.1073/pnas.0508723103.
- Wiik, R., Andersen, K., Uglenes, I., & Egidius, E. (1989). Cortisol-induced increase in susceptibility of Atlantic salmon, *Salmo salar*, to *Vibrio salmonicida*, together with effects on the blood cell pattern. *Aquaculture*, 83(3-4): 201-215. DOI: 10.1016/0044-8486(89)90033-1.
- Witeska, M. (2015). Anemia of Teleost Fish. *Bulletin of the European Association of Fish Pathologists*, 35(4):148-160.
- Witeska, M., Kondera, E., Ługowska, K., Bojarski, B. (2022). Hematological methods in fish – Not only for beginners. *Aquaculture*, 547: 1-17. DOI: 10.1016/j.aquaculture.2021.737498.
- Xiao, Z., Li, X., Xue, M., Zhang, M., Liu, W., Fan, Y., Chen, X., Chu, Z., Gong, F., Zeng, L., & Zhou, Y. (2022). *Vibrio metschnikovii*, a Potential Pathogen in Freshwater-Cultured Hybrid Sturgeon', *Animals*, 12(9): 1-14. DOI: 10.3390/ani12091101.
- Xie, J., Bu, L., Jin, S., Wang, X., Zhao, Q., Zhou, S., & Xu, Y. (2020). Outbreak of vibriosis caused by *Vibrio harveyi* and *Vibrio alginolyticus* in farmed seahorse *Hippocampus kuda* in China. *Aquaculture*, 523: 1-9. DOI: 10.1016/j.aquaculture.2020.735168.
- Yada, T., Hirano, T. & Grau, E.G. (1994). Changes in Plasma Levels of the Two Prolactins and Growth Hormone during Adaptation to Different Salinities in the Euryhaline Tilapia, *Oreochromis niloticus*. *General and Comparative Endocrinology*, 93: 214-223. DOI: 10.1006/gcen.1994.1025
- Yanuhar, U., Nurcahyo, H., Widiyanti, L., Junirahma, N.S. Caesar, N.R., & Sukoso, S. (2022). In vivo test of *Vibrio alginolyticus* and *Vibrio harveyi* infection in the humpback grouper (*Cromileptes altivelis*) from East Java Indonesia. *Veterinary World*, 15: 1269-1282. DOI: 10.14202/vetworld.2022.1269-1282.
- Yuhana, S., Suprpto, H., Soegianto, A., Dalahi, F., Mahardika, K., Zafran, Z., & Mastuti, I. (2019). The hematological response of cantang hybrid grouper (*Epinephelus fuscoguttatus* x *Epinephelus lanceolatus*) injected with extracellular product, intracellular component and whole cell vaccine of *Vibrio alginolyticus*. *AACL Bioflux*, 12(6): 2273-2285.
- Zapata, A., Diez, B., Cejalvo, T., Gutiérrez-De Frías, C., & Cortés, A. (2006). Ontogeny of the immune system of fish. *Fish and Shellfish Immunology*, 20(2), pp. 126-136. DOI: 10.1016/j.fsi.2004.09.005.

Zhang, X.H., He, X. & Austin, B. (2020). *Vibrio harveyi*: a serious pathogen of fish and invertebrates in mariculture. *Marine Life Science and Technology*, 2(3): 231–245. DOI: 10.1007/s42995-020-00037-z.

Zhao, M.L., Chi, H. & Sun, L. (2017). Neutrophil extracellular traps of *Cynoglossus semilaevis*: Production characteristics and antibacterial effect. *Frontiers in Immunology*, 8(MAR): 1–9. DOI: 10.3389/fimmu.2017.00290.

Growth Performance, Digestive Enzymes Activities and Gut Microbiota of Malaysian Mahseer, *Tor tambroides* Fingerlings Affected by Various Probiotics Concentrations

SING YING CHUA^{1*}, MOHAMMAD BODRUL MUNIR², FATHURRAHMAN LANANAN³,
ROSLIANAH ASDARI^{1*}

¹ Faculty of Resource Science and Technology, Universiti Malaysia Sarawak, 94300 Kota Samarahan, Sarawak, Malaysia; ² Faculty of Agriculture, Universiti Islam Sultan Sharif Ali, Senaut Campus, Jalan Tutong, Tutong TB1741, Negeri Brunei Darussalam; ³ East Coast Environmental Research Institute, Universiti Sultan Zainal Abidin, 21300 Kuala Nerus, Terengganu, Malaysia

*Corresponding author: singying0397@hotmail.com, aroslianah@unimas.my

Received: 25 July 2024

Accepted: 8 November 2024

Published: 31 December 2024

ABSTRACT

The most valued freshwater fish in Malaysia is the Malaysian mahseer, *Tor tambroides*, also known as Empurau. Due to the extended growing period, innovative feeding management is required to maintain fish health. This study looked at the effect of Lacto-sacc, a feed additive and antibiotic replacement made up of *Lactobacillus acidophilus*, *Saccharomyces cerevisiae* and *Enterococcus faecium*, on *T. tambroides* fingerlings' growth performance, digestive enzyme activities and gut microbiota. A total of 600 fingerlings, each weighing $6.53 \text{ g} \pm 0.17 \text{ g}$, were allocated into twelve 650 L tanks, with 50 fingerlings per tank. Over a period of 20 weeks, the fish were fed four different diets: 0% Lacto-sacc as control (A), 0.5% Lacto-sacc (B), 1.0% Lacto-sacc (C), and 1.25% Lacto-sacc (D), with each diet replicated in three tanks. Although statistic revealed no significant differences in growth performance among treatment group ($p > 0.05$), but it is noteworthy that fingerlings of *T. tambroides* were fed a diet containing 0.5% Lacto-sacc exhibited a trend toward improved growth performance with value higher SGR, along with elevated lipase and protease activities than other groups. Fusobacteria, Proteobacteria, Bacteroidetes, Firmicutes were the top four phyla in the gut microbiota of *T. tambroides*, accounting for more than 95%, with Fusobacteria dominating at around 70% of the gut microbiota. *Cetobacterium*, *ZOR0006*, *Brevinema*, and *Aeromonas* were the most common genera detected. *T. tambroides* fed a 0.5% Lacto-sacc (B) diet had lower Fusobacteria abundance while increasing other dominating bacteria compared to other treatments. Although there is no significant difference in gut microbiota, the gut microbiota of *T. tambroides* fed probiotics was more consistently disturbed and diversified, indicating less species dominance. The addition of Lacto-sacc, particularly at a concentration of 0.5%, appeared to enhance growth performance and increase the activity of digestive enzymes compared to the diet without Lacto-sacc, although the results were not statistically significant.

Keywords: Digestive enzyme, growth performance, gut microbiota, Lacto-sacc, *Tor tambroides*

Copyright: This is an open access article distributed under the terms of the CC-BY-NC-SA (Creative Commons Attribution-NonCommercial-ShareAlike 4.0 International License) which permits unrestricted use, distribution, and reproduction in any medium, for non-commercial purposes, provided the original work of the author(s) is properly cited.

INTRODUCTION

Tor tambroides is known to be one of the most valuable riverine fish in Southeast Asia. The fish species which is found in Malaysia and Indonesia shares the same genus with *T. douronensis* and *T. tambra* (Lau *et al.*, 2021a). Due to its excellent commercial and conservation value, high market demand, and high flesh quality, it has significant potential in aquaculture, with market prices reaching up to USD 200 per kg in 2013, depending on grade and size (Redhwan *et al.*, 2022). However, despite its unique texture and taste, the slow-

growing variant of *T. tambroides*, has low seed production which fails to meet the market demand, as they usually grow only to an average size of 800 g when reared in pond culture in around 33 months (Zomorni *et al.*, 2022). According to the Red List of Threatened Species provided by The International Union for Conservation of Nature (IUCN), study on *T. tambroides* population is still insufficient, though the population trend has decreased, primarily due to invasion events, massive destruction of habitats, and overfishing to fulfil market demand (Kottelat *et al.*, 2018).

In order to maintain the health of *T. tambroides*, which is a slow-growing fish, it is necessary to provide a feed that contains balanced nutrients and can support the fish's well-being over a prolonged period of time. Probiotics have been found to be effective in enhancing growth performance and boosting overall fish health through better nutrient uptake and enhanced immunity towards infectious diseases. The inclusion of probiotics in the diets of juvenile fish can provide nutritional and health benefits by detoxifying and denaturing indigestible compounds in feeds using hydrolytic enzymes, as well as stimulating the immunity of fishes (Bandyopadhyay *et al.*, 2015). Tachibana *et al.* (2021) found that feeding Nile Tilapia with probiotic strains of *Bacillus licheniformis* and *Bacillus subtilis* resulted in better overall net return and a 0.5 - 2% increase in fish production when compared to the control group. One commonly used probiotic in aquaculture is a lactic acid bacterium known as *Lactobacillus acidophilus*. The *Lactobacillus* genus has a long shelf life and good resistancy to environmental conditions, making it an ideal choice for aquaculture operations (Soltani *et al.*, 2017). *L. acidophilus* is found naturally as part of the microbiota at the larval, fry, and fingerling stages of fish development since they can be isolated from the skin, gills, and gut (Ige, 2013). *Saccharomyces cerevisiae*, on the other hand, is a type of Brewers' yeast with high protein content and can be used to compensate amino acid and vitamin deficiencies in fish diets. This microorganism is pathogenic and is capable of resisting bile and lower pH. *S. cerevisiae* also contains immunostimulating compounds such as β -1,3-glucans, mannan-oligosaccharides (MOS) and chitin. These compounds can boost the immune response of fish and serve as a live food and fish meal replacement (Vallejos-Vidal *et al.*, 2016; Risjani *et al.*, 2021).

The selection of safe probiotic candidates is of utmost importance. Lacto-sacc is probiotics mixture produced by AllTech Biotechnology for livestock use. Several studies involving Nile Tilapia, Koi Carp, rabbit, broiler chicken, turkey and quail hens have been conducted using *L. acidophilus* and *S. cerevisiae* combination (Gippert *et al.*, 1992; Mahajan *et al.*, 2000; Sotirov *et al.*, 2001; Abou Zied *et al.*, 2003; Dhanaraj *et al.*, 2010; Wan Alias *et al.*, 2023; Hannan *et al.*, 2024). Lacto-sacc had proven by these studies that able to improve the growth

performance of the host, enhance the feed utilization and immune response, reduce pathogen and improve digestive health and nutrient digestibility. Hannan *et al.* (2024) study proven that inclusion of Lacto-sacc to diet also significantly enhance the immune responses and increase survival rate when challenged with pathogen such as *Vibrio parahaemolyticus* in gravid mud crab.

Additionally, it is crucial to establish the appropriate probiotic dosage before introducing it to the intensive aquaculture industry to avoid the risk of accidental overdose (Ige, 2013). Overdosing probiotics can lead to unwanted side effects and unnecessary costs, while underdosing probiotics may result in incurring costs without achieving the desired outcome of targeted parameters (Nikoskelainen *et al.*, 2001; Ghosh *et al.*, 2007).

Research conducted by Asaduzzaman *et al.* (2018a and 2018b), Hossain *et al.* (2022) and Wan Alias *et al.* (2023) are known to use probiotics on *T. tambroides*. Conversely, studies on the gut microbiota of *T. tambroides* have also been carried out to compare gut microbiota between wild and captive *T. tambroides*, batches of *T. tambroides* from different culture farms and also diseased and healthy *T. tambroides* (Tan *et al.*, 2019; Iehata *et al.*, 2021; Lau *et al.*, 2021b). To date, there is still no published report on the effect of Lacto-sacc on the gut microbiota of the *T. tambroides*. The current study aims to determine the effects of different Lacto-sacc concentration on growth performance, digestive enzyme activities and gut microbiota of *T. tambroides*.

MATERIALS & METHODS

Experimental Fish and Husbandry Condition

The *T. tambroides* fingerlings were obtained from Puri Johan Agro Sdn Bhd at Serian, Sarawak at the size of 1–1.5 inch per fingerlings. The fish were fed with commercial catfish pellet (Uni-President, T502SV), which contain 40% crude protein and 5–8% crude fat, during the 8 weeks of acclimation prior to the experiment. A total of 12 High Density Polyethylene (HDPE) tanks, each with a capacity of 650 L, were utilized for running the current study. The tanks were stocked with experimental fish, which had an average weight and length of 6.53 ± 0.17 g

and 7.23 ± 0.14 cm, at a rate of 50 fingerlings per tank. Feeding was carried out twice per day at 08:30 and 16:30 at 5% of the average fish body weight for 20 weeks. The *in-situ* water quality measurements such as water temperature, pH and dissolved oxygen levels of the tanks were monitored twice daily.

Diet Preparation

Experimental diets containing 40% protein and 12% lipid were prepared with varying levels of Lacto-sacc (AllTech, Inc., USA) supplementation. The Lacto-sacc supplementation contains probiotics

concentration was *S. cerevisiae* 3.80×10^9 CFU/lb, *L. acidophilus* 2.10×10^8 CFU/lb, *Enterococcus faecium* 1.50×10^8 CFU/lb. A total of four diets were formulated; 0% Lacto-sacc as control diet (A), 0.5% Lacto-sacc (B), 1.0% Lacto-sacc (C), and 1.25% Lacto-sacc (D). As shown in Table 1, all the raw ingredients were mixed with water and then pelleted with a pelletiser before drying the pellets in an oven at 35°C for 48 hours. Dried pellets were packed and stored in a -20 °C freezer and will only be defrosted before feeding. The proximate composition was analysed for experimental diets, as shown in Table 1.

Table 1. Feed formulation used in *Tor tambroides* feeding trial

Ingredient (g/kg)	Control (A)	0.5% Lacto-sacc (B)	1.0% Lacto-sacc (C)	1.25% Lacto-sacc (D)
Fish Meal ¹	594.00	594.00	594.00	594.00
Corn Starch	287.60	287.60	287.60	287.60
Fish Oil	17.4	17.4	17.4	17.4
Palm Oil	40.00	40.00	40.00	40.00
Cellulose	11.00	6.00	1.00	1.00
CMC ²	10.00	10.00	10.00	7.50
Vitamin mix	20.00	20.00	20.00	20.00
Mineral mix	20.00	20.00	20.00	20.00
Lacto-sacc mixture	0.00	5.00	10.00	12.50
Proximate Composition (%)				
Protein	41.82	40.41	40.82	41.74
Lipid	12.99	13.34	11.43	11.78
Moisture	7.23	7.7	6.93	6.27
Ash	4.13	4.13	4.27	4.33
Fibre	0.27	0.27	0.33	0.33
NFE	33.65	34.15	36.22	35.55
Gross Energy (J/g)	18418	19109.5	18988.5	18921

¹ Sri Putra Trading, Alor Star, Kedah. Crude protein 67.38%; Crude fat 10.03%

² CMC: carboxymethyl cellulose

Relative Protein Digestibility

The relative protein digestibility (RPD) was determined *in vitro* using the pH drop method and carried out according to the Munir *et al.* (2016) method. Six fish were randomly collected from each tank, forming 18 fish per treatment, and dissected after 4 hours of feeding. The casein was chosen as standard. The RPD was calculated using the formula Eq. (1):

$$RPD = \{(-\Delta\text{pH feedstuff}) / (-\Delta\text{pH casein})\} \times 100 \text{ Eq.(1)}$$

Digestive Enzymes Activity Assay

The crude intestinal enzyme extraction method

was carried out according to Munir *et al.* (2016) with modification. The fish gut was rinsed with 4 °C cold distilled water and cut into pieces, then weighed. The gut was then mixed with 4 °C cold phosphate buffer saline (PBS) at a ratio of 1:10 in a 50 ml centrifuge tube and homogenized using a homogenizer. Subsequently, the mixture was centrifuged at 12000 RPM for 15 minutes at 4 °C. The supernatants were then transferred into 2 ml centrifuge tubes and stored in a -80 °C deep freezer. The activity of digestive enzymes (amylase, lipase, and protease) was assessed using the Sigma-Aldrich MAK009, MAK046 and PF0100 kits, respectively according to the manufacturer's instructions.

Data Collection

Growth and survival parameter was determined. Measurements were taken by weighing each fish fingerling at four weeks intervals. Ten fish were selected from each tank, and their total length, standard length and body weight were recorded. The final weight of each fish was measured at the end of the experiment. The relative growth (RG)[Eq.(2)], specific growth rate (SGR)[Eq.(3)] and survival rate (SR)[Eq.(4)] were calculated using the following equations:

$$RG (\%): 100 \left(\frac{\text{Final Weight} - \text{Initial Weight}}{\text{Initial Weight}} \right) \quad \text{Eq.(2)}$$

$$SGR (\%/day): 100 \left(\frac{\ln \text{Final Weight} - \ln \text{Initial Weight}}{\text{Nos. of Days}} \right) \quad \text{Eq.(3)}$$

$$SR (\%): 100 \left(\frac{\text{Final Number of Fish}}{\text{Initial Number of Fish}} \right) \quad \text{Eq.(4)}$$

DNA Extraction

Fish were rinsed with 4 °C cold autoclaved distilled water and wiped dry before dissection. The gut was cut from the end of the stomach to the anus and cut into smaller pieces in a microcentrifuge tube. The DNA extraction was performed with the Qiagen DNeasy Powersoil Pro Kit. The concentration of eluted DNA was checked using Nanodrop (DeNovix, USA). DNA sample purity around 1.8 at 260 nm/280 nm with a concentration of more than 20 ng/μl was used for further experiments.

Library Preparation and Sequencing

The V3-V4 hypervariable regions of 16S rRNA genes of gut microbiota were selected for Polymerase Chain Reaction (PCR). PCR amplification was carried out using the following primers: the forward primer 5' CCTACGGGNGGCWGCAG 3' and the reverse primer 5' GACTACHVGGGTATCTAATCC 3'. The PCR reaction mixture (25 μl) was prepared with 12.5 μl of 2X KAPA HiFi HotStart ReadyMix, 5 μl of 10 μM Forward Primer, 5 μl of 10 μM Reverse Primer and 2.5 μl of DNA template. The PCR amplification conditions included an initial denaturation at 95 °C for 3 minutes, followed by 25 cycles of denaturation at 95 °C for 30 seconds, annealing at 55 °C for 30 seconds, elongation at 72 °C for 30 seconds, and final elongation at 72 °C for 5 minutes.

The DNA samples were sequenced using an Illumina MiSeq platform. The DNA samples were subjected to library preparation before

sequencing. The amplicons underwent purification and were linked with distinctive index adapter pairs using the Nextera XT Index kit. Following this, the indexed DNA libraries underwent purification using Agencourt AMPure XP (Beckman Coulter, USA). The concentration of these libraries was determined using a Qubit dsDNA HS Assay Kit and a Qubit 2.0 Fluorometer (Thermo Fisher Scientific, USA). At the same time, their size was confirmed using the Agilent 2100 Bioanalyzer (Agilent, USA). Subsequently, the libraries were standardized and combined for subsequent MiSeq sequencing (2 X 300 bp paired-end).

Data Analysis

The significance of growth performance, RPD, and digestive enzyme activities was analysed using One-way Analysis of Variance (ANOVA) at a 95% significance difference. Analysis was carried out using IBM SPSS Statistics Version 25.

The MiSeq sequencing data were analysed using Quantitative Insights into Microbial Ecology (QIIME 2 v2020.8) and was installed on Linux Ubuntu System v18.04. The sequence was quality checked with FastQC v0.11.5 before further analysis to ensure sequences were of good quality. Adapter sequences were removed from both paired-end forward and reverse reads using the cutadapt command before trimming chimeric sequences. The Divisive Amplicon Denoising Algorithm 2 (DADA2) was utilized to denoise, and filter chimeric sequences based on the parametric model that infers true biological sequences from reads. Forward and reverse reads were individually denoised and merged before removing chimeric sequences using 'removeChimeraDenovo', resulting in the formation of Amplicon Sequence Variants (ASVs). Clustered ASVs were then summarised into various taxonomic levels based on GreenGenes database at a 99% identity threshold.

The statistical analysis was examined into two sections, which are alpha diversity and beta diversity. The alpha diversity index parameter chosen was Shannon, Chao1 and Simpson to evaluate the species richness and diversity of each treatment among the gut microbiota of *T. tambroides*. The beta diversity analysis aims to quantify the difference in species composition among the gut microbiota of *T. tambroides*.

Weighted UniFrac was selected for Principal Coordinate Analysis (PCoA) to visualize the variation in gut microbiota composition across different treatments. One-way ANOVA at 95% significance difference was chosen for the check significance of gut microbiota relative abundance of phyla and genera of *T. tambroides*.

RESULTS

Growth Performance, Relative Protein Digestibility and Digestive Enzyme Activities of *T. tambroides*

The presence of Lacto-sacc has been shown to influence the growth performance of fish, with the probiotic concentration listed in Table 2. The statistical analysis revealed no significant difference in all growth performance and survival rate among the treatment groups ($p>0.05$). However, it is noteworthy that treatment B (0.5% Lacto-sacc) exhibited a trend toward improved performance and survival rate with value consistently higher in weight gain, RG, SGR and SR than other treatment groups. These observations indicate that, although not statistically significant, treatment B may offer potential benefits that should be investigated further. As shown in Table 2, the results indicated a trend observed that 0.5% Lacto-sacc was the ideal concentration for raising *T. tambroides* fingerlings, followed by 1.0% Lacto-sacc, 1.25% Lacto-sacc, and control (0% Lacto-sacc), based on their high weight gain, RG, SGR and SR. The addition of probiotics positively influenced growth performance.

Although there was no significant effect ($p>0.05$) found between treatments for amylase and protease activity using One Way ANOVA in Table 3, numerically higher digestive enzyme activities were observed in all probiotic treatments compared to the control group. Treatment D recorded the highest amylase activity, followed by C, B, and A. For protease activity, treatment B showed highest value, followed by C, D, and A. Notably, treatment B had a statistically significant effect ($p<0.05$) on lipase activity, exhibiting higher levels compared to the other treatments.

Gut Microbiota of *T. tambroides*

The sample extracted from *T. tambroides* was quantified for good quality that concentration

was more than 20ng/ μ l, and the purity of the sample OD260/280 was around 1.8 to 2.0. The sequencing depth was normalised for all *T. tambroides* samples as a plateau was observed when the curve flattened gradually, as the sequencing depth is adequate for capturing the diversity present in each sample. Alpha diversity assesses the richness and evenness of species within a specific area without considering differences between areas or samples. As shown in Table 4, the Shannon, Chao1 and Simpson index were shown for each treatment. Treatment B had the highest Shannon (2.8394) and Simpson index (0.8981), while treatment D had the highest Chao1 index (112.3333). Conversely, treatment C had the lowest Shannon, Chao1 and Simpson index.

The 12 samples of *T. tambroides* were observed at Principle Coordinate 1 vs Principle Coordinate 2 in Figure 1. The figure shows that the overall distribution distance between gut microbiota diversity of *T. tambroides* was closely related. Some samples were more dispersed, and A1 at the lower part, and C3 at the upper part of the plot.

Gut Taxonomy of *T. tambroides*

The gut taxonomy data for 12 samples of *T. tambroides* were categorized into their respective groups, the group means were calculated and summarised for each top 10 phyla (Table 5) and genera level (Table 6). No significant differences were found between treatments in both the top 10 phyla and genera of gut microbiota of *T. tambroides*.

The phylum Fusobacteria dominated the gut microbiota of *T. tambroides*. The relative abundance of Fusobacteria varied between 71.79% to 78.31%, with treatment B exhibiting the lowest abundance and treatment A having the highest abundance. On the other hand, the highest Proteobacteria abundance was found in treatment B and the highest Bacteroidetes found in treatment D. Spirochaetes was absent in treatment D.

The most abundant genus found in the gut microbiota of *T. tambroides* was *Cetobacterium*, followed by *ZOR0006*, *Brevinema*, Uncultured and *Aeromonas*. The highest *Cetobacterium* abundance (77.31%) was found in treatment A, and the lowest abundance (71.79%) was

observed in treatment B. The second most abundance genus found was *ZOR0006*, which varied from 2.20% to 6.78%, with the lowest being treatment D and the highest abundance

being treatment B. The *Brevinema* was absent in treatment D, and the highest abundance was found in treatment B

Table 2. Growth performance parameter of *Tor tambroides* fingerlings

Parameter	Control (A)	0.5% Lacto-sacc (B)	1.0% Lacto-sacc (C)	1.25% Lacto-sacc (D)
Initial Weight, g	6.52±0.09	6.48±0.16	6.55±0.11	6.57±0.22
Final Weight, g	17.36±0.45	18.14±0.89	17.94±1.33	17.79±1.38
Weight Gain, g	10.84±0.57	11.66±0.97	11.39±1.43	11.23±1.36
RG ¹ , %	166.28±9.44	180.64±18.12	174.76±24.84	170.85±20.23
SGR ² , %	0.70±0.03	0.73±0.04	0.72±0.06	0.71±0.05
SR ³ , %	98.67±0.67	99.33±0.67	100±0.00	98.67±1.33
VSI ⁴	8.28±0.52	8.81±0.77	8.81±0.49	8.98±0.35
HSI ⁵	0.44±0.08	0.60±0.05	0.53±0.11	0.59±0.08
IPF ⁶	0.83±0.28	0.66±0.15	1.57±0.33	1.70±0.26

Values are the means of triplicate groups ± S.E.

¹RG: Relative Growth

²SGR: Specific Growth Rate

³SR: Survival Rate

⁴VSI: Viscerosomatic Index

⁵HSI: Hepatosomatic Index

⁶IPF: Intra-peritoneal Fat

Table 3. Digestive enzyme activities of *Tor tambroides* fingerlings

Parameter	Control (A)	0.5% Lacto-sacc (B)	1.0% Lacto-sacc (C)	1.25% Lacto-sacc (D)
RPD	42.06±5.97	56.12±11.37	52.44±11.78	52.65±12.31
Amylase, nmole/min/ml	2059.62±102.03	2821.63±1126.14	3591.27±1664.69	3886.90±371.16
Lipase, nmole/min/ml	14.51±1.38 ^a	62.90±8.80 ^b	24.50±1.69 ^a	21.17±2.47 ^a
Protease, ug/ml	2700.25±170.18	3173.87±826.72	2969.48±481.47	2929.54±309.62

Values are the means of triplicate groups ± S.E. Data with a different superscript in same row indicate significant differences (p<0.05).

¹ One unit of amylase is the amount of amylase that cleaves ethylidene-pNP-G7 to generate 1.0 µmole of p-nitrophenol per minute at 25 °C.

² One unit is the amount of lipase that generates 1.0 µmol glycerol from triglycerides per mg of protein per minute at 37 °C.

Table 4. Summary of alpha diversity of *Tor tambroides* gut microbiota

Treatment	Shannon index	Chao1 index	Simpson index
Control (A)	2.7017	110.667	0.8859
0.5% Lacto-sacc (B)	2.8394	96.0000	0.8981
1.0% Lacto-sacc (C)	2.6704	88.3333	0.8840
1.25% Lacto-sacc (D)	2.8360	112.3333	0.8958

Table 5. The relative abundance for top 10 phyla detected in Phase 1 *Tor tambroides* gut

Phylum	Control (A)	0.5% Lacto-sacc (B)	1.0% Lacto-sacc (C)	1.25% Lacto-sacc (D)
Fusobacteria	78.3133 ± 3.5158	71.7900 ± 7.0800	78.2700 ± 8.8803	73.9833 ± 3.1083
Proteobacteria	7.0667 ± 3.1086	8.0633 ± 4.3664	6.7867 ± 0.8756	7.6000 ± 4.7219
Bacteroidetes	7.9333 ± 10.4787	7.1733 ± 2.8856	9.4200 ± 4.6252	13.0633 ± 6.0600
Firmicutes	3.5833 ± 3.2124	7.6167 ± 3.9730	4.7200 ± 4.6627	2.3967 ± 2.0467
Spirochaetes	1.9767 ± 3.2012	4.4767 ± 7.7538	0.0267 ± 0.0462	0 ± 0
Actinobacteria	1.3233 ± 0.9592	0.3733 ± 0.3347	0.2400 ± 0.1054	1.9400 ± 2.3601
Planctomycetes	0.3867 ± 0.2367	0.2500 ± 0.4330	0.1467 ± 0.1185	0.4667 ± 0.5807
Verrucomicrobia	0.1033 ± 0.1274	0.1167 ± 0.0586	0.3267 ± 0.4535	0.4167 ± 0.4565
Chlamydiae	0.0267 ± 0.0379	0.0200 ± 0.0346	0.0067 ± 0.0115	0.0467 ± 0.0808
Cyanobacteria	0.0367 ± 0.0551	0.0067 ± 0.115	0 ± 0	0.0233 ± 0.0404

Table 6. The relative abundance for top 10 genera detected in Phase 1 *Tor tambroides* gut

Genus	Control (A)	0.5% Lacto-sacc (B)	1.0% Lacto-sacc (C)	1.25% Lacto-sacc (D)
<i>Cetobacterium</i>	77.3133 ± 5.1683	71.7900 ± 7.0800	78.2700 ± 8.880	73.9833 ± 3.1083
<i>ZOR0006</i>	3.2333 ± 3.4469	6.7800 ± 4.0661	3.6700 ± 3.7326	2.2033 ± 2.0410
<i>Brevinema</i>	1.9767 ± 3.201	4.4767 ± 7.7538	0.0267 ± 0.0462	0 ± 0
<i>Uncultured</i>	7.1600 ± 9.0179	5.9567 ± 1.8700	8.4700 ± 5.5209	11.6733 ± 5.5256
<i>Aeromonas</i>	1.8967 ± 0.9577	3.4000 ± 1.0714	2.0033 ± 0.8394	1.7367 ± 0.9182
<i>Bacteroides</i>	0.9033 ± 1.2989	0.7733 ± 0.4692	0.5667 ± 0.0551	0.8500 ± 0.4349
<i>Macellibacteroides</i>	0.4667 ± 0.2103	0.7733 ± 0.3844	1.5033 ± 1.0111	1.5000 ± 1.5862
<i>Mycobacterium</i>	0.7433 ± 0.8846	0.0933 ± 0.1365	0.0467 ± 0.0808	0.8300 ± 1.0306
<i>Dechloromonas</i>	0.4000 ± 0.3345	0.4233 ± 0.5689	0.2100 ± 0.2456	0.6900 ± 0.6986
<i>Plesiomonas</i>	0.6867 ± 0.8171	0.2900 ± 0.0400	0.2367 ± 0.1234	0.1433 ± 0.1401

DISCUSSION

Growth Performance, Relative Protein Digestibility and Digestive Enzyme Activities of *T. tambroides*

Although no significant difference in growth performance was observed between treatments in this study, various other studies have reported a positive effect on growth when using higher concentrations of probiotics. For instance, Soltani *et al.* (2017) found that common carp exhibited significant growth improvement when administered 1.2×10^6 CFU of *L. plantarum*,

while Abou Zied *et al.* (2003) observed significant growth enhancement in Nile Tilapia with 0.1% Lacto-sacc, and Abass *et al.* (2018) reported improved growth performance in Nile Tilapia with 7% yeast. However, these outcomes can be affected by various factors, including species, life stage, dosage, and experimental conditions, as noted by Hosseini *et al.* (2016), who suggested assessing different probiotics for desired species.

In contrast, higher probiotic concentrations do not always result in a positive effect on growth compared to lower concentrations. For

instance, Hosseini *et al.* (2016) found that the growth performance and survival of goldfish, *Carassius auratus gibelio* were not affected by the concentration of *L. acidophilus*. A report by Nikoskelainen *et al.* (2001) also shows that administering a high dosage of *L. rhamnosus* at 10^{12} CFU does not enhance the resistance of rainbow trout to furunculosis compared to a lower dose of 10^9 CFU. Additionally, Pooramini *et al.* (2009) also discovered that feed with 5% and 10% yeast yield similar results in terms of growth for rainbow trout.

Additionally, *S. cerevisiae* can enhance nutrient digestibility and improve the overall health of the intestinal mucosa and the density of intestinal villi. At the same time, MOS stimulates the growth of beneficial bacteria, such as *Lactobacilli*, which improve food digestion and assimilation (Abass *et al.*, 2018). *L. acidophilus* has been reported to enhance growth performance, mucosal immune response, and stress resistance and modulate intestinal microbiota towards beneficial bacteria (Hoseinifar *et al.*, 2015). Furthermore, Hosseini *et al.* (2016) have found that dietary *L. acidophilus* could help in reducing the ghrelin gene, an appetite-related gene in the intestinal tract of goldfish, resulting in reduced body glucose levels and overall appetite.

The highest survival rate, 100% was demonstrated by 1.0% Lacto-sacc (C), followed by 99.33% in 0.5% Lacto-sacc (B) and 98.67% in both 1.25% Lacto-sacc (D) and 0% Lacto-sacc (A). The death fish in treatment 0.5% Lacto-sacc (B) and 1.25% Lacto-sacc (D) resulted from overfeeding larger fish. The death in the control group, 0% Lacto-sacc (A) was found to be pop eye infection and red spot symptoms that happened in week 13 in tank A2 (second replicate of control group) and week 17 in tank A3 (third replicate). Two additional fish in tank A2 exhibited similar symptoms. The introduction of probiotics in fish diets improved survival rates as reported by Abass *et al.* (2018) and Hoseinifar *et al.* (2015).

Better digestive enzyme activity was observed in fish treated with probiotics compared to the control group, indicating that probiotics could enhance fish digestion. Gram-positive bacteria such as *Lactobacillus* sp. could increase intestine enzymatic activity by secreting exogenous enzymes that are beneficial to the

digestion process (Akter *et al.*, 2019). The intake of *L. acidophilus* has been associated with the increase of lactic acid bacteria, resulting in changes in both amylase and lipase activity. Moreover, *L. acidophilus* has also been proven to effectively improve dish digestive enzyme activities (Akter *et al.*, 2019; Mohammadian *et al.*, 2019). According to Mohapatra *et al.*, (2012), most probiotics are able to trigger essential fatty acid production through the secretion of lipid digesting enzymes. Digestive enzymes such as amylase, lipase, and protease can also be produced by lactic acid bacteria (Askarian *et al.*, 2012). In a study by Darafsh *et al.* (2020), Persian sturgeon fed with *S. cerevisiae* showed higher amylase, protease, and lipase activities compared to the control group.

The introduction of probiotics also increases the population of beneficial microbes and microbial enzymes that promote feed digestibility and absorption. As a result, the growth performance of fish will be improved (Allameh *et al.*, 2017). The best results were observed in 0.5% Lacto-sacc in terms of growth, protease and lipase activity. Treatment B shows high protease activity which helps in protein digestion (Table 3). Probiotic dosage does not have noticeable effects on fish enzymes because there were no significant differences in the bacteria retained in the gut among the fish in treatments (Dawood *et al.*, 2019).

However, the treatment showed not significantly on growth performance and amylase and protease activity might be due to short duration of the probiotics feeding trial as *Tor tambroides* is slow growing fish. Also, *T. tambroides* prefer flowing and clean water environment. To maintain a good water quality for *T. tambroides*, 50% of the water in the closed tank was changed daily. However, this water change may disrupt the nutrient flow and lead to the loss of nutrient and probiotics, potentially affecting the fish's nutrient uptake and leading to no significant differences between treatments.

As seen in a study on Nile Tilapia, a higher concentration (0.1%) of Lacto-sacc yields better results than lower concentration (0.05%) Lacto-sacc (Zied *et al.*, 2003). The combination of both *L. acidophilus* and *S. cerevisiae* at a concentration of 0.25% has been shown to effectively improve the growth performance and microbial load in the gut of Koi Carp, with

brewer's yeast at a concentration of 0.5% showing the best results (Dhanaraj *et al.*, 2010). Given that a higher initial concentration was used in this experiment, the optimal concentration of Lacto-sacc may fall between 0.1% and 0.5%. Higher concentration of probiotics will not always result in better growth and improvement in physiological status, while overdosing might lead to higher costs and undesired effects (Soltani *et al.*, 2017). As Lacto-sacc becomes dominant in the gut, the gut microbiota may become imbalanced. This will induce *L. acidophilus* to produce bacteriocins while also fermenting lactose into lactic acid. These processes will reduce the pH within the gut which will then eliminate both harmful and beneficial bacteria. Therefore, a Lacto-sacc diet of more than 0.5% concentration is unnecessary for *T. tambroides* feeding since there will not be any improvements to the growth and digestive enzyme activities.

Gut Microbiota of *T. tambroides*

In Alpha diversity, treatment B has the highest Shannon Index that indicating higher diversity and more even distribution of species abundance compared to other treatment. Treatment D showed highest Chao 1 indexes value representing they had highest species richness. For Simpson index, CP1 had the lowest Simpson Index value indicating they had higher diversity, and all species were more equally abundant. Treatment B that has the highest Shannon and Simpson index but with lower Chao1 index can be interpreted as treatment has mix of both abundant and rare species with fewer estimated total species and dominance of a few species that cause uneven distribution.

Beta Diversity was shown by the Principal Coordinate Analysis (PCoA) that visualized patterns in dissimilarity. Most of the samples were close clustering, which means most of the samples were more similar to each other microbial community composition. For the distal treatment that more far apart from other samples are more dissimilar microbial communities with others.

The total relative abundance of Fusobacteria, Proteobacteria, Bacteroidetes and Firmicutes were more than 95% of the total gut microbiota of the *T. tambroides*. The most abundant phyla that had been found in the gut microbiota of *T.*

tambroides of both phases were Fusobacteria, Proteobacteria, Bacteroidetes and Firmicutes, similar with studies of Tan *et al.* (2019) and Lau *et al.* (2021b) on *T. tambroides*. However, in study of Lau *et al.* (2021b) with microbiome analysis of gut bacterial communities of healthy and diseased *T. tambroides* studies, Proteobacteria was the most abundant among them all. In contrast, in studies by Tan *et al.* (2019) on wild and captive *T. tambroides*, Fusobacteria was highest abundant (26.8%) but almost similar to an abundance of Firmicutes (25.8%) and Proteobacteria (25.2%).

Fusobacteria can be found in most abundance in the gut, and this finding agrees with some studies with different fish species (Mathai *et al.*, 2021; Zhang *et al.*, 2021). Fusobacteria, particularly *Cetobacterium* were found to be prevalent in gut of microbiota of freshwater fish and account for more than 70% of the gut microbial fish community in many fish species (Van Kessel *et al.*, 2011; Ray *et al.*, 2017; Xie *et al.*, 2022). The decrease in the abundance of Fusobacteria including *Cetobacterium* might because of *Saccharomyces cerevisiae*, *Lactobacillus acidophilus* and Fusobacteria which played a crucial role in carbohydrates fermentation. In the meantime, Ofek *et al.* (2022) study found that Proteobacteria was increased at the expense of Fusobacteria in the intestine of diseased fish. Also, study of Siddik *et al.* (2022) found out that the abundance of Proteobacteria and Firmicutes increased when fed with *Saccharomyces cerevisiae* and *Lactobacillus casei* on juvenile barramundi. Among top 10 genera, there are 3 genera belongs to Proteobacteria which were *Aeromonas*, *Dechloromonas* and *Plesiomonas*.

Firmicutes, characterized as advantageous intestinal bacteria, it recognized for positive impact on the growth performance, immunity, digestion, and disease resistance in aquatic animals (Xu *et al.*, 2021). In the study, the *ZOR0006* was a genus of phylum Firmicutes and were observed as second most abundance genus. While in Duperron *et al.* (2019), Foucault *et al.* (2022) and Gallet *et al.* (2023) studies, the two most prevalent gut associated bacteria on the medaka fish were *Cetobacterium* and *ZOR0006*. In the study conducted by Ofek *et al.* (2022), the abundance of *ZOR0006* was greater (9.0%) in intestine of healthy tilapia compared diseased tilapia, constituting only one-third of the

abundance observed in healthy fish intestine. Spirochaetes were absent in treatment D. *Brevinema* was present at top 10 genera, member of the phylum Spirochaetes and it was suggested as opportunistic pathogen. However, this bacterium was a conditional pathogen that occurrence of intestinal diseases only when found high abundance in intestine (Kong *et al.*, 2023).

It is noticeable that the more preferred concentration in growth performance which is treatment B has lower *Cetobacterium* and higher other more abundance bacteria. As shown in alpha diversity, they are more even distributed and more diverse than other treatment. In accordance with the diversity resistance hypothesis, a microbial community that exhibits greater diversity is more likely to include a species possessing antagonistic traits toward an invader or pathogen (Xiong *et al.*, 2019). Also, study of Yang *et al.* (2023) found out that diseased yellow catfish has significant lower gut microbial richness and diversity than healthy individuals.

Although the study results were not statistically different in most of the bacteria between treatment, and comparing to the control group, generally probiotics treated group were decreased in abundance of Fusobacteria and increased in Proteobacteria, Bacteroidetes, Firmicutes. The elevation of the other bacteria levels may be attributed to the decrease of the Fusobacteria abundance which might be due to nutrient competition such as carbohydrate as they have overlapping nutrient utilization ability with probiotics. The introduction of Lacto-sacc bring beneficial effect to the gut, resulting increase in these beneficial bacteria and bring more even distributed gut microbiota.

CONCLUSION

This study demonstrated that adding 0.5% Lacto-sacc to the diet of *T. tambroides* fingerlings improved growth performance and digestive enzyme activity when compared to the control (0% Lacto-sacc) and other treatment groups. However, no additional benefits were observed at concentrations greater than 0.5%. Fusobacteria, Proteobacteria, Bacteroidetes, Firmicutes were the top four phyla in the gut microbiota of *T. tambroides*, accounting for more than 95%, with Fusobacteria dominating at

around 70% of the gut microbiota. *Cetobacterium*, *ZOR0006*, *Brevinema*, and *Aeromonas* were the most common genera detected. *T. tambroides* fed a 0.5% Lacto-sacc diet had lower Fusobacteria abundance while increasing other bacteria compared to other treatments. Although there is no significant in gut microbiota, the gut microbiota of *T. tambroides* fed probiotics was likewise more consistently disturbed and diversified, indicating less species dominance. Future research should focus on the appropriate Lacto-sacc concentration to enhance cost efficiency, as well as the long-term effects of probiotics on growth.

ACKNOWLEDGEMENTS

This project was funded by the Ministry of Higher Education (MOHE), Malaysia through Fundamental Research Grant Scheme (FRGS) FRGS/1/2019/WAB01/UNIMAS/03/2.

DECLARATION OF INTERESTS

The authors have declared that there are no potential conflicts of interest. The data produced and/or analysed in this study can be obtained from the corresponding author upon request.

REFERENCES

- Abass, D.A., Obirikorang, K.A., Campion, B.B., Edziyie, R.E. & Skov, P.V. (2018). Dietary supplementation of yeast (*Saccharomyces cerevisiae*) improves growth, stress tolerance, and disease resistance in juvenile Nile tilapia (*Oreochromis niloticus*). *Aquaculture International*, 26: 843-855. DOI: 10.1007/s10499-018-0255-1
- Abou Zied, R., Abd El-Maksoud, A. & Ali, A. (2003). Effect of virginiamycin or lacto-sacc on the growth performance of Nile tilapia fish during the nursing period. *Egyptian Journal of Nutrition and Feeds*, 6: 481-489.
- Akter, M.N., Hashim, R., Sutriana, A., Siti Azizah, M.N. & Asaduzzaman, M. (2019). Effect of *Lactobacillus acidophilus* supplementation on growth performances, digestive enzyme activities and gut histomorphology of striped catfish (*Pangasianodon hypophthalmus* Sauvage, 1878) juveniles. *Aquaculture Research*, 50(3): 786-797. DOI: <https://doi.org/10.1111/are.13938>
- Allameh, S., Noaman, V. & Nahavandi, R. (2017). Effects of probiotic bacteria on fish performance.

- Advanced Techniques in Clinical Microbiology*, 1(2): 11.
- Asaduzzaman, M.D., Iehata, S., Akter, S., Kader, M.A., Ghosh, S.K., Khan, M.N.A. & Abol-Munafi, A.B. (2018a). Effects of host gut-derived probiotic bacteria on gut morphology, microbiota composition and volatile short chain fatty acids production of Malaysian Mahseer *Tor tambroides*. *Aquaculture Reports*, 9: 53-61. DOI: 10.1016/j.aqrep.2017.12.003
- Asaduzzaman, M., Sofia, E., Shakil, A., Haque, N.F., Khan, M.N.A., Ikeda, D., Kinoshita, S. & Abol-Munafi, A.B. (2018b). Host gut-derived probiotic bacteria promote hypertrophic muscle progression and upregulate growth-related gene expression of slow-growing Malaysian Mahseer *Tor tambroides*. *Aquaculture Reports*, 9: 37-45. DOI:10.1016/j.aqrep.2017.12.001
- Askarian, F., Zhou, Z., Olsen, R.E., Sperstad, S. & Ringø, E. (2012). Culturable autochthonous gut bacteria in Atlantic salmon (*Salmo salar L.*) fed diets with or without chitin. Characterization by 16S rRNA gene sequencing, ability to produce enzymes and in vitro growth inhibition of four fish pathogens. *Aquaculture*, 326: 1-8. DOI: 10.1016/j.aquaculture.2011.10.016
- Bandyopadhyay, P., Mishra, S., Sarkar, B., Swain, S.K., Pal, A., Tripathy, P.P. & Ojha, S.K. (2015). Dietary *Saccharomyces cerevisiae* boosts growth and immunity of IMC *Labeo rohita* (Ham.) juveniles. *Indian Journal of Microbiology*, 55: 81-87. DOI: 10.1007/s12088-014-0500-x
- Darafsh, F., Soltani, M., Abdolhay, H.A. & Shamsaei Mehrejan, M. (2020). Improvement of growth performance, digestive enzymes and body composition of Persian sturgeon (*Acipenser persicus*) following feeding on probiotics: *Bacillus licheniformis*, *Bacillus subtilis* and *Saccharomyces cerevisiae*. *Aquaculture Research*, 51(3): 957-964. DOI: 10.1111/are.14440
- Dawood, M.A., Magouz, F.I., Salem, M.F. & Abdel-Daim, H.A. (2019). Modulation of digestive enzyme activity, blood health, oxidative responses and growth-related gene expression in GIFT by heat-killed *Lactobacillus plantarum* (L-137). *Aquaculture*, 505: 127-136. DOI: 10.1016/j.aquaculture.2019.02.053
- Dhanaraj, M., Haniffa, M., Singh, S.A., Arockiaraj, A.J., Ramakrishnan, C.M., Seetharaman, S. & Arthimanju, R. (2010). Effect of probiotics on growth performance of koi carp (*Cyprinus carpio*). *Journal of Applied Aquaculture*, 22(3): 202-209. DOI: 10.1080/10454438.2010.
- Duperron, S., Halary, S., Habiballah, M., Gallet, A., Huet, H., Duval, C., Bernard, C. & Marie, B. (2019). Response of fish gut microbiota to toxin-containing cyanobacterial extracts: a microcosm study on the medaka (*Oryzias latipes*). *Environmental Science & Technology Letters*, 6(6): 341-347. DOI: 10.1021/acs.estlett.9b00297.s004
- Foucault, P., Gallet, A., Duval, C., Marie, B. & Duperron, S. (2022). Gut microbiota and holobiont metabolome composition of the medaka fish (*Oryzias latipes*) are affected by a short exposure to the cyanobacterium *Microcystis aeruginosa*. *Aquatic Toxicology*, 253: 106329. DOI: 10.1016/j.aquatox.2022.106329
- Gallet, A., Halary, S., Duval, C., Huet, H., Duperron, S. & Marie, B. (2023). Disruption of fish gut microbiota composition and holobiont's metabolome during a simulated *Microcystis aeruginosa* (Cyanobacteria) bloom. *Microbiome*, 11(1): 108. DOI: 10.1186/s40168-023-01558-2
- Ghosh, S., Sinha, A. & Sahu, C. (2007). Effect of probiotic on reproductive performance in female livebearing ornamental fish. *Aquaculture Research*, 38(5): 518-526. DOI: 10.1111/j.1365-2109.2007.01696.x
- Gippert, T., Virag, G. & Nagy, I. (1992). Lacto-Sacc in rabbit nutrition. *Journal of Applied Rabbit Research*, 15: 1101-1101.
- Hannan, M.A., Munir, M.B., Asdari, R., Islam, M.S., Lima, R.A., Islam, H.R., Rashid, M.H., & Hing, H.W.Y. (2024). Dietary lacto-sacc stimulates the immune response of gravid mud crab (*Scylla olivacea*). *Comparative Immunology Reports*, 7, 200156.
- Hoseinifar, S.H., Roosta, Z., Hajimoradloo, A. & Vakili, F. (2015). The effects of *Lactobacillus acidophilus* as feed supplement on skin mucosal immune parameters, intestinal microbiota, stress resistance and growth performance of black swordtail (*Xiphophorus helleri*). *Fish & Shellfish Immunology*, 42(2): 533-538. DOI: 10.1016/j.fsi.2014.12.003
- Hossain, M.K., Ishak, S.D., Ambok-Bolong, A.M., Noordin, N.M., Iehata, S. & Kader, M.A. (2022). Effect of intestinal autochthonous *Enterococcus faecalis* on the growth performance, gut morphology of Malaysian mahseer (*Tor tambroides*) and protection against *Aeromonas hydrophila*. *International Aquatic Research*, 14(1): 1-12.

- Hosseini, M., Miandare, H.K., Hoseinifar, S.H. & Yarahmadi, P. (2016). Dietary *Lactobacillus acidophilus* modulated skin mucus protein profile, immune and appetite genes expression in gold fish (*Carassius auratus gibelio*). *Fish & Shellfish Immunology*, 59: 149-154. DOI: 10.1016/j.fsi.2016.10.026
- Iehata, S., Nosi, M.Z., Danish-Daniel, M. & Sharifah, N.E. (2021). Gut microbiome associated with cultured Malaysian mahseer *Tor tambroides*. *Aquaculture, Conservation & Legislation*, 14(1): 46-58.
- Ige, B.A. (2013). Probiotics use in intensive fish farming. *African Journal of Microbiology Research*, 7(22): 2701-2711. DOI: 10.5897/AJMRx12.021
- Kong, Y., Liao, Z., Ma, X., Liang, M., Xu, H., Mai, K. & Zhang, Y. (2023). Response of intestinal microbiota of tiger puffer (*Takifugu rubripes*) to the fish oil finishing strategy. *Microorganisms*, 11(1): 208. DOI: doi.org/10.3390/microorganisms11010208
- Kottelat, M., Pinder, A. & Harrison, A. (2018). *Tor Tambroides*. Cambridge, UK: International Union for Conservation of Nature. <https://www.iucnredlist.org/species/187939/91076554>
- Lau, M.M.L., Lim, L.W.K., Ishak, S.D., Abol-Munafi, A.B. & Chung, H.H. (2021a). A review on the emerging asian aquaculture fish, the Malaysian Mahseer (*Tor tambroides*): Current status and the way forward. *Proceedings of the Zoological Society*, 74(2): 227-237. DOI: 10.1007/s12595-021-00368-4
- Lau, M.M.L., Kho, C.J.Y., Lim, L.W.K., Sia, S.C., Chung, H.H., Lihan, S. & Apun, K. (2021b). Microbiome analysis of gut bacterial communities of healthy and diseased Malaysian mahseer (*Tor tambroides*). *bioRxiv*, 2021-12. DOI: 10.1101/2021.12.08.471852
- Mahajan, P., Sahoo, J. & Panda, P. (2000). Effect of probiotic (Lacto-Sacc) feeding and seasons on the different quality characteristics of poultry meat. *Indian Journal of Poultry Science*, 35(3): 297-301.
- Mathai, P.P., Byappanahalli, M.N., Johnson, N.S. & Sadowsky, M.J. (2021). Gut microbiota associated with different sea lamprey (*Petromyzon marinus*) life stages. *Frontiers in Microbiology*, 12: 706683. DOI: 10.3389/fmicb.2021.706683
- Mohammadian, T., Nasirpour, M., Tabandeh, M.R., Heidary, A.A., Ghanei-Motlagh, R. & Hosseini, S.S. (2019). Administrations of autochthonous probiotics altered juvenile rainbow trout *Oncorhynchus mykiss* health status, growth performance and resistance to *Lactococcus garvieae*, an experimental infection. *Fish & Shellfish Immunology*, 86: 269-279. DOI: 10.1016/j.fsi.2018.11.052
- Mohapatra, S., Chakraborty, T., Prusty, A., Das, P., Paniprasad, K. & Mohanta, K. (2012). Use of different microbial probiotics in the diet of rohu, *Labeo rohita* fingerlings: effects on growth, nutrient digestibility and retention, digestive enzyme activities and intestinal microflora. *Aquaculture Nutrition*, 18(1): 1-11. DOI: 10.1111/j.1365-2095.2011.00866.x
- Munir, M.B., Hashim, R., Chai, Y.H., Marsh, T.L. & Nor, S.A.M. (2016). Dietary prebiotics and probiotics influence growth performance, nutrient digestibility and the expression of immune regulatory genes in snakehead (*Channa striata*) fingerlings. *Aquaculture*, 460: 59-68. DOI: 10.1016/j.aquaculture.2016.03.041
- Nikoskelainen, S., Ouwehand, A., Salminen, S. & Bylund, G. (2001). Protection of rainbow trout (*Oncorhynchus mykiss*) from furunculosis by *Lactobacillus rhamnosus*. *Aquaculture*, 198 (3-4): 229-236. DOI: 10.1016/S0044-8486(01)00593-2
- Ofek, T., Lalzar, M., Izhaki, I. & Halpern, M. (2022). Intestine and spleen microbiota composition in healthy and diseased tilapia. *Animal Microbiome*, 4(1): 50. DOI: 10.1186/s42523-022-00201-z
- Pooramini, M., Kamali, A., Hajimoradloo, A., Alizadeh, M. & Ghorbani, R. (2009). Effect of using yeast (*Saccharomyces cerevisiae*) as probiotic on growth parameters, survival and carcass quality in rainbow trout *Oncorhynchus mykiss* fry. *International Aquatic Research*, 1(1): 39.
- Ray, C., Bujan, N., Tarnecki, A., Davis, A.D., Browdy, C. & Arias, C.R. (2017). Analysis of the gut microbiome of Nile tilapia *Oreochromis niloticus* L. fed diets supplemented with Previda® and Saponin. *Journal of Fisheries Sciences.com*, 11(2): 36-45. DOI: 10.21767/1307-234x.1000116
- Redhwan, A.I., Rao, S.N., Mohamad-Zuki, N.A., Kari, A., Kamarudin, A.S., Ismail, N., Nguang, S.I., Ha, H.C., Yong, W.S., Yong, F.H. & Komilus, C.F. (2022). Mahsheers in Malaysia: A Review of Feed for Cultured *Tor tambroides* and *Tor tambra*. *Bioscience Research*, 19(1): 349-359.
- Risjani, Y., Mutmainnah, N., Manurung, P. & Wulan, S.N. (2021). Exopolysaccharide from

- Porphyridium cruentum* (purpureum) is not toxic and stimulates immune response against vibriosis: The assessment using zebrafish and white shrimp *Litopenaeus vannamei*. *Marine drugs*, 19 (3): 133. DOI: 10.3390/md19030133
- Siddik, M.A., Foysal, M.J., Fotedar, R., Francis, D.S. & Gupta, S.K. (2022). Probiotic yeast *Saccharomyces cerevisiae* coupled with *Lactobacillus casei* modulates physiological performance and promotes gut microbiota in juvenile barramundi, *Lates calcarifer*. *Aquaculture*, 546: 737346. DOI: 10.1016/j.aquaculture.2021.737346
- Soltani, M., Abdy, E., Alishahi, M., Mirghaed, A.T. & Hosseini-Shekarabi, P. (2017). Growth performance, immune-physiological variables and disease resistance of common carp (*Cyprinus carpio*) orally subjected to different concentrations of *Lactobacillus plantarum*. *Aquaculture International*, 25: 1913-1933. DOI: 10.1007/s10499-017-0164-8
- Sotirov, L., Denev, S., Tsachev, I., Lalev, M., Oblakova, M. & Porfirova, Z. (2001). Effect of different growth promoters on lysozyme and complement activity. II. Studing in turkeys. *Revue de medecine veterinaire*, 152(1): 67-70.
- Tachibana, L., Telli, G.S., Dias, D.D.C., Goncalves, G.S., Guimaraes, M.C., Ishikawa, C.M., Cavalcante, R.B., Natori, M.M., Fernandez Alarcon, M.F. & Tapia-Paniagua, S. (2021). *Bacillus subtilis* and *Bacillus licheniformis* in diets for Nile tilapia (*Oreochromis niloticus*): Effects on growth performance, gut microbiota modulation and innate immunology. *Aquaculture Research*, 52(4): 1630-1642. DOI: 10.1111/are.15016
- Tan, C.K., Natrah, I., Suyub, I.B., Edward, M.J., Kaman, N. & Samsudin, A.A. (2019). Comparative study of gut microbiota in wild and captive Malaysian Mahseer (*Tor tambroides*). *Microbiology Open*, 8(5): e00734. DOI: 10.1002/mbo3.734
- Vallejos-Vidal, E., Reyes-López, F., Teles, M. & MacKenzie, S. (2016). The response of fish to immunostimulant diets. *Fish & Shellfish Immunology*, 56: 34-69. DOI: 10.1016/j.fsi.2016.06.028
- Van Kessel, M.A., Dutilh, B.E., Neveling, K., Kwint, M.P., Veltman, J.A., Flik, G., Jetten, M. S., Klaren, P.H. & Op den Camp, H.J. (2011). Pyrosequencing of 16S rRNA gene amplicons to study the microbiota in the gastrointestinal tract of carp (*Cyprinus carpio* L.). *AMB Express*, 1(1): 1-9. DOI: 10.1186/2191-0855-1-41
- Wan Alias, F.S.L., Munir, M.B., Asdari, R., Hannan, A. & Hasan, J. (2023). Dietary lacto-sacc improved growth performance, food acceptability, body indices, and basic hematological parameters in empurau (*Tor tambroides*) fries reared in the aquaponics system. *Journal of Applied Aquaculture*, 35(4): 1131-1153. DOI: 10.1080/10454438.2022.2095239
- Xie, M., Xie, Y., Li, Y., Zhou, W., Zhang, Z., Yang, Y., Olsen, R.E., Ringo, E., Ran, C. & Zhou, Z. (2022). Stabilized fermentation product of *Cetobacterium somerae* improves gut and liver health and antiviral immunity of zebrafish. *Fish & Shellfish Immunology*, 120: 56-66. DOI: 10.1016/j.fsi.2021.11.017
- Xiong, J.B., Nie, L. & Chen, J. (2019). Current understanding on the roles of gut microbiota in fish disease and immunity. *Zoological Research*, 40(2): 70-76.
- Xu, Y., Li, Y., Xue, M., Yang, T., Luo, X., Fan, Y., Meng, Y., Liu, W., Lin, G., Li, B., Zeng, L. & Zhou, Y. (2021). Effects of dietary *Saccharomyces cerevisiae* YFI-SC2 on the growth performance, intestinal morphology, immune parameters, intestinal microbiota, and disease resistance of Crayfish (*Procambarus clarkia*). *Animals*, 11(7): 1963. DOI: 10.3390/ani11071963
- Yang, J., Lin, Y., Wei, Z., Wu, Z., Zhang, Q., Hao, J., W.S. & Li, A. (2023). *Edwardsiella ictaluri* almost completely occupies the gut microbiota of fish suffering from Enteric septicemia of catfish (Esc). *Fishes*, 8(1): 30. DOI: 10.3390/fishes8010030
- Zhang, Y., Wen, B., Meng, L.J., Gao, J.Z. & Chen, Z.Z. (2021). Dynamic changes of gut microbiota of discus fish (*Symphysodon haraldi*) at different feeding stages. *Aquaculture*, 531: 735912. DOI: 10.1016/j.aquaculture.2020.735912
- Zomorni, M.S., Hai, C.T., Redhwan, A.I. & Komilus, C.F. (2022). Efficacy of black soldier fly (*Hermetia illucens*) larvae meal as feed on growth performance for juvenile Javan Mahseer (*Tor tambra*). *Journal of Agrobiotechnology*, 13(1): 118-130. DOI: 10.37231/jab.2022.13.1s.321

Morphology and Molecular Characterisation of *Karenia mikimotoi* (Dinophyceae) from Sabah Malaysian Borneo, with a Focus on the Second Internal Transcribed Spacer (ITS2) of Ribosomal RNA gene

SHERYL UNCHA ANDREW CHIBA¹, SING TUNG TENG*¹, SAMSUR MOHAMAD¹,
NURSYAHIDA ABDULLAH¹, ING KUO LAW¹, PO TEEN LIM² & CHUI PIN LEAW²

¹Faculty of Resource Science and Technology, Universiti Malaysia Sarawak, Kota Samarahan, 94300 Sarawak, Malaysia; ²Bachok Marine Research Station, Institute of Ocean and Earth Sciences, University of Malaya, 16310 Bachok, Kelantan, Malaysia

* Corresponding author: tsteng@unimas.my

Received: 17 July 2024

Accepted: 8 November 2024

Published: 31 December 2024

ABSTRACT

The first recorded bloom of *Karenia mikimotoi* (initially *Gymnodinium mikimotoi*) occurred off the coast of Japan in 1934, causing mass mortality of shellfish and fish. This event highlighted the devastating impact of *K. mikimotoi* blooms and marked a turning point in harmful algal bloom (HAB) research, driving studies on its identification, biology, toxicology, and effects on marine life and ecosystems. The past reported bloom events in Southeast Asia have raised public concerns, leading to further investigation into the occurrence and geographical distribution of *K. mikimotoi* in the region. As of yet, there is no recorded evidence of *K. mikimotoi* blooms in Malaysian waters. This prompts the investigation of the occurrence and distribution of *K. mikimotoi* in Malaysia, and this study represents the first record of *K. mikimotoi* in Malaysian waters. In this study, clonal cultures of *K. mikimotoi* isolated from Sepanggar Bay, Sabah were examined using light microscopy (LM) and scanning electron microscopy (SEM) to observe its morphological features. Cells of *K. mikimotoi* from Malaysian Borneo exhibited a typical dorso-ventrally flattened body with bi-lobed and linear apical grooves on the cell apex. Molecular characterisation of the strains based on the internal transcribed spacer (ITS) region and large-subunit (LSU) ribosomal DNA revealed close phylogenetic relationships with other strains of *K. mikimotoi* from other regions, forming a monophyletic clade that positioned as sister to *K. brevis*, supporting the species identity of *K. mikimotoi*. The secondary structure of the ITS2 RNA transcript revealed a universal structure with four major helices. Structural comparison between *K. mikimotoi* and its relatives revealed four to six hemi-compensatory base changes. The results demonstrated the efficacy of ITS2 secondary structure information in delimiting species in *Karenia*. The detailed morphology and molecular characteristics of *K. mikimotoi* were revealed, for the first time, from the coastal waters of Malaysian Borneo.

Keywords: Kareniaceae, Malaysia, phylogeny, ribosomal RNA gene, rRNA transcript

Copyright: This is an open access article distributed under the terms of the CC-BY-NC-SA (Creative Commons Attribution-NonCommercial-ShareAlike 4.0 International License) which permits unrestricted use, distribution, and reproduction in any medium, for non-commercial purposes, provided the original work of the author(s) is properly cited.

INTRODUCTION

The genus *Karenia* G. Hansen & Moestrup, 2000 (order: Gymnodiniales; family: Kareniaceae) is a group of athecate dinoflagellates that contribute to the harmful algal bloom (HAB) phenomena (Cen *et al.*, 2020). Some species of *Karenia* have been reported to cause mass fatalities of marine animals and massive fish mortality, leading to significant economic losses in marine and coastal aquaculture (Davis, 1948; Gunter *et al.*, 1948; Flewelling *et al.*, 2005; Li *et al.*, 2019). The genus *Karenia* also poses threats to public health through neurotoxic shellfish poisoning (NSP) and respiratory illnesses

(Watkins *et al.*, 2008; Heil & Steidinger, 2009; Hoagland *et al.*, 2009).

The lack of comprehensive taxonomical study for *Karenia* species has become critically important since the discovery of red tides that killed marine life. Recently, a new *Karenia* species called *K. hui* had been described from China (Cen *et al.*, 2024). Over three decades, the taxonomical classification of the genus *Karenia* has progressed significantly, and as of now, the genus *Karenia* consists of eleven recognised species namely *Karenia asterichroma*, *K. bicuneiformis* (synonym: *K. bidigitata*), *K. brevis*, *K. brevisulcata*, *K. concordia*, *K. cristata*, *K. hui*, *K. longicanalis* (synonym: *K.*

umbella), *K. mikimotoi*, *K. papilionacea*, and *K. selliformis* (Guiry and Guiry, 2023; Cen *et al.*, 2024).

Naked dinoflagellates of genus *Karenia* were previously classified under genus *Gymnodinium* before genus *Karenia* was established (Bergholtz *et al.*, 2006; Caruana & Amzil, 2018). The historical taxonomic of *K. mikimotoi* became a state of turmoil, particularly after the strain isolated from European waters was identified as *Gyrodinium* cf. *aureolum* (Hulburt, 1957; Gentien, 1998). Strains discovered from different areas of Japan were named as *Gymnodinium* sp., *G. sp. 1* and *G. type-'65* but were later re-assessed and re-described as *K. mikimotoi* (Fukuyo *et al.*, 2002). In 1984, additional strains from Japan were named *Gymnodinium nagasakiense* owing to the dissimilar morphology traits as *G. mikimotoi* under light microscopy (Takayama & Adachi, 1984), and *Gyrodinium nagasakiense*, based on singular displacement with European *G. cf. aureolum* (Tangen, 1977; Takayama & Adachi, 1984; Partensky *et al.*, 1988). Molecular studies later confirmed that *Gymnodinium nagasakiense* and *Gyrodinium nagasakiense* were actually identical to *Gymnodinium mikimotoi* (Hansen *et al.*, 2000). Comprehensive morphological, molecular, and pigment analyses on the European *G. cf. aureolum* and *G. mikimotoi* were performed and had reached a consensus that European *G. cf. aureolum* was conspecific with *G. mikimotoi* (Hansen *et al.*, 2000; Tang *et al.*, 2008). A re-evaluation by Daugbjerg *et al.* (2000) highlighted the presence of a straight apical groove as a unique feature of all *Karenia* species which was morphologically distinct than that of *Gymnodinium* sensu stricto, thus, separating *Karenia* species from genus *Gymnodinium*. Consequently, *Gymnodinium mikimotoi* was reclassified as *Karenia mikimotoi* (Daugbjerg *et al.*, 2000).

K. mikimotoi (formerly known as *Gymnodinium mikimotoi*) was described from Gokasho Bay, Japan (Oda, 1935). The name “mikimotoi” was given to this species in reference to Mikimoto Kōkichi, the “Pearl King” who was known inside and outside the Japanese empire for pearl cultivation in Gokasho Bay (Eunson, 1955; Ericson, 2016). Over the course of more than 80 years, this HAB-forming dinoflagellate species has caused mass mortalities in marine life worldwide, mainly in

the coastal waters of Europe and Asia (Li *et al.*, 2019).

In the Asian region, blooms of *K. mikimotoi* have been reported since the 1930s. Several areas in Japan have documented the blooms of this species (Oda, 1935; Takayama & Adachi, 1984; Yanagi *et al.*, 1995; Matsuyama *et al.*, 1999; Siswanto *et al.*, 2013; Li *et al.*, 2019). In Gokasho Bay, Honshu, Japan, the *K. mikimotoi* blooms in 1934 caused mortalities of fish and shellfish (Oda, 1935). In Omura Bay, Nagasaki, a *K. mikimotoi* bloom was associated with fish and shellfish deaths in 1965 (Takayama & Adachi, 1984). In Suo-Nada and Iyo-Nada, Japan, a *K. mikimotoi* bloom in 1985 caused significant damage to the fisheries, with financial losses exceeding 10 million USD (Yanagi *et al.*, 1995). From 1981 to 1985, *K. mikimotoi* was reported in Korean coastal waters (Park *et al.*, 2013). In 1989, a bloom of *K. mikimotoi* associated with a fish kill event occurred in Indian waters (D'Silva *et al.*, 2012). In the Bolinao-Anda area, Pangasinan province in the Philippines, high biomass of *K. mikimotoi* was occasionally reported, but no fish kills were observed (Yñiguez *et al.*, 2021). In 1998, *K. mikimotoi* blooms was reported in Hong Kong waters (Lu & Hodgkiss, 2004), this red tide caused significant losses to about two-thirds (estimated 1000 out of 1500) of mariculture farms, with an estimated financial loss of 315 million HKD (40 million USD). Following the first bloom in the coastal waters of China, the bloom areas of *K. mikimotoi* were observed to spread from Guangdong province to Tianjin city, and the provinces of Zhejiang, Fujian, Hebei, and Jiangsu (Baohong *et al.*, 2021). Blooms of *K. mikimotoi* in China have become frequent in the East China Sea, including the Changjiang River estuary and the coastal areas of Zhejiang and Fujian Provinces, almost every year since 2002 (Li *et al.*, 2017). In 2011 and 2014, *K. mikimotoi* caused patches of water discoloration along the east Johor Strait, Singapore (Leong *et al.*, 2015).

Within the Southeast Asian region, Vietnam, Singapore, and Philippines are the countries that have reported the occurrences of *K. mikimotoi* (Larsen & Nguyen, 2004; Leong *et al.*, 2015; Azanza and Benico, 2017; Yñiguez *et al.*, 2021). The presence of the species was first reported in Vietnamese coastal waters in a sampling survey in 1999. As reported by Leong *et al.* (2015), a

high biomass of *K. mikimotoi* (>200 cells mL^{-1}) was observed along east Johor Strait in 2011. Following the first occurrence of *K. mikimotoi* in Singapore waters, bloom patches of this dinoflagellate were subsequently detected in Punggol Marina and Changi Sailing Club (Leong *et al.*, 2015). The observation in Changi Sailing Club recorded the cell densities of $>5,000$ cells mL^{-1} (Leong *et al.*, 2015). The most recent bloom of *K. mikimotoi* in east Johor Strait, Singapore was observed in 2016, with the highest cell density exceeding 8,000 cells mL^{-1} (Kok & Leong, 2019). In Bolinao-Anda, Philippines, a very high abundance of *K. mikimotoi* were reported but no fish kill observed (Azanza & Benico, 2017). The increasing frequency and intensity of *K. mikimotoi* blooms in Southeast Asia is a continuous concern due to the adverse ecological impacts associated with this harmful dinoflagellate (Yñiguez *et al.*, 2021).

Although there have been widespread occurrences of mass mortalities of aquatic animals globally, notably in Southeast Asia, there is no documented evidence of *K. mikimotoi* blooms in Malaysian waters. While *K. mikimotoi* blooms have not been reported in Malaysia, harmful algal bloom (HAB) monitoring on *K. mikimotoi* is crucial because this species has the potential to form harmful blooms that can lead to mass fish deaths and pose a serious threat to both marine life and aquaculture. Therefore, it is essential to collect scientific information to shed light on the presence of this harmful athecate dinoflagellate in Malaysia, particularly in the coastal waters of Borneo, as part of HAB monitoring. This study, thus, aims to document the occurrence of *K. mikimotoi* in Borneo, by

opportunistic sampling in Sepanggar Bay, Sabah, Malaysian Borneo, followed by single cells isolation and culture establishment of the Kareniaceae-like cells. The clonal cultures were subsequently characterized by means of advanced morphological and molecular approaches. The species was identified based on the morphological traits examined through light and scanning electron microscopy, and further supported by molecular phylogenetic analysis of large subunit (LSU) and internal transcribed spacer (ITS) of the ribosomal RNA gene. The secondary structure of ITS2 transcript was modelled for *Karenia* species to infer the phylogenetic relationships. This study reports, for the first time, the detailed morphology and molecular characteristics of *K. mikimotoi* in Borneo's coastal waters.

MATERIALS & METHODS

Sampling Site and Algal Cultivation

Seawater samples were collected at Sepanggar Bay, Sabah ($6^{\circ}5'27.9''\text{N}$ $116^{\circ}7'38.4''\text{E}$) (Figure 1) using a 20- μm mesh-size plankton net and brought back to the laboratory for incubation. Single cell isolation (Hoshaw, 1973) from the seawater sample was carried out under light microscope Olympus BX51 (Olympus, Tokyo, Japan). The cells were grown in General-Purpose Medium (GPM) (Loeblich, 1975) and were kept in a temperature-controlled growth chamber at 25°C and light intensity of $100 \mu\text{mol m}^{-2} \text{s}^{-1}$ under a 12:12 h light:dark regime (Kon *et al.*, 2017). The culture established was deposited in the UNIMAS Harmful Algae Culture Collection with strain name KMSPBUD5.

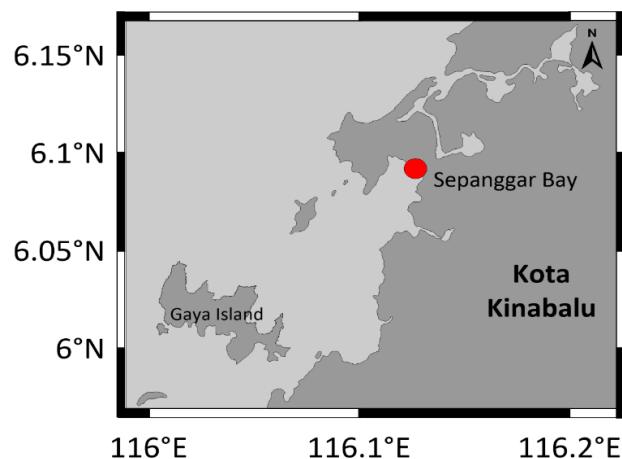


Figure 1. Map of Sabah, Malaysian Borneo showing the sampling site in this study

Light and Scanning Electron Microscopy

Live cells were examined under an Olympus BX51 light and fluorescence microscope (Olympus, Tokyo, Japan) to record the morphometric measurements, and positions of chloroplast and nucleus. Cells were stained with 0.1% SYBR Safe DNA stain (Invitrogen, MA, USA) to observe the nucleus under a fluorescence microscope using 450–490 nm excitation and 510–550 nm emission. For scanning electron microscopic observation, cells were fixed with 1% acidic Lugol's and 1% glutaraldehyde overnight (Nézan *et al.*, 2014) and dehydrated in a graded ethanol series of 10%, 30%, 50%, 75%, 90%, 95%, and absolute ethanol. Samples were critical-point dried using the K850 Critical Point Dryer (Quorum, Laughton, United Kingdom), sputter-coated with gold palladium, and observed under a JEOL JSM-6510 Analytical Scanning Electron Microscope (JEOL, Tokyo, Japan).

DNA Extraction, Gene Amplification, Purification and Sequencing

Exponential-phased cells were harvested for genomic DNA extraction following the protocol of the DNeasy^R Plant Mini Kit (Qiagen, Hilden, Germany). The large subunit (LSU) of ribosomal RNA gene (rDNA) was amplified using the primer pair, D1R (5'-ACC CGC TGA ATT TAA GCA TA-3') and D3Ca (5'-ACG AAC GAT TTG CAC GTC AG-3') (Scholin *et al.*, 1994). The internal transcribed spacer (ITS) region was amplified using a primer pair designed *in silico* in this study, *viz.* SDINOITSF (5'-TCG TAA CAA GGT TTC CGT AGG TG-3') and Smalldino ITS2R (5'-GGT ACT TGT TTG CTA TCG GTC TCG-3').

For gene amplification using Polymerase Chain Reaction (PCR), 1× PCR buffer (Promega, Madison, WI, USA), 1.5 mM MgCl₂, 0.2 mM dNTPs (Qiagen, Hilden, Germany), 0.5 μM each primer, 2.5 U *Taq* DNA polymerase (Promega), and 10–100 ng μL⁻¹ DNA were mixed in a 25 μL PCR cocktail. Gene amplification was performed in a Mastercycler[®] nexus GX2 thermocycler (Eppendorf, Hamburg, Germany). Gel electrophoresis was run at 75V for 25 min and illustrated in an E-Box gel documentation imaging (Vilber, Marne-la-

Vallée, France). The amplicons were purified using the Promega Wizard[®] PCR Preps DNA Purification System (Madison, Wisconsin, United States) and Sanger sequencing were undertaken by Apical Scientific Sdn. Bhd. (Selangor, Malaysia).

Phylogenetic Analysis

Maximum Parsimony (MP), Maximum Likelihood (ML), and Bayesian Inference (BI) were used to infer the phylogenetic relationships between *K. mikimotoi* and its close relatives. PAUP* ver. 4.0b.10 (Swofford, 2003) was used for MP and ML runs. For the MP run, heuristic searches of 1,000 random-addition replications and branch-swapping with tree-bisection reconnection (TBR) were performed. Bootstrap analysis was performed with 1,000 bootstrap replications and 100 random sequence additions per bootstrap replicate. Heuristic searches and branch-swapping with 100 random addition replications in TBR were used for ML analysis. MrBayes 3 (Ronquist and Huelsenbeck, 2003) was used to run BI. The Akaike information criterion from jModelTest 2.1.10 (Darriba *et al.*, 2012) was used to determine the best-fit model of ML and BI. FigTree v1.4.3 (Rambaut, 2007) was used to visualise the phylogenetic trees.

ITS2 Secondary Structure Modelling

ITS2 secondary structure of *Karenia* species was modelled from the ITS sequences based on the 5.8S–28S interaction identified at the proximal stem of the structure. The ITS2 secondary structure of *Karenia* species was predicted using the free energy minimization in RNAstructure v6.4 (Ali *et al.*, 2023). The ITS2 RNA transcripts were modelled by homology modelling workflow (Wolf *et al.*, 2005), using the ITS2 Database (Koetschan *et al.*, 2012; Merget *et al.*, 2012). The ITS2 secondary structure was illustrated in VARNA (Darty *et al.*, 2009). The multiple sequence-structure alignment of *Karenia* ITS2 was generated in an ITS sequence structure-specific scoring matrix (Seibel *et al.*, 2006) in 4SALE v1.7 (Seibel *et al.*, 2006, 2008). The compensatory base change (CBC) and hemi-compensatory base change (hCBC) were identified in 4SALE (Wolf *et al.*, 2005; Seibel *et al.*, 2006, 2008).

RESULTS

Morphological Characterisation of *K. mikimotoi*

The morphotype of *K. mikimotoi* was observed and identified in this study using single culture strain.

K. mikimotoi (Miyake & Kominami ex Oda) G. Hansen & Moestrup

Morphology: Cells are broadly ovoid, 22.1–27.4 μm long ($25 \pm 1.6 \mu\text{m}$; $n = 30$) and 17.2–23.9 μm

wide ($21 \pm 2.3 \mu\text{m}$, $n = 30$). Cells are dorso-ventrally flattened, the epicone is conical and slightly smaller than the hemispherical hypocone, hypocone is with two lobes (Figure 2(a)–2(c)). The ellipsoidal nucleus is situated at the left side of the hypocone near the edge of cell, slightly extended into the epicone (Figure 2(d)–2(e)). The straight and wide apical groove is situated slightly above the sulcal intrusion extending to the dorsal of epicone, creating a slight indentation at the cell apex (Figure 2(a)–2(c), 2(f)–2(h)).

Locality: Sepanggar Bay ($6^{\circ}5'27.9''$ N $116^{\circ}7'38.4''$ E), Sabah, Borneo, Malaysia

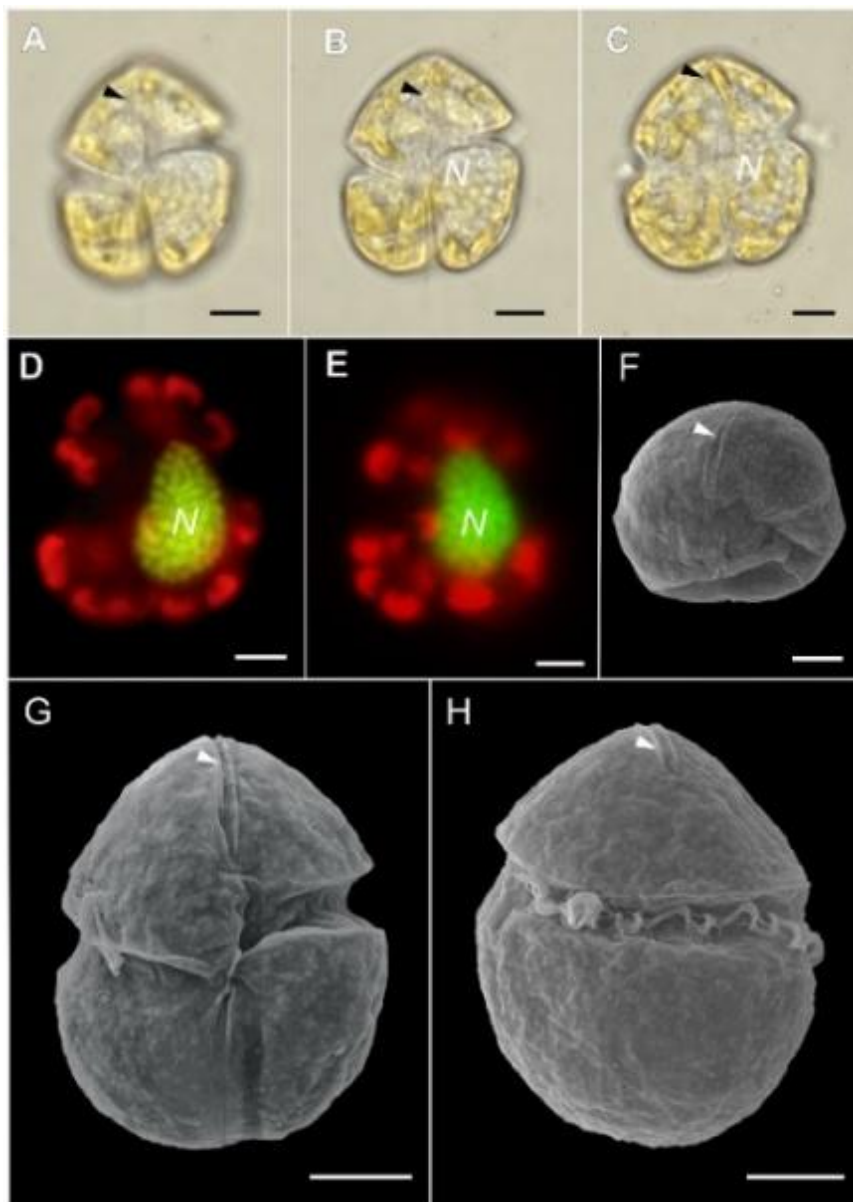


Figure 2. *Karenia mikimotoi*. (a-e) LM. Live cells showing apical groove (arrowhead) and nucleus (N). (d-e) SYBR Safe-stained cells with an ellipsoid nucleus (N) located on the left side of the hypocone nearing the edge of the cell. (f-h) SEM. Straight apical groove (arrowhead) in apical (f), ventral (g), and (h) dorsal views. Scales, 5 μm

Molecular Characterisation of *K. mikimotoi*

The LSU and ITS sequences of *K. mikimotoi* obtained in this study were deposited in the NCBI GenBank (LSU: PP993796 and ITS: PP993794). The D1–D3 region of the LSU and ITS rDNAs of *K. mikimotoi* were used to reconstruct the phylogenetic inferences of *Karenia* species. Similar tree topologies using MP, ML, and BI, were yielded from both phylogenetic trees, with the ML tree topologies showing the inferences (LSU, Figure 3; ITS, Figure 4). In the phylogenetic trees of this study, the *K. mikimotoi* from Sabah was notably positioned within a clade that included *K. mikimotoi* strains from previous studies. Both phylogenetic analyses revealed that *K. mikimotoi* formed a sister clade to *K. brevis* (ML bootstrap values/BI posterior probabilities, 100/100% in LSU tree, Figure 3; 94/99% in ITS tree, Figure 4). Grouping of *K. mikimotoi*, *K. brevis*, and *K. selliformis* was consistent in both LSU and ITS phylogenetic trees (Figure 3; Figure 4). The LSU tree (Figure 3) inferred monophyletic groups of (*K. selliformis*, *K. brevisulcata*, and *K. cristata*) (100/100%, Figure 3), and (*K. papilionacea*, *K. bidigitata* and *K. asterichroma*) (100/82%, Figure 3). In ITS tree (Figure 4), *K. selliformis*, *K. longicanalis* (synonym: *K. umbella*) and *K. aureolum* had formed a monophyletic clade (100/100%, Figure 4), which was paraphyletic to *K. papilionaceae* (100/100%; Figure 4). The molecular phylogenetic trees of this study also revealed the monophyletic clade of *Asterodinium gracile* and *K. papilionacea* (100/82%, Figure 3; 100/100%, Figure 4), and the position of *Brachidinium capitatum* within the clade of *Karenia*.

ITS2 Secondary Structure of *Karenia*

ITS2 secondary structure of five *Karenia* species *viz.* *K. mikimotoi*, *K. brevis*, *K. selliformis*, *K. longicanalis* and *K. papilionaceae* were modelled. The ITS2 RNA transcripts of *Karenia* Clade I comprised of *K. mikimotoi*, *K. brevis* and *K. selliformis* (Figure 5), and *Karenia* Clade II consisted of *K. longicanalis* and *K. papilionaceae* (Figure 6). Comparison of the compensatory base changes (CBCs) and hemi-compensatory base changes (hCBCs) of *K. mikimotoi* to the closely related species were mapped on the transcripts. The pairwise

structural comparison between *K. mikimotoi* and *K. brevis* (Figure 5) showed four hCBCs (in Helix I, G-U↔G-C; Helix II, A-C↔A-U, G-G↔G-U; Helix III, G-C↔G-U), and no CBC was detected. When comparing *K. mikimotoi* with *K. selliformis* (Figure 5), six hCBCs were revealed (in Helix I, G-U↔G-C, U-A↔U-C; Helix II, C-G↔G-G, A-C↔A-U; Helix III, G-C↔G-U, G-C↔A-C), no CBC was detected. When *K. brevis* was compared to *K. selliformis* (Figure 5), four hCBCs (in Helix I, U-A↔U-C; Helix II, C-G↔G-G, G-U↔G-C; Helix III, G-C↔A-C) and no CBC showed. Pairwise structural comparison of *K. longicanalis* and *K. papilionacea* (Figure 6) revealed three CBCs (in Helix IV, G-C↔U-G, A-U↔U-A, G-C↔A-U). The comparison of ITS2 RNA transcript of *K. longicanalis* and *K. papilionacea* (Figure 6) also showed ten hCBCs (in Helix I, U-G↔C-G, C-G↔U-G, U-G↔U-A; Helix II, C-G↔U-G; Helix III, U-G↔C-G, G-C↔G-U, G-C↔G-U, U-G↔C-G, G-U↔A-U, G-U↔A-U).

DISCUSSION

Morphology and Molecular Characterisation of *K. mikimotoi*

Cells of *K. mikimotoi* from Borneo coastal waters was within the similar size range as reported in previous studies of *K. mikimotoi* from distinct geographical region (Table 1). *K. mikimotoi* of Sabah was 22 to 27 µm long and 17 to 24 µm wide, and the cell sizes was within the range of previously reported *K. mikimotoi* which had cell sizes ranges between 20 and 38 µm long, 16 and 30 µm wide (Oda, 1935; Hansen *et al.*, 2000; Haywood *et al.*, 2004; Iwataki *et al.*, 2022). Species of *Karenia* are morphologically variable but share common traits such as a dorso-ventrally flattened body, an elliptical or pentagonal cell shape, a straight apical groove, and sometimes an apical carina (Oda, 1935; Botes *et al.*, 2003; de Salas *et al.*, 2004; Haywood *et al.*, 2004; Escobar-Morales & Hernández-Becerril, 2015; Hansen *et al.*, 2000; Iwataki *et al.*, 2022), and typically described having conical epicone and hemispherical hypocone (Oda, 1935; Haywood *et al.*, 2004; Hansen *et al.*, 2000; Iwataki *et al.*, 2022). with key features including a straight apical groove on the epicone and no ventral pore (Daugbjerg *et al.*, 2000).

Table 1. Morphological comparison of *Karenia mikimotoi* observed in this study and previous studies (n.d. = no data)

Reference(s)	In this study	Iwataki <i>et al.</i> (2022)	Hansen <i>et al.</i> (2000)	Oda (1935); Haywood <i>et al.</i> (2004)
Cell length (μm)	22.1–27.4 (25.0 \pm 1.6)	24.6–35.1 (31.2 \pm 3.0)	23.9–37.7 (32.8 \pm 3.4)	20.0–30.0 (24.8 \pm 0.4)
Cell width (μm)	17.2–23.9 (21.0 \pm 2.3)	21.9–30.9 (26.8 \pm 2.4)	21.6–36.4 (30.6 \pm 3.8)	16.0–30.0 (20.9 \pm 0.3)
Cell shape	Broadly ovoid and dorso-ventrally flattened, with conical epicone and two-lobed hemispherical hypocone	Conical epicone, hemispherical hypocone, dorsoventrally flattened	Conical or hemispherical epicone, hemispherical hypocone	Broadly ovoid and flattened dorsal abdomen, with wide conical epicone and two-lobed flakes hypocone
Nucleus	Ellipsoid, located on the left side of hypocone nearing the edge of cell	Round in the left hypocone, or ellipsoid in the left of the cell	Elongated, reniform or pyriform, situated in the left part of the cell	Ellipsoid, located on the left side of hypocone nearing the edge of cell
Sulcal intrusion	Present	Present, anterior was shallow and distal end was open	Present, narrow but widened slightly towards the antapex to slightly above epicone	Present at epicone
Ventral pore	Absent	n.d.	n.d.	n.d.
Apical groove	Straight, wide, slightly above sulcal intrusion extending to dorsal epicone	Straight	Delicate, narrow, situated to the left of sulcal axis extending from slightly above sulcal extension on the ventral side of cell way down the dorsal side of epicone	Straight, slightly above right side of the starting point of the sulcal intrusion extending to the dorsal epicone

Previous studies on *K. mikimotoi* (Oda, 1935; Haywood *et al.*, 2004; Hansen *et al.*, 2000; Iwataki *et al.*, 2022) documented a visible apical groove, linear and narrow in shape that extended slightly above the sulcus intrusion to the dorsal side of the epicone. This is similar to the apical groove of *K. mikimotoi* observed in this study. Previous studies did not record the presence of a ventral pore (Oda, 1935; Hansen *et al.*, 2000; Haywood *et al.*, 2004; Iwataki *et al.*, 2022), which was confirmed to be absent in *K. mikimotoi* as recorded in this study. The position of nucleus was one of the distinguishing characteristics for identifying *K. mikimotoi* (Tangen & Bjornland, 1981; Haywood *et al.*,

2004; Wolny *et al.*, 2024). A few studies had documented that the nucleus in *K. mikimotoi* was located at the left side of the cell (Hansen *et al.*, 2000; Iwataki *et al.*, 2022; Wolny *et al.*, 2024). The position of nucleus of *K. mikimotoi* observed in this study was similar with the previous reports on this species.

The combination of morphological and molecular characterisation was utilized in this study to further support the species identification of *K. mikimotoi*. As an athecate dinoflagellate, *K. mikimotoi* is delicate and prone to deformation or even cell lysis during preservation (Krock *et al.*, 2009). Therefore, the identification of

Karenia species often requires observation of live samples, as preserved samples may be ambiguous and make it difficult to obtain morphological features and morphometric data (de Salas *et al.*, 2003; Bergholtz *et al.*, 2006; Wayne *et al.*, 2007). Identifying *K. mikimotoi* with microscope is challenging owing to its smaller cell size, minimal morphological divergence from other *Karenia* species under light microscope, and low cell abundance during non-bloom periods (Friedheim, 2016; Zhang *et al.*, 2022). According to Haywood *et al.* (2004), microscopic identification of *K. mikimotoi* may be determined by cell size and nucleus position, while emphasises that molecular phylogenetic analysis is crucial in resolving difficulties in species identification. Molecular methods such as DNA sequencing of rDNA ITS and LSU region supports morphological data from light microscopy for more precise and reliable of species identification (Yuan *et al.*, 2012).

Molecular data not only aids in species delineation but also for facilitating comprehensive species characterisation and taxonomic classification (Monaco & Prouzet, 2015). *K. mikimotoi* is phylogenetically closer to *K. brevis*, and the results of this study agreed with past studies demonstrating the close relationship between *K. mikimotoi* and *K. brevis* (Ok *et al.*, 2023). In addition, Benico *et al.* (2019) had documented *A. gracile* affinity to *K. papilionacea* and was closely related to *Karenia* species. The phylogenetic analysis in Henrichs *et al.* (2011) study had revealed the placement of *B. capitatum* in the *Karenia* clade. The placement of *A. gracile* and *B. capitatum* in the clade of genus *Karenia* was also revealed in this study and these findings had provided support for the inclusion of genera *Asterodinium* and *Brachidinium* in Kareniaceae family as reported in previous studies (Henrichs *et al.*, 2011; Benico *et al.*, 2019).

ITS2 Secondary Structure of *Karenia*

This study is the first to analyse and compare the ITS2 secondary structure of *Karenia* species to obtain a clearer understanding of the genetic relationships between species within this genus. The modelling of ITS2 secondary structures in *Karenia* revealed four highly conserved universal helices (I–IV). Helices I and IV are the most evolutionarily variable helices and are particularly useful for comparing species and

subspecies, while helices II and III are more conserved in the lower taxonomic levels and differ from other eukaryotic ITS2 structures (Coleman, 2009).

In the molecular characterization of *K. mikimotoi*, *K. brevis*, and *K. selliformis*, phylogenetic analysis (Figure 3; Figure 4) reveals their separation into three distinct species lineages. This is further supported by the presence of hemi-compensatory base changes (hCBCs) when comparing their ITS2 transcripts (Figure 5). In a study on *Fukuyoa paulensis*, no compensatory base changes (CBCs) were detected among the clades, but an hCBC was observed in the most divergent clade (Laza-Martínez *et al.*, 2016). In the present study, four hCBCs were identified between *K. mikimotoi* and *K. brevis* ITS2 transcripts, and six hCBCs were found in comparisons between *K. mikimotoi* and *K. selliformis* ITS2 transcripts (Figure 5). The presence of additional hCBCs increases genetic divergence between species, leading to their classification as separate species (Wolf *et al.*, 2013). In other words, hCBCs play a crucial role in species divergence and represent a key step in speciation (Rousset *et al.*, 1991; Wolf *et al.*, 2013; Metzger *et al.*, 2017). To further support the use of hCBCs as molecular markers in the ITS2 transcript, Teng *et al.* (2015) applied hCBCs to define new species identities in *Pseudo-nitzschia*.

Besides, based on ITS2 secondary structure and CBCs analyses *K. longicanalis* is distinct from *K. papilionacea* by having three CBCs and ten hCBCs (Figure 6). Different species are more easily classified when CBCs are present in the homologous modelling of the ITS2 secondary structure (Coleman, 2003; Müller *et al.*, 2007). The CBC information can be useful in evaluating species delineation, but divergence of ITS2 sequences due to hybridisation and polyploidisation can lead to misleading inferences of true homology between taxa and accurate phylogenetic reconstruction (Alvarez & Wendel, 2003). A good indicator of distinct species is the presence of at least one CBC (Müller *et al.*, 2007; Wolf *et al.*, 2013).

The taxa are classified as different species when CBCs or hCBCs are present in the homology modelling (Coleman, 2003; Müller *et al.*, 2007). The predicted ITS2 secondary structure is sufficient to demarcate closely

related species, especially pseudo-cryptic and cryptic species (Amato *et al.* 2007, Müller *et al.*, 2007). In this study, the presence of hCBCs can be used as a diagnostic feature of species delineation in *Karenia* when CBCs are absent.

The presence of CBCs or hCBCs of ITS2 transcript in this study can serve as supporting information in species delimitation among *Karenia* species.

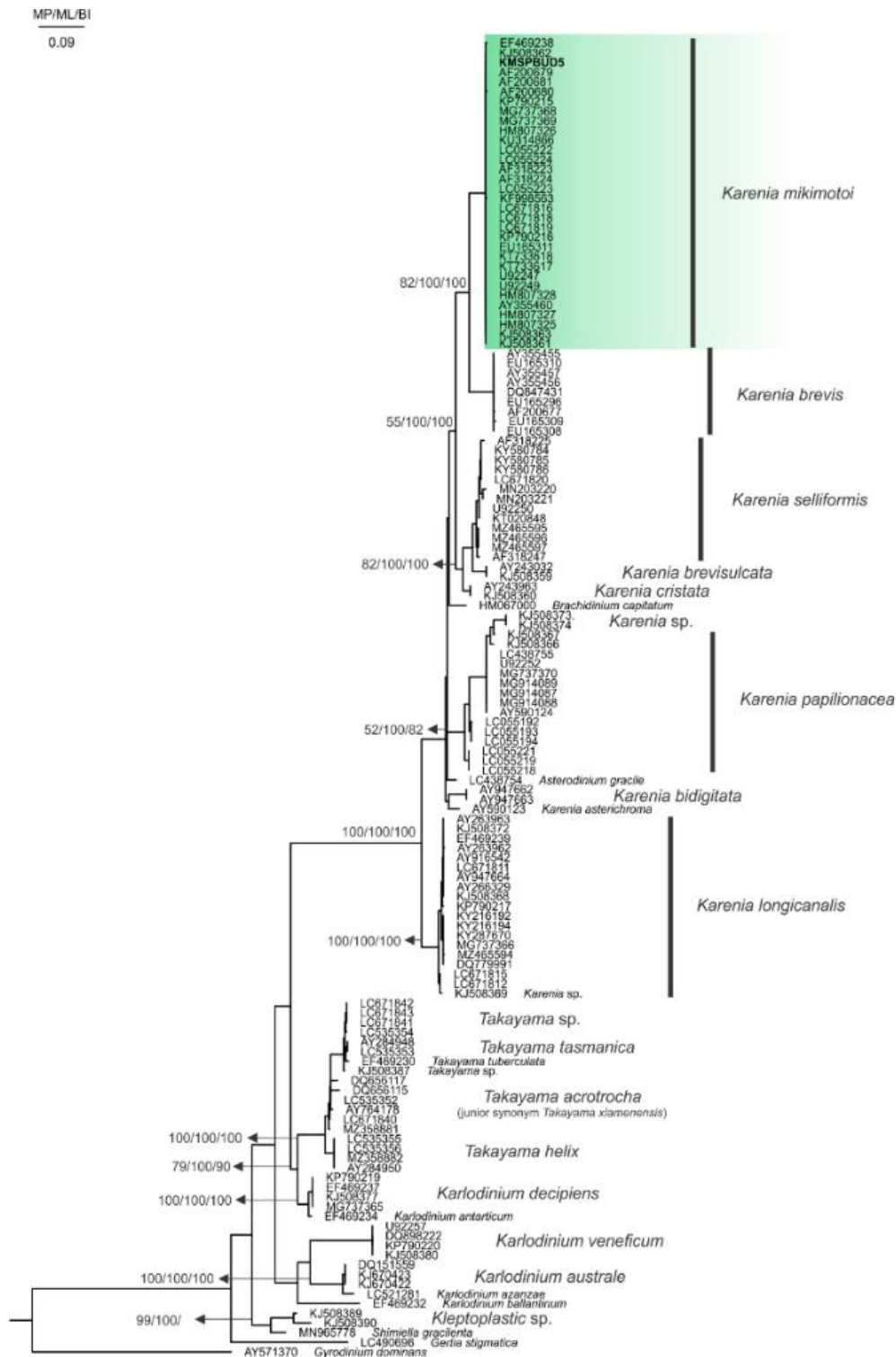


Figure 3. Phylogeny tree inferred from maximum likelihood (ML) based on *Karenia* LSU rDNA datasets. Nodal supports are bootstrap values of maximum parsimony (MP), maximum likelihood (ML), and posterior probability of BI; only values >50% support are indicated. The studied species are in bold. *Gyrodinium dominans* was chosen as the outgroup

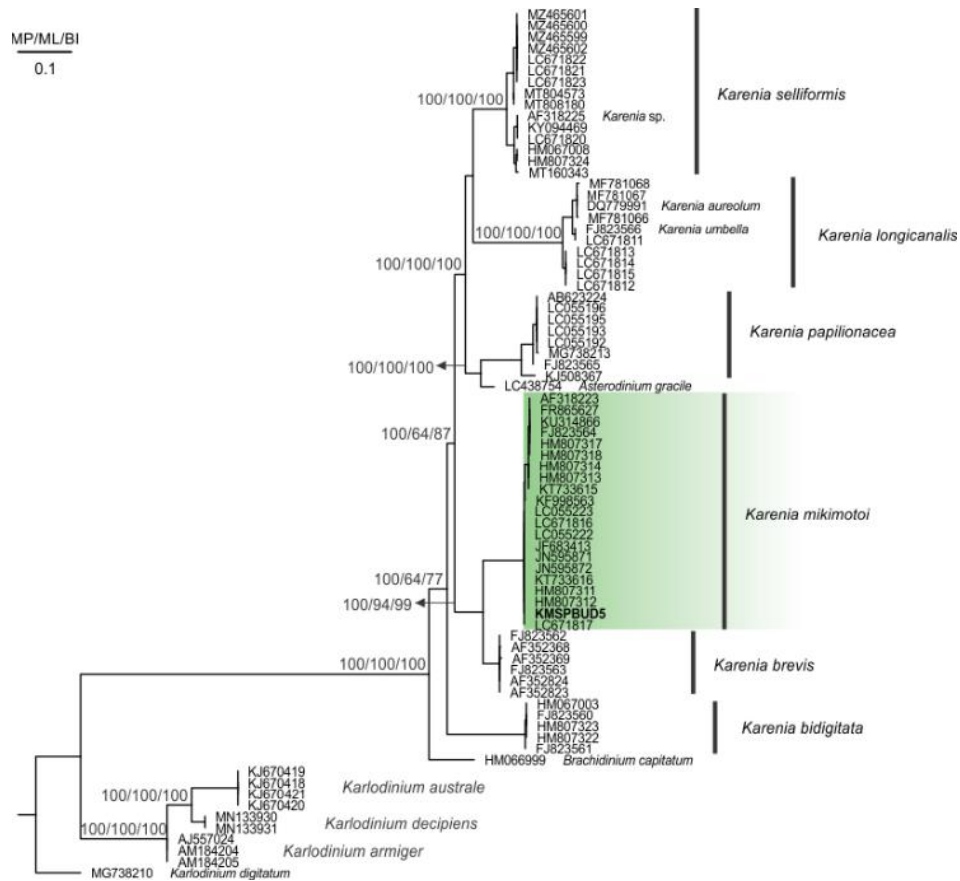


Figure 4. Phylogeny tree inferred from maximum likelihood (ML) based on *Karenia* ITS2 rDNA datasets. Nodal supports are bootstrap values of maximum parsimony (MP), maximum likelihood (ML), and posterior probability of BI; only values >50% support are indicated. The studied species are in bold. *Karlodinium digitatum* was chosen as the outgroup

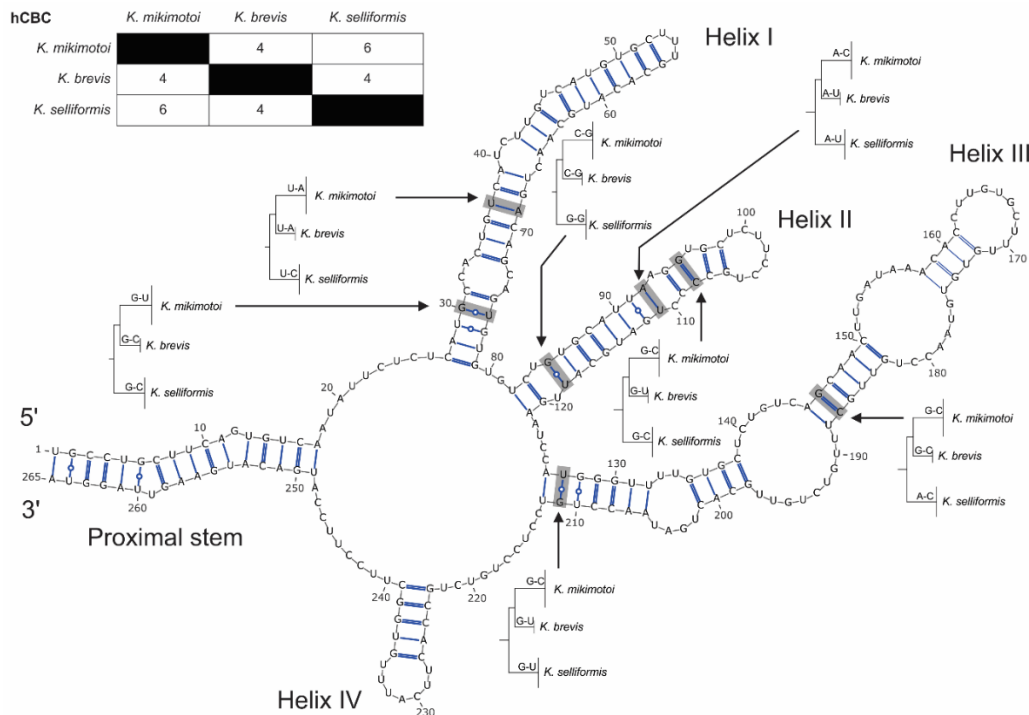


Figure 5. ITS2 RNA transcripts of *Karenia mikimotoi* with closely related species, viz. *Karenia brevis* and *Karenia selliformis*. Shaded rectangles indicate hCBCs

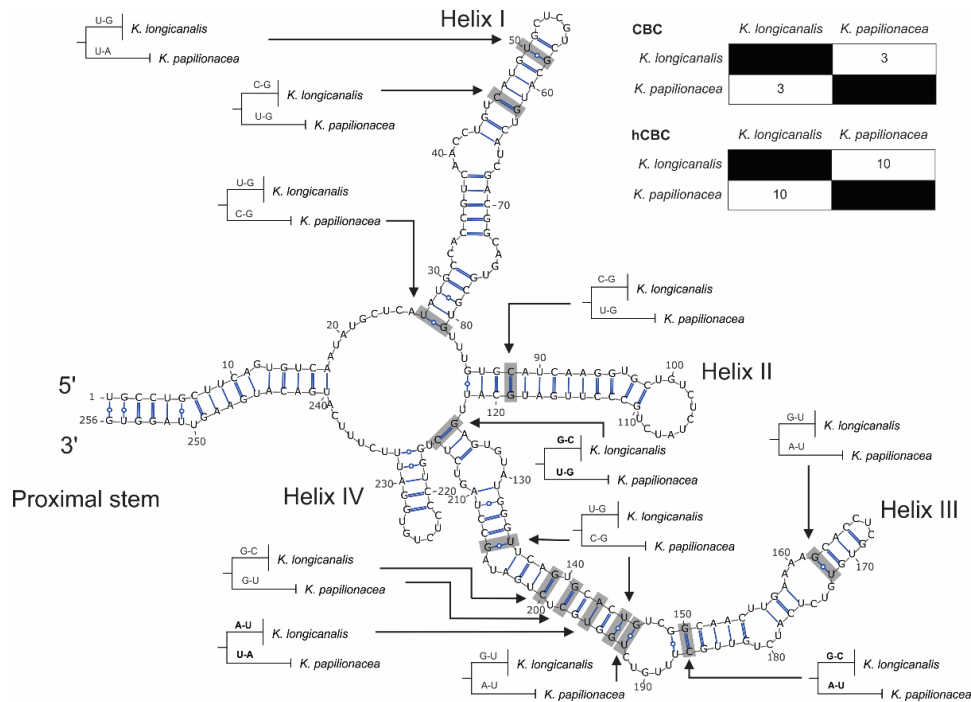


Figure 6. ITS2 RNA transcripts of *Karenia longicanalis* with closely related species, viz. *Karenia papilionacea*. Shaded rectangles indicate CBCs or hCBCs. Bolded indicate CBCs

Geographical Distribution and Bloom Events of *K. mikimotoi* in Asia

The bloom-forming dinoflagellate species *K. mikimotoi* has been documented in temperate coastal waters along the coasts of Atlantic, Pacific, and Indian Oceans (Li *et al.*, 2019). Although *K. mikimotoi* is documented for the first time in Borneo coastal waters in this study, it has a long history of widespread distribution with detrimental impacts on marine life in other Asian countries, for instances, Japan, China, Singapore, Vietnam, Korea and India. First report of *K. mikimotoi* was during red tides in 1934 in Japan, where this toxic species was associated with fish and shellfish kills along the shore of Gokasho Bay, Honshu (Oda, 1935). Since then, *K. mikimotoi* was reported to bloom from 1991 to 1995 in several areas in Japan, including Tanabe Bay, Hoketsu Bay, Suo-Nada, near Ie-shima islands, and Hiroshima Bay (Nakamura *et al.*, 1995; Koizumi *et al.*, 1996; Kimura *et al.*, 1999; Matsuyama *et al.*, 1999). Among all the affected countries, China is the most affected by the blooms of *K. mikimotoi*. The first discovery of *K. mikimotoi* in China dates back to 1998 in Daya Bay and the Pearl River estuary (Baohong *et al.*, 2021). Since then, *K. mikimotoi* blooms have recurred over 120 times in China, becoming an annual calamity even in current 21st century (Baohong *et al.*,

2021; Zhang *et al.*, 2023). The longest period of *K. mikimotoi* bloom recorded in China was in the Yangtze River estuary, lasting for 72 days in 2006 (Baohong *et al.*, 2021). In 2012, 22 blooms of *K. mikimotoi* were observed affecting Zhejiang Province, Fujian Province, and Guangdong Province (Baohong *et al.*, 2021). *K. mikimotoi* has also been documented in several Southeast Asian countries, including Singapore (Leong *et al.*, 2015; Kok & Leong, 2019) and Vietnam (Larsen & Nguyen, 2004). Park *et al.* (2013) documented the occurrence of *K. mikimotoi* on the Geoje coast of Korea. In India, *K. mikimotoi* blooms were linked to fish kills along the Kerala coast in 2004 (D'Silva *et al.*, 2012), Cochin Barmouth in 2009 (Hartman *et al.*, 2014), Gulf of Mannar in 2013 (Babu *et al.*, 2016), and Kochi estuary (Kumar *et al.*, 2018). The distribution of *K. mikimotoi* is believed to be facilitated by ballast water carried by international vessels. A study by Wang *et al.* (2010, as cited in Wang *et al.*, 2022) linked the movement and subsequent invasion of *K. mikimotoi* into new regions of the China Sea to ballast water transport, highlighting the role of shipping in the spread of this species. The detection of *K. mikimotoi* in Sabah, especially near the international port at Sepangar Bay, Kota Kinabalu, further highlights its extensive distribution via ballast water.

Table 2. Summary of red-tides attributed to *K. mikimotoi* in Asia with detrimental effects to marine life (n.d. = no data)

Year	Area	Adverse effects	Reference
1934	Japan; Gokasho Bay, Honshu	Fish, shellfish mortality Fish gills disorder, mucus spawn	Oda (1935)
1965	Japan; Omura Bay, Nagasaki	Fish, shellfish mortalities	Takayama and Adachi (1984)
1972	Japan; Omura Bay, Nagasaki	n.d.	Hirayama (1972); Gentien (1998)
1981	Korea; Geoje coast	n.d.	Park <i>et al.</i> (2013)
1985	Japan; Suo-Nada and Iyo-Nada	Fisheries damage >10 million US\$	Yanagi <i>et al.</i> (1995)
1989	India; Kodi, Karnataka	Fish mortality	D'Silva <i>et al.</i> (2012)
1991	Japan; Tanabe Bay	n.d.	Nakamura <i>et al.</i> (1995)
1992	Japan; Hoketsu Bay	n.d.	Koizumi <i>et al.</i> (1996)
1992	Japan; Suo-Nada	n.d.	Kimura <i>et al.</i> (1999)
1993	Japan; Suo-Nada	n.d.	Kimura <i>et al.</i> (1999)
1994	Japan; near Ie-shima Islands	n.d.	Nakamura <i>et al.</i> (1995)
1995	Japan; Hiroshima Bay	Shellfish mortality	Matsuyama <i>et al.</i> (1999)
1998	China; Pearl River estuary and Daya Bay	Fish mortality	Dickman (2000); Qi <i>et al.</i> (2004)
2002	China; Fujian coast	Fish, shellfish mortalities	Li <i>et al.</i> (2017)
2003	China; East China Sea coast	n.d.	Li <i>et al.</i> (2017)
2003	China; Zhejiang Province	n.d.	Baohong <i>et al.</i> (2021)
2004	China; Tianjin and Yellow River estuary	n.d.	Baohong <i>et al.</i> (2021)
2004	China; Bohai Sea and East China Sea	n.d.	Li <i>et al.</i> (2017)
2004	India; Kerala coast	Fish mortality	D'Silva <i>et al.</i> (2012)
2004	Vietnam coast	n.d.	Larsen and Nguyen (2004)
2005	China; Yangtze River estuary, Bohai Bay and Zhejiang Province	n.d.	Baohong <i>et al.</i> (2021)
2005	China; East China Sea coast and Pearl River estuary	Fish, shellfish mortalities	Li <i>et al.</i> (2009); Li <i>et al.</i> (2010); Li <i>et al.</i> (2017)
2006	China; East China Sea coast	n.d.	Li <i>et al.</i> (2017)
2006	China; Yangtze River estuary and Zhejiang Province	n.d.	Baohong <i>et al.</i> (2021)
2007	China; Bohai Sea and East China Sea	n.d.	Li <i>et al.</i> (2017)
2008	China; East China Sea coast	n.d.	Li <i>et al.</i> (2017)
2008	Japan; Suo-Nada and Beppu Bay	Fish mortality	Siswanto <i>et al.</i> (2013)
2009	China; East China Sea coast	n.d.	Li <i>et al.</i> (2017)
2009	India; Cochin barmouth	Fish mortality	Hartman <i>et al.</i> (2014)
2010	China; East China Sea coast	n.d.	Li <i>et al.</i> (2017)
2010	Japan; Beppu Bay	n.d.	Siswanto <i>et al.</i> (2013)
2011	Singapore; Johor Straits	n.d.	Leong <i>et al.</i> (2015)
2012	China; East China Sea coast	Abalone, fish mortalities	Li <i>et al.</i> (2017)
2012	China; Zhejiang Province and Fujian Province	n.d.	Baohong <i>et al.</i> (2021)
2013	India; Gulf of Mannar	Fish mortality	Babu <i>et al.</i> (2016)
2014	Singapore; Johor Straits	n.d.	Leong <i>et al.</i> (2015)
2014	Japan; Imari Bay	n.d.	Aoki <i>et al.</i> (2017)
2014	China; East China Sea coast	n.d.	Li <i>et al.</i> (2019)
2015	Japan; Hakodate Bay	Abalone, fish, squid mortalities	Shimada <i>et al.</i> (2016)
2015	China; East China Sea coast	n.d.	Li <i>et al.</i> (2019)
2015	Japan; Sasebo Bay	n.d.	Higo <i>et al.</i> (2017)
2015	India; Kochi estuary	n.d.	Kumar <i>et al.</i> (2018)
2017	China; Zhejiang Province	n.d.	Baohong <i>et al.</i> (2021)
2017	Philippines; Bolinao-Anda, Pangasinan	High abundance yet no fish kill reported	Azanza and Benico (2017); Yñiguez <i>et al.</i> , 2021
2018	China; East China Sea coast	Fish, abalone mortality	Li <i>et al.</i> (2019)
2022	Malaysia; Sabah, Borneo	n.d.	This study

CONCLUSION

In this study, we discovered *K. mikimotoi*, for the first time, in Malaysia Borneo. This suggests the prevalence of this toxic athecate dinoflagellate in our waters that require attention for monitoring of HABs in Malaysia. Therefore, further studies on the diversity and distribution of *Karenia* in Malaysia are recommended to determine the diversity and distribution of *Karenia* in Malaysia as well as to assess the potential risk of toxic dinoflagellate *Karenia* occurrence especially in finfish and shellfish mariculture area in the country.

ACKNOWLEDGEMENTS

We would like to acknowledge the Universiti Malaysia Sarawak for supports and this work was funded by the Ministry of Higher Education, Malaysia, Fundamental Research Grant Scheme (FRGS) (FRGS/1/2020/WAB11/UNIMAS/03/2). This work forms parts of the master project of Sheryl Uncha anak Andrew Chiba.

REFERENCES

- Ali, S.E., Mittal, A. & Mathews, D.H. (2023). RNA secondary structure analysis using RNAstructure. *Current Protocols*, 3, e846. DOI: 10.1002/cpz1.846
- Amato, A., Kooistra, W.H., Ghiron, J.H., Mann, D.G., Pröschold, T., & Montresor, M. (2007). Reproductive isolation among sympatric cryptic species in marine diatoms. *Protist*, 158(2), 193–207. DOI: 10.1016/j.protis.2006.10.001
- Azanza, R.V. & Benico, G.A. (2017). “Fish kills” in the Philippines associated with harmful algal blooms (HABs). *Proceedings of the Tenth EASTHAB Symposium*.
- Babu, M.J., Geetha, P. & Soman, K.P. (2016). MODIS-aqua data based detection and classification of algal blooms along the coast of India using RLS classifier. *Procedia Computer Science*, 93, 424-430. DOI: 10.1016/j.procs.2016.07.238
- Baohong, C., Kang, W., Huige, G. & Hui, L. (2021). *Karenia mikimotoi* blooms in coastal waters of China from 1998 to 2017. *Estuarine, Coastal and Shelf Science*, 249, 107034. DOI: 10.1016/j.ecss.2020.107034
- Benico, G., Takahashi, K., Lum, W.M. & Iwataki, M. (2019). Morphological variation, ultrastructure, pigment composition and phylogeny of the star-shaped dinoflagellate *Asterodinium gracile* (Kareniaceae, Dinophyceae). *Phycologia*, 5(4), 405-418. DOI: 10.1080/00318884.2019.1601948
- Bergholtz, T., Daugbjerg, N. & Fernández, M. (2006). On the identity of *Karlodinium veneficum* and description of *Karlodinium armiger* sp. nov. (Dinophyceae), based on light and electron microscopy, nuclear-encoded LSU rDNA, and pigment composition. *Journal of Phycology*, 42, 170-193. DOI: 10.1111/j.1529-8817.2006.00187.x
- Botes, L., Sym, S. & Pitcher, G. (2003). *Karenia cristata* sp. nov. and *Karenia bicuneiformis* sp. nov. (Gymnodiniales, Dinophyceae): two new *Karenia* species from the South African Coast. *Phycologia*, 42, 563-571. DOI: 10.2216/i0031-8884-42-6-563.1
- Caruana, A. M. N. & Amzil, Z. (2018). Chapter 13 - Microalgae and Toxins. In: *Microalgae in Health and Disease Prevention* (Levine, I. A. and Fleurence, J., 1st ed.), pp. 263-305. London: Academic Press.
- Cen, J., Wang, J., Huang, L., Ding, G., Qi, Y., Cao, R., Cui, L. & Lü, S. (2020). Who is the “murderer” of the bloom in coastal waters of Fujian, China, in 2019? *Journal of Oceanology and Limnology*, 38, 722-732. DOI: 10.1007/s00343-020-9290-8
- Cen, J., Lu, S., Moestrup, Ø., Jiang, T., Ho, K. C., Li, S., Li, M., Huan, Q. & Wang, J. (2024). Five *Karenia* species along the Chinese coast: with the description of a new species, *Karenia hui* sp. nov. (Kareniaceae, Dinophyta). *Harmful Algae*, 137, 102645. DOI: 10.1016/j.hal.2024.102645
- Coleman, A.W. (2003). ITS2 is a double-edged tool for eukaryote evolutionary comparisons. *Trends in Genetics*, 19, 370-375. DOI: 10.1016/S0168-9525(03)00118-5
- Coleman, A.W. (2009). Is there a molecular key to the level of “biological species” in eukaryotes? A DNA guide. *Molecular Phylogenetics and Evolution*, 50, 197-203. DOI: 10.1016/j.ympev.2008.10.008
- D’Silva, M.S., Anil, A.C., Naik, R.K. & D’Costa, P.M. (2012). Algal blooms: a perspective from the coasts of India. *Natural Hazards*, 63, 1225-1253. DOI: 10.1007/s11069-012-0200-3
- Darriba, D., Taboada, G.L., Doallo, R. & Posada, D. (2012). jModelTest 2: more models, new heuristics and parallel computing. *Nature Methods*, 9, 772. DOI: 10.1038/nmeth.2109

- Darty, K., Denise, A., & Ponty, Y. (2009). VARNA: Interactive drawing and editing of the RNA secondary structure. *Bioinformatics*, 25(15), 1974–1975. DOI: 10.1093/bioinformatics/btp250
- Daugbjerg, N., Hansen, G., Larsen, J. & Moestrup, Ø. (2000). Phylogeny of some of the major genera of dinoflagellates based on ultrastructure and partial LSU rDNA sequence data, including the erection of three new genera of unarmoured dinoflagellates. *Phycologia*, 39, 302-317. DOI: 10.2216/i0031-8884-39-4-302.1
- Davis, C.C. (1948). *Gymnodinium brevis* sp. nov., a cause of discolored water and animal mortality in the Gulf of Mexico. *Botanical Gazette*, 109, 358-360. DOI: 10.1086/335561
- de Salas, M.F., Bolch, C.J.S., Botes, L., Nash, G., Wright, S.W. & Hallegraeff, G.M. (2003). *Takayama* gen. nov. (Gymnodiniales, Dinophyceae), a new genus of unarmored dinoflagellates with sigmoid apical grooves, including the description of two new species. *Journal of Phycology*, 39, 1233-1246. DOI: 10.1111/j.0022-3646.2003.03-086.x
- de Salas, M.F., Bolch, C.J.S. & Hallegraeff, G. M. (2004). *Karenia umbella* sp. nov. (Gymnodiniales, Dinophyceae), a new potentially ichthyotoxic dinoflagellate species from Tasmania, Australia. *Phycologia*, 43, 166-175. DOI: 10.2216/i0031-8884-43-2-166.1
- Ericson, K. (2016). Making space for red tide: discoloured water and the early twentieth century bayscape of Japanese pearl cultivation. *Journal of the History of Biology*, 50, 393-423. DOI: 10.1007/s10739-016-9443-x
- Escobar-Morales, S. & Hernández-Becerril, D. (2015). Free-living marine planktonic unarmoured dinoflagellates from the Gulf of Mexico and the Mexican Pacific. *Botanica Marina*, 58, 9-22. DOI: 10.1515/bot-2014-0084
- Eunson, R. (1955). *The Pearl King: The Fabulous Story of Mikimoto*. New York: Greenberg.
- Flewelling, L.J., Naar, J.P., Abbott, J.P., Baden, D.G., Barros, N.B., Bossart, G.D., Bottein, M.-Y.D., Hammond, D.G., Haubold, E.M., Heil, C.A., Henry, M.S., Jacocks, H.M., Leighfield, T.A., Pierce, R.H., Pitchford, T.D., Rommel, S.A., Scott, P.S., Steidinger, K.A., Truby, E.W., Van Dolah, F.M. & Landsberg, J.H. (2005). Red tides and marine mammal mortalities. *Nature*, 435, 755-756. DOI: 10.1038/nature435755a
- Friedheim, S. (2016). Comparison of species identification methods: DNA barcoding versus morphological taxonomy. *Journal of Microbiology & Experimentation*, 3(1), 00082. DOI: 10.15406/jmen.2016.03.00082
- Fukuyo, Y., Imai, I., Kodama, M. & Tamai, K. (2002). Red tides and other harmful algal blooms in Japan. In: Taylor, F. J. R. and Trainer, V. L. (eds.) *Harmful algal blooms in the PICES region of the North Pacific*. Sidney, B.C., Canada: Institute of Ocean Sciences.
- Gentien, P. (1998). Bloom dynamics and ecophysiology of the *Gymnodinium mikimotoi* species complex. *Physiological ecology of harmful algal blooms*, 155-173.
- Guiry, M.D. & Guiry, G.M. (2023). AlgaeBase. World-wide electronic publication. Available: <https://www.algaebase.org>.
- Gunter, G., Williams, R.H., Davis, C.C. & Smith, F.G.W. (1948). Catastrophic mass mortality of marine animals and coincident phytoplankton bloom on the West Coast of Florida, November 1946 to August 1947. *Ecological Monographs*, 18, 309-324. DOI: 10.2307/1948622
- Hansen, G., Daugbjerg, N. & Henriksen, P. (2000). Comparative study of *Gymnodinium mikimotoi* and *Gymnodinium aureolum*, comb. nov. (= *Gyrodinium aureolum*) based on morphology, pigment composition, and molecular data. *Journal of Phycology*, 36(2), 394-410. DOI: 10.1046/j.1529-8817.2000.99172.x
- Hartman, S.E., Hartman, M.C., Hydes, D.J., Smythe-Wright, D., Gohin, F., & Lazure, P. (2014). The role of hydrographic parameters, measured from a ship of opportunity, in bloom formation of *Karenia mikimotoi* in the English Channel. *Journal of Marine Systems*, 139: 455-463. DOI: 10.1016/j.jmarsys.2014.07.001
- Haywood, A.J., Steidinger, K.A., Truby, E.W., Bergquist, P.R., Bergquist, P.L., Adamson, J. & Mackenzie, L. (2004). Comparative morphology and molecular phylogenetic analysis of three new species of the genus *Karenia* (Dinophyceae) from New Zealand. *Journal of Phycology*, 40(1), 165-179. DOI: 10.1111/j.0022-3646.2004.02-149.x
- Heil, C.A. & Steidinger, K.A. (2009). Monitoring, management, and mitigation of *Karenia* blooms in the eastern Gulf of Mexico. *Harmful Algae*, 8, 611-617. DOI: 10.1016/j.hal.2008.11.006

- Henrichs, D.W., Olson, R.J., Sosik, H.M. & Campbell, L. (2011). Phylogenetic analysis of *Brachidinium capitatum* (Dinophyceae) from the Gulf of Mexico indicates membership in the Kareniaceae. *Journal of Phycology*, 47(2), 366-374. DOI: 10.1111/j.1529-8817.2011.00960.x
- Hoagland, P., Jin, D., Polansky, L.Y., Kirkpatrick, B., Kirkpatrick, G., Fleming, L.E., Reich, A., Watkins, S.M., Ullmann, S.G. & Backer, L.C. (2009). The costs of respiratory illnesses arising from Florida gulf coast *Karenia brevis* blooms. *Environmental Health Perspectives*, 117(8), 1239–1243. DOI: 10.1289/ehp.0900645
- Hoshaw, R.W. (1973). Methods for microscopic algae. *Handbook of phycological methods: culture methods*, 53-68.
- Hulburt, E.M. (1957). The taxonomy of unarmored Dinophyceae of shallow embayments on Cape Cod, Massachusetts. *The Biological Bulletin*, 112, 196-219. DOI: 10.2307/1539198
- Iwataki, M., Lum, W.M., Kuwata, K., Takahashi, K., Arima, D., Kuribayashi, T., Kosaka, Y., Hasegawa, N., Watanabe, T., Shikata, T., Isada, T., Orlova, T.Y. & Sakamoto, S. (2022). Morphological variation and phylogeny of *Karenia selliformis* (Gymnodiniales, Dinophyceae) in an intensive cold-water algal bloom in eastern Hokkaido, Japan. *Harmful Algae*, 114, 102204. DOI: 10.1016/j.hal.2022.102204
- Kimura, B., Kamizono, M., Etoh, T., Koizumi, Y., Murakami, M. & Honjo, T. (1999). Population development of the red tide dinoflagellate *Gymnodinium mikimotoi* in inshore waters of Japan. *Plankton Biology and Ecology*, 46(1), 37-47.
- Koetschan, C., Hackl, T., Müller, T., Wolf, M., Förster, F. & Schultz, J. (2012). ITS2 database IV: interactive taxon sampling for internal transcribed spacer 2 based phylogenies. *Molecular Phylogenetics and Evolution*, 63: 585–588.
- Koizumi, Y., Uchida, T. & Honjo, T. (1996). Diurnal vertical migration of *Gymnodinium mikimotoi* during a red tide in Hoketsu Bay, Japan. *Journal of Plankton Research*, 18(2), 289-294. DOI: 10.1093/plankt/18.2.289
- Kok, J.W.K. & Leong, S.C.Y. (2019). Nutrient conditions and the occurrence of a *Karenia mikimotoi* (Kareniaceae) bloom within East Johor Straits, Singapore. *Regional Studies in Marine Science*, 27, 100514. DOI: 10.1016/j.rsma.2019.100514
- Kon, N.F., Lau, W.L.S., Hii, K.S., Law, I.K., Teng, S.T., Lim, H.C., Takahashi, K., Gu, H., Lim, P.T. & Leaw, C.P. (2017). Quantitative real-time PCR detection of a harmful unarmoured dinoflagellate, *Karlodinium australe* (Dinophyceae). *Phycological Research*, 65, 291-298. DOI: 10.1111/pre.12186
- Krock, B., Pitcher, G., Ntuli, J. & Cembella, A. (2009). Confirmed identification of gymnodimine in oysters from the west coast of South Africa by liquid 145 chromatography-tandem mass spectrometry. *African Journal of Marine Science*, 31, 113-118. DOI: 10.2989/AJMS.2009.31.1.12.783
- Kumar, P.S., Kumaraswami, M., Rao, G.D., Ezhilarasan, P., Sivasankar, R., Rao, V.R. & Ramu, K. (2018). Influence of nutrient fluxes on phytoplankton community and harmful algal blooms along the coastal waters of southeastern Arabian Sea. *Continental Shelf Research*, 161, 20-28. DOI: 10.1016/j.csr.2018.04.012
- Larsen, J. & Nguyen, N.L. (2004). Potentially toxic microalgae of Vietnamese waters. *Opera Botanica*, 140, 5-216.
- Laza-Martínez, A., David, H., Riobó, P., Miguel, I. & Orive, E. (2016). Characterization of a Strain of *Fukuyoa paulensis* (Dinophyceae) from the Western Mediterranean Sea. *Journal of Eukaryotic Microbiology*, 63(4), 481–497. DOI: 10.1111/jeu.12292
- Li, X., Yan, T., Lin, J., Yu, R. & Zhou, M. (2017). Detrimental impacts of the dinoflagellate *Karenia mikimotoi* in Fujian coastal waters on typical marine organisms. *Harmful Algae*, 61, 1-12. 137. DOI: 10.1016/j.hal.2016.11.011
- Li, X., Yan, T., Yu, R. & Zhou, M. (2019). A review of *Karenia mikimotoi*: Bloom events, physiology, toxicity and toxic mechanism. *Harmful Algae*, 90, 101702. DOI: 10.1016/j.hal.2019.101702
- Loeblich, A. R. (1975). A seawater medium for dinoflagellates and the nutrition of *Cachonina niel*. *Journal of Phycology*, 11, 80-86. DOI: 10.1111/j.1529-8817.1975.tb02752.x
- Leong, S., Yew, C., Peng, L. L., Moon, C. S., Kit, J. K. W. & Ming, S. T. L. (2015). Three new records of dinoflagellates in Singapore's coastal waters, with observations on environmental conditions associated with microalgal growth in the Johor Straits. *Raffles Bulletin of Zoology*, 31, 24-36.
- Matsuyama, Y., Uchida, T. & Honjo, T. (1999). Effects of harmful dinoflagellates, *Gymnodinium*

- mikimotoi* and *Heterocapsa circularisquama*, red-tide on filtering rate of bivalve molluscs. *Fisheries Science*, 65, 248-253. DOI: 10.2331/fishsci.65.248
- Merget, B., Koetschan, C., Hackl, T., Förster, F., Dandekar, T., Müller, T., Schultz, J., & Wolf, M. (2012). The ITS2 Database. *Journal of Visualized Experiments*, (61), 3806. DOI: 10.3791/3806
- Metzger, B.P.H., Wittkopp, P.J. & Coolon, J.D. (2017). Evolutionary dynamics of regulatory changes underlying gene expression divergence among *Saccharomyces* species. *Genome Biology and Evolution*, 9(4), 843-854. DOI: 10.1093/gbe/evx035
- Monaco, A. & Prouzet, P. (2015). *Marine Ecosystems: Diversity and Functions*. Wiley.
- Müller, T., Philippi, N., Dandekar, T., Schultz, J., & Wolf, M. (2007). Distinguishing species. *RNA*, 13(9), 1469–1472. DOI: 10.1261/rna.617107
- Nakamura, Y., Suzuki, S. & Hiromi, J. (1995). Population dynamics of heterotrophic dinoflagellates during a *Gymnodinium mikimotoi* red tide in the Seto Inland Sea. *Marine Ecology Progress Series*, 125, 269-277.
- Nézan, E., Siano, R., Boulben, S., Six, C., Bilien, G., Chèze, K., Duval, A., Le Panse, S., Quéré, J. & Chomérat, N. (2014). Genetic diversity of the harmful family Kareniaceae (Gymnodiniales, Dinophyceae) in France, with the description of *Karlodinium gentienii* sp. nov.: A new potentially toxic dinoflagellate. *Harmful Algae*, 40, 75-91. DOI: 10.1016/j.hal.2014.10.006
- Oda M. (1935). The red tide of *Gymnodinium mikimotoi* n.sp. (MS.) and the effect of altering copper sulphate to prevent the growth of it. *Zoological Society of Japan*, 47(555): 35-48.
- Ok, J.H., Jeong, H.J., Lim, A.S., Kang, H.C. You, J.H., Park, S.A. & Eom, S.H. (2023). Lack of mixotrophy in three *Karenia* species and the prey spectrum of *Karenia mikimotoi* (Gymnodiniales, Dinophyceae). *Algae*, 38(1), 39-55. DOI: 10.4490/algae.2023.38.2.28
- Park, J., Jeong, H.J., Yoo, Y.D. & Yoon, E.Y. (2013). Mixotrophic dinoflagellate red tides in Korean waters: distribution and ecophysiology. *Harmful Algae*, 30, S28-S40. DOI: 10.1016/j.hal.2013.10.004
- Partensky, F., Vaultot, D., Couté, A. & Sournia, A. (1988). Morphological and nuclear analysis of the bloom-forming dinoflagellates *Gyrodinium cf. aureolum* and *Gymnodinium nagasakiense*. *Journal of Phycology*, 24(3), 408-415. DOI: 10.1111/j.1529-8817.1988.tb04484.x
- Rambaut, A. (2007). FigTree, a graphical viewer of phylogenetic trees.
- Ronquist, F. & Huelsenbeck, J.P. (2003). MrBayes 3: Bayesian phylogenetic inference under mixed models. *Bioinformatics*, 19, 1572-1574. DOI: 10.1093/bioinformatics/btg180
- Ronquist, F., Teslenko, M., van der Mark, P., Ayres, D.L., Darling, A., Höhna, S., Larget, B., Liu, L., Suchard, M.A. & Huelsenbeck, J.P. (2012). MrBayes 3.2: efficient Bayesian phylogenetic inference and model choice across a large model space. *Systematic Biology*, 61, 539-542. DOI: 10.1093/sysbio/sys029
- Rousset, F., Pélandakis, M. & Solognac, M. (1991). Evolution of compensatory substitutions through G-U intermediate state in *Drosophila* rRNA. *Proceedings of the National Academy of Sciences of the United States of America*, 88, 10032-10036. DOI: 10.1073/PNAS.88.22.10032.
- Seibel, P.N., Müller, T., Dandekar, T., Schultz, J. & Wolf, M. (2006). 4SALE – a tool for synchronous RNA sequence and secondary structure alignment and editing. *Bioinformatics*, 7(498). DOI: 10.1186/1471-2105-7-498
- Seibel, P.N., Müller, T., Dandekar, T. & Wolf, M. (2008). Synchronous visual analysis and editing of RNA sequence and secondary structure alignments using 4SALE. *BMC Research Notes*, 1(91). DOI: 10.1186/1756-0500-1-91
- Seibel, P., Müller, T., Dandekar, T. & Wolf, M. (2008). Synchronous visual analysis and editing of RNA sequence and secondary structure alignments using 4SALE. *BMC Research Notes*, 1: 91.
- Siswanto, E., Ishizaka, J., Tripathy, S.C. & Miyamura, K. (2013). Detection of harmful algal blooms of *Karenia mikimotoi* using MODIS measurements: a case study of Seto-Inland Sea, Japan. *Remote Sensing of Environment*, 129, 185-196. DOI: 10.1016/j.rse.2012.11.012
- Swofford, D.L. (2003). PAUP* Phylogenetic Analysis Using Parsimony (*and Other Methods). Version 4. <http://paup.csit.fsu.edu/>.
- Takayama, H. & Adachi, R. (1984). *Gymnodinium nagasakiense* sp. nov., a red-tide forming

- dinophyte in the adjacent waters of Japan. *Bulletin of Plankton Society of Japan*, 31, 7-14.
- Tangen, K. (1977). Blooms of *Gyrodinium aureolum* (Dinophyceae) in North European waters, accompanied by mortality in marine organisms. *Sarsia*, 63, 123-133. DOI: 10.1080/00364827.1977.10411330
- Tangen, K. & Bjornland, T. (1981). Observations on pigments and morphology of *Gyrodinium aureolum* Hulburt, a marine dinoflagellate contain 19^hhexanoyloxyfucoxantin as the main carotenoid. *Journal of Plankton Research*, 3, 389-401. DOI: 10.1093/plankt/3.3.389
- Tang, Y.Z., Egerton, T.A., Kong, L. & Marshall, H.G. (2008). Morphological variation and phylogenetic analysis of the dinoflagellate *Gymnodinium aureolum* from a tributary of Chesapeake Bay. *J. Eukaryot. Microbiol.* 55, 91-99. DOI: 10.1111/j.1550-7408.2008.00305.x
- Teng, S.T., Lim, P.T., Lim, H.C., Rivera-Vilarelle, M., Quijano-Scheggia, S., Takata, Y., Quilliam, M.A., Wolf, M., Bates, S.S. & Leaw, C.P. (2015). A non-toxicogenic but morphologically and phylogenetically distinct new species of *Pseudonitzschia*, *P. sabit* sp. nov. (Bacillariophyceae). *Journal of Phycology*, 51, 706-725. DOI: 10.1111/jpy.12318
- Wang, Q., Lin, L., Chen, X., Wu, W. & Wu, H. (2022). Transportation of bloom forming species in ballast water by commercial vessels at Yangshan deep water port. *Ocean and Coastal Management*, 219, 106045. DOI: 10.1016/j.ocecoaman.2022.106045
- Watkins, S.M.A.R., Fleming, L.E. & Hammond, R. (2008). Neurotoxic shellfish poisoning. *Marine Drugs*, 6, 431-455. DOI: 10.3390/md20080022
- Wayne, L.R., Vandersea, M.W., Kibler, S.R., Reece, K.S., Stokes, N.A., Lutzoni, F. M., Yonish, B.A., West, M.A., Black, M.N.D. & Tester, P.A. (2007). Recognizing dinoflagellate species using ITS rDNA sequences. *Journal of Phycology*, 43, 344-355. DOI: 10.1111/j.1529-8817.2006.00305.x
- Wolf, M., Achtziger, M., Schultz, J., Dandekar, T., & Müller, T. (2005). Homology modeling revealed more than 20,000 rRNA internal transcribed spacer 2 (ITS2) secondary structures. *RNA*, 11(11), 1616-1623. DOI: 10.1261/rna.2144205
- Wolf, M., Chen S., Song, J., Ankenbrand, M., & Müller, T. (2013). Compensatory base changes in ITS2 secondary structures correlate with the biological species concept despite intragenomic variability in ITS2 sequences - a proof of concept. *PLoS One*, 8(6), e66726. DOI: 10.1371/journal.pone.0066726
- Wolny, J.L., Whereat, E.B., Egerton, T.A., Gibala-Smith, L.A., McKay, J.R., O'Neil, M., Wazniak, C.E. & Mulholland, M.R. (2024). The occurrence of *Karenia* species in mid-Atlantic coastal waters: data from the Delmarva Peninsula, USA. *Harmful Algae*, 132, 102579. DOI: 10.1016/j.hal.2024.102579
- Yanagi, T., Yamamoto, T., Koizumi, Y., Ikeda, T., Kamizono, M. & Tamori, H. (1995). A numerical simulation of red tide formation. *Journal of Marine Systems*, 6, 269-285. DOI: 10.1016/0924-7963(94)00030-K
- Yñiguez, A.T., Lim, P.T., Leaw, C.P., Jipanin, S.J., Iwataki, M., Benico, G. & Azanza, R.V. (2021). Over 30 years of HABs in the Philippines and Malaysia: what have we learned? *Harmful Algae*, 102, 101776. DOI: 10.1016/j.hal.2021.101776
- Yuan, J., Mi, T., Zhen, Y., & Yu, Z. (2012). Development of a rapid detection and quantification method of *Karenia mikimotoi* by real-time quantitative PCR. *Harmful Algae*, 17, 83-91. DOI: 10.1016/J.HAL.2012.03.004
- Zhang, W., Zhang, Q., Smith, K.F., Qiu, L., Liu, C., Yin, X. & Liu, Q. (2022). Development of specific DNA barcodes for the Dinophyceae family Kareniaceae and their application in the South China Sea. *Frontiers in Marine Science*, 9. DOI: 10.3389/fmars.2022.851605
- Zhang, Y., Song, X. & Zhang, P. (2023). Combined effects of toxic *Karenia mikimotoi* and hypoxia on the juvenile abalone *Haliotis discus hannai*. *Journal of Shellfish Research*, 42(2), 373-379. DOI: 10.2983/035.042.0207

Potential of Local Microorganisms Solution from Chicken Manure as a Bioactivator in Liquid Waste Treatment from the Fish Cracker Processing Industry

HAMDANI ABDULGANI^{*1,2}, HADIYANTO³ & SUDARNO⁴

¹Doctoral Program of Environmental Science, School of Postgraduate Studies, Universitas Diponegoro Semarang, Indonesia; ² Faculty of Engineering, Universitas Wiralodra, Indramayu, Indonesia; ³Chemical Engineering Department, Faculty of Engineering, Universitas Diponegoro, Semarang; ⁴Environmental Engineering Department, Faculty of Engineering, Universitas Diponegoro, Semarang

*Corresponding author: dani.gani@unwir.ac.id

Received: 31 January 2024

Accepted: 13 September 2024

Published: 31 December 2024

ABSTRACT

The wastewater produced by traditional food industry is a source of problem due to its high levels of organic compounds pollutant that can increase the level of chemical oxygen demand (COD) and biological oxygen demand (BOD) values that exceed the established wastewater quality standard thresholds. The difficulty in removing high concentrations of organic material through conventional waste treatment necessitates the use of special treatment methods using local microorganisms' solution as bioactivators to accelerate the decomposition of organic compounds. This research aims to identify bacteria in local microorganisms' solution with potential applications in reducing organic compounds by its enzymatic activities. Based on the research results, among the 42 isolates examined, six isolates demonstrated the ability to hydrolyze starch, protein and fat based on qualitative tests. These isolates belong to the genus *Bacillus* based on partial sequencing of 16S rRNA gene. The qualitative tests confirmed the potential of these isolates as they exhibited enzymatic activities that showed potential to reduce organic compounds.

Keywords: amylase, lipase, molecular identification, organic compounds, protease

Copyright: This is an open access article distributed under the terms of the CC-BY-NC-SA (Creative Commons Attribution-NonCommercial-ShareAlike 4.0 International License) which permits unrestricted use, distribution, and reproduction in any medium, for non-commercial purposes, provided the original work of the author(s) is properly cited.

INTRODUCTION

Waste from the food industry can pose issues as it contains substantial amounts of carbohydrates, proteins, fats, oils, mineral salts and chemical residues. The high content of organic compounds in liquid waste from the food industry can serve as nutrients for microbial growth, potentially leading to a reduction in dissolved oxygen in water. If liquid waste is released into water without undergoing proper processing, it can pollute the water, damage the aquatic ecosystem and threaten the availability of clean water (Gameissa *et al.*, 2012). Furthermore, the presence of organic waste in liquid waste from the food industry can lead to human health problems. The difficulty in removing high concentrations of organic material through conventional waste treatment necessitates the use of special treatment methods (Pervez *et al.*, 2021).

To prevent these negative impacts, it is crucial to process liquid waste before

discharging it into the environment. Wastewater treatment technology can be implemented through various methods, including physical, chemical and biological approaches. One of the most effective strategies involves utilizing biological methods with microorganisms (Zaman *et al.*, 2020). The addition of microorganisms as bioactivators, accelerates the decomposition of organic compounds. Importantly, bioactivators are environmentally friendly as they lack dangerous or toxic ingredients. In wastewater treatment, bioactivators play a crucial role in preventing odors, significantly increasing the metabolic rate of bacteria, and enhancing the decomposition of organic compounds. These bioactivators can be derived from local microorganisms solution (Yunilas *et al.*, 2022).

Local microorganisms solution is a fermented liquid that contains micro and macro nutrients, along with bacteria that have the potential to decompose organic matter (Hadi, 2019). Local microorganisms' solution contains

rice washing water as its source of carbohydrates, palm sugar and coconut water as a source of glucose, and chicken manure as a source of microorganisms (Indasah & Muhith, 2020). Carbohydrates are a source of energy for microorganisms, including glucose which is a simple sugar that is easily metabolized by microorganisms (Sandle, 2016). Chicken manure is one of the organic materials that can be used in producing local microorganisms' solution. The presence of organic compounds in liquid waste can be significantly reduced because these compounds serve as an energy source for microorganisms, leading to the production of enzymes that break down the organic material. Enzymes such as amylase break down carbohydrates, protease breaks down proteins and lipase breaks down fats and oils. While local microorganisms solution is commonly used as a bioactivator in organic compost production, its potential in processing liquid waste has not been thoroughly explored. This research aimed to identify bacteria in local microorganisms solution with potential applications in liquid waste treatment, allowing these bacteria to be utilized as bioactivators.

MATERIALS AND METHODS

Local Microorganisms Solution Production

Local microorganisms' solution production from chicken manure was carried out by aerobic and anaerobic fermentation. The chicken manure was crushed and mixed with palm sugar, water from rice rinsing, and coconut water. Fermentation was carried out for 14 days aerobically and anaerobically. The aerobic fermentation was carried out by incubating the local microorganisms mixture in jerry cans and the oxygen was supplied from a hose. The anaerobic fermentation was carried out by local microorganisms fermentation in tightly closed jerry cans with a hose attached on top of the jerry can that connected to a bottle which contains clean water so that the air from outside did not enter the jerry can to keep the anaerobic incubation.

Isolating Bacteria from Local Microorganisms Solution

The fermented local microorganism solution samples were serially diluted up to 10^{-5} dilutions. A total of 100 μ l aliquots from the

dilution 10^{-3} to 10^{-5} were taken and spread onto a nutrient agar plate and incubated for 24 hours at 37 °C.

Characterization of Isolated Bacteria

Isolated colonies from the samples were characterized by identifying the morphology of the colonies in terms of shape, edges, elevation, colour and Gram staining procedure were conducted for microscopic identification.

Qualitative Screening of Potential Bacteria

The starch agar and Lugol's solution were used for screening amylolytic bacteria, skim milk agar for screening proteolytic bacteria, while olive oil or fish oil and rhodamin B medium for screening lipolytic bacteria. Bacteria that showed a clear zone around its colony on starch agar and skim milk agar were selected as potential strains. Bacteria that grew on oil medium and showed orange luminescence under UV light were also selected as potential strains.

Molecular Identification of Potential Isolates

The potential isolates were chosen for molecular identification using the 16S rRNA genes based on the outcome of enzymatic screening. The selected bacterial isolates were cultured in nutrient broth (NB) at 37 °C for 24 h. The supernatant was extracted from the cultures after they were centrifuged for 5 min at 10,000 rpm. A 10% Chelex solution in ddH₂O (500 μ l) was added. The cultures were then heated for 5 min at 95 °C, vortexed, and then heated for an additional 5 min at 95 °C. The culture was centrifuged once again for 15 min at 10,000 rpm, and the DNA-containing supernatant was then moved to a new microtube (Gautam, 2022). The extracted DNA was amplified using My Taq HS Red DNA Polymerase (Bioline) by following the manufacturer's instructions. The amplified products were shipped to Genetika Science, Indonesia for further DNA sequencing process. The retrieved sequences were aligned and compared in order to determine the closest evolutionary relatives using the Basic Local Alignment Search Tool (BLAST) in the National Centre for Biotechnology Information (NCBI) GenBank. The software Molecular Evolutionary Genetics Analysis (MEGA) X was

utilized for both sequence alignment and phylogenetic identification.

RESULTS AND DISCUSSION

There were 42 isolated bacteria from chicken manure, as shown in Table 1. All of the isolates were further tested for its enzymatic activity by a qualitative test. The result showed various enzymatic activity results. There are 22 isolates

showing positive results on the amylase screening, 38 isolates showing positive results on the protease screening and 20 isolates showing positive results on the lipase screening. The 10 isolates that show positive results on the 3 enzymatic screening were selected for lipase screening with fish oil and it all showed positive results (Table 1). Based on the Gram staining procedure, all isolates are rod-shaped and belong to the Gram-positive group.

Table 1. Qualitative enzymatic screening of bacteria from local microorganisms from chicken manure

Bacteria isolate code	Amylase screening	Protease screening	Lipase screening using olive oil	Lipase screening using fish oil*
A1	-	+	-	
A2	-	+	-	
A3	-	+	+	
A4	+	-	+	
A5	-	+	+	
A6	+	+	-	
A7	-	+	+	
A8	+	+	-	
A9	-	-	-	
A10	-	+	+	
A11	+	+	+	+
A12	-	+	+	
A13	-	+	+	
A14	-	+	+	
A15	-	+	-	
A16	+	+	+	+
A17	+	+	-	
A18	+	+	-	
A19	+	+	-	
A20	+	+	-	
A21	+	+	+	+
A22	+	+	+	+
A23	+	+	+	+
A24	+	+	+	+
B1	+	+	-	
B2	+	+	-	
B3	-	+	-	
B4	-	-	-	
B5	-	+	+	
B6	-	+	+	
B7	-	+	-	
B8	+	+	+	+
B9	-	+	-	
B10	+	+	+	+
B11	+	+	+	+
B12	+	+	-	
B13	+	+	-	
B14	-	+	-	
B15	+	+	-	
B16	-	+	-	
B17	-	-	-	
B18	+	+	+	+

Notes:

- (+) shows positive result, (-) shows negative result
- The lipase screening using fish oil was only conducted to the isolates that have shown positive results on amylase, protease and lipase screening.

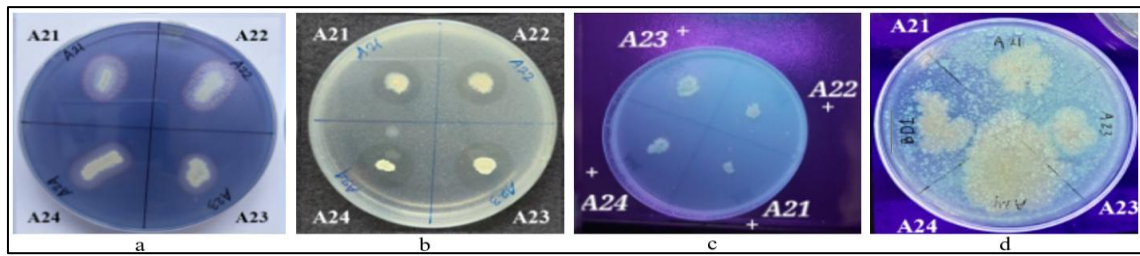


Figure 1. a) Presence of a clear zone around the microbial colony on the starch agar after addition of Lugol's solution indicates that the isolate secretes amylolytic enzymes; b) Presence of a clear zone around the microbial colony on the skim milk agar indicates that the isolate secretes proteolytic enzymes; c) Microbial colony that shows orange fluorescence under UV light indicates that the isolate secretes lipolytic enzymes on olive oil media; d) Microbial colony that showed orange fluorescence under UV light indicates that the isolate secretes lipolytic enzymes on fish oil media.

Screening of Amylolytic Bacteria

Amylase is an enzyme that hydrolyzes starch into simpler sugars, such as glucose and maltose (Sundarram & Murthy, 2014). Among the 42 isolates, 23 isolates showed the ability to hydrolyze starch (Table 1) by the formation of a clear zone around the bacterial colony after 24 h of incubation after the addition of Lugol's solution to the Starch Agar medium (Figure 1a). Brust *et al.* (2020) explained that iodine binding to amylose results in a dark blue color, whereas binding with amylopectin results in a reddish-brown color. The presence of a clear zone indicates the decomposition of starch in the medium, preventing iodine from binding to the starch.

Screening of Proteolytic Bacteria

Protease is an enzyme that can hydrolyze proteins or peptides by breaking the peptide bonds that links amino acid residues in proteins, resulting in shorter peptides and amino acids (Razzaq *et al.*, 2019). Based on research conducted, there were 40 bacterial isolates that could hydrolyze protein (Table 1) by the formation of a clear zone around the bacterial colony after incubation for 24 h on Skim Milk Agar medium (Figure 1b). Pratika *et al.* (2021) stated that a clear zone can form in media containing protein if the inoculated bacteria have proteolytic ability.

Screening of Lipolytic Bacteria

Lipase is an enzyme that can hydrolyze ester bonds in water-insoluble substrates, such as fat compounds (triglycerides), into diglycerides, monoglycerides and fatty acids (Lim *et al.*,

2022). Among the 42 isolates, there were 21 bacterial isolates that could hydrolyze fat (Table 1). It is indicated by the color of bacterial colonies that glow orange when observed under UV light after being incubated for 24 h in media containing olive oil and rhodamine B (Figure 1c). Bartasun *et al.* (2013) stated that rhodamine B binds to free fatty acids that have been decomposed from olive oil by the lipase enzyme, so that it can produce orange fluorescent light when exposed to UV light.

Further screening on 10 bacteria on media containing fish oil showed that the isolated bacteria also have the ability to break down the fat compounds that present in fish oil (Figure 1d). The composition in plant oil and animal oil are different. Olive oil has high content of fatty acids with high level of monounsaturated fatty acids (MUFA), containing up to 85% unsaturated fatty acid with high oleic acid content, linoleic acid and palmitoleic acid and 14% of saturated fatty acid such as palmitic acid and stearic acid (Jimenez-Lopez *et al.*, 2020). Meanwhile fish oil contains saturated fatty acids, MUFAs and PUFAs (Huang *et al.*, 2018). In crude fish oil, the dominant saturated fatty acid is palmitic acid in 21.21 – 26.63% the dominant unsaturated fatty acid is oleic acid in 19.78 – 27.11% and dominant PUFA are eicosapentaenoic acid (EPA) in 6.02 – 9.97%, and docosahexaenoic acid (DHA) in 17.00 – 20.83% (Mgbechidinma *et al.*, 2023). Based on the enzymatic screening results of the isolates that have been conducted, six isolates with the potential to degrade amylase, protein and fat were selected for identification due to their distinct morphological characteristics from each isolate.

Molecular Identification

The phylogenetic tree generated from the 16S rDNA gene sequences of the six isolates showed that the isolates came from the same genus, namely *Bacillus*, with isolate A11 having the highest homology with *Bacillus tequilensis* strain 10b (NR 104919.1), A23 having the highest homology with *Bacillus velezensis* strain ES1-02 (OQ566944.1), A24 having highest homology with *Bacillus amyloliquefaciens* strain NBRC 15535 (NR 041455.1), B8 has the highest homology with *Bacillus amyloliquefaciens* strain W36 (MN922613.1), B10 has the highest homology with *Bacillus subtilis* strain IAM 12118 (NR 112116.2) and B18 has the highest homology with *Bacillus siamensis* KCTC 13613 strain PD-A10 (NR 117274.1). Homology data for isolates and bacteria in GenBank can be seen in Table 2.

The dominance of the *Bacillus* in local microorganisms from chicken manure can be attributed to its prolific growth in the intestines, playing a crucial role in maintaining digestive ecological balance (Su *et al.*, 2020). Previous research by Abinaya *et al.* (2015) has shown that cow dung contains a consortium which has species that were used in wastewater treatment, such as *Pseudomonas aeruginosa*, *P. putida*, *Aspergillus niger*, *Bacillus cereus* and *B. subtilis*. Local microorganisms of chicken

manure are representatives of all five species (Figure 2 and Figure 3).

Bacillus is a gram-positive bacteria that are rod-shaped and endospore-forming. It has the capability to ferment glucose and exploit a wide variety of organic and inorganic substances as nutritional sources. *Bacillus* can be either obligate aerobes which are dependent on oxygen, or facultative anaerobes which can survive in the lack of oxygen (Logan & Vos, 2015). The optimal temperature for its growth is 25 – 40 °C (Hlordzi *et al.*, 2020), and for the pH, it varies between species and varieties, e.g. pH of *B. subtilis* ranges in 5.0 – 9.0 (Gauvry *et al.*, 2021), *B. amyloliquefaciens* ranges in 5.0 – 9.0 (Gotor-Vila *et al.*, 2017), *B. siamensis* ranges in 4.5 – 9.0 (Sumpavapol *et al.*, 2010), *B. tequilensis* ranges in 5.5 – 8.0 (Gatson *et al.*, 2006) and *B. velezensis* ranges in 5.0 – 10.0 (Ji *et al.*, 2021). In response to nutritional or environmental stresses, *Bacillus* produces highly resilient dormant endospores that exhibit resistance to cold, heat, disinfectants, radiation and desiccation. *Bacillus* plays a role in regulating various water quality parameters, including physical aspects like total dissolved solids, and chemical factors such as pH, chemical oxygen demand and biological oxygen demand. They also contribute to mitigating oil spills and maintaining microbial balance (Hlordzi *et al.*, 2020).

Table 2. Molecular identification of potential strain

Bacteria isolate code	Strain	Max score	E-value	Percent identity	GenBank accession
A11	<i>Bacillus tequilensis</i> strain 10b	1544	0.0	98.52%	NR 104919.1
A23	<i>Bacillus velezensis</i> strain ES1-02	2233	0.0	97.77%	OQ566944.1
A24	<i>Bacillus amyloliquefaciens</i> strain NBRC 15535	1770	0.0	98.41%	NR 041455.1
B8	<i>Bacillus amyloliquefaciens</i> strain W36	2123	0.0	97.75%	MN922613.1
B10	<i>Bacillus subtilis</i> strain IAM 12118	1812	0.0	99.30%	NR 112116.2
B18	<i>Bacillus siamensis</i> KCTC 13613 strain PD-A10	1517	0.0	97.42%	NR 117274.1

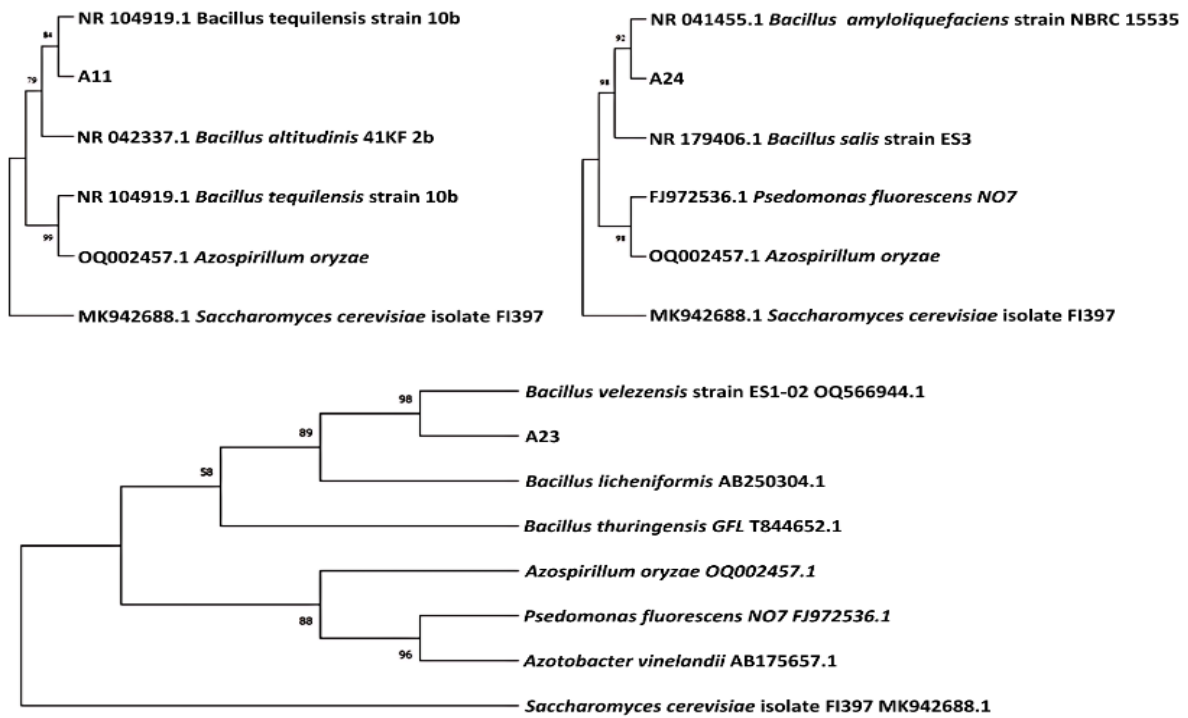


Figure 2. Phylogenetic analysis of identified isolates A11, A23, A24

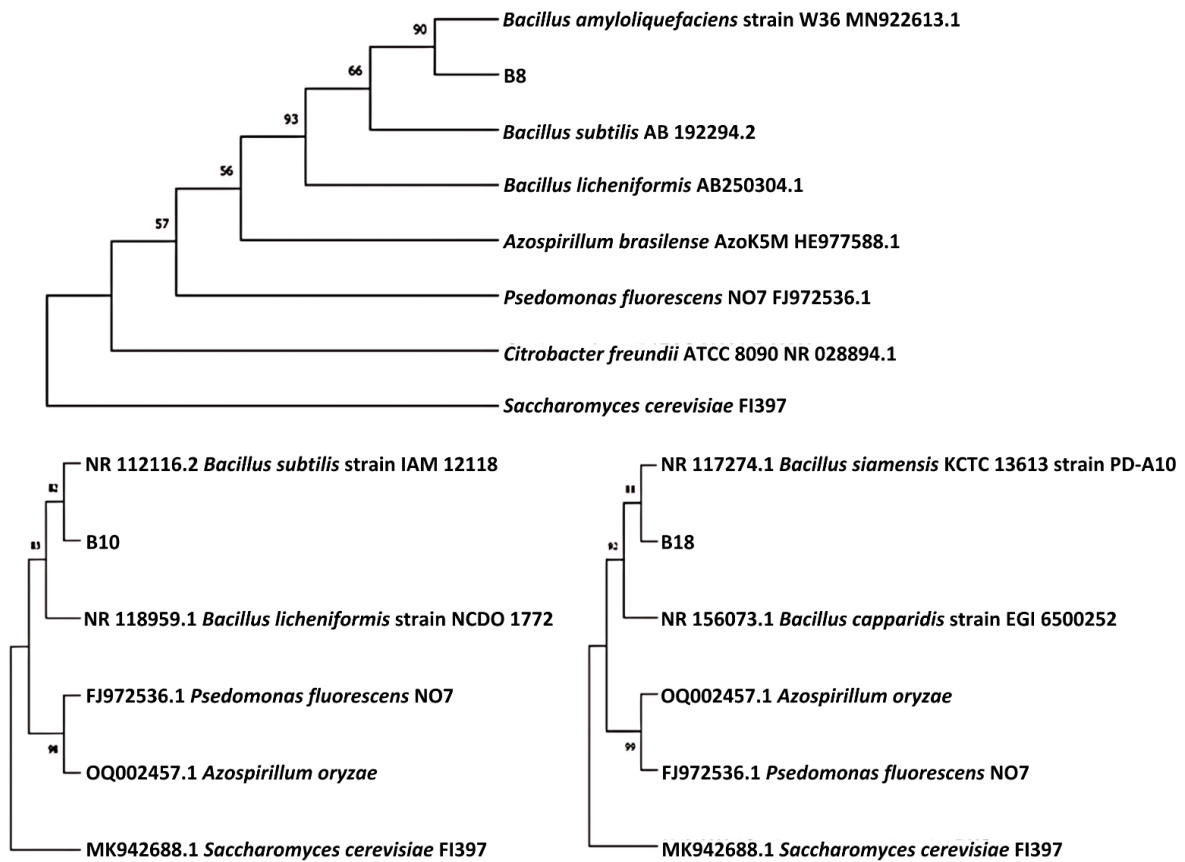


Figure 3. Phylogenetic analysis of identified isolates B8, B10 and B18

Based on previous research, various species of bacteria from the genus *Bacillus* have potential in waste treatment applications. In a study by Othman *et al.* (2023), *B. B. tequilensis*, for instance, shows the ability to degrade ammonia in aquaculture liquid waste with a degradation rate of 89.9% on 100 - 500 mg/L of ammonia concentration (Wang *et al.*, 2023). *B. velezensis* has demonstrated potential in treating various types of wastewater, such as slaughter wastewater (Deng *et al.*, 2022), brewery wastewater (Agunbiade *et al.*, 2022), and pulp and paper wastewater (Nair *et al.*, 2020). *velezensis* was utilized for processing domestic liquid waste from various human activities, encompassing residential, industrial, commercial, livestock and agricultural sectors. The common contaminants found in this liquid waste include organic compounds, nitrogen, phosphorus, heavy metals and other chemical compounds. The analysis conducted by Othman *et al.* (2023) on chemical oxygen demand (COD) levels in the treated domestic liquid waste revealed a decrease after 216 h, from 24 mg/L up to 16.90 mg/L. Additionally, total suspended solid (TSS) analysis showed a significant reduction in the amount of suspended solids from 7.50 mg/L up to 6.41 mg/L. *B. amyloliquefaciens* has shown the ability to treat domestic wastewater by decreasing the concentration of TSS from 2300 mg/L to 1400 mg/L and COD from 925 mg/L up to 133 mg/L (El-Bestawy *et al.*, 2014). *B. subtilis* has demonstrated its efficacy in treating domestic liquid waste with a reduction in biochemical oxygen demand (BOD) values by over 85% until lower than 20 mg/L within two weeks (Meekwamdee *et al.*, 2023). Furthermore, its application has been found to decrease the total value of organic compounds decreased from 86.58 mg/L to 12.74 mg/L, with an efficiency of 85.29% (Anggraini *et al.*, 2019) and significantly increase the denitrification rate with a nitrate decomposition percentage of up to 96%, reducing nitrate concentration to 3.2 mg/L (Rahimi *et al.*, 2020). In a study conducted by Prasad & Manjunath (2011), the utilization of a bacterial consortium including *B. subtilis*, *B. licheniformis*, *B. amyloliquefaciens*, *Serratia marcescens*, *Pseudomonas aeruginosa* and *Staphylococcus aureus*, was examined for the treatment of liquid waste generated by various industrial processes, decreasing BOD from 3500 mg/L to less than 20 mg/L in 12 days. The application of the *B. siamensis* strain ZF1-1 to

livestock waste with high levels of nitrogen and ammonia resulted in a significant reduction from 1277.41 mg/L, with total nitrogen concentration decreased to 22.22% and ammonia to 37.50% (Chen *et al.*, 2020). Additionally, Mehetre *et al.* (2019) found that *B. siamensis* possesses the ability to synthesize bio-surfactant agents, aiding in the binding of waste containing fats and oils.

Additionally, previous research by Sahendra *et al.* (2021) showed that cow dung can be used as an adsorbent in liquid waste processing with COD values of 12 mg/L, BOD 28.72 mg/L, TSS 26.67 mg/L and pH of 6, but there were no mentions of possible microorganisms that were present in the cow dung. Another research by Safitri *et al.* (2015) shows that the use of bacterial consortium including *Bacillus coagulans*, *B. licheniformis*, *B. pumilus*, *B. subtilis*, *Nitrosomonas* sp. and *Pseudomonas putida* were able to reduce the amount of pollutant from industrial wastewater up to 71.93% of BOD, 64.30% of COD, 94.85% of TSS, and 88.58% of ammonia. Research from John *et al.* (2020) has also used bacterial consortium consisting of *B. cereus*, *B. amyloliquefaciens* and *P. stutzeri* to maintain ammonia and nitrite below toxic level in aquaculture wastewater. Biswas *et al.* (2022) has also utilized bacterial consortium consisting of various genera dominated by *Bacillus*, *Vibrio* and *Staphylococcus* species for petrochemical wastewater treatment to reduce up to 88% of BOD content.

CONCLUSION

Based on the research results, among the 42 isolated bacteria from local microorganisms of chicken manure, six bacteria isolates demonstrated the ability to hydrolyze starch, protein and fat based on qualitative tests. These isolates, A11, A23, A24, B8, B10 and B18, all belong to the *Bacillus* genus. The qualitative tests confirmed the potential of these isolates as they exhibited enzymatic activities. Considering their ability, these isolates show promising potential as a bioactivator in the liquid waste treatment.

ACKNOWLEDGEMENTS

Authors would like to thank Wiralodra University, Indramayu for providing funding for this research work.

REFERENCES

- Abd-Elhalim, B.T., Gamal, R.F., El-Sayed, S.M. & Abu-Hussien, S.H. (2023). Optimizing alpha-amylase from *Bacillus amyloliquefaciens* on bread waste for effective industrial wastewater treatment and textile desizing through response surface methodology. *Scientific Reports*, 13(1): p.19216. DOI: 10.1038/s41598-023-46384-6.
- Agunbiade, M., Oladipo, B., Ademakinwa, A.N., Awolusi, O., Adesiyun, I.M., Oyekola, O., Oloade, O. & Ojo, A. (2022). Bioflocculant produced by *Bacillus velezensis* and its potential application in brewery wastewater treatment. *Scientific Reports*, 12(1). DOI: 10.1038/s41598-022-15193-8.
- Anggraini, S. I., Arfiati, D. & Nursyam, H. (2019). Effectiveness of *Bacillus subtilis* bacteria as a total organic matter reducer in catfish pond (*Clarias gariepinus*) cultivation. *International Journal of Biotech Trends and Technology*, 9(2): 7–10. DOI: 10.14445/22490183/ijbtt-v9i2p602.
- Bartasun, P., Cieśliński, H., Bujacz, A., Wierzbicka-Woś, A. & Kur, J. (2013). A study on the interaction of rhodamine B with methylthioadenosine phosphorylase protein sourced from an Antarctic soil metagenomic library. *PLoS One*, 8(1): p.e55697. DOI: 10.1371/journal.pone.0055697.
- Beric, T., Urdaci, M., Stankovic, S. & Knezevic-Vukcevic, J. (2009). RAPD analysis of genetic diversity and qualitative assessment of hydrolytic activities in a collection of *Bacillus* sp. isolate. *Archives of Biological Sciences*, 61(4): 645–652. DOI: 10.2298/abs0904645b.
- Biswas, T., Banerjee, S., Saha, A., Bhattacharya, A., Chanda, C., Gantayet, L.M., Bhadury, P. & Chaudhuri, S.R. (2022). Bacterial consortium based petrochemical wastewater treatment: from strain isolation to industrial effluent treatment. *Environmental Advances*, 7: 100132. DOI: 10.1016/j.envadv.2021.100132.
- Brust, H., Orzechowski, S., & Fettke, J. (2020). Starch and glycogen analyses: methods and techniques. *Biomolecules*, 10(7): 1020. DOI: 10.3390/biom10071020.
- Chen, M., Li, A., Yang, M., Zhang, M., Zhou, L. & Zhu, H. (2020). Analysis of a heterotrophic nitrification bacteria isolated from livestock and poultry wastewater and its nitrogen removal characteristics. *Modern Food Science and Technology*, 10: 50–58.
- Deng, J., Jia, M., Zeng, Y. Q., Li, W., He, J., Ren, J., Bai, J., Zhang, L., Li, J. & Yang, S. (2022). Enhanced treatment of organic matter in slaughter wastewater through live *Bacillus velezensis* strain using nano zinc oxide microsphere. *Environmental Pollution*, 292: 118306. DOI: 10.1016/j.envpol.2021.118306.
- Earl, A.M., Losick, R. and Kolter, R. (2008). Ecology and genomics of *Bacillus subtilis*. *Trends in microbiology*, 16(6): pp.269-275. DOI: 10.1016/j.tim.2008.03.004.
- El-Bestawy, E. (2014). Decontamination of Domestic Wastewater Using Suspended Individual and Mixed Bacteria in Batch System. *Journal of Bioremediation & Biodegradation*, 05(05). DOI: 10.4172/2155-6199.1000231.
- Gameissa, M.W. & Suprihatin, N.S.I. (2012). Pengolahan tersier Limbah Cair Industri Pangan dengan Teknik Elektrokoagulasi Menggunakan Elektroda Stainless Steel. *Agro Industri Indonesia*, 1(1): 31–37.
- Gatson, J.W., Benz, B.F., Chandrasekaran, C., Satomi, M., Venkateswaran, K. & Hart, M.E. (2006). *Bacillus tequilensis* sp. nov., isolated from a 2000-year-old Mexican shaft-tomb, is closely related to *Bacillus subtilis*. *International Journal of Systematic and Evolutionary Microbiology*, 56 (7): 1475–1484. DOI: 10.1099/ijs.0.63946-0.
- Gautam, A. (2022). *DNA Isolation by Chelex method in DNA and RNA isolation techniques for non-experts*. Cham: Springer International Publishing. pp. 79–84.
- Gauvry, E., Mathot, A. G., Couvert, O., Leguérinel, I. & Coroller, L. (2021). Effects of temperature, pH and water activity on the growth and the sporulation abilities of *Bacillus subtilis* BSB1. *International Journal of Food Microbiology*, 337: 108915. DOI: 10.1016/j.ijfoodmicro.2020.108915.
- Gotor-Vila, A., Teixidó, N., Sisquella, M., Torres, R. & Usall, J. (2017). Biological characterization of the biocontrol agent *Bacillus amyloliquefaciens* CPA-8: The effect of temperature, pH and water activity on growth, susceptibility to antibiotics and detection of enterotoxigenic genes. *Current Microbiology*, 74(9): 1089–1099. DOI: 10.1007/s00284-017-1289-8.
- Hadi, R.A. (2019). Pemanfaatan MOL (Mikroorganisme Lokal) dari Materi yang Tersedia di Sekitar Lingkungan. *Agrosience (AGSCI)*, 9(1): 93. DOI:

- 10.35194/agsci.v9i1.637.
- Hlordzi, V., Kuebutornye, F.K.A., Afriyie, G., Abarike, E.D., Lu, Y., Chi, S. & Anokyewaa, M.A. (2020). The use of *Bacillus* species in maintenance of water quality in aquaculture: A review. *Aquaculture Reports*, 18: 100503. DOI: 10.1016/j.aqrep.2020.100503.
- Huang, T.H., Wang, P.W., Yang, S.C., Chou, W.L. & Fang, J.Y. (2018). Cosmetic and therapeutic applications of fish oil's fatty acids on the skin. *Marine Drugs*, 16(8): 256. DOI: 10.3390/md16080256.
- Hui, C., Guo, X., Sun, P., Khan, R.A., Zhang, Q., Liang, Y. & Zhao, Y.H. (2018). Removal of nitrite from aqueous solution by *Bacillus amyloliquefaciens* biofilm adsorption. *Bioresource Technology*, 248: 146–152. DOI: 10.1016/j.biortech.2017.06.176.
- Indasah, I. & Muhith, A. (2020). Local Microorganism From “Tape” (Fermented Cassava) In composition and its effect on physical, chemical and biological quality in environmental. IOP Conference Series: *Earth and Environmental Science*, 519: 012003. DOI: 10.1088/1755-1315/519/1/012003.
- Ji, C., Wang, X., Song, X., Zhou, Q., Li, C., Chen, Z., Gao, Q., Li, H., Li, J., Zhang, P. & Cao, H. (2021). Effect of *Bacillus velezensis* JC-K3 on endophytic bacterial and fungal diversity in wheat under salt stress. *Frontiers in Microbiology*, 12. DOI: 10.3389/fmicb.2021.802054.
- Jimenez-Lopez, C., Carpena, M., Lourenço-Lopes, C., Gallardo-Gomez, M., Lorenzo, J.M., Barba, F.J., Prieto, M.A. & Simal-Gandara, J. (2020). Bioactive compounds and quality of extra virgin olive oil. *Foods*, 9(8): 1014. DOI: 10.3390/foods9081014.
- John, E.M. Krishnapriya, K. & Sankar, T. (2020). Treatment of ammonia and nitrite in aquaculture wastewater by an assembled bacterial consortium. *Aquaculture*, 526: 735390. DOI: 10.1016/j.aquaculture.2020.735390.
- Lim, S.Y., Steiner, J.M. & Cridge, H. (2022). Lipases: it's not just pancreatic lipase! *American Journal of Veterinary Research*, 83(8). DOI: 10.2460/ajvr.22.03.0048.
- Logan, N.A. & Vos, P.D. (2015). *Bacillus*. *Bergey's manual of systematics of archaea and bacteria*, pp.1-163. DOI: 10.1002/9781118960608.gbm00530.
- Meekwamdee, B., Suebsaiprom, W. & Chunhachart, O. (2023). Study on effective of *Bacillus subtilis* for domestic wastewater treatment in the royal thai army chemical department area. *Journal of Namibian Studies: History Politics Culture*, 33. DOI: 10.59670/jns.v33i.1014.
- Mehetre, G. T., Dastager, S. G. & Dharne, M. S. (2019). Biodegradation of mixed polycyclic aromatic hydrocarbons by pure and mixed cultures of biosurfactant producing thermophilic and thermo-tolerant bacteria. *Science of the Total Environment*, 679: 52–60. DOI: 10.1016/j.scitotenv.2019.04.376.
- Mgbechidinma, C.L., Zheng, G., Baguya, E.B., Zhou, H., Okon, S.U. & Zhang, C. (2023). Fatty acid composition and nutritional analysis of waste crude fish oil obtained by optimized milder extraction methods. *Environmental Engineering Research*, 28(2). DOI: 10.4491/eer.2022.034.
- Nair, A.S., Al-Bahry, S. & Sivakumar, N. (2020). Co-production of microbial lipids and biosurfactant from waste office paper hydrolysate using a novel strain *Bacillus velezensis* ASN1. *Biomass Conversion and Biorefinery*, 10(2): pp.383-391. DOI: 10.1007/s13399-019-00420-6.
- Othman, M.F., Abu Hasan, H., Muhamad, M.H. & S. Babaqi, B. (2023). Biopolishing of Domestic Wastewater Using Polyvinyl Alcohol – Supported Biofilm of Bacterial Strain *Bacillus velezensis* Isolate JB7. *Journal of Ecological Engineering*, 24(8): 33–42. DOI: 10.12911/22998993/165780.
- Pervez, M.N., Mishu, M.R., Stylios, G.K., Hasan, S.W., Zhao, Y., Cai, Y., Zarra, T., Belgiorno, V. & Naddeo, V. (2021). Sustainable treatment of food industry wastewater using membrane technology: A short review. *Water*, 13(23): p.3450. DOI: 10.3390/w13233450.
- Prasad, M.P. & Manjunath, K. (2011). Comparative study on biodegradation of lipid-rich wastewater using lipase producing bacterial species. *Indian Journal of Biotechnology*, 10: 121–124.
- Pratika, M., Ananda, M. & Suwastika, I.N. (2021). Protease activity from bacterial isolates of *Nepenthes maxima* reinw. ex nees. *Journal of Physics: Conference Series*, 1763(1): 012092. DOI: 10.1088/1742-6596/1763/1/012092
- Rahimi, S., Modin, O., Roshanzamir, F., Neissi, A., Saheb Alam, S., Seelbinder, B., Pandit, S., Shi, L. & Mijakovic, I. (2020). Co-culturing *Bacillus subtilis* and wastewater microbial community in a bio-electrochemical system enhances

- denitrification and butyrate formation. *Chemical Engineering Journal*, 397: 125437. DOI: 10.1016/j.cej.2020.125437.
- Ravel J. & Fraser C.M. (2005). Genomics at the genus scale. *Trends Microbiol*, 13(3): 95-97. DOI: 10.1016/j.tim.2005.01.004.
- Razzaq, A., Shamsi, S., Ali, A., Ali, Q., Sajjad, M., Malik, A. & Ashraf, M. (2019). Microbial proteases applications. *Frontiers in Bioengineering and Biotechnology*, 7. DOI: 10.3389/fbioe.2019.00110.
- Safitri, R., Priadie, B., Miranti, M. and Astuti, A.W. (2015). Ability of bacterial consortium *Bacillus coagulans*, *Bacillus licheniformis*, *Bacillus pumilus*, *Bacillus subtilis*, *Nitrosomonas* sp., and *Pseudomonas putida* in bioremediation of Waste Water in Cisirung Waste Water Treatment Plant. *AgroLife Scientific Journal*, 4(1): 146-152.
- Sahendra, S.L., Hamsyah, R.A. & Sa'diyah, K., (2021). Pengolahan Limbah Cair Pabrik Gula Menggunakan Adsorben dari Kotoran Sapi dan Ampas Tebu. *Chemical Engineering Research Articles*, 4(1): pp.31-38. DOI: 10.25273/cheesa.v4i1.8416.31-38.
- Sandle, T. (2016). *Pharmaceutical Microbiology*. Woodhead Publishing. DOI: 10.1016/c2014-0-00532-1.
- Sondhi, S., Kumar, D., Angural, S., Sharma, P. & Gupta, N. (2018). Enzymatic approach for bioremediation of effluent from pulp and paper industry by thermo alkali stable laccase from *Bacillus tequilensis* SN4. *Journal of Commercial Biotechnology*, 23(4). DOI: 10.5912/jcb799.
- Su, Y., Liu, C., Fang, H. & Zhang, D. (2020). *Bacillus subtilis*: a universal cell factory for industry, agriculture, biomaterials and medicine. *Microbial Cell Factories*, 19 (1). DOI: 10.1186/s12934-020-01436-8.
- Sundarram, A. & Murthy, T.P.K. (2014). α -amylase production and applications: a review. *Journal of Applied & Environmental Microbiology*, 2(4): pp.166-175. DOI: 10.12691/jaem-2-4-10.
- Sumpavapol, P., Tongyonk, L., Tanasupawat, S., Chokesajjawatee, N., Luxananil, P., and Visessanguan, W. (2010). *Bacillus siamensis* sp. nov., isolated from salted crab (poo-khem) in Thailand. *International Journal of Systematic and Evolutionary Microbiology*, 60(10):2364–2370. DOI: 10.1099/ij.s.0.018879-0.
- Turnbull PCB. (1996). *Bacillus*. In: Baron S, editor. *Medical microbiology*. 4th ed. galveston (TX): University of Texas Medical Branch at Galveston. Chapter 15. PMID: 21413260.
- Wang, Z., Liu, H. & Cui, T. (2023). Identification of a strain degrading ammonia nitrogen, optimization of ammonia nitrogen degradation conditions, and gene expression of key degrading enzyme nitrite reductase. *Fermentation*, 9(4): 397. DOI: 10.3390/fermentation9040397.
- Yunilas, Y., Siregar, A.Z., Mirwhandhono, E., Purba, A., Fati, N., & Malvin, T. (2022). Potensi dan Karakteristik Larutan Mikroorganisme Lokal (MOL) Berbasis Limbah Sayur sebagai Bioaktivator dalam Fermentasi. *Journal of Livestock and Animal Health*, 5(2), 53–59. DOI: 10.32530/jlah.v5i2.540.
- Zaman, B., Sutrisno, E., Sudarno, S., Simanjutak, M.N. & Krisnanda, E. (2020). Natural Soil as Bio-activator for Wastewater Treatment System. *IOP Conference Series: Earth and Environmental Science*, 448(1): 012032. DOI: 10.1088/1755-1315/448/1/012032.

Antagonistic Potential of a Phosphate Solubilizing Bacteria (*B. cereus* PS1.1, *B. cereus* PS1.2, *B. cereus* PS1.4) Against the Patogent Fungus *Ganoderma* sp. Isolated from Basal Stem of Oil Palm (*Elaeis guineensis* Jacq.) with Rot Disease

SITI KHOTIMAH*, RAHMAWATI, MUKARLINA & ADE INDRIANI

Faculty of Mathematics and Natural Sciences, Tanjungpura University, Pontianak, West Kalimantan, Indonesia

*Corresponding author: siti.khotimah@fmipa.untan.ac.id

Received: 25 April 2024

Accepted: 6 September 2024

Published: 31 December 2024

ABSTRACT

Ganoderma sp. is a pathogenic fungus whose attack can cause basal stem rot disease of oil palm (*Elaeis guineensis* Jacq.). Disease control using phosphate solubilizing bacteria (PSB), namely *Bacillus cereus* can be an alternative to biological control. The purpose of this study was to determine the antagonistic ability of PSB (*B. cereus* PS1.1, *B. cereus* PS1.2, *B. cereus* PS1.4) in inhibiting the growth of *Ganoderma* sp. BP1 and changes in hyphal morphology of *Ganoderma* sp. BP1 after antagonistic testing. The research was conducted from January to May 2023 at the Microbiology Laboratory, Department of Biology, Faculty of Mathematics and Natural Sciences, Tanjungpura University, Pontianak. Antagonist testing used a completely randomized design (CRD) with the treatments consisted of *Ganoderma* sp. BP1 (negative control), 1% hexaconazole fungicide (positive control), PSB isolates PS1.1, PS1.2 and PS1.4. The test method used the dual culture on *Sabouraud Dextrose Agar* (SDA) media with each treatment repeated four times so that 20 experimental units were obtained. The results showed that PSB isolate PS1.4 had strong inhibition with an inhibition zone diameter of 11.01 mm, while isolates PS1.1 and PS1.2 had moderate inhibition with inhibition zone diameters of 9.43 mm and 9.45 mm, respectively, against *Ganoderma* sp. BP1. Hyphal morphology changes in of *Ganoderma* sp. BP1 that occurred after the antagonist test consist of lysed hyphae, twisted hyphae, hook-like hyphal tips, curly hyphae, bulbous hyphae, branched hyphae and bent hyphal ends.

Keywords: Antagonistic test, *Bacillus cereus*, biological control, *Ganoderma* sp., inhibition zone, phosphate solubilizing bacteria (PSB).

Copyright: This is an open access article distributed under the terms of the CC-BY-NC-SA (Creative Commons Attribution-NonCommercial-ShareAlike 4.0 International License) which permits unrestricted use, distribution, and reproduction in any medium, for non-commercial purposes, provided the original work of the author(s) is properly cited.

INTRODUCTION

Oil palm (*Elaeis guineensis* Jacq.) is a leading plantation commodity in Indonesia, especially West Kalimantan. Based on the economic sector, this plantation crop is useful as a producer of edible oil, industrial oil and biofuel (biodiesel) (Rosmegawati, 2021). The problem faced by oil palm plantations in Indonesia to date is the increasing attack of basal stem rot disease (BSR) caused by the pathogen *Ganoderma boninense*. Losses caused by *G. boninense* attacks can reach 50% (Prasetyo *et al.*, 2008). The attack of *G. boninense* causes the death of more than 80% of the entire population in several plantations in Indonesia, and the result of the transmission of this pathogen causes a decrease in oil palm production per unit area (Susanto *et al.*, 2013).

Basal stem rot is a soil borne fungus that attacks old and young plants (Ummi, 2018). The fungus *G. boninense* can attack oil palms at the nursery and production stages. Oil palms that are not handled properly at the beginning of their growth/nursery, the pathogen will spread throughout the planting area (Semangun, 2008). Efforts to control the pathogen *G. boninense* are still being developed to overcome the BSR problem.

The most common effort to control the pathogen *G. boninense* is using synthetic pesticides, but the unwise use of pesticides will cause environmental residues, various health problems, and other ecological balance disorders (Istikorini, 2002). The use of environmentally friendly biological agents is an effort that can be made, one of which is using phosphate solubilizing bacteria (PSB). Plants that

experience phosphorus (P) nutrient deficiency make plants susceptible to disease, so the use of PSB can be used as a biocontrol that can improve root health and plant growth through its protection against disease so that it plays an important role in suppressing plant diseases (Sela *et al.*, 2022).

Bacteria that act as phosphate solvents in soil have been found, including those from the *Bacillus* genus (Ekowati *et al.*, 2022). The *Bacillus* genus is able to compete with pathogens by producing several secondary metabolites such as antibiotics, siderophores, bacteriocins and extracellular enzymes, inducing plant resistance compounds and producing antibiotic compounds such as chitinase enzymes that can hydrolyze fungal cell walls (Javandira *et al.*, 2013). Exposure to these antimicrobial compounds can cause the hyphae of pathogenic fungi to become abnormal in the form of lysed hyphae, twisted hyphae, curled hyphae, dwarf hyphae, branched hyphae and twisted hyphae, meaning that these antagonistic bacteria are able to compete with pathogenic fungi (Asril, 2011).

Research on biological control in the research of Mahmud *et al.* (2020) showed that *T. virens* has a high inhibition against *G. boninense* of 73.5% in vitro. Fitriatin *et al.* (2020) stated that the phosphate solubilizing microbial group (*Pseudomonas mallei*, *P. cepacea*, *B. subtilis*, *B. megaterium*, *Penicillium* sp. and *Aspergillus niger*) was able to inhibit *Fusarium* sp. antagonistically. Research by Asril *et al.* (2022) stated that PSB with isolate code EF. NAP8 has antagonistic activity against acacia plant pathogenic fungi, namely *Ganoderma philippii* and *Fusarium oxysporum* with a percentage inhibition of 34.44% and 33.33%, respectively.

PSB isolates (*B. cereus* PS1.1, *B. cereus* PS1.2, *B. cereus* PS1.4) isolated from peat soil in Teluk Bakung Village, Ambawang District, Kubu Raya Regency were able to dissolve phosphate with a phosphate solvent index ranging from 1.1-2.9 (Khotimah, 2021). Based on this description, it is necessary to further study the local PSB isolates (*B. cereus* PS1.1, *B. cereus* PS1.2, *B. cereus* PS1.4) in inhibiting the growth of the fungus *Ganoderma* sp. BP1 isolated from the basal of rotten-symptomatic oil palm trunks in West Kalimantan.

MATERIALS AND METHODS

Media Preparation

A total of four media were used in this study, namely Potato Dextrose Agar (PDA) (Merck) + ciprofloxacin 0.01 g, Pikovskaya's Agar (PA) (HiMedia), Nutrient Broth (NB) (Merck) and Sabouraud Dextrose Agar (SDA) (Merck). PDA as fungal media, PA as media for rejuvenating phosphate-solubilizing bacteria, NB as phosphate-solubilizing bacteria suspension media, and SDA as antagonist test media. The media were sterilized using an autoclave at 121 °C pressure 1 atm for 15 minutes (Atlas, 2004; Waluyo, 2008).

Rejuvenation of Phosphate-Solubilizing Bacteria

Isolates of phosphate solubilizing bacteria (*B. cereus* PS1.1, *B. cereus* PS1.2, *B. cereus* PS1.4) (collection of Microbiology laboratory, Department of Biology, Faculty of Mathematics and Natural Sciences, Tanjungpura University by Khotimah, 2021), then inoculated on Pikovskaya's agar media by taking 1 ose of bacterial colonies. The isolate obtained was then scratched into a test tube containing Pikovskaya's agar media. Bacterial isolates that have been scratched on slanted agar media are incubated at room temperature for 24 hours (Yati, 2019).

Rejuvenation *Ganoderma* sp.

The hyphae of *Ganoderma* sp. BP1 (isolated from the basal of oil palm trunks with rotten symptoms in oil palm plantations in Sungai Nipah Village, Teluk Pakedai District, Kubu Raya Regency), were taken and inoculated using a straight ose needle at three points on PDA media in a petri dish, then incubated for 7 days at room temperature (Purnamasari *et al.*, 2012).

Preparation of Test Suspension of Phosphate-Solubilizing Bacteria

Culture of phosphate solubilizing bacteria *B. cereus* that has been rejuvenated was taken 1 ose, then inoculated in 50 mL of NB media and incubated at room temperature for 12 hours using a shaker at 120 rpm. The 12-hour-old bacterial suspension was then measured for optical density using a UV-Vis

spectrophotometer with a wavelength of 600 nm until the absorbance value was 0.8-1 (Son *et al.*, 2012) with an estimated number of bacteria in the suspension of 1.5×10^8 CFU cells/mL (Claudia *et al.*, 2021).

Antagonism Testing of Phosphate-Solubilizing Bacterial Isolate *Bacillus cereus* against *Ganoderma* sp.

The method used refers to Suryanto *et al.* (2016), namely the modified dual culture method using SDA media by observing the direct interaction that occurs between antagonistic agents and pathogens. Culture of *Ganoderma* sp. BP1 was cut using a sterile cork borer with a diameter of 6 mm, then placed on 20 mL of SDA media in the center of the Petri dish (negative control). *Ganoderma* sp. was first grown to ± 20 mm in diameter on the third day (Nisa *et al.*, 2020). Sterile Whatman No.1 paper with a diameter of 6 mm was soaked into a suspension of antagonistic bacteria that had an optical density

with an absorbance value of 0.8-1 or soaked with 1% hexaconazole fungicide (0.1 mL of fungicide plus distilled water diluted to 10 mL) (positive control) for 30 minutes. The filter paper was then placed on the edge of the petri dish within 3 cm each on the left and right from the center of the fungal colony (Flori *et al.*, 2020; Sakinah & Enny, 2014). Observations of the diameter of the antagonism power were observed until *Ganoderma* sp. BP1 in the negative control filled the petri dish (Nisa *et al.*, 2020), namely on the sixth day. The scheme of laying the test of antagonistic bacteria and pathogenic fungi can be seen in (Figure 1). Observations of inhibition diameter were measured from the first day after planting into SDA media until the sixth day. How to calculate the diameter of inhibition using the following formula : Diameter of inhibition = $\frac{y-x}{2}$ (Suryanto *et al.*, 2016). According to David and Stout (1971), the ability of antagonism can be grouped into four categories of inhibition based on the diameter of the inhibition (Table 1).

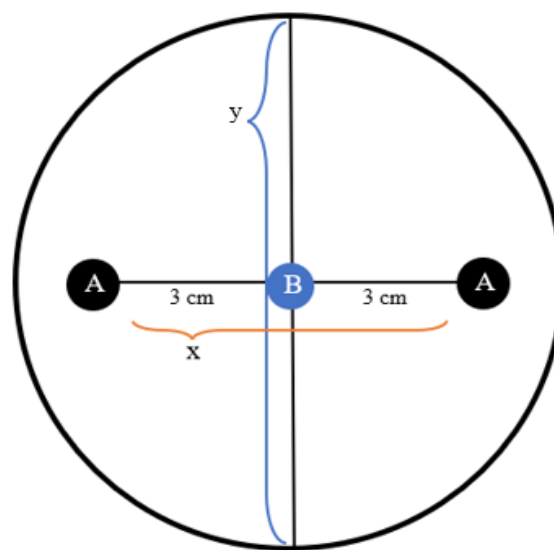


Figure 1. Schematic of the placement of antagonistic bacteria and pathogenic fungi. (A). Filter paper soaked with antagonistic bacteria, (B). Culture of pathogenic fungi (Suryanto *et al.*, 2016)

Table 1. Category of inhibition diameter

Diameter of inhibition (mm)	Category (David dan Stout 1971)
> 20 mm	Very strong
11-20 mm	Strong
6-10 mm	Moderate
≤ 5 mm	Weak

Observation of Mycelium of Pathogenic Fungus After Antagonist Test

Observation of fungal mycelium is done in two ways, namely visually and microscopically. Visual observation is done by looking at the growth zone of the fungal mycelium. Microscopic observations were made by observing the tip of the fungal mycelium in the inhibition zone. The surface of the SDA media containing the tip of the mycelium of *Ganoderma* sp. fungus inhibited by phosphate solubilizing bacteria was cut 1x1 cm, then placed on a glass object and covered with a cover glass (Suryanto *et al.*, 2012). Hyphae were observed under a light microscope with a magnification of 400× and examined for the presence or absence of abnormal morphology of the fungus mycelium, such as bending of the tip of the mycelium, broken mycelium, split mycelium, branched mycelium, lysed mycelium or stunted mycelium growth (Lorito *et al.*, 1993). According to Halo *et al.*, (2019) hyphae with abnormal morphology can be bent hyphae, hook-like hyphal ends, narrowed hyphae, lysed hyphae, swollen hyphae and hyphae with protrusions.

Data Analysis

Data analysis using one-way analysis of variance (ANOVA) at the 95% confidence level, if it shows a significant effect, then the Duncan Multiple Range test will be carried out at the 5% level using SPSS 26.0 software (Dendang, 2015).

RESULTS

Antagonistic Test of Phosphate-Solubilizing Bacterial Isolates *Bacillus cereus* against *Ganoderma* sp.

The results of the antagonistic test observed on the sixth day after incubation between phosphate-solubilizing bacterial isolates (*B. cereus* PS1.1, *B. cereus* PS1.2, *B. cereus* PS1.4) against *Ganoderma* sp. BP1 fungal isolates on SDA media showed inhibition in the treatment (Figure 2).

Based on the measurement of the diameter of the inhibition of PSB isolates (*B. cereus* PS1.1, *B. cereus* PS1.2, *B. cereus* PS1.4) against the fungus *Ganoderma* sp. BP1, the highest inhibition diameter with a very strong inhibition category in treatment P2 (positive control), namely using 1% hexaconazole fungicide by 24.50 mm, strong inhibition category in treatment P5 (*B. cereus* PS1.4 vs. *Ganoderma* sp. BP1) by 11.01 mm, and the moderate inhibition category in the P3 treatment (*B. cereus* PS1.1 vs *Ganoderma* sp. BP1) at 9.43 mm and P4 (*B. cereus* PS1.2 vs *Ganoderma* sp. BP1) at 9.45 mm (Table 2). The results of ANOVA analysis showed that each treatment had a significant difference in inhibition diameter ($P < 0.05$), meaning that there was a significant effect on the average inhibition diameter. Based on the results of the Duncan Multiple Range test at the 95% confidence level, it is known that treatment P1 (negative control) is significantly different from P2 (positive control), P3 (*B. cereus* PS1.1 vs *Ganoderma* sp. BP1), P4 (*B. cereus* PS1.2 vs *Ganoderma* sp. BP1) and P5 (*B. cereus* PS1.4 vs *Ganoderma* sp. BP1). Treatment P2 (positive control) was significantly different from treatment P1 (negative control), P3 (*B. cereus* PS1.1 vs *Ganoderma* sp. BP1), P4 (*B. cereus* PS1.2 vs *Ganoderma* sp. BP1) and P5 (*B. cereus* PS1.4 vs *Ganoderma* sp. BP1). Treatment P3 was not significantly different from treatment P4 (*B. cereus* PS1.2 vs *Ganoderma* sp. BP1) but significantly different from P1 (negative control), P2 (positive control) and P5 (*B. cereus* PS1.4 vs *Ganoderma* sp. BP1).

Table 2. Mean diameter of inhibition against *Ganoderma* sp. BP1 on the sixth day after incubation

Treatments	Mean diameter of inhibition on day six ± SD (mm)	Category David dan Stout (1971)
P1 (<i>Ganoderma</i> sp.)	0,00±0,00 ^a	No Inhibition
P2 (Fungisida Heksakonazol 1% vs <i>Ganoderma</i> sp. BP1)	24,50±0,31 ^b	Very Strong
P3 (<i>B. cereus</i> PS1.1 vs <i>Ganoderma</i> sp. BP1)	9,43±0,58 ^c	Moderate
P4 (<i>B. cereus</i> PS1.2 vs <i>Ganoderma</i> sp. BP1)	9,45±0,81 ^c	Moderate
P5 (<i>B. cereus</i> PS1.4 vs <i>Ganoderma</i> sp. BP1)	11,01±1,17 ^d	Strong

Notes: Mean numbers followed by the same letter in the same column indicate results that are not significantly different in the Duncan test at the 95% confidence level

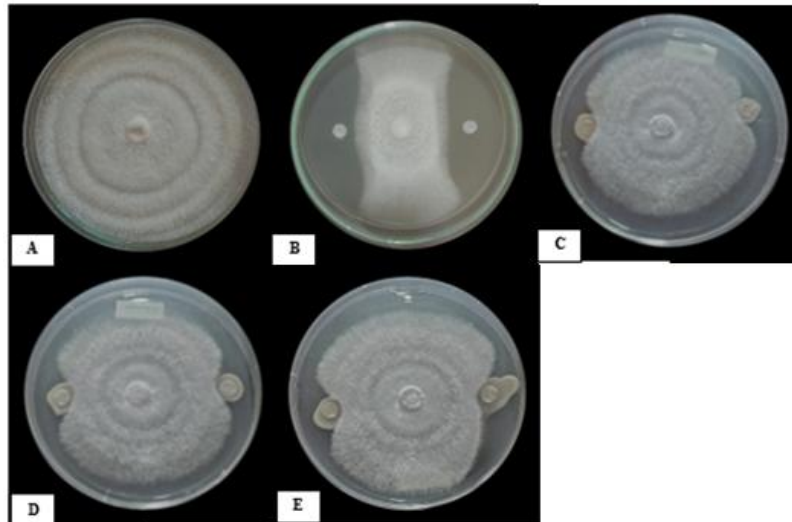


Figure 2. Antagonistic test results of phosphate-solubilizing bacteria (*B. cereus* PS1.1, *B. cereus* PS1.2, *B. cereus* PS1.4) against *Ganoderma* sp. BP1 on the sixth day after incubation. (a). Negative control, (b). Positive control, (c). *B. cereus* PS1.1 vs *Ganoderma* sp. BP1, (d). *B. cereus* PS1.2 vs *Ganoderma* sp. BP1, (e). *B. cereus* PS1.4 vs *Ganoderma* sp. BP1

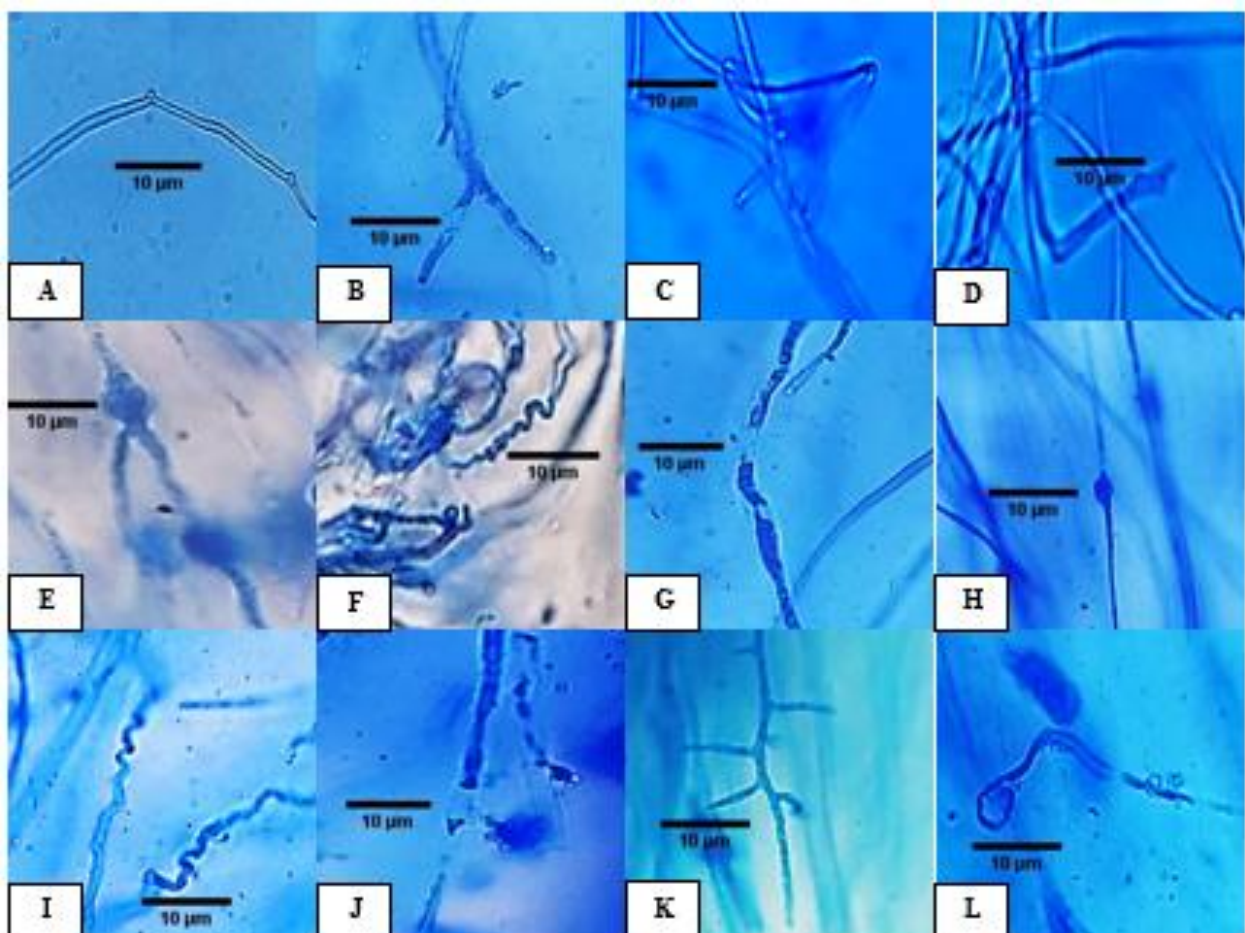


Figure 3. Abnormal hyphae shape on *Ganoderma* sp. BP1 after antagonistic test. (a). Normal hyphae (negative control); 1% hexaconazole effect (positive control): (b). Lysed hyphae, (c). Twisted Hyphae, (d). Hook-like hyphae tip; effect of isolate PS1.1: (e). Round-shaped Hyphae, (f). Curly hyphae; effect of isolate PS1.2: (g). Lysed hyphae, (h). Round-shaped hyphae, (i). Curly hyphae; effect of isolate PS1.4: (j). Lysed hyphae, (k). Branched hyphae, (l). Tip of hyphae bent. Scale = 10µm, magnification = 400×

Treatment P5 (*B. cereus* PS1.4 vs *Ganoderma* sp. BP1) was significantly different from treatments P1 (negative control), P2 (positive control), P3 (*B. cereus* PS1.1 vs *Ganoderma* sp. BP1) and P4 (*B. cereus* PS1.2 vs *Ganoderma* sp. BP1) (Table 2).

Microscopic Hyphae of *Ganoderma* sp. after Antagonist Test

Microscopic observations to see the abnormal hyphal morphology of *Ganoderma* sp. BP1 were made on the seventh day. Due to the antagonistic activity of phosphate solubilizing bacteria (*B. cereus* PS1.1, *B. cereus* PS1.2, *B. cereus* PS1.4), the hyphae of *Ganoderma* sp. BP1 experienced abnormal growth. Treatment P1 (negative control) had normal *Ganoderma* sp. BP1 hyphae. Treatment P2 (positive control) caused lysed hyphae, twisted hyphae, and hook-like hyphal tips. Treatment P3 (*B. cereus* PS1.1 vs *Ganoderma* sp. BP1) caused round hyphae, and curly hyphae. Treatment P4 (*B. cereus* PS1.2 vs *Ganoderma* sp. BP1) caused lysed hyphae, round hyphae, and curly hyphae. Treatment P5 (*B. cereus* PS1.4 vs *Ganoderma* sp. BP1) caused lysed hyphae, branched hyphae and bent hyphae tips (Figure 3).

DISCUSSION

PSB isolates (*B. cereus* PS1.1, *B. cereus* PS1.2, *B. cereus* PS1.4) were tested against *Ganoderma* sp. BP1 fungus to see their inhibitory ability. The inhibition ability of each treatment began on the fourth day after the pathogenic fungus *Ganoderma* sp. BP1 was inoculated until the negative control *Ganoderma* sp. BP1 filled the petri dish on the sixth day. Treatment P1 (negative control) *Ganoderma* sp. BP1 colonies without treatment of PSB bacteria (*B. cereus* PS1.1, *B. cereus* PS1.2, *B. cereus* PS1.4) grew well because there was no competition so that the nutrients were fulfilled. Based on the antagonist test, the three PSB isolates (*B. cereus* PS1.1, *B. cereus* PS1.2, *B. cereus* PS1.4) and the positive control using hexaconazole 1% were able to suppress the growth of *Ganoderma* sp. BP1 (Figure 2) with varying diameters of inhibition (Table 2). This condition states that PSB isolates have the ability as antagonistic agents against the pathogenic fungus *Ganoderma* sp. BP1 through their ability to produce several growth inhibitory compounds. According to Loekas (2008), antagonistic

bacteria release an inhibitory compound that can lyse the membranes of pathogenic fungi and disrupt their metabolic systems, so that the pathogenic fungi no longer have the ability to infect their host plants.

The results of measurements and observations showed that the treatment of PSB isolate P5 (*B. cereus* PS1.4 vs *Ganoderma* sp. BP1) had a strong inhibition category, and the treatments P3 (*B. cereus* PS1.1 vs *Ganoderma* sp. BP1) and P4 (*B. cereus* PS1.2 vs *Ganoderma* sp. BP1) had a moderate inhibition category (Table 2). The difference in the diameter of inhibition of each treatment of PSB isolates is thought to be because PSB isolates have different levels of ability to produce antimicrobial compounds. The size of the inhibition diameter produced is thought to be influenced by the sensitivity of the fungi and bacteria tested, the suspension of bacterial culture and the amount of antimicrobial compounds produced by bacteria. According to Cappucino & Sherman (2013), there are factors that affect the formation of inhibition zones, namely the speed of growth of the test microbes, the number of microbes tested, the level of microbial sensitivity to antimicrobial compounds, as well as the diffusion ability of antimicrobial compounds into the media and their interaction with the tested microbes. The ability of each bacterial isolate to inhibit the growth of *Ganoderma* sp. fungi is likely due to the antimicrobial compounds produced by each PSB isolate.

The results of measurements and observations of treatment P2 (1% hexaconazole vs *Ganoderma* sp. BP1) have a very strong inhibition category. Hexaconazole is a potential fungicide that is often used in oil palm plantations to control basal stem root (BSR) disease caused by *Ganoderma boninense* (Maznah *et al.*, 2015). Hexaconazole is a systemic, protectant and eradicant fungicide of the triazole class (Kalam and Mukherjee, 2001). Systemic eradication power to all parts of the plant, namely through xylem vessels (Djojsumarto, 2008). The mechanism of action of triazole class fungicides is based on inhibition of ergosterol biosynthesis. Ergosterol is a compound derived from sterols and is a specific membrane constituent component in fungi that are not found in other microorganisms (Pratiwi, 2002). Triazole fungicides are known to have

broad-spectrum efficacy against *Ascomycetes*, *Basidiomycetes*, and *Deuteromycetes* fungi (Wahyuni *et al.*, 2018).

Microscopic observations to see the abnormal hyphal morphology of *Ganoderma* sp. BP1 after the antagonist test were carried out on the seventh day. The antagonistic mechanism that occurs results in changes in the hyphal structure of the *Ganoderma* sp. BP1 fungus caused by PSB (*B. cereus* PS1.1, *B. cereus* PS1.2, *B. cereus* PS1.4) and hexaconazole fungicide. Treatment P1 (negative control) of *Ganoderma* sp. BP1 hyphae looked normal (Figure 3a) due to the absence of competition with antagonistic bacteria. The P2 treatment (1% hexaconazole vs *Ganoderma* sp. BP1) caused hyphae lysis, hyphae twisting and hook-like hyphae tips (Figures 3b, c, d). The abnormal hyphae are thought to be due to the active ingredient compound of the fungicide hexaconazole causing changes in the hyphal structure by disrupting its shape and function. Situmorang *et al.* (2015) stated that fungicides that enter important parts of the fungus will indeed interfere with the function of these parts and work to change the shape and composition of the cell wall by limiting essential enzymes in the cell or changing the metabolic rate, but does not mean inhibiting all enzymes produced by the fungus. Hexaconazole which is a systemic fungicide can cause disruption of fungal cell wall synthesis, cell membrane synthesis and function, also affects energy generation in cells and metabolic intermediates, disrupts lipid synthesis and cell nucleus function (Sijpesteijn, 1970).

Treatment P3 (*B. cereus* PS1.1 vs *Ganoderma* sp. BP1) caused round hyphae and curly hyphae (Figures 3e, f). Treatment P4 (*B. cereus* PS1.2 vs *Ganoderma* sp. BP1) caused lysed hyphae, round hyphae and curly hyphae (Figures 3g, h, i). Treatment P5 (*B. cereus* PS1.4 vs *Ganoderma* sp. BP1) caused lysed hyphae, branched hyphae, and bent hyphal tips (Figures 3j, k, l). The abnormal hyphae that occurred were thought to be due to antifungal compounds produced by the PSB isolates and due to the defense mechanism of *Ganoderma* sp. BP1 against PSB. Lysis of hyphae indicates that PSB isolates are able to hydrolyze the cell wall of *Ganoderma* sp. Pathogenic fungal hyphae that experience swelling are thought to be a defense mechanism of the pathogen against isolate attack (Asril *et al.*, 2022).

Ganoderma sp. BP1, which experienced abnormal hyphal growth after antagonistic testing, could be caused by secondary metabolite compounds and volatile compounds produced by PSB. Research by Hu *et al.* (2023) tested *Bacillus cereus* CF4-51 against *Sclerotinia sclerotiorum*, the results showed that the volatile compounds from *B. cereus* CF4-51 produced and the most influential were 1,2-Benzenedicarboxylic acid and bis(2-methylpropyl) ester which were able to cause damage to the cell membrane and cell wall of the fungus resulting in cytoplasmic leakage which could change the hyphal structure. These volatile compounds can also change the permeability of the fungal cell membrane so that these compounds can enter the cytoplasm of the pathogen which further damages the cell wall and changes its shape. *S. sclerotiorum* cells exposed to volatile compounds also form swollen rounded hyphae sections so that with this structure the pathogenic fungus fails to invade the plant (Hu *et al.*, 2023).

The result of abnormal hyphae that undergo changes in shape such as branched hyphae, curly hyphae, and bent hyphal ends is also thought to be caused by compounds produced by PSB which result in changes in the gene expression of pathogenic fungi. According to Liu *et al.* (2018) and Takayama *et al.* (2010) that volatile compounds are able to affect the expression of genes (e.g., SsSac, Ss-SI2, SsSOP1, and SsAMS2) associated with hyphal pole growth. Results suggest that such volatile compounds impact the expression of genes involved in hyphal pole integrity and budding. *Bacillus* also produces lipopeptides capable of binding to lipid membranes in cells, disrupting permeability and producing structural damage. Fengycin and iturin produced can open pores in the plasma membrane and can damage fungal hyphae. The activity of iturin is based on osmotic disruption while fengycin inhibits phospholipase (Aranda, 2005) as a result the structure of the fungal cell wall can undergo abnormal changes in shape.

Research by Surendran *et al.* (2017), stated that *G. boninense* hyphae exposed to phenolic compounds, namely 1 mM 2,6-dimethoxy benzoic acid, produced hyphae of *G. boninense* that branched a lot and inhibited hyphal growth. Research by Widiyanti *et al.* (2018), stated that antagonistic endophytic bacteria affect the

morphology of *G. boninense* mycelia, namely mycelia curling, curling in reverse direction and thinning. Secondary metabolite compounds produced by endophytic bacterial isolates that affect the growth and morphology of *G. boninense* mycelia can allegedly be utilized to control basal stem rot disease in oil palm plants. Lytic enzymes such as chitinase and glucanase also play a role in the process of hyphal lysis. Bacteria that cause lysis activity in pathogens are one of the mechanisms that indicate disease biocontrol (Asril et al., 2022).

CONCLUSION

Three isolates of phosphate solubilizing bacteria (*B. cereus* PS1.1, *B. cereus* PS1.2, *B. cereus* PS1.4) have the ability to inhibit the growth of the pathogenic fungus *Ganoderma* sp. BP1 isolated from the basal of oil palm with rot disease. Isolate PS1.4 is the isolate that has the highest inhibition diameter of 11.01 mm with a strong inhibition category, while isolates PS1.1 and PS1.2 are isolates that have inhibition diameter of 9.43 mm and 9.45 mm respectively with moderate category. Three isolates of phosphate solubilizing bacteria (*B. cereus* PS1.1, *B. cereus* PS1.2, *B. cereus* PS1.4) caused the hyphae of *Ganoderma* sp. BP1 to become abnormal, namely round hyphae, curly hyphae, lysed hyphae, branched hyphae and bent hyphal tips.

REFERENCES

- Aranda, F.J., Teruel, J.A. & Ortiz, A. (2005). Further aspects on the hemolytic activity of the antibiotic lipopeptide iturin A. *Biochimica et Biophysica Acta (BBA) Biomembranes*, 1713(1):51-56.
- Asril, M. (2011). *Kemampuan bakteri tanah dalam menghambat pertumbuhan Ganoderma boninense dan Fusarium oxysporum secara in vitro dan uji penghambatan penyakit layu fusarium pada benih cabai merah*. (Thesis). Universitas Sumatera Utara, Medan.
- Asril, M., Lisafitri, Y. & Siregar, B.A. (2022). Antagonism activity of phosphate solubilizing bacteria against *Ganoderma philippii* and *Fusarium oxysporum* of Acacia plants. *Journal of Multidisciplinary Applied Natural Science*, 2(2):82-89. DOI: 10.47352/jmans.2774-3047.118
- Atlas, R.M. (2004). *Handbook of Microbiological Media*, Third Edition. Boca Raton: CRC Press.
- Cappucino, J.G. & Sherman, N. (2013). *Manual Laboratorium Mikrobiologi*. Jakarta: EGC. Penerjemah: Miftahurrahmah N. Ed ke- 8.
- Claudia, K.M., Nursyirwani, N. & Effendi, I. (2021). Biodegradability of proteolytic bacteria in Mangrove ecosystems. *Journal of Coastal and Ocean Sciences*, 2(2): 120-126. DOI: 10.31258/jocos.2.2.120-126.
- David, W.W. & Stout, T.R. (1971). Disc plate method of microbiological antibiotic assay. *Microbiology*, 22(4): pp.659-665.
- Dendang, B. (2015). *Uji antagonisme Trichoderma sp. terhadap Ganoderma sp. yang menyerang tanaman Sengon secara in vitro*. *Jurnal Penelitian Kehutanan Wallacea*, 4(2): 147-156.
- Djojosumarto, P. (2008). *Panduan Lengkap Pestisida dan Aplikasinya*. Jakarta Pusat: Agro Media.
- Ekowati, C.N., Shintia, R., Umar, S. & Irawan, B. (2022). The potential of soil bacterial isolates from Liwa Botanical Gardens, West Lampung as phosphate solubilizing bacteria. *Jurnal Ilmiah Biologi Eksperimen dan Keanekaragaman Hayati (J-BEKH)*, 9(1): 83-89., DOI: 10.23960/jbekh.v9i1.203.
- Fitriatin, B.N, Dewi, Y.W. & Sofyan, E.T. (2020). Antagonism activity of phosphate solubilizing microbes and nitrogen fixing bacteria toward *Fusarium* sp. *International Journal of Environment, Agriculture and Biotechnology*, 5(6): 1538-1540.
- Flori, F., Mukarlina, M. & Rahmawati, R. (2020). *Potensi antagonis isolat bakteri Bacillus spp. asal rizosfer tanaman Lada (Piper nigrum L.) sebagai agen pengendali jamur Fusarium sp.* *Jurnal Biologi Makassar*, 5(1): 111-120.
- Halo, B.A., Al-Yahyai, R.A., Maharachchikumbura, S.S. & Al- Sadi, A.M. (2019). *Talaromyces variabilis* interferes with *Pythium aphanidermatum* growth and suppresses *Pythium* induced damping off of Cucumbers and Tomatoes. *Scientific reports*, 9(1): 1-10. DOI: 10.1038/s41598-019-47736-x.
- Hu, J., Dong, B., Wang, D., Meng, H., Li, X. & Zhou, H. (2023). Genomic and metabolic features of *Bacillus cereus*, inhibiting the growth of *Sclerotinia sclerotiorum* by synthesizing secondary metabolites. *Archives of Microbiology*, 205(1): 8. DOI: 10.1007/s00203-022-03351-5.

- Istikorini, Y. (2002). *Pengendalian penyakit tumbuhan secara hayati yang ekologis dan berkelanjutan*. Makalah Falsafah Saint (PPs 702). Bogor: Institut Pertanian Bogor.
- Javandira, C., Aini, L.Q. & Abadi, A.L. (2013). *Pengendalian penyakit busuk lunak umbi Kentang (*Erwinia carotovora*) dengan memanfaatkan agens hayati *Bacillus subtilis* dan *Pseudomonas fluorescens**. *Jurnal Hama dan Penyakit Tumbuhan*, 1(1): 90-97.
- Kalam, A. & Mukherjee, A.K. (2001). Influence of hexaconazole, carbofuran, and ethion on soil microflora and dehydrogenase activities in soil and intact cell. *Indian Journal of Experimental Biology*, 39: 90-94.
- Khotimah, S. (2021). *Potensi jamur dan bakteri pendegradasi selulosa serta bakteri pelarut fosfat, penambat nitrogen non symbiosis, dan penghasil IAA pada berbagai tingkatan kematangan gambut sebagai kandidat biofertilizer*. (Dissertation). Brawijaya University, Malang.
- Liu, L., Wang, Q., Zhang, X., Liu, J., Zhang, Y. & Pan, H. (2018). Ssams2 a gene encoding GATA transcription factor, is required for appressoria formation and chromosome segregation in *Sclerotinia sclerotiorum*. *Frontiers in Microbiology*, 9: 418172. DOI: 10.3389/fmicb.2018.03031
- Loekas, S. (2008). *Pengantar Pengendalian Hayati Penyakit Tanaman*. Jakarta: PT. Raja Grafindo Persada.
- Lorito, M.G., Harman, E., Hayes, C.K., Broadway, R.M., Tronsmo, S.L. & Woo, Di Pietro, A. (1993). Chitinolytic enzymes produced by *Trichoderma harzianum*: antifungal activity or purified endochitinase and chitobiosidase. *Phytopathol*, 83(3): 302-307.
- Mahmud, Y., Cindy, R. & Syukra, I. (2020). Efektivitas *Trichoderma virens* dalam mengendalikan *Ganoderma boninense* di pre nursery Kelapa Sawit pada medium gambut. *Jurnal Agroekoteknologi*, 11(1): 11-16.
- Maznah, Z., Halimah, M., Ismail, S. & Idris, A.S. (2015). Dissipation of the fungicide hexaconazole in oil palm plantation. *Environmental Science and Pollution Research*. 22(24): 19648-19657. DOI:10.1007/s11356-015-5178-z.
- Nisa, M., Aini, F. & Maritsa, H.U. (2020). *Aktivitas antagonistik bakteri selulolitik asal rhizosfer Kelapa Sawit (*Elaeis guineensis* Jacq.) terhadap *Ganoderma boninense* Pat. Al-Kaunyah: Jurnal Biologi*, 13(1): 9-19.
- Prasetyo, E.A., Susanto, A. & Utomo, C. (2008). *Metode penghindaran penyakit busuk pangkal batang Kelapa Sawit (*Ganoderma boninense*) dengan sistem lubang tanam besar*. *Jurnal Penelitian Kelapa Sawit*, 16(2): 77-86.
- Pratiwi, A.R. (2002). *Deteksi ergosterol sebagai indikator kontaminasi cendawan pada tepung terigu*. *Jurnal Teknologi Industri Pangan*, 8(3): 256-259.
- Purnamasari, M.I., Prihatna, C., Gunawan, A.W. & Suwanto, A. (2012). *Isolasi dan identifikasi secara molekuler *Ganoderma* spp. yang berasosiasi dengan penyakit busuk pangkal batang di Kelapa Sawit*. *Jurnal Fitopatologi Indonesia*, 8(1): 9-15.
- Rosmegawati. (2021). *Peran aspek teknologi pertanian Kelapa Sawit untuk meningkatkan produktivitas produksi Kelapa Sawit*. *Jurnal Agrisia*, 13(2): 73-90.
- Sakinah, A.L. & Enny, Z. (2014). *Resistensi *Azotobacter* terhadap $HgCl_2$ yang berpotensi menghasilkan enzim merkuri reductase*. *Jurnal Sains dan Seni Pomits*, 3(2): 84-86.
- Sela, F.M., Rianto, F. & Syahputra, E. (2022). *Pemanfaatan bakteri pelarut fosfat dalam mengendalikan penyakit hawar pelepah pada Padi Cihayang Merah*. *Jurnal Sains Pertanian Equator*, 11(4): 225-232.
- Semangun, H. (2008). *Penyakit-Penyakit Tanaman Perkebunan di Indonesia*. Yogyakarta: Universitas Gadjah Mada.
- Sijpesteijn, A.K. (1970). Biochemical modes of action of agricultural fungicides. *World Review of Pest Control*, 9: 85-93.
- Situmorang, Y.A., Bakti, D. & Hasanuddin. (2015). *Dampak beberapa fungisida terhadap pertumbuhan koloni jamur *Metarhizium anisopliae* (Metch) Sorokin di laboratorium*. *Jurnal Online Agroekoteknologi*, 1(3): 147-159.
- Son, B., Yun, J., Lim, J.A., Shin, H., Heu, S. & Ryu, S. (2012). Characterization of LysB4, an endolysin from the *Bacillus cereus*-infecting bacteriophage B4. *BMC microbiology*, 12(1): 1-9. DOI: 10.1186/1471-2180-12-33.
- Surendran, A., Siddiqui, Y., Saud, H.M., Ali, N.S. & Manickam, S. (2017). The antagonistic effect of phenolic compounds on ligninolytic and

- cellulolytic enzymes of *Ganoderma boninense*, causing basal stem rot in oil palm. *International Journal of Agriculture & Biology*, 19(6): 1437-1446. DOI: 10.17957/IJAB/15.0439.
- Suryanto, D., Wibowo, R.H., Siregar, E.B.M. & Munir, E. (2012). A possibility of chitinolytic bacteria utilization to control basal stems disease caused by *Ganoderma boninense* in oil palm seedling. *African Journal of Microbiology Research*, 6(9): 2053-2059. DOI: 10.5897/AJMR11.1343.
- Suryanto, D., Yeldi, N. & Munir, E. (2016). Antifungal activity of endophyte bacterial isolates from torch Ginger (*Etilingera elicitator* (Jack.) RM Smith) root to some pathogenic fungal isolate. *International Journal of Pharm Tech Research*, 9(8): 340-347.
- Susanto, A., Prasetyo, A.E., Priwiratama, H., Wening, S. & Suriyanto, S. (2013). *Ganoderma boninense* penyebab penyakit busuk batang atas Kelapa Sawit. *Jurnal Fitopatologi Indonesia*, 9(4), 123-123.
- Takayama, Y., Mamnun, Y.M., Trickey, M., Dhut, S., Masuda, F., Yamano, H., Toda, T. & Saitoh, S. (2010). Hsk1- and SCFPof3-dependent proteolysis of *S. pombe* Ams2 ensures histone homeostasis and centromere function. *Developmental Cell*, 18(3-3): 385-396.
- Umami, N. (2018). *Uji Bakteri Antagonis Terhadap Perkembangan Penyakit Busuk Pangkal Batang Kelapa Sawit (Ganoderma boninense Pat.) di Laboratorium*. (Thesis), Universitas Sriwijaya, Palembang.
- Wahyuni, M., Simanjuntak, J.H. & Sitompul, I.O. (2018). *Efektivitas fungisida berbahan aktif heksakonazol terhadap penyakit jamur akar putih bibit tanaman karet (Hevea brasiliensis)*. *Agrotekma: Jurnal Agroteknologi dan Ilmu Pertanian*, 3(1), 1-10.
- Waluyo, L. (2008). *Teknik Metode Dasar Mikrobiologi*. Malang: Universitas Muhammadiyah. Malang Press.
- Widiantini, F., Yulia, E. & Nasahi, C. (2018). *Potensi antagonisme senyawa metabolit sekunder asal bakteri endofit dengan pelarut metanol terhadap jamur G. boninense Pat.* *Agrikultura*, 29(1): 55-60.
- Yati, T. (2019). *Kemampuan Bakteri Rizosfer Kelapa Sawit di PT Bumitama Gunajaya Agro, Kalimantan sebagai Antagonis Jamur Ganoderma boninense Pat. Dan Pemacu Pertumbuhan Tanaman*. [Thesis], Universitas Lampung, Lampung.

Physico-Chemical Properties and Mineral Identification of Salt Licks Soil in Segaliud Lokan Forest Reserve

SITI NUR ANISA MOHAMAD MAIDIN¹, JEPHTE SOMPUD², ISMAIL ABD RAHIM¹, MOHD. SANI SARJADI¹ & BABA MUSTA^{1*}

¹Faculty of Science and Natural Resources, Universiti Malaysia Sabah, 88400 Kota Kinabalu, Sabah, Malaysia; ²Faculty of Tropical Forestry, Universiti Malaysia Sabah, 88400 Kota Kinabalu, Sabah, Malaysia

*Corresponding author: babamus@ums.edu.my

Received: 16 December 2023 Accepted: 11 September 2024 Published: 31 December 2024

ABSTRACT

This study intended to describe the physicochemical and mineralogical properties of salt licks discovered in Segaliud Lokan Forest Reserve. The salt licks in this forest reported to be visited and used by wildlives via camera trap studies. In order to understand this wildlife's behavior, the physicochemical and mineralogical properties of the salt lick especially the salt lick soil are important to determine the cause of the wildlife visitation. Five salt licks area as well as controlled soils were selected. Water and rock samples were also collected for the comparison study. The physical characteristic of licks soil shows pH ranges from slightly acidic to alkaline, high moisture content (23.30% – 59.35%), wide range of organic matter content (0.38% – 9.65%) and electrical conductivity range between 41.82 $\mu\text{S}/\text{cm}$ to 243.32 $\mu\text{S}/\text{cm}$ which is higher than the controlled soils. The soil texture from the salt licks soils is mostly classified as loam. The result of chemical analysis shows that the concentration of elements is higher in the lick soil compared to the controlled soil such as Ca (1101.92 mg/kg – 11551.64 mg/kg), K (767.32 mg/kg – 2432.11 mg/kg), Na (85.83 mg/kg – 754.20 mg/kg), Mg (986.05 mg/kg – 5843.29 mg/kg) and P (47.23 mg/kg – 290.215 mg/kg). Water samples from salt licks area are rich in Ca (637.67 mg/L – 3074.25 mg/L) and Na (572.35 mg/L – 2554.63 mg/L) compared to river nearby. The mineral analysis indicated the appearance of clay such as illite, chlorite and smectite. As a conclusion, the salt lick soil's pH varies from slightly acidic to alkaline (5.38 – 8.98) compared to controlled soils (4.54), The salt lick surface soils also show higher percentage of moisture content (69.38%) and soil electrical conductivity (78.41%) difference compared to controlled soils. Meanwhile the organic matter percentage in salt lick soils is slightly lower (48.85%) than the controlled soils (51.11%). The salt lick soils also exhibit higher elements concentration than the controlled soils such as average concentration of Ca (96.14%), K (86.09%), Na (89.51%) Mg (91.38%) and P (86.78%).

Keywords: Mineralogy, physico-chemical properties, salt lick, soil, water

Copyright: This is an open access article distributed under the terms of the CC-BY-NC-SA (Creative Commons Attribution-NonCommercial-ShareAlike 4.0 International License) which permits unrestricted use, distribution, and reproduction in any medium, for non-commercial purposes, provided the original work of the author(s) is properly cited.

INTRODUCTION

Salt licks are places where animals visit the place for geophagic activities (Panichev *et al.*, 2012; Lazarus *et al.*, 2019). Natural occurring salt licks can be identified by bite marks or foot prints of animals in the wild (Lameed & Adetola 2012; Molina *et al.*, 2014) whereas artificial salt licks are made by humans in the form of blocked or bagged for farming purposes (Brightsmith, 2004). Natural mineral licks often exist along river banks (Kreulen, 1985; Diamond *et al.*, 1999) and also can be found within forest which is located away from the rivers (Matsubayashi *et al.*, 2007; Tobler *et al.*, 2009).

The frequent usage of natural licks by wildlife has resulted in many studies focusing on describing the physical characteristic of the salt lick, chemical and mineralogical composition and types of animals visiting the salt licks (Molina *et al.*, 2014; Matsubayashi *et al.*, 2007). Previous studies suggest that geophagy activities is a process where wildlife supplementing their diet with several nutrients such as N, Ca, C, P, Mg, Na, K, Fe, Cu, Zn, Cl or I (Matsubayashi *et al.*, 2007; Ayotte *et al.*, 2006). Apart from mineral intake for their diets, wildlife also visits salt licks to counter the adsorption of dietary toxin by ingesting certain types of clay such as kaolinite (Kreulen, 1985; Diamond *et al.*, 1999)

and act as buffering capacity (Kreulen, 1985; Ayotte *et al.*, 2006).

Buffering capacity defined as the ability of solution to counteract pH changes. For example, in terms of livestock studies conducted by Rolinec *et al.* (2018) indicated that the piglet's stomachs is higher than the optimal range because the first feed is colostrum, and for pigs as a standard protein, it is considered the protein of sow's milk, which can be affected by the health status of sows (Rolinec *et al.*, 2012). Irregular intake of large amount of feed may increase the pH values of the stomach above 5 and may persist for a few days (Lawlor *et al.*, 2005). Increased gastric pH in weaned pigs leads to decreased digestion and also diarrhea (Yen, 2000). When this situation is applied in wildlife's diet, visiting the salt licks is the only way to counteract the dietary toxin and to keep healthy.

Beside from functioning as mineral resources, salt lick area is considered as critical and crucial for wildlife (Primack, 1993). It has significant influence on the density and structure of population, distribution of wildlife and carrying capacity of habitats (Montenegro, 2004). Salt licks are also believed to attract large number of wild animal species (Blake *et al.*, 2010). Types of species visiting salt licks are mammals and birds, specifically frugivores and herbivores to consume soil or drink water (Kreulen, 1985; Diamond *et al.*, 1999). Composition of species visiting salt lick and frequency of visitation may vary from one lick to another lick (Tobler *et al.*, 2009). The variation is due to the abundance level of mineral composition in the soil or water between different salt lick (Abrahams, 1999).

Only a few studies have been conducted in Southeast Asia, especially Malaysia regarding the relationship between natural licks and wildlife distribution (Matsubayashi *et al.*, 2007). Specifically, studies focusing on the physico-chemical properties and elements concentration of salt licks in Sabah are lacking. Thus, the aim of this work is to determine the physico-chemical properties and elements concentration as well as mineral identification found in salt lick soils in Segaliud Lokan Forest Reserve and to compare the elements concentration between lick soils and non-lick soils. In addition, this

study reveals key information about the elements concentration in salt lick soils engulf by wildlife.

MATERIALS AND METHODS

Description of Study Area

The study area was performed at Segaliud Lokan Forest Reserve (SLFR) located in Sandakan, Sabah bound to latitude 05° 25'' N - 05° 35'' N and longitude 117° 30'' E - 117° 37'' E as shown in Figure 1. The sampling location are selected based on the salt lick locality found in the forest reserve. Located in tropical climate, the soil is exposed to high weathering (Ling *et al.*, 2023) and leaching of bases minerals. This study area consists of two rock formations. The oldest rock unit found is Kulapis Formation, aged Eocene to Middle Miocene. Kulapis Formation is composed entirely of consolidated redbed marine sediments where the interbedded sandstone and mudstone are red in colour (Clennell, 1991). The main lithologies for this formation are greywacke, sublitharenite, calcareous lithic arenite and laminated mudstone (Hutchison, 2005). Both the salt lick soils and controlled soils are taken from the same formation. The salt lick soil locations were chosen based on the camera trap that show the presence of wildlife using the licks whereas the controlled soil location were sampled approximately 500 m away from the salt lick location. The main difference of the salt lick areas and control area is the presence of wildlife engulfing the soils. The lack of wildlife in the control areas indicates that the location is not crucial in supporting the well-being of the animals.

Soil, Water and Rock Sampling

This study uses two types of soil sampling; vertically and horizontal subsurface sampling. These types of sampling were used to identify the variation of mineral content on the surface and according to depth. For salt lick soil samples, vertical sampling is done by using a one-meter-long PVC pipe which is hit using a hammer until it reaches the hard bedrock depth. The pipe is then sealed on both ends to prevent any contamination. Collected core samples were extruded once it reached the laboratory and subdivided into 5 cm and 10 cm intervals depending on the depth obtained. Horizontal

sampling is performed by removing a thin layer of the top soil before collecting the soil samples around 1 kg each. The depth for the horizontal soil sample is 5 cm deep from the soil surface. Controlled soil samples were also taken approximately 500 m away from salt lick area for comparison in physico-chemical properties and elements concentration with salt lick soils. The soil samples were stored in an airtight ziplock bags to avoid contamination. Water samples were taken from the running surface water or any water collected on the surface of the licks (Figure 2). The bottle and cap were rinsed

using the water sample before collecting for water samples. Nitric acids (2%) were added into the water samples for preservation. Fresh rock samples were also taken as hand specimen. One rock sample (weathered sandstone) was taken from the outcrop found in salt lick SL59 and two rock samples (sandstone and mudstone) were taken from SL60. The rest of the rock samples were taken from outcrop along the forest road in the study area. All samples were labelled accordingly. A total of 34 salt lick soil, 5 controlled soil, 17 water samples and 5 rock samples were collected.

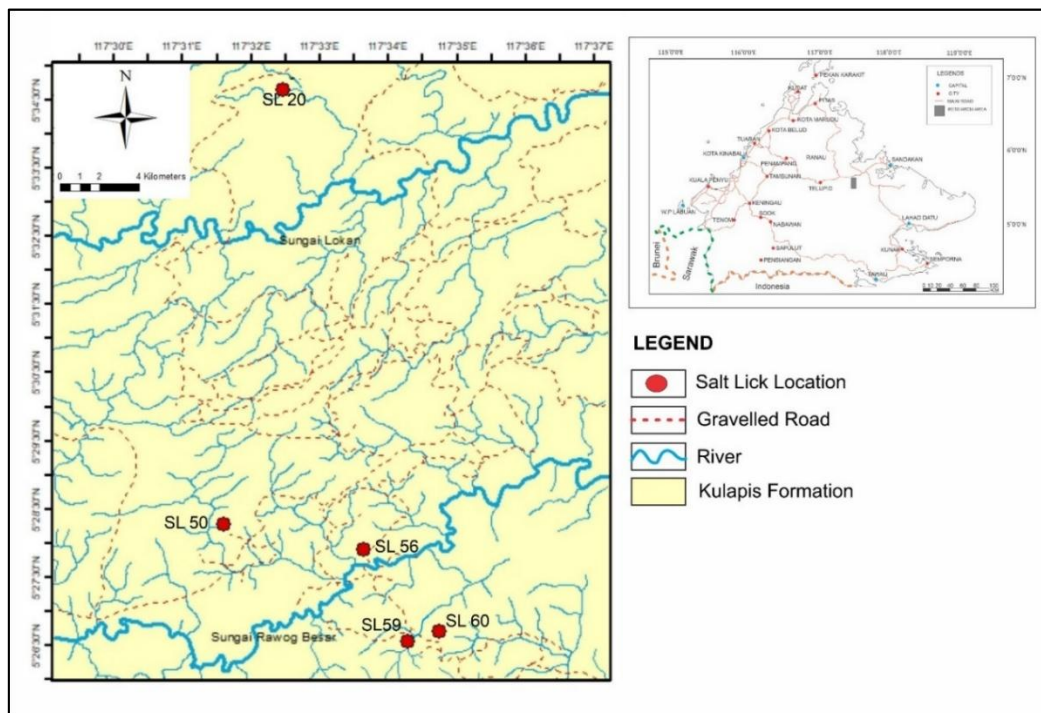


Figure 1. Geological map of study and sampling stations in Segaliud Lokan Forest Reserve



Figure 2. Water sampling carried out over a small flowing river cutting through salt lick SL59

Experimental Analysis

As soon as the samples reach the laboratory, the samples were tested for physico-chemical parameter analysis (pH, moisture content, organic matter and electrical conductivity). The soil samples were later air-dried as preparation for particle size distribution (texture) by following the British Standard method (BS1377:1990). The water samples were placed in the refrigerator as soon as it reached the laboratory. The test conducted for the water samples are pH, electrical conductivity, total dissolved solids and elements concentration.

The metal digestion process for soil samples were conducted using HCl: HNO₃ (aqua regia) mixture with 1:3 ratio based on the USEPA 6010D method. One gram of air dried, powdered and sieved through 63 µm mesh soil sample were weighed and added with 14 ml aqua regia solution and left overnight. The sample were then filtered through the Whatman 0.45 µm cellulose nitrate filter membrane to remove any suspended particles for cations analysis. Water samples were also filtered and diluted in the same manner. The Inductively Coupled Plasma (ICP- OES) were performed using Perkin Elmer Optima model 5300DV Spectrometer. Before performing an ICP OES analysis, a standard dilution stock solution of 100 mg/L as made in accordance with the International Certified Reference Materials (CRM) to calibrate the instrument. The standard reference materials (SRM) analysis calculations were performed with an accuracy range of 80%-120% in order to assess the acid digestion method's appropriateness. Five reagent blanks were analyzed to determine the contamination before proceed to the ICP-OES analysis. All soil samples and water samples were performed in triplicate. The sample were analyzed to detect Ca, K, Na, Mg and P. Reading establish were recorded by the spectrometer and raw data were generated by the WinLab32 software.

Petrographic analysis was conducted using a petrographic microscope LEICA DM2500 by observing thin sections. Scanning Electron Microscopy (SEM) test were conducted to examined the morphology of the clay found in the soil samples. Five grams of air-dried soil

samples were used for SEM analysis. The soil samples were coated using gold coater. Sample analysis was performed using JEOL JSM- 35 6100 microscope and Link An 10/855 Analyser.

RESULTS AND DISCUSSION

Physico-chemical Properties

The salt lick soils range from slightly acidic to slightly basic (pH 5.38 – 8.98) in nature whereas the controlled soil shows acidic soil (pH 4.54). The ranges for moisture content (25.28 - 39.00%) and organic matter (0.38 - 5.28%) shows higher value than the controlled soil (Table 1). The electrical conductivity for salt lick soil also shows higher reading ranges between 41.82 µS/cm to 243.32 µS/cm compared to controlled soil (50.31 µS/cm). The higher values of moisture content (69.38%) supported by the higher percent of particle size of clay and silt particles than sand (Table 1). The percentage of the particle size varies from each salt licks. Soils with finer particles (clay and silt) have a larger surface area than those with coarser particles, and a large surface area allows soil to hold a more water (Chakraborty and Mistri 2015).

The surface soil of salt lick SL56 was gravelled as shown in Figure 3. The surface soil was also submerged in water (Figure 4) believed to be sourced from a spring (Figure 5). This confirms the high moisture content (%) and organic matter (%) with animal's excrement in the vicinity of the samples taken. The electrical conductivity for mud lick soils similarly exhibited higher reading compare to controlled soils indicating the concentration of salts is greater (Othaman *et al.*, 2020). With exception of SL59 where electrical conductivity reading (41.82 µS/cm) vary with the rest of the licks (167.31 µS/cm - 243.32 µS/cm). Lower electrical conductivity values suggest that less soluble salts are readily available in the soil (Othaman *et al.*, 2020). The existence of salt licks area was depending on the accumulation of salt. Jakovljević *et al.* (2003) reported that salt found in the salt lick areas were the products of weathering depending on the weathering rate and leaching rate of the weathered resulting products.

Table 1. Mean value for physico-chemical parameters and elemental concentration analysis for soil samples.

Sample	pH	MC (%)	OM (%)	EC (uS/cm)	Particle Size (%)				Concentration (mg/kg)					
					Sand	Silt	Clay	Texture	Ca	K	Na	Mg	P	
Surface Soil														
SL20 (n=4)	8.98	25.28	0.38	236.58	34.80	35.04	30.18	Clay Loam	8318.50	2432.11	529.04	5843.29	261.78	
SL50 (n=5)	6.95	39.00	3.92	243.32	31.30	36.61	32.11	Clay Loam	11551.64	1456.29	199.60	2501.74	256.29	
SL56 (n=3)	6.04	36.00	5.28	224.39	52.60	29.39	18.01	Sandy Loam	1101.92	980.54	154.56	1442.14	128.48	
SL59 (n=6)	5.38	36.28	4.80	41.82	53.50	26.92	19.24	Sandy Loam	1252.95	767.32	85.83	986.05	47.23	
SL60 (n=6)	7.53	23.30	2.50	167.31	16.1	58.19	25.68	Silt Loam	2807.07	1920.97	647.67	4825.05	273.83	
Controls (n=5)	4.51	17.04	3.79	51.72	46.40	30.96	22.29	Loam	1006.254	1220.702	189.424	1470.738	141.572	
Subsurface Soil														
SL59 (1) (n=2)	6.57	54.62	9.40	51.05	85.30	2.95	11.74	Loamy Sand	2204.215	760.705	83.305	1373.79	128.235	
SL59 (2) (n=2)	6.63	50.36	6.86	61.44	60.15	19.25	20.60	Sandy Clay Loam	2129.445	965.45	123.645	1701.525	173.23	
SL59 (3) (n=2)	6.59	48.22	8.87	71.76	55.57	25.94	18.49	Sandy Loam	2216.025	977.975	122.115	1705.71	207.73	
SL59 (4) (n=2)	6.59	59.35	9.65	75.09	43.85	31.54	24.62	Loam	2435.78	1105.42	149.23	1806.945	290.215	
SL60 (a) (n=2)	8.32	27.95	2.05	94.32	16.29	61.02	22.69	Silt Loam	3901.57	2253.80	577.98	5573.05	bdl	
SL60 (b) (n=2)	8.44	30.10	2.11	94.92	16.96	62.84	20.20	Silt Loam	3756.79	2158.61	607.55	5592.49	78.58	
SL60 (c) (n=2)	8.77	31.56	1.74	133.68	12.58	33.21	54.21	Loam	4333.21	2216.83	754.20	5613.35	174.85	
1	0cm-10cm		30cm-40cm					a	0cm-5cm	bdl	below detection limit			
2	10cm-20cm							b	5cm-10cm					
3	20cm-30cm							c	10cm-15cm					

**Figure 3.** Gravelled environment of salt lick SL56



Figure 4. The surface soil of SL56 was wet believed to be influenced by spring water nearby



Figure 5. Spring found in salt lick SL56

SL56 and SL59 soil exhibit slightly higher organic matter content with 26.09% and 23.70% difference compared to other salt lick for surface soils. In addition, SL59 soil profile show high organic matter content found at depth 10-20 cm (6.86%), 20-30 cm (8.87%) and 30-40 cm (9.65%) respectively. The occurrence of small stream on the surface soil of SL59 contribute to the organic matter in the soil. Small stream flowing through the lick causing the soil to be constantly saturated with water lead to poor aeration and low oxygen. This condition causes low mineralization rate because microorganisms in the soil became inactive or eventually die. Long term exposure to the water saturated soil with low decomposition rate potentially producing high organic matter content (Bot & Benites, 2005). This situation also explained the soil condition in SL56 where a spring existed in the lick area (Figure 5) thus resulting in higher organic matter (5.28%) in the soil.

Generally, the salt lick soil and control soil show texture variation. This indicates that each lick is different from each other and function differently (Abrahams, 1999). SL20 and SL50 soil texture show clay loam whereas SL56 and SL59 show sandy loam and SL60 shows silt loam. Different percentage of soil particle distribution will affect adsorption. Soil with smaller particle size has high surface area thus greater adsorption capacity (Mandzhieva *et al.*, 2014). Eventhough SL56 and SL59 contain more sand, presence of organic matter and the total percentage of combined value between silt and clay particles ensure enough major elements in the soil (Table 1). This is because fine-textured soils usually have a greater exchange capacity than coarse soils because of a higher proportion of colloids. Most chemical interactions in the soil occur on colloid surfaces because of their charged surfaces (McCauley *et al.*, 2005).

Only two salt licks were selected for profile soil sampling. It is because these two salt lick provide sufficient depth for vertical sampling with approximately 15 cm to 20 cm deep respectively (Table 1). Soil pH value for both salt lick shows small range indicating the soil pH is well buffered (Malik & Haq, 2022). There are no significant changes in pH value between each layer (Table 1). The soil moisture content and organic matter shows fluctuation within depth. This is influenced by the distribution of silt and clay as shown in Table 1 which shows variation

across depth (Matus, 2021). SL60 salt lick soil is alkaline (pH 8.32-8.77) with stable pH too. The moisture content and organic matter showing shifting trend with every interval. Low clay percentage in the upper layer (20.20%-22.69%) is the reason for low moisture content as clay has good water retention (Kumari & Mohan, 2021). Decreasing organic matter with depth is due to increasing soil pH as growing condition of microorganism in alkaline environment is poor, resulting low biological oxidation of organic matter (Primavesi, 1984). Both salt lick shows steadily increasing electrical conductivity with increasing depth indicating presence of high concentration of readily available salts (Othaman *et al.*, 2020) such as calcium, potassium, sodium and magnesium as shown in Table 1.

Elemental Concentration

The selected major elements in this study are calcium (Ca), potassium (K), sodium (Na), magnesium (Mg) and phosphorus (P). The concentration of the elements varies for each salt lick. Generally, concentration of phosphorus (P) is the lowest element concentration (47.23 mg/kg – 385.43 mg/kg) found in licks and controlled soils within this study area followed by sodium (Na) (85.83 mg/kg – 529.04 mg/kg). The average elements concentration for SL56 show slightly lower compared to average elements concentration of controlled soils. This result was obtained because one out of three soil samples taken displays low concentration of several elements such as Ca (186.14 mg/kg), Mg (753.21 mg/kg) and P (66.47 mg/kg) which affect the total average concentration. The other two soil samples of SL56 show high concentration of Ca (1559.80 mg/kg), Mg (1786.60 mg/kg) and P (159.48 mg/kg).

SL20, SL50 and SL59 show high concentration of calcium (Ca) whereas SL56 and SL60 are concentrated with magnesium (Mg). In terms of potassium (K), sodium (Na) and phosphorus (P) concentration, SL20 and SL60 were both show greater concentration compared to other salt lick soils (Table 1). Elements concentration in lick SL59 relatively within the same range of the controlled soils average concentration. This phenomenon can be explained by the existence of small stream flowing through the lick. Continuous stream

flows cause elements to leach from soils into the water body and be carried away (Lu *et al.*, 2017).

This study shows that the concentrations of calcium were high (1101.92 mg/kg- 11551.64 mg/kg) in the salt lick soils. Parent rocks such as sandstone tends to have acidic pH value thus forming acidic soil (Osman, 2013) due to the presence of high silica which is acidic in nature (Kelesoglu *et al.*, 2012). Existence of calcium in acidic background derived from the decomposition process of animals, microorganism and plants that cause calcium to be mineralized and release back into the soil (Jaiswal *et al.*, 2021). This situation is observed in SL56 and SL59 with acidic soil (pH 5.38 – 6.04) compared to the rest of the licks. Neutral to slightly alkaline lick shows high concentration of calcium. Plant roots also leak minerals, sugars and components like calcium back into the soil (Brunner & Bachafen, 1998). Plants growing on Kulapis Formation beds have the possibilities to absorb calcium from the soil because Kulapis Formation consists of calcareous lithic arenite sandstone (Hutchison, 2005) which is characterized by high concentration of calcium

carbonates. This is particularly true in this study where SL20, SL50 and SL60 soils pH values were between those ranges (8.98, 6.96 and 7.53 respectively).

Potassium concentration in SL56 (980.54 mg/kg) and SL59 (767.32 mg/kg) are low in value. Slightly acidic sandy soil contains low potassium ion due to leaching processes (Anderson, 1974) and low potassium bearing mineral such as illite (Mengel *et al.*, 2001). Acidic soil pH displayed by both licks (6.04, 5.38) provide an environment for cation exchange capacity (CEC) competition due to concentration of H^+ is higher and the presence of easily soluble aluminum (Al^{3+}) (Ross & Ketterings, 1995). These two elements will displace other exchangeable cations (K^+) (Rahman *et al.*, 2018) causing the cations move into the soil solution and increase the potential of leaching. In contrast, SL20, SL50 and SL60 exhibited high concentration of potassium (2432.11 mg/kg, 1456.29 mg/kg and 1920.97 mg/kg). This may be due to the existence of illite clay in the soils as illite is the source for potassium (Reitemeier, 1957).



Figure 6. Butterfly observed on the surface soil of salt lick SL59

In this study, the sodium concentrations of the salt lick soils were in range with the controlled soils except for SL20 and SL60 licks. Both of this lick potentially visited by wildlife to nourish their sodium diet. Low concentrations of sodium were observed in SL59 (85.83 mg/kg) but presence of flocks of butterflies on the salt lick soils were noticed (Figure 6). This situation is similar as reported by Sim *et al.*, (2020). This indicates that, the licks play their role as sources of nutrients for wildlife even with low concentration of certain mineral compare to other minerals. Klaus *et al.* (1998) in his research found that the concentration of sodium in lick soils is lower from controlled soil. This phenomenon may arise due to an antagonistic element such as higher calcium concentration tends to exchange sodium in leaching processes (Carrow & Duncan, 2012). Calcium is a divalent cation readily take the place of excess sodium ions which is a monovalent cation occupying the exchange sites of soil colloids. The strength of cation retention by soil particles increases with increasing ion charge and decreasing hydrated ion radius (Bohn *et al.*, 2001). The ease of cation removal from specific colloids has been represented by 'lyotropic series', $\text{Th}^{4+} > \text{Fe}^{3+} > \text{Al}^{3+} > \text{Cu}^{2+} > \text{Ba}^{2+} > \text{Sr}^{2+} > \text{Ca}^{2+} > \text{Mg}^{2+} > \text{Cs}^+ > \text{Rb}^+ > \text{K}^+ = \text{NH}_4^+ > \text{Li}^+ > \text{Na}^+$, in the order of decreasing strength of retention (Mitchell and Soga, 2005). The relative extent of adsorption or desorption of ions primarily depend on the valence; for instance, Na^+ can be easily replaced by Ca^{2+} .

Second most abundant elements observed in the lick soils is magnesium. Among the elements found to be magnesium bearing mineral are chlorite, dolomite, montmorillonite, pyroxene and vermiculite (Scheffer *et al.*, 1966). Thus, weathering of these minerals will enrich the soil with magnesium. Higher amount of magnesium in SL20 (5843.29 mg/kg), SL50 (2501.74 mg/kg) and SL60 (4825.05 mg/kg) is caused by the favorable environment for cation exchange capacity for magnesium take place. Furthermore, the red beds of Kulapis Formation indicate an iron rich source probably influenced by the nearby ophiolite at the northwest of the formation (Hutchison, 2005). Kulapis Formation at the east Bidu-bidu Hills constitutes interbedded pale greyish-red sandstones and chocolate brown mudstone (Newton-Smith, 1967). The Bidu-bidu Hills is the only massive ultrabasic rock found in the study area. The

uplifted ophiolites were overlain by serpentinite conglomerates (Newton-Smith, 1967; Hutchison and Tungal, 1991). Thus, this justifies the source of magnesium in Kulapis Formation and supported by the occurrence of mafic mineral observed in the petrographic and mineralogy analysis of this study.

Higher magnesium levels are found in clay soils due to the presence of easily weathered ferromagnesian mineral (Osman, 2013) such as chlorite in the salt lick soil (Figure 8). This explain the higher magnesium concentration in clay texture shown in SL20, SL50 and SL60 samples. Magnesium is a base cation (Havlin, 2005) thus explaining correlation between higher soil pH in SL20 (8.98) and SL60 (7.53) and the exchangeable calcium (8318.60 mg/kg) and magnesium (5843.29 mg/kg) (Yost & Hartemink, 2019). Generally, magnesium shows similar ion exchange with the calcium (Mikkelsen, 2010).

In acidic and sandy soil such as SL56 and SL59, magnesium is easily leach due to higher exchangeable of aluminum and H^+ in the soil (Metson, 1974; Senbayram *et al.*, 2015). Therefore, higher acidity of soil will lower the magnesium concentration. Coarse soil texture which is high in sand particle percentage increases the removal of magnesium due to the low binding capacity in sand (Senbayram *et al.*, 2015). The presence of flowing stream in SL59 also lead to the lower concentration of magnesium in the lick. Water will cause dilution of elements concentration in the area and flowing river has the potential to bring ions out of the salt lick areas through the leaching process (Lu *et al.*, 2017) further influencing the low concentration of elements in the soil.

As the least concentration observed in the soil, phosphorus is an element that is directly affected by pH. In acidic condition, phosphate ion tend to react quickly with aluminum and iron to form less soluble salt whereas in alkaline condition, phosphate ion react rapidly with calcium and magnesium to form less soluble compound (Jensen, 2010). Neutral soils (SL50) provide conducive environment for phosphorus availability. Alkaline soils (SL20 and SL60) are rich in Ca^{2+} and Mg^{2+} which adsorbs phosphorus and precipitate (Prasad & Chackraborty, 2019). For instance, the precipitation of calcium phosphate occurs when the calcium and

phosphorus sources interact at increasing pH of the medium (Avramenko *et al.*, 2023).

Element concentration for soil profile analysis shows that generally all the elements for both soil profile in SL59 and SL60 increasing as the depth increase (Table 1). Exception for calcium where the concentration fluctuates and also potassium for SL60. Nutrient leaching such as magnesium (Mengel *et al.*, 2001) occurs downward soil profile following the movement of water (Lehmann & Schroth, 2002) thus supporting the finding of this study where nutrient concentration is higher in the subsurface soil compare to the surface soil (Table 1).

Table 2 shows the concentration for water samples. Generally, controlled water samples show less mineral content compared to lick's water. Phosphorus is undetectable in both controlled and river. The amount of phosphorus in lick's water sample are too low (0.01 mg/l – 0.03 mg/l). Obviously, average concentration of calcium is relatively high in lick's water (1566.10 mg/kg). The high average concentrations of calcium were also recorded in Rawog river (952.07 mg/kg) and Sg. 50 river (1081.93 mg/kg). Both rivers are located away from the salt lick areas, suggesting the contribution of rich calcium bedrocks to the calcium concentration in the water. According to Otobo (1995) where the concentration and relative abundance of ions in river waters (that is, its chemical composition) is highly variable and depends mainly on the nature of the bedrock, precipitation and evaporation–crystallization

processes. This demonstrated that the Kulapis Formation beds as one of the sources of calcium in the study area as calcium leached from the weathering processes.

Apart from calcium, sodium concentration is also high in lick's water sample (568.45 mg/l – 2554.63 mg/l) implying that the elements are leached from the soil into water body. High amount of sodium in the water proposing that wildlife visit the licks for water intake rich in sodium. Exception for SL20 where the amount of potassium (571.68 mg/kg) and magnesium (771.98 mg/kg) are rather high compared to other licks indicating leaching process occurs rapidly in the area.

Petrography and Mineralogy

Three sandstones and two mudstones were collected for petrography analysis. A sandstone sample was collected from the outcrop found in SL59 area and 2 rock samples (a sandstone and a mudstone) were collected in the vicinity of salt lick SL60 area. The sandstones varies from fine to coarse grained. The grains are rounded to subrounded, are well to moderately sorted (Figure 7a and 7b). The matrix percentage is less than 10% represented by brownish colour observed under the microscope. The petrography of mudstone analysis shows that the mudstone is made up of very fine grained minerals and clay minerals as matrix (Figure 7c). Chlorite was also present in the mudstone based on its greenish colour (Figure 7d).

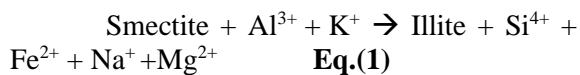
Table 2. Chemical properties of water sample (average values) of licks, control and river nearby

Sample	Concentration (mg/L)				
	Ca	K	Na	Mg	P
SL20 (n=2)	2715.39 ± 1857.50	571.68 ± 4.50	250.44 ± 656.70	771.98 ± 415.44	bdl
SL50 (n=1)	3074.25	9.29	2554.63	10.32	0.01
SL56 (n=1)	1855.25	5.35	568.45	6.45	0.03
SL59 (n=2)	637.67 ± 39.27	7.19 ± 0.00	572.35 ± 3.59	3.98 ± 0.00	bdl
Controls (n=6)	361.20 ± 639.33	2.05 ± 0.81	4.38 ± 0.87	5.00 ± 2.23	bdl
Sg. 50 (n=2)	1081.93 ± 14.99	1.96 ± 0.02	7.40 ± 0.08	4.48 ± 0.01	bdl
Rawog river (n=3)	952.07 ± 174.57	3.76 ± 0.75	10.01 ± 0.04	4.09 ± 0.09	bdl

Bdl: below detection limit

Plagioclase was also detected in very small amount and heavily weathered (Figure 7e) as well as microcline feldspar (Figure 7f) in sandstone. Authigenic mineral such as muscovite and chlorite are also observed in the sample as an elongated sheet like structure (Figure 7g). The muscovite grain changes in direction due to the strong movement of quartz grain (Worden & Burley, 2003).

Figure 8 shows the scanning electron microscopy (SEM) results conducted on salt lick soil samples for the identification of major minerals or clays, their morphology and structures. The minerals identified that made up the lick soil composition are chlorite, illite and smectite. It is clearly visible that smectites are abundant in lick soils, showing an Okal leaf structure (Figure 8a) (Abu El-Ezz *et al.*, 2012). The individual grain is poorly defined due to diffuse outlines and curled edges forming flower like structure (Abu El-Ezz *et al.*, 2012). It can be regarded as aggregates with foliated and lamellar structure as a result of the expulsion of water and gas during compaction and oxidation of organic matter (Keller, 1985). As observed from the thin section, the feldspar grain had undergone intense weathering. Dissolution of alkali feldspar will produce aluminum ion and silica in aqueous form (Huggett, 2005). According to Huggett (2005), dissolution of K feldspar will yield Al^{3+} and K^+ which will react with smectite to form illite-smectite and ultimately illite:

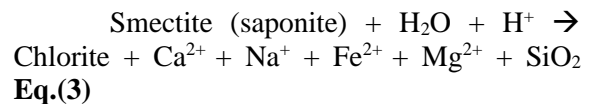
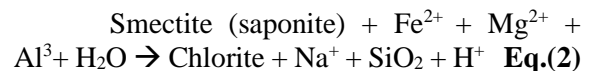


Potassium ion for the illitization was supplied mainly from the alteration of K feldspar within the sandstone and from mica within the shales (Kumar *et al.*, 2016). Abundance of potassium can be seen from the elemental concentration analysis. Both aluminium and potassium ions will react with smectite to form illite-smectite and eventually illite in the later. This process is known as illitization.

Illitization occurs in sediments enriched in K-feldspar (Worden & Morad, 2000). Illite occurs with different morphologies according to the potassium supersaturation during precipitation (Weibel *et al.*, 2020). The pattern of illite-smectite shown in Figure 8a appear as crooked scaly and partly foliated. In contrast to Figure 8b

where the illite shows fibrous structure indicating of rapid growth during burial (Mullin, 2001). The formation of fibrous illite requires higher thermal exposures compare to that of the illite formation by smectite illitization (Stroker & Harris, 2009). Thus, the existence of fibrous illite in this study proves that Kulapis Formation was exposed to high thermal environment during burial.

Chlorite was also found in the salt lick soil samples. The chlorite minerals occur as poorly developed plates with irregular outlines or ragged edges and it shapes shows a high magnesium type chlorite (Hillier, 1994) (Figure 8c). Chlorite also exhibits edge to face, face-to-face (Figure 8d) and edge-to-edge contacts (Wilson *et al.*, 2014). According to Wilson *et al.* (2014) less developed chlorite crystal structures indicate authigenic origin. Smectite transforms into chlorite in alkaline condition that rich in iron and magnesium ion (Chen *et al.*, 2011). Chloritization is a process where smectite reacts with Fe^{2+} , Mg^{2+} and water to transform into chlorite. According to Chang *et al.* (1986):



Chlorite sources include transformation of detrital Fe-rich berthierine, transformation of Mg-rich smectite (Wilson *et al.*, 2014). The specific origin of chlorite controls its composition. Chlorite in marine sandstones is originated from berthierine source, whereas chlorite from the continental sandstones originated from smectite (Berger *et al.*, 2009; Worden *et al.*, 2020). Following the findings of SEM analysis, it is confirmed that the chlorite found in this study is originated from smectite.

The clay minerals composition in soil suggest that made up soil shows that the salt lick soils supply a good amount of nutrients. The dissolution of smectite contributes calcium, sodium, magnesium and silica into the soils (Metz *et al.*, 2005). Illite is in potassium (Barre *et al.*, 2007) whereas chlorite contains abundant iron and magnesium (Deer *et al.*, 2013).

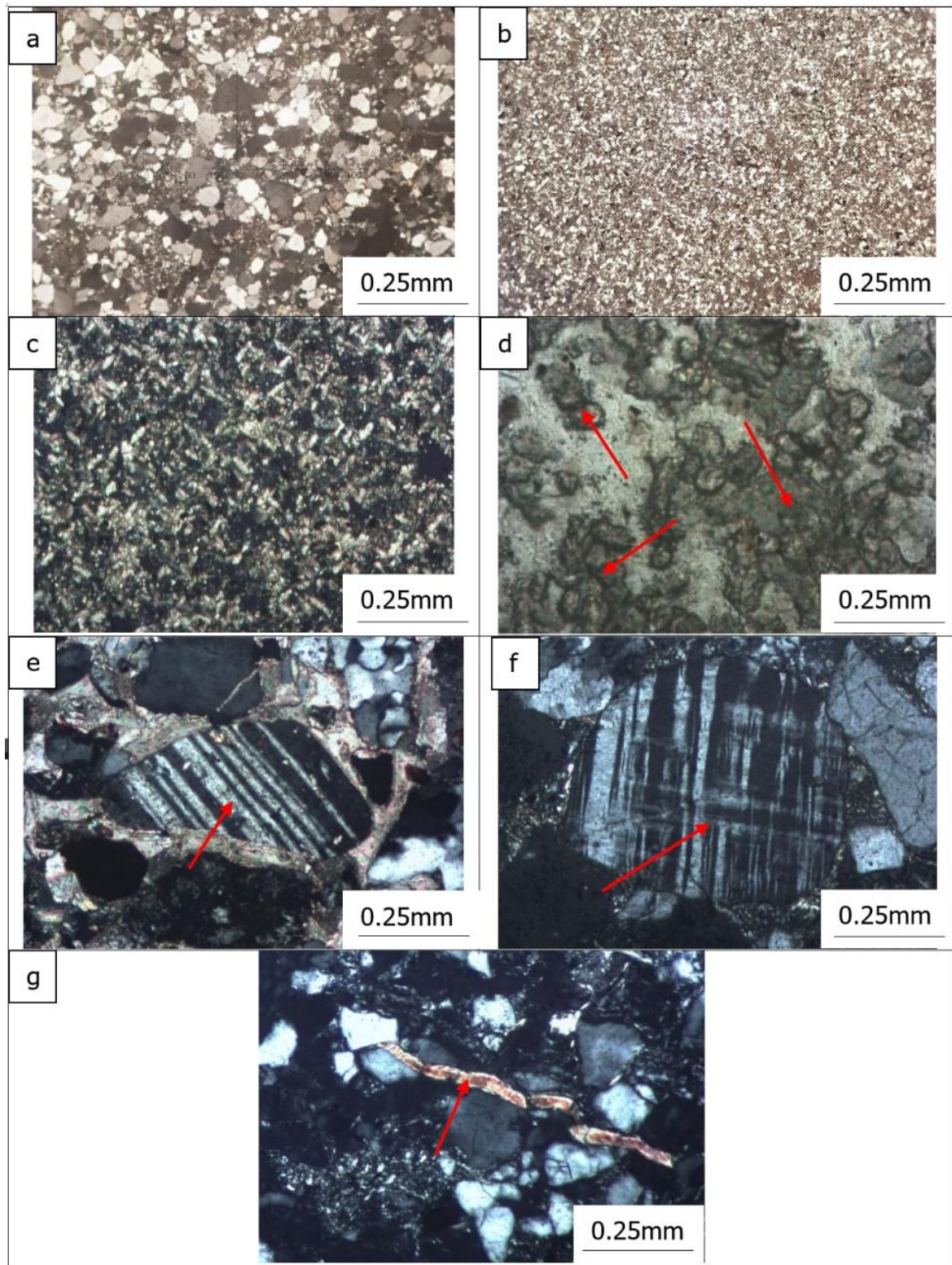


Figure 7. (a) Coarse grain sandstone. (b) Fine grained sandstone. (c) Fine-grained mudstone. (d) Greenish chlorite mineral (red arrows). (e) Heavily weathered plagioclase feldspar (red arrow). (f) Microcline feldspar (red arrow). (g) Muscovite mineral shows elongated shape (red arrow)

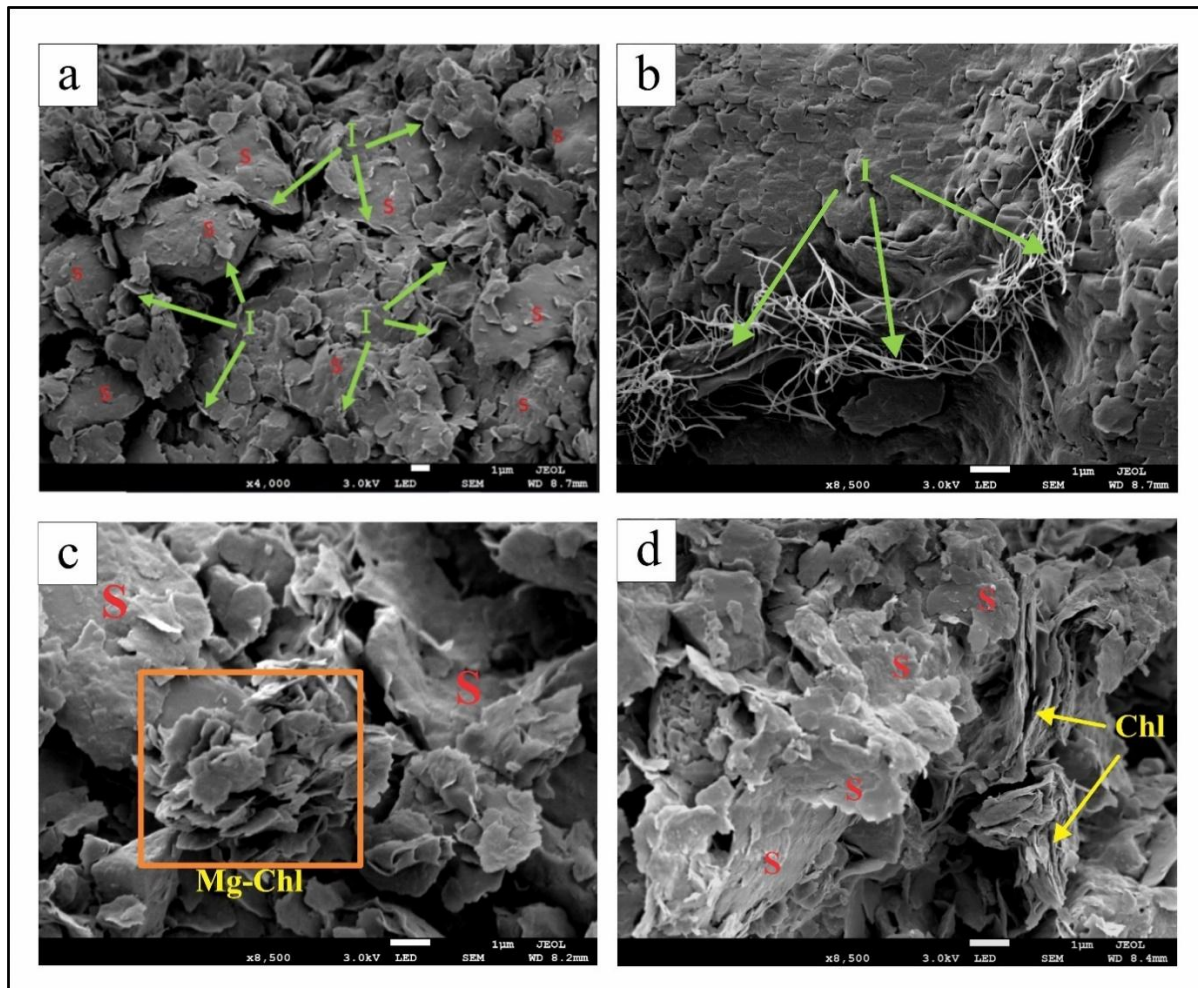


Figure 8. (a) Smectite showing curved leaf like structure with illite appear crooked scaly and foliated partly. (b) Fibrous illite. (c) Less developed Mg-rich chlorite indicates authigenic chlorite (orange box). (d) Chlorite mineral shows parallel structure surrounded by smectite. (Chl= chlorite; I= Illite; S= smectite)

CONCLUSION

In summary, salt lick soil shows slightly acidic to alkaline, high moisture content, high organic matter and high electrical conductivity values compared to control soils. Soil texture for salt lick soils best describe as loam. All lick soils and water samples express high concentration of essential mineral such as calcium, potassium, sodium, magnesium and phosphorus compared to control sites. Although overall elements concentration is slightly low in SL56 and SL59 samples, these two licks served their purpose as nutrient source as sodium seeking species were spotted at the sites. The presence of flowing river in the latter lick also possibly the reason for wildlife visitation. Types of clay such as chlorite, illite, and smectite further contribute to the presence and concentration of the elements in the salt lick of this area. Comparison with the published report in Deramakot Forest Reserve,

Kulapis Formation in the present study shows a wider range of element concentration. The findings give insight on the variation of element concentration in salt lick soils of the same rock formation. Therefore, this study serves as a geochemical baseline data on the distribution of elements concentration of salt lick soils especially in Kulapis Formation.

ACKNOWLEDGMENTS

The authors would like to thank KTS Plantation Sdn. Bhd. and Universiti Malaysia Sabah for the guidance and financial support with matching grant (Code Project GKP0023-2018 and GUG0469-1/2020). All laboratories works were done in the laboratories at Faculty of Science and Natural Resources and Centre of Instrumentation and Science Services, Universiti Malaysia Sabah (UMS), Kota Kinabalu, Sabah.

REFERENCES

- Abrahams, P.W. (1999). The chemistry and mineralogy of three savanna lick soils. *Journal of Chemical Ecology*, 25: 2215-2228. DOI: 10.1023/A:1020861505138
- Abu El-Ezz, A.R., Abdou, A.A. & Temraz, M.G.M. (2012). The petrography, mineralogy, and hydrocarbon potential of the shales of the duwi formation, Abu Tartur, South Western Desert, Egypt. *Petroleum Science and Technology*, 30(22): 2373-2382. DOI: 10.1080/10916466.2010.499404
- Anderson, G. D. (1974). Potassium responses of various crops in East Africa. Potassium in tropical crops and soils.
- Avramenko, M., Nakashima, K., Takano, C. & Kawasaki, S. (2023). Soil improvement using calcium phosphate compounds as a novel sustainable method: A review. *GEOMATE Journal*, 24(101): 68-75. DOI: 10.21660/2023.101.g12142
- Ayotte, J.B., Parker, K.L., Arocena, J.M. & Gillingham, M.P. (2006). Chemical composition of lick soils: functions of soil ingestion by four ungulate species. *Journal of Mammalogy*. 87(5): 878-888. DOI: 10.1644/06-MAMM-A-055R1.1
- Barre, P., Velde, B. & Abbadie L. (2007). Dynamic role of “illite-like” clay minerals in temperate soils: facts and hypotheses. *Biogeochemistry*, 82: 77-88. DOI: 10.1007/s10533-006-9054-2
- Berger, A., Gier, S. & Krois, P. (2009) Porosity-preserving chlorite cements in shallow-marine volcanoclastic sandstones: Evidence from Cretaceous sandstones of the Sawan gas field, Pakistan. *AAPG bulletin*, 93(5): 595-615. DOI: 10.1306/01300908096
- Blake, J., Guerra, J., Mosquera, D., Torres, R., Loiselle, B. & Romo D. (2010). Use of mineral licks by white-bellied spider monkeys (*Ateles belzebuth*) and red howler monkeys (*Alouatta seniculus*) in eastern Ecuador. *International Journal of Primatology*, 31: 471–483. DOI: 10.1007/s10764-010-9407-5
- Bohn, H.L., McNeal, B.L. & O'Connor, G.A. (2001). *Soil chemistry*. John Wiley and Sons. New York.
- Bot, A. & Benites J. (2005). *The importance of soil organic matter: Key to drought-resistant soil and sustained food production (No. 80)*. Food & Agriculture Org.
- Brightsmith, D.J. (2004). Effects of weather on parrot geophagy in Tambopata, Peru. *The Wilson Bulletin*, 116(2): 134-145. DOI: 10.1676/03-087B
- Brunner, U. & Bachofen, R. (1998). The biogeochemical cycles of phosphorus: a review of local and global consequences of the atmospheric input. *Toxicological & Environmental Chemistry*, 67(1-2): 171-188. DOI: 10.1080/02772249809358612
- Carrow, R.N. & Duncan, R.R. (2012). *Saline and sodic turfgrass soils*. CRC Press Taylor & Francis Group Boca Raton. 1-415.
- Chakraborty, K. & Mistri, B. (2015). Importance of soil texture in sustenance of agriculture: a study in Burdwan-I CD Block, Burdwan, West Bengal. *Eastern Geographer*, 21(1): 475-482.
- Chang, H.K., Mackenzie, F.T. & Schoonmaker, J. (1986). Comparisons between the diagenesis of dioctahedral and trioctahedral smectite, Brazilian offshore basins. *Clays and Clay Minerals*. 34:407–423. DOI: 10.1346/CCMN.1986.0340408
- Chen, G., Du, G., Zhang, G., Wang, Q., Lv, C. & Chen, J. (2011). Chlorite cement and its effect on the reservoir quality of sandstones from the Panyu low-uplift, Pearl River Mouth Basin. *Petroleum Science*. 8:143–150. DOI: 10.1007/s12182-011-0127-z
- Clennell, B. (1991). The origin and tectonic significance of melanges in Eastern Sabah, Malaysia. *Journal of Southeast Asian Earth Sciences*, 6 (3-4): 407-429. DOI: 10.1016/0743-9547(91)90085-C
- Deer, W.A., Howie, R.A. & Zussman, J. (2013). *An introduction to Rock-Forming Minerals, 3rd edition*. The Mineralogical Society, London. 498.
- Diamond, J., Bishop, K.D., Gilardi, J.D. (1999). Geophagy in New Guinea birds. *Ibis*. 141(2): 181-193. DOI: 10.1111/j.1474-919X.1999.tb07540.x
- Havlin, J.L. (2005). Fertility. In: Hillel D, Hatfield JL. (Eds.) *Encyclopedia of Soils in the Environment*. 3: 10–19. DOI: 10.1016/B0-12-348530-4/00228-9
- Hillier, S. (1994). Pore-lining chlorites in siliciclastic reservoir sandstones: electron microprobe, SEM and XRD data, and implications for their origin. *Clay Minerals*. 29(4): 665-679. DOI: 10.1180/claymin.1994.029.4.20

- Huggett, J.M. (2005). *Sedimentary rocks: Clays and their diagenesis*. Encyclopedia of Geology. Elsevier. 62-70. DOI: 10.1016/B0-12-369396-9/00311-7
- Hutchison, C.S. (2005). *Geology of North-West Borneo Sarawak, Brunei and Sabah*. Elsevier B.V. Netherlands.
- Hutchison, C.S. & Tunghah, S. (1991). Sabah serpentinite sandstone and conglomerate. *Geological Society Malaysia Newsletter (Warta)*. 17: 59–64.
- Jaiswal, L.K., Singh, P., Singh, R.K., Nayak, T., Tripathi, Y.N., Upadhyay, R.S. & Gupta, A. (2021). *Effects of salt stress on nutrient cycle and uptake of crop plants*. Physiology of salt stress in plants: Perception, signalling, omics and tolerance mechanism, 129-153. DOI: 10.1002/9781119700517.ch8
- Jakovljević, M.D., Kostić, N.M. & Antić-Mladenović, S. B. (2003). The availability of base elements (Ca, Mg, Na, K) in some important soil types in Serbia. *Proceedings for Natural Sciences, Matica Srpska Novi Sad*, 104: 11-21. DOI: 10.2298/ZMSPN0304011J
- Jensen, T.L. (2010). *Soil pH and the Availability of Plant Nutrients*. International Plant Nutrition Institute (IPNI).
- Kelesoglu, S., Volden, S., Kes, M. & Sjöblom, J. (2012). Adsorption of naphthenic acids onto mineral surfaces studied by quartz crystal microbalance with dissipation monitoring (QCM-D). *Energy & Fuels*, 26(8): 5060-5068. DOI: 10.1021/ef300612z
- Klaus, G., Klaus-Hügi, C. & Schmid, B. (1998). Geophagy by large mammals at natural licks in the rain forest of the Dzanga National Park, Central African Republic. *Journal of Tropical Ecology*, 14(6): 829-839. DOI: 10.1017/S0266467498000595
- Keller, W.D. (1985). The nascence of clay minerals. *Clays and Clay Minerals*, 33(3): 161-172.
- Kreulen, D.A. (1985). Lick use by large herbivores: a review of benefits and banes of soil consumption. *Mammal Review*, 15(3): 107-123. DOI: 10.1111/j.1365-2907.1985.tb00391.x
- Kumar, S., Gupta, R.C. & Shrivastavan, S. (2016). Strength, abrasion and permeability studies on cement concrete containing quartz sandstone coarse aggregates. *Construction and Building Materials*, 125: 884-891. DOI: 10.1016/j.conbuildmat.2016.08.106
- Kumari, N. & Mohan, C. (2021). Basics of clay minerals and their characteristic properties. *Clays and Clay Minerals*, 24: 1-29. DOI: 10.5772/intechopen.97672
- Lameed, A.G. & Adetola, J.O. (2012). Species-diversity utilization of salt lick sites at Borgu Sector of Kainji Lake National Park, Nigeria. *Biodiversity enrichment in a diverse world*, 2(3): 35-62. DOI: 10.5772/51089.
- Lawlor, P.G., Lynch, P.B., Caffrey, P.J., O'Reilly, J.J. & O'Connell, M.K. (2005). Measurements of the acid-binding capacity of ingredients used in pig diets. *Irish Veterinary Journal*, 58(8): 447-452. DOI: 10.1186/2046-0481-58-8-447
- Lazarus, B.A., Che-Amat, A., Abdul Halim Shah, M.M., Hamdan, A., Abu Hassi, H., Mustaffa Kamal, F., Azizan, T.R.P.T., Noor, M.H.M., Mustapha, N.M. & Ahmad, H. (2021). Impact of natural salt lick on the home range of Panthera tigris at the Royal Belum Rainforest, Malaysia. *Scientific Reports*, 11(1): 1-8. DOI: 10.1038/s41598-021-89980-0
- Lehmann, J. & Schroth, G. (2002). *Nutrient leaching. In Trees, Crops and Soil Fertility: Concepts and Research Methods*. Wallingford UK: CABI publishing. DOI: 10.1079/9780851995939.0151
- Ling, S.Y., Asis, J. & Musta, B. (2023). Distribution of metals in coastal sediment from northwest sabah, Malaysia. *Heliyon*, 9(2). DOI: 10.1016/j.heliyon.2023.e13271
- Lu, H., Cao, L., Liang, Y., Yuan, J., Zhu, Y., Wang, Y., Gu, Y. & Zhao, Q. (2017). Mineral-leaching chemical transport with runoff and sediment from severely eroded rare-earth tailings in southern China. *Solid Earth*, 8(4): 845-855. DOI: 10.5194/se-8-845-2017
- Malik, Z.A. & Haq, S.M. (2022). Soil chemical properties-variation with altitude and forest composition: A case study of Kedarnath wildlife Sanctuary, Western Himalaya (India). *Journal of Forest and Environmental Science*, 38(1): 21-37. DOI: 10.7747/JFES.2022.38.1.21
- Mandzhieva, S., Minkina, T., Pinskiy, D., Bauer, T. & Sushkova, S. (2014). The role of soil's particle-size fractions in the adsorption of heavy metals. *Eurasian Journal of Soil Science*, 3(3): 197-205. DOI: 10.18393/ejss.16003

- Matsubayashi, H., Lagan, P., Majalap, N., Tangah, J., Sukor, J.R.A. & Kitayama, K. (2007). Importance of natural licks for the mammals in Bornean inland tropical rain forests. *Ecological Research*, 22(5): 742-748. DOI: 10.1007/s11284-006-0313-4
- Matus, F.J. (2021). Fine silt and clay content is the main factor defining maximal C and N accumulations in soils: a meta-analysis. *Scientific Reports*, 11(1): 6438. DOI: 10.1038/s41598-021-84821-6
- McCauley, A., Jones, C. & Jacobsen, J. (2005). Basic soil properties. *Soil and Water Management Module*. Montana State University.1(1): 1-12.
- Mengel, K., Kirkby, E.A., Kosegarten, H. & Appel T. (2001). *Principles of Plant Nutrition*. Springer, Dordrecht. 553-571.
- Metson, A.J. (1974). Magnesium in New Zealand soils. I. Some factors governing the availability of soil magnesium: a review. *New Zealand Journal of Experimental Agriculture*. DOI: 10.1080/03015521.1974.10427689
- Metz, V., Amram, K. & Ganor, J. (2005). Stoichiometry of smectite dissolution reaction. *Geochimica et Cosmochimica Acta*, 69: 1755-1772. DOI: 10.1016/j.gca.2004.09.027
- Mikkelsen, R. (2010). *Soil and Fertilizer Magnesium*. Better Crops. 94(2): 26-28.
- Mitchell, J. K. & Soga, K. (2005). *Fundamentals of Soil Behaviour*. 3rd ed. John Wiley and Sons. New York.
- Molina, E., León, T.E. & Armenteras, D. (2014). Characteristics of natural salt licks located in the Colombian Amazon foothills. *Environmental Geochemistry and Health*, 36: 117-129. DOI: 10.1007/s10653-013-9523-1
- Montenegro, O.L. (2004). *Natural licks as keystone resources for wildlife and people in Amazon*. (PhD Thesis), University of Florida. Florida, USA.
- Mullin, J.W. (2001). *Crystallization* (Vol. 124). Butterworth-Heinemann.
- Newton-Smith, J. (1967). Geology and mineral resources of the Bidu-Bidu Hills area, Sabah, East Malaysia. *Borneo Region Geological Survey Malaysia Report*. 15: 109.
- Osman, K.T. (2013). *Soil as a Part of the Lithosphere*. In: Soils. Springer, Dordrecht. DOI: 10.1007/978-94-007-5663-2_2
- Othaman, N.C., Isa, M.M., Ismail, R.C., Ahmad, M.I. & Hui, C.K. (2020). Factors that affect soil electrical conductivity (EC) based system for smart farming application. *AIP Conference Proceedings*, 2203(1): 020055. DOI: 10.1063/1.5142147
- Otobo, A. J. T. 1995. *The Ecology and Fishery of the Pygmy Herring Sierratherissa leonensis (Thys van Dan Audenaerde, 1969) (Clupeidae) in the Nun River and Taylor Creek of the Niger Delta*. Doctoral dissertation. University of Port Harcourt.
- Panichev, A.M., Golokhvast, K.S., Gulkov, A.N. & Chekryzhov, I.Y. (2012). Geophagy in animals and geology of kudurs (mineral licks): A review of Russian publications. *Environmental Geochemistry and Health*, 35(1): 133–152. DOI: 10.1007/s10653-012-9464-0
- Prasad, R. & Chakraborty D. (2019). *Phosphorus basics: Understanding phosphorus forms and their cycling in the soil*. Alabama Coop. Ext. Syst. <https://www.aces.edu/blog/topics/crop-production/understanding-phosphorus-forms-and-their-cycling-in-the-soil>. Accessed on 24 May 2021.
- Primack, R. (1993). *Essential of conservation biology*. Sinauer Associates Inc. Sunderland, Massachusetts.
- Primavesi, A. (1984). *Manejo ecológico del suelo: La agricultura en regiones tropicales*. 5ta Edición. El Ateneo. Rio de Janeiro, Brazil.
- Rahman, M.A., Lee, S.H., Ji, H.C., Kabir, A.H., Jones, C.S. & Lee, K.W. (2018). Importance of mineral nutrition for mitigating aluminum toxicity in plants on acidic soils: current status and opportunities. *International Journal of Molecular Sciences*, 19(10): 3073. DOI: 10.3390/ijms19103073
- Reitemeier, R.F. (1957). *Soil potassium and fertility*. The Yearbook of Agriculture. States Department of Agriculture. Washington
- Rolinec, M., Bíro, D., Gálik, B., Šimko, M. & Juráček, M. (2012). Immunoglobulins in colostrum of sows with porcine reproductive and respiratory syndrome – PRRS. *Journal of Central European Agriculture*, 13(2): 303-311. DOI: 10.5513/JCEA01/13.2.1049
- Rolinec, M., Bíro, D., Gálik, B., Šimko, M., Juráček, M. & Hanušovský, O. (2018). Essential amino acids index of sow's colostrum. *Journal of Central*

- European Agriculture*, 19(1): 95-101. DOI: 10.5513/JCEA01/19.1.2028
- Ross, D.S. & Ketterings, Q. (1995). *Recommended methods for determining soil cation exchange capacity*. Recommended soil testing procedures for the northeastern United States. 493(101): 62
- Scheffer, F., Schachtschabel, P., Blume, H.P. & Thiele-Bruhn, S. (1966). *Lehrbuch der bodenkunde (Vol. 13)*. Stuttgart: Enke. DOI: 10.1007/978-3-662-49960-3
- Senbayram, M., Gransee, A., Wahle, V. & Thiel, H. (2015). Role of magnesium fertilisers in agriculture: plant–soil continuum. *Crop and Pasture Science*, 66(12): 1219-1229. DOI: 10.1071/CP15104
- Sim, S.F., Azlan, J.M., Rahman, N.A.H.M.A., Lihan, S. & Kang, P.L. (2020). Mineral characteristics of tropical salt licks in Sarawak, The northwest of Borneo island. *Journal of Sustainability Science and Management*, 15(8): 53-62. DOI: 10.46754/jssm.2020.12.005
- Stroker, T. & Harris, N. (2009). K-Ar dating of authigenic illites: Integrating diagenetic history of the Mesa Verde Group, Piceance Basin, NW Colorado (abs.). *AAPG Annual Meeting*, 18: 206.
- Tobler, M.W., Carrillo-Percestequi, S.E. & Powell, G. (2009). Habitat use, activity patterns and use of mineral licks by five species of ungulate in south-eastern Peru. *Journal of Tropical Ecology*, 25(3): 261-270. DOI: 10.1017/S0266467409005896
- Weibel, R., Nielsen, M.T., Therkelsen, J., Jakobsen, F.C., Bjerager, M., Mørk, F., Mathiesen, A., Hovikoski, J., Pedersen, S.S., Johannessen, P.N. & Dybkjær, K. (2020). Illite distribution and morphology explaining basinal variations in reservoir properties of Upper Jurassic sandstones, Danish North Sea. *Marine and Petroleum Geology*, 116: 104290. DOI: 10.1016/j.marpetgeo.2020.104290
- Wilson, M. J., Wilson, L., Patey, I. & Shaw, H. (2014). The influence of individual clay minerals on formation damage of reservoir sandstones: a critical review with some new insights. *Clay Minerals*, 49(2): 147-164. DOI: 10.1180/claymin.2014.049.2.02
- Worden, R.H. & Burley S.D. (2003). *Sandstone diagenesis: the evolution of sand to stone*. Sandstone diagenesis: Recent and ancient. 1-44. DOI: 10.1002/9781444304459.ch
- Worden, R.H. & Morad, S. (2000). *Quartz cementation in oil field sandstones: a review of the key controversies*. Quartz cementation in sandstones. 1-20. DOI: 10.1002/9781444304237.ch1
- Worden, R.H., Griffiths, J., Wooldridge, L.J., Utley, J. E.P., Lawan, A. Y., Muhammed, D.D., Simon, N. & Armitage, P.J. (2020). Chlorite in sandstones. *Earth-Science Reviews*, 204: 103105.
- Yen, J.T. (2000). Anatomy of the digestive system and nutritional physiology. In: Edited by Lewis, A.J., Southern, L.L., eds. *Swine Nutrition (Second edition)*. Boca Raton: CRC Press.
- Yost, J.L. & Hartemink, A.E. (2019). Soil organic carbon in sandy soils: A review. *Advances in Agronomy*, 158: 217-310. DOI: 10.1016/bs.agron.2019.07.004

Synthesis, Antibacterial Properties and Molecular Docking of Nitrobenzoylthiourea Compounds and their Copper(II) Complex

NURINA ASYURA BINTI MOHD YUNUS¹, MAYA ASYIKIN MOHAMAD ARIF^{1*} & FAZIA MOHAMAD SINANG^{2*}

¹Chemistry Programme, Faculty of Resource Science and Technology, Universiti Malaysia Sarawak, 94300 Kota Samarahan, Sarawak, Malaysia; ²Resource Biotechnology Programme, Faculty of Resource Science and Technology, Universiti Malaysia Sarawak, 94300 Kota Samarahan, Sarawak, Malaysia

*Corresponding authors: mamasyikin@unimas.my; msfazia@unimas.my

Received: 21 February 2024 Accepted: 25 September 2024 Published: 31 December 2024

ABSTRACT

The rise of multidrug-resistant microbial pathogens has increased the demand for highly effective antibiotics. Five nitrobenzoylthiourea ligands (**1–5**) with amino acid side chains and their corresponding Cu(II) complexes (**6–10**) were synthesised with yields ranging from 43% to 90%. The successful synthesis of ligands **1–5** were confirmed by the absence of the $\nu(\text{NCS})$ stretching band and the presence of the $\nu(\text{NH})$ band, indicating the complete reaction of all (NCS) with a series of amino acids as well as the appearance of two N-H signals in the ¹H NMR spectra of all the synthesised ligands. On the other hand, the shift of the (C=O) carboxylic peaks in the Cu(II) complexes suggested successful coordination of ligands to the metal ion *via* the carboxylate group. The antibacterial activities of these compounds were tested against six bacteria: *Staphylococcus aureus*, *Bacillus cereus*, *Listeria monocytogenes*, *Escherichia coli*, *Klebsiella pneumoniae*, and *Pseudomonas aeruginosa* using the disc diffusion method. The Cu(II) complexes (**6–10**) exhibited enhanced antibacterial activity compared to the ligands (**1–5**), especially against gram-negative bacteria (*E. coli*, *K. pneumoniae*, and *P. aeruginosa*). For example, compound **4** showed moderate activity against *K. pneumoniae* with a 14 mm inhibition zone while its Cu(II) complexes, **8** recorded better inhibition against *K. pneumoniae* with a 16 mm inhibition zone. Molecular docking studies on all complexes (**6–10**) also revealed higher binding affinity with targeted proteins with binding energy between -10.4 kcal/mol to -9.0 kcal/mol, in comparison with ligand **2** and **4** with the binding energy of only -7.7 kcal/mol (against *S. aureus*) and -6.9 kcal/mol (against *K. pneumoniae*). The enhanced antibacterial activity of all complexes correlates with the higher binding affinity obtained for all complexes. Hence, this study concludes that the nitrobenzoylthiourea derivatives, and particularly their Cu(II) complexes can show potential as antibacterial agent although more thorough investigation are required to develop these compounds into useful drugs.

Keywords: Antibacterial agents, binding affinity, Cu(II) complexes, nitrobenzoylthiourea

Copyright: This is an open access article distributed under the terms of the CC-BY-NC-SA (Creative Commons Attribution-NonCommercial-ShareAlike 4.0 International License) which permits unrestricted use, distribution, and reproduction in any medium, for non-commercial purposes, provided the original work of the author(s) is properly cited.

INTRODUCTION

The discovery of new medications has accelerated in recent decades as the prevalence of germs resistant to antibiotics has increased (Fair & Tor, 2014). This is due the negligent use of antibiotic, which resulted in the evolution of multidrug resistance bacteria (Mohler *et al.*, 2017). Microorganisms develop a variety of mechanisms to limit antimicrobial efficiency, including altering target sites, decreasing cellular permeability to allow for drug penetration, enzymatic destruction of antimicrobial substances, and biofilm development (Idrees *et al.*, 2020). As a result, demand for highly resistant antibiotics increased, and it is critical to conduct rapid

evaluations of potential drugs. On the other hand, the vast array of biological activities of the thiourea-based compound has sparked considerable interest among researchers, with the expectation that modification of ligands and their coordination *via* metal ions would increase their resistance to multidrug-resistant microbial pathogens and influence the drug's microbiological properties. Moreover, metal ions are positively charged and act as electrophiles whereas biological molecules such as DNA and protein are electron-rich and tend to bind and interact with biological molecules (Boros *et al.*, 2020).

Thiourea derivatives have garnered considerable attention as versatile ligands in a variety of applications due to their unique ability

to coordinate with a variety of transition metal ions as monodentate or bidentate ligands and to coordinate with metal centres as neutral, monoanionic, or dianionic ligands to form a stable complex (Wakshlak *et al.*, 2015; Mohapatra *et al.*, 2021). The ability of multiband coordination is dependent on the presence of a donor heteroatom such as oxygen, nitrogen or sulphur, in the ligand. With the presence of two units of reactive primary amide group, thiourea has been found to be a suitable precursor in the synthesis of a variety of their derivatives as well as an excellent chelating agent to metals through S and O, and it has demonstrated a wide range of biological activity, including antibacterial and antifungal activity (Ikokoh *et al.*, 2015; Mohapatra *et al.*, 2021). Thiourea functionality as versatile precursor derives from its ability to form stable hydrogen bonds with recognition elements of biological targets, including proteins, enzymes and receptor as the hydrogen bond network is essential for stabilizing ligand-receptor interaction (Ronchetti *et al.*, 2021). Consequently, reactive functional groups of thiourea, such as amino, imino, and thiol, can play important roles as precursor in the synthesis of organic molecules for various biological applications, as demonstrated in bacteriostatic activities, where they can be protonated under acidic conditions and reacted with the carboxyl and phosphate groups of the bacterial surface, resulting in prominent antibacterial activity (Ngaini *et al.*, 2012; Halim & Ngaini, 2017). Additionally, thiourea is employed as an active ingredient in pharmaceuticals, which increases the usability of their derivatives as they will pose no adverse risk to natural living bodies (Ohammad, 2018).

Metal complexes are thought to exert their effect through the inhibition of enzymes, interaction with intracellular biomolecules, increased lipophilicity and modification of cell membrane functions (Malik *et al.*, 2018). Metal complex considerably improved the results given by thiourea ligand alone. On the other hand, copper(II) was specifically chosen due to its well-known antimicrobial properties. Copper exposure has been shown to impair the integrity of the bacterial cell wall, resulting in the microorganism's mortality (Montero *et al.*, 2019), while also increasing their susceptibility to copper ions, which cause metabolic dysfunction. According to Arendsen and coworkers (2019), when copper ions reach a

critical intracellular concentration, the plasma membrane becomes increasingly permeable, allowing important cell content including nucleotides, amino acids, and potassium. Moreover, attachment of amino acids may be advantageous as these are biomolecules that play a critical role in a variety of biological functions (Raheel *et al.*, 2016) and have been used to enhance the efficacy (*in vitro*) of existing drugs (Idrees *et al.*, 2020).

In this study, five new monobenzoyl thiourea derivatives were synthesised *via* the reaction of 4-nitrobenzoyl isothiocyanate with tryptophan, methionine, valine, alanine, and cysteine. The effect of complexation with copper(II) metal in their antibacterial activity was analysed against three gram-positive and three gram-negative bacteria. The contribution of newly synthesised nitrobenzoyl thiourea bearing amino acid side chain and their copper(II) complexes in the antibacterial study were emphasised with molecular docking analysis. Even if the incorporation of copper(II) ion does not improve the antibacterial activity directly, it may lead to compounds that can potentially inhibit virulence mechanisms of highly resistant pathogens as this study is important in drug discovery for the medical industry.

MATERIALS & METHODS

Materials

4-nitrobenzoyl chloride, potassium thiocyanate (KSCN) powder, tryptophan, methionine, serine, valine, L-alanine, cysteine, silver(I) nitrate, copper(II) chloride, potassium hydroxide (KOH), distilled acetone, ethanol, acetonitrile, ethyl acetate, propanol, methanol, hexane, dichloromethane, chloroform, cyclohexanol, nitromethane, tetrahydrofuran, diethyl ether, toluene, petroleum ether is of reagent grade and used without purification. Acetone was distilled over magnesium sulfate anhydrous.

Instrumentation and Analytical Characterisation of Thiourea Compounds

Characterisation of pure thiourea compounds were conducted using Fourier Transform Infrared Spectrometry (FTIR) Perkin-Elmer Spectrum (GX2000) spectrometer. The FTIR spectra (ν/cm^{-1}) of all compounds were determined using Attenuated Total Reflection

(ATR) technique. The CHNS elemental analysis of thiourea ligands and complexes were performed using Thermo Scientific™ FlashSmart™ Elemental Analyser. The ^1H and ^{13}C NMR spectroscopy (JEOL ECA 500 MHz) were used to confirm the chemical structure of thiourea ligands by identifying the H and C present in the synthesised compounds. All NMR spectra were recorded in DMSO- d_6 solutions and the chemical shifts were reported in δ (ppm).

Synthesis of Thiourea Ligands

Synthesis of ((4-nitrobenzoyl)carbamothioyl)tryptophanato (1)

4-nitrobenzoyl chloride (0.01 mol, 1.86 g) and potassium thiocyanate (0.01 mol, 0.97 g) were dissolved in 120 mL of distilled acetone. The solution was stirred for 1 hour until white precipitate formed. The white precipitate, potassium chloride (KCl) was removed while the filtrate formed was kept for the next step. A 0.01 mol (2.04 g) of tryptophan was added to the filtrate solution and the solution mixture was heated to reflux for three days (72 hours) at 65 °C before being filtered, ultimately yielding only the targeted compounds while eliminating unwanted products. The mixture was allowed to cool at room temperature and the filtrate was left to evaporate at room temperature for several days. After several days, orange solid was formed and collected as compound **1** (3.357 g, 81.40%). Compound was purified by recrystallisation using ethanol/dichloromethane (2:1) ratio. FTIR ν_{max} 3412 (N-H), 1717 (C=O carboxylic), 1674 (C=O amide), 1514 (C=C aromatic), 854 (C=S), 1159 (C-N). Calcd. for ($\text{C}_{19}\text{H}_{16}\text{N}_4\text{O}_5\text{S}$); C: 55.33%, H: 3.91%, N: 13.58%, S: 7.77%, found: C: 55.72%, H: 4.18%, N: 13.87%, S: 6.51%. ^1H NMR (500 MHz; DMSO- d_6) δ 11.89 (1H, s, NH), 11.04 (1H, d, $J = 7.6$ Hz, NH), 10.92 (1H, d, NH), 8.28 (2H, d, $J = 4.6$ Hz, Ar-H), 8.03 (2H, d, $J = 1.5$ Hz, Ar-H), 7.49 (1H, d, $J = 7.6$ Hz, Ar-H), 7.29 (1H, d, $J = 7.6$ Hz, Ar-H), 7.14 (1H, d, $J = 2.3$ Hz, Ar-H), 7.01 (1H, t, $J = 7.6$ Hz, Ar-H), 6.90 (1H, t, $J = 7.6$ Hz, Ar-H), 2.47 (1H, q, $J = 1.8$ Hz, CH), 2.06 (2H, d, $J = 6.1$ Hz, CH_2). ^{13}C -NMR (125 MHz; DMSO- d_6) δ 180.2 (C=SNH), 172.3 (C=OOH), 167.5 (C=ONH), 150.3 (Ar-C), 138.5 (Ar-C), 136.6 (Ar-C), 130.7 (Ar-C), 127.9-108.9 (Ar-C), 58.9 (CH), 26.7 (CH_2).

Synthesis ((4-nitrobenzoyl)carbamothioyl)

methioninato (2)

The procedure for compound **1** was repeated using methionine (0.01 mmol, 1.49 g). After several days, yellow solid was formed and collected as compound **2** (2.899 g, 81.11%). Compound was purified through washing with distilled water. FTIR ν_{max} 3218 (N-H), 1722 (C=O carboxylic), 1508 (C=O amide), 1508 (C=C aromatic), 853 (C=S), 1156 (C-N). Calcd. for ($\text{C}_{13}\text{H}_{15}\text{N}_3\text{O}_5\text{S}_2$); C: 43.69%, H: 4.23%, N: 11.76%, S: 17.94%, found: C: 43.71%, H: 4.22%, N: 11.82%, S: 17.76%. ^1H NMR (500 MHz; DMSO- d_6) δ 11.88 (1H, s, NH), 11.09 (1H, d, $J = 7.4$ Hz, NH), 8.27-8.31 (2H, m, Ar-H), 8.09-8.12 (2H, m, Ar-H), 4.97 (1H, dd, $J = 12.6, 6.9$ Hz, CH), 2.51 (2H, q, $J = 7.5$ Hz, CH_2), 2.46 (2H, t, $J = 1.7$ Hz, CH_2), 2.03 (3H, s, CH). ^{13}C -NMR (125 MHz; DMSO- d_6) δ 180.7 (C=SNH), 172.3 (C=OOH), 167.4 (C=ONH), 150.3 (Ar-C), 138.2 (Ar-C), 130.8 (Ar-C), 123.8 (Ar-C), 57.2 (CH), 30.9 (CH_2), 29.7 (CH_2), 15.2 (CH_3).

Synthesis of ((4-nitrobenzoyl)carbamothioyl)valinato (3)

The procedure for compound **1** was repeated using valine (0.01 mol, 1.17 g). After several days, milky white solid was formed and collected as compound **3** (2.912 g, 89.51%). Compound was purified by recrystallisation using propanol/dichloromethane (2:1) ratio. FTIR ν_{max} 3237 (N-H), 1716 (C=O carboxylic), 1672 (C=O amide), 1521 (C=C aromatic), 854 (C=S), 1163 (C-N). Calcd. for ($\text{C}_{13}\text{H}_{15}\text{N}_3\text{O}_5\text{S}$); C: 47.99%, H: 4.65%, N: 12.92%, S: 9.86%, found: C: 48.06%, H: 4.73%, N: 12.97%, S: 8.26%. ^1H NMR (500 MHz; DMSO- d_6) δ 11.93 (1H, s, NH), 11.17 (1H, d, $J = 7.7$ Hz, NH), 8.28 (2H, d, $J = 8.9$ Hz, Ar-H), 8.11 (2H, d, $J = 8.9$ Hz, Ar-H), 2.46 (1H, t, $J = 1.7$ Hz, CH), 2.27-2. (1H, m, CH), 0.91-0.98 (6H, m, 2 CH_3). ^{13}C -NMR (125 MHz; DMSO- d_6) δ 181.1 (C=SNH), 171.8 (C=OOH), 167.8 (C=ONH), 150.4 (Ar-C), 138.4 (Ar-C), 130.8 (Ar-C), 123.8 (Ar-C), 63.2, 30.7 (CH), 19.2, 18.6 (CH_3).

Synthesis of ((4-nitrobenzoyl)carbamothioyl)alaninato (4)

The procedure for compound **1** was repeated using alanine (0.01 mol, 0.89 g). After several days, orange-brick solid was formed and

collected as compound **4** (2.363 g, 79.5%). Compound was purified by recrystallisation using ethanol/dichloromethane (2:1) ratio. FTIR ν_{\max} 3281 (N-H), 1709 (C=O carboxylic), 1659 (C=O amide), 1532 (C=C aromatic), 847 (C=S), 1167 (C-N). Calcd. for (C₁₁H₁₁N₃O₅S); C: 44.44%, H: 3.73%, N: 14.13%, S: 10.79%, found: C: 44.84%, H: 3.97%, N: 14.58, S: 8.68%. ¹H-NMR (500 MHz, DMSO-d₆) δ 11.88 (1H, s, NH), 11.11 (1H, d, *J* = 6.9 Hz, NH), 8.28 (1H, d, *J* = 8.9 Hz, Ar-H), 8.09 (1H, d, *J* = 8.9 Hz, Ar-H), 4.83-4.77 (1H, m, CH), 1.46 (3H, d, *J* = 7.2 Hz, CH₃). ¹³C-NMR (125 MHz, DMSO-d₆) δ 180.1 (C=SNH), 173.4 (C=OOH), 167.6 (C=ONH), 150.3 (Ar-C), 138.5 (Ar-C), 130.7 (Ar-C), 123.9 (Ar-C), 17.7 (CH₃).

Synthesis of ((4-nitrobenzoyl)carbamothioyl) cysteinato (5)

The procedure for compound **1** was repeated using cysteine (0.01 mol, 1.2116 g). After several days, orange solid was formed and collected as compound **5** (2.706 g, 82.15%). Compound was purified by recrystallisation using ethanol/hexane (1:2). FTIR ν_{\max} 3113 (N-H), 1716 (C=O carboxylic), 1668 (C=O amide), 1519 (C=C aromatic), 848 (C=S), 1157 (C-N). Calcd. for (C₁₁H₁₁N₃O₅S₂); C: 40.11%, H: 3.37%, N: 12.76%, S: 19.47%, found: C: 40.43%, H: 3.57%, N: 14.07%, S: 16.49%. ¹H-NMR (500 MHz, DMSO-d₆) δ 11.90 (1H, s, NH), 11.21 (1H, d, *J* = 7.4 Hz, NH), 8.27 (1H, d, *J* = 5.2 Hz, Ar-H), 8.09 (1H, d, *J* = 8.9 Hz, Ar-H), 3.57 (1H, dd, *J* = 11.7, 9.5 Hz, CH), 2.46 (2H, t, *J* = 1.9 Hz, CH₂). ¹³C-NMR (125 MHz; DMSO-d₆) δ 172.4 (C=SNH), 166.3 (C=OOH), 149.9 (C=ONH), 142.3 (Ar-C), 136.9 (Ar-C), 130.6 (Ar-C), 124.0 (Ar-C), 57.2 (CH), 32.9 (CH₂).

Synthesis of Copper(II) Complexes of Thiourea

Synthesis and Characterisation Data of di((4-nitrobenzoyl)carbamothioyl) tryptophanato copper(II) (6)

Compound **1** (0.206 g, 0.5 mmol) was dissolved in 10 ml of ethanol followed by continuous stirring to make sure all ligand was dissolved. A (2.2 mL 0.5 mmol) of KOH was added into the solution and the mixture was stirred at room temperature for 30 minutes. A metal solution of CuCl₂.2H₂O (0.043 g, 0.25 mmol) in 2 mL of

distilled water was later added into the solution containing ligand and KOH before the mixture was stirred for another 24 hours. Then, the mixture was filtered out and left to evaporate for few days to give out brownish precipitate of complex **6** (0.18 g, 68.70%). The complex was then subjected to purification with distilled water. FTIR ν_{\max} 3170 (N-H), 1681 (C=O amide), 1520 (C=C aromatic), 853 (C=S), 1171 (C-N). Calcd. for (C₃₈H₄₈CuN₈O₁₉S₂); C: 43.53%, H: 4.61%, N: 10.69%, S: 6.12%, found: C: 43.16%, H: 3.85%, N: 10.62%, S: 6.61%.

Synthesis and Characterisation Data of di((4-nitrobenzoyl)carbamothioyl)methionato copper(II) (7)

The procedure for the synthesis of complex **7** was repeated using ligand **2** (0.357 g, 1.0 mmol), KOH (4.7 mL 1.0 mmol) and CuCl₂.2H₂O (0.085 g, 0.5 mmol). After few days, green precipitate of complex **7** (0.239 g, 57.59 %) was obtained. FTIR ν_{\max} 2986 (N-H), 1682 (C=O amide), 1523 (C=C aromatic), 854 (C=S), 1169 (C-N). Calcd. for (C₂₆H₃₄CuN₆O₁₃S₄); C: 37.61%, H: 4.13%, N: 10.12%, S: 15.45%, found: C: 37.25%, H: 3.73%, N: 10.52%, S: 15.61%.

Synthesis of di((4-nitrobenzoyl)carbamothioyl)valinatocopper(II) (8)

The procedure for the synthesis of complex **8** was repeated using compound **3** (0.325 g, 1.0 mmol), KOH (4.7 mL 1.0 mmol) and CuCl₂.2H₂O (0.085 g, 0.5 mmol). After few days, brownish precipitate of complex **8** (0.261 g, 65.10%) was obtained. FTIR ν_{\max} 2964 (N-H), 1679 (C=O amide), 1519 (C=C aromatic), 853 (C=S), 1166 (C-N). Calcd. for (C₂₆H₃₈CuN₆O₁₅S₂); C: 38.92%, H: 4.77%, N: 10.48%, S: 7.99%, found: C: 48.73%, H: 4.30%, N: 10.85%, S: 9.21%.

Synthesis of di((4-nitrobenzoyl)carbamothioyl)alaninatocopper(II) (9)

The procedure for the synthesis of complex **9** was repeated using compound **4** (0.193 g, 0.65 mmol), KOH (3.1 mL 0.65 mmol) and CuCl₂.2H₂O (0.0554 g, 0.325 mmol). After few days, brownish precipitate of complex **9** (0.137 g, 55.24%) was obtained. FTIR ν_{\max} 3116 (N-H), 1671 (C=O amide), 1519 (C=C aromatic), 854 (C=S), 1170 (C-N). Calcd. for

(C₂₂H₃₂CuN₆O₁₆S₂); C: 34.58%, H: 4.22%, N: 11.00%, S: 8.39%, found: C: 34.30%, H: 3.90%, N: 11.04%, S: 9.89%.

Synthesis of di((4-nitrobenzoyl)carbamothioyl)tcysteinatocopper(II) (10)

The procedure for the synthesis of complex **10** was repeated using compound **5** (0.157 g, 0.48 mmol), KOH (2.3 mL, 0.48 mmol) and CuCl₂·2H₂O (0.041 g, 0.24 mmol). After few days, brownish precipitate of complex **10** (0.131 g, 76.15%) was obtained. FTIR ν_{\max} 3072 (N-H), 1703 (C=O carboxylic), 1651 (C=O amide), 1523 (C=C aromatic), 851 (C=S), 1168 (C-N). Calcd. for (C₂₂H₂₀CuN₆O₁₀S₄); C: 36.69%, H: 2.80%, N: 11.67%, S: 17.81%, found: C: 36.64%, H: 3.08%, N: 12.26%, S: 12.75%.

Antimicrobial Activity Test

All synthesised compounds were evaluated for antibacterial activity using the disc diffusion method against three gram-positive bacteria (*Staphylococcus aureus*, *Bacillus cereus*, *Listeria monocytogenes*) and three gram-negative bacteria (*Escherichia coli*, *Klebsiella pneumoniae*, *Pseudomonas aeruginosa*). All bacteria were cultured in Mueller Hinton broth and incubated at 37 °C with stirring for 24 hours. The bacterial suspension was adjusted to 0.5 McFarland standard and 20 μ L of the inoculum was spread uniformly onto Mueller Hinton agar using a sterile cotton swab. The disc with different concentrations (50 ppm, 100 ppm, 150 ppm, 200 ppm, 250 ppm, 500 ppm and 1000 ppm) of synthesized compounds dissolved in DMSO were placed onto the Mueller Hinton agar. The DMSO was used as negative control (Halim & Ngaini, 2016). Meanwhile, penicillin, vancomycin, ampicillin, tetracycline, ceftazidime and imipenem were used as the standard antibiotic for *Staphylococcus aureus*, *Bacillus cereus*, *Listeria monocytogenes*, *Escherichia coli*, *Klebsiella pneumoniae*, *Pseudomonas aeruginosa* respectively. Each antibiotic was selected based on its established efficacy as a standard treatment for the corresponding bacterial strain. Subsequently, the plates were incubated at 37 °C for 24 hours. After the incubation, the clear inhibition zone was observed, and the diameter of the inhibition zone was measured in millimetre (mm).

Molecular Docking Study

The crystal structures of the targeted bacterial proteins, *S. aureus* (PDB entry: 4xwa), *B. cereus* (PDB entry: 5bca), *K. pneumoniae* (PDB entry: 5xun), and *P. aeruginosa* (PDB entry: 7ci4) were retrieved in PDB format from the RCSB Protein Data Bank. The protein was prepared using AutoDock Tools-1.5.7 by adding polar hydrogen atoms, removing water molecules, and ensuring the structure was appropriately formatted. The prepared protein structure was saved as a pdbqt file. The synthesised ligand structures were generated using Chemdraw software and were later converted to pdbqt files using a variety of software programs, including Molview, Open Babel, and the AutoDock Tools program. Docking simulations were performed with AutoDock Vina using default grid box parameters (40 \times 40 \times 40, 0.375 Å spacing) provided by AutoDock Tools (Trott & Olson, 2010). These parameters automatically center the grid on the protein's binding pocket. The grid coordinates were (14.743, -0.047, 14.858) for *S. aureus*, (40.132, 23.825, 36.938) for *B. cereus*, (-28.095, 7.000, 19.029) for *K. pneumoniae*, and (26.335, -8.649, 21.505) for *P. aeruginosa*. These default settings are designed to maximise the likelihood of identifying potential binding interactions across the protein surface, particularly in exploratory docking studies where the exact binding site may not be well-defined. Following that, molecular docking was performed using AutoDock Vina (Pingaew *et al.*, 2018), which efficiently handles the docking process within the grid parameters. The docking process was managed with command prompt, and the binding poses were visualized with PyMOL (Schrodinger, 2016), an open-source molecular visualization tool used to identify hydrogen bonds and other key interactions between the synthesised compounds and amino acid residues of the protein (Roche Allred *et al.*, 2017). Factors such as the conformation within protein binding site, binding affinity, and the number of hydrogen bond interactions with protein residues were investigated for better understanding.

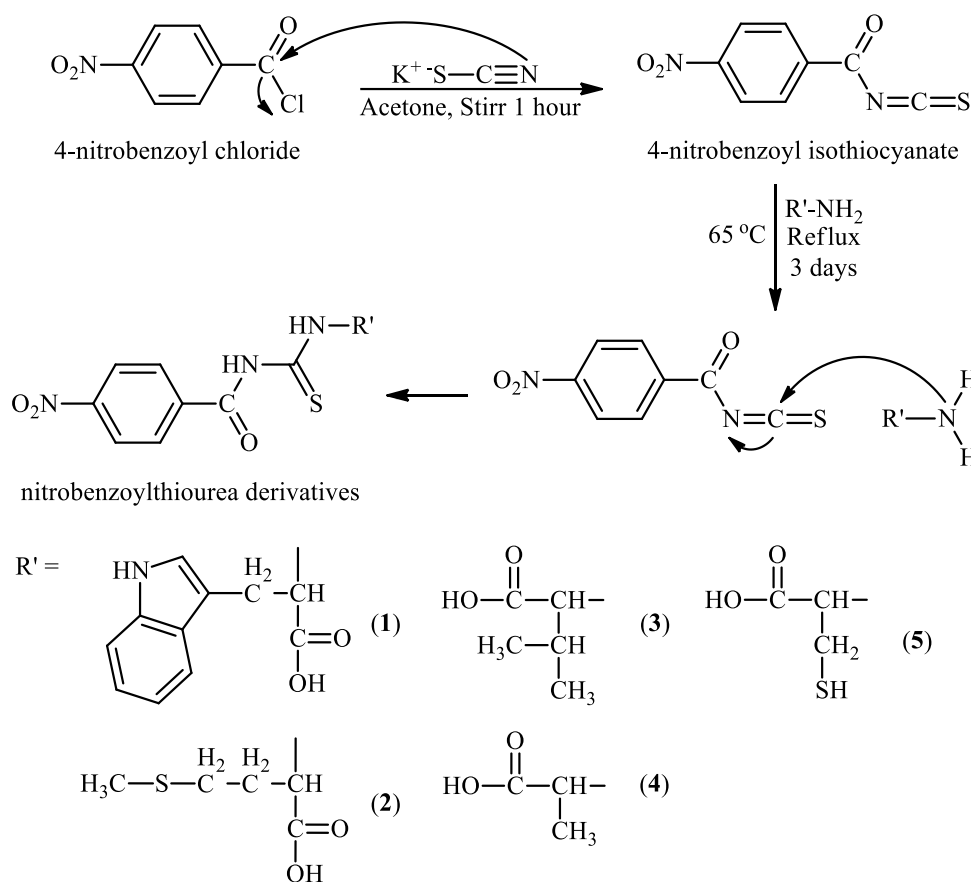
RESULTS & DISCUSSION

Thiourea Ligands

Thiourea ligands were synthesised *via* a sequence of nucleophilic substitution reactions, involving thiocyanate and isothiocyanate intermediates. Initially, the thiocyanate anion

(SCN⁻) serves as a nucleophile, attacking the carbonyl carbon of 4-nitrobenzoyl chloride. This interaction facilitates the displacement of the chloride ion, thereby yielding 4-nitrobenzoyl isothiocyanate. Subsequently, a primary amine (R'-NH₂), which is the amino acid series engages in a nucleophilic attack on the electrophilic carbon of the isothiocyanate group (N=C=S) within the 4-nitrobenzoyl

isothiocyanate. This nucleophilic addition leads to the formation of a thiourea linkage (-NH-C=S), resulting in the corresponding nitrobenzoylthiourea derivatives. Thiourea derivatives (**1-5**) were successfully synthesized with the percentage yields of 81.40%, 81.11%, 89.51%, 79.5% and 82.15% respectively. The synthesis pathway of the thiourea ligand was depicted in scheme 1.



Scheme 1: Synthesis pathway of thiourea ligand (**1-5**)

All synthesised compounds were characterised using CHNS elemental analysis, FT-IR, ¹H and ¹³C NMR spectroscopy. The elemental analysis data of ligand **1-5** are shown in Table 1. The FT-IR spectra showed the successful formation of thiourea compounds through the absence of ν(NCS) group at 2000 cm⁻¹ to 2400 cm⁻¹ and the presence of expected absorption at 3100 cm⁻¹ to 3400 cm⁻¹ attributed to ν(NH) band (Fakhar *et al.*, 2018). This result from the conversion of (NCS) to (NH) which also indicates that all (NCS) has reacted with the amino acid. For ligands (**1-5**), the ν(C=O) stretching of carboxylic were observed at 1722 cm⁻¹ to 1709 cm⁻¹. Apart from that, distinctive peaks were also observed between 1681 cm⁻¹ to

1659 cm⁻¹ that attributed to the presence of ν(C=O) of amide group of ligands (**1-5**) respectively. These distinctive peak apparently were decreased in frequency compared to ordinary amides absorption range due to the formation of intramolecular hydrogen bond interaction (Khairul *et al.*, 2016) between the hydrogen atom of thio-amide group (H-N-C=S) and the oxygen atom of carbonyl group (C=O) (Fakhar *et al.*, 2018). Moreover, the C=O group (benzoyl) occurred at 1681 to 1659 cm⁻¹ which was lower than the usual carbonyl group at 1760-1685 cm⁻¹, is due to the conjugation towards the benzene ring and the hydrogen bond formation with NH (Li *et al.*, 2010). Table 2 summarises the important bands observed in the FTIR

spectra of nitrobenzoylthiourea derivatives (**1-5**).

The ^1H NMR and ^{13}C NMR spectroscopic analysis was performed for all nitrobenzoylthiourea ligands (**1-5**). For ^1H NMR two (NH) peaks can be observed which represent resonance of (CONH) and (CSNH). The proton resonance of (CONH) in which the proton bonded to carbonyl group can be noticed at higher chemical shift compared to the resonance of (CSNH) in which the proton is bonded to thiocarbonyl group. This might be due to electron withdrawing effect of oxygen and sulphur (Hassan *et al.*, 2011), and the presence of deshielding aromatic ring near (CONH) group making it more deshielded and exist downfield at higher frequency compared to proton of (CSNH). The chemical shifts of the two (N-H) signals were distinct, owing to the existence and

influence of the electron withdrawing group and intramolecular hydrogen bond in the molecule (Saeed *et al.*, 2010; Raheel *et al.*, 2016). Distinctive multiple resonances at δ_{H} 8.28-8.09 ppm were observed due to the presence of proton of the aromatic group. Apart from that, the formation of thiourea ligands were confirmed by the appearance of carbon peak signals. The carbon peaks of (CONH) were more deshielded and present at the most downfield frequency followed by the carbon of (COOH) and (CSNH) due to the higher electronegativity value of oxygen compared to sulphur atom. The spectra of ^{13}C NMR exhibited carbonyl (C=O) at δ_{C} 172.4-181.0 ppm and δ_{C} 166.3-173.3 ppm corresponding to (CONH) and (C=OO) respectively. The successful formation of thiourea compound was also confirmed by the signal at δ_{C} 149.9-167.8 ppm represents (CSNH) thiocarbonyl.

Table 1. CHNS elemental analysis of nitrobenzoylthiourea derivatives 1-5

Thiourea	Molecular Formula	Molecular Weight	Measured value (Theoretical Value)			
			% Carbon	% Hydrogen	% Nitrogen	% Sulphur
1	$\text{C}_{19}\text{H}_{16}\text{N}_4\text{O}_5\text{S}$	414.42	55.72(55.33)	4.18(3.91)	13.87(13.58)	6.51(7.77)
2	$\text{C}_{13}\text{H}_{15}\text{N}_3\text{O}_5\text{S}_2$	357.41	43.71(43.69)	4.22(4.23)	11.82(11.76)	17.76(17.94)
3	$\text{C}_{13}\text{H}_{15}\text{N}_3\text{O}_5\text{S}$	325.34	48.16(47.99)	4.73(4.65)	12.97(12.92)	8.26(9.86)
4	$\text{C}_{11}\text{H}_{11}\text{N}_3\text{O}_5\text{S}$	297.29	44.84(44.44)	3.97(3.73)	14.53(14.13)	8.68(10.79)
5	$\text{C}_{11}\text{H}_{11}\text{N}_3\text{O}_5\text{S}_2$	329.35	40.43(40.11)	3.57(3.37)	14.07(12.76)	16.49(19.47)

Table 2. Important bands observed in the FTIR spectra of nitrobenzoylthiourea derivatives 1-5

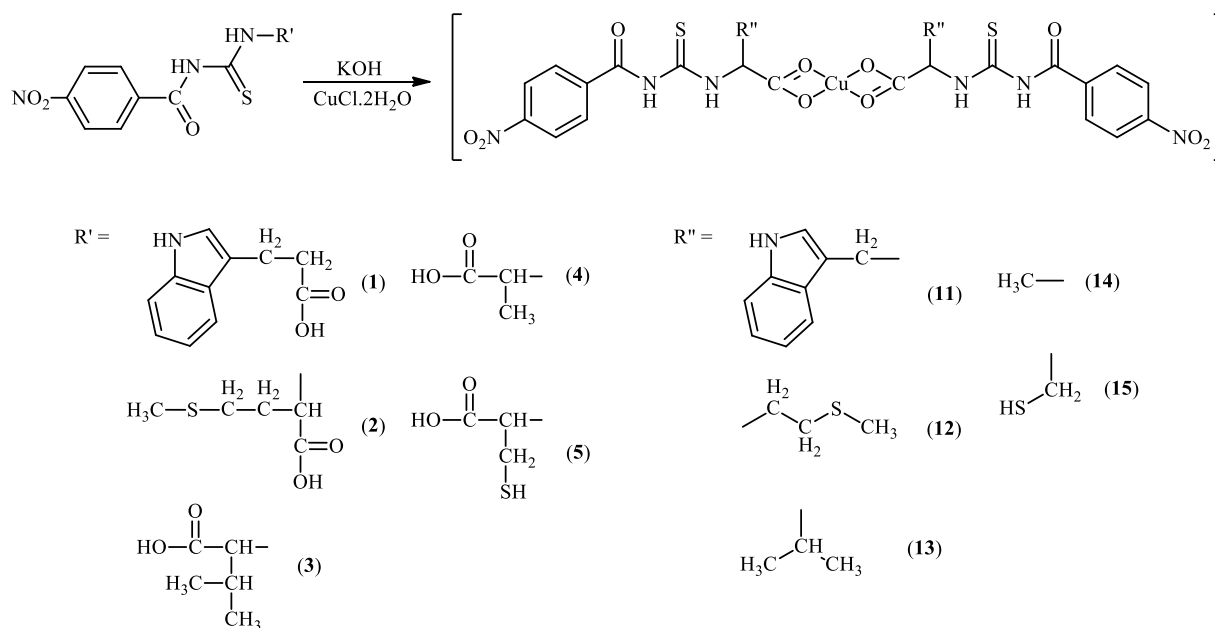
Thiourea ligand	$\nu(\text{NH})$	$\nu(\text{C=O})$ carboxylic	$\nu(\text{C=O})$ amide	$\nu(\text{C=C})$ aromatic	$\nu(\text{C=S})$	$\nu(\text{CN})$
1	3412	1716	1674	1514	854	1159
2	3218	1722	1681	1508	853	1156
3	3237	1716	1672	1521	854	1163
4	3281	1709	1659	1532	847	1167
5	3113	1716	1668	1519	848	1157

Copper(II) Complexes of Thiourea

Copper(II) complexes were synthesised through a process that involved the deprotonation of the

carboxylic acid group present in the nitrobenzoylthiourea ligands. This deprotonation step generates a carboxylate anion, which then facilitates the coordination of copper(II) ions to form stable copper(II) thiourea complexes *via* chelation. Copper(II) complexes (**6-10**) were successfully synthesised with satisfactory percentage yield of 68.7%, 57.6%,

65.1%, 55.2% and 76.2%, respectively. Scheme 2 illustrated the synthesis pathway of copper(II) complexes (**6-10**).



Scheme 2: Synthesis pathway of copper(II) complexes of thiourea (6-10)

The CHNS elemental analysis data of copper(II) complexes (**6-10**) are in good agreement with the theoretical value as showed in Table 3. FTIR analysis of copper(II) complexes (**6-10**) was conducted to demonstrate significant changes in the functional group stretching vibrations upon complexation, as evidenced by the shifting of the designated peaks and intensities in their spectra. These changes confirm the coordination sites of ligands (**1-5**) to the metal ions in the complex. In addition, the shifts experienced by the $\nu(\text{C}=\text{O})$ carboxylic ($1709\text{--}1722\text{ cm}^{-1}$) towards lower region ($1671\text{--}1703\text{ cm}^{-1}$) in the IR spectrum of (**6-10**) possibly indicate the coordination to the Cu(II) metal centre through the carboxylate binding site to form the thiourea complexes. The shifting of the peak towards the lower region was due to the deprotonation that induced the delocalisation of the electron and conforming the coordination through oxygen (Mishra *et al.*, 2012). In addition, the decrease in shifting frequency observed in complex (**10**), compared to its free ligand, suggests a reduction in the bond order of

the $\text{C}=\text{O}$ bond upon coordination to the copper(II) metal (Welch *et al.*, 2022). The carbonyl of $\nu(\text{C}=\text{O})$ of amide group showed slight chemical shift from 1659 cm^{-1} to 1681 cm^{-1} in the free ligand to 1651 cm^{-1} to 1682 cm^{-1} of metal complexes. In addition, there was very little to no variable shift of $\nu(\text{C}=\text{S})$ and $\nu(\text{C}-\text{N})$ in the complex in comparison to the free ligands. This observation suggests that the $(\text{C}=\text{S})$ group does not form any coordinate covalent bond with the metal ions. This interpretation is consistent with the unchanged spectral features between the free ligands and the complex, indicating that the chemical environment around these functional groups remains largely unaffected by metal coordination. The FTIR stretching vibration values of copper(II) complexes (**6-10**) were shown in Table 4. Due to the paramagnetic nature of copper(II) complexes, ^1H and ^{13}C NMR experiments was not performed on all of the copper(II) complexes. The paramagnetic properties of the complexes could cause severe broadening of NMR signals, making NMR an ineffective method for their analysis.

Table 3. CHNS elemental analysis of thiourea complex 6-10

Complex	Molecular Formula	Molecular Weight (g/mol)	Measured value (Theoretical Value)
---------	-------------------	--------------------------	------------------------------------

			% C	% H	% N	% S
6	C ₃₈ H ₃₂ CuN ₈ O ₁₀ S ₂	888.38	43.16 (43.53)	3.85 (4.61)	10.62 (10.69)	6.61 (6.12)
7	C ₂₆ H ₃₀ CuN ₆ O ₁₀ S ₄	778.36	37.25 (37.61)	3.73 (4.13)	10.52 (10.12)	15.61 (15.45)
8	C ₂₆ H ₂₈ CuN ₆ O ₁₀ S ₂	712.21	48.73 (38.92)	4.30 (4.77)	10.85 (10.48)	9.21 (7.99)
9	C ₂₂ H ₂₀ CuN ₆ O ₁₀ S ₂	656.10	34.30 (34.58)	3.90 (4.22)	11.04 (11.00)	9.89 (8.39)
10	C ₂₂ H ₂₀ CuN ₆ O ₁₀ S ₄	720.23	36.64 (36.69)	3.08 (2.80)	12.26 (11.67)	12.75 (17.81)

Table 4. FTIR spectrum of thiourea complex 6-10

Thiourea complexes	v(NH)	v(C=O) amide	v(C=C) aromatic	v(C=S)	v(CN)
6	3170	1681	1520	853	1171
7	2986	1682	1523	854	1169
8	2964	1679	1519	853	1166
9	3116	1671	1519	854	1170
10	3072	1651	1523	851	1168

Antibacterial Activity

The antibacterial activity of all produced compounds at different concentrations (150 ppm, 250 ppm, 500 ppm, and 1000 ppm) was determined using the disc diffusion method. The compounds (**1-10**) were tested against several bacteria, including *Staphylococcus aureus*, *Bacillus cereus*, *Listeria monocytogenes*, *Escherichia coli*, *Klebsiella pneumoniae*, and *Pseudomonas aeruginosa*. Standard antibiotics were used as positive controls, and DMSO served as the negative control (Ngaini & Mortadza, 2019). The results were classified as mild (6-13 mm) or moderate (14-16 mm) based on the inhibition zones (Halim & Ngaini, 2017). The antibacterial activity of thiourea compounds (**1-10**) against gram-positive bacteria is summarized in Table 5.

Notably, all ligands showed little bactericidal activity against gram-positive bacteria at concentrations below 500 ppm. This low activity

could be due to steric hindrance caused by bulky groups, such as the tryptophan and nitrobenzoyl groups in ligand **1**, which block the interaction between the compound's active sites and the bacterial receptor sites (Smith, 2017; Fakhar *et al.*, 2018). As lipophilicity is a key factor in a compound's bioactivity (Arslan *et al.*, 2009), steric hindrance decreases lipophilicity, making it harder for the compound to penetrate bacterial cell membranes, thus reducing the antibacterial activity (Ngaini *et al.*, 2012).

However, at both 500 ppm and 1000 ppm, ligands **1** and **2** showed mild antibacterial activity against gram-positive bacteria (*B. cereus*, *L. monocytogenes*, and *S. aureus*). Ligand **2**'s activity may be due to the longer aliphatic chain in its structure, which increases biological activity by enhancing lipophilicity (Liang *et al.*, 2018; Fatima *et al.*, 2017).

The incorporation of copper(II) into the thiourea complexes (**6-10**) led to more effective

inhibition of gram-positive bacteria. At both 500 ppm and 1000 ppm, all complexes showed antibacterial activity, particularly against *S. aureus*, with complex **8** showing the highest activity. The copper(II) complexes also significantly increased antibacterial activity of complex **9** and **10** against *B. cereus* compared to their free ligands **4** and **5**. This improved activity could possibly be due to the effect of chelation, which reduces metal ion polarity and increases lipophilicity, allowing better penetration through bacterial cell membranes (Sumrra *et al.*, 2014; Ramesh *et al.*, 2016).

For gram-negative bacteria, the thiourea ligands (**1-5**) showed no activity at concentration below 500 ppm, except for ligand **4**, which had notable activity against *K. pneumoniae* starting at 150 ppm. This could possibly be due to the smaller size of alanine that enhance the antibacterial activity, which is in agreement with the data reported by Madabhushi *et al.* (2014). Ligands **2**, **3**, and **5** showed only mild activity at 500 ppm and 1000 ppm. Copper(II) complexes (**6-10**), however, showed mild to moderate

activity against gram-negative bacteria, with complex **9** being the most active at concentrations below 500 ppm. This further demonstrates the role of metal ions in enhancing antibacterial effects (Boros *et al.*, 2020; Claudel *et al.*, 2020). The metal-ligand complex increases lipophilicity, helping the complex penetrate bacterial cell membranes and deactivate bacteria (Liang *et al.*, 2018; Arendsen *et al.*, 2019). The antibacterial activity of the thiourea compounds (**1-10**) against gram-negative bacteria is shown in Table 6.

Overall, metal complexes exhibited better antibacterial activity than free ligands, especially against gram-positive bacteria, which are generally more susceptible to antibacterial agents due to their cell wall structure (Mukherjee *et al.*, 2017). Complex **10** was the most effective against gram-positive bacteria, while complex **9** showed the highest inhibition against gram-negative bacteria. The inhibition zones for the thiourea ligands (**1-5**) and copper(II) complexes (**6-10**) are shown in Figures 1- 4.

Table 5. Zone of inhibition (mm) of thiourea compounds (1-10) on gram positive bacteria

Concentration (ppm)	Zone of Inhibition (mm)											
	<i>S. aureus</i>				<i>B. cereus</i>				<i>L. monocytogenes</i>			
	150	250	500	1000	150	250	500	1000	150	250	500	1000
1	-	-	-	-	-	-	8	9	-	-	-	-
2	-	-	10	10	-	-	-	-	-	-	7.5	9
3	-	-	-	-	-	-	-	-	-	-	-	-
4	-	-	-	-	-	-	-	-	-	-	-	-
5	-	-	-	-	-	-	-	-	-	-	-	-
6	-	-	7	11	-	-	-	-	-	-	-	-
7	-	-	7	10	-	-	-	-	7.5	7.5	7.5	7.5
8	-	-	13	15	-	-	-	-	-	-	-	-
9	-	-	9	15	-	-	9.5	10	-	-	-	-
10	9.5	9.5	9.5	10	-	-	8	9.5	-	-	-	-

DMSO (-): 6.5 mm

Standard antibiotic (+):

Penicillin = 17 mm

Vancomycin = 15 mm

Ampicillin = 19 mm

*Note: (-) = No activity

Table 6. Zone of inhibition (mm) of synthesized compound on gram negative bacteria

	Zone of Inhibition (mm)		
	<i>E. coli</i>	<i>K. pneumoniae</i>	<i>P. aeruginosa</i>

Compound	Concentration (ppm)				Concentration (ppm)				Concentration (ppm)			
	150	250	500	1000	150	250	500	1000	150	250	500	1000
1	-	-	-	-	-	-	-	-	-	-	-	-
2	-	-	-	7	-	-	8	8	-	-	9	12
3	-	-	-	-	-	-	7	7	-	-	-	-
4	-	-	-	-	12	13	13	14	-	-	-	-
5	-	-	-	-	-	-	10	11	-	-	-	-
6	-	-	8	9.5	-	-	-	-	-	-	-	-
7	7	7	7	9	-	-	8	8	-	-	-	7.5
8	8	8	8	8	-	-	12	16	-	-	-	-
9	7	7.5	8.5	9	7	7.5	8.5	9	-	8	8	8
10	-	-	7.5	7.5	-	-	-	7	-	-	8	9

DMSO (-): 6.5 mm
 Standard antibiotic (+):
 Tetracycline = 19 mm
 Cefazidime = 17 mm
 Imipenem = 17 mm

*Note: (-) = No activity

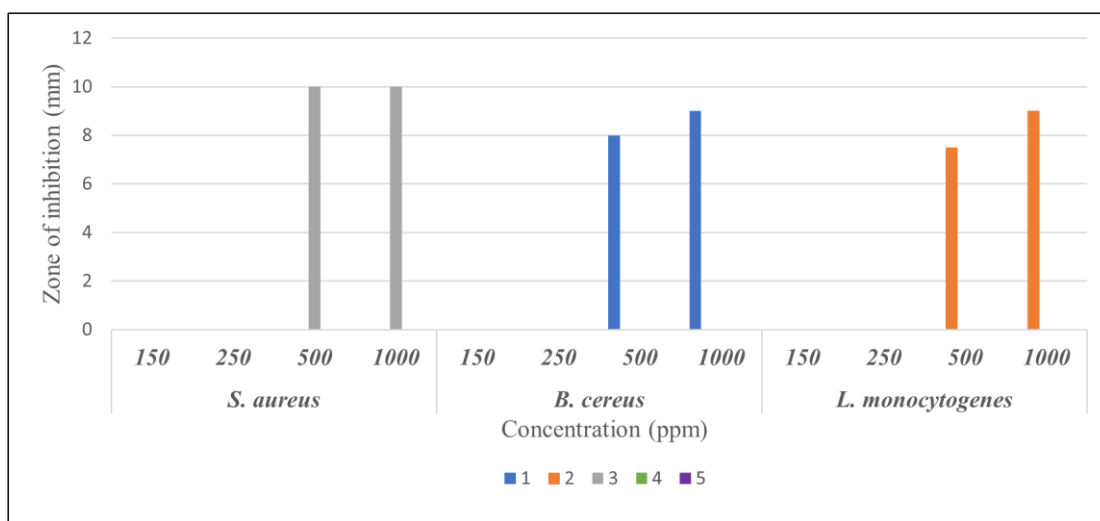


Figure 1. The zone of inhibition (mm) of thiourea ligand (1-5) on gram-positive bacteria

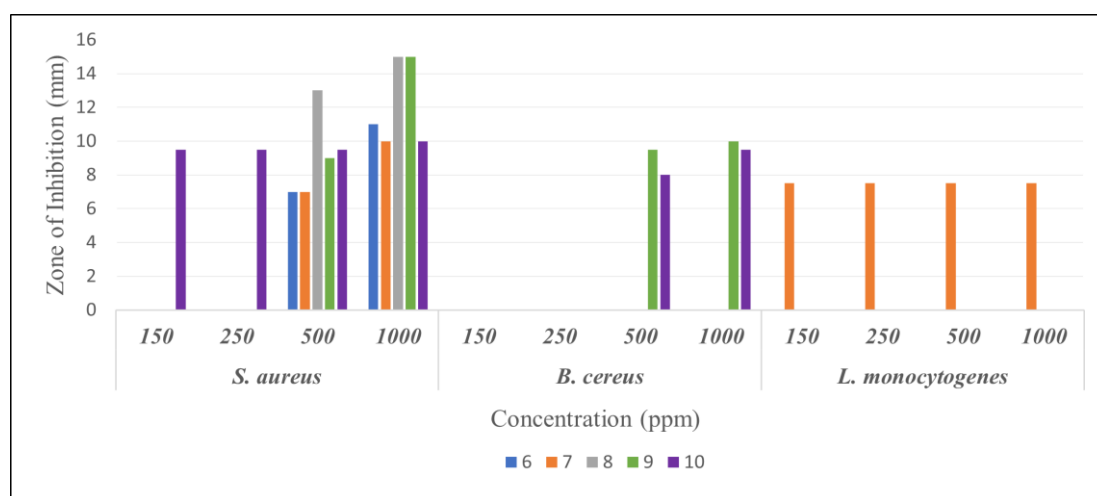


Figure 2. The zone of inhibition (mm) of thiourea copper(II) complex (6-10) on gram-positive bacteria

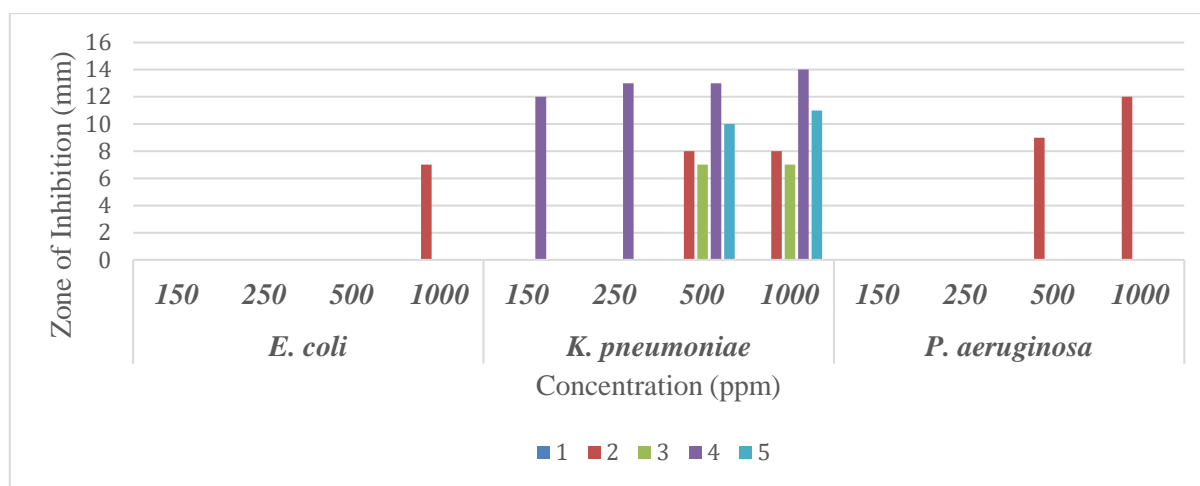


Figure 3. The zone of inhibition (mm) of thiourea ligand (1-5) on gram-negative bacteria

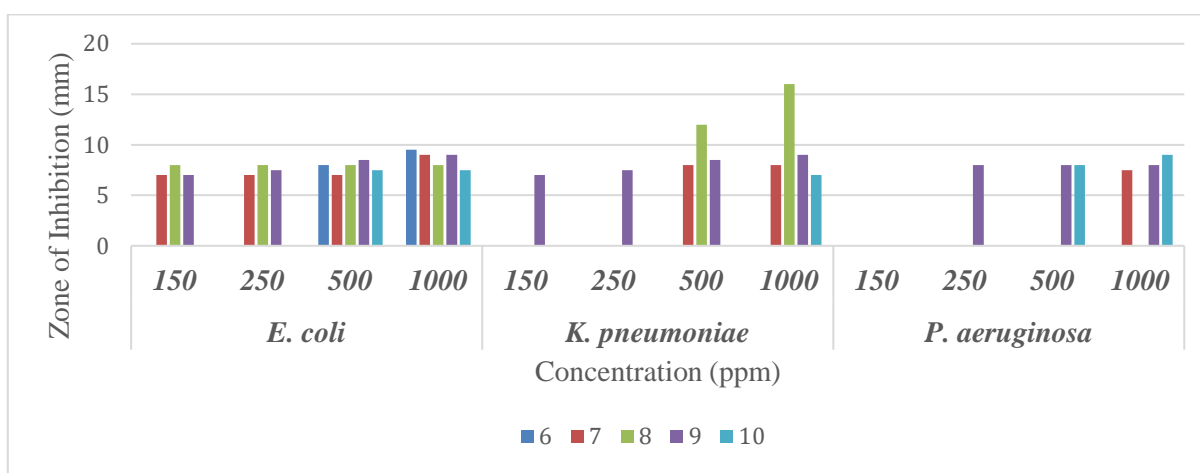


Figure 4. The zone of inhibition (mm) of thiourea copper(II) complex (6-10) on gram-negative bacteria

Molecular Docking Study

Molecular docking was employed to predict the interactions between synthesised compounds (ligand and complexes) and targeted proteins at the atomic level, aiding in understanding the mode of action in antibacterial activity (Echeverria *et al.*, 2017). In this study, we focused on the compounds with the inhibition zones of 10 mm or greater from the antibacterial studies to prioritise candidates with the highest antibacterial potency. The findings from the docking studies were used to provide an insight on what are the possible factors that contribute to the antibacterial properties of the selected compounds, such as the binding affinity (docking score), interaction between the compounds and the proteins (e.g hydrogen bonds, hydrophobic interaction etc) or how well the compounds fit into the binding pockets. The targeted proteins for this study were PDB ID

4XWA (*S. aureus*), PDB ID 7ci4 (*P. aeruginosa*), PDB ID 5xun (*K. pneumoniae*) and PDB ID 5BCA (*B. cereus*), which are highly crucial for the survival of the named bacteria (Mahone & Goley., 2020; Bush & Bradford., 2016; Zeng & Lin., 2013; Ambade *et al.*, 2023).

For free ligand **2**, the obtained binding energy against *S. aureus* and *P. aeruginosa*, were -7.7 kcal/mol and -6.7 kcal/mol respectively, while the obtained binding energy for free ligand **4** against *K. pneumoniae* was -6.7 kcal/mol. The binding energies obtained were consistent with the mild antibacterial activity of these compounds against the respected bacteria. Comparison was also made with the free amino acids that present in free ligand **2** which is methionine against both *S. aureus* and *P. aeruginosa*, which results in the binding energy of -4.4 kcal/mol and -3.8 kcal/mol respectively. Likewise, the same experiment was conducted

on alanine, an amino acid block of free ligand **4** which resulted in the binding energy of -3.9 kcal/mol. These data shows that the presence of thiourea moiety in the synthesised compounds, **2** and **4** could possibly result in the formation of more hydrogen bonds that contributed to the enhanced binding affinity of the synthesised compounds with the targeted protein receptors (Ngaini *et al.*, 2020). An illustration of the molecular docking for the interactions of the ligands and the receptors is depicted in Figure 5-7 while the molecular binding pocket of ligand **2** docked with *S. aureus* and *P. aeruginosa* as well as ligand **4** docked with *K. pneumoniae* is shown in Figure 8.

On the other hand, the copper(II) complexes (**6-10**) were shown to have stronger binding affinity to the targeted proteins with lower binding energy compared to the free ligands **2** and **4**. Of all the copper(II) complexes studied, complex **6** showed the strongest binding affinity with the lowest binding energies of -10.4 kcal/mol, followed by complex **9** (-9.8 kcal/mol), **8** (-9.4 kcal/mol), **10** (-9.3 kcal/mol) and **7** (-9.0 kcal/mol) (Table 8). The molecular

binding pocket of *S. aureus* docked with complex **6-10** is illustrated in Figure 9. The 3D Pymol Modelling shows that complex **6** formed ten hydrogen bonds with nine important amino acid residues of protein PDB ID 4XWA (*S. aureus*), particularly between the metal-bound oxygen with the -NH groups of SER-175 in the enzyme's binding pocket that could possibly be the key interaction that contributed to the inhibitory activity. These interactions, especially with polar substituents like -NO₂, -NH, and C=O groups, can enhance the binding stability and are likely responsible for the observed biological activity (Maalik *et al.*, 2019; Souza *et al.*, 2021). The 3D Pymol Modelling for other complexes in shown in Table 9 to 11. Nevertheless, there was no π - π interaction observed between the aromatic ring of the inhibitor and bacteria, although there are some aromatic rings present in the compounds. Although this data provides some insights to the inhibition of the bacteria, it is still not conclusive and have some limitations and more thorough investigation should be made particularly on the inhibition mechanism of the synthesised compounds.

Table 7. The molecular docking results for thiourea ligand **2**, **4** and its respected antibiotic with *S. aureus* (PDB entry: 4xwa), *P. aeruginosa* (PDB entry: 7ci4) and *K. pneumoniae* (PDB entry: 5xun) including the binding affinity and important amino acid residues of proteins that interact with the compounds

Ligand	PDB entry	Binding score value (kcal/mol)	Important Residue
2	4xwa	-7.7	Gly12, Ser13, Gly14, Lys15 and Thr16
2	7ci4	-6.7	Glu55 and Arg272
4	5xun	-6.9	Thr64, Thr93 and Tyr86
Methionine	4xwa	-4.4	Thr16, Gly14, Ser13 and Cys15
Methionine	7ci4	-3.8	Asn251 and Asp89
Alanine	5xun	-3.9	Arg96 and Ser66

Table 8. The molecular docking results for thiourea complex **6**, **7**, **8**, **9** and **10** with *S. aureus* (PDB entry: 4xwa), *B. cereus* (PDB entry: 5bca) and *K. pneumoniae* (PDB entry: 5xun) including the binding affinity score and important amino acid residues of proteins that interact with the compounds

Complex	PDB entry	Binding score value (kcal/mol)	Important Residue
6	4xwa	-10.4	Ser180, Arg48, Ser 175, Glu11, Thr16, Lys15, Gly14, Ser13 and Gly12
7	4xwa	-9.0	Thr16, Lys15, Ser13, Gly12, Glu11 and Ser175
8	4xwa	-9.4	Ser180, Arg48, Ser175, Arg92 and Lys15
9	4xwa	-9.8	Ser180, Asn173, Glu11, Lys15, Ser175 and Gly176
10	4xwa	-9.3	Ser180, Arg48, Ser 175, Glu11, Thr16, Lys15, Gly14 and Ser13
9	5bca	-8.3	Tyr343, Lys379, Arg380 and Ala444
8	5xun	-9.2	Cys69, Asn88, Ser66 and Arg96

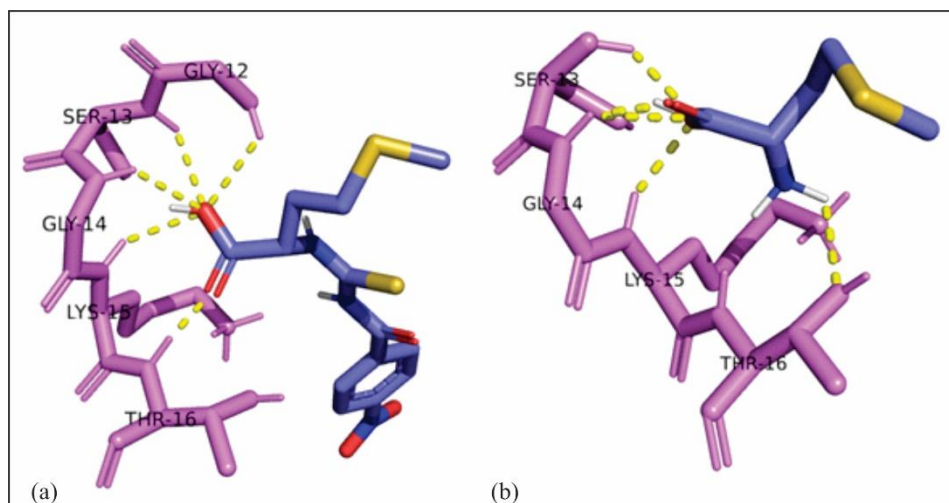


Figure 5. The 3D representation of the interactions for *S. aureus* (PDB ID: 4xwa) docked with (a) ligand 2 and (b) methionine.

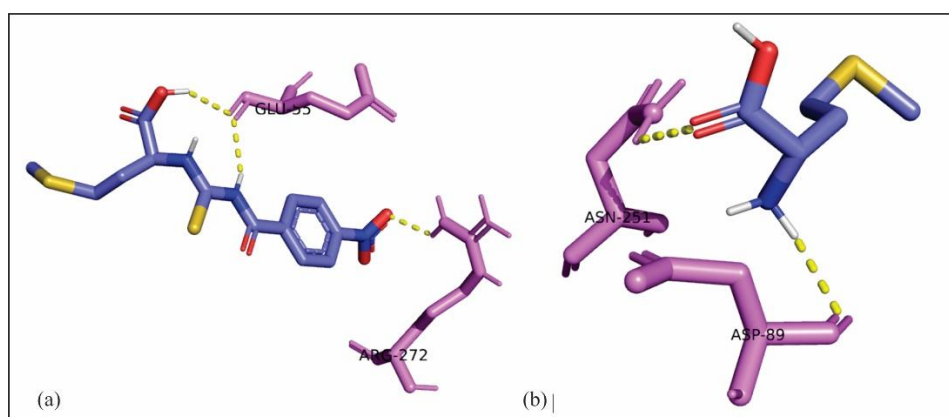


Figure 6. The 3D representation of the interactions for *P. aeruginosa* (PDB entry: 7ci4) docked with (a) ligand 2 and (b) methionine

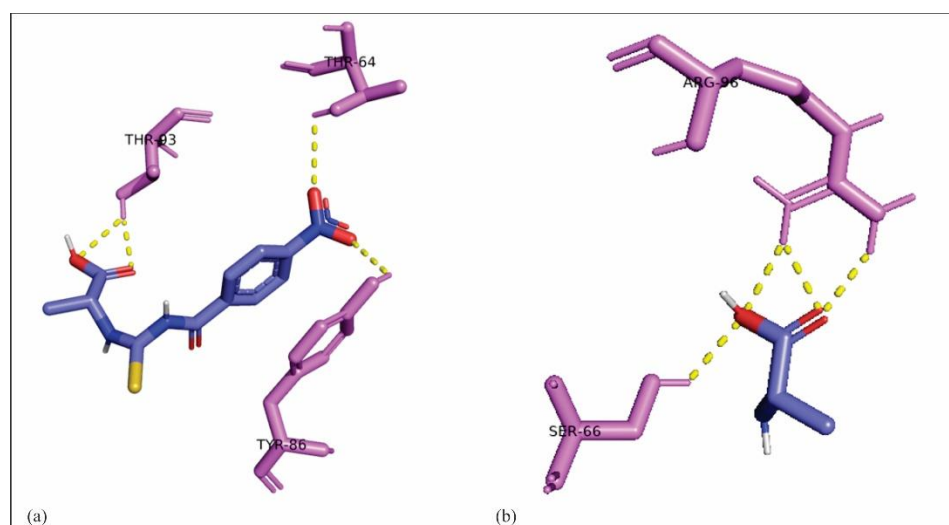


Figure 7. The 3D representation of the interactions for *K. pneumoniae* (PDB entry: 5xun) docked with (a) ligand 4 and (b) alanine

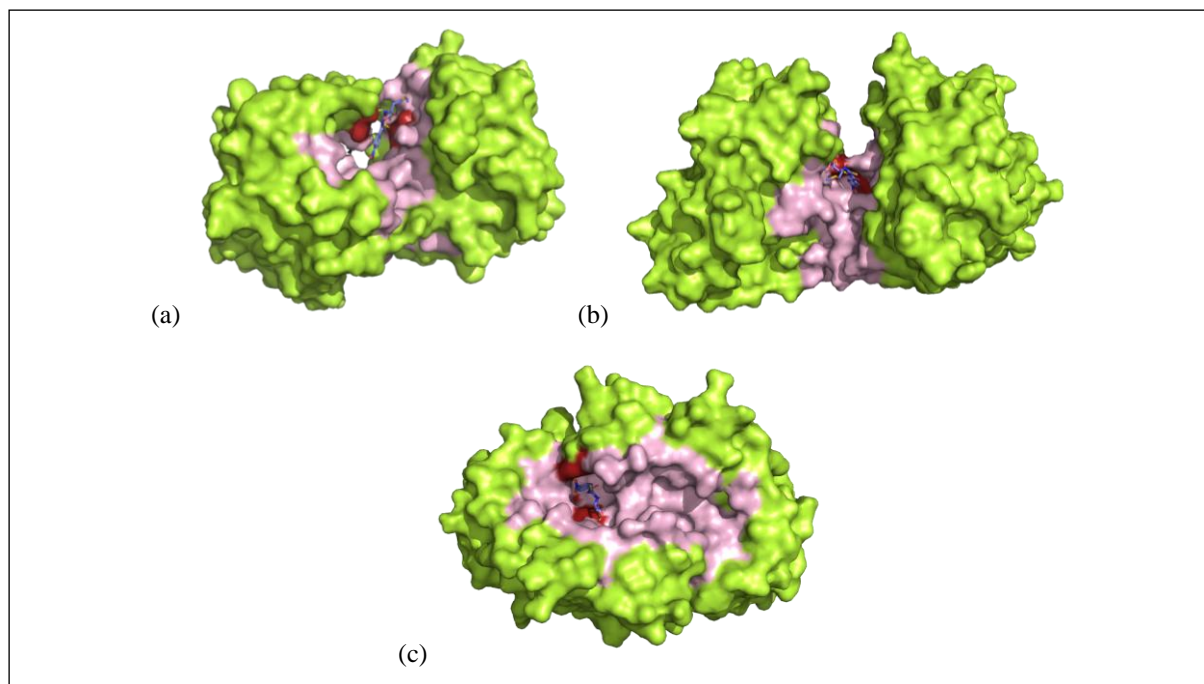


Figure 8. The molecular binding pocket of (a) ligand 2 docked with *S. aureus*, (b) ligand 2 docked with *P. aeruginosa* and (c) ligand 4 docked with *K. pneumoniae*

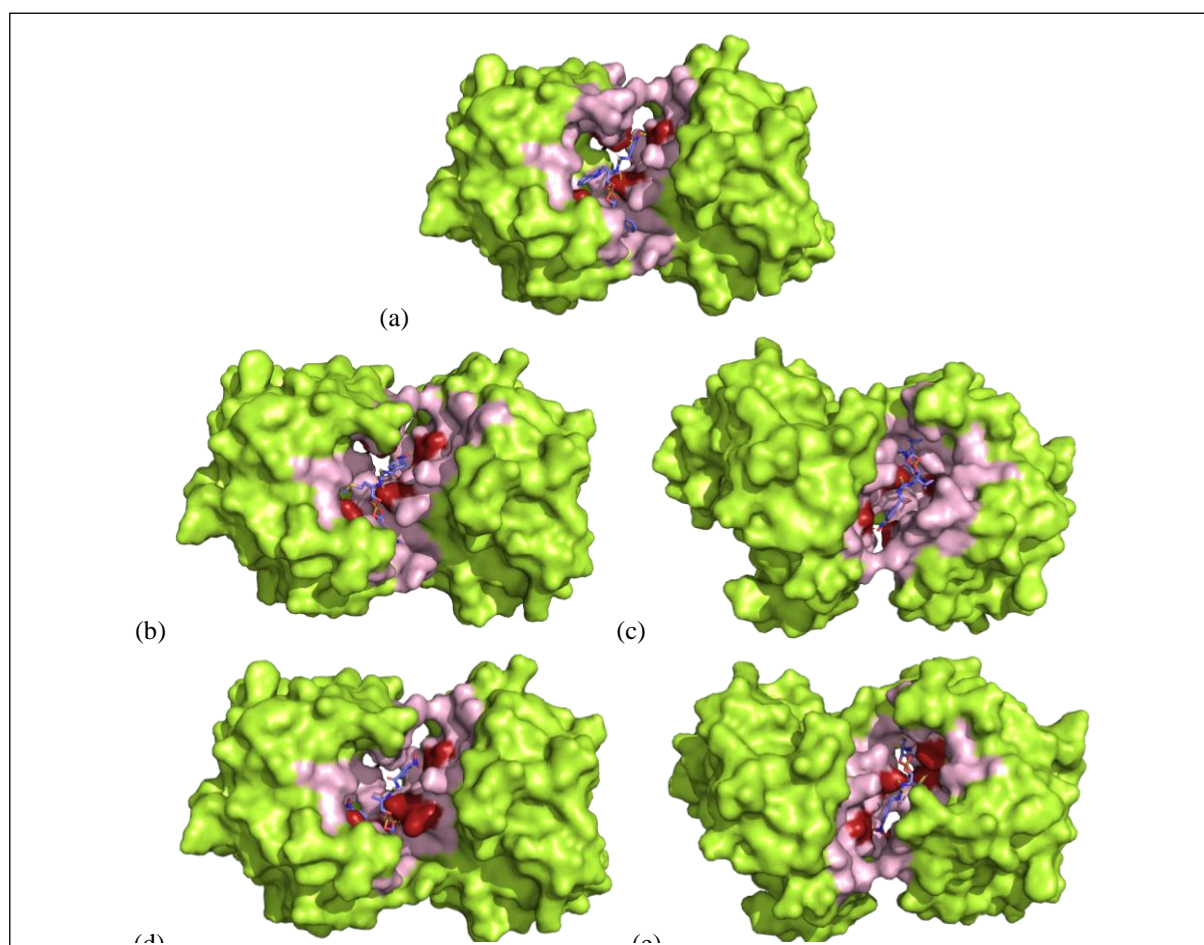


Figure 9. The molecular binding pocket of *S. aureus* docked with (a) complex 6, (b) complex 7, (c) complex 8, (d) complex 9 and (e) complex 10

Table 9. 3D docking illustration between complex 6, 7, 8, 9 and 10 against *S. aureus* (PDB entry: 4xwa)

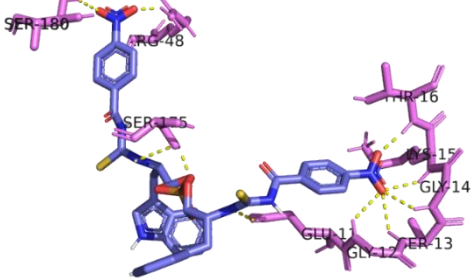
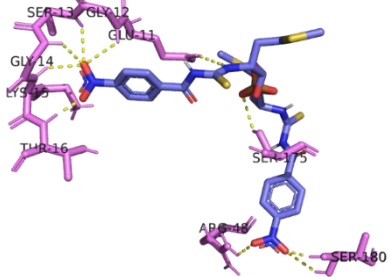
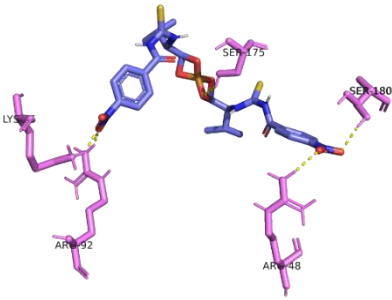
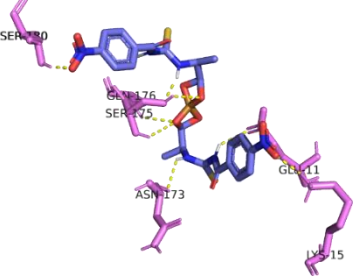
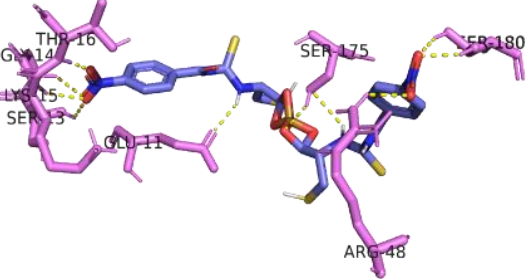
Complex	Binding poses (kcal/mol)	PyMol Modelling
6	-10.4	
7	-9.0	
8	-9.4	
9	-9.8	
10	-9.3	

Table 10. 3D docking illustration between complex 9 against *B. cereus* (PDB entry: 5bca)

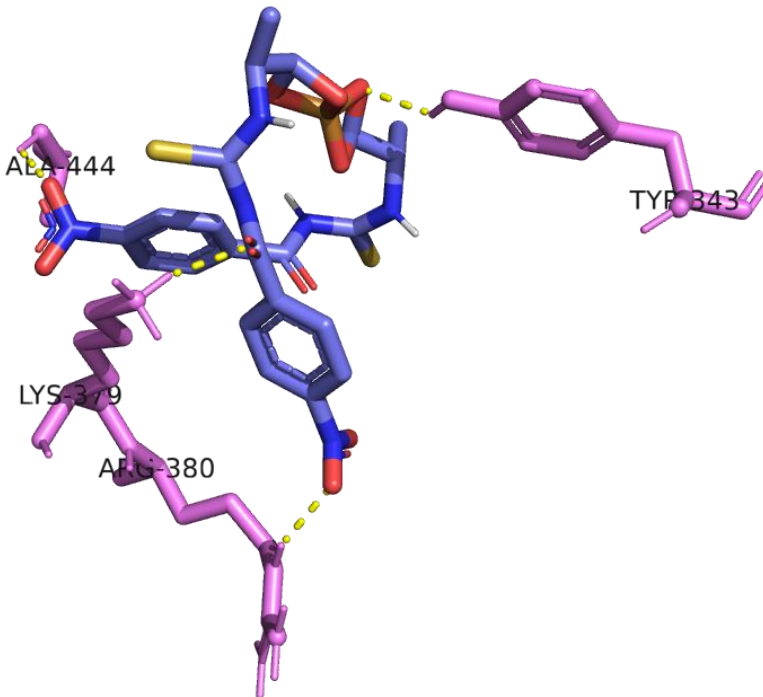
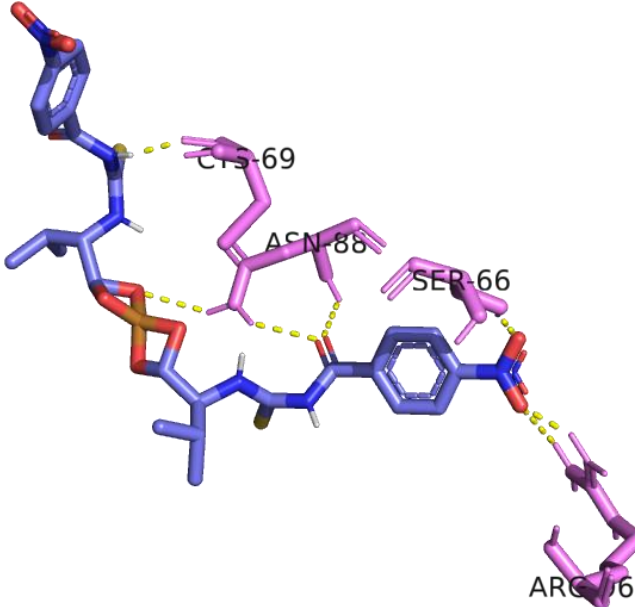
Complex	Binding poses (kcal/mol)	PyMol Modelling
9	-8.3	

Table 11. 3D docking illustration between complex 7 against *K. pneumoniae* (PDB entry: 5xun)

Complex	Binding poses (kcal/mol)	Pymol Modelling
7	-9.2	

CONCLUSION

In conclusion, nitrobenzoylthiourea derivatives were synthesised via one-pot reactions between nitrobenzoyl chloride, potassium thiocyanate and a series of chosen amino acids in acetone solvent under reflux conditions in moderate to high yields. On the other hand, Cu(II) complexes were prepared from the deprotonation of carboxylic acid moiety of the ligands and subsequent reaction with Cu(II) chloride with moderate yield. From the present studies, the incorporation of Cu(II) ions has enhanced the antibacterial activity of the free ligands which was measured based on the inhibition zones against both gram-positive and gram-negative bacteria. In the case of gram-positive bacteria, at 1000 ppm, complex **8** and **9** both inhibited the growth of *S. aureus* with 15 mm inhibition zones. Likewise, complex **8** also inhibited the growth of *K. pneumoniae* at the concentration of 1000 ppm with inhibition zone of 16 mm. Docking studies were conducted only on ligands and complexes that shown 10 mm and greater inhibition zone to provide some insights on what factors that could possibly contributed to the antibacterial activity. Complexes **6-10** have shown good binding energies between -10.4 kcal/mol to -9.0 kcal/mol and these findings correlates to the enhanced antibacterial activity of the copper(II) complexes synthesised.

The present study has several limitations. First, the scope of the research is confined to the molecular docking of four specific protein structures (PDB IDs: 4xwa, 7ci4, 5xun and 5bca), which may not represent the full range of possible interactions. Additionally, the accuracy of the docking predictions is inherently limited by the resolution of the protein structures used and the constraints of the computational algorithms. Furthermore, this study relies on available crystallographic data, which may not fully capture dynamic conformational changes in proteins. Consequently, experimental validation is necessary to confirm the predicted interactions. Future studies could extend these findings by including more diverse protein-ligand complexes and employing enhanced molecular dynamics simulations.

Supporting Materials Summary

The characterization data FTIR spectrometer, ¹H and ¹³C NMR spectroscopy on each of

compound for this article can be accessed as supplementary data.

ACKNOWLEDGEMENT

The work is financially supported through E07/SpMYRA/1713/2018. We are thankful to Universiti Malaysia Sarawak for the Zamalah scholarship awarded to the first author.

REFERENCES

- Ambade, V., Ambade, S., Sharma V. & Sanas, P. (2023). Comparison between Amino Acid Profiling of Structural Proteins of earliest and recent omicron strain of SARS-CoV-2 and Nutritional Burden on COVID-19 patients. *Human Nutrition & Metabolism*, 34: 200220. DOI: <https://doi.org/10.1016/j.hnm.2023.200220>
- Arendsen, L.P., Thakar, R. & Sultan, A. H. (2019). The use of copper as an antimicrobial agent in health care, including obstetrics and gynecology. *Clinical Microbiology Reviews*, 32(4): 25-18. DOI: 10.1128/CMR.00125-18
- Arslan, H., Duran, N., Borekci, G., Ozer, C.K. & Akbay, C. (2009). Antimicrobial activity of some thiourea derivatives and their nickel and copper complexes. *Molecules*, 14(1): 519–527. DOI: 10.3390/molecules14010519
- Azócar, M.I., Gómez, G., Levín, P., Paez, M., Muñoz, H. & Dinamarca, N. (2014). Review: Antibacterial behavior of carboxylate silver(I) complexes. *Journal of Coordination Chemistry*, 67: 3840–3853. DOI: 10.3390/molecules23071629
- Boros, E., Dyson, P.J. & Gasser, G. (2020). Classification of metal-based drugs according to their mechanisms of action. *Chemistry*, 6(1): 41–60. DOI: 10.1016/j.chempr.2019.10.013
- Bush, K., and Bradford, P. A. (2016). β -Lactams and β -lactamase inhibitors: an overview. *Cold Spring Harb. Perspect. Med.* 6: 295–306. DOI: 10.1101/cshperspect.a025247
- Claudel, M., Schwarte, J.V. & Fromm, K.M. (2020). New antimicrobial strategies based on metal complexes. *Chemistry*, 2(4): 849–899. DOI: <https://doi.org/10.3390/chemistry2040056>
- Drzewiecka-Antonik, A., Rejmak, P., Klepka, M., Wolska, A., Chrzanowska, A. & Struga, M. (2020). Structure and anticancer activity of Cu(II)

- complexes with (bromophenyl)thiourea moiety attached to the polycyclic imide. *Journal of Inorganic Biochemistry*, 212(6): 8-16. DOI: <https://doi.org/10.1016/j.jinorgbio.2020.111234>
- Echeverría, J., Urzúa, A., Sanhueza, L. & Wilkens, M. (2017). Enhanced antibacterial activity of ent-labdane derivatives of salvic acid (7 α -hydroxy-8(17)-ent-labden-15-oic acid): effect of lipophilicity and the hydrogen bonding role in bacterial membrane interaction. *Molecules*, 22(7): 1-19. DOI: 10.3390/molecules22071039
- Fair, R. J. & Tor, Y. (2014). Antibiotics and bacterial resistance in the 21st century. *Perspectives in Medicinal Chemistry*, 6: 25–64. DOI: <https://doi.org/10.4137/pmc.s14459>
- Fakhar, I., Hussien, N.J., Sapari, S., Bloh, A.H., Yusoff, S.F.M., Hasbullah, S.A., Yamin, B.M., Mutalib, S.A., Shihab, M.S. & Yousif, E. (2018). Synthesis, x-ray diffraction, theoretical and antibacterial studies of bis-thiourea secondary amine. *Journal of Molecular Structure*, 1159: 96–102. DOI: <https://doi.org/10.1016/j.molstruc.2018.01.032>
- Fatima, T., Haque, R.A., Razali, M.R., Ahmad, A., Asif, M., Khadeer Ahamed, M.B. & Abdul Majid, A.M.S. (2017). Effect of lipophilicity of wingtip groups on the anticancer potential of mono N-heterocyclic carbene silver(I) complexes: Synthesis, crystal structures and in vitro anticancer study. *Applied Organometallic Chemistry*, 31(10): 1–13. DOI: <https://doi.org/10.1002/aoc.3735>
- Halim, A.A.N. & Ngaini, Z. (2017). Synthesis and characterization of halogenated bis(acylthiourea) derivatives and their antibacterial activities. *Phosphorus, Sulfur and Silicon and the Related Elements*, 192(9): 1012–1017. DOI: <https://doi.org/10.1080/10426507.2017.1315421>
- Halim, A.N.A. & Ngaini, Z. (2016). Synthesis and bacteriostatic activities of bis(Thiourea) derivatives with variable chain length. *Journal of Chemistry*, 2016(3): 1-7. DOI: <https://doi.org/10.1155/2016/2739832>
- Hassan, I.N., Yamin, B.M., Daud, W.R.W. & Kassim, M. B. (2011). Synthesis, spectral characterisation and crystal structural of 1-(2-morpholinoethyl)-3-(3-phenylacryloyl)thiourea. *International Journal of Physical Sciences*, 6(35): 7898–7903. DOI: <https://doi.org/10.5897/IJPS11.1458>
- Idrees, M., Mohammad, A.R., Karodia, N. & Rahman, A. (2020). Multimodal role of amino acids in microbial control and drug development. *Antibiotics*, 9(6): 1–23. DOI: <https://doi.org/10.3390/antibiotics9060330>
- Ikokoh, P.P.A., Onigbanjo, H.O., Adedirin, O., Akolade, J.O., Uzo, A. & Fagbohun, A. (2015). Synthesis and antimicrobial activities of copper(I) thiourea and silver(I) thiourea. *Open Journal of Research*, 2(2): 086-091.
- Khairul, W.M., Tukimin, N. & Rahamathullah, R. (2016). Synthesis, characterization and electrical properties of N-([4-(aminophenylethynyl)toluene]-N'-(cinnamoyl)thiourea (AECT) as single molecular conductive film. *Sains Malaysiana*, 45(5): 825–831.
- Li, Z., Zhang, Y. & Wang, Y. (2010). Synthesis and characterization of N-benzoyl-N' - carboxyalkyl substituted thiourea derivatives. *Phosphorus, Sulfur, and Silicon and the Related Elements*, 178(2): 293-297. DOI: <https://doi.org/10.1080/10426500307952>
- Liang, X., Luan, S., Yin, Z., He, M., He, C., Yin, L., Zou, Y., Yuan, Z., Li, L., Song, X., Lv, C. & Zhang, W. (2018). Recent advances in the medical use of silver complex. *European Journal of Medicinal Chemistry*, 157: 62–80. DOI: <https://doi.org/10.1016/j.ejmech.2018.07.057>
- Maalik, A., Rahim, H., Saleem, M., Fatima, N., Rauf, A., Wadood, A., Malik, M. I., Ahmed, A., Rafique, H., Zafar, M. N., Riaz, M., Rasheed, L. & Mumtaz, A. (2019). Synthesis, antimicrobial, antioxidant, cytotoxic, antiurease and molecular docking studies of N-(3-trifluoromethyl)benzoyl-N'-aryl thiourea derivatives. *Bioorganic Chemistry*, 88(5): 1-9. DOI: <https://doi.org/10.1016/j.bioorg.2019.102946>
- Madabhushi, S., Mallu, K., Vangipuram, V., Kurva, S., Poornachandra, Y. & Kumar, C. (2014). Synthesis of novel benzimidazole functionalized chiral thioureas and evaluation of their antibacterial and anticancer activities. *Bioorganic & Medicinal Chemistry Letters*, 24(20): 4822-4825. DOI: <https://doi.org/10.1016/j.bmcl.2014.08.064>
- Mahone C.R. & Goley E.D. Bacterial cell division at a glance. (2020). *J Cell Sci*. 133(7): jcs237057. DOI: <https://doi.org/10.1242/jcs.237057>

- Malik, M.A., Dar, O.A., Gull, P., Wani, M.Y. & Hashmi, A. A. (2018). Heterocyclic Schiff base transition metal complexes in antimicrobial and anticancer chemotherapy. *Medicinal Chemistry*, 9(3): 409–436. DOI: <https://doi.org/10.1039/c7md00526a>
- Mishra, A., Ninama, S., Sharma, P., Soni, N. & Awate, R. (2020). Synthesis, characterization, molecular docking and antimicrobial activity of copper(II) complexes of metronidazole and 1,10-phenanthroline. *Inorganica Chimica Acta*, 510: 6–11. DOI: <https://doi.org/10.1016/j.ica.2020.119744>
- Mohapatra, S.S., Dwibedy, S.K. & Padhy, I. (2021). Polymyxins, the last-resort antibiotics: Mode of action, resistance emergence, and potential solutions. *Journal of Biosciences*, 46(3): 1-18. DOI: <https://doi.org/10.1007/s12038-021-00209-8>
- Möhler, J.S., Kolmar, T., Synnatschke, K., Hergert, M., Wilson, L.A., Ramu, S., Elliott, A.G., Blaskovich, M.A.T., Sidjabat, H.E., Paterson, D. L., Schenk, G., Cooper, M. A. & Ziora, Z. M. (2017). Enhancement of antibiotic-activity through complexation with metal ions - combined ITC, NMR, enzymatic and biological studies. *Journal of Inorganic Biochemistry*, 167: 134–141. DOI: <https://doi.org/10.1016/j.jinorgbio.2016.11.028>
- Montero, D. A., Arellano, C., Pardo, M., Vera, R., Gálvez, R., Cifuentes, M., Berasain, M. A., Gómez, M., Ramírez, C. & Vidal, R. M. (2019). Antimicrobial properties of a novel copper-based composite coating with potential for use in healthcare facilities. *Antimicrobial Resistance and Infection Control*, 8(2019): 1-10. DOI: <https://doi.org/10.1186/s13756-018-0456-4>
- Mukherjee, I., Ghosh, A., Bhadury, P. & De, P. (2017). Side-chain amino acid-based cationic antibacterial polymers: investigating the morphological switching of a polymer-treated bacterial cell. *ACS Omega*, 2(4): 1633–1644. DOI: 10.1021/acsomega.7b00181
- Ngaini, Z., Mohd Arif, M.A., Hussain, H., Mei, E.S., Tang, D. & Kamaluddin, D. H. A. (2012). Synthesis and antibacterial activity of acetoxybenzoyl thioureas with aryl and amino acid side chains. *Phosphorus, Sulfur and Silicon and the Related Elements*, 187(1): 1–7. DOI: <https://doi.org/10.1080/10426507.2011.562398>
- Ngaini, Z. & Mortadza, N.A. (2019). Synthesis of halogenated azo-aspirin analogues from natural product derivatives as the potential antibacterial agents. *Natural Product Research*, 33(24): 3507–3514. DOI: <https://doi.org/10.1080/14786419.2018.1486310>
- Ngaini, Z., Rasin, F., Wan Zullkiplee, W.S.H. & Abd Halim, A. N. (2020). Synthesis and molecular design of mono aspirinate thiourea-azo hybrid molecules as potential antibacterial agents. *Phosphorus, Sulfur and Silicon and the Related Elements*, 196(3): 275–282. DOI: <https://doi.org/10.1080/10426507.2020.1828885>
- Ohammad, B. (2018). Synthesis, structure and spectroscopic properties of oxovanadium tris (3, 5-dimethylpyrazolyl) borate aroylthiourea complexes. *Sains Malaysiana*, 47(8): 1775–1785. DOI: <http://dx.doi.org/10.17576/jsm-2018-4708-16>
- Pingaew, R., Prachayasittikul, V., Anuwongcharoen, N., Prachayasittikul, S., Ruchirawat, S. & Prachayasittikul, V. (2018). Synthesis and molecular docking of N, N'-disubstituted thiourea derivatives as novel aromatase inhibitors. *Bioorganic Chemistry*, 79: 171-178.
- Raheel, A., Imtiaz-Ud-Din, Badshah, A., Rauf, M.K., Tahir, M.N., Khan, K.M., Hameed, A. & Andleeb, S. (2016). Amino acid linked bromobenzoyl thiourea derivatives: Syntheses, characterization and antimicrobial activities. *Journal of the Chemical Society of Pakistan*, 38(5): 959–964.
- Roche Allred, Z. D., Tai, H., Bretz, S. L. & Page, R. C. (2017). Using PyMOL to explore the effects of pH on noncovalent interactions between immunoglobulin g and protein a: a guided-inquiry biochemistry activity. *Biochemistry and Molecular Biology Education*, 45(6): 528–536. DOI: <https://doi.org/10.1002/bmb.21066>
- Ramesh, P., Revathi, M., H.A.A., Mohammeda, N. A. A., Siddappa, S., Reddy, P.M. & Pasha, C. (2016). Copper(II) complexes of new carboxamide ligands: synthesis, spectroscopic and antibacterial study. *International Journal of Advanced Research in Chemical Science*, 3(8): 1–8. DOI: <http://dx.doi.org/10.20431/2349-0403.0308001>
- Ronchetti, R., Moroni, G., Carotti, A., Gioiello, A. & Camaioni, E. (2021). Recent advances in urea and thiourea-containing compounds: focus on innovative approaches in medicinal chemistry and organic synthesis. *RSC Medicinal Chemistry*, 12(7): 1046–1064.
- Saeed, S., Rashid, N., Jones, P.G., Ali, M. & Hussain, R. (2010). Synthesis, characterization and biological evaluation of some thiourea derivatives bearing benzothiazole moiety as potential

- antimicrobial and anticancer agents. *European Journal of Medicinal Chemistry*, 45(4): 1323–1331.
- Schrödinger (2016). The PyMOL Molecular Graphics System, Version 1.8 Schrödinger, LLC.
- Smith, M. (2017). Antibiotic Resistance Mechanisms. *Journeys in Medicine and Research on Three Continents Over 50 Years*, 2017: 95–99.
- Souza, R.A.C., Costa, W.R.P., de F. Faria, E., Bessa, M. A.d.S., Menezes, R.de P., Martins, C.H.G., Maia, P.I.S., Deflon, V.M. & Oliveira, C.G. (2021). Copper(II) complexes based on thiosemicarbazone ligand: Preparation, crystal structure, Hirshfeld surface, energy framework, anti mycobacterium activity, in silico and molecular docking studies. *Journal of Inorganic Biochemistry*, 223(4): 1-13.
- Sumrra, S.H., Ibrahim, M., Ambreen, S., Imran, M., Danish, M. & Rehmani, F.S. (2014). Synthesis, spectral characterization, and biological evaluation of transition metal complexes of bidentate N, O donor schiff bases. *Bioinorganic Chemistry and Applications*, 2014: 1-11.
- Trott, O. & Olson, A.J. (2010). AutoDock Vina: improving the speed and accuracy of docking with a new scoring function, efficient optimization, and multithreading. *Journal of computational chemistry*, 31(2): 455–461. DOI: <https://doi.org/10.1002/jcc.21334>
- Wakshlak, R.B. K., Pedahzur, R. & Avnir, D. (2015). Antibacterial activity of silver-killed bacteria: the “zombies” effect. *Scientific Reports*, 5: 1–5.
- Welch, E.F., Rush, K.W., Arias, R.J. & Blackburn, N.J. (2022). Copper monooxygenase reactivity: Do consensus mechanisms accurately reflect experimental observations? *Journal of Inorganic Biochemistry*, 231(12): 1-12. DOI: <https://doi.org/10.1016/j.jinorgbio.2022.111780>
- Zeng, X. & Lin, J. (2013). Beta-lactamase induction and cell wall metabolism in Gram-negative bacteria. *Frontiers in microbiology*, 4: 128. DOI: <https://doi.org/10.3389/fmicb.2013.00128>

Red Seaweed Carrageenan: A Comprehensive Review of Preparation in Cosmetics - An In Depth Analysis

NAZIRAH MINGU¹, NUR HASLINDA ABDUL MAIL¹, HASMADI MAMAT², MD SHAFIQUZZAMAN SIDDIQUEE³, MOHD HAFIZ ABD MAJID¹ & MOHD SANI SARJADI^{*1}

¹Faculty of Science and Natural Resources, Universiti Malaysia Sabah, Jalan UMS, 88400 Kota Kinabalu, Sabah, Malaysia; ²Faculty of Food Science and Nutrition, Universiti Malaysia Sabah, Jalan UMS, 88400 Kota Kinabalu, Sabah, Malaysia; ³Biotechnology Research Institute, Universiti Malaysia Sabah, Jalan UMS, 88400 Kota Kinabalu, Sabah, Malaysia

*Corresponding author: msani@ums.edu.my

Received: 1 July 2024

Accepted: 24 September 2024

Published: 31 December 2024

ABSTRACT

Carrageenan, an extract from red seaweed (*Rhodophyta*), has many uses in cosmetics, and this literature review delves into them all. Due to its superior gelling, thickening, and stabilizing properties, carrageenan, a polysaccharide with a wide range of chemical structures, has been utilized in various industries throughout history. In recent years, the cosmetics industry has shown growing interest in harnessing the potential of carrageenan, driven by the increasing demand for natural and sustainable ingredients. This review provides a comprehensive examination of the botanical background, types of carrageenan, and the most effective extraction methods for obtaining the key bioactive compounds that enhance its functionality in cosmetic formulations. The functional properties of carrageenan in cosmetics are discussed in depth, including its gelling and thickening capabilities, moisturizing effects, and stability enhancement. Additionally, its biological activities, such as antioxidant and anti-inflammatory properties, contribute to its appeal as a valuable ingredient in skincare products. Formulation considerations, including compatibility with a wide range of cosmetic ingredients and optimal concentrations, are explored to facilitate the development of effective products. The review also addresses the incorporation of carrageenan into cosmetic formulations, along with safety and regulatory aspects, ensuring a comprehensive understanding of the product's conformity with industry standards. In conclusion, the review provides an overview of current challenges, potential future research directions, and case studies showcasing the incorporation of carrageenan into cosmetic products. This review aims to serve as a valuable resource for researchers, formulators, and industry professionals interested in the innovative use of carrageenan in the evolving landscape of cosmetic science by synthesizing existing knowledge and identifying gaps in the current scientific literature.

Keywords: Carrageenan, cosmetic, red seaweed (*Rhodophyta*)

Copyright: This is an open access article distributed under the terms of the CC-BY-NC-SA (Creative Commons Attribution-NonCommercial-ShareAlike 4.0 International License) which permits unrestricted use, distribution, and reproduction in any medium, for non-commercial purposes, provided the original work of the author(s) is properly cited.

INTRODUCTION

Cosmetics, encompassing a wide variety of personal care products, constitute an essential aspect of daily grooming routines and play a crucial role in enhancing and maintaining the aesthetic appeal of the human body (Kalasariya *et al.*, 2021). These products are currently undergoing a transformative shift, driven by an increasing emphasis on sustainability and consumer demand for natural alternatives (Ferreira *et al.*, 2022). In addition to their role in facilitating self-expression and boosting confidence, cosmetics are also leading the way in this development.

The cosmetics industry is experiencing a surge in the utilization of bioactive compounds derived from natural sources, reflecting a broader societal trend towards environmentally friendly products (Prajaputra *et al.*, 2024). Customers are becoming increasingly conscious of the environmental impact of their choices, thus seeking products aligned with their ethical principles (Khalil *et al.*, 2017). This trend is exemplified by the adoption of ingredients such as carrageenan from red seaweed (Batista *et al.*, 2020), underscoring the industry's commitment to offering aesthetically pleasing options that are both environmentally friendly and sustainable (Shi *et al.*, 2020), catering to individual well-being and ecological responsibility alike.

Carrageenan is a sulfated polysaccharide derived from various species of red seaweed (Shi *et al.*, 2020). It is highly sought after in the cosmetic industry due to its excellent gelling and thickening properties (Tarman *et al.*, 2020). The extraction process involves a series of meticulous steps, beginning with the collection of red seaweed, typically found in large quantities in coastal regions worldwide (Pessarrodona *et al.*, 2020). Before undergoing extraction, this natural resource is meticulously cleaned and dried. The extraction process typically involves alkaline treatment or other specialized methods (Firdayanti *et al.*, 2023).

Due to the abundance of red seaweed in coastal areas, carrageenan extraction is a sustainable practice that requires minimal land use and freshwater resources compared to the extraction of plant-based ingredients from terrestrial sources (Bukhari *et al.*, 2023). Given the growing demand for sustainable sourcing in the cosmetics industry, carrageenan aligns well with this trend (Gerber *et al.*, 1958).

Furthermore, carrageenan's appeal stems from its natural derivation and high biocompatibility, making it an ideal candidate for the production of clean and environmentally friendly beauty products sought by conscientious consumers (Hamasuna *et al.*, 1994). Its versatility extends beyond gelling and thickening; carrageenan also moisturizes and conditions the skin, enhancing its desirability for use in various cosmetic formulations (He *et al.*, 2019), including haircare (Ismail *et al.*, 2020), skincare (Janowicz *et al.*, 2023), and other personal care products (Jiménez-Escrig *et al.*, 2013).

The significance of incorporating natural ingredients into cosmetic formulations cannot be emphasized enough (Jing *et al.*, 2021). With a rising consumer demand for products free from synthetic additives, chemicals, and potential irritants (Ju *et al.*, 2023), the allure of natural ingredients extends beyond environmental concerns (Khoobakht *et al.*, 2024). They offer unique advantages for skin health and product efficacy (Pangestuti *et al.*, 2021). In this landscape, carrageenan emerges as a standout ingredient, sourced from botanical origins and boasting a versatile array of functionalities (Gerber *et al.*, 1958). It presents an enticing

option for formulators seeking to align with current beauty industry trends and values.

The aim of this review is to extensively examine the utilization of carrageenan extract from red seaweed in cosmetic production. By delving into extraction methods, functional properties, biological activities, formulation considerations, safety aspects, and regulatory implications associated with carrageenan, we move forward to deepen understanding of its potential in the cosmetics industry. Through this investigation, the review endeavors to furnish researchers, formulators, and industry professionals with valuable insights to navigate the convergence of natural ingredients and cosmetic science more effectively.

Chemical Composition of Seaweed

Based on the research conducted by Ghada and Armany on the chemical composition of seaweed from the Mediterranean Sea coast in Egypt, chemical analyses have been carried out to identify the elements present in various types of red seaweed sourced from different sampling locations along the Mediterranean Sea (El-said *et al.*, 2013).

The study likely involved collecting samples of red seaweed from multiple locations along the Egyptian coast of the Mediterranean Sea (El-said *et al.*, 2013; Lim *et al.*, 2021). These samples would have been subjected to various chemical analyses to determine their elemental composition. Analytical techniques such as atomic absorption spectroscopy (AAS), inductively coupled plasma mass spectrometry (ICP-MS), or X-ray fluorescence spectroscopy (XRF) may have been employed to quantify the concentration of elements present in the seaweed samples (Lim *et al.*, 2021).

The chemical composition analysis would have provided valuable insights into the elemental content of the red seaweed (Montaser *et al.*, 2021; Mostafavi *et al.*, 2020), including essential nutrients such as potassium, magnesium, calcium, and trace elements like iodine, selenium, and zinc as shown in Table 1. Additionally, the presence of potentially harmful elements or heavy metals may have been investigated to assess the seaweed's safety for consumption or utilization in various

applications (Núñez-Santiago *et al.*, 2011; Laokelis *et al.*, 2022).

The research findings would contribute to our understanding of the nutritional value, environmental quality, and potential industrial

applications of red seaweed from the Mediterranean Sea coast in Egypt (El-said *et al.*, 2013). They could also inform future studies on seaweed utilization, marine biodiversity conservation, and sustainable resource management in coastal ecosystems.

Table 1. Distributions of selected elements and carbohydrate contents in different red seaweed species

Sample of red seaweed	Nutritional value for some seaweed (mg/g)					Carbohydrates
	Ca	Mg	Na	K	F	
<i>Gracilaria compressa</i>	3.33	1.73	29.08	4.46	40.97	116.23
<i>Gracilaria verrucosa</i>	0.94	0.29	22.80	8.17	113.12	111.46
<i>Pterocladia capillacea</i>	3.05	2.08	17.92	8.32	177.88	96.37
<i>Hypnea musciformis</i>	3.79	1.15	24.22	8.22	50.90	111.72

Based on the results of chemical analysis from the research, various critical elements present in seaweed contribute to its nutritional value, which varies depending on the type of seaweed and its growth conditions. Calcium, a vital mineral found in seaweed, plays a crucial role in promoting skeletal health and serves as a valuable dietary source (Al-Nahdi *et al.*, 2019). It is essential for the development and maintenance of strong bones and teeth, with adequate consumption aiding in bone density and helping to prevent disorders such as osteoporosis, particularly among aging populations (Ningrum *et al.*, 2021). Additionally, calcium is involved in various physiological functions, including muscular contraction, neuronal transmission, and blood coagulation (Otero *et al.*, 2021).

Moving on to magnesium, another essential mineral found in seaweed, it serves as a cofactor for enzymes involved in the conversion of food into energy. Consumption of seaweed as a source of magnesium contributes to increased energy synthesis and utilization in cells, thereby aiding metabolic activities. Similar to calcium, magnesium is crucial for muscle and nerve function, assisting in muscle contraction and relaxation, which is integral for maintaining muscle health and preventing disorders such as muscle cramps (Hamzalıoğlu *et al.*, 2016). Furthermore, magnesium has potential benefits for cardiovascular health, as it helps regulate blood pressure and maintain a regular heartbeat (Hong *et al.*, 2021).

Sodium and potassium are also essential elements found in seaweed, playing roles in fluid balance, neuron function, and overall cellular health. Both sodium and potassium are important

electrolytes involved in regulating water balance within and surrounding cells (Huang *et al.*, 2022; Jönsson *et al.*, 2023). Adequate intake of these components as part of a balanced diet contributes to optimal hydration levels, critical for cellular function, nutrient transport optimization, and waste disposal efficiency. Additionally, seaweed contains trace levels of fluorine, contributing to overall dietary fluorine consumption, which aids in the remineralization of dental enamel and helps maintain good oral hygiene (Kaur *et al.*, 2022; Waseem *et al.*, 2023).

Furthermore, seaweed has a high carbohydrate content compared to other elements, serving as a key source of energy. Polysaccharides found in seaweed, including agar and carrageenan in red seaweeds and ulvans in green seaweeds, offer sustained energy release, enhancing metabolic activity and overall vitality (Wells *et al.*, 2016). Additionally, seaweed carbohydrates, particularly dietary fiber, promote intestinal health by promoting regular bowel movements, preventing constipation, and maintaining a healthy gut microbiota (Wijesinghe *et al.*, 2019). Due to its complex composition, seaweed carbohydrates may also help manage blood sugar levels by allowing for a more gradual release of glucose into the system (Xu *et al.*, 2023).

Optimized Methods for Extracting Carrageenan

Carrageenan is a polysaccharide extracted from red seaweed (Rhodophyta) and is widely used in various industries, including food, pharmaceuticals, cosmetics, and biotechnology, due to its gelling, thickening, and stabilizing properties (Al-Nahdi *et al.*, 2019; Laokelis *et al.*,

2022). There are several methods used to extract carrageenan from red seaweed, and these methods can vary based on factors such as the type of seaweed, extraction efficiency, and desired properties of the carrageenan (Ningrum *et al.*, 2021). These methods can vary in terms of efficiency, yield, and the quality of carrageenan produced. Researchers often optimize these methods based on factors such as the type of seaweed, desired properties of carrageenan, and industrial scalability. Additionally, advancements in extraction technologies continue to improve efficiency and sustainability in carrageenan production (Xu *et al.*, 2023).

The extraction process of carrageenan from red seaweed is meticulously executed, involving several crucial steps. Initially, seaweed is carefully harvested from coastal regions, with common species including *Chondrus crispus* or *Euclima cottonii* (Al-Nahdi *et al.*, 2019). Following harvest, thorough cleaning is undertaken to eliminate contaminants such as sand and epiphytes. Subsequently, the seaweed may undergo pre-treatment, often involving immersion in an alkaline solution to soften cell walls for easier extraction (Liu *et al.*, 2022). Careful drying follows to reduce moisture content, preparing the seaweed for the extraction phase (Entezari *et al.*, 2022).

Based on Figure 1, during the extraction process, the dried seaweed undergoes an alkaline treatment, typically employing potassium hydroxide (KOH) (Ferdiansyah *et al.*, 2023). This treatment dissolves the carrageenan previously present in the seaweed. Subsequently, carrageenan precipitation occurs by adding an acid, usually potassium chloride (KCl), causing the carrageenan to solidify and separate from the solution (Yuan & Song, 2005). Post-precipitation, the produced carrageenan undergoes washing to remove residual salts and impurities before being dried (Zaitseva *et al.*, 2022), yielding a purified carrageenan product ready for utilization across various industries, including cosmetics.

This extraction method is crucial to ensure the isolation of carrageenan in a form suitable for diverse applications, owing to its exceptional gelling and thickening properties as summary in Table 2.

Alkaline Extraction Method

This method involves treating the red seaweed with an alkaline solution, typically potassium hydroxide (KOH) or sodium hydroxide (NaOH), to solubilize the carrageenan. After alkaline treatment, the mixture is heated to facilitate carrageenan extraction. The carrageenan is then precipitated from the solution by adding an acid, such as hydrochloric acid (HCl) or sulfuric acid (H₂SO₄). The precipitated carrageenan is then washed and dried to obtain the final product (Loukelis *et al.*, 2022).

Acid Extraction method

In this method, the red seaweed is treated with a dilute acid, such as hydrochloric acid (HCl) or sulfuric acid (H₂SO₄), to dissolve the carrageenan. The mixture is then heated to aid in the extraction process. Once the carrageenan is extracted, it is precipitated by adding a base, such as calcium carbonate (CaCO₃) or potassium carbonate (K₂CO₃), to neutralize the acid. The precipitated carrageenan is then washed and dried (Núñez-Santiago *et al.*, 2011; Laokelis *et al.*, 2022).

Hot Water Extraction Method

This method involves boiling the red seaweed in water to extract carrageenan. The mixture is then filtered to remove solid residues, and the filtrate containing carrageenan is concentrated by evaporation. Carrageenan is then precipitated by adding alcohol, such as isopropyl alcohol or ethanol, to the concentrated solution. The precipitated carrageenan is collected, washed, and dried (Liu *et al.*, 2022; Entezari *et al.*, 2022).

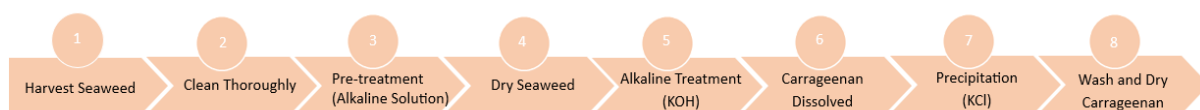


Figure 1. The eight (8) extraction process of carrageenan

Table 2. Summary of extraction carrageenan process from red seaweed

Extraction Method	Method steps	Reagent Related**	Industry Related	Applications [Ref.]
Alkaline	<ul style="list-style-type: none"> • Treatment with Alkaline Solution • Heating and Facilitation of Extraction • Precipitation with Acid • Washing and >Drying of Carrageenan 	<ul style="list-style-type: none"> • Potassium hydroxide (KOH) or sodium hydroxide (NaOH) as alkaline solution • Hydrochloric acid (HCl) or sulfuric acid (H₂SO₄) as acid for precipitation 	<p>Food Industry: Carrageenan extracted via this method is commonly used as a stabilizer and thickening agent in dairy products like ice cream and chocolate milk.</p> <p>Pharmaceutical Industry: Utilized as a gelatinous substance in pharmaceutical formulations, including capsules and tablets.</p>	Applied Phycology (Kaur <i>et al.</i> , 2022; Wells <i>et al.</i> , 2016; Thiviya <i>et al.</i> , 2022)
Acid	<ul style="list-style-type: none"> • Dissolution with Dilute Acid • Heating to Aid Extraction • Neutralization and Precipitation • Washing and Drying of Carrageenan 	<ul style="list-style-type: none"> • Hydrochloric acid (HCl) or sulfuric acid (H₂SO₄) as acid for dissolution • Calcium carbonate (CaCO₃) or potassium carbonate (K₂CO₃) as base for precipitation 	<p>Biotechnology: Carrageenan extracted via this method finds applications in tissue engineering and drug delivery systems.</p> <p>Cosmetic Industry: Used as a thickening agent and stabilizer in lotions, creams, and shampoos.</p>	Agricultural and Food Chemistry (Núñez-Santiago <i>et al.</i> , 2011; Laokelis <i>et al.</i> , 2022).
Hot Water	<ul style="list-style-type: none"> • Boiling and Extraction in Water • Filtration and Concentration • Precipitation with Alcohol • Washing and Drying of Carrageenan 	<ul style="list-style-type: none"> • Water as solvent for extraction • Isopropyl alcohol or ethanol as alcohol for precipitation • Optionally, salt solutions (e.g., sodium chloride) for salting out 	<p>Biomedical Engineering: Carrageenan extracted via this method is utilized in the development of wound dressings and scaffolds for tissue regeneration.</p> <p>Nutraceuticals: Used as a dietary supplement due to its potential health benefits, including its role in promoting digestive health.</p>	Marine Drugs (Tarman <i>et al.</i> , 2020; Pangestuti <i>et al.</i> , 2021; Pacheco-Quito <i>et al.</i> , 2020; El-Beltagi <i>et al.</i> , 2022; López-Hortas <i>et al.</i> , 2021; Peñalver <i>et al.</i> , 2020; Wan-Loy <i>et al.</i> , 2016)
Enzyme-Assisted	<ul style="list-style-type: none"> • Cell Wall Breakdown with Enzymes • Further Solubilization and Recovery • Precipitation and Processing • Washing and Drying of Carrageenan 	<ul style="list-style-type: none"> • Specific enzymes such as cellulase or pectinase for cell wall degradation • Alkaline solution (e.g., KOH or NaOH) or acid solution (e.g., HCl or H₂SO₄) for further extraction 	<p>Biopharmaceuticals: Carrageenan extracted via this method is utilized in the formulation of controlled-release drug delivery systems.</p> <p>Bioremediation: Used in environmental applications for the removal of heavy metals from wastewater.</p>	Biotechnology and Bioengineering (Tarman <i>et al.</i> , 2020; Entezari <i>et al.</i> , 2022; Kanlayavattanukul <i>et al.</i> , 2015)
Microwave-Assisted	<ul style="list-style-type: none"> • Utilization of Microwave Irradiation • Enhanced Extraction Efficiency • Precipitation and Processing • Washing and Drying of Carrageenan 	<ul style="list-style-type: none"> • Water or alkaline solution as solvent for extraction • Isopropyl alcohol or ethanol as alcohol for precipitation • Optionally, salt solutions (e.g., sodium chloride) for salting out 	<p>Food Packaging: Carrageenan extracted via this method is employed as a coating material for food packaging films to improve their mechanical and barrier properties.</p> <p>Agriculture: Utilized as a bio-stimulant in agriculture for enhancing plant growth and stress tolerance.</p>	Chemical Technology and Biotechnology (Tarman <i>et al.</i> , 2020; Entezari <i>et al.</i> , 2022; Kanlayavattanukul <i>et al.</i> , 2015)

** These reagents and chemicals play crucial roles in each extraction method, aiding in the solubilization, precipitation, and purification of carrageenan from red seaweed. The specific choice and concentration of these chemicals may vary depending on factors such as the seaweed species, extraction conditions, and desired properties of the extracted carrageenan.

Enzyme-Assisted Extraction Method

Enzyme-assisted extraction involves using specific enzymes, such as cellulase or pectinase, to break down cell wall components of the red seaweed and release carrageenan. After enzyme treatment, the mixture is typically subjected to further extraction steps such as alkaline or acid treatment to solubilize and recover carrageenan. The extracted carrageenan is then precipitated and processed similarly to other extraction methods (Otero *et al.*, 2021).

Microwave-Assisted Extraction Method

This method utilizes microwave irradiation to enhance the extraction efficiency of carrageenan. Red seaweed is mixed with a suitable solvent, such as water or alkaline solution, and subjected to microwave irradiation. The microwave energy helps to break down cell walls and facilitate the release of carrageenan into the solvent. After extraction, carrageenan is precipitated, washed, and dried (Entezari *et al.*, 2022).

Types of Carrageenan and their Properties

Carrageenan, derived from red seaweed, is categorized into three main types: kappa, iota, and lambda, each with distinct properties and applications in cosmetics.

Kappa Carrageenan: Known for its strong gelling abilities, kappa carrageenan is a key ingredient in hair styling products like gels and mousses, providing firm textures (Figure 2). It helps create stable and resilient shapes, crucial for long-lasting hold in these products.

Iota Carrageenan: This type forms soft, elastic gels, making it ideal for lotions, creams, and moisturizers. Its ability to impart a smooth, luxurious feel on the skin enhances the sensory experience of cosmetic products.

Lambda Carrageenan: Unlike kappa and iota, lambda carrageenan does not gel but significantly increases viscosity. It is widely used in creams and emulsions to improve consistency and stability without forming a gel (refer to Figure 2).

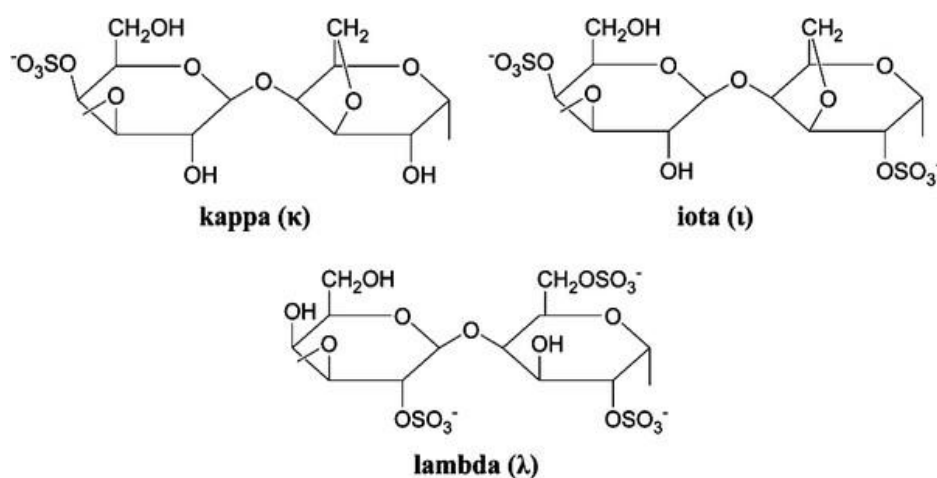


Figure 2. Chemical structure of kappa, iota and lambda carrageenans

Biological Activities

In addition to its role in enhancing texture and stability, carrageenan possesses significant biological activities that render it invaluable in cosmetic formulations (Núñez-Santiago *et al.*, 2011; Bagal-Kestwal *et al.*, 2019).

The inherent properties of this polysaccharide make it a highly sought-after addition to personal care and skincare products. Renowned for its antioxidant properties,

carrageenan plays a pivotal role in combating oxidative stress on the skin (Wang *et al.*, 2024). Antioxidants aid in neutralizing free radicals and mitigating damage caused by environmental factors, making them particularly relevant in cosmetics designed for anti-aging or protective purposes (El-Beltagi *et al.*, 2022; Pinheiro *et al.*, 2023).

Furthermore, carrageenan exhibits anti-inflammatory properties, making it an excellent choice for soothing and calming irritated or

sensitive skin (Obafemi *et al.*, 2021; Fransiska *et al.*, 2021). These anti-inflammatory attributes align with the increasing demand for skincare products tailored to address conditions such as inflammation or redness. Moreover, carrageenan serves as a humectant, facilitating skin moisture retention and contributing to hydration (Kanlayavattanakul *et al.*, 2015). As such, it holds importance as a key component in moisturizers and formulations intended to hydrate the skin (Liu *et al.*, 2023), thereby enhancing the overall skin-conditioning performance of cosmetic products.

Given its diverse biological activities, carrageenan transcends its role as a mere texturizing agent; it emerges as an active ingredient with positive implications for skin health and the overall effectiveness of cosmetic products within the industry.

Protein

Seaweeds are renowned for being rich sources of protein, with the concentration varying depending on factors such as species, seasonal cycle, and environmental fluctuations. These proteins encompass essential amino acids, along with glycine, alanine, proline, arginine, glutamic acid, and aspartic acid (McKim *et al.*, 2019). Among the three main types of seaweeds - green, red, and brown - red seaweeds boast the highest protein concentration, reaching up to 47%. In comparison, brown seaweeds typically contain protein concentrations ranging from 24% to 35%, while green seaweeds fall within a similar range (Míšková *et al.*, 2021; Morais *et al.*, 2021). Interestingly, the protein concentration of red

seaweeds rivals that of other protein-rich foods such as soybeans, cereals, eggs, and fish.

Lipid

Seaweeds harbor lipids, albeit with a low concentration ranging from 0.5% to 5.0% of dry weight samples as shown in Table 3 (Peñalver *et al.*, 2020). Despite this modest concentration, seaweeds are esteemed as rich sources of lipids, notably containing a high proportion of unsaturated fatty acids, including Eicosapentaenoic acid (as n-3 PUFAs) and Arachidonic acid (as n-6 PUFAs) (Petikirige *et al.*, 2022)

Further examination from Table 3 reveals that red seaweeds exhibit the lowest lipid content (0.64-5.0) %, followed by brown (0.38-11.91) % and green seaweeds (1.57-13.04) %. The variation in total lipid content can be attributed to factors such as geographic location, temperature, light intensity, seasonal changes, salinity, and species interactions (Priyadarshi *et al.*, 2022).

Seaweeds are rich reservoirs of beneficial lipids, including a diverse array of sterols such as cholesterol and clionasterol (Rioux *et al.*, 2017). These sterols are renowned for their bioactivity, offering numerous health benefits including cancer prevention, weight management, antioxidant effects, and protection against tumors (Yuan and Song, 2021), viruses, and cardiovascular diseases (Roohinejad *et al.*, 2017). Fucosterol and isofucosterol emerge as prominent players among these seaweed sterols (Shannon E *et al.*, 2022; Safwa *et al.*, 2023).

Table 3. Chemical composition of seaweeds based on different species

Species	Chemical composition of seaweed (% dry weight)		
	Protein	Lipid	Ash
Green seaweed	32.70-3.30	13.04-1.57	27.50-19.59
Brown seaweed	25.70-5.40	11.91-0.38	39.30-20.71
Red seaweed	47.0-2.30	5.0-0.64	44.03-17.50

Vitamins

Seaweeds boast a diverse array of vitamins, including fat-soluble vitamins such as vitamin A, vitamin D, vitamin E, and provitamin A, as well as water-soluble vitamins like vitamin C, various B vitamins (including vitamin B12, vitamin B6, vitamin B3, vitamin B2, and vitamin B), pantothenic acid, niacin, riboflavin, and folic

acid (Chauhan *et al.*, 2016; Obafemi *et al.*, 2021). However, the levels of vitamins in seaweeds may vary depending on the species, with some seaweeds exhibiting lower levels of certain vitamins (Lim *et al.*, 2021).

Different types of seaweeds-green, red, and brown-each possess their own unique strengths when it comes to vitamins. Green seaweeds are

particularly rich in vitamin E, while red seaweeds excel in providing vitamin C. Brown seaweeds stand out for their contribution of essential vitamin B3 (Rioux *et al.*, 2017). Interestingly, seaweeds also contain vitamin B12, a nutrient often scarce in plant-based foods, with various seaweed families containing differing amounts of this vital vitamin (Salido *et al.*, 2024).

Pigments

Pigments play a crucial role in controlling photosynthesis, as well as the growth and development of plants (Shannon E *et al.*, 2022). There are three main types of pigments: chlorophylls, carotenoids, and phycobilins. Chlorophylls, particularly chlorophyll a, are essential elements in photosynthesis, with green seaweeds containing the highest quantity of chlorophyll. Carotenoids and phycobilins serve as accessory pigments, transferring energy to chlorophyll a. Brown macrophytes are distinguished by their fucoxanthin content, while red ones are renowned for their phycobilins (Smyth *et al.*, 2021).

In the realm of food, color is a vital aspect, with pigments playing a crucial role. Primarily, pigments are utilized as natural dyes, reflecting a growing consumer preference for health-conscious choices. Natural pigments are regarded as health-promoting ingredients, offering numerous beneficial functions and serving as promising alternatives to synthetic dyes and ingredients. Additionally, due to their nutraceutical properties, pigments exhibit biological activities that significantly impact human health (Qin, 2018; Thiviya *et al.*, 2022).

Metals and Iodine

Given seaweeds' propensity for bioaccumulating metals, their consumption raises concerns regarding the potential transfer of high-risk metals to humans in relation to chemical pollution. Thus, it is imperative to comprehend the metal concentrations present in seaweed. Various factors, such as the seaweed's habitat and the surrounding water quality, influence the levels of metals within them. Typically, green macrophytes exhibit higher metal bioaccumulation compared to red and brown macrophytes (Jia *et al.* 2014; Sanjeewa *et al.*, 2016). In Europe, the European Union

Recommendation has proposed regulations for controlling the presence of arsenic, cadmium, iodine, lead, and mercury in seaweed, halophilic plants, and seaweed-based products.

Of particular importance is iodine, as some seaweed species contain elevated levels of this element. While excessive iodine intake may contribute to thyroid diseases, it is essential for the synthesis of thyroid hormones. Studies conducted by the Spanish Agency for Food Safety and Nutrition (AESAN) have revealed that processing methods, such as freezing or drying, can affect the iodine content of seaweeds. In France, a maximum iodine content of 2000 mg kg⁻¹ DW is recommended for all seaweed species. However, pregnant women, individuals with heart or renal conditions, and those with thyroid disorders (especially those taking iodine-related medications) should exercise caution when consuming iodine or iodine-derived products (Otero *et al.*, 2021).

Application and Formulation Considerations

The application and formulation considerations of carrageenan in cosmetic products underscore its versatile role in achieving specific textural and performance characteristics while meeting formulation requirements. Thanks to its unique gelling properties, carrageenan proves to be a valuable ingredient across a range of cosmetic products, including lotions, creams, and gels, where it imparts desired smoothness and consistency. Its ability to form and stabilize gels enhances both the tactile experience and visual appeal of the final product.

Furthermore, carrageenan demonstrates compatibility with a wide array of cosmetic ingredients, affording formulators the flexibility to create diverse formulations without compromising stability or efficacy. Its compatibility extends to formulations based on either water or oil (Fransiska *et al.*, 2021), rendering it suitable for use in various cosmetic products.

Formulation considerations for carrageenan involve optimizing its concentration according to the specific requirements of the cosmetic product to achieve optimal results. Formulators can manipulate carrageenan concentration to attain desired texture, viscosity, and stability without negatively affecting the performance of

other ingredients (Shannon *et al.*, 2022; Safwa *et al.*, 2023). Its versatility makes it an ideal candidate for combination with other natural ingredients commonly used in cosmetics, enabling the creation of holistic formulations that align with consumer demand for clean and environmentally friendly beauty products.

Beyond its role as a texturizing agent, carrageenan contributes to the overall sensorial experience provided by cosmetic products (Rioux *et al.*, 2017; Salido *et al.*, 2024). Enhancing spread ability and absorbability, it not only improves product effectiveness but also enhances customer satisfaction (Liu *et al.*, 2023). Formulators can leverage carrageenan to create

aesthetically pleasing products that resonate with market trends emphasizing functionality and a natural, environmentally conscious appeal.

Specific Chemical Content

Red seaweed, like other types of seaweed, contains a variety of bioactive compounds that offer benefits for cosmetic applications. While the specific chemical content may vary between different species of seaweed, red seaweed is known for containing unique compounds that contribute to its skincare properties as shown in Figure 3. Here are some of the key chemicals found in red seaweed, along with their cosmetic benefits.

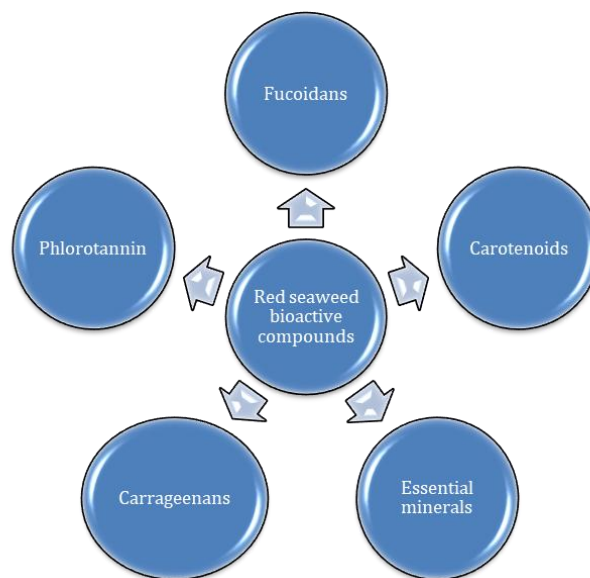


Figure 3. Several of chemicals found in red seaweed, along with their cosmetic benefits

Carrageenans

Red seaweed is rich in carrageenans, a type of sulfated polysaccharide. Carrageenans have excellent emollient properties, making them valuable in moisturizing creams, lotions, and masks. They form a protective barrier on the skin, helping to retain moisture and prevent dryness. Additionally, carrageenans have a soothing effect on the skin, making them suitable for calming irritated or inflamed skin.

Fucoidans

Fucoidans are another type of polysaccharide found in red seaweed. They have antioxidant and anti-inflammatory properties, which can help protect the skin from environmental damage and

reduce redness and inflammation. Fucoidans also promote collagen synthesis and skin regeneration, making them beneficial for anti-aging and wound healing formulations.

Phlorotannins

Phlorotannins are polyphenolic compounds found in red seaweed that possess strong antioxidant properties. They help neutralize free radicals generated by UV radiation and other environmental stressors, thereby protecting the skin from premature aging and oxidative damage. Phlorotannins also have skin-brightening effects, making them useful in formulations targeting hyperpigmentation and uneven skin tone.

Carotenoids

Red seaweed contains carotenoids, including β -carotene and astaxanthin, which are responsible for its red coloration. Carotenoids have potent

antioxidant properties and help protect the skin from UV-induced damage. They also contribute to the skin's natural radiance and can enhance the appearance of dull or tired skin. Figure 4 show the chemicals structure of β -Carotene.

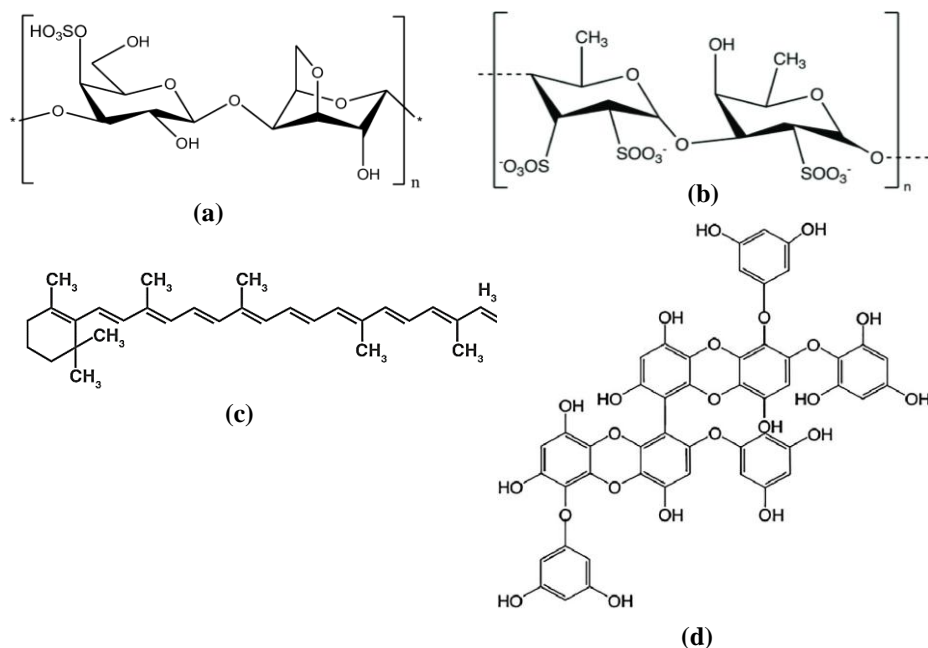


Figure 4. Chemical structures of; (a) Kappa - carrageenan; (b) Fucoidan; (c) Phlorotannin; (2,7'-phloroglucinol-6,6'-biecckol) and (d) β -carotene

Essential Minerals

Red seaweed is a rich source of essential minerals such as calcium, magnesium, potassium, and iron. These minerals play crucial roles in maintaining skin health and function. Calcium helps regulate skin cell turnover and hydration, magnesium supports enzymatic processes involved in collagen synthesis, potassium (Núñez-Santiago *et al.*, 2011; Laokelis *et al.*, 2022) helps maintain electrolyte balance in skin cells, and iron contributes to oxygen transport and energy metabolism in the skin.

Compared to other types of seaweed, red seaweed is particularly prized in cosmetics for its high content of carrageenans, fucoidans, and phlorotannins, which offer unique benefits such as enhanced moisturization, anti-inflammatory

effects, and antioxidant protection. However, it's worth noting that the specific chemical composition and concentrations of bioactive compounds can vary between different species of red seaweed and even within the same species due to factors like geographical location, environmental conditions, and harvesting methods.

Natural and Sustainable Sourcing

With growing consumer demand for natural and sustainable skincare ingredients, red seaweed extracts offer an attractive option for cosmetic manufacturers. Seaweed cultivation is environmentally friendly and requires minimal land and freshwater resources compared to traditional agricultural crops. Table 4 shows the summary of cosmetic application based on the bioactive compound in the red seaweeds.

Table 4. Cosmetic application, bioactive and elements present in the red seaweeds

Cosmetic Application [Ref.]	Bioactive	Bioactive Compounds	Chemicals/ Elements
Moisturizing Properties (Zaitseva <i>et al.</i> , 2022; Pinheiro <i>et al.</i> , 2023)	<ul style="list-style-type: none"> Red seaweed extracts are known for their hydrating and moisturizing effects on the skin. Studies have identified polysaccharides and peptides in red seaweed that help improve skin hydration by forming a protective barrier, reducing transepidermal water loss, and enhancing skin elasticity. 	Polysaccharides (e.g., carrageenans, agarans), peptides	Sulfur-containing compounds, such as sulfated polysaccharides
Anti-Aging Effects (Janowicz <i>et al.</i> , 2023; Pangestuti <i>et al.</i> , 2021; Waseem <i>et al.</i> , 2023; Priyadarshi <i>et al.</i> , 2022)	<ul style="list-style-type: none"> Certain compounds found in red seaweed, such as phlorotannins and carotenoids, possess antioxidant properties. These antioxidants help neutralize free radicals, which are known to cause oxidative stress and contribute to skin aging. Research suggests that incorporating red seaweed extracts into cosmetic formulations may help reduce the appearance of wrinkles, fine lines, and other signs of aging. 	Phlorotannins, carotenoids	Polyphenols, fucoxanthin, astaxanthin
Anti-Inflammatory and Soothing Properties (Obafemi <i>et al.</i> , 2021)	<ul style="list-style-type: none"> Red seaweed extracts contain bioactive compounds like fucoidans and sulfated polysaccharides, which exhibit anti-inflammatory properties. These compounds can help soothe irritated skin, reduce redness, and alleviate symptoms of conditions like eczema and psoriasis. Cosmetics containing red seaweed extracts may therefore be beneficial for individuals with sensitive or inflamed skin. 	Fucoidans, sulfated polysaccharides	Fucose, galactose, sulfate esters
Skin Brightening and Pigmentation Reduction (Pangestuti <i>et al.</i> , 2021; Montaser <i>et al.</i> , 2021; Liu <i>et al.</i> , 2023)	<ul style="list-style-type: none"> Some studies have explored the potential of red seaweed extracts in skin brightening formulations. Certain compounds in red seaweed, such as arbutin and phycobiliproteins, have been found to inhibit melanin production and reduce hyperpigmentation, leading to a more even skin tone. 	Arbutin, phycobiliprotein	Phenolic compounds, bilirubin-like pigments
Wound Healing and Regenerative Effects (Batista <i>et al.</i> , 2020; Jing <i>et al.</i> , 2021; Montaser <i>et al.</i> , 2021)	<ul style="list-style-type: none"> Red seaweed extracts have been investigated for their wound healing properties. Compounds like carrageenan and fucoidans promote the proliferation of skin cells, accelerate wound closure, and stimulate collagen synthesis, thereby aiding in tissue repair and regeneration. 	Carrageenans, fucoidans	Carrageenan oligosaccharides, fucose-containing sulfated polysaccharides
UV Protection (Gerber <i>et al.</i> , 1958)	<ul style="list-style-type: none"> Certain red seaweed species produce compounds like mycosporine-like amino acids (MAAs), which have UV-absorbing properties. Incorporating these compounds into cosmetic formulations may help provide additional protection against UV-induced skin damage, including sunburn and photoaging. 	Mycosporine-like amino acids	Amino acids (e.g., glycine, glutamine), imino acids

Safety, Regulatory Aspects & Challenges

When integrating carrageenan into cosmetic formulations, considerations regarding safety, regulatory compliance, and related challenges are imperative to ensure the quality of the final product and the well-being of its users. Initially, carrageenan is generally regarded as safe for use in cosmetics, with numerous studies affirming its safety within specified concentrations. However, concerns arise regarding its potential degradation into smaller molecules, known as poligeenan, under specific conditions (McKim *et al.*, 2019). This raises safety concerns, particularly at higher concentrations or when formulated in certain ways. To ensure the safe and effective use of carrageenan in cosmetics, regulatory bodies such as the Food and Drug Administration (FDA) in the United States, the European Commission, and similar agencies worldwide have established limits and specifications for its usage (Morais *et al.*, 2021).

In the cosmetics industry, challenges associated with carrageenan include potential interactions with other components, leading to formulation instability or decreased product effectiveness (Shannon *et al.*, 2019). With consumer awareness regarding ingredients on the rise, there's a growing demand for transparent labeling and communication regarding the presence of carrageenan in cosmetic products (Smyth *et al.*, 2021). Despite its benefits, significant obstacles persist in utilizing carrageenan in cosmetic formulations. These hurdles encompass compliance with evolving regulations, addressing consumer concerns regarding safety and sustainability, and ongoing research to validate its efficacy and safety.

A comprehensive approach is necessary, giving equal weight to consumer safety and product innovation, to navigate these challenges and leverage the benefits carrageenan offers in the cosmetics industry, such as its natural origin, versatility, and advantageous properties (Thiviya *et al.*, 2022). This entails striking a delicate balance between addressing regulatory requirements, meeting consumer expectations, and harnessing carrageenan's potential in cosmetic formulations effectively.

With regard to carrageenan, formulation considerations, safety aspects, and regulatory

dynamics underscore the importance of maintaining a balanced approach. While enhancing product texture and stability, carrageenan also contributes to the broader narrative of environmentally conscious beauty (Wan-Loy *et al.*, 2016). As the cosmetics industry continues to evolve, carrageenan emerges as a promising and innovative component, aligning with sustainability demands and consumer expectations (Pimentel *et al.*, 2017).

To navigate carrageenan's future in the cosmetics industry effectively, ongoing research, collaboration between regulatory bodies and industry stakeholders, and transparent communication with consumers are essential (Qin *et al.*, 2018). Commitment to rigorous safety assessments and continuous monitoring of industry practices is crucial to address challenges such as degradation and formulation interactions. Carrageenan plays a pivotal role in formulating products that not only meet stringent safety standards but also resonate with evolving beauty consumer values and preferences.

CONCLUSION

In conclusion, the utilization of carrageenan extract derived from red seaweed in cosmetic product production exemplifies the dynamic intersection of natural ingredients and the advancement of cosmetic science. Through a comprehensive examination of its types, biological activities, and extraction methods, it becomes evident that carrageenan holds multifaceted potential within the cosmetics sector. Among the various extraction techniques, the optimal method for obtaining the most important bioactive compounds has been identified, which maximizes its effectiveness in cosmetic applications. Its versatility in gelling, thickening, and providing skin benefits aligns well with the increasing consumer preference for clean and environmentally friendly beauty products. Given the dynamic landscape of the cosmetic industry driven by sustainability and natural ingredient trends, carrageenan stands poised to significantly influence the development of future beauty formulations that are both clean and efficacious. As the cosmetics industry embraces innovation and sustainability, carrageenan's role is set to expand, making it a

key player in shaping the future of clean and effective beauty products.

ACKNOWLEDGEMENTS

The authors would like to thank Universiti Malaysia Sabah for the financial support, provided through the Cluster Research Grant DKP0035.

REFERENCES

- Al-Nahdi, Z.M., Al-Alawi, A., & Al-Marhobi, I. (2019). The effect of extraction conditions on chemical and thermal characteristics of kappa-carrageenan extracted from *Hypnea bryoides*. *Journal of Marine Sciences*, 1: 5183261. 1-10. DOI:10.1155/2019/5183261
- Bagal-Kestwal, D.R., Pan, M.H., & Chiang, B.H. (2019). Properties and applications of gelatin, pectin, and carrageenan gels. *Bio monomers for green polymeric composite materials*, 117-140. DOI:10.1002/9781119301714.ch6
- Batista, M.P., Gonçalves, V.S., Gaspar, F.B., Nogueira, I.D., Matias, A.A., & Gurikov, P. (2020). Novel alginate-chitosan aerogel fibres for potential wound healing applications. *International Journal of Biological Macromolecules*, 156: 773-782. DOI:10.1016/j.ijbiomac.2020.04.089
- Bauer, S., Jin, W., Zhang, F., & Linhardt, R.J. (2021). The application of seaweed polysaccharides and their derived products with potential for the treatment of Alzheimer's disease. *Marine drugs*, 19(2): 89. DOI:10.3390/md19020089
- Bukhari, N.T.M., Rawi, N.F.M., Hassan, N.A.A., Saharudin, N.I., & Kassim, M.H.M. (2023). Seaweed polysaccharide nanocomposite films: A review. *International Journal of Biological Macromolecules*, 245: 125486. 1-13. DOI:10.1016/j.ijbiomac.2023.125486
- Chauhan, P.S., & Saxena, A. (2016). Bacterial carrageenases: an overview of production and biotechnological applications. *3 Biotech*, 6(2): 146. 1-18. DOI:10.1007/s13205-016-0461-3
- El-Beltagi, H.S., Mohamed, A.A., Mohamed, H.I., Ramadan, K.M., Barqawi, A.A., & Mansour, A.T. (2022). Phytochemical and potential properties of seaweeds and their recent applications: A review. *Marine drugs*, 20(6): 342. 1-49. DOI:10.3390/md20060342
- El-Said, G.F., & El-Sikaily, A. (2013). Chemical composition of some seaweed from Mediterranean Sea coast, Egypt. *Environmental Monitoring and assessment*, 185, 6089-6099. DOI:10.1007/s10661-012-3009-y
- Entezari, T., Zarei, M., Jamekhorshid, A., Mohammadzadeh, M.R., & Entezam, M. (2022). Purification and characterization of carrageenan extracted from persian gulf *laurencia snyderiae* red algae. *Applied Food Biotechnology*, 9(3): 239-249. DOI:10.22037/afb.v9i3.37367
- Ferdiansyah, R., Abdassah, M., Zainuddin, A., Rachmaniar, R., & Chaerunisaa, A.Y. (2023). Effects of alkaline solvent type and pH on solid physical properties of carrageenan from *Eucheuma cottonii*. *Gels*, 9(5): 397. 1-14. DOI:10.3390/gels9050397
- Ferreira, M., Matos, A., Couras, A., Marto, J., & Ribeiro, H. (2022). Overview of cosmetic regulatory frameworks around the world. *Cosmetics*, 9(4): 72. 1-15. DOI:10.3390/cosmetics9040072
- Firdayanti, L., Yanti, R., Rahayu, E.S., & Hidayat, C. (2023). Carrageenan extraction from red seaweed (*Kappaphycopsis cottonii*) using the bead mill method. *Algal Research*, 69: 102906.
- Fransiska, D., Darmawan, M., Sinurat, E., Sedayu, B.B., Wardhana, Y.W., Herdiana, Y., & Setiana, G.P. (2021). Characteristics of oil in water (o/w) type lotions incorporated with kappa/iota carrageenan. *IOP Conference Series: Earth and Environmental Science*, 715, (1): 012050.
- Gerber, P., Dutcher, J.D., Adams, E.V., & Sherman, J.H. (1958). Protective effect of seaweed extracts for chicken embryos infected with influenza B or mumps virus. *Proceedings of the Society for Experimental Biology and Medicine*, 99(3): 590-593.
- Hamasuna, R., Eizuru, Y., & Minamishima, Y. (1994). Inhibition by iota-carrageenan of the spread of murine cytomegalovirus from the peritoneal cavity to the blood plasma. *Journal of General Virology*, 75(1): 111-116. DOI:10.1099/0022-1317-75-1-111
- Hamzalıoğlu, A., & Gökmen, V. (2024). Interaction between bioactive carbonyl compounds and asparagine and impact on acrylamide. *Acrylamide in Food*, Academic Press. 433-455.
- He, D., Zhao, A.S., Su, H., Zhang, Y., Wang, Y.N., Luo, D., Li, J.A. & Yang, P. (2019). An injectable scaffold based on temperature-responsive

- hydrogel and factor-loaded nanoparticles for application in vascularization in tissue engineering. *Journal of Biomedical Materials Research Part A*, 107(10): 2123-2134. DOI:10.1002/jbm.a.36723
- Hong, D.D., Hien, H.M., & Son, P.N. (2007). Seaweeds from Vietnam used for functional food, medicine and biofertilizer. *Journal of Applied Phycology*, 19: 817-826.
- Huang, Z., Bi, R., Musil, S., Pétursdóttir, Á. H., Luo, B., Zhao, P., Tan, X. & Jia, Y. (2022). Arsenic species and their health risks in edible seaweeds collected along the Chinese coastline. *Science of the Total Environment*, 847: 157429. 1-12.
- Ismail, M.M., & Amer, M.S. (2021). Characterization and biological properties of sulfated polysaccharides of *Corallina officinalis* and *Pterocladia capillacea*. *Acta Botanica Brasilica*, 34: 623-632.
- Janowicz, M., Galus, S., Ciurzyńska, A., & Nowacka, M. (2023). The potential of edible films, sheets, and coatings based on fruits and vegetables in the context of sustainable food packaging development. *Polymers*, 15(21): 4231.
- Jia, X., Yang, J., Wang, Z., Liu, R., & Xie, R. (2014). Polysaccharides from *Laminaria japonica* show hypoglycemic and hypolipidemic activities in mice with experimentally induced diabetes. *Experimental Biology and Medicine*, 239(12): 1663-1670.
- Jiménez-Escrig, A., & Sánchez-Muniz, F. J. (2000). Dietary fibre from edible seaweeds: Chemical structure, physicochemical properties and effects on cholesterol metabolism. *Nutrition Research*, 20(4): 585-598.
- Jiménez-Escrig, A., Gómez-Ordóñez, E., & Rupérez, P. (2011). Seaweed as a source of novel nutraceuticals: sulfated polysaccharides and peptides. *Advances in Food and Nutrition Research*, 64: 325-337.
- Jing, X., Sun, Y., Liu, Y., Ma, X., & Hu, H. (2021). Alginate/chitosan-based hydrogel loaded with gene vectors to deliver polydeoxyribonucleotide for effective wound healing. *Biomaterials Science*, 9(16): 5533-5541. DOI:10.1039/D1BM00911G
- Jönsson, M., Maubert, E., Merkel, A., Fredriksson, C., Karlsson, E. N., & Wendin, K. (2024). A sense of seaweed: Consumer liking of bread and spreads with the addition of four different species of northern European seaweeds. A pilot study among Swedish consumers. *Future Foods*, 9: 100292.
- Ju, J., Yang, J., Zhang, W., Wei, Y., Yuan, H., & Tan, Y. (2023). Seaweed polysaccharide fibers: Solution properties, processing and applications. *Journal of Materials Science & Technology*, 140: 1-18.
- Kalasariya, H. S., Yadav, V. K., Yadav, K. K., Tirth, V., Algahtani, A., Islam, S., & Jeon, B. H. (2021). Seaweed-based molecules and their potential biological activities: An eco-sustainable cosmetics. *Molecules*, 26(17): 5313.
- Kanlayavattanukul, M., & Lourith, N. (2015). Biopolysaccharides for skin hydrating cosmetics. *Polysaccharides: Bioactivity and Biotechnology*; Springer International Publishing: New York, NY, USA, 1867-1892.
- Kaur, M., Kala, S., Parida, A., & Bast, F. (2023). Concise review of green algal genus *Monostroma* Thuret. *Journal of Applied Phycology*, 35(1): 1-10.
- Khalil, H. P. S. A., Tye, Y. Y., Saurabh, C. K., Leh, C. P., Lai, T. K., Chong, E. W. N., Nurul Fazita, M. R., Mohd Hafiidz, J., Banerjee, A. & Syakir, M.I. (2017). Biodegradable polymer films from seaweed polysaccharides: A review on cellulose as a reinforcement material. *Express Polymer Letters*, 11(4): 244-265.
- Khoobakht, F., Khorshidi, S., Bahmanyar, F., Hosseini, S.M., Aminikhah, N., Farhoodi, M., & Mirmoghtadaie, L. (2024). Modification of mechanical, rheological and structural properties of agar hydrogel using xanthan and locust bean gum. *Food Hydrocolloids*, 147: 109411. DOI:10.1016/j.foodhyd.2023.109411
- Kumari, P., Kumar, M., Gupta, V., Reddy, C. R. K., & Jha, B. (2010). Tropical marine macroalgae as potential sources of nutritionally important PUFAs. *Food Chemistry*, 120(3): 749-757. DOI:10.1016/j.foodchem.2009.11.006
- Lee, K.Y., & Mooney, D.J. (2012). Alginate: properties and biomedical applications. *Progress in Polymer Science*, 37(1): 106-126.
- Lim, C., Yusoff, S., Ng, C.G., Lim, P.E., & Ching, Y.C. (2021). Bioplastic made from seaweed polysaccharides with green production methods. *Journal of Environmental Chemical Engineering*, 9(5): 105895.

- Liu, F., Duan, G., & Yang, H. (2023). Recent advances in exploiting carrageenans as a versatile functional material for promising biomedical applications. *International Journal of Biological Macromolecules*, 235: 123787.
- Liu, Y., An, D., Xiao, Q., Chen, F., Zhang, Y., Weng, H., & Xiao, A. (2022). A novel κ -carrageenan extracting process with calcium hydroxide and carbon dioxide. *Food Hydrocolloids*, 127: 107507.
- López-Hortas, L., Flórez-Fernández, N., Torres, M. D., Ferreira-Anta, T., Casas, M. P., Balboa, E. M., Falque, E. & Domínguez, H. (2021). Applying seaweed compounds in cosmetics, cosmeceuticals and nutricosmetics. *Marine Drugs*, 19(10): 552. 1-30. DOI:10.3390/md19100552
- Loukelis, K., Papadogianni, D., & Chatzinikolaidou, M. (2022). Kappa-carrageenan/chitosan/gelatin scaffolds enriched with potassium chloride for bone tissue engineering. *International Journal of Biological Macromolecules*, 209: 1720-1730.
- McKim, J.M., Willoughby Sr, J.A., Blakemore, W.R., & Weiner, M.L. (2019). Clarifying the confusion between poligeenan, degraded carrageenan, and carrageenan: A review of the chemistry, nomenclature, and in vivo toxicology by the oral route. *Critical Reviews in Food Science and Nutrition*, 59(19): 3054-3073.
- Míšková, Z., Salek, R. N., Křenková, B., Kůrová, V., Němečková, I., Pachlová, V., & Buňka, F. (2021). The effect of κ - and ι -carrageenan concentrations on the viscoelastic and sensory properties of cream desserts during storage. *LWT*, 145: 111539.
- Montaser, A.S., Jlassi, K., Ramadan, M.A., Sleem, A.A., & Attia, M.F. (2021). Alginate, gelatin, and carboxymethyl cellulose coated nonwoven fabrics containing antimicrobial AgNPs for skin wound healing in rats. *International Journal of Biological Macromolecules*, 173: 203-210.
- Morais, T., Cotas, J., Pacheco, D., & Pereira, L. (2021). Seaweeds compounds: an ecosustainable source of cosmetic ingredients. *Cosmetics*, 8(1): 8.
- Mostafavi, F.S., & Zaeim, D. (2020). Agar-based edible films for food packaging applications-A review. *International Journal of Biological Macromolecules*, 159: 1165-1176.
- Ningrum, A.M., & Chasani, A.R. (2021). Numerical phenetic and phylogenetic relationships in silico among brown seaweeds (Phaeophyceae) from Gunungkidul, Yogyakarta, Indonesia. *Biodiversitas Journal of Biological Diversity*, 22(6): 3057-3064
- Núñez-Santiago, M.D.C., Tecante, A., Garnier, C., & Doublier, J.L. (2011). Rheology and microstructure of κ -carrageenan under different conformations induced by several concentrations of potassium ion. *Food Hydrocolloids*, 25(1): 32-41.
- Obafemi, C.A., Adegbite, O.B., Fadare, O.A., Iwalewa, E.O., Omisore, N.O., Sanusi, K., Ylmaz, Y. & Ceylan, Ü. (2021). Tryptanthrin from microwave-assisted reduction of isatin using solid-state-supported sodium borohydride: DFT calculations, molecular docking and evaluation of its analgesic and anti-inflammatory activity. *Heliyon*, 7(1): 1-13.
- Otero, P., Carpena, M., Garcia-Oliveira, P., Echave, J., Soria-Lopez, A., García-Pérez, P., Fraga-Corral, M., Cao, H., Nie, S., Xiao, J., Simal-Gandara, J. & Prieto, M. A. (2021). Seaweed polysaccharides: Emerging extraction technologies, chemical modifications and bioactive properties. *Critical Reviews in Food Science and Nutrition*, 63(13): 1901-1929. DOI:10.1080/10408398.2021.1969534
- Pacheco-Quito, E.M., Ruiz-Caro, R., & Veiga, M.D. (2020). Carrageenan: drug delivery systems and other biomedical applications. *Marine Drugs*, 18(11): 583.
- Pangestuti, R., Shin, K.H., & Kim, S.K. (2021). Anti-photoaging and potential skin health benefits of seaweeds. *Marine Drugs*, 19(3): 172.
- Peñalver, R., Lorenzo, J.M., Ros, G., Amarowicz, R., Pateiro, M., & Nieto, G. (2020). Seaweeds as a functional ingredient for a healthy diet. *Marine Drugs*, 18(6): 301.
- Pessarrodona, A., Assis, J., Filbee-Dexter, K., Burrows, M.T., Gattuso, J.P., Duarte, C.M., Krause-Jensen, D., Moore, P. J., Smale, D.A. & Wernberg, T. (2022). Global seaweed productivity. *Science Advances*, 8(37): eabn2465.1-10. DOI:10.1126/sciadv.abn2465
- Petikirige, J., Karim, A., & Millar, G. (2022). Effect of drying techniques on quality and sensory properties of tropical fruits. *International Journal of Food Science & Technology*, 57(11): 6963-6979.
- Pimentel, F.B., Alves, R.C., Rodrigues, F., & PP Oliveira, M.B. (2017). Macroalgae-derived ingredients for cosmetic industry - An update. *Cosmetics*, 5(1): 2.

- Pinheiro, J.L.S., Rodrigues, L.H.M., da Silva, L.D., dos Santos, V.M.R., Gomes, D.A., da Silva Chagas, F. D., Venes, J. & Damasceno, R. O. S. (2023). Sulfated iota-carrageenan from marine alga *Agardhiella ramosissima* prevents gastric injury in rodents via its antioxidant properties. *Algal Research*, 77: 103371. 1-12 DOI:10.1016/j.algal.2023.103371
- Prajaputra, V., Isnaini, N., Maryam, S., Ernawati, E., Deliana, F., Haridhi, H.A., Fadli, N., Karina, S., Agustina, S., Nurfadillah, N., Arisa, I.I., Desiyana, L.S. & Bakri, T.K. (2024). Exploring marine collagen: Sustainable sourcing, extraction methods, and cosmetic applications. *South African Journal of Chemical Engineering*, 47(1): 197-211. DOI: 10.1016/j.sajce.2023.11.006
- Priyadarshi, R., Purohit, S.D., Roy, S., Ghosh, T., Rhim, J.W., & Han, S.S. (2022). Antiviral biodegradable food packaging and edible coating materials in the COVID-19 era: A mini-review. *Coatings*, 12(5): 577.
- Qiao, D., Zhang, Y., Lin, L., Li, K., Zhu, F., Wang, G., Xi, G., Jiang, F., Zhang, B. & Xie, F. (2023). Revealing the role of λ -carrageenan on the enhancement of gel-related properties of acid-induced soy protein isolate/ λ -carrageenan system. *Food Hydrocolloids*, 150: 109608. 1-8. DOI:10.1016/j.foodhyd.2023.109608
- Qin, Y. (2018). Seaweed hydrocolloids as thickening, gelling, and emulsifying agents in functional food products. In *Bioactive seaweeds for food applications*. Academic Press. 135-152
- Rioux, L.E., Beaulieu, L., & Turgeon, S.L. (2017). Seaweeds: A traditional ingredients for new gastronomic sensation. *Food hydrocolloids*, 68: 255-265.
- Rodríguez-Bernaldo de Quirós, A., & López-Hernández, J. (2021). An overview on effects of processing on the nutritional content and bioactive compounds in seaweeds. *Foods*, 10(9): 2168.
- Roohinejad, S., Koubaa, M., Barba, F. J., Saljoughian, S., Amid, M. & Greiner, R. (2017). Application of seaweeds to develop new food products with enhanced shelf-life, quality and health-related beneficial properties. *Food Research International*, 99: 1066-1083.
- Safwa, S.M., Ahmed, T., Talukder, S., Sarker, A., & Rana, M.R. (2023). Applications of non-thermal technologies in food processing Industries-A review. *Journal of Agriculture and Food Research*, 100917.
- Salido, M., Soto, M., & Seoane, S. (2023). Seaweed: Nutritional and gastronomic perspective. A review. *Algal Research*, 103357.
- Sanjeewa, K.K.A., Kim, E. A., Son, K.T. & Jeon, Y.J. (2016). Bioactive properties and potentials cosmeceutical applications of phlorotannins isolated from brown seaweeds: A review. *Journal of Photochemistry and Photobiology B: Biology*, 162: 100-105.
- Shannon, E., & Abu-Ghannam, N. (2019). Seaweeds as nutraceuticals for health and nutrition. *Phycologia*, 58(5): 563-577.
- Shannon, E., Conlon, M., & Hayes, M. (2022). The prebiotic effect of Australian seaweeds on commensal bacteria and short chain fatty acid production in a simulated gut model. *Nutrients*, 14(10): 2163. DOI:10.3390/nu14102163
- Shi, F., Chang, Y., Shen, J., Chen, G. & Xue, C. (2023). A comparative investigation of anionic polysaccharides (sulfated fucan, ι -carrageenan, κ -carrageenan, and alginate) on the fabrication, stability, rheology, and digestion of multilayer emulsion. *Food Hydrocolloids*, 134: 108081.
- Smyth, P.P. (2021). Iodine, seaweed, and the thyroid. *European Thyroid Journal*, 10(2): 101-108. DOI:10.1159/000512971
- Tafuro, G., Costantini, A., Baratto, G., Francescato, S., Busata, L., & Semenzato, A. (2021). Characterization of polysaccharidic associations for cosmetic use: Rheology and texture analysis. *Cosmetics*, 8(3): 62.
- Tarman, K., Sadi, U., Santoso, J., & Hardjito, L. (2020). Carrageenan and its enzymatic extraction. *Encyclopedia of Marine Biotechnology*, 1: 147-159.
- Thiviya, P., Gamage, A., Gama-Arachchige, N.S., Merah, O., & Madhujith, T. (2022). Seaweeds as a source of functional proteins. *Phycology*, 2(2): 216-243.
- Wang, Q., Zhou, C., Xia, Q., Pan, D., Du, L., He, J., Sun, Y., Geng, F. & Cao, J. (2024). pH sensitive cold-set hydrogels based on fibrinogen hydrolysates/carrageenan: Insights of rheology, coacervation, microstructure and antioxidant ability. *Food Hydrocolloids*, 147: 109377: DOI:10.1016/j.foodhyd.2023.109377
- Wan-Loy, C., & Siew-Moi, P. (2016). Marine algae as a potential source for anti-obesity agents. *Marine Drugs*, 14(12): 222.

- Waseem, M., Khan, M. U., Majeed, Y., Ntsefong, G. N., Kirichenko, I., Klopova, A., Trushov, P. & Lodygin, A. (2023). Seaweed-based films for sustainable food packaging: properties, incorporation of essential oils, applications, and future directions. *Slovak Journal of Food Sciences/Potravinarstvo*, 17(1). DOI:10.5219/1908
- Wells, M. L., Potin, P., Craigie, J. S., Raven, J. A., Merchant, S. S., Helliwell, K. E., Smith, A.G., Camire, M.E. & Brawley, S. H. (2017). Algae as nutritional and functional food sources: revisiting our understanding. *Journal of Applied Phycology*, 29: 949-982. DOI 10.1007/s10811-016-0974-5
- Wijesinghe, W.A.J.P., & Jeon, Y.J. (2012). Enzyme-assistant extraction (EAE) of bioactive components: a useful approach for recovery of industrially important metabolites from seaweeds: A Review, *Fitoterapia*, 83(1): 6-12. DOI:10.1016/j.fitote.2011.10.016
- Xu, J., Liao, W., Liu, Y., Guo, Y., Jiang, S., & Zhao, C. (2023). An overview on the nutritional and bioactive components of green seaweeds. *Food Production, Processing and Nutrition*, 5(1): 18. 1-21. DOI:10.1186/s43014-023-00132-5
- Yuan, H., & Song, J. (2005). Preparation, structural characterization and in vitro antitumor activity of kappa-carrageenan oligosaccharide fraction from *Kappaphycus striatum*. *Journal of Applied Phycology*, 17: 7-13. DOI:10.1007/s10811-005-5513-8
- Zaitseva, O.O., Sergushkina, M.I., Khudyakov, A.N., Polezhaeva, T.V., & Solomina, O.N. (2022). Seaweed sulfated polysaccharides and their medicinal properties. *Algal Research*, 68: 102885. 1-35. DOI:10.1016/j.algal.2022.102885
- Zhang, Y., Song, B., Wang, X., Zhang, W., Zhu, H., Pang, X., Wang, Y., Xie, N., Zhang, S. & Lv, J. (2023). Rheological properties and microstructure of rennet-induced casein micelle/ κ -carrageenan composite gels. *LWT*, 178: 114562. 1-10. DOI:10.1016/j.lwt.2023.114562

REVIEW PAPER

The Danger of Foot and Mouth Disease in Livestock – A Review

ASWIN RAFIF KHAIRULLAH¹, SHENDY CANADYA KURNIAWAN², MUSTOFA HELMI EFFENDI^{3*}, OTTO SAHAT MARTUA SILAEN⁴, IKECHUKWU BENJAMIN MOSES⁵, ABDULLAH HASIB⁶, SANCAKA CHASYER RAMANDINIANTO⁷, DANIAH ASHRI AFNANI⁸, AGUS WIDODO⁹, KATTY HENDRIANA PRISCILIA RIWU¹⁰, REICHAN LISA AZ ZAHRA¹¹ & SHEILA MARTY YANESTRIA¹²

¹Research Center for Veterinary Science, National Research and Innovation Agency (BRIN). Jl. Raya Bogor Km. 46 Cibinong, Bogor 16911, West Java, Indonesia; ²Master Program of Animal Sciences, Department of Animal Sciences, Specialisation in Molecule, Cell and Organ Functioning, Wageningen University and Research. Wageningen 6708 PB, Netherlands; ³Division of Veterinary Public Health, Faculty of Veterinary Medicine, Universitas Airlangga. Jl. Dr. Ir. H. Soekarno, Kampus C Mulyorejo, Surabaya 60115, East Java, Indonesia; ⁴Doctoral Program in Biomedical Science, Faculty of Medicine, Universitas Indonesia. Jl. Salemba Raya No. 6 Senen, Jakarta 10430, Indonesia; ⁵Department of Applied Microbiology, Faculty of Science, Ebonyi State University. Abakaliki 480211, Nigeria; ⁶School of Agriculture and Food Sustainability, The University of Queensland. Gatton, QLD, 4343, Queensland; ⁷Lingkar Satwa Animal Care Clinic. Jl. Sumatera No. 31L, Gubeng, Surabaya 60281, East Java, Indonesia; ⁸Department of Microbiology and Parasitology, Faculty of Veterinary Medicine, Universitas Pendidikan Mandalika. Jl. Pemuda No. 59A, Dasan Agung Baru, Mataram 83125, West Nusa Tenggara, Indonesia; ⁹Department of Health, Faculty of Vocational Studies, Universitas Airlangga. Jl. Dharmawangsa Dalam Selatan No. 28-30, Kampus B Airlangga, Surabaya 60115, East Java, Indonesia; ¹⁰Department of Veterinary Public Health, Faculty of Veterinary Medicine, Universitas Pendidikan Mandalika. Jl. Pemuda No. 59A, Dasan Agung Baru, Mataram 83125, Nusa Tenggara Barat, Indonesia; ¹¹Profession Program in Veterinary Medicine, Faculty of Veterinary Medicine, Universitas Airlangga. Jl. Dr. Ir. H. Soekarno, Kampus C Mulyorejo, Surabaya 60115, East Java, Indonesia; ¹²Faculty of Veterinary Medicine, Universitas Wijaya Kusuma Surabaya. Jl. Dukuh Kupang XXV No.54, Dukuh Kupang, Dukuh Pakis, Surabaya 60225, East Java, Indonesia

*Corresponding authors: mhelmiEFFENDI@gmail.com

Received: 15 August 2023

Accepted: 11 June 2024

Published: 31 December 2024

ABSTRACT

The FMD virus, also known as FMDV, is a member of the Picornaviridae family of the genus Aphthovirus. There are seven immunologically distinct FMD virus serotypes, known as Asia-1, A, C, O, South-African Territories (SAT) -1, -2, and -3. The disease's clinical symptoms include the development of vesicles on the lips, tongue, palate, tooth pads, nose, coronary band, gums, and interdigital spaces. There are many viral, host, and environmental factors that affect the epidemiology of FMD, including variations in viral virulence, particle stability in diverse microenvironments, and possible long-term survival. FMD can spread in a variety of ways, including through human contact with contaminated milk tankers or animal transport vehicles, the use of contaminated animal goods, equipment, or vehicles, or by the transmission of windborne viruses. Foot and mouth illness is not considered to be a serious public health hazard because the infection seems to be rare and the effects are self-limiting. Since the cost of disease control is added to the direct economic losses brought on by animal deaths, decreased milk production, and slowed animal growth rates, FMD epidemics indirectly harm the economy. Some of the techniques used to control FMD epidemics include mobility restrictions, quarantines, the death of infected and exposed animals, and cleaning and disinfecting impacted buildings, equipment, and vehicles.

Keywords: Foot and mouth disease, infectious disease, livestock, virus

Copyright: This is an open access article distributed under the terms of the CC-BY-NC-SA (Creative Commons Attribution-NonCommercial-ShareAlike 4.0 International License) which permits unrestricted use, distribution, and reproduction in any medium, for non-commercial purposes, provided the original work of the author(s) is properly cited.

INTRODUCTION

A highly contagious viral illness that affects animals with cloven hooves, foot and mouth disease (FMD) epidemics have a significant negative financial impact on the global livestock business (Chanchaidechachai *et al.*, 2022). This disease can attack livestock and wild animals such as cattle, sheep, buffalo, goats, pigs, deer, elephants, and camels (Rodríguez-Habibe *et al.*, 2020). The illness sometimes produces epidemics in once free nations and is endemic in portions of South America, Africa, the Middle East, and Asia (Jamal & Belsham, 2013). About 77% of the world's total livestock population is estimated to be affected by FMD; thus, making it one of the important illnesses that need to be reported to the World Organization for Animal Health (Knight-Jones *et al.*, 2017). The livestock sector has been seriously threatened by this since the sixteenth century (Longjam *et al.*, 2011).

An Italian monk named Hieronymus Fracastorius gave the earliest account of foot and mouth disease (FMD) in cattle in Venice in 1514 (Jamal & Belsham, 2013). Affected animals refuse to eat, display reddened oral mucosa, and have vesicles on their paws and in their mouths. Morbidity due to FMD can reach 90-100% among susceptible animal populations; however, most infected animals recover as mortality is generally low, especially in adult animals (1 – 5%) (Teifke *et al.*, 2012). This description, made 500 years ago, bears a strong resemblance to FMD when viewed today. An estimated 77 – 80% of the global livestock-keeping regions, especially in Asia, Africa, the Middle East, and some regions in South America have been affected by this disease.

Globally, FMD continues to afflict more than 100 nations, and its distribution largely corresponds to economic progress (Pattnaik *et al.*, 2012). The FMD virus (FMDV), which is a member of the Picornaviridae family of the genus Aphthovirus, is known for causing FMD (Malik *et al.*, 2017). There are seven different FMDV serotypes known: Asia 1, O, A, C, SAT1, SAT2, and SAT3 (Ranaweera *et al.*, 2019; Paton *et al.*, 2021). FMDV samples from the South African FMD outbreak were found to include the SAT1, SAT2, and SAT3 FMDV serotypes (Fana *et al.*, 2021). Asian serotype 1 was discovered in Pakistan. Meanwhile, the last serotype C was detected in Kenya and Brazil (Wekesa *et al.*,

2015). Cloven hooves play a critical epidemiological function in keeping the virus in the environment, even though FMD can inadvertently infect a wide range of host species (Grubman & Baxt, 2004).

Clinically, the disease manifests as the development of vesicles on the lips, tongue, palate, tooth pads, snout, coronary band, gums, and interdigital spaces (Arzt *et al.*, 2011). Additionally prevalent are drooling, depression, lameness, and anorexia, which have a negative impact on livestock systems productivity and efficiency (Jori *et al.*, 2021). Significant economic effects from these epidemics may include decreased milk and meat output, maintenance expenses, power outages, limitations on the trade in animals and animal products, and high implementation costs for control efforts (Espinosa *et al.*, 2020). The current requirement for mass slaughter of diseased animals and possible contacts when an outbreak arises in an FMD-free area also makes FMD a problem for animal welfare (Bradhurst *et al.*, 2019).

Even though FMD rarely results in the death of older animals, the virus can induce major cardiac lesions in young animals with a significant mortality rate of 20% or higher. FMD typically has a fatality rate below 5% (Mahmoud & Galbat, 2017). The main obstacles to containing this condition and the reasons it is regarded as the most feared viral disease are its high prevalence of transmission, wide geographic distribution, broad host range, ability to identify carrier status, antigenic diversity that results in poor cross-immunity, and relatively short duration of immunity (Shurbe *et al.*, 2022). The main issues with controlling this disease include a lack of surveillance, inadequate diagnostic tools, and ineffective control strategies (Maree *et al.*, 2014). Throughout the year, there are still periodic reports of these breakouts.

This disease has been wiped out in more affluent nations, but the disease's spread to underdeveloped nations that are often free of it can result in significant economic losses (Limon *et al.*, 2020). FMD outbreaks frequently recur in these nations despite the implementation of prevention and control strategies like a combination of stamp policies, increased biosecurity, preventative or emergency

vaccinations, movement restrictions, strengthened surveillance, education programs, and community outreach (Blacksell *et al.*, 2019). Due to disparities in animal health priorities, varied resources, and varying logistical capabilities, these techniques are adopted and enforced inconsistently among nations, which leads to partial or no results (Gordon *et al.*, 2022).

The FMD virus is regarded as a serious global health issue. The goal of this review is to provide a comprehensive explanation of the etiology, pathophysiology, epidemiology, diagnosis, clinical symptoms, transmission, impact on public health, economic impact, and control measures against the development of FMD in livestock. This review's information was compiled to present recent scientific research, identify knowledge gaps and study restrictions surrounding FMD disease, and provide current scientific literature.

Etiology

The Foot and Mouth Disease Virus (FMDV) is the sole genus-level representative of the Aphthovirus genus that belongs to the Picornaviridae family and the first viral pathogen to be recognized (Malik *et al.*, 2017). There are seven immunologically distinct FMDV virus serotypes, identified as A, O, C, Asia-1, South-African Territories (SAT) -1, -2, and -3, which include more than 65 subtypes (Ranaweera *et al.*, 2019). Type O stood for the Oise in France, while Type A stood for Allemagne (Germany). The type C is then referred to as the supplementary type in Germany (Jamal & Belsham, 2013). About 30 years later, researchers at The Pirbright Institute, United Kingdom in England identified 3 novel FMDV serotypes called SAT1, SAT2, and SAT3 in samples taken from an FMD outbreak in South Africa (Banda *et al.*, 2022). First identified in a sample from Pakistan was a seventh serotype called Asia 1 (Longjam *et al.*, 2011).

A single-stranded RNA with a positive charge and a length of roughly 8500 nucleotides is found inside the viral particle, or virion (Gao *et al.*, 2016). These are icosahedral particles with a smooth surface that have a diameter of about 30 nm. The structural proteins VP1, VP2, VP3, and VP4 are each present in 60 copies (Dong *et*

al., 2021). The fourth structural protein (MW8.5 kDa) is internal, whereas the first three (MW24 kDa) include a surface component. Additionally, virions typically contain one or two VP0 units, which are the forerunners of VP2 and VP4 (Park *et al.*, 2022). The structural protein VP1-3 folds into eight strands that join to create the majority of the capsid structure, forming a 13-barrel wedge shape (Longjam *et al.*, 2011). The FMDV's three-dimensional structure has shown notable surface features made of loops between the G and H strands of VP1 (Burman *et al.*, 2006).

Located inside the capsid is the VP4 protein. Loops connecting the 13-barrel VP1-3 strands make up the virion's outer surface (Yuan *et al.*, 2017). FMDV lacks surface gorges or pits, which are receptor binding sites for enteroviruses and cardioviruses. This makes it different from other picornaviruses (Wang *et al.*, 2015). The channel on the fivefold axis of this virion, which facilitates the entry of tiny molecules like Cscl into the capsid and gives FMDV the highest buoyant density among the picornaviruses, is another characteristic of this organism (Yuan *et al.*, 2017). The trypsin-sensitive region of VP1 contains the FMDV's primary cell attachment site and immunodominant region, which are both situated in solvent-exposed regions of the virion surface (Lawrence *et al.*, 2013). Previous serological research showed that one of the main antigenic regions of the virus, the highly variable VP1 region, which is comprised of residues 135 to 155, is shared by various FMDV serotypes (Ludi *et al.*, 2014).

Pathogenesis

After the virus enters the animal's body through the digestive and respiratory tracts, it replicates in the lymphoid tissue, particularly in the upper respiratory tract, before entering the bloodstream and circulating for three to five days (Rodríguez-Habibe *et al.*, 2020). Prior to the virus entering the bloodstream and the onset of clinical symptoms, the virus can be found in the oropharynx one to three days earlier. The virus then travels and replicates through the circulation in its predilected epithelial tissues, including the heart muscle in young animals, between the nails, female animal nipples, and the tongue (Dash *et al.*, 2010). The virus was ejected from infected animals two days before clinical

signs manifested (the virus in milk was discovered four days prior to the onset of clinical signs), and considerable amounts of the virus were no longer expelled 4 – 5 days after vesicles developed (Stenfeldt *et al.*, 2016a). Skin wounds typically recover in 10 days, but animals with secondary infections need longer time of about 2 weeks to recover (Dillon, 2011).

The epithelium turns pale and gradually fills with fluid on the first day that clinical indications in the form of skin lesions occur. On the second day, the vesicles burst, and a layer of epithelium with distinct borders could be seen at the lesion's edges and at its red base. On the third day, the lesion's edges are hazy and the ground turns a faint crimson tint; fibrin deposition starts. On the fourth day, fibrin deposition increased in size and epithelial tissue started to regrow around the lesion's margins (Mohebbi *et al.*, 2017). The scars are still visible as pale areas even though the lesions are typically healed by day 10 and scar tissue has formed by day 7. Although the age of lesions can be determined, the accuracy will decrease since the rate of lesions healing varies between animals (Gornik *et al.*, 2019). Due to their smaller size compared to cattle, lesions in goats and sheep are typically more challenging to observe. Additionally, these small ruminants frequently have leg lesions in the coronary band of the leg, which are typically milder lesions (Muthukrishnan *et al.*, 2020). In pigs, foot lesions are more frequently observed to identify the age of the lesions (Stenfeldt *et al.*, 2016a).

Even though ruminants have immunity to the FMD virus, virus particles can still be discovered in their oropharynx up to 28 days after infection, and 50% of ruminants may develop persistent infection (Stenfeldt *et al.*, 2016b). Animals whose oropharynx is still found to have the virus after 28 days post-infection are referred to as disease-carrying animals (Jamal & Belsham, 2013). Cattle, small ruminants, African buffalo, and Asian water buffalo have all been observed to be chronic carriers of the virus for up to five years, three years, and nine months, respectively, although pigs are not thought to be such persistent carriers (Bertram *et al.*, 2018). The amount of viral excretion in carriers is variable (not constant), and it gets smaller over time. With the exception of the African buffalo, which is considered to have contributed to the FMD outbreak in Zimbabwe in 1989 and 1991, the

epidemiological significance of these carriers (especially cattle and small ruminant animals such as pigs) in disease transmission is unknown (Guerrini *et al.*, 2019).

Epidemiology

The epidemiology of FMD is complicated and is influenced by a variety of viral, host, and environmental factors, including variations in viral virulence (lesional severity, number, and duration of viral shedding), stability of the particles in different microenvironments, and potential long-term persistence (Paton *et al.*, 2018). The host species (cattle, sheep, water buffalo, goats, pigs, deer, antelope, and bison), nutritional and immunological state, population densities, animal migration, and contact between various domestic and wild host species and animals that might mechanically transport the virus are other factors that affect FMDV replication and transmission (Ranjan *et al.*, 2016). The environment can act as a geographical barrier to the spread of a virus or, on the other hand, it can promote transmission of a virus when the correct climatic circumstances are present (Bessell *et al.*, 2008). The tremendous potential for FMDV variation and adaptation in this multifactorial scenario has mimicked complicated evolutionary patterns discovered by molecular epidemiological investigations, which are mostly based on nucleotide sequencing of capsid protein genes (Caridi *et al.*, 2021).

Various regions of Asia, Africa, the Middle East, and South America are plagued with foot and mouth disease (Maree *et al.*, 2014). While serotypes O and A are common, SAT virus is primarily found in Africa (with sporadic incursions into the Middle East), and Asia 1 is now solely found in Asia (Bachanek-Bankowska *et al.*, 2018). FMDV is not present in Western Europe, New Zealand, Australia, Greenland, Iceland, North and Central America (Brown *et al.*, 2021). However, FMD has not been detected in North America for more than 60 years despite recent outbreaks in Western Europe (where eradication efforts have been successful) (Valarcher *et al.*, 2008). The last FMD outbreak occurred in the US in 1929, whereas it has not occurred in Canada or Mexico since the 1950s (Jamal & Belsham, 2013). After being proclaimed cured of the disease in 1986, an FMD

outbreak returned to Indonesia recently in 2022 (Sutawi *et al.*, 2023).

FMDV serotypes are not evenly distributed around the world. The virus strains O, A, and C have persistent and aggressive distribution patterns throughout Europe, America, Asia, and Africa (Woldemariyam *et al.*, 2023). However, FMDV serotype C may no longer exist outside of laboratories because the last FMDV serotype C infection was documented in Ethiopia in 2005 (Ayelet *et al.*, 2009). Sub-Saharan Africa is typically the only place where the SAT1-3 virus is found (Wubshet *et al.*, 2019). The three continental reservoirs in Asia, Africa, and South America, which can be further divided into seven primary infectious viral pools, are currently maintaining the worldwide burden of FMDV infection (Woldemariyam *et al.*, 2023). Each of these seven primary infectious viral pools has at least three different serotypes of the virus, and because circulating viruses are mostly found in these local reservoirs, local strains have developed that are sometimes (as with type A and SAT viruses) difficult to control without specialized testing and vaccinations (Ludi *et al.*, 2014).

Diagnosis

The control and eradication of disease in endemic areas depend on an accurate diagnosis of FMDV infection. Clinical indicators are typically utilized to make the initial diagnosis of FMD, but these can be easily mistaken for those of other vesicular illnesses. Therefore, breeders must identify illness symptoms quickly and report them to the appropriate veterinary authorities to confirm. Samples of suspected disease should also be sent to a reference laboratory for confirmation (Ding *et al.*, 2013). Important support for FMD control and vaccination campaigns is provided by quick and accurate laboratory data generation (Capozzo *et al.*, 2023). However, because of inefficient cold chains and prolonged transport times, samples that laboratories acquire from many impoverished nations may be of low quality (Blacksell *et al.*, 2019). These circumstances render laboratory diagnosis unreliable, necessitating the use of a diagnostic instrument that is suited for the situation to enable quick diagnosis and the implementation of the necessary controls (van Vuren *et al.*, 2022).

The following ideas form the foundation of the majority of current diagnostic methods for FMD detection: Viral isolation involving proliferation in susceptible cell cultures is used to identify the infectious agent, use of an FMDV-specific antibody or capture reagent in an Enzyme-linked Immunosorbent Assay (ELISA) technique for viral antigen detection, genetic analysis of nucleotide sequences and reverse transcription polymerase chain reaction (RT-PCR)-based viral nucleic acid detection, detection of FMDV-specific antibodies in animals that have already been exposed to the virus (Rémond *et al.*, 2002). Typically, sera determined to be positive by ELISA are confirmed by Virus Neutralization Test (VNT) (Ma *et al.*, 2011). These methods are especially appropriate for well-equipped labs, which are typically national or regional reference labs.

For instance, the use of viral cell culture systems necessitates educated people, a biosafety level 3 (BSL-3) laboratory, and cautious handling of samples to prevent cross-contamination and environmental contamination (Artika & Ma'roef, 2017). A high-quality sample is necessary for successful viral isolation, which also calls for transportation conditions from the sampling location to the lab (Burrell *et al.*, 2017). In diagnostic labs in endemic areas, it is simple to deploy both solid-phase competition ELISA and liquid-phase inhibitory ELISA for the serological detection of FMDV-specific antibodies to structural proteins (Cao *et al.*, 2022).

Clinical Symptoms

The intensity of clinical indications can range from moderate or subclinical to severe, depending on the virus type, exposure dose, age and species of the infected animal, and degree of host immunity. Death is uncommon, with the exception of young animals, who can pass away through malnutrition or multifocal myocarditis (Hammond *et al.*, 2021). Most adult animals recover in two to three weeks, however subsequent infections can prolong recovery (Park *et al.*, 2022). Morbidity can be close to 100%. The mortality rate is typically 1% to 5% for adults, but 20% or more for young lambs, piglets, and calves (Mahmoud *et al.*, 2017). Recovery typically takes two weeks in simple cases.

Cattle

The most severe FMD symptoms are found in highly productive dairy cows found in developed nations (Lyons *et al.*, 2015). The following signs and symptoms appear after 24 hours: pyrexia, anorexia, chills, decreased milk production for a couple of days, smacking of the lips, drooling, grinding of teeth, limping, kicking, or stamping of the feet. These symptoms are caused by vesicles (aphthae) between the coronary bands and claws, and in the mucous membranes of the buccal and nasal cavities. Vesicles can burst in the mammary glands and leave behind erosions (Shmeiger *et al.*, 2021). Recovery typically takes 8 to 15 days. There are several complications, including tongue erosion, superinfection of lesions, nail distortion, mastitis and a persistent disruption of milk production, myocarditis, infertility, abortion, a persistent loss of weight, and loss of heat regulation. Myocarditis causes the death of young animals (Tufani, 2013).

Sheep and Goat

Many diseased sheep or goats could not show any symptoms or may only have one lesion. Typical symptoms include fever and mild to severe lameness in one or more legs. Vesicles develop on the feet, in the coronary bands, and in the interdigital gaps, but they may burst or become concealed by foot lesions from other causes (Muthukrishnan *et al.*, 2020). Mouth lesions typically present as shallow erosions and are frequently undetectable or severe. It is typical for sheep and goats to be milked to exhibit pyrexia and agalactia. Several epidemics resulted in the death of numerous ewes. Young animals can die without showing any clinical symptoms (Kitching & Hughes, 2002).

Pigs

Pigs exposed to concrete in particular can experience pyrexia, develop severe leg lesions, and become lame with detached claws (Perez & Willeberg, 2017). Vesicles frequently develop at pressure sites on the legs, particularly along the knuckles. There may be dry lesions on the tongue and vesicular lesions on the muzzle (Stenfeldt *et al.*, 2016a). Piglets younger than 8 weeks of age are especially susceptible to sudden death from heart failure in young pigs up to 14 weeks of age (Moreno-Torres *et al.*, 2022).

Transmission

There are numerous ways that FMD can spread, including human contact with contaminated equipment, animal transport vehicles, milk tankers, animal products, vehicles, and windborne virus transmission (Auty *et al.*, 2019). One of the main ways that FMD spreads is by the aerosol route, which involves passing the disease from one animal to another (Brown *et al.*, 2022). Virus concentrations in downstream air are primarily determined by meteorological factors. The quantity and species of afflicted animals, the type of virus, the environment, and the species and number of animals under the wind are all factors that determine how quickly an infection spreads through the air (Subramaniam *et al.*, 2022). Inhibiting the spread of disease-causing aerosols during the rainy season are persistent downpours, high relative humidity, and humid winds. Additionally, during this season, strong rains or flooding in some locations hinder the movement and transportation of animals from one place to another (Rahman *et al.*, 2020).

The number of FMD outbreaks rises in the winter because of environmental factors that favor dry weather, dry winds, and low to moderate temperatures (Hegde *et al.*, 2014). Viral infections may spread more quickly among susceptible animal populations as a result of these favorable environmental conditions (Mielke & Garabed, 2020). Due to the summer's oppressive heat, there are fewer FMD outbreaks (Hagerman *et al.*, 2018). Additionally, migration to new pastures, large-scale movements and animal groupings, as well as cow and buffalo exhibits, are all associated with seasonal peaks in FMD prevalence (Wubshet *et al.*, 2019). Cattle are regarded as an indication of this illness because they are typically the first species to exhibit FMD symptoms (Mohebbi *et al.*, 2017). Because the minimum 20TCID₅₀ (tissue culture infective dose) of virus is needed to initiate infection in these animals (cattle and buffalo), they are extremely sensitive to infection (Walz *et al.*, 2020).

Pigs are regarded as a reinforcing host for the illness due to their high airborne virus transmission rates and relative resistance to airborne infection (Valarcher *et al.*, 2008). Sheep and cattle both excrete airborne viruses at a

similar rate, but due to sheep's smaller respiratory volume than cattle, it is believed that they are less susceptible to airborne infections (Marcos *et al.*, 2019). Sheep are thought of as maintenance hosts since they do not often exhibit conventional clinical symptoms or cardinal indicators that are similar to those of other airborne diseases (Stenfeldt *et al.*, 2019). Conditions that are conducive to the spread of this disease include low relative humidity (>60%), dim sunlight, a lack of heavy rain, and slow and consistent wind speed and direction (Brown *et al.*, 2022).

FMD virus can be shed into blood, milk, pharynx, rectum, and vagina before the appearance of clinical manifestations of disease in infected cows (Suchowski *et al.*, 2021). The possibility exists for raw milk to spread the virus both inside the farm and from farm to farm because the virus is shed into the milk before the dairy cows exhibit clinical signs of sickness (Shaban *et al.*, 2022). Further study is required in areas including virus emission, particle size and virus content, virus challenge times, and meteorological consequences to better understand airborne FMD transmission and its significance in upcoming outbreaks. The genetic and antigenic diversity of FMDV is one of its most crucial characteristics.

Public Health Impact

Humans can also contract FMDV, which has moderate flu-like symptoms as well as conjunctivitis symptoms, small vesicular eruptions on the skin, and tissue erosion (Dillon, 2011). Most of the symptoms are extremely mild, self-limiting, and unnoticeable. When handling infected or suspect animals and conducting laboratory sample processing, precautions should be used (Longjam *et al.*, 2011). Since the infection seems to be uncommon and the consequences are moderate, foot and mouth disease is not seen as a severe public health issue (Knight-Jones *et al.*, 2017). There have only been a relatively small number of clinical cases, even though many persons who previously worked with FMDV in vaccine labs or other settings generated antibodies to this virus (Di Giacomo *et al.*, 2022). One lab reported only 2 occurrences in more than 50 years, and a significant FMD vaccine manufacturer found 3 cases among its employees (Chanchaidechachai *et al.*, 2022). Perhaps exposure to extremely high

levels of virus or predisposing circumstances is required for infection.

Between 1921 and 1969, there were reports of more than 40 human instances of FMD that were confirmed in labs (Bauer, 1997). Vesicular lesions and influenza-like symptoms are among the signs and symptoms of this illness, which is often mild, transient, and self-limiting (Wong *et al.*, 2020). Some human cases are known to enter via wound infection, with the initial lesion forming at the site of inoculation (Prempeh *et al.*, 2001). There are also claims that three veterinarians purposefully exposed themselves to the FMD virus by consuming tainted unpasteurized milk for three days (Shaban *et al.*, 2022). Another study claimed that youngsters may be more likely than adults to contract the virus (Dubie & Negash, 2021). The FMD virus is present in the vesicles from an infected individual, despite their being no reports of person-to-person transmission (Li *et al.*, 2021).

Economic Impact

The genetic makeup of the animals (usually their expressed genotype which were inherited from their parents) in a country, common livestock management techniques, costs for inputs and products used in livestock production, and the country's ability to produce livestock for export markets are all factors that affect the prevalence and danger of disease attack (Adamchick *et al.*, 2021). Disease impact is not the same in all countries and livestock populations as a result of these differences. Live animal commerce between FMD-affected and FMD-free nations is prohibited (Knight-Jones *et al.*, 2017). The EU, US, and Japan often have the highest pricing for FMD-free meat, with prices being 50% higher on average (Dinku & Matsuda, 2018). Additionally, trade in cattle products is prohibited. Only processed, canned goods may be shipped in the event of the usual outbreak; however, boneless meat may be exported if FMD is effectively controlled by vaccination administered by an experienced veterinary service capable of identifying an outbreak (Paton *et al.*, 2009).

FMD outbreaks damage the economy indirectly since the cost of disease control adds to the direct economic losses brought on by animal fatalities, decreased milk output, and slowed animal growth rates (de Menezes *et al.*,

2023). A nation that has been identified as having FMD will face barriers in international trade due to the disease's ease of spread, particularly when dealing with products derived from animals that may carry the FMD virus (Auty *et al.*, 2019). The socioeconomic circumstances of those impacted by limitations on the movement of animals and animal products are likewise impacted by FMD epidemics (Naranjo & Cosivi, 2013). To stop the spread of the virus when FMD first appeared in the UK in 2001, around 6.2 million animals were euthanised (Davies, 2002). The outbreak in Japan in 2010 resulted in 290 thousand animals having to be slaughtered (Muroga *et al.*, 2012), while in South Korea as many as 3.47 million animals were slaughtered in 2010 to 2011 (Park *et al.*, 2013). According to a 2013 study, the annual economic losses caused by lower productivity and the cost of FMD vaccine range from 6.5 to 21 billion US dollars worldwide (Alhaji *et al.*, 2020).

Control And Preventive Measures

In a region endemic with FMD, quick action is crucial for controlling an outbreak. Veterinarians should adhere to their local and national illness reporting procedures when they uncover or suspect this disease (Eschbaumer *et al.*, 2020). Import restrictions aid in preventing the spread of FMDV from endemic regions to diseased animals or tainted food fed to animals (Woldemariyam *et al.*, 2023). Particularly concerning is food waste provided to pigs. FMDV can be killed by heat treatment, which also lowers the danger of outbreaks; nevertheless, several nations have outright banned feeding because it is impossible to ensure that proper heat treatment techniques are followed (Kristensen *et al.*, 2021). The WOAHA has published guidelines for eradicating FMDV from animal products such as dairy, meat, leather, and wool (Marcos & Perez, 2019). Recently, a global FMD control campaign was launched to lower the spread of the virus and the incidence of this disease (Naranjo & Cosivi, 2013).

Among the steps employed to contain FMD epidemics include quarantine and mobility restrictions, the killing of afflicted and exposed animals, and the cleaning and disinfection of impacted buildings, machinery, and vehicles (Clemmons *et al.*, 2021). Euthanasia of animals at risk of infection and immunization are

possible further interventions (Costa & Akdeniz, 2019). Infected carcasses must be safely disposed of using methods such as rendering, burying, or burning (Guan *et al.*, 2010). The carcass should not be fed to carnivores, including dogs and cats, which may become infected with the virus in raw tissue (Waters *et al.*, 2021). To stop the virus from spreading mechanically, rats and other vectors can be eliminated (Auty *et al.*, 2019). People who have been exposed to FMDV may be advised to refrain from contact with vulnerable animals for a while, as well as decontaminating clothing and other personal items (Orsel & Bouma, 2009). To avoid virus entry, farms that are not infected should implement good biosecurity practices (Fountain *et al.*, 2018).

During some outbreaks, vaccination can be used to prevent the spread of FMDV or to save some animals (such as zoo animals) (Muleme *et al.*, 2013). The choice to utilize vaccination is complicated and depends on the outbreak's scientific, economic, political, and social considerations (Rawdon *et al.*, 2018). Additionally, vaccines are utilized in endemic regions to safeguard animals from sickness (Railey & Marsh, 2019). The FMDV vaccination (such as the use of live-attenuated vaccines, DNA vaccines, peptide vaccines, and live viral vector vaccines) only offers protection against the serotype it contains; to provide appropriate protection, the vaccine strain must also be modified to account for field strains (Singh *et al.*, 2019).

CONCLUSION

FMD is considered to be a significant global veterinary concern especially as the FMD virus sub-lineages have been recognized to evolve into novel strains with the capacity to escape vaccination and result into major livestock epidemics. Limitations on the transportation of animals and animal products have an influence on people whose socioeconomic conditions are affected by FMD epidemics. Farms that are not afflicted should employ appropriate biosecurity procedures to prevent virus entry. Finally, it is imperative to continue implementing measures and research studies directed at vaccine matching, vaccine design improvement, vaccine quality control, and continued surveillance in order to control and to keep track of FMD virus epidemiology and transmission.

ACKNOWLEDGEMENTS

The authors would like to thank the Faculty of Veterinary Medicine, Universitas Airlangga, Indonesia and National Research and Innovation Agency (BRIN), Indonesia.

REFERENCES

- Adamchick, J., Rich, K.M. & Perez, A.M. (2021). Assessment of the risk of foot and mouth disease among beef cattle at slaughter from east african production systems. *Viruses*, 13(12): 2407. DOI: 10.3390%2Fv13122407
- Alhaji, N.B., Amin, J., Aliyu, M.B., Mohammad, B., Babalobi, O.O., Wungak, Y. & Odetokun, I.A. (2020). Economic impact assessment of foot-and-mouth disease burden and control in pastoral local dairy cattle production systems in Northern Nigeria: A cross-sectional survey. *Preventive Veterinary Medicine*, 177(1): 104974. DOI: 10.1016/j.prevetmed.2020.104974
- Artika, I.M. & Ma'roef, C.N. (2017). Laboratory biosafety for handling emerging viruses. *Asian Pacific Journal of Tropical Biomedicine*, 7(5): 483-491. DOI: 10.1016/j.apjtb.2017.01.020
- Arzt, J., Baxt, B., Grubman, M.J., Jackson, T., Juleff, N., Rhyan, J., Rieder, E., Waters, R. & Rodriguez, L.L. (2011). The pathogenesis of foot-and-mouth disease II: viral pathways in swine, small ruminants, and wildlife; myotropism, chronic syndromes, and molecular virus-host interactions. *Transboundary and Emerging Diseases*, 58(4): 305-326. DOI: 10.1111/j.1865-1682.2011.01236.x
- Auty, H., Mellor, D., Gunn, G. & Boden, L.A. (2019). The risk of foot and mouth disease transmission posed by public access to the countryside during an outbreak. *Frontiers in Veterinary Science*, 6(1): 381. DOI: 10.3389/fvets.2019.00381
- Ayelet, G., Mahapatra, M., Gelaye, E., Egziabher, B.G., Rufeal, T., Sahle, M., Ferris, N.P., Wadsworth, J., Hutchings, G.H. & Knowles, N.J. (2009). Genetic characterization of foot-and-mouth disease viruses, Ethiopia, 1981-2007. *Emerging Infectious Diseases*, 15(9): 1409-1417. DOI: 10.3201%2Fid1509.090091
- Bachanek-Bankowska, K., Di Nardo, A., Wadsworth, J., Henry, E.K.M., Parlak, Ü., Timina, A., Mischenko, A., Qasim, I.A., Abdollahi, D., Sultana, M., Hossain, M.A., King, D.P. & Knowles, N.J. (2018). Foot-and-Mouth disease in the middle east caused by an a/asia/g-vii virus lineage, 2015-2016. *Emerging Infectious Diseases*, 24(6): 1073-1078. DOI: 10.3201%2Fid2406.170715
- Banda, F., Shilongo, A., Hikufe, E.H., Khaiseb, S., Kabajani, J., Shikongo, B., Set, P., Kapapero, J.K., Shoombe, K.K., Zaire, G., Kabilika, S., Quan, M., Fana, E.M., Mokopasetso, M., Hyera, J.M.K., Wadsworth, J., Knowles, N.J., Nardo, A.D. & King, D.P. (2022). The first detection of a serotype O foot-and-mouth disease virus in Namibia. *Transboundary and Emerging Diseases*, 69: e3261-e3267. DOI: 10.1111/tbed.14561
- Bauer, K. (1997). Foot- and-mouth disease as zoonosis. *Archives of Virology Supplementum*, 13(1): 95-97. DOI: 10.1007/978-3-7091-6534-8_9
- Bertram, M.R., Vu, L.T., Pauszek, S.J., Brito, B.P., Hartwig, E.J., Smoliga, G.R., Hoang, B.H., Phuong, N.T., Stenfeldt, C., Fish, I.H., Hung, V.V., Delgado, A., VanderWaal, K., Rodriguez, L.L., Long, N.T., Dung, D.H. & Arzt, J. (2018). Lack of transmission of foot-and-mouth disease virus from persistently infected cattle to naïve cattle under field conditions in Vietnam. *Frontiers in Veterinary Science*, 5(1): 174. DOI: 10.3389/fvets.2018.00174
- Bessell, P.R., Shaw, D.J., Savill, N.J. & Woolhouse, M.E. (2008). Geographic and topographic determinants of local FMD transmission applied to the 2001 UK FMD epidemic. *BMC Veterinary Research*, 4(1): 40. DOI: 10.1186/1746-6148-4-40
- Blacksell, S.D., Siengsan-Lamont, J., Kamolsiripichaiorn, S., Gleeson, L.J. & Windsor, P.A. (2019). A history of FMD research and control programmes in Southeast Asia: lessons from the past informing the future. *Epidemiology and Infection*, 147: e171. DOI: 10.1186/1746-6148-4-40
- Bradhurst, R., Garner, G., East, I., Death, C., Dodd, A. & Kompas, T. (2019). Management strategies for vaccinated animals after an outbreak of foot-and-mouth disease and the impact on return to trade. *PLoS ONE*, 14(10): e0223518. DOI: 10.1371%2Fjournal.pone.0223518
- Brown, E., Nelson, N., Gubbins, S. & Colenutt, C. (2022). Airborne transmission of foot-and-mouth disease virus: A review of past and present perspectives. *Viruses*, 14(5): 1009. DOI: 10.3390/v14051009

- Brown, V.R., Miller, R.S., McKee, S.C., Ernst, K.H., Didero, N.M., Maison, R.M., Grady, M.J. & Shwiff, S.A. (2021). Risks of introduction and economic consequences associated with African swine fever, classical swine fever and foot-and-mouth disease: A review of the literature. *Transboundary and Emerging Diseases*, 68(4): 1910-1965. DOI: 10.1111/tbed.13919
- Burrell, C.J., Howard, C.R. & Murphy, F.A. (2017). Laboratory diagnosis of virus diseases. *Fenner and White's Medical Virology*, 135-154. DOI: 10.1016%2FB978-0-12-375156-0.00010-2
- Burman, A., Clark, S., Abrescia, N.G., Fry, E.E., Stuart, D.I. & Jackson, T. (2006). Specificity of the VP1 GH loop of foot-and-mouth disease virus for alphavirus integrins. *Journal of Virology*, 80(19): 9798-9810. DOI: 10.1128%2FJVI.00577-06
- Cao, Y., Li, K., Xing, X., Zhu, G., Fu, Y., Bao, H., Bai, X., Sun, P., Li, P., Zhang, J., Ma, X., Wang, J., Zhao, Z., Li, D., Liu, Z. & Lu, Z. (2022). Development and validation of a competitive elisa based on bovine monoclonal antibodies for the detection of neutralizing antibodies against foot-and-mouth disease virus serotype A. *Journal of Clinical Microbiology*, 60(4): e0214221. DOI: 10.1128/jcm.02142-21
- Capozzo, A.V., Vosloo, W., de Los Santos, T., Pérez, A.M. & Pérez-Filgueira, M. (2023). Editorial: Foot-and-mouth disease epidemiology, vaccines and vaccination: moving forward. *Frontiers in Veterinary Science*, 10(1): 1231005. DOI: 10.3389/fvets.2023.1231005
- Caridi, F., Cañas-Arranz, R., Vázquez-Calvo, Á., de León, P., Calderón, K.I., Domingo, E., Sobrino, F. & Martín-Acebes, M.A. (2021). Adaptive value of foot-and-mouth disease virus capsid substitutions with opposite effects on particle acid stability. *Scientific Reports*, 11(1): 23494. DOI: 10.1038/s41598-021-02757-3
- Chanchaidechachai, T., Saatkamp, H., Inchaisri, C. & Hogeveen, H. (2022). Analysis of epidemiological and economic impact of foot-and-mouth disease outbreaks in four district areas in thailand. *Frontiers in Veterinary Science*, 9(1): 904630. DOI: 10.3389/fvets.2022.904630
- Clemmons, E.A., Alfson, K.J. & Dutton, J.W. (2021). Transboundary animal diseases, an overview of 17 diseases with potential for global spread and serious consequences. *Animals*, 11(7): 2039. DOI: 10.3390%2Fani11072039
- Costa, T. & Akdeniz, N. (2019). A review of the animal disease outbreaks and biosecure animal mortality composting systems. *Waste Management*, 90(1): 121-131. DOI: 10.1016/j.wasman.2019.04.047
- Dash, P., Barnett, P.V., Denyer, M.S., Jackson, T., Stirling, C.M., Hawes, P.C., Simpson, J.L., Monaghan, P. & Takamatsu, H.H. (2010). Foot-and-mouth disease virus replicates only transiently in well-differentiated porcine nasal epithelial cells. *Journal of Virology*, 84(18): 9149-9160. DOI: 10.1128%2FJVI.00642-10
- Davies, G. (2002). The foot and mouth disease (FMD) epidemic in the United Kingdom 2001. *Comparative Immunology, Microbiology and Infectious Diseases*, 25(5-6): 331-343. DOI: 10.1016/s0147-9571(02)00030-9
- de Menezes, T.C., Filho, J.B.S.F. & Countryman, A.M. (2023). Potential economic impacts of foot-and-mouth disease in Brazil: A case study for Mato Grosso and Paraná. *Journal of the Agricultural and Applied Economics Association*, 1-16. DOI: 10.1002/jaa2.73
- Di Giacomo, S., Bucafusco, D., Schammas, J.M., Pega, J., Miraglia, M.C., Barrionuevo, F., Capozzo, A.V. & Perez-Filgueira, D.M. (2022). Assessment on different vaccine formulation parameters in the protection against heterologous challenge with FMDV in Cattle. *Viruses*, 14(8): 1781. DOI: 10.3390%2Fv14081781
- Dillon, M.B. (2011). Skin as a potential source of infectious foot and mouth disease aerosols. *Proceedings: Biological Sciences*, 278(1713): 1761-1769. DOI: 10.1098%2Frspsb.2010.2430
- Ding, Y.Z., Chen, H.T., Zhang, J., Zhou, J.H., Ma, L.N., Zhang, L., Gu, Y. & Liu, Y.S. (2013). An overview of control strategy and diagnostic technology for foot-and-mouth disease in China. *Virology Journal*, 10(1): 78. DOI: 10.1186%2F1743-422X-10-78
- Dinku, S.Y. & Matsuda, T. (2018). Evaluating the impact of the bse and fmd outbreaks on meat demand: An engel curve analysis of japanese daily data. *Japanese Society of Agricultural Technology Management*, 25(1): 1-12. DOI: 10.20809/seisan.25.1_1
- Dong, H., Lu, Y., Zhang, Y., Mu, S., Wang, N., Du, P., Zhi, X., Wen, X., Wang, X., Sun, S., Zhang, Y. & Guo, H. (2021). A heat-induced mutation on VP1 of foot-and-mouth disease virus serotype o enhanced capsid stability and immunogenicity.

- Journal of Virology*, 95(16): e0017721. DOI: 10.1128/jvi.00177-21
- Dubie, T. & Negash, W. (2021). Seroprevalence of bovine foot and mouth disease (FMD) and its associated risk factors in selected districts of Afar region, Ethiopia. *Veterinary Medicine and Science*, 7(5): 1678-1687. DOI: 10.1002/vms3.574
- Eschbaumer, M., Vögtlin, A., Paton, D.J., Barnabei, J.L., Sanchez-Vazquez, M.J., Pituco, E.M., Rivera, A.M., O'Brien, D., Nfon, C., Brocchi, E., Kassimi, L.B., Lefebvre, D.J., López, R.N., Maradei, E., Duffy, S.J., Loitsch, A., De Clercq, K., King, D.P., Zientara, S., Griot, C. & Beer, M. (2020). Non-discriminatory exclusion testing as a tool for the early detection of foot-and-mouth disease incursions. *Frontiers in Veterinary Science*, 7(1): 552670. DOI: 10.3389/fvets.2020.552670
- Espinosa, R., Tago, D. & Treich, N. (2020). Infectious diseases and meat production. *Environmental and Resource Economics*, 76: 1019-1044. DOI: 10.1007/s10640-020-00484-3
- Fana, E.M., Mpoloka, S.W., Leteane, M., Seoke, L., Masoba, K., Mokopasetso, M., Rapharing, A., Kabelo, T., Made, P. & Hyera, J. (2021). A five-year retrospective study of foot-and-mouth disease outbreaks in Southern Africa, 2014 to 2018. *Veterinary Medicine International*, 2021(1): 7438809. DOI: 10.1155/2021/7438809
- Fountain, J., Woodgate, R., Rast, L. & Hernández-Jover, M. (2018). Assessing biosecurity risks for the introduction and spread of diseases among commercial sheep properties in New South Wales, Australia, using foot-and-mouth disease as a case study. *Frontiers in Veterinary Science*, 5(1): 80. DOI: 10.3389/fvets.2018.00080
- Gao, Y., Sun, S.Q. & Guo, H.C. (2016). Biological function of Foot-and-mouth disease virus non-structural proteins and non-coding elements. *Virology Journal*, 13(1): 107. DOI: 10.1186/s12985-016-0561-z
- Gordon, L.G., Porphyre, T., Muhanguzi, D., Muwonge, A., Boden, L. & Bronsvort, B.M.C. (2022). A scoping review of foot-and-mouth disease risk, based on spatial and spatio-temporal analysis of outbreaks in endemic settings. *Transboundary and Emerging Diseases*, 69(6): 3198-3215. DOI: 10.1111/tbed.14769
- Gornik, H.L., Persu, A., Adlam, D., Aparicio, L.S., Azizi, M., Boulanger, M., Bruno, R.M., de Leeuw, P., Fendrikova-Mahlay, N., Froehlich, J., Ganesh, S.K., Gray, B.H., Jamison, C., Januszewicz, A., Jeunemaitre, X., Kadian-Dodov, D., Kim, E.S., Kovacic, J.C., Mace, P., Morganti, A., Sharma, A., Southerland, A.M., Touzé, E., van der Niepen, P., Wang, J., Weinberg, I., Wilson, S., Olin, J.W. & Plouin, P.F. (2019). First international consensus on the diagnosis and management of fibromuscular dysplasia. *Vascular Medicine*, 24(2): 164-189. DOI: 10.1177/1358863x18821816
- Grubman, M.J. & Baxt, B. (2004). Foot-and-mouth disease. *Clinical Microbiology Reviews*, 17(2): 465-493. DOI: 10.1128/cmr.17.2.465-493.2004
- Guan, J., Chan, M., Grenier, C., Brooks, B.W., Spencer, J.L., Kranendonk, C., Coppes, J. & Clavijo, A. (2010). Degradation of foot-and-mouth disease virus during composting of infected pig carcasses. *Canadian Journal of Veterinary Research*, 74(1): 40-44.
- Guerrini, L., Pfukenyi, D.M., Etter, E., Bouyer, J., Njagu, C., Ndhlovu, F., Bourgarel, M., de Garine-Wichatitsky, M., Foggin, C., Grosbois, V. & Caron, A. (2019). Spatial and seasonal patterns of FMD primary outbreaks in cattle in Zimbabwe between 1931 and 2016. *Veterinary Research*, 50(1): 73. DOI: 10.1186/s13567-019-0690-7
- Hagerman, A.D., South, D.D., Sondgerath, T.C., Patyk, K.A., Sanson, R.L., Schumacher, R.S., Delgado, A.H. & Magzamen, S. (2018). Temporal and geographic distribution of weather conditions favorable to airborne spread of foot-and-mouth disease in the coterminous United States. *Preventive Veterinary Medicine*, 161(1): 41-49. DOI: 10.1016/j.prevetmed.2018.10.016
- Hammond, J.M., Maulidi, B. & Henning, N. (2021). Targeted FMD Vaccines for Eastern Africa: The AgResults foot and mouth disease vaccine challenge project. *Viruses*, 13(9): 1830. DOI: 10.3390%2Fv13091830
- Hegde, R., Gomes, A.R., Giridhar, P., Kowalli, S., Shivashankar, B.P., Sudharshana, K.J., Nagaraj, K., Sesharao, R., Mallinath, K.C., Shankar, B.P., Nagaraj, D., Seema, C.M., Khan, T.A., Nagaraj, G.V., Srikala, K., Dharanesh, N.K., Venkatesha, M.D. & Renukprasad, C. (2014). Epidemiology of foot and mouth disease in Karnataka state, India: a retrospective study. *Virusdisease*, 25(4): 504-509. DOI: 10.1007%2F13337-014-0239-3
- Jamal, S.M. & Belsham, G.J. (2013). Foot-and-mouth disease: past, present and future. *Veterinary Research*, 44(1): 116. DOI: 10.1186/1297-9716-44-116

- Jori, F., Hernandez-Jover, M., Magouras, I., Dürr, S. & Brookes, V.J. (2021). Wildlife–livestock interactions in animal production systems: what are the biosecurity and health implications? *Animal Frontiers*, 11: 8-19. DOI: 10.1093/af/vfab045
- Kitching, R.P. & Hughes, G.J. (2002). Clinical variation in foot and mouth disease: sheep and goats. *Revue Scientifique et Technique de*, 21(3): 505-512. DOI: 10.20506/rst.21.3.1342
- Knight-Jones, T.J.D., McLaws, M. & Rushton, J. (2017). Foot-and-Mouth disease impact on smallholders - what do we know, what don't we know and how can we find out more? *Transboundary and Emerging Diseases*, 64(4): 1079-1094. DOI: 10.1111/tbed.12507
- Kristensen, T., Belsham, G.J. & Tjørnehøj, K. (2021). Heat inactivation of foot-and-mouth disease virus, swine vesicular disease virus and classical swine fever virus when air-dried on plastic and glass surfaces. *Biosafety and Health*, 3(4): 217-223. DOI: 10.1016/j.bsheal.2021.07.002
- Lawrence, P., Pacheco, J.M., Uddowla, S., Hollister, J., Kotecha, A., Fry, E. & Rieder, E. (2013). Foot-and-mouth disease virus (FMDV) with a stable FLAG epitope in the VP1 G-H loop as a new tool for studying FMDV pathogenesis. *Virology*, 436(1): 150-161. DOI: 10.1016/j.virol.2012.11.001
- Li, K., Wang, C., Yang, F., Cao, W., Zhu, Z. & Zheng, H. (2021). Virus-Host Interactions in Foot-and-Mouth Disease Virus Infection. *Frontiers in Immunology*, 12(1): 571509. DOI: 10.3389/fimmu.2021.571509
- Limon, G., Ulziibat, G., Sandag, B., Dorj, S., Purevtseren, D., Khishgee, B., Basan, G., Bandi, T., Ruuragch, S., Bruce, M., Rushton, J., Beard, P.M. & Lyons, N.A. (2020). Socio-economic impact of foot-and-mouth disease outbreaks and control measures: An analysis of Mongolian outbreaks in 2017. *Transboundary and Emerging Diseases*, 1(1): 1-16. DOI: 10.1111/tbed.13547
- Longjam, N., Deb, R., Sarmah, A.K., Tayo, T., Awachat, V.B. & Saxena, V.K. (2011). A brief review on diagnosis of foot-and-mouth disease of livestock: Conventional to molecular tools. *Veterinary Medicine International*, 2011(1): 905768. DOI: 10.4061/2F2011%2F905768
- Ludi, A.B., Horton, D.L., Li, Y., Mahapatra, M., King, D.P., Knowles, N.J., Russell, C.A., Paton, D.J., Wood, J.L.N., Smith, D.J. & Hammond, J.M. (2014). Antigenic variation of foot-and-mouth disease virus serotype A. *Journal of General Virology*, 95(2): 384-392. DOI: 10.1099/2Fvir.0.057521-0
- Lyons, N.A., Alexander, N., Stärk, K.D., Dulu, T.D., Rushton, J. & Fine, P.E.M. (2015). Impact of foot-and-mouth disease on mastitis and culling on a large-scale dairy farm in Kenya. *Veterinary Research*, 46(1): 41. DOI: 10.1186/s13567-015-0173-4
- Ma, L.N., Zhang, J., Chen, H.T., Zhou, J.H., Ding, Y.Z. & Liu, Y.S. (2011). An overview on ELISA techniques for FMD. *Virology Journal*, 8(1): 419. DOI: 10.1186/1743-422x-8-419
- Mahmoud, M.A. & Galbat, S.A. (2017). Outbreak of foot and mouth disease and peste des petits ruminants in sheep flock imported for immediate slaughter in Riyadh. *Veterinary World*, 10(2): 238-243. DOI: 10.14202/vetworld.2017.238-243
- Malik, N., Kotecha, A., Gold, S., Asfor, A., Ren, J., Huiskonen, J.T., Tuthill, T.J., Fry, E.E. & Stuart, D.I. (2017). Structures of foot and mouth disease virus pentamers: Insight into capsid dissociation and unexpected pentamer reassociation. *PLoS Pathogens*, 13: e1006607. DOI: 10.1371/journal.ppat.1006607
- Marcos, A. & Perez, A.M. (2019). Quantitative risk assessment of foot-and-mouth disease (FMD) virus introduction into the fmd-free zone without vaccination of argentina through legal and illegal trade of bone-in beef and unvaccinated susceptible species. *Frontiers in Veterinary Science*, 6(1): 78. DOI: 10.3389/fvets.2019.00078
- Maree, F.F., Kasanga, C.J., Scott, K.A., Opperman, P.A., Melanie, C., Sangula, A.K., Raphael, S., Yona, S., Wambura, P.N., King, D.P., Paton, D.J. & Rweyemamu, M.M. (2014). Challenges and prospects for the control of foot-and-mouth disease: an African perspective. *Veterinary medicine (Auckland, N.Z.)*, 5: 119-138. DOI: 10.2147/2FVMRR.S62607
- Mielke, S.R. & Garabed, R. (2020). Environmental persistence of foot-and-mouth disease virus applied to endemic regions. *Transboundary and Emerging Diseases*, 67(2): 543-554. DOI: 10.1111/tbed.13383
- Mohebbi, M.R., Barani, S.M. & Mahravani, H. (2017). An uncommon clinical form of foot-and-mouth disease in beef cattle presented with corneal skin lesions. *Iranian Journal of Veterinary Research*, 18(4): 291-293.

- Moreno-Torres, K.I., Delgado, A.H., Branan, M.A., Yadav, S., Stenfeldt, C. & Arzt, J. (2022). Parameterization of the durations of phases of foot-and-mouth disease in pigs. *Preventive Veterinary Medicine*, 202(1): 105615. DOI: 10.1016/j.prevetmed.2022.105615
- Muleme, M., Barigye, R., Khaitsa, M.L., Berry, E., Wamono, A.W. & Ayebazibwe, C. (2013). Effectiveness of vaccines and vaccination programs for the control of foot-and-mouth disease in Uganda, 2001-2010. *Tropical Animal Health and Production*, 45(1): 35-43. DOI: 10.1007/s11250-012-0254-6
- Muroga, N., Hayama, Y., Yamamoto, T., Kurogi, A., Tsuda, T. & Tsutsui, T. (2012). The 2010 foot-and-mouth disease epidemic in Japan. *The Journal of Veterinary Medical Science*, 74(4): 399-404. DOI: 10.1292/jvms.11-0271
- Muthukrishnan, M., Balasubramanian, N.S. & Alwar, S.V. (2020). Experimental Infection of Foot and Mouth Disease in Indian Sheep and Goats. *Frontiers in Veterinary Science*, 7(1): 356. DOI: 10.3389/fvets.2020.00356
- Naranjo, J. & Cosivi, O. (2013). Elimination of foot-and-mouth disease in South America: lessons and challenges. *Philosophical Transactions of the Royal Society B*, 368(1623): 20120381. DOI: 10.1098/rstb.2012.0381
- Orsel, K. & Bouma, A. (2009). The effect of foot-and-mouth disease (FMD) vaccination on virus transmission and the significance for the field. *Canadian Veterinary Journal*, 50: 1059-1063.
- Park, J.H., Lee, K.N., Ko, Y.J., Kim, S.M., Lee, H.S., Shin, Y.K., Sohn, H.J., Park, J.Y., Yeh, J.Y., Lee, Y.H., Kim, M.J., Joo, Y.S., Yoon, H., Yoon, S.S., Cho, I.S. & Kim, B. (2013). Control of foot-and-mouth disease during 2010-2011 epidemic, South Korea. *Emerging Infectious Diseases*, 19(4): 655-659. DOI: 10.3201/eid1904.121320
- Park, S.Y., Jin, J.S., Kim, D., Kim, J.Y., Park, S.H., Park, J.H., Park, C.K. & Ko, Y.J. (2022). Development of Monoclonal Antibody to Specifically recognize VP0 but not VP4 and VP2 of foot-and-mouth disease virus. *Pathogens*, 11(12): 1493. DOI: 10.3390/pathogens11121493
- Paton, D.J., Gubbins, S. & King, D.P. (2018). Understanding the transmission of foot-and-mouth disease virus at different scales. *Current Opinion in Virology*, 28(1): 85-91. DOI: 10.1016/j.coviro.2017.11.013
- Paton, D.J., Di Nardo, A., Knowles, N.J., Wadsworth, J., Pituco, E.M., Cosivi, O., Rivera, A.M., Kassimi, L.B., Brocchi, E., de Clercq, K., Carrillo, C., Maree, F.F., Singh, R.K., Vosloo, W., Park, M.K., Sumption, K.J., Ludi, A.B. & King, D.P. (2021). The history of foot-and-mouth disease virus serotype C: the first known extinct serotype?, *Virus Evolution*, 7: veab009. DOI: 10.1093/ve/veab009
- Paton, D.J., Sumption, K.J. & Charleston, B. (2009). Options for control of foot-and-mouth disease: knowledge, capability and policy. *Philosophical Transactions of the Royal Society B*, 364(1530): 2657-2667. DOI: 10.1098/rstb.2009.0100
- Pattnaik, B., Subramaniam, S., Sanyal, A., Mohapatra, J.K., Dash, B.B., Ranjan, R. & Rout, M. (2012). Foot-and-mouth disease: Global status and future road map for control and prevention in India. *Agricultural Research*, 1: 132-147. DOI: 10.1007/978-11259-022-10010-z
- Perez, A.M. & Willeberg, P.W. (2017). Editorial: Foot-and-Mouth disease in Swine. *Frontiers in Veterinary Science*, 4: 133. DOI: 10.3389/fvets.2017.00133
- Prempeh, H., Smith, R. & Müller, B. (2001). Foot and mouth disease: the human consequences. The health consequences are slight, the economic ones huge. *BMJ*, 322(7286): 565-566. DOI: 10.1136/bmj.322.7286.565
- Rahman, A.K.M.A., Islam, S.K.S., Sufian, M.A., Talukder, M.H., Ward, M.P. & Martínez-López, B. (2020). Foot-and-Mouth disease space-time clusters and risk factors in Cattle and Buffalo in Bangladesh. *Pathogens*, 9(6): 423. DOI: 10.3390/pathogens9060423
- Railey, A.F. & Marsh, T.L. (2019). A Rational explanation of limited FMD vaccine uptake in endemic regions. *Pathogens*, 8(4): 181. DOI: 10.3390/pathogens8040181
- Ranaweera, L.T., Wijesundara, U.K., Jayarathne, H.S., Knowles, N., Wadsworth, J., Mioulet, V., Adikari, J., Weebadde, C. & Sooriyapathirana, S.S. (2019). Characterization of the FMDV-serotype-O isolates collected during 1962 and 1997 discloses new topotypes, CEY-1 and WCSA-1, and six new lineages. *Scientific Reports*, 9(1): 14526. DOI: 10.1038/s41598-019-51120-0
- Ranjan, R., Biswal, J.K., Subramaniam, S., Singh, K.P., Stenfeldt, C., Rodriguez, L.L., Pattnaik, B.

- & Arzt, J. (2016). Foot-and-Mouth disease virus-associated abortion and vertical transmission following acute infection in Cattle under natural conditions. *PLoS One*, 11(12): e0167163. DOI: 10.1371/journal.pone.0167163
- Rawdon, T.G., Garner, M.G., Sanson, R.L., Stevenson, M.A., Cook, C., Birch, C., Roche, S.E., Patyk, K.A., Forde-Folle, K.N., Dubé, C., Smylie, T. & Yu, Z.D. (2018). Evaluating vaccination strategies to control foot-and-mouth disease: a country comparison study. *Epidemiology and Infection*, 146(9): 1138-1150. DOI: 10.1017/S0950268818001243
- Rémond, M., Kaiser, C. & Lebreton, F. (2002). Diagnosis and screening of foot-and-mouth disease. *Comparative Immunology, Microbiology & Infectious Diseases*, 25(5-6): 309-320. DOI: 10.1016/S0147-9571(02)00028-0
- Rodríguez-Habibe, I., Celis-Giraldo, C., Patarroyo, M.E., Avendaño, C. & Patarroyo, M.A. (2020). A Comprehensive Review of the Immunological Response against Foot-and-Mouth Disease Virus Infection and Its Evasion Mechanisms. *Vaccines (Basel)*, 8(4): 764. DOI: 10.3390/Vvaccines8040764
- Shaban, A.K., Mohamed, R.H., Zakaria, A.M. & Baheeg, E.M. (2022). Detection of foot-and-mouth disease virus in raw milk in Menofia Governorate and its effect on reproductive hormones and physiochemical properties of milk. *Veterinary World*, 15(9): 2202-2209. DOI: 10.14202/Vvvetworld.2022.2202-2209
- Shmeiger, Z., Miculitzki, M., Gelman, B., Vaxman, I. & Goshen, T. (2021). The Effect of Foot and Mouth Disease Morbidity Influencing Periparturient Diseases and Culling on Nir Yitzhak Dairy Cattle Farm. *Israel Journal of Veterinary Medicine*, 76(1): 27-34.
- Shurbe, M., Simeon, B., Seyoum, W., Muluneh, A., Tora, E. & Abayneh, E. (2022). Seroprevalence and associated risk factors for foot and mouth disease virus seropositivity in cattle in selected districts of Gamo zone, Southern Ethiopia. *Frontiers in Veterinary Science*, 9: 931643. DOI: 10.3389/Vvfvets.2022.931643
- Singh, R.K., Sharma, G.K., Mahajan, S., Dhama, K., Basagoudanavar, S.H., Hosamani, M., Sreenivasa, B.P., Chaicumpa, W., Gupta, V.K. & Sanyal, A. (2019). Foot-and-Mouth disease virus: Immunobiology, advances in vaccines and vaccination strategies addressing vaccine failures-An Indian perspective. *Vaccines (Basel)*, 7(3): 90. DOI: 10.3390/Vvaccines7030090
- Stenfeldt, C., Eschbaumer, M., Rekant, S.I., Pacheco, J.M., Smoliga, G.R., Hartwig, E.J., Rodriguez, L.L. & Arzt, J. (2016a). The foot-and-mouth disease carrier state divergence in Cattle. *Journal of Virology*, 90(14): 6344-6364. DOI: 10.1128/jvi.00388-16
- Stenfeldt, C., Pacheco, J.M., Brito, B.P., Moreno-Torres, K.I., Branam, M.A., Delgado, A.H., Rodriguez, L.L. & Arzt, J. (2016b). Transmission of Foot-and-Mouth Disease Virus during the Incubation Period in Pigs. *Frontiers in Veterinary Science*, 3(1): 105. DOI: 10.3389/Vvfvets.2016.00105
- Stenfeldt, C., Pacheco, J.M., Singanallur, N.B., Vosloo, W., Rodriguez, L.L. & Arzt, J. (2019). Virulence beneath the fleece; a tale of foot-and-mouth disease virus pathogenesis in sheep. *PLoS One*, 14(1): e0227061. DOI: 10.1371/journal.pone.0227061
- Subramaniam, S., Mohapatra, J.K., Sahoo, N.R., Sahoo, A.P., Dahiya, S.S., Rout, M., Biswal, J.K., Ashok, K.S., Mallick, S., Ranjan, R., Jana, C. & Singh, R.P. (2022). Foot-and-mouth disease status in India during the second decade of the twenty-first century (2011-2020). *Veterinary Research Communications*, 46(4): 1011-1022. DOI: 10.1007/s11259-022-10010-z
- Suchowski, M., Eschbaumer, M., Teifke, J.P. & Ulrich, R. (2021). After nasopharyngeal infection, foot-and-mouth disease virus serotype A RNA is shed in bovine milk without associated mastitis. *Journal of Veterinary Diagnostic Investigation*, 33: 997-1001. DOI: 10.1177/10406387211022467
- Sutawi, Wahyudi, A., Malik, A., Suyatno, Hidayati, A., Rahayu, I.D. & Hartatie, E.S. (2023). Re-emergence of foot and mouth disease outbreak in Indonesia: A review. *Advances in Animal and Veterinary Sciences*, 11(2): 263-270. DOI: 10.17582/journal.aavs/2023/11.2.264.271
- Teifke, J.P., Breithaupt, A. & Haas, B. (2012). Foot-and-mouth disease and its differential diagnoses. *Tierärztliche Praxis Ausgabe G: Grosstiere – Nutztiere*, 40(4): 225-237.
- Tufani, N.A. (2013). Complications of foot and mouth disease in cattle and their clinical management. *Progress Research*, 8(1): 127-129.
- Valarcher, J.F., Leforban, Y., Rweyemamu, M., Roeder, P.L., Gerbier, G., Mackay, D.K., Sumption, K.J., Paton, D.J. & Knowles, N.J. (2008). Incursions of foot-and-mouth disease virus into Europe between 1985 and 2006.

- Transboundary and Emerging Diseases*, 55(1): 14-34. DOI: 10.1111/j.1865-1682.2007.01010.x
- van Vuren, P.J., Singanallur, N.B., Keck, H., Eschbaumer, M. & Vosloo, W. (2022). Chemical inactivation of foot-and-mouth disease virus in bovine tongue epithelium for safe transport and downstream processing. *Journal of Virological Methods*, 305(1): 114539. DOI: 10.1016/j.jviromet.2022.114539
- Walz, E., Evanson, J., Sampedro, F., VanderWaal, K. & Goldsmith, T. (2020). Planning "Plan B": the case of moving cattle from an infected feedlot premises during a hypothetical widespread fmd outbreak in the United States. *Frontiers in Veterinary Science*, 6(1): 484. DOI: 10.3389/fvets.2019.00484
- Wang, G., Wang, Y., Shang, Y., Zhang, Z. & Liu, X. (2015). How foot-and-mouth disease virus receptor mediates foot-and-mouth disease virus infection. *Virology Journal*, 12(1): 9. DOI: 10.1186%2Fs12985-015-0246-z
- Waters, R.A., Wadsworth, J., Mioulet, V., Shaw, A.E., Knowles, N.J., Abdollahi, D., Hassanzadeh, R., Sumption, K. & King, D.P. (2021). Foot-and-mouth disease virus infection in the domestic dog (*Canis lupus familiaris*), Iran. *BMC Veterinary Research*, 17(1): 63. DOI: 10.1186/s12917-021-02769-1
- Wekesa, S.N., Sangula, A.K., Belsham, G.J., Tjornehoj, K., Muwanika, V.B., Gakuya, F., Mijele, D. & Siegismund, H.R. (2015). Characterisation of recent foot-and-mouth disease viruses from African buffalo (*Syncerus caffer*) and cattle in Kenya is consistent with independent virus populations. *BMC Veterinary Research*, 11(1): 17. DOI: 10.1186/s12917-015-0333-9
- Woldemariyam, F.T., Kariuki, C.K., Kamau, J., De Vleeschauwer, A., De Clercq, K., Lefebvre, D.J. & Paeshuysse, J. (2023). Epidemiological dynamics of foot-and-mouth disease in the horn of Africa: The role of virus diversity and animal movement. *Viruses*, 15(4): 969. DOI: 10.3390/v15040969
- Wong, C.L., Yong, C.Y., Ong, H.K., Ho, K.L. & Tan, W.S. (2020). Advances in the diagnosis of foot-and-mouth disease. *Frontiers in Veterinary Science*, 7(1): 477. DOI: 10.3389/fvets.2020.00477
- Wubshet, A.K., Dai, J., Li, Q., & Zhang, J. (2019). Review on outbreak dynamics, the endemic serotypes, and diversified topotypic profiles of foot and mouth disease virus isolates in Ethiopia from 2008 to 2018. *Viruses*, 11(11): 1076. DOI: 10.3390/v11111076
- Yuan, H., Li, P., Ma, X., Lu, Z., Sun, P., Bai, X., Zhang, J., Bao, H., Cao, Y., Li, D., Fu, Y., Chen, Y., Bai, Q., Zhang, J. & Liu, Z. (2017). The pH stability of foot-and-mouth disease virus. *Virology Journal*, 14(1): 233. DOI: 10.1186/s12985-017-0897-z

The Gut Microbiomes of Wild Rodents within Forested Environments in Sarawak, Borneo

MUHAMMAD AMIN IMAN AZMI^{*1}, JULIUS WILLIAM-DEE¹, MUHD AMSYARI MORNI^{1,2},
NUR AFIQAH AQILAH AZHAR¹, NOR AL-SHUHADAH SABARUDIN¹, EMY RITTA
JINGGONG¹, SYAMZURAINI ZOLKAPLEY¹, CHENG-SIANG TAN³, FAISAL ALI ANWARALI
KHAN^{*1}

¹Faculty of Resource Science and Technology, Universiti Malaysia Sarawak, 94300, Kota Samarahan, Sarawak, Malaysia; ²Institute of Biodiversity and Environmental Conservation, Universiti Malaysia Sarawak, 94300, Kota Samarahan, Sarawak, Malaysia; ³Centre for Tropical and Emerging Diseases, Faculty of Medicine and Health Sciences, Universiti Malaysia Sarawak, 94300, Kota Samarahan, Sarawak, Malaysia

*Corresponding authors: muhdaminiman@gmail.com; akfali@unimas.my

Received: 1 August 2024

Accepted: 18 December 2024

Published: 31 December 2024

ABSTRACT

The gut microbiota of rodents is shaped by highly diverse bacterial communities. Within the gut environment, there are core gut bacteria that are responsible for facilitating essential bodily processes while maintaining the health of the host rodents. Currently, research on the gut microbiota of wild rodents in Borneo remains limited, especially those encompassing the potential influence of environmental factors. Through the Next-Generation Sequencing (NGS) performed using Oxford Nanopore Technologies, a total of 1052 bacterial genera were detected from 16 rodent individuals of six rodent species. These bacteria were found to be prevalent in the gut microbiota of wild rodents in forested regions. Several bacterial families of importance belonging to the phylum Bacillota were identified, including Lachnospiraceae (18%), Lactobacillaceae (20%) and Oscillospiraceae (19%). They were found to have a high relative abundance when compared with other bacterial families. The diversity of gut microbes among individual rodents showed no significant differences. However, the gut microbiome composition of wild rodents appears to have been influenced by the host species and their life stages. The outcome of this study allows for a better understanding of the prevailing core microbiome members shared across multiple wild rodent individuals within forested areas.

Keywords: Gut microbiota, Malaysia Borneo, Next-generation sequencing, rodent

Copyright: This is an open access article distributed under the terms of the CC-BY-NC-SA (Creative Commons Attribution-NonCommercial-ShareAlike 4.0 International License) which permits unrestricted use, distribution, and reproduction in any medium, for non-commercial purposes, provided the original work of the author(s) is properly cited.

INTRODUCTION

The gut microbiota of rodents is a complex ecosystem of microorganisms inhabiting their gastrointestinal tracts. It comprises high bacterial diversity, collectively forming a dynamic and intricate community (Coyte & Rakoff-Nahoum, 2019). The gut bacterial community plays a crucial role in maintaining the health of the host by facilitating essential processes such as digestion, nutrient absorption, colonisation resistance and immune system regulation (Kinross *et al.*, 2011; Valdes *et al.*, 2018; Hou *et al.*, 2022). The gut microbiome may potentially influence wildlife behaviour through chemical signalling and impacts on the host nervous system (Archie & Tung, 2015). Hence, the symbiotic relationship between these microorganisms and their host allows the formation of a stable bacterial community,

comprising of gut microbiota that contribute to the various physiological processes of wild rodents.

The core gut microbiota refers to the bacteria that would define the overall microbiome composition of the host (Risely, 2020; Perlman *et al.*, 2022; Sharon *et al.*, 2022). These microbes could be essential in sustaining the overall gut microbial community while ensuring host survival. However, identifying keystone taxa that help shape the ecological structure of the gut microbiome is difficult, as highlighted by Perlman *et al.* (2022). Instead, a more suitable approach would be to determine recurring microbiome members in multiple individual hosts to gain an understanding of their significance. The concurrent bacterial taxa found across different individuals, even in an otherwise variable microbial community, could

presumably be considered members of the core gut microbiome (Turnbaugh *et al.*, 2007).

The gut microbiome diversity of rodents could exhibit variation among different host individuals (Viney, 2019). This diversity is shaped by a combination of host genetics and environmental factors (Campbell *et al.*, 2012), and studies have demonstrated that seasonal changes in rodents' diet can lead to short-term shifts in their gut microbial communities (Maurice *et al.*, 2015). Furthermore, the ageing process of rodents was found to significantly alter the composition and diversity of their gut microbiome in the long-term (Fenn *et al.*, 2023). Despite these insights, the specific environmental factors directly influencing gut microbiome diversity in rodents are still not well understood. Environmental factors that are distinct to the rodents' natural habitat could play a role in shaping their gut microbiome composition (Teng *et al.*, 2022).

The characterisation of the gut microbiome within wild rodents would contribute to a better understanding on the intricate relationships between the bacterial community and their rodent hosts. Currently, research on the gut microbiota of wild rodents in Malaysia remains limited, especially those encompassing the potential influence of environmental factors. Recent studies have instead focused on gut

microbiome studies of other endangered mammals such as flying foxes (Mohd-Yusof *et al.*, 2022), tigers (Khairulmunir *et al.*, 2023; Gani *et al.*, 2024) and primates (Jose, *et al.*, 2024; Sariyati *et al.*, 2024). Thus, the main objectives of this study are to taxonomically identify the gut microbiome of wild rodents and to determine the potential environmental factors that could shape their gut microbial diversity.

MATERIALS AND METHODS

Study Sites

The study sites consist of multiple mixed dipterocarp forested areas situated in both protected and non-protected regions of Sarawak, Borneo (Figure 1). The chosen locations host a variety of native forest rodent species, adapted to their respective habitats within the study sites. Among the protected areas are Gunung Gading National Park (N1°41'27.0" E109°50'45.0") and Lambir Hills National Park (N4°11'57.5" E114°02'34.3"), while Marup Atas Engkilili (N1°07'08.3" E111°38'15.8"), Ulu Poi Kanowit (N1°57'09.9" E112°13'23.0"), and Sungai Sibau Kapit (N2°00'02.7" E112°56'16.4") represent the non-protected areas (Supplementary Table 2). Rodent trapping was carried out from October 2021 to March 2023.

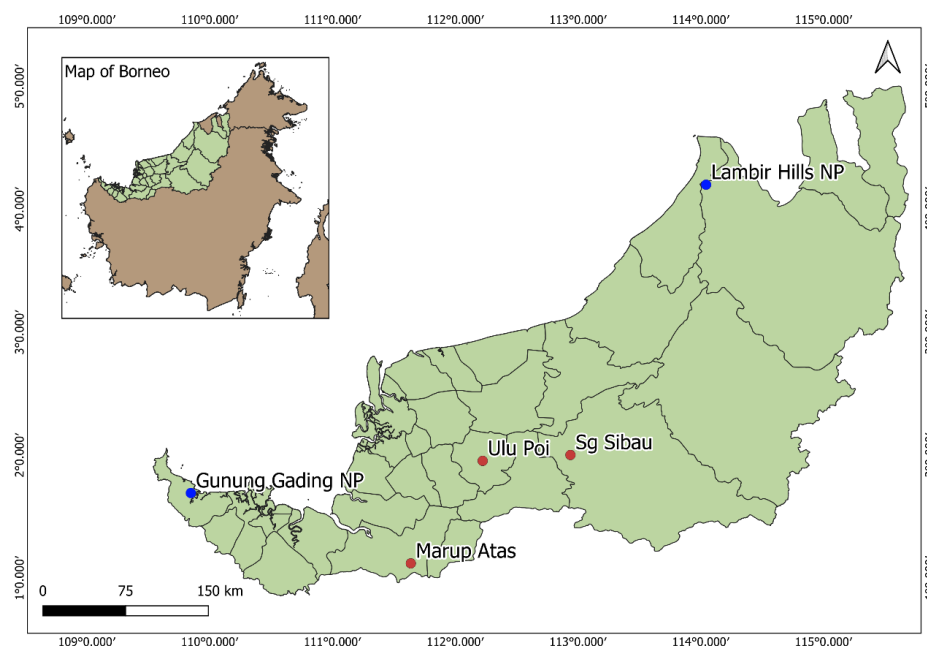


Figure 1. Map of sampling sites in Sarawak, highlighted in green (QGIS v3.21). Non-protected areas are marked with red dots while protected areas are marked as blue

Sampling Methods

Each sampling site involved five nights of trapping, with a total of 50 cage traps and 120 Sherman traps being used for the rodent trapping. The same traps were deployed at each site and sanitised beforehand using 70% ethanol to kill microorganisms and bleach to degrade the DNA of previously trapped rodents. The traps were baited with banana covered with peanut butter. The traps were checked from 0900 hours to 1200 hours, as well as from 1400 hours to 1700 hours, with bait replacement occurring every two days. Morphological measurements of the captured rodents, including head body, tail ventral, ear, hindfoot, sex, weight and life stages, were also recorded. Then, the rodents were transferred to separate sterilised breathable containers to avoid cross contamination during faecal collection. The rodents were identified in the field using descriptions and keys from Payne *et al.* (1985) and Phillipps and Phillipps (2018). Molecular methods were later used to confirm the species identification due to the presence of several cryptic species. Fresh faecal samples were collected using sterile forceps as soon as the rodents defecate in the sterilised containers. The faecal samples of each captured rodent were transferred to sterilised 1.5 ml collection tube containing RNAlater (Ambion, USA) using sterilised forceps. The collection tubes containing faecal samples were immediately stored in a cooler box. Upon arrival at the laboratory, the sample was promptly transferred to a -20 °C freezer for DNA preservation and stability.

DNA Extraction and Molecular Species Identification

A QIAmp PowerFecal Pro DNA Kit (Qiagen, Germany) was used according to the manufacturer's protocol to extract the DNA from collected rodent faecal samples. The extracted DNA was amplified through polymerase chain reaction (PCR), targeting the cytochrome *b* region of the mtDNA. The primer set used were LGL 765 (5'-GAA AAA CCA YCG TTG TWA TTC AAC T-3') and LGL 766 (5'-GTT TAA TTA GAA TYT YAG CTT TGG G-3') (Bickham *et al.*, 1995). The PCR conditions were: pre-denaturation at 94 °C for 7 minutes, 34 cycles of: denaturation at 92 °C for 1 minute, annealing at 50 °C for 1 minute and extension at 72 °C for 1 minute, followed by 72

°C final extension for 7 minutes. The PCR products were sent to a commercial sequencing company for purification and sequencing (Apical Scientific, Malaysia). Sequencher 4.1.4 (Gene Code, USA) was then used to clean the obtained DNA sequences and the NCBI Basic Local Alignment Search Tool (BLAST) was used for species identification based on the lowest E-values of the uploaded sequences. The lower E-values indicate high degree of similarity between sequences defined by many identical residues and few substitutions or gaps (Kerfeld & Scott, 2011). Finally, the DNA sequences, along with sequences from GenBank were analysed in MEGA-X 10.2.4 software to generate a Maximum-Likelihood phylogenetic tree and calculate the pairwise genetic distance between rodent individuals subjected to Kimura two-parameter model (Kimura, 1980). The sequences of the sampled rodents were submitted to the GenBank and Sequence Read Archive databases (Supplementary Table 3).

Next-Generation Sequencing

A DeNovix DS-11 Spectrophotometer (Denovix, Delaware, USA) was used for quantification of the extracted faecal DNA as preparation for nanopore sequencing. DNA with a concentration above 20 µg/ml and a purity ratio between 1.8 and 2.0 at 260 nm and 280 nm absorbance are considered to have passed the quality check. The PCR amplification of 16S rRNA gene (27F and 1482R) were done using 16S Barcoding Kit (SQK-RAB204) from Oxford Nanopore Technologies, United Kingdom (ONT). The quality of PCR products were checked and only passed products (concentration above 20 µg/ml; absorbance ratio between 1.8 and 2.0 at 260/280 ratio) proceeded to sample pooling and library preparation following the manufacturer's protocol (ONT). The Flow Cell Priming Kit (EXP-FLP002) was then used to prime the flow cell (R9.4.1) and load the samples. Lastly, a MinION Mk1C sequencer (ONT) was used to perform nanopore sequencing for around 17 hours for each sequencing run.

Data Analysis

FASTQ files of the 16S rRNA sequences were obtained using Guppy 5.1.12 (ONT), which is the basecaller integrated in the MinKNOW 21.11.6 (ONT) operating system. The EPI2ME

(ONT) application was used to perform taxonomic classification of bacterial species according to the National Center for Biotechnology Information (NCBI) taxonomic records at 95% confidence threshold. Reads below the threshold of the default quality score of 7 were excluded. The range of the library sizes was between ~25,000 and ~1,300,000 reads. The R package phyloseq (McMurdie & Holmes, 2013) was used to normalise the dataset to the library with the lowest number of reads for further analysis using the rarefying method. The gut microbiome of rodents was visualised using the MiscMetabar package (Taudière, 2023) to produce a Sankey chart. Also, the ggplot2 package (Wickham, 2011) was used to produce an abundance graph of bacterial genera for each rodent individual. Alpha diversity was estimated using the Shannon index and plots of diversity indices were done using the phyloseq package (McMurdie & Holmes, 2013).

RESULTS

A total of 16 rodent individuals (15 adult; 1 juvenile) belonging to six different species from various study sites were used in this study (Table 1). Among the sites, Sungai Sibau Kapit had the highest number of rodent captures, with a total of five individuals. For the lowest number of sampled rodents, Gunung Gading National Park and Lambir Hills National Park recorded only two individuals each. Furthermore, Sungai Sibau Kapit had the highest diversity as four species were caught during rodent sampling. In contrast, Gunung Gading National Park recorded just one species. The phylogenetic tree and genetic distances between rodent's species (K2P)

confirm the species identification of the wild rodents (Table 2; Figure 2).

The combined gut microbiome of all rodent individuals was distinguished at different taxonomic levels (Figure 3). After filtering, the average read length of all sequences of bacteria were around 1,500 bp. Overall, the most abundant phylum across all rodent species is Bacillota (formerly Firmicutes) which represents around 78% of the total abundance. The three most dominant bacterial families belong to this phylum, which includes Lachnospiraceae (18%), Lactobacillaceae (20%) and Oscillospiraceae (19%). At the genus level, a total of 1052 bacterial genera were detected, with the most abundant consisting of *Ruminococcus* (12.2%), *Ligilactobacillus* (8.9%), and *Lactobacillus* (7.2%) (Table 3). Comparing each rodent individual, their gut microbiome composition did not adhere to a strict pattern (Figure 4). The relative abundance of these predominant genera differs from each rodent individual. In particular, one juvenile rodent individual from Lambir Hills National Park (L1) had genus *Ligilactobacillus* (77.8%) as the most dominant genus.

The estimated alpha diversity, based on the Shannon diversity index values, displayed variation among the gut microbiomes of all rodent individuals, ranging from 2.2 in Lambir Hills National Park to 5.0 in Sungai Sibau Kapit (Figure 5). Non-parametric Kruskal-Wallis test was used to assess the differences between alpha diversity according to each study site and revealed these differences were not significant ($p < 0.05$).

Table 1. Number of individuals of rodent species from Gunung Gading National Park (GGNP), Lambir Hills National Park (LHNP), Marup Atas Engkilili (MAE), Sungai Sibau Kapit (SSK) and Ulu Poi Kanowit (UPK)

Rodent Species	GGNP	LHNP	MAE	SSK	UPK
<i>Maxomys surifer</i>	0	0	0	1	0
<i>Maxomys tajuddini</i>	0	0	2	1	1
<i>Maxomys whiteheadi</i>	2	0	1	0	0
<i>Niviventer cremoriventer</i>	0	1	1	2	1
<i>Rattus tanezumi</i>	0	0	0	0	1
<i>Sundamys muelleri</i>	0	1	0	1	0
Total	2	2	4	5	3

Table 2. Average percentage of K2P genetic distance values among rodent species based on cytochrome *b* gene

No.	Rodent Species	1	2	3	4	5	6
1	<i>Maxomys surifer</i>	-					
2	<i>Maxomys tajuddini</i>	14.5	-				
3	<i>Maxomys whiteheadi</i>	12.6	9.7	-			
4	<i>Niviventer cremoriventer</i>	16.6	16.3	15.9	-		
5	<i>Rattus tanezumi</i>	16.5	17.3	16.5	16.2	-	
6	<i>Sundamys muelleri</i>	17.8	18.0	17.0	17.2	15.9	-

Table 3. Relative abundance table in percentages of the top 23 most abundant bacterial genera (>1% overall relative abundance) according to rodent species

Bacterial Genera	<i>Maxomys surifer</i> (n=1)	<i>Maxomys tajuddini</i> (n=4)	<i>Maxomys whiteheadi</i> (n=3)	<i>Niviventer cremoriventer</i> (n=5)	<i>Rattus tanezumi</i> (n=1)	<i>Sundamys muelleri</i> (n=2)	Overall
<i>Ruminococcus</i>	9.69	5.68-26.8	2.59-12.5	0.76-14.2	5.54	22.5-40.4	12.2
<i>Ligilactobacillus</i>	0.26	0.03-0.12	0.06-0.10	0.03-77.8	0.38	0.03-0.09	8.93
<i>Lactobacillus</i>	11.61	3.64-9.17	11.6-25.5	0.03-1.49	4.66	1.00-8.11	7.19
<i>Blautia</i>	5.37	1.91-8.80	0.97-5.49	0.45-11.38	3.62	1.93-3.59	4.07
<i>Lachnospirillum</i>	5.87	2.91-12.1	1.27-3.97	0.41-7.80	2.96	1.87-2.59	3.68
<i>Flintibacter</i>	3.12	1.82-5.28	0.66-2.76	0.24-2.80	6.22	3.24-4.80	2.80
<i>Limosilactobacillus</i>	1.59	0.75-5.46	2.10-4.04	0.03-4.33	6.12	1.11-3.42	2.62
<i>Flavonifractor</i>	2.18	2.40-3.48	1.31-3.00	0.22-4.00	4.82	2.43-3.79	2.52
<i>Clostridium</i>	3.57	1.09-3.05	1.09-6.40	0.34-3.03	1.90	1.11-2.11	2.19
<i>Duncaniella</i>	1.90	0.64-2.13	2.45-3.81	0.39-5.74	4.77	0.56-0.91	2.04
<i>Klebsiella</i>	0.06	0.38-3.35	1.00-7.38	0.07-11.9	0.09	0.06	1.89
<i>Anaerostipes</i>	0.96	1.41-4.21	0.55-1.34	0.26-6.39	1.55	1.37-2.31	1.72
<i>Muribaculum</i>	1.61	0.52-1.89	2.17-3.32	0.34-4.53	3.30	0.33-0.54	1.70
<i>Prevotella</i>	0.68	0.37-2.80	0.83-4.52	0.06-2.80	3.38	1.54-2.72	1.59
<i>Romboutsia</i>	4.85	0.02-4.06	0.02-11.1	0.01-1.65	0.13	0.03-0.14	1.49
<i>Lacrimispora</i>	1.03	0.92-3.13	0.20-1.45	0.40-2.82	1.53	1.10-3.40	1.48
<i>Escherichia</i>	0.31	0.29-3.13	0.84-1.71	0.13-3.73	0.18	0.16-0.27	1.43
<i>Intestinimonas</i>	2.26	1.01-2.23	0.52-2.35	0.10-1.44	1.85	1.82-1.86	1.35
<i>Lachnospira</i>	0.82	0.21-3.42	0.07-0.29	0.06-3.98	0.77	0.63-1.39	1.16
<i>Phascolarctobacterium</i>	0.74	0.00-3.59	0.00-5.61	0.00-0.17	0.00	0.69-2.25	1.08
<i>Bacillus</i>	1.06	0.79-1.28	0.82-1.08	0.98-1.55	1.11	0.61-1.03	1.07
<i>Bacteroides</i>	1.92	0.25-2.63	0.87-3.62	0.28-0.94	1.02	0.38-0.61	1.06
<i>Anaerobutyricum</i>	0.52	0.53-3.47	0.14-0.87	0.12-2.69	1.18	0.64-1.26	1.00

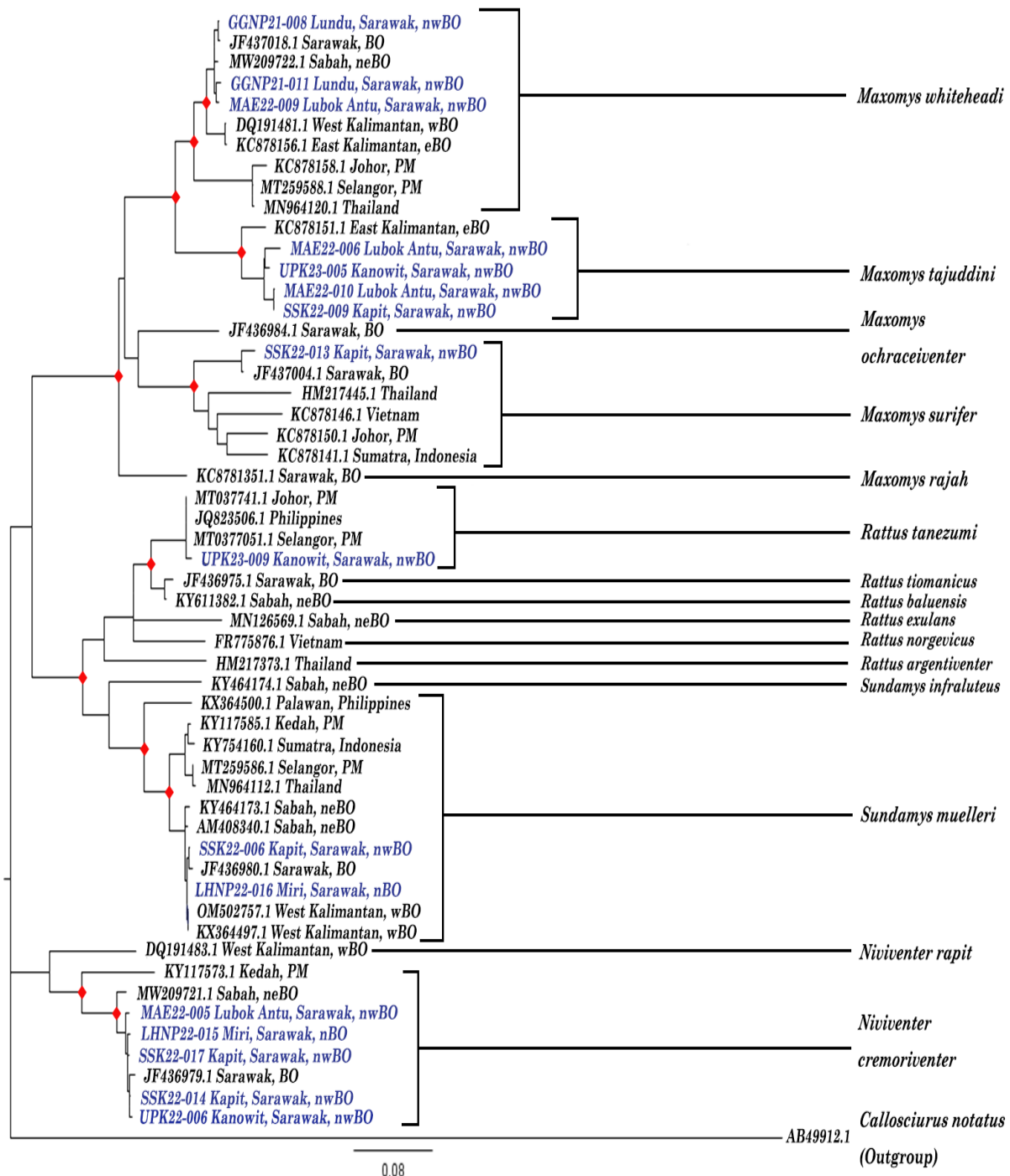


Figure 2. Maximum-Likelihood phylogenetic tree of sequenced rodent individuals highlighted in blue font. Red diamonds indicate nodes with bootstrap values >90. (PM = Peninsular Malaysia, BO = Borneo, nBO = North Borneo, nwBO = Northwest Borneo, neBO = Northeast Borneo, wBO = West Borneo, eBO = East Borneo)

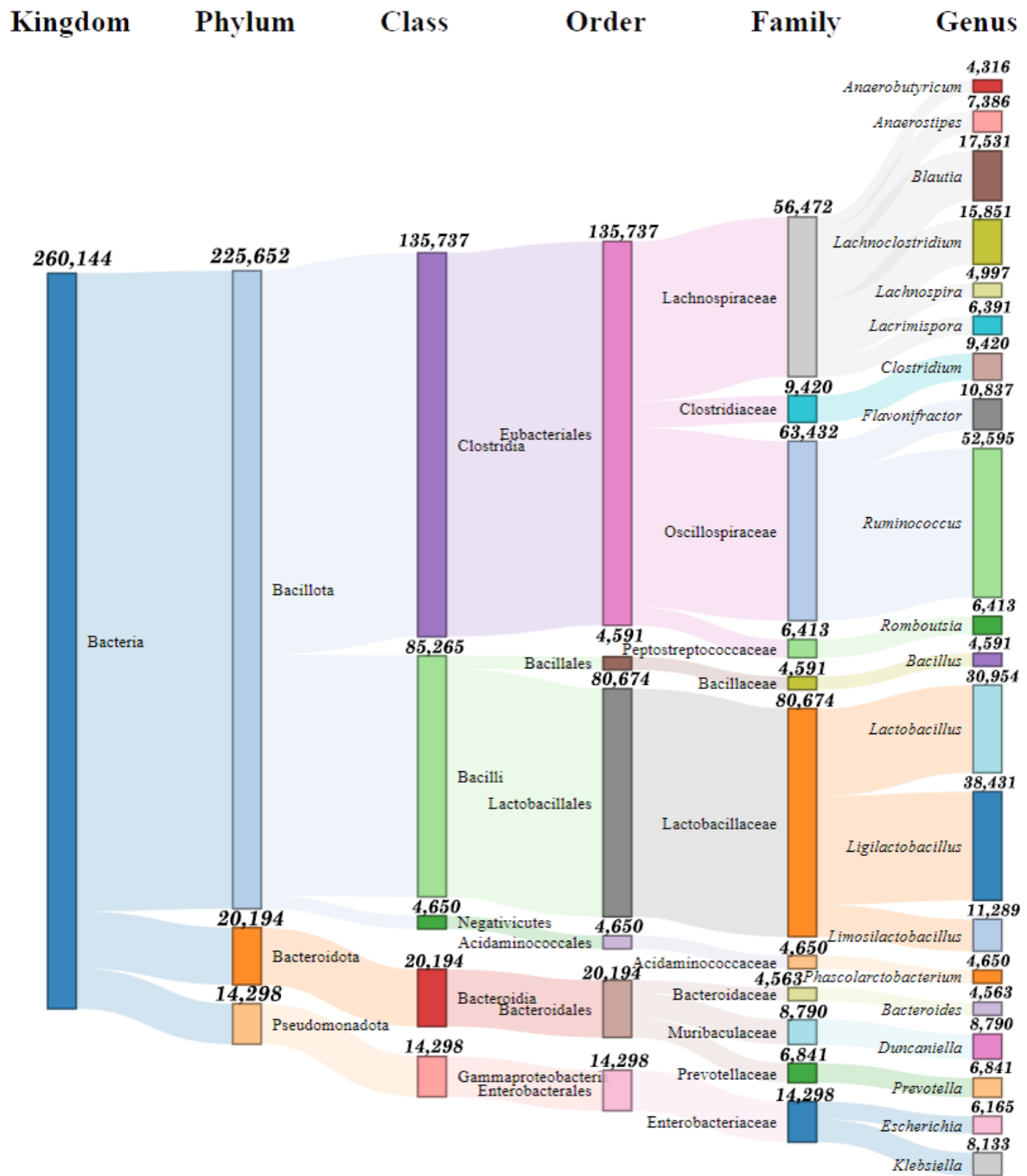


Figure 3. Sankey chart of combined gut microbiome composition of all rodent individuals (n = 16) according to different taxa levels. Only bacterial genera with relative abundance of >1% were shown. Number above nodes indicate the number of reads assigned for each taxon

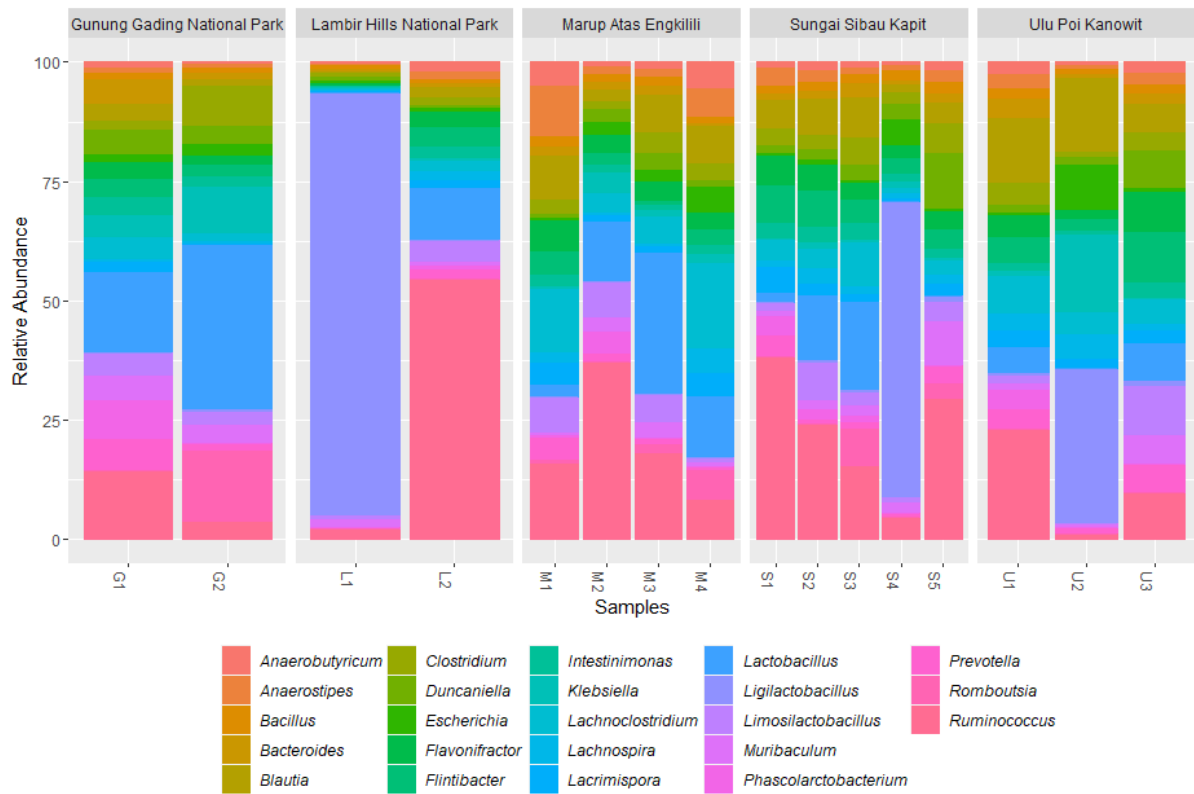


Figure 4. Abundance bar plots of the top 23 most abundant bacterial genera from rodent individuals across different localities. The top 23 genera were selected as they represent >1% of the relative abundance of the total bacterial abundance. Abbreviations of samples follow Supplementary Table 1

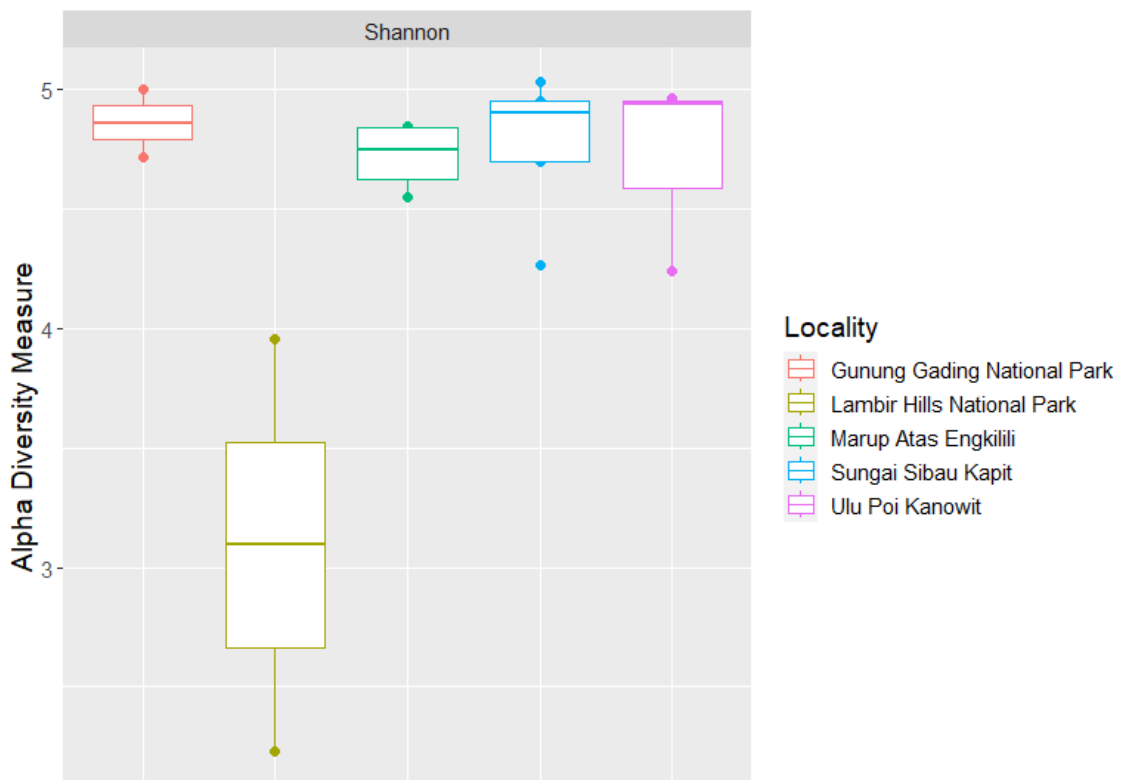


Figure 5. Box plot of Shannon diversity index of the gut microbiome of rodent individuals across different study sites

DISCUSSION

The gut microbiomes across different rodent individuals have shown patterns of variation, indicating the presence of distinct bacterial communities. Various factors, including dietary preferences, host genetics, and environmental exposures, have been reported to contribute to the observed heterogeneity (Campbell *et al.*, 2012; Maurice *et al.*, 2015). However, a consistent finding throughout all these microbiomes is the dominance of the Bacillota phylum. Similarly, recent studies have identified Bacillota, previously recognised as Firmicutes, as one of the most abundant bacterial phyla within the gut microbiota of wild rodents (Weldon *et al.*, 2015; Jahan *et al.*, 2021). These microbes are commonly found within the mammalian gut microbiota, contributing to the regulation of the host's immune system and the development of the gut epithelium (Leser & Mølbak, 2009).

One of the most abundant bacterial family observed in the gut microbiota of rodents was Oscillospiraceae. This family is also recognised as Ruminococcaceae, which is considered as a heterotypic synonym to Oscillospiraceae (Euzéby, 2010). Members of this bacterial family, alongside Lachnospiraceae, are common in the gut environment and plays a vital role in digestion and nutrient absorption. They were found to be specialised for degrading complex plant material through enzymatic activities (Biddle *et al.*, 2013). The genus *Ruminococcus*, belonging to the family Oscillospiraceae, is the most abundant genus observed across all rodent individuals. Studies have shown that *Ruminococcus* is a constituent of the rodent core gut bacteria based on their significant abundance (Wang *et al.*, 2019). The high prevalence of this bacteria observed in wild rodents could have potential importance to their feeding behaviours (e.g., Kohl *et al.*, 2022). Forest rodents in Borneo have very specialised diets and lifestyles (Phillipps & Phillipps, 2018). Since most of the rodent species found in this study typically inhabit forested areas, the presence of *Ruminococcus* may suggest that the readily abundant vegetation leads them to consume a substantial amount of plant material.

Lachnospiraceae is also a prominent bacterial family and is represented by multiple genera at varying abundances. Among these, the genus

Blautia was observed as the most highly present genus. Liu *et al.* (2021) have highlighted the nutritional benefits of some *Blautia* species for their probiotic properties in mammals. However, they have also stated that further research is required due to the lack of comprehensive review concerning this genus. Although it was observed at relatively low abundance, another noteworthy bacterial genus within the same Lachnospiraceae family is *Anaerobutyricum*. Similar to *Blautia*, certain strains of *Anaerobutyricum* could potentially serve as probiotics, and recent studies have undergone preclinical testing in mice models for medical use (Wortelboer *et al.*, 2022). The presence of various Lachnospiraceae members within the gut microbiota suggests their pivotal role as a component of the bacterial community, and further research on the significance of this family could contribute to advancements in wildlife and humans in general.

Another dominant bacterial family is Lactobacillaceae which recorded the highest abundance for the overall combined gut microbiome of wild rodents. This family represents the lactic acid bacteria that are responsible for metabolising lactose within the gut environment (König & Fröhlich, 2017). This includes the genus *Lactobacillus* which were found to be significantly higher in reproductively active wild female rodents (Maurice *et al.*, 2015). Notably, the gut microbiota of a juvenile *Niviventer cremoriventer* individual from Lambir Hills National Park was observed to be predominantly *Ligilactobacillus*, another genus from the family Lactobacillaceae that was formerly known as the *Lactobacillus salivarius* group (Zheng *et al.*, 2020). It is possible that *Ligilactobacillus* could share similar properties with *Lactobacillus* as lactic acid bacteria. The relative abundance of *Ligilactobacillus* in the other adult *N. cremoriventer* individuals were noticeably lower (0% to 39.8%) than the juvenile individual (77.8%). The prevalence of this genus in the gut of the young rodent could imply its significance during infancy, potentially contributing to the digestion of maternal milk.

Several potentially pathogenic bacterial genera were detected at low abundance in multiple rodent individuals from various localities. This includes *Bacillus*, *Bacteroides*, *Clostridium*, and *Escherichia*. Certain species

from these genera are considered pathogenic to humans as they can cause illnesses and can be transmitted to both humans and animals through multiple pathways (e.g., direct contact with infected animals or ingestion of contaminated food or water) (Wexler, 2007; Erickson, 2016; Carlson *et al.*, 2019; Fagre *et al.*, 2022). While the combined abundance of these bacteria is lower than that of the other bacterial taxa, their prevalence in all wild rodent individuals indicates the potential existence of a commensal relationship between them. These bacteria may possess the capability to coexist within the established bacterial community in the rodent gut microbiota, capitalising on the nutrient-rich environment derived from the gut microbiota (Bäumler & Sperandio, 2016). Nevertheless, rodents are recognised as reservoir hosts for pathogenic bacteria, and conducting specific analyses that emphasise the prevalence of pathogenic bacteria occurring at low abundances could lead to a better understanding of their transmission dynamics.

The interactions between specific environmental factors and the composition of the wild rodent gut microbiome remains largely unknown. Shifting the focus towards the dietary behaviours and the vegetation composition of the natural habitat would help determine the factors that contribute to the variations in the gut microbial communities within mammals (e.g., Fan *et al.*, 2022). However, it is apparent that the host rodent species plays a substantial role in shaping their gut microbiota. For instance, in *Maxomys* species, *Lactobacillus* is one of the most dominant taxa with a relative abundance ranging from 3.64% to 25.50%. In contrast, for other rodent genera (*Niviventer*, *Sundamys* and *Rattus*), the relative abundance of *Lactobacillus* falls between 0.03% to 8.11%. Anders *et al.* (2021) reported similar findings, noting clear differences in the gut microbiome compositions among three wild rodent species (*Apodemus speciosus*, *A. argenteus* and *Myodes rufocanus*). The monophyletic relationship among *Maxomys* individuals implies that the phylogenetic similarity of rodent species may reflect their gut microbiome composition. According to Wang *et al.* (2022), gut microbiota among individuals of the same species from two distant locations are more similar, compared to individuals of closely related species within the same geographical area. However, the habitats are similar overall, with the main differences being in annual

temperature and precipitation. Nevertheless, due to the higher number of rodent individuals within genus *Maxomys*, this assumption needs to be treated with caution. On the other hand, the life stage of the rodents seems to affect their gut microbiota based on the observed low alpha diversity exhibited by the juvenile *N. cremoriventer* individual from Lambir Hills National Park. As highlighted by Fenn *et al.* (2023), microbiome alpha diversity increases with age for wild rodents as there is a positive shift in species richness. This pattern might arise due to the incomplete development of the bacterial community within the gut environment of young rodents.

The characterisation of the combined core gut microbiota in this study may not accurately reflect the microbiome composition of distinct rodent species. Given the non-invasive nature of faecal sampling, it is recommended to obtain a larger sample size that encompasses a diverse range of wild rodent species and accounts for different life stages. This approach would yield a more comprehensive understanding on the dynamics of the host-specific core gut microbiome, especially with an increased number of representatives for each species. Furthermore, including more localities with distinct habitat types and incorporating additional environmental data into the characterisation of the rodents' gut microbiome would provide insights into the constituents that influence the structure of the bacterial community (e.g., Lobato-Bailón *et al.*, 2023). Determining the effects of distinct habitats on the rodent gut microbiome could have significant implications for zoonotic disease risks, as certain environmental factors may potentially influence pathogenic bacteria transmission.

CONCLUSION

This study effectively characterises the gut microbiome of multiple wild rodents inhabiting forested areas in Sarawak, Borneo as bacteria with high relative abundance hold potential as core constituents of the rodent gut microbiome. Furthermore, it appears that the gut microbiome composition of wild rodents is influenced by the host rodent species and their life stages, as evidenced by the abundance patterns of certain bacterial taxa.

ACKNOWLEDGEMENTS

The authors sincerely thank Sarawak Research and Development Council for their funding and support (GL/F07/SRDC/05/2021; RDCRG02/CAT/2020/_33), and Sarawak Forestry Corporation for the permission to conduct our work in Sarawak (Permit No. SFC.810-4/6/1 (2021) and Park Permit No. WL 21/2021). We also thank Faculty of Resource Science and Technology at Universiti Malaysia Sarawak (UNIMAS) and its staff for assisting in logistics and laboratory support. UNIMAS also supported some of the authors through the Zamalah Graduate Scholarship and Postgraduate Research Grant (F07/PGRG/2046/2020). Lastly, we are thankful for FAAK lab members for their cooperation and commitment during the sampling process for this study. The substance of this manuscript was submitted by MAIA to the Faculty of Resource Science and Technology, Universiti Malaysia Sarawak as partial fulfilment of the M.Sc. degree in Zoology.

REFERENCES

- Anders, J.L., Moustafa, M.A.M., Mohamed, W.M.A., Hayakawa, T., Nakao, R., & Koizumi, I. (2021). Comparing the gut microbiome along the gastrointestinal tract of three sympatric species of wild rodents. *Scientific Reports*, 11(1), 19929. DOI:10.1038/s41598-021-99379-6
- Archie, E.A., & Tung, J. (2015). Social behavior and the microbiome. *Current Opinion in Behavioral Sciences*, 6: 28-34. DOI: 10.1016/j.cobeha.2015.07.008
- Bäumler, A.J., & Sperandio, V. (2016). Interactions between the microbiota and pathogenic bacteria in the gut. *Nature*, 535(7610): 85-93. DOI:10.1038/nature18849
- Bickham, J.W., Wood, C.C., & Patton, J.C. (1995). Biogeographic implications of cytochrome b sequences and allozymes in sockeye (*Oncorhynchus nerka*). *Journal of Heredity*, 86(2): 140-144. DOI:10.1093/oxfordjournals.jhered.a111544
- Biddle, A., Stewart, L., Blanchard, J., & Leschine, S. (2013). Untangling the genetic basis of fibrolytic specialization by Lachnospiraceae and Ruminococcaceae in diverse gut communities. *Diversity*, 5(3): 627-640. DOI:10.3390/d5030627
- Campbell, J.H., Foster, C.M., Vishnivetskaya, T., Campbell, A.G., Yang, Z.K., Wymore, A., Palumbo, A.V., Chesler, E.J., & Podar, M. (2012). Host genetic and environmental effects on mouse intestinal microbiota. *The ISME Journal*, 6(11): 2033-2044. DOI:10.1038/ismej.2012.54
- Carlson, C.J., Kracalik, I.T., Ross, N., Alexander, K.A., Hugh-Jones, M.E., Fegan, M., Elkin B.T., Epp, T., Shury, T.K., Zhang, W., Bagirova, M., Getz, W.M., & Blackburn, J.K. (2019). The global distribution of *Bacillus anthracis* and associated anthrax risk to humans, livestock and wildlife. *Nature Microbiology*, 4(8), 1337-1343. DOI:10.1038/s41564-019-0435-4
- Coyte, K.Z., & Rakoff-Nahoum, S. (2019). Understanding competition and cooperation within the mammalian gut microbiome. *Current Biology*, 29(11): R538-R544. DOI:10.1016/j.cub.2019.04.017
- Erickson, M.C. (2016). Overview: Foodborne pathogens in wildlife populations. In: Jay-Russell, M., & Doyle, M.P. (eds.), *Food Safety Risks from Wildlife: Challenges in Agriculture, Conservation, and Public Health*. Cham: Springer. pp. 1-30. DOI:10.1007/978-3-319-24442-6_1
- Euzéby, J. (2010). List of new names and new combinations previously effectively, but not validly, published. *International Journal of Systematic and Evolutionary Microbiology*, 60(3): 469-472. DOI:10.1099/ijs.0.022855-0
- Fagre, A.C., Cohen, L.E., Eskew, E.A., Farrell, M., Glennon, E., Joseph, M.B., Frank, H.K., Ryan, S.J., Carlson, C.J., & Albery, G.F. (2022). Assessing the risk of human-to-wildlife pathogen transmission for conservation and public health. *Ecology Letters*, 25(6), 1534-1549. DOI:10.1111/ele.14003
- Fan, C., Zhang, L., Jia, S., Tang, X., Fu, H., Li, W., Liu, C., Zhang, H., Cheng, Q., & Zhang, Y. (2022). Seasonal variations in the composition and functional profiles of gut microbiota reflect dietary changes in plateau pikas. *Integrative Zoology*, 17(3): 379-395. DOI:10.1111/1749-4877.12630
- Fenn, J., Taylor, C., Goertz, S., Wanelik, K.M., Paterson, S., Begon, M., Jackson, J., & Bradley, J. (2023). Discrete patterns of microbiome variability across timescales in a wild rodent population. *BMC Microbiology*, 23(1): 1-17. DOI:10.1186/s12866-023-02824-x
- Gani, M., Mohd-Ridwan, A.R., Sitam, F.T., Kamarudin, Z., Selamat, S.S., Awang, N.M.Z., Karuppannan, K.V., & Md-Zain, B. M. (2024).

- Habitat shapes the gut microbiome diversity of Malayan tigers (*Panthera tigris jacksoni*) as revealed through metabarcoding 16S rRNA profiling. *World Journal of Microbiology and Biotechnology*, 40(4), 111. DOI:10.1007/s11274-023-03868-x
- Hou, K., Wu, Z.X., Chen, X.Y., Wang, J.Q., Zhang, D., Xiao, C., Zhu, D., Koya, J.B., Wei, L., Li, J., & Chen, Z.S. (2022). Microbiota in health and diseases. *Signal Transduction and Targeted Therapy*, 7(1): 135. DOI:10.1038/s41392-022-00974-4
- Jahan, N.A., Lindsey, L.L., Kipp, E.J., Reinschmidt, A., Heins, B.J., Runck, A.M., & Larsen, P.A. (2021). Nanopore-based surveillance of zoonotic bacterial pathogens in farm dwelling peridomestic rodents. *Pathogens*, 10(9): 1183. DOI:10.3390/pathogens10091183
- Jose, L., Lee, W., Hanya, G., Tuuga, A., Goossens, B., Tangah, J., Matsuda, I., & Kumar, V.S. (2024). Gut microbial community in proboscis monkeys (*Nasalis larvatus*): Implications for effects of geographical and social factors. *Royal Society Open Science*, 11(7), 231756. DOI:10.1098/rsos.231756
- Kerfeld, C.A., & Scott, K.M. (2011). Using BLAST to teach “E-value-tionary” concepts. *PLoS Biology*, 9(2): e1001014. DOI:10.1371/journal.pbio.1001014
- Khairilmunir, M., Gani, M., Karuppanan, K.V., Mohd-Ridwan, A.R., & Md-Zain, B.M. (2023). High-throughput DNA metabarcoding for determining the gut microbiome of captive critically endangered Malayan tiger (*Pantheratigrisjacksoni*) during fasting. *Biodiversity Data Journal*, 11, e104757. DOI:10.3897/BDJ.11.e104757
- Kimura, M. (1980). A simple method for estimating evolutionary rate of base substitutions through comparative studies of nucleotide sequences. *Journal of Molecular Evolution*, 16: 111-120. DOI:10.1007/BF01731581
- Kinross, J.M., Darzi, A.W., & Nicholson, J.K. (2011). Gut microbiome-host interactions in health and disease. *Genome Medicine*, 3: 1-12. DOI:10.1186/gm228
- Kohl, K.D., Dieppa-Colón, E., Goyco-Blas, J., Peralta-Martínez, K., Scafidi, L., Shah, S., Zawacki, E., Barts, N., Ahn, Y., Hedayati, S., Secor, S.M., & Rowe, M.P. (2022). Gut microbial ecology of five species of sympatric desert rodents in relation to herbivorous and insectivorous feeding strategies. *Integrative and Comparative Biology*, 62(2): 237-251. DOI:10.1093/icb/icac045
- König, H., & Fröhlich, J. (2017). Lactic acid bacteria. In: König, H., Uden, G., & Fröhlich, J. (eds.), *Biology of Microorganisms on Grape, in Must and in Wine*. Cham: Springer. pp. 3-41. DOI:10.1007/978-3-319-60021-5
- Leser, T.D., & Mølbak, L. (2009). Better living through microbial action: the benefits of the mammalian gastrointestinal microbiota on the host. *Environmental Microbiology*, 11(9): 2194-2206. DOI:10.1111/j.1462-2920.2009.01941.x
- Liu, X., Mao, B., Gu, J., Wu, J., Cui, S., Wang, G., Zhao, J., Zhang, J., & Chen, W. (2021). *Blautia*—a new functional genus with potential probiotic properties? *Gut Microbes*, 13(1): 1875796. DOI:10.1080/19490976.2021.1875796
- Lobato-Bailón, L., García-Ulloa, M., Santos, A., Guixé, D., Camprodon, J., Florensa-Rius, X., Molleda, R., Manzano, R., Ribas, M.P., Espunyes, J., Dias-Alves, A., Marco, I., Migura-García, L., & Martínez-Urtaza, J. (2023). The fecal bacterial microbiome of the Kuhl’s pipistrelle bat (*Pipistrellus kuhlii*) reflects landscape anthropogenic pressure. *Animal Microbiome*, 5(1): 1-14. DOI:10.1186/s42523-023-00229-9
- Maurice, C.F., Knowles, S.C., Ladau, J., Pollard, K.S., Fenton, A., Pedersen, A.B., & Turnbaugh, P.J. (2015). Marked seasonal variation in the wild mouse gut microbiota. *The ISME Journal*, 9(11): 2423-2434. DOI:10.1038/ismej.2015.53
- McMurdie, P.J., & Holmes, S. (2013). phyloseq: An R package for reproducible interactive analysis and graphics of microbiome census data. *PLoS ONE*, 8(4): e61217. DOI:10.1371/journal.pone.0061217
- Mohd-Yusof, N.S., Abdul-Latiff, M.A.B., Badrulisham, A.S., Othman, N., Yaakop, S., Md-Nor, S., & Md-Zain, B.M. (2022). First report on metabarcoding analysis of gut microbiome in Island Flying Fox (*Pteropus hypomelanus*) in island populations of Malaysia. *Biodiversity Data Journal*, 10, e69631. DOI:10.3897/BDJ.10.e69631
- Payne, J., Francis, C.M., & Phillipps, K. (1985). *A field guide to the mammals of Borneo*. Kota Kinabalu: The Sabah Society.
- Perlman, D., Martínez-Álvaro, M., Morais, S., Altshuler, I., Hagen, L.H., Jami, E., Roehle, R., Pope, P.B., & Mizrahi, I. (2022). Concepts and consequences of a core gut microbiota for animal growth and development. *Annual Review of*

- Animal Biosciences*, 10: 177-201. DOI:10.1146/annurev-animal-013020-020412
- Phillipps, Q., & Phillipps, K. (2018). *Phillipps field guide to the mammals of Borneo*. 2nd Edition. Oxford, UK: John Beaufoy Publishing.
- Risely, A. (2020). Applying the core microbiome to understand host–microbe systems. *Journal of Animal Ecology*, 89(7): 1549-1558. DOI:10.1111/1365-2656.13229
- Sariyati, N.H., Othman, N., Abdullah-Fauzi, N.A.F., Chan, E., Md-Zain, B.M., Karuppanan, K.V., & Abdul-Latiff, M.A.B. (2024). Characterizing the gastrointestinal microbiome diversity in endangered Malayan Siamang (*Symphalangus syndactylus*): Insights into group composition, age variability and sex-related patterns. *Journal of Medical Primatology*, 53(5), e12730. DOI:10.1111/jmp.12730
- Sharon, I., Quijada, N.M., Pasolli, E., Fabbri, M., Vitali, F., Agamennone, V., Dötsch, A., Selberherr, E., Grau, J.H., Meixner, M., Liere, K., Ercolini, D., de Filippo, C., Caderni, G., Brigidi, P., & Turroni, S. (2022). The core human microbiome: Does it exist and how can we find it? A critical review of the concept. *Nutrients*, 14(14): 2872. DOI:10.3390/nu14142872
- Taudière, A. (2023). MiscMetabar: Miscellaneous functions for metabarcoding analysis. Retrieved January 16, 2024, from <https://github.com/adrietaudiere/MiscMetabar>.
- Teng, Y., Yang, X., Li, G., Zhu, Y., Zhang, Z. (2022). Habitats show more impacts than host species in shaping gut microbiota of sympatric rodent species in a fragmented forest. *Frontiers in Microbiology*, 13: 811990. DOI:10.3389/fmicb.2022.811990
- Turnbaugh, P.J., Ley, R.E., Hamady, M., Fraser-Liggett, C.M., Knight, R., & Gordon, J.I. (2007). The human microbiome project. *Nature*, 449(7164): 804-810. DOI:10.1038/nature06244
- Valdes, A.M., Walter, J., Segal, E., & Spector, T.D. (2018). Role of the gut microbiota in nutrition and health. *BMJ*, 361: k2179. DOI:10.1136/bmj.k2179
- Viney, M. (2019). The gut microbiota of wild rodents: Challenges and opportunities. *Laboratory Animals*, 53(3): 252-258. DOI:10.1177/0023677218787538
- Wang, J., Lang, T., Shen, J., Dai, J., Tian, L., & Wang, X. (2019). Core gut bacteria analysis of healthy mice. *Frontiers in Microbiology*, 10: 887. DOI:10.1128/AEM.00794-10
- Wang, Z., Zhang, C., Li, G., & Yi, X. (2022). The influence of species identity and geographic locations on gut microbiota of small rodents. *Frontiers in Microbiology*, 13: 983660. DOI:10.3389/fmicb.2022.983660
- Weldon, L., Abolins, S., Lenzi, L., Bourne, C., Riley, E.M., & Viney, M. (2015). The gut microbiota of wild mice. *PLoS ONE*, 10(8): e0134643. DOI: 10.1371/journal.pone.0134643
- Wexler, H. M. (2007). *Bacteroides*: The good, the bad, and the nitty-gritty. *Clinical Microbiology Reviews*, 20(4), 593-621. DOI:10.1128/cmr.00008-07
- Wickham, H. (2011). ggplot2. *Wiley Interdisciplinary Reviews: Computational Statistics*, 3(2): 180-185. DOI:10.1002/wics.147
- Wortelboer, K., Koopen, A.M., Herrema, H., de Vos, W.M., Nieuwdorp, M., & Kemper, E.M. (2022). From fecal microbiota transplantation toward next-generation beneficial microbes: The case of *Anaerobutyricum soehngenii*. *Frontiers in Medicine*, 9: 1077275. DOI:10.3389/fmed.2022.1077275
- Zheng, J., Wittouck, S., Salvetti, E., Franz, C.M., Harris, H.M., Mattarelli, P., O'Toole, P.W., Pot, B., Vandamme, P., Walter, J., Watanabe, K., Wuyts, S., Felis, G.E., Gänzle, M.G., & Lebeer, S. (2020). A taxonomic note on the genus *Lactobacillus*: Description of 23 novel genera, emended description of the genus *Lactobacillus* Beijerinck 1901, and union of Lactobacillaceae and Leuconostocaceae. *International Journal of Systematic and Evolutionary Microbiology*, 70(4): 2782-2858. DOI:10.1099/ijssem.0.004107

Chemistry Profile and Biological Activity of *Camposperma auriculatum* Extracts

RINI MUHARINI^{*1}, IRA LESTARI¹, ERSANDO¹, MASRIANI¹, YANA AISYA PUTRI¹,
FEBRILIA GERINA¹, ANTONIUS RB OLA²

¹Study Program of Chemistry Education, Faculty of Teacher Training and Education, Tanjungpura University, Pontianak, Indonesia; ²Chemistry Department, Faculty of Science and Engineering, University of Nusa Cendana, Kupang, Indonesia

*Corresponding author: rini.muharini@fkip.untan.ac.id

Received: 21 November 2023 Accepted: 24 July 2024 Published: 31 December 2024

ABSTRACT

As our ongoing investigation for bioactive natural products from tropical plant, we performed preliminary study on one of important tropical plants in West Kalimantan, Terentang putih, *Camposperma auriculatum*. The aims were to determine effective solvent used for extraction, chemistry profile, total phenolic content, free-radical scavenging, cytotoxicity, and anti-termite activities of leaves, stems, and roots extracts of *C. auriculatum*. Variation of solvent for extraction was selected based on its polarisation, namely, ethanol, ethyl acetate, and *n*-hexane. The effectiveness of solvent was determined by observing the rendemen of each extract, where amount of sample and solvent volume, duration of extraction, temperature, and maceration technique were controled. Determination of total phenolic content was performed using Folin-Ciocalteu method. IC₅₀ value for free-radical scavenging activity was calculated by plotting standard concentration and absorption data observed through DPPH method. Cytotoxicity evaluation was performed to each ethanolic extract against 4T1 cancer cell line using MTT assay. Anti-termite activity was conducted against *Coptotermes curvignathus* by calculating percentage of termite mortality and paper weight loss. This research showed that ethanol solvent was the most effective extraction solvent giving the highest yield in each part of plant. Phytochemically, all extracts showed that they contain phenolics and alkaloids. Ethanolic extract of stems showed the highest total phenolic content with 737.6 ± 0.56 ppm (GAE) and the most active as free-radical scavenger with IC₅₀ value of 135.51 ± 0.91 ppm. Meanwhile, the roots extract exhibited pronounce cytotoxicity toward 4T1 cancer cell line with IC₅₀ value of 1.55 ± 3.29 µg/ml and high selectivity index. Furthermore, the roots extract displayed most active as anti-termite as well as antifeedant. Hitherto, this study is the first report on phytochemistry and biological activity from leaves, stems, and roots of *C. auriculatum*. Moreover, this plant can be explored further for its potential on medicinal and agricultural industries.

Keywords: Anti-proliferative, anti-termite, *Camposperma auriculatum*, free-radical scavenging, phytochemical investigation

Copyright: This is an open access article distributed under the terms of the CC-BY-NC-SA (Creative Commons Attribution-NonCommercial-ShareAlike 4.0 International License) which permits unrestricted use, distribution, and reproduction in any medium, for non-commercial purposes, provided the original work of the author(s) is properly cited.

INTRODUCTION

Camposperma auriculatum, known as Terentang putih by local, is one of tropical plants found abundant on peat swamp forest of primary forest in West Kalimantan. Beside for its wood, local people traditionally used young leaves of this plant for treating burn skin. In Johor, shoots and roots were prepared for treating coughing with blood (Sabran *et al.*, 2016). Meanwhile, leaves and roots were used as herbal remedies for stomach ache and headache (Ismail *et al.*, 2015). The oil produced from the wood was reported having irritation effect on skin (Sanusi *et al.*, 2018)

To the best of our knowledge, there is little information related with secondary metabolites and its bioactivity from *C. auriculatum*. The only information about chemical compounds from *C. auriculatum* was from Lamberton's research dated back more than 60 years ago. It mentioned the isolation of a 5-hydroxycyclohex-2-en-one from *C. auriculatum* oil (Lamberton, 1958). This type of alkylhydroxycyclohexenones was reported also to be found in *Camposperma zeylanica* Thwaites leaves (Edireweera *et al.*, 2018). The compounds were campospermenone A, B, and C, in which exhibited promising antiproliferative towards several breast cancer cell lines (Edireweera *et al.*, 2018).

As our ongoing exploration and investigation on bioactive compound from tropical plant, we performed preliminary study on *C. auriculatum* collected at Sungai Pinang village, Melawi district, West Kalimantan. This paper described the extraction results on leaves, stems, and roots of *C. auriculatum* by using different polarity solvents, determination of total phenolic contents, free-radical scavenging activity, and anti-termite properties of each ethanolic extract.

MATERIALS AND METHODS

Plant Material Preparation and Extraction

The leaves, stems, and roots of *C. auriculatum* were collected in October 2020 at Sungai Pinang village, Melawi district, West Kalimantan. Its specimens were determined and deposited at Herbarium Bogor, Bogor, with code number B-1559/IPH.3/KS/XII/2020. The maceration technique was performed to each part of plant by using ethanol, ethyl acetate, and *n*-hexane as solvent. Each resulted extract was concentrated using rotary vacuum evaporator (Buchii, Germany) and calculated for its rendement.

Chemistry Profile Evaluation

Aliquote of each extract was screened phytochemically using several specific reagents for phenolics, alkaloids, triterpenoids, and steroids, as well as thin layer chromatography (TLC) techniques with CeSO₄ 1.5% as a universal TLC visualization reagent. Reverse phase HPLC (Agilent EZChrom Elite 1220, USA) was used to identify constituents profile contained in each extract.

Determination of Total Phenolic Content

Total phenolic content of each extract were determined using Folin-Ciocalteu assay described previously (Armania *et al.*, 2013) with some modification. Gallic acid was used as comparison. The absorption data of the mixture of each extract (10 mg/ml) with Folin-Ciocalteu reagent was observed with UV Spectrophotometer at λ 765 nm. Measurement to each extract was done in two replicates. Total phenolic content was represented as milligram gallic acid equivalent per gram extract (mgGAE/g extract).

Free-radical Scavenging Assay

Free-radical scavenging evaluation for each extract were done by conducting TLC-DPPH method described by Ciesla (2015). IC₅₀ values were determined by using DPPH method (Gulcin & Alwasel, 2023). Ascorbic acid was used as a positive control. Correlation between total phenolic content and antioxidant was carried out using Pearson's correlation with $p=0.05$.

Cytotoxicity Assay

Cytotoxicity evaluation of each ethanolic extract was conducted on 4T1 cancer cell line, a murine mammary carcinoma cell line from BALB/cfC3H mouse, using MTT assay with modification (Damasuri *et al.*, 2020). Each ethanolic extract was prepared as a mixture of one hundred μ l of culture medium in various concentration (31.25 – 500 μ g/ml) on 96-well microplate. Cisplatin was used as positive control. The medium culture without extract was played as negative control. The assay was done in triplicate. Absorbance for each well was measured using ELISA microplate reader at λ 570 nm. The absorbance values were directly proportional to the number of live cells. The viability was calculated using formula as in Eq. (1):

$$\% \text{ viability} = 100\% - \left(\frac{A_s - A_e}{A_s - A_b} \right) \times 100\% \quad \text{Eq. (1)}$$

where A_s is absorbance of cell control, A_e is absorbance of extract, and A_b is absorbance of media control. IC₅₀ values were determined by probit analysis on log concentrations and percentage of viability. The selectivity index (SI) was determined by comparing IC₅₀ ratio in Vero cell versus 4T1 cells (Rollando *et al.*, 2022). Selectivity index will be considered high when its value is higher than 3.

Anti-termite Assay

Anti-termite evaluation was performed by feeding termites *Coptotermes curvignathus* with filter paper Whatman No.1 (d = 3 cm) impregnated with extract using previously described procedure (Adfa *et al.*, 2017) with slight modification. About 30 workers and 3 soldiers of termites were employed. Negative

control was Whatman filter paper without extract. Each day, termite condition was checked. After 21 days, the number of dead termites were calculated for its percentage mortality with formula as in Eq. (2):

$$\% \text{ termite mortality} = \frac{\text{number of dead termites after treatment}}{\text{number of termites before treatment}} \times 100\% \quad \text{Eq. (2)}$$

In the same time, percentage of paper weight loss was determined to observe how many termites consumed their food. It can be calculated using Eq. (3):

$$\% \text{ paper weight loss} = \frac{\text{paper weight before treatment} - \text{paper weight after treatment}}{\text{berapaper weight before treatment}} \times 100\% \quad \text{Eq. (3)}$$

Finally, calculation of absolute antifeedant coefficient for each extract experiment was performed in order to determine antifeedant activity with formula as in Eq. (4):

$$A = \frac{KK - EE}{KK + EE} \times 100\% \quad \text{Eq. (4)}$$

where A is absolute antifeedant coefficient, KK is paper weight loss of control paper, EE is paper weight loss of extract impregnated paper.

Statistics Analysis

All measurements were done in replication. Data represented as a mean and a standard deviation. The mean difference between obtained data were determined using t-test with p value < 0.05.

RESULTS AND DISCUSSION

Extraction's process began with preparation of leaves, stems, and roots of *C. auriculatum* as dried powder 165.0, 579.9, and 135.0, g respectively. Each sample was divided equally to be macerated with ethanol, ethyl acetate, and *n*-hexane to give nine extracts all together (Figure 1). The volume of solvent, maceration duration, and number of shaking the mixture were controlled and made to be exactly the same with each other. Therefore, the effect of given solvent can be observed.

Ethanol, ethyl acetate, and *n*-hexane extract of each sample were analysed by comparing its rendements and phytochemical profiles. Based

on rendement, ethanol extract gave the highest yield compared to ethyl acetate and *n*-hexane extract (Table 1). Theoretically, organic solvent will take secondary metabolites with similar polarity out from plant cell tissue (Sticher, 2008), in which ethanol, as universal polar organic solvent, is able to extract almost all secondary metabolites contained in plant cell. This is related with the size of ethanol that small enough to break the membrane of plant cell (Tzanova *et al.*, 2020). Further analysis on rendement of each extract obtained that ethanolic extract from *C. auriculatum* roots gave the highest rendement with 8.31%, indicating roots part contained the highest content of secondary metabolites. This data suggested that *C. auriculatum* likely deposited its secondary metabolites more in roots part other than leaves or stems. Moreover, rendement analysis showed that leaves possessed more semi polar to non polar compounds than polar compounds. The yield of ethyl acetate extract from leaves was quite similar to ethanol extract, whereas its *n*-hexane extract gave more than 2%. Thus, *C. auriculatum* stems and roots were suggested to have more polar compounds rather than non polar compounds (Table 1). This suggestion was supported by TLC and HPLC chromatogram analyses on each extract.

Phytochemical screening test showed that the leaves possessed phenolic, alkaloid, terpenoids, and steroids (Table 2). The existence of terpenoids and steroids in leaves was particularly detected in ethyl acetate and *n*-hexane extracts. The roots extract showed that phenolics and alkaloids were dominant secondary metabolites in this part of plant. Previous study reported that secondary metabolites isolated from genus Camnospermae were phenolics and terpenoids. They were lanaroflavon (**1**), a flavonoid isolated from *C. panamense* leaves (Weniger *et al.*, 2004); camnospermenone A (**2**), camnospermenone B (**3**), camnospermenone C (**4**), isolated from *C. zeylanica* Thwaites leaves (Ediriweera *et al.*, 2018); and 5-hydroxy-cyclohex-2-en-one (**5**), isolated from *C. auriculatum* oil (Lamberton, 1958) (Figure 2). Thus, the finding of the existence of alkaloids, where it is prevailing in root part of *C. auriculatum*, becomes new phytochemical information for this genus.

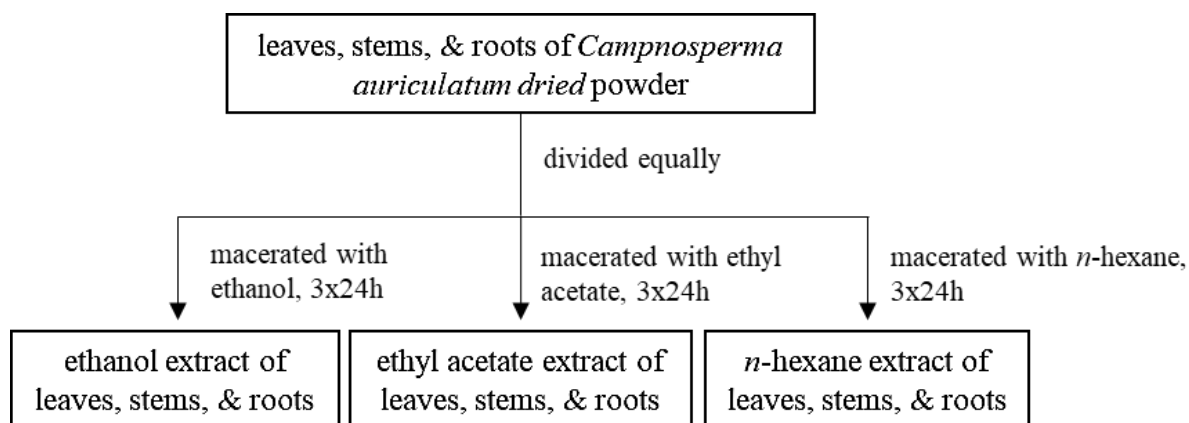


Figure 1. Procedure scheme of leaves, stems, and roots of *C. auriculatum* extraction

Table 1. Rendement yield of each extract

Part of plant	Extract	Amount (g)	Rendement (%)
leaves	Ethanol	3.68	6.69
	Ethyl acetate	3.35	6.08
	<i>n</i> -Hexane	1.64	2.98
stems	Ethanol	3.36	1.73
	Ethyl acetate	0.63	0.32
	<i>n</i> -Hexane	0.58	0.30
roots	Ethanol	3.74	8.31
	Ethyl acetate	0.98	2.19
	<i>n</i> -Hexane	0.19	0.43

Table 2. Phytochemical screening result using several specific reagents towards each extract

Extracts*	Specific Reagent**			
	a	b	c	d
CDE	+	+	++	-
CDA	++	+	+	+
CDH	-	++	+	+
CBE	++	+	-	-
CBA	+	+	-	-
CBH	-	-	+	-
CAE	++	+++	-	-
CAA	++	+++	-	-
CAH	-	+	-	-

*CDE = ethanol leaves extract, CDA = ethyl acetate leaves extract, CDH = *n*-hexane leaves extract, CBE = ethanol stems extract, CBA = ethyl acetate stems extract, CBH = *n*-hexane stems extract, CAE = ethanol roots extract, CAA = ethyl acetate roots extract, CAH = *n*-hexane roots extract

**a = FeCl₃ 5% reagent; b = Mayer reagent; c = salkowsky reagent; d = liebermann-burchard reagent; +, ++, +++ = positive result with increasing concentration; - = negative result

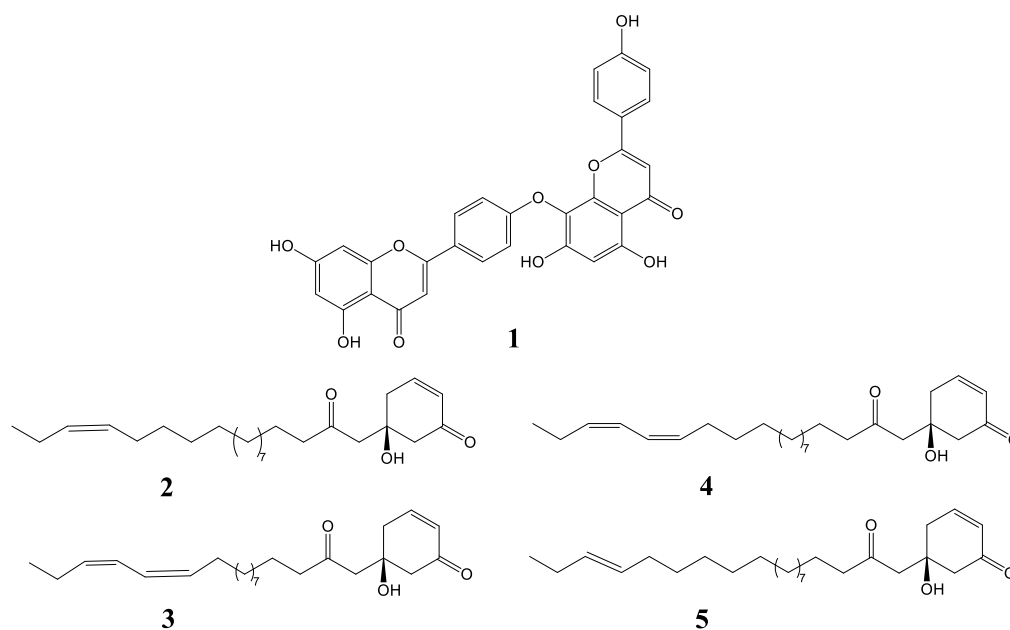


Figure 2. Reported compounds isolated from genus *Camptospermae*

Thin layer chromatography (TLC) technique was performed to analyse chromatogram profile from each extract. Two eluent systems with different polarity (*n*-hexane – ethyl acetate, 8 : 2; chloroform 100%) were used to give better understanding on TLC chromatogram. The chromatogram showed that ethanolic leaves extract differed than that ethanolic stems and roots extracts, by giving spots on non polar region with retention factor above 0.7 (Figure 3). Further, the HPLC chromatogram profile of each ethanolic extract showed similar pattern

(Figure 4), particularly for roots and stems extracts. Meanwhile, ethanolic leaves extract chromatogram slightly differed by showing overlapping peaks at retention time 12.5 – 15 minutes (more non polar region). Combining this data with phytochemical screening's result gave facts that phenolics and alkaloids detected in each extract possessed similar polarity and variation. Meanwhile, peaks at retention time 12.5 – 15 minutes in ethanolic leaves extract's chromatogram might belong to terpenoids or steroids.

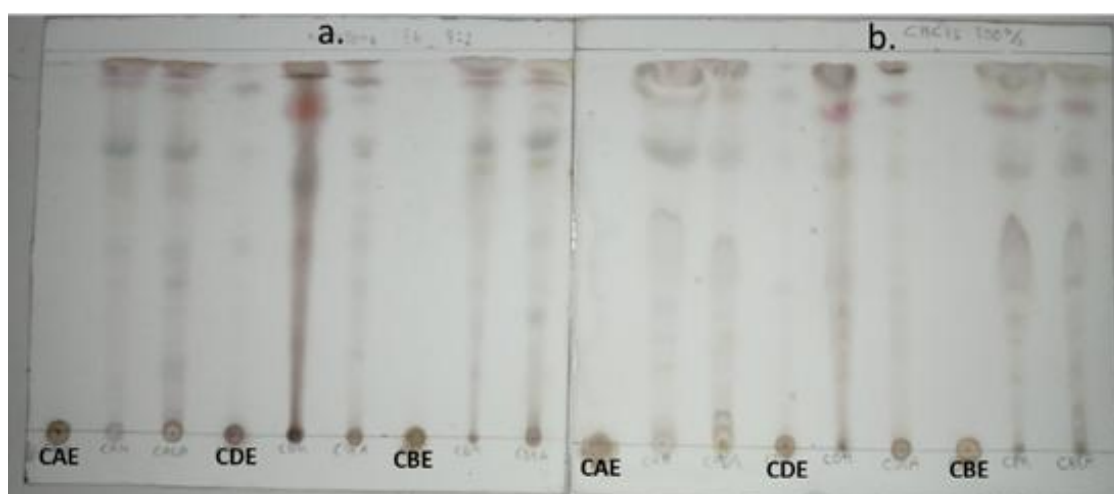


Figure 3. TLC chromatogram for ethanol extract of roots (CAE), leaves (CDE), dan stems (CBE) after spraying with CeSO_4 1.5% with eluent sistem *n*-hexane – ethyl acetate, 8 : 2 (a), and chloroform 100% (b)

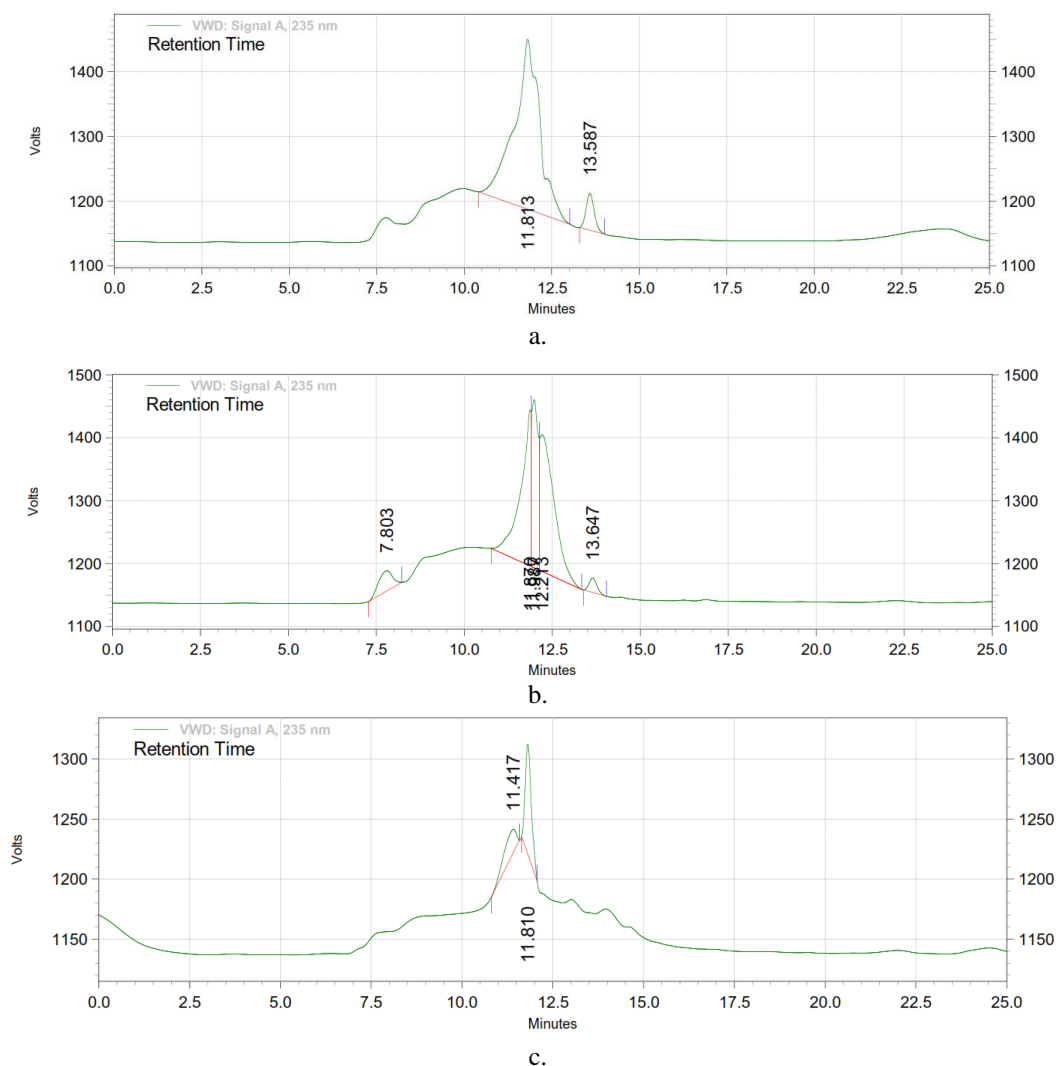


Figure 4. HPLC profile of ethanol roots (a), stems (b), and leaves (c) extracts

Total phenolic content (TPC) from ethanol stems extract was higher than from the ethanol roots and leaves extract. This finding was interesting because FeCl_3 5% test for phenolics of the stems extract showed less intense color than from the roots. In this case, this proved that TPC determination is important to describe quantitatively the amount of phenolics in the plant extract.

Antioxidant evaluation was performed using DPPH assay and showed that ethanol extract of stems and roots exhibited potential antioxidant activity with IC_{50} values of 135.66 and 194.54 ppm (Table 3). Free-radical scavenging activity of an extract or a compound was reported to have strong correlation with other biological activities, such as cytotoxicity,

antiinflammation, antidiabetes, anticancer, and antiviral (Lesjak *et al.*, 2018; Grigalius *et al.*, 2017). In this case, both extracts were predicted to show good results in other bioactivity assays. Therefore, further bioactivity evaluation toward these extracts was necessary to be performed. Correlation analysis between free-radical scavenging activity and total phenolic content of these extracts indicated that there was strong correlation between both variable ($r = -0.93$). This data indicated that phenolics contained in leaves, stems, and roots of *C. auriculatum* were responsible for radical scavenging activity showed by these extracts. Thus, this study showed that phenolics contribute on free-radical scavenging activity in the plant extract (Muharini, 2021).

4T1 breast cancer cell line is one type of breast cancer cell that commonly used in preclinical research, particularly for studying breast cancer metastasis (Nakayama *et al.*, 2021). Cytotoxic activity could be categorized into four groups. They are high cytotoxic ($IC_{50} < 20 \mu\text{g/ml}$), moderate cytotoxic ($21 \mu\text{g/ml} \leq IC_{50} \leq 200 \mu\text{g/ml}$), weak cytotoxic ($201 \mu\text{g/ml} \leq IC_{50} \leq 500 \mu\text{g/ml}$), and no cytotoxic activity ($IC_{50} > 500 \mu\text{g/ml}$) (Damasuri *et al.*, 2020). Based on this classification, the evaluation result showed that ethanol roots extract exhibited high cytotoxicity, stems extract possessed moderate cytotoxicity, and leaves extract is inactive toward 4T1 cancer cell lines (Table 4). Nevertheless, both roots and stems extracts possessed high selectivity with SI index more than three. Thus, the result indicated that latter extracts has pronounce potential for biopharmaceutical purposes.

Camposperma auriculatum plant is woody plant used by local for furniture and traditional house floor because it sustains toward termites. The activity of anti-termite was classified into seven categories as very strong (mortality (m) $\geq 95\%$), fairly strong ($75\% \leq m \leq 95\%$), sufficiently strong ($60\% \leq m \leq 75\%$), moderate ($40\% \leq m \leq 60\%$), weak ($25\% \leq m \leq 40\%$), quite weak ($5\% \leq m \leq 25\%$), and inactive ($m < 5\%$)

(Priyono, 1998). Anti-termite evaluation toward leaves, stems, and roots extracts showed that all of extracts are extremely active against *C. curvignathus*, where roots extract exhibited the most active as antitermite (Table 4). Meanwhile termite's resistance towards extract-impregnated paper was observed through paper weight loss and calculated for antifeedant absolute coefficient (Ohmura *et al.*, 2000). There are four criteria of antifeedant activity, i.e very strong ($75\% \leq \text{antifeedant (A)} \leq 100$), strong ($50\% \leq A < 75\%$), moderate ($25\% \leq A < 50\%$), and inactive ($0 \leq A < 25\%$) (Dungani *et al.*, 2012). Calculation of antifeedant absolute coefficient towards paper weight loss of each extract showed that roots extract exhibited pronounce antifeedant activity. On the other side, the anti-termite activity of leaves and stems extracts was due to the toxicity of its constituents towards *C. carvignathus*. By comparing the anti-termite activity of leaves, stems, and roots extracts, it can be suggested that the constituents responsible for anti-termite contained in roots extract differed from those in leaves and stems extracts. Furthermore, it revealed that the ethanol leaves extract is toxic toward termites *C. carvignathus*, but non-toxic toward 4T1 cancer cell lines. Nevertheless, these findings confirm well the utility of this plant as furniture or house flooring material.

Table 3. Total phenolic contents (TPC) and free-radical scavenging activity data of each ethanolic extract of *C. auriculatum*

Extracts ^a	Free-radical scavenging activity ^b (IC_{50} , ppm)	TPC ^b (GAE, ppm)
CDE	> 1000	151.6 \pm 0.19
CBE	135.51 \pm 0.91	737.6 \pm 0.56
CAE	194.54 \pm 1.63	420.3 \pm 69.07

^aCDE = ethanol leaves extract, CBE = ethanol stems extract, CAE = ethanol roots extract

^ba mean and standard deviation in two replicates

Table 4. Cytotoxicity Data of *C. auriculatum* extracts

Extracts	IC_{50} ($\mu\text{g/ml}$)		Selectivity Index
	4T1	Vero	
CAE	1.55 \pm 3.29	100.66 \pm 4.42	64.94
CBE	51.15 \pm 1.82	547.32 \pm 3.48	10.70
CDE	> 500	> 500	1

CONCLUSION

This study on *C. auriculatum* showed that ethanolic roots extract contained the highest content of secondary metabolites. In general,

major secondary metabolites in *C. auriculatum* were phenolics and alkaloids. Meanwhile, the ethanol stems extract showed the highest amount of phenolics based on its TPC value, which also exhibited the highest radical

scavenging activity. It can be concluded that ethanolic stems and roots extracts of *C.auriculatum* were promising to be natural sources for searching antioxidants. All ethanolic extracts exhibited pronounce anti-termite activity, with the ethanolic roots extract gave antifeedant property. These results are able to give a hint for further investigation toward *C. auriculatum* plant. Hitherto, there was no antioxidant and anti-termite of phenolic or alkaloids reported from *C. auriculatum* previously. Thus, further investigation on secondary metabolites from leaves, stems, and roots of *C. auriculatum* was necessary to be done thoroughly.

ACKNOWLEDGEMENTS

We are extremely grateful to Faculty of Teacher Training and Education, Tanjungpura University, for providing financial support through DIPA 2023 grant and the laboratory facilities.

REFERENCES

- Adfa, M., Sanusi, A., Manaf, S., Gustian, I. & Banon, C. (2017). Antitermitic activity of *Cinnamomum parthenoxylon* leaves against *Coptotermes curvignathus*. *Oriental Journal of Chemistry*, 33(6): 3063-3068. DOI: 10.13005/ojc/330646
- Armania, N., Saiful, L., Noorhidayah, S., Safinar, I., Biau, J., Wei, K., Noreen, H. & Hamid, A. (2013). *Dillenia suffruticosa* exhibited antioxidant and cytotoxic activity through induction of apoptosis and G 2 / M cell cycle arrest. *Journal of Ethnopharmacology*, 146(2): 525-535. DOI: 10.1016/j.jep.2013.01.017
- Cieřla, L.M., Waksmundzka-Hajnos, M., Wojtunik, K.A. & Hajnos, M. (2015). Thin-layer chromatography coupled with biological detection to screen natural mixtures for potential drug leads. *Phytochemistry Letters*, 11: 445-454. DOI: 10.1016/j.phytol.2015.02.005
- Damasuri, A.R., Sholikhah, E.N. & Mustofa. (2020). Cytotoxicity of ((E)-1-(4-aminophenyl)-3-phenylprop-2-en-1-one) on HeLa cell line. *Indonesian Journal of Pharmacology and Therapy*, 1(2): 54-59. DOI:10.22146/ijpther.606
- Dungani, R., Bhat, I. ul H., Abdul Khalil, H.P.S., Naif, A. & Hermawan, D. (2012). Evaluation of antitermitic activity of different extracts obtained from Indonesian teakwood (*Tectona grandis* L.f). *BioResources*, 7(2): 1452–1461. DOI: 10.15376/biores.7.2.1452-1461
- Ediriweera, M.K., Jayarathna, P., Tennekon, K.H., Samarakoon, S.R., Thabrew, I. & Karunanayake, E.H. (2018). Campnospermonone A, B, and C, three new cytotoxic alkylhydroxycyclohexanones from *Campnosperma zeylanica* Thawaites leaves. *Phytochemistry Letters*, 24: 114-119. DOI: 10.1016/j.phytol.2018.01.018.
- Grigallius, I. & Petrikaite, V. (2017). Relationship between antioxidant and anticancer activity of trihydroxyflavones. *Molecules*, 22: 2169. DOI: 10.3390/molecules22122169
- Gulcin, İ. & Alwaseel, S.H. (2023). DPPH Radical Scavenging Assay. *Processes*, 11: 2248 DOI: 10.3390/pr11082248
- Ismail, I., Linatoc, A.C., Mohamed, M., & Tokiman, L. (2015). Documentation of medicinal plants traditionally used by the Jakun people of endaurompin (Peta) for treatments of malaria-like symptoms. *Jurnal Teknologi*, 77(31): 63-69. DOI: 10.11113/jt.v77.6908.
- Lamberton, J.A. (1958). Studies of the optically active compounds of *Anacardiaceae exudates*, V. Further investigation of the exudate from *Campnosperma auriculata* Hook F. *Australian Journal of Chemistry*, 12(2): 224-233. DOI: 10.1071/CH9590224.
- Lesjak, M., Beara, I., Simin, N., Pintac, D., Majkic, T., Bekvalac, K., Orcic, D. & Mimika-Dukic, N. (2018). Antioxidant and anti-inflammatory activities of quercetin and its derivatives. *Journal of Functional Foods*, 40: 68-75. DOI: 10.1016/j.jff.2017.10.04
- Muharini, R., Lestari, I. & Masriani. (2021). Antioxidant-phenolic content correlation of phenolics rich fraction from *Dillenia suffruticosa* wood bark. *Pharmaciana*, 11(2): 283-292. DOI: 10.12928/pharmaciana.v11i2.20674
- Nakayama, J., Han, Y., Kuroiwa, Y., Azuma, K., Yamamoto, Y. & Semba, K. (2021). The in vivo selection method in breast cancer metastasis. *International Journal of Molecular Sciences*, 22(4): 1-19. DOI: 10.3390/ijms22041886
- Ohmura, W., Doi, S., Aoyama, M. & Ohara, S. (2000). Antifeedant activity of flavonoids and related compounds against the subterranean termite *Coptotermes formosanus* Shiraki. *Journal*

- of *Wood Science*, 46(2): 149-153. DOI: 10.1007/BF00777362
- Prijono, D. (1998). Insecticidal activity of meliaceous extracts against *Crocidolomia binotalis* Zeller (Lepidoptera: Pyralidae). *Buletin Hama Dan Penyakit Tumbuhan*, 10(1): 1-7.
- Rollando, R., Monica, E. & Aftoni, M. H. (2022). In vitro Cytotoxic Potential of *Sterculia quadrifida* Leaf Extract Against Human Breast Cancer Cell Lines. *Tropical Journal of Natural Product Research*, 6(8): 1228-1232. DOI: 10.26538/tjnpr/v6i8.12
- Sabran, S. F., Mohamed, M., & Abu Bakar, M. F. (2016). Ethnomedical knowledge of plants used for the treatment of tuberculosis in Johor, Malaysia. *Evidence-Based Complementary and Alternative Medicine*, Article ID 2850845. DOI: 10.1155/2016/2850845
- Sanusi, S. B., Bakar, M. F. A., Mohamed, M., Sabran, S. F., Norazlimi, N. A., & Isha, A. (2018). Antimycobacterial activity and potential mechanism of action of *Camptosperma auriculatum* shoot extract. *AIP Conference Proceedings* 2016, 020129. DOI: 10.1063/1.5055531
- Sticher, O. (2008). Natural Product Isolation. *Natural Product Reports*, 25 (3): 517-554.
- Tzanova, M., Atanasov, V., Yaneva, Z., Ivanova, D., & Dinev, T. (2020). Selectivity of current extraction techniques for flavonoids from plant materials. *Processes*, 8(10): 1-30. DOI: 10.3390/pr8101222
- Weniger, B., Vothron-Senecheau, C., Arango, G.J., Kaiser, M., Brun, R., & Anton, R. (2004). A bioactive biflavonoid from *Camptosperma panamense*. *Fitoterapia*, 75: 764-767. DOI: 10.1016/j.fitote.2004.09.015.

Farmers' Perception Towards Agroforestry Practices in Siburan

JACKLIN ANAK MATHEW, MUHAMMAD HIBATULLAH BIN JAMALI, VANISHRI KALY
SITTHAN, ROMIA RONA TAGANG & MOHAMAD HILMI IBRAHIM*

Agrotechnology Programme, Faculty of Resource Science and Technology, Universiti Malaysia Sarawak, 94300,
Kota Samarahan, Sarawak, Malaysia

*Corresponding author: imhilmi@unimas.my

Received: 13 April 2024

Accepted: 1 November 2024

Published: 31 December 2024

ABSTRACT

Climate change increasingly affects agricultural output and productivity, prompting a search for resilient and sustainable land use practices. Among these, agroforestry has gained recognition as a crucial strategy, offering mitigation against climate change and providing environmental, economic, and social benefits. Agroforestry is a practice that integrates trees and crops for sustainable land management to mitigate climate change and generate income. Although there are successful pilot projects for wet rice cultivation in Kampung Skuduk and Kampung Chupak, agroforestry activities in the paddy fields have yet to be documented. Therefore, it is crucial to introduce agroforestry practices to farmers in order to diversify their income sources and aid in their adaptation to climate change. Thus, this study aimed to determine farmers' perception towards agroforestry, as it will influence farmers' attitudes and the likelihood of them adopting agroforestry practices to adopt agroforestry practice. Data was gathered via structured questionnaire interviews, employing a five-point Likert scale to evaluate respondents' views on agroforestry. The data were analysed using SPSS and the trend of the composite score was used to interpret the five-point Likert scale data. The results show that the respondents have a positive attitude toward agroforestry practices. They also expected awareness-raising activities and workshops on agroforestry, indicating that they are willing to learn more about these practices. Eighty percent of respondents who do not practice agroforestry are interested in practicing agroforestry if there are no obstacles. This positive attitude indicates that farmers in the study area are ready and willing to practice agroforestry if there are no obstacles, because a positive attitude towards an agricultural innovation will increase the likelihood of adoption.

Keywords: Agroforestry, attitude, climate change, paddy farmers, perception

Copyright: This is an open access article distributed under the terms of the CC-BY-NC-SA (Creative Commons Attribution-NonCommercial-ShareAlike 4.0 International License) which permits unrestricted use, distribution, and reproduction in any medium, for non-commercial purposes, provided the original work of the author(s) is properly cited.

INTRODUCTION

Agricultural productivity, crop choice, and food security are affected by climate change worldwide (Vaghefi *et al.*, 2016). The increasing volatility of climate variables such as temperature fluctuations, changes in precipitation patterns, soil moisture variability, floods, droughts, and other natural calamities directly undermines the sustainability of agricultural systems on economic, social, and environmental fronts (Tang, 2019). These changes, particularly in yield, cultivated land area, and crop value, challenge the long-term viability of agricultural practices, threatening the stability of food systems and economic security (Vaghefi *et al.*, 2016). In response, agroforestry has emerged as a promising land use strategy, recognized for its potential to combat climate change's adverse effects while offering various

environmental, economic, and social benefits (Brown *et al.*, 2018).

Agroforestry is a method of integrating trees with crops to address environmental, economic, and societal issues (Köthke *et al.*, 2022). Numerous studies have shown that agroforestry practices can contribute to carbon sequestration and maintain soil health and ecosystem integrity (Castle *et al.*, 2022). A study by Santos *et al.* (2019) found that agroforestry systems provide up to 45-65 % benefits for biodiversity and ecosystem services. These ecological advantages fortify the environment and translate into tangible social and economic gains for farmers, providing increased profitability and sustainability. The potential of agroforestry to deliver financial benefits is undeniable, as it improves soil quality, enhances crop yields, and diversifies income sources (Castle *et al.*, 2022).

Agroforestry is a well-established practice in paddy cultivation across Southeast Asian countries, including Vietnam, Indonesia, the Philippines, Myanmar, Laos, and Thailand, where it has proven instrumental in mitigating the impacts of climate change (Wangpakapattanawong *et al.*, 2017). However, despite its proven success, agroforestry activities have yet to be documented in the paddy fields in Kampung Skuduk and Kampung Chupak. These villages are successful pilot projects for wet rice cultivation in Sarawak (Kong, 2014), and rice cultivation is one of the most important economic activities in Siburan. Farmers who only grow rice on their farms are considered more vulnerable to climate and market shocks (Wangpakapattanawong *et al.*, 2017). This is because monocropping increases exposure to risks such as floods and droughts. Trees, by contrast, offer greater resilience against these extreme weather events, providing a buffer that rice alone cannot. Farmers who integrate tree crops are able to maintain food production and income even when rice yields face challenges. Therefore, it is important to provide farmers in Kampung Skuduk and Kampung Chupak with opportunities to diversify their sources of income and thus help them adapt to the climate change crisis.

However, before introducing agroforestry to farmers, it is crucial to determine their attitudes towards agroforestry practices to ensure the successful implementation of agroforestry. This is because the first step in the decision-making process when adopting new practices depends on their knowledge of the practice, e.g. how to

apply it and what results it brings in terms of products, yields, potential environmental benefits, risks and costs (Rogers *et al.*, 2014). This knowledge then forms the basis for a person's perceptions and attitudes towards the practice (Meijer *et al.*, 2014). Knowledge refers to the information and understanding about agroforestry, while perception refers to the farmer's view based on their needs and experiences. Both knowledge and perception determine the farmer's attitude toward agroforestry (Meijer *et al.*, 2014). Therefore, this study aimed to determine perceptions and attitudes toward agroforestry practices. Few studies conducted in Bangladesh and Malaysia indicate that most farmers have a positive attitude toward agroforestry, especially middle-aged farmers who prefer to adopt agroforestry techniques (Islam *et al.*, 2021; Sheikh *et al.*, 2021).

METHODOLOGY

Study Area

This study was conducted in Kampung Skuduk and Kampung Chupak, located in the Siburan district, about 32 kilometers (about 19.88 miles) from Kuching, the capital of Sarawak (Figure 1). These two villages are primarily inhabited by the Bidayuh ethnic group, who rely heavily on paddy cultivation as their main economic activity (personal communication). According to the records from the Siburan District Agriculture Department, there are 89 registered paddy farmers in the area in 2023.

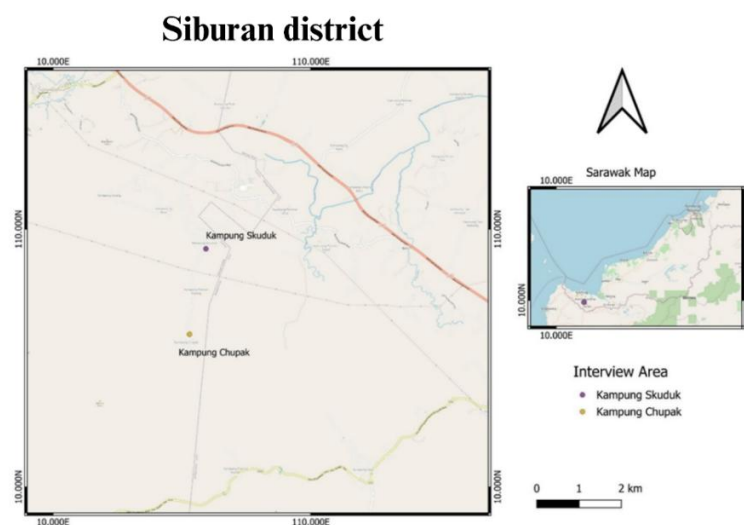


Figure 1. The location of study area, Kampung Skuduk and Kampung Chupak

Questionnaire Interview

A formal questionnaire interview was conducted targeting the registered rice farmers listed by the Jabatan Pertanian Daerah Siburan (Siburan District Department of Agriculture). Five trained enumerators were tasked with administering the questionnaires. Before the survey, the enumerators were familiarised with the questionnaire and the study's objectives. The questionnaires consisted of seven sections:

1. Socio-demographic information about the respondents
2. Information about rice cultivation
3. Respondent's perception of rice cultivation
4. Awareness and knowledge about agroforestry practices
5. Respondent's awareness of the benefits of agroforestry
6. Respondent's perception of agroforestry practices
7. The challenges in adapting agroforestry practices

The socio-demographics of the respondents were collected during the interview and their perceptions were rated using a five-point Likert scale (1 = strongly agree, 2 = agree, 3 = neutral, 4 = disagree, 5 = strongly disagree). Before eliciting their views on agroforestry, respondents were provided with a comprehensive explanation of the concept and its associated benefits.

Data Analysis

The socio-demographics of the respondents were analysed using IBM SPSS Statistic 27. The responses to the Likert scale were analysed using the method of Alonazi *et al.* (2019). Weighted means were calculated for the Likert scales, from Strongly Agree=1 to Strongly Disagree=5 (see Table 1), so that the tendency of the composite scores could be determined (Alonazi *et al.*, 2019).

Table 1. Weighted means for five-point Likert scale adapted from Alonazi *et al.* (2019)

Weighted Mean	Result
1 - 1.79	Strongly agree
1.8 - 2.59	Agree
2.60 - 3.39	Neutral
3.4 - 4.19	Disagree
4.2 - 5	Strongly disagree

RESULTS

Socio-Demographic of the Respondents in the Study Area and their Perception Towards Agroforestry

Table 2 shows the socio-demographic data of the paddy farmers who participated in this study. Of the 89 registered farmers, 43 responses were obtained, and the analysis revealed that 42% of respondents actively engaged in agroforestry, while 58% did not (Figure 2). Gender distribution among the surveyed group indicates a predominance of male farmers (63%), with females constituting 37%. Most of the respondents were older than 65 years old (49%), and most of them were married (91%). Most of the farmers in Kampung Skuduk and Kampung Chupak belong to the older generation, so most of them have been cultivating paddy for more

than 21 years (74%). As most of the respondents belonged to the Bidayuh ethnic group (77%), many of them practised the Christian faith (98%). Most of the respondents (72%) have formal education, i.e. they have completed primary or high school, and only 1% of the respondents have higher education. Meanwhile, 26% of respondents have no formal education. More than half of the respondents primarily engaged in rice farming as their main occupation (84%), and most of them (84%) have a monthly income of less than RM1300.

Most respondents indicated a solid inclination to recommend agroforestry practices to their friends or acquaintances (WM = 1.60). They strongly agreed that agroforestry should be practised in agriculture (WM = 1.51), as shown in Table 3. The respondents also anticipated increased awareness programs, and skill-

development workshops focused on agroforestry practices (WM = 1.40 for both). The results of this study show that the respondents have a positive perception and attitude towards agroforestry practices after being informed about

the benefits of agroforestry. Moreover, 80% of the respondents who do not practice agroforestry were interested in practising agroforestry if there were no obstacles (Figure 3).

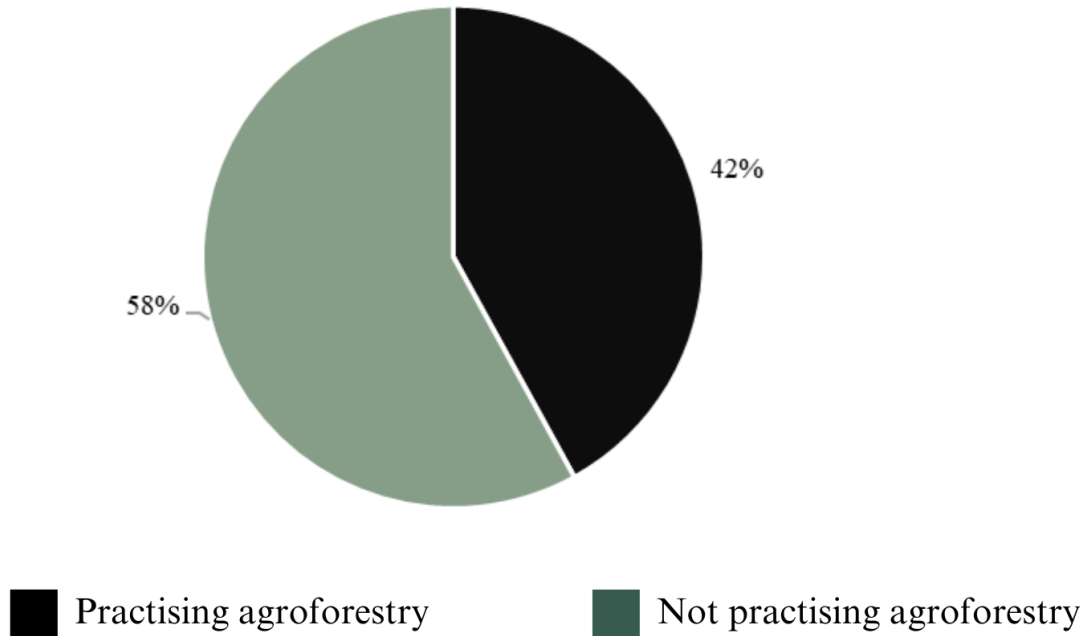


Figure 2. Respondents practising agroforestry and not practising agroforestry

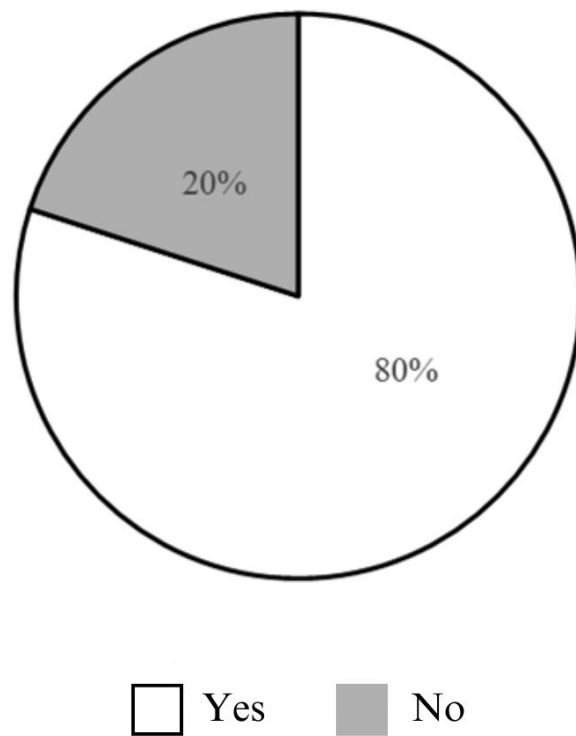


Figure 3. Non agroforestry practitioners that interested in practising agroforestry if there are no obstacles

Table 2. Socio-demographic of respondents in Kampung Skuduk and Kampung Chupak, Siburan, Sarawak

	Variables	No. of Respondents (%)
1.	Gender	
	Female	16 (37%)
	Male	27 (63%)
2.	Age	
	35 – 44	1 (2%)
	45 – 54	10 (23%)
	55 – 64	11 (26%)
	≥ 65	21 (49%)
3.	Marital Status	
	Single	1 (2%)
	Married	39 (91%)
	Divorce/Widow	3 (7%)
4.	Race	
	Iban	4 (9%)
	Bidayuh	33 (77%)
	Cina	4 (9%)
	Orang Ulu	1 (2%)
	Others	1 (2%)
5.	Religion	
	Christian	42 (98%)
	Islam	1 (2%)
6.	Education	
	No Formal Education	11 (26%)
	Formal education	31 (72%)
	Higher education	1 (2%)
7.	Paddy Cultivation Status	
	Full Time	36 (84%)
	Part Time	7 (16%)
8.	Income	
	Less than RM 1300	36 (84%)
	RM 1300 – RM 1400	5 (12%)
	RM 1401 – RM 1700	1 (2%)
	More than RM 1701	1 (2%)
9.	Experience	
	5 – 10 years	6 (14%)
	11 – 20 years	5 (12%)
	≥ 21 Years	32 (74%)

Table 3. Farmers' perception on agroforestry practices. Weighted means for the Likert Scale were calculated and the weighted mean tendency was determined (Refer Table 1)

Descriptions	Weighted mean	Result
Recommending agroforestry practice to acquaintances	1.60	Very likely to recommend
Agroforestry practice must be practised in agriculture	1.51	Strongly agree
More awareness activity on agroforestry must be organized	1.40	Very anticipating
Workshop skills on agroforestry practices must be organized	1.40	Very anticipating

DISCUSSION

Respondents' Socio-Demographics and Their Attitude Towards Agroforestry Practice

The respondent's socio-demographics play a crucial role in determining their perceptions and attitudes towards adopting or rejecting new ideas (Phondani *et al.*, 2020). Various studies have shown that socioeconomic characteristics significantly influence adoption behaviour in relation to new practices. Various studies have shown that socioeconomic characteristics significantly influence adoption behaviour in relation to new practices. Education plays a crucial role in shaping respondents' perceptions and attitudes toward agroforestry because it enables farmers to comprehend the knowledge associated with this practice. This understanding is the foundation for individuals' perceptions and attitudes about agroforestry (Meijer *et al.*, 2014). Given that most respondents in this study have formal education, they may find it easier to understand and adopt agroforestry if provided with the proper information.

After learning about the benefits of agroforestry, most respondents expressed a desire to recommend these practices to their acquaintances. They believe that agroforestry should be adopted in the agriculture sector, as they recognise its potential to improve land productivity and quality of life. These findings indicate that they are likely to recommend agroforestry to others and have a higher tendency to apply agroforestry in the future. Furthermore, their anticipation of awareness activities and workshops indicates a willingness to learn about agroforestry practices. This positive attitude demonstrates that the farmers in the study area are willing and ready to adopt agroforestry, provided there are no significant obstacles. This finding is further supported by the fact that the majority (80%) of respondents not currently practising agroforestry expressed interest in doing so. Such positive attitudes towards agricultural innovations increased the likelihood of adoption, whereas negative attitudes typically lower adoption probabilities (Meijer *et al.*, 2014).

CONCLUSION

In summary, the farmers in Kampung Chupak and Kampung Skuduk have a positive attitude

towards agroforestry. They express a desire for awareness activities and skills workshops related to agroforestry, indicating their willingness to learn more about this sustainable practice. This positive attitude suggests that farmers in the study area are ready and willing to practise agroforestry if there are no obstacles. A positive attitude towards agricultural innovation will increase the likelihood of adoption. Therefore, the government and the private sector should collaborate to disseminate knowledge and information about agroforestry to the community, as a lack of understanding can hinder the adoption of agroforestry.

ACKNOWLEDGEMENT

The authors acknowledge [Universiti Malaysia Sarawak (UNIMAS) for the PILOT Research Grant Scheme (UNI/F07/PILOT/85193/2022)] for supporting this project and appreciation to the Jabatan Pertanian Daerah Siburan (Siburan District Agriculture Department) for the cooperation during the data collection and connecting us with the farmers. We would also like to thank all respondents who participated in the data collection for their cooperation. We would also like to thank the enumerators who participated in the interviews: Muhammad Hibatullah Bin Jamali, Selvana Eyra Felix, Prisceila Chong and Monica Moi Anak Melike.

REFERENCES

- Alonazi, M., Beloff, N. & White, M. (2019). Exploring determinants of m-government services: A study from the citizens' perspective in Saudi Arabia. *Proceedings of the 2019 Federated Conference on Computer Science and Information Systems*, 18, pp.627–631. DOI: 10.15439/2019f75
- Brown, S.E., Miller, D.C., Ordonez, P.J., & Baylis, K. (2018). Evidence for the impacts of agroforestry on agricultural productivity, ecosystem services, and human well-being in high-income countries: A systematic map protocol. *Environmental Evidence*, 7(1): DOI: 10.1186/s13750-018-0136-0
- Castle, S., Miller, D., Merten, N., Ordonez, P. & Baylis, K. (2022). Evidence for the impacts of agroforestry on ecosystem services and human well-being in high-income countries: A systematic map. *Environmental Evidence*, 11(1): DOI: 10.1186/s13750-022-00260-4

- Islam, M., Aktar, L., Jubair, S., Dey, T. & Biswas, R. (2021). Addressing farmers' perceptions, attitudes, and constraints to adopt agroforestry adjacent to the coastal belt of Sundarbans, Bangladesh. *European Journal of Agriculture and Food Sciences*, 3(4): 78–88. DOI: 10.24018/ejfood.2021.3.4.304
- Kong, J. (2014). Wet paddy programme benefits 200 farmers. *Borneo Post Online*. Retrieved February 21, 2024, from <https://www.theborneopost.com/2014/08/19/wet-paddy-programme-benefits-200-farmers/>
- Köthke, M., Ahimbisibwe, V., & Lippe, M. (2022). The evidence base on the environmental, economic and social outcomes of agroforestry in patchy—An evidence review map. *Frontiers in Environmental Science*, 10: 925477. DOI: 10.3389/fenvs.2022.925477
- Meijer, S.S., Catacutan, D., Ajayi, O.C., Sileshi, G.W. & Nieuwenhuis, M. (2014). The role of knowledge, attitudes and perceptions in the uptake of agricultural and agroforestry innovations among smallholder farmers in sub-Saharan Africa. *International Journal of Agricultural Sustainability*, 13(1): 40–54. DOI: 10.1080/14735903.2014.912493
- Mwase, W., Sefasi, A., Njoloma, J., Nyoka, B. I., Manduwa, D. & Nyaika, J. (2015). Factors affecting adoption of agroforestry and evergreen agriculture in Southern Africa. *Environment and Natural Resources Research*, 5(2): 148–154. DOI: 10.5539/enrr.v5n2p148
- Phondani, P.C., Maikhuri, R.K., Rawat, L.S. & Negi, V.S. (2020). Assessing farmers' perception on criteria and indicators for sustainable management of indigenous agroforestry systems in Uttarakhand, India. *Environmental and Sustainability Indicators*, 5. DOI: 10.1016/j.indic.2019.100018
- Rogers, E.M., Singhal, A., & Quinlan, M.M. (2014). Diffusion of innovations. In *An integrated approach to communication theory and research* (pp. 432–448). Routledge.
- Santos, P.Z.F., Crouzeilles, R., & Sansevero, J. B.B. (2019). Can agroforestry systems enhance biodiversity and ecosystem service provision in agricultural landscapes? A meta-analysis for the Brazilian Atlantic Forest. *Forest Ecology and Management*, 433: 140–145. DOI: 10.1016/j.foreco.2018.10.064
- Sheikh, R., Islam, M., Sharmin, A., Biswas, R. & Kumar, J. (2021). Sustainable agroforestry practice in Jessore district of Bangladesh. *European Journal of Agriculture and Food Sciences*, 3(1): 1–10. DOI: 10.24018/ejfood.2021.3.1.150
- Tang, K.H.D. (2019). Climate change in Malaysia: Trends, contributors, impacts, mitigation and adaptations. *Science of the Total Environment*, 650(2): 1858–1871. DOI: 10.1016/j.scitotenv.2018.09.316
- Vaghefi, N., Shamsudin, M.N., Radam, A., & Rahim, K.A. (2016). Impact of climate change on food security in Malaysia: economic and policy adjustments for rice industry. *Journal of Integrative Environmental Sciences*, 13(1): 19–35. DOI: 10.1080/1943815X.2015.1112292
- Wangpakapattanawong, P., Finlayson, R., Öborn, I., Roshetko, J.M., Sinclair, F.L., Shono, K., Borelli, S., Hillbrand, A. & Conigliar, M. (2017). Agroforestry in rice-production landscapes in Southeast Asia: A practical manual. *Food and Agriculture Organization of the United Nations Regional Office for Asia and the Pacific World Agroforestry Centre (ICRAF)*.

Optimizing Silicon Application for Enhancing Growth and Chlorophyll Concentration in Pepper Plants (*Piper nigrum* L.) Cultivar Kuching

NUR AINU FARHAH RABAE¹, XIAOLEI JIN², LEE CHUEN NG¹ & SITI NORDAHLIAWATE MOHAMED SIDIQUE^{3*}

¹Biointeractions and Crop Health Research Interest Group, Faculty of Fisheries and Food Sciences, Universiti Malaysia Terengganu, 21030 Kuala Nerus, Terengganu, Malaysia; ²Department of Biological Sciences, National Sun Yat-Sen University, Leinai Road, Kaohsiung, 80424 Taiwan; ³Institute of Tropical Biodiversity and Sustainable Development, Universiti Malaysia Terengganu, 21030 Kuala Nerus, Terengganu, Malaysia

*Corresponding author: dahliasidique@umt.edu.my

Received: 29 June 2024

Accepted: 1 December 2024

Published: 31 December 2024

ABSTRACT

Silicon is known to play a central role in regulating various aspects of plant growth and development, including nutrient uptake, root formation, and growth. Silicon is the second most abundant element found in soil primarily as neutral, monomeric silicic acid, which is the biologically available form for plant uptake. Although silicon is not considered an essential nutrient for the basic life cycle of most plants, its availability can significantly benefit plant health, growth, and stress tolerance. However, previous research has mainly focused on plants grown in silicon, and silicon occurs naturally as silicon dioxide (SiO₂), and is not in a form that is easily absorbed by plants. Therefore, this study investigates the effects of silicon (Si) in silicic acid form (H₄O₄Si) on the growth and chlorophyll concentration of pepper (*Piper nigrum* L.) seedlings, particularly the Kuching variety. The Si application had been applied once a week with five different concentrations via root applications; T1 [0.5% Si (v/v)], T2 [1.5% Si (v/v)], T3 [2.0% Si (v/v)], T4 [1.5% potassium silicate (v/v)] as positive control and T5 [negative control (without silicon)] on pepper cutting-grown plants. Growth parameters such as plant height, stem diameter and chlorophyll concentration were observed and collected. Our results showed that the treatment with Si nutrients is promising, as the Si-treated pepper clones showed faster and more robust growth compared to the control plants in the early growth stages. The results indicate that a 0.5% Si concentration (v/v) effectively maintains the high chlorophyll content over four weeks, in contrast to the decreasing trend observed in the control group. This study thus presents the first report on the application of Si in *P. nigrum* L., demonstrating the feasibility of Si uptake and growth enhancement in pepper plants. The results suggest a stepwise application of Si, starting with low concentrations (0.5% Si v/v) via the root in the early growth stages to strengthen young plants before transplanting to the field. However, foliar spraying could also be considered in future studies as the silicon is absorbed faster compared to root application. Further studies on the passive defence structure (physical barriers such as cuticle, wax, and trichomes) are needed to prove that it can repel pathogens and insects.

Keywords: Chlorophyll concentration, *Piper nigrum*, growth enhancement, silicon, silicic acid, Terengganu

Copyright: This is an open access article distributed under the terms of the CC-BY-NC-SA (Creative Commons Attribution-NonCommercial-ShareAlike 4.0 International License) which permits unrestricted use, distribution, and reproduction in any medium, for non-commercial purposes, provided the original work of the author(s) is properly cited.

INTRODUCTION

The pepper plant, scientifically known as *Piper nigrum* L. and often referred to as the "king of spices," because of its active ingredient piperine, which has various pharmacological effects and offers numerous health benefits (Srinivasan, 2007). The cultivation of black pepper is widespread in various Asian countries, including Malaysia, where the pepper plant is one of the four most economically important agricultural crops after palm, rubber and cocoa (Joy *et al.*, 2007; Damanhour & Ahmad, 2014; Abdulla *et al.*, 2015). In Malaysia, there are seven commonly cultivated varieties: "Semongok Aman", "Semongok Emas", "Kuching", "Sarikei", "Semongok Perak", "Uthirancotta", "Nyerigai", and "PN129" (Paulus, 2011). In Sarawak, the most

common varieties are Sarikei and Kuching (Ravindran *et al.*, 2000). Kuching grows faster and higher yielding than Sarikei (Paulus & Sim, 2005), making it the predominant variety in Sarawak and Johor (Paulus, 2011). However, Kuching is highly susceptible to diseases such as Phytophthora foot rot, blackberry, Fusarium wilt, root-knot, and wrinkle leaf (Paulus, 2011). Despite other widely grown varieties such as "Semongok Perak", "Semongok Emas" and "Semongok Aman", Kuching remains the most widely grown variety in Malaysia.

Malaysia considered the fifth largest pepper producer in the world (Malaysia Pepper Board, 2022), relies mainly on Sarawak, which contributes 98% of the country's annual production (Adam *et al.*, 2018). The average domestic consumption of pepper

in 2017-2021 was 10, 891 tonnes (Malaysia's Open Data Portal, 2022). Domestic consumption of pepper increased from 12,000 tonnes in 2014 to 13,500 tonnes in 2015 (Adam *et al.*, 2018). Black pepper production has declined since the early 1980s, primarily due to pest infestations and disease outbreaks in field plantations (Chen *et al.*, 2010). Moreover, due to biotic and abiotic stress factors, farmers have difficulty in procuring healthy planting materials, resulting in minimised pepper yields (Sharma & Kalloo, 2004). Consequently, this has resulted in an annual reduction of approximately 2% in the total pepper cultivation area (Adam *et al.*, 2018).

There is therefore a need to promote the growth and development of plants, e.g. by administering silicon (Si) application, which can reportedly help to improve plants' resistance to disease. For example, rock melon and strawberry growers have added Si to the irrigation system to increase plant defenses against diseases such as powdery mildew (Samuels *et al.*, 1991; Menzies *et al.*, 1992; Belanger *et al.*, 2003; Ouellette *et al.*, 2017). Numerous studies have reported the promotion of root development by the combined application of salicylic acid (SA) and Si fertilization. SA, a phenolic compound, is known to regulate plant growth and development in several areas, including nutrient uptake and root initiation and growth (Wani *et al.*, 2016; Khan *et al.*, 2017; Pasternak *et al.*, 2019). SA exposure has been shown to stimulate the development of adventitious, primary, and lateral roots in numerous plant species (Yang *et al.*, 2013; Pasternak *et al.*, 2019). Similarly, the beneficial effects of Si fertilization on plants have been extensively documented (Laane, 2017), including its regulatory role in enhancing the uptake of other essential plant nutrients (Ma & Yamaji, 2006; Liang *et al.*, 2007; Al-Wasfy, 2013; Deshmukh *et al.*, 2017). It is known that Si strengthens the cell walls of plants, and thus potentially increases resistance to biotic and abiotic stress factors such as pests, diseases, and drought, while at the same time increasing plant quality and yield.

However, conventional Si sources, especially silicon dioxide, can pose problems for pepper plants in terms of uptake. To solve this problem, a technology called Silicic Acid Agro Technology (SAAT) has been introduced for the application of Si in agricultural crops (Laane, 2017). SAAT has shown promising efficacy in facilitating Si uptake, even in crops that were previously unable to absorb Si efficiently, including non-accumulating Si plants (Epstein, 1994; Laane, 2017). The application of Si can improve plant growth parameters by increasing

root growth, root mass, stem length and diameter, plant height, number of shoots and leaf area (Laane, 2017), which would indirectly increase plant yield potential. Plant height is an important indicator of plant growth, biomass production and yield potential in cereals and wheat (Martin *et al.*, 2017). In addition, the Si content of wheat grown under salt stress was determined.

Si can be applied to plants either by foliar spraying or by watering into the soil. However, Si in the form of silicic acid can be applied via foliar spraying in lower concentrations during the vegetative stage and act as a growth promoter (Lanne, 2017). To date, Si has not been recognized as an essential plant nutrient, although it can promote plant growth and agricultural production (Zellener *et al.*, 2021). However, the Association of American Plant Food Control Officials (AAPFCO) recognizes Si and classifies it as a beneficial substance. Si products are also approved by the Organic Materials Review Institute (OMRI) for use in organic farming. Nevertheless, there are only few studies on the use of Si in the pepper plant. The aim of this study was therefore to determine the effect of Si applications on the growth of pepper plant in the early growth phase. This is the first report on the application of silicon (in the form of silicic acid) to pepper plants, *P. nigrum* L.

MATERIALS AND METHODS

Experimental Plot

The experimental plot is located at pepper plantation in Setiu, Terengganu, Malaysia (5°32'1N, 102° 57' 15E). The experimental plot was set up in a randomized complete block design (RCBD). The duration for this study was two months starting on August 2018 until October 2018.

Pepper plants, variety Kuching, had been selected in this study due to the most widely grown cultivar and it is readily accessible. It also has vigorous growth and high yield production. Each treatment was conducted with three replicates. For irrigation and fertilization, pepper plants were irrigated using a drip irrigation system. Irrigation was scheduled twice a day automatically by drip tape. Additionally, this study followed the Standard Operating Procedures (SOP) for planting procedures, irrigation, and fertilization in black pepper plantations. These procedures were based on the guidelines provided by the Agriculture Department of Lembah Bidong, ensuring that all practices were aligned with established agricultural standards.

Silicon Nutrient Treatments

Five different silicon (Si) concentration were applied to cutting-grown pepper plants: T1 (0.5% Si v/v), T2 (1.5% Si v/v), T3 (2.0% Si v/v), T4 (1.5% potassium silicate) as positive control and T5 (control without silicon) as negative control. The dilution of Si nutrients was calculated using the standard dilution formula, $M_1V_1 = M_2V_2$; where M_1 = initial percentage of solution, V_1 = volume needed for dilution, M_2 = final percentage of solution, V_2 = final volume needed for the experiment. A total of fifty pepper plants were given Si in the form of monosilicic acid (72% of SIKA, Taiwan) once a week as root treatments. The Si was prepared on the day of application and all seedlings had been given 40 ml of the Si solution.

Plant Growth Assessments

Throughout the study, the plant growth of the seedlings was measured twice a month. Plant growth was assessed by stem diameter, plant height and leaf chlorophyll concentration. Plant height was measured using tape measure (cm), while stem diameter was measured using a digital vernier caliper and chlorophyll content was measured using a Konica Minolta chlorophyll meter. Chlorophyll content data were measured three times per plant and 10 leaves per treatment.

Statistical Analysis

All data were analyzed using analysis of variance (ANOVA) in SPSS Statistics 20. Comparison with the mean values of the control and the treatment was performed using Tukey's HSD test at a significance level of $p < 0.05$ (95% confidence level). A Pearson correlation coefficient was performed to evaluate the relationship between treatment and pepper plant height, stem diameter and chlorophyll concentration (SPAD).

RESULTS AND DISCUSSION

The effect of Si application on pepper plants showed a promising result for stem cutting seedling growth and development.

Plant Height Response to Silicon Treatments

The results showed a significant difference ($p < 0.05$) in increment of plant height between the Si treatments over a four-week period (Figure 1). The plant height increment showed that T1 (0.5% Si v/v) consistently had the highest plant height across all weeks and thus showed the most significant growth

development. From week 1 until week 4; 13.2 cm, 29.4 cm, 38.9 cm and 51.7 cm, respectively. Plants without Si (T5) showed the slowest growth from week 1 to week 4 (4.4 cm, 8.9 cm, 11.7 cm and 12.7 cm, respectively) (Figure 1). In week 1, treatments T2 (1.5% Si v/v), T3 (2.0% Si v/v), and T4 (1.5% Psi v/v) had similar plant heights, ranging from 5 to 10 cm, with no significant differences between them.

All Si-treated pepper plants were growing faster than control plants and the range from the highest to the lowest (on week-4); T1 (51.7 cm) > T2 (39.5 cm) > T3 (30.9 cm) > T4 (27.9 cm) > T5 (12.7 cm) (Figure 1). The pepper seedlings treated with Si showed a positive result and had enhanced plant growth. Control treatment show no significant correlation between Si and plant height over the four weeks. The correlation coefficients range in Week 3 ($r [8] = [-0.58]$, $p = [0.077]$) and in Week 4 $r [8] = [0.19]$, $p = [0.60]$, indicating weak and negative relationships for most weeks (Table 1). In T1 (0.5% Si), weak negative correlations were observed throughout all weeks, with r values ranging from -0.539 to 0.130. (Table 1). The application of 1.5% Si shows a transition from negative correlations in Weeks 1 and 2 ($r = -0.495$ and -0.552 , respectively) to a statistically significant positive correlation in Week 3 $r [8] = [0.67]$, $p = [0.05]$ (Table 1). This suggests that by Week 3, the pepper plants responded positively to Si application.

Higher Si concentrations may bring fewer positive effects on plant height for several reasons, despite its overall benefits to plant growth. One possible explanation is that excessive Si application can alter the balance of other essential nutrients and water uptake, potentially limiting growth. At high concentrations, Si can interfere with normal physiological processes, including the regulation of plant hormones like gibberellins, which play a key role in promoting stem elongation and overall plant height (Sah *et al.*, 2022). Therefore, while Si promotes growth at optimal levels, overapplication can shift the plant's resources more towards stress resistance and structural reinforcement rather than height growth (Shivaraj *et al.*, 2022)

Similar findings from previous studies by Jufri *et al.* (2016) and Suhaizan *et al.* (2017) that have been confirmed that Si-treated chili plants exhibit greater leaf length and showed significant improvements in vegetative growth compared to control plants. In addition, similar growth-promoting effects of Si have been observed in other crops such as rice, tomatoes, cucumbers, coffee and strawberry (Ma & Yamaji, 2006; Silva *et al.*, 2010; Ouellette *et al.*, 2017). Suhaizan *et al.* (2023) reported that the

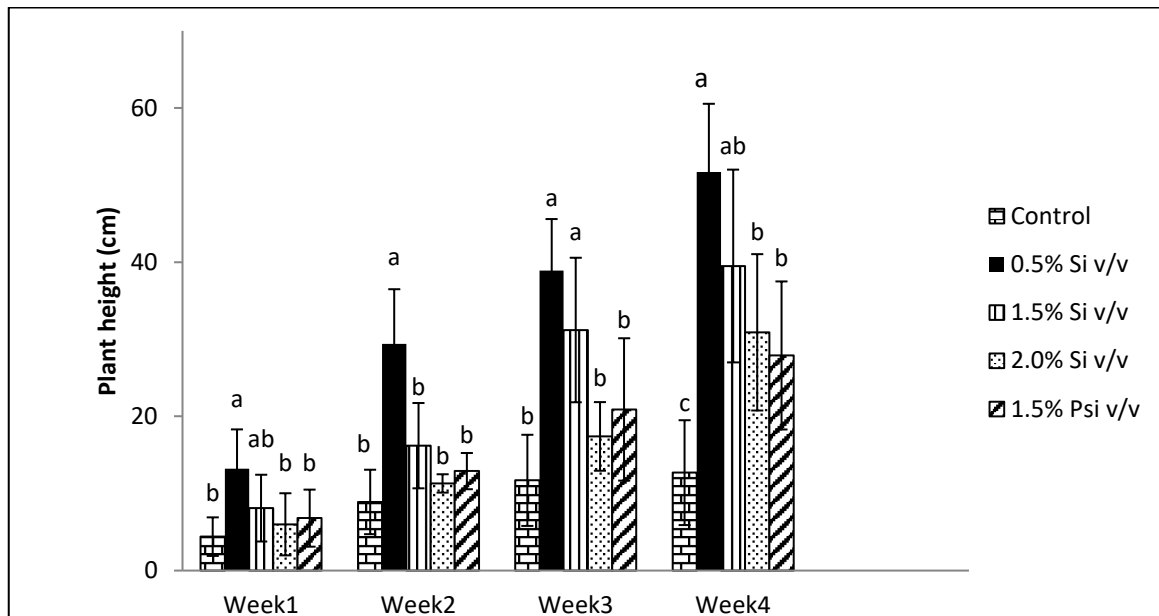


Figure 1. Pepper plant height increment (cm) from week-1 until week-4 grown from stem cutting seedlings. Silicon was applied once a week by root application. The treatments: T1 (0.5% Si v/v), T2 (1.5% Si v/v), T3 (2.0% Si v/v), T4 (1.5% potassium silicate) as positive control and T5 (control without silicon) as negative control

Table 1. Pearson correlation coefficients between treatments and pepper plant height

		W1	W2	W3	W4
Plant Height	Controls	-0.321	-0.316	-0.584	0.190
	0.5% Si	-0.390	-0.452	-0.539	0.130
	1.5% Si	-0.495	-0.552	0.665*	0.190
	2.0% Si	-0.662*	-0.234	0.808**	-0.62
	1.5% PSi	-0.702*	0.858**	-0.668*	0.156

*Correlation is significant at the 0.05 level (2-tailed)

**Correlation is significant at the 0.01 level (2-tailed)

impact of Si nutrient application on the growth of chili plants grown using a fertigation system. The study tested different Si concentrations (0 ppm, 108 ppm, 180 ppm, and 360 ppm) and evaluated their effects on various growth parameters, including stem diameter and plant height. The findings showed that Si significantly enhanced the growth performance of chili plants. The highest concentration (360 ppm) resulted in the greatest increase in stem diameter, plant biomass, and Si accumulation in stems and fruits. From this study, it suggests that Si application improves structural growth and helps chili plants better withstand abiotic stress, enhancing overall plant development. Other study by Gong *et al.* (2003) reported that wheat plants grown in pots with Si application showed greater plant height and leaf area compared to control plants without Si. While peppers were previously considered low silicon accumulators (Epstein, 1994), the application of Si in the form of silicic acid has now been shown to enable pepper plants to uptake Si, providing significant benefits. In this study, Si-treated pepper seedlings grown faster and healthier compared to control plants during the early stages of development.

Si plays a crucial role in regulating plant growth and development, affecting various aspects such as nutrient uptake, root formation, and growth (Ma & Yamaji, 2006; Liang *et al.*, 2007; Al-Wasfy, 2013; Wani *et al.*, 2016; Deshmukh *et al.*, 2017; Khan *et al.*, 2017; Pasternak *et al.*, 2019). However, studies back then were mostly focusing on Si effects on plants cultivated in solution culture (with controlled microclimate or lab condition) while there were limited studies on plants cultivated in soil medium and large scale-field (with natural microclimate).

Stem Diameter Response to Silicon Treatments

There were no significant differences ($p > 0.05$) in stem diameter for all treatments. The T2 treatments showed the widest in increment of stem diameter on the first week (0.5 mm) compared to other Si treatment and control. But by week 3 and week 4, the T1 (0.5% Si v/v) treatment showed a significant increase in stem diameter compared to the control and other treatments. T1 was 2.8 mm whereas control was only 1.5 mm (Figure 2). Other Si treatments had intermediate stem diameters, while the 1.5% Psi v/v treatment consistently showed the lowest stem

diameter by week 3 and week 4 (Figure 2). Unexpectedly, the lowest Si concentration (T1) had increased (stem diameter) faster than other treatments [0.4 mm (week 1), 1.2 mm (week 2), 2.1 mm (week 3) and 2.8 mm (week 4)] (Figure 2). The increment rank of stem diameter on week-4; T1 [2.8mm]> T2 [2.1 mm]> T3 [1.9 mm]> T4 (1.7 mm) > T5 (1.5 mm) (Figure 2). Results from Table 2 show that T2 shows a gradual increase in correlation

strength from Week 1 to Week 4, transitioning from a negligible correlation in Week 1 $r [8] = [-0.05]$, $p = [0.08]$ to a significant positive correlation in Week 3 $r [8] = [0.477]$, $p = [0.49]$ (Table 2). This indicates that 1.5% Si had a delayed but beneficial effect on stem diameter, which became more pronounced as the study progressed. The increase in stem diameter by Week 3 might suggest that 1.5% Si concentration optimally supports structural growth at this stage.

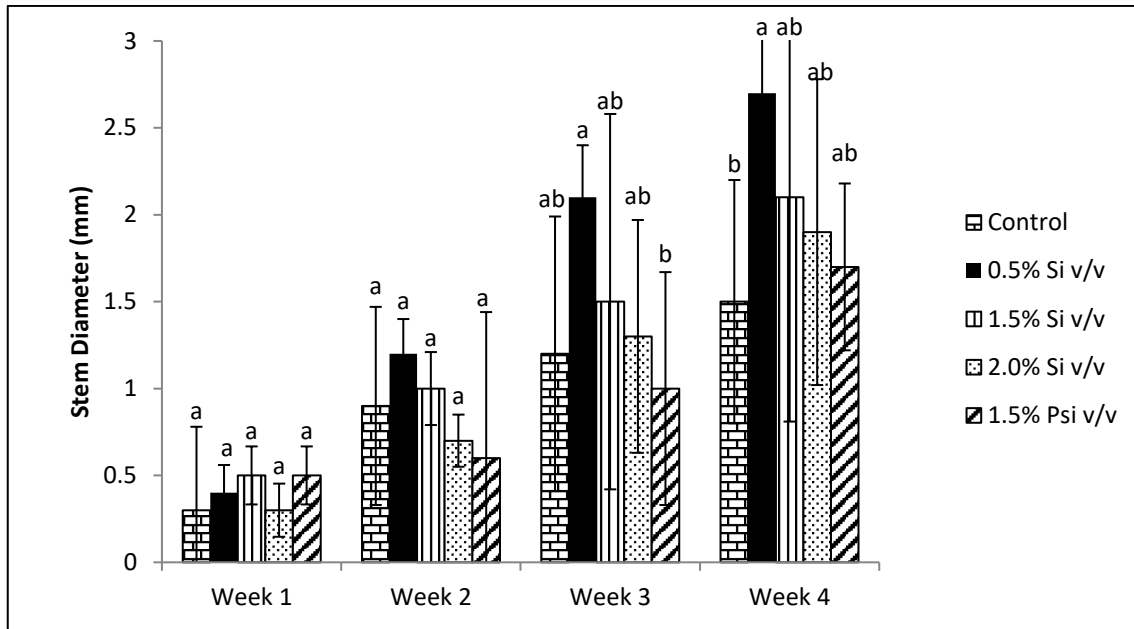


Figure 2. Pepper plant stem diameter increment (mm) from week-1 until week-4 grown from stem cutting seedlings. Silicon was applied once a week by root applications. The treatments: T1 (0.5% Si v/v), T2 (1.5% Si v/v), T3 (2.0% Si v/v), T4 (1.5% potassium silicate) as positive control and T5 (control without silicon) as negative control

Table 2. Pearson correlation coefficients between treatments and pepper plant stem diameter

		W1	W2	W3	W4
Stem-diameter	Controls	-0.419	-0.584	-0.628	0.723*
	0.5% Si	-0.141	0.050*	0.060**	0.013**
	1.5% Si	-0.048	0.054*	0.477*	0.492
	2.0% Si	0.109	0.098	0.144	0.416
	1.5% P _{Si}	-0.244	-0.205	-0.164	-0.454

*Correlation is significant at the 0.05 level (2-tailed)

**Correlation is significant at the 0.01 level (2-tailed)

These results indicate that the T1 concentration is most effective in increasing stem diameter over the course of four weeks. The control and the other Si treatments had moderate effects, while the potassium silicate treatment was the least effective in promoting stem diameter growth.

In rice plants, Si has been shown to increase resistance to fungal attack by strengthening the stem base and promoting cell elongation (Wakabayashi et al., 2002; Liang et al., 2013). In addition, Si depots such as silica gel, contribute to the strengthening of cereal stems and leaves by increasing the number of silicate cells and Si content in the stem, even at elevated nitrogen levels (Fallah, 2012). The observed

improvement in stem strength following Si supplementation is consistent with previous studies demonstrating the positive effects of Si on plant biomechanics and structure. Consequently, the presence of Si can increase stem strength and reduce stem lodging, especially during periods of increased peppercorn production.

Chlorophyll Concentration (SPAD) Response to Silicon Treatments

There were no significant differences ($p > 0.05$) in chlorophyll concentration were observed between all Si treatments (Figure 3). At week 1, all treatments, including the control, had similar chlorophyll

concentrations, approximately 60 SPAD units. Nevertheless, pepper plants treated with Si generally had higher chlorophyll content (SPAD) compared to the control plants (Figure 3). Chlorophyll content was higher in T1 (65.7 SPAD) at week 3 (Figure 3), whereas pepper plant treated with T2 has the highest chlorophyll concentration on week 2 (54.9 SPAD) (Figure 3). The T5 had the lowest chlorophyll content (38.1 SPAD) on week 3 (Figure 3). Results indicated that there was no relationship between control treatment and chlorophyll concentration (SPAD in week 1 $r [7] = [-0.39]$, $p = [.18]$ and week 3 $r [7] = [-0.63]$, $p = [.037]$ (Table 3). For T1, correlation coefficients fluctuate over the study period, showing a positive correlation in Week 1 $r [7] = 0.445$, $p =$

$[.024]$ and weak negative correlations in subsequent weeks (Weeks 2, 3, and 4) (Table 3). None of the correlations are statistically significant ($p > 0.05$), suggesting that T3 had little effect on chlorophyll concentration throughout the study. This finding aligns with other studies indicating that high Si concentrations may not significantly impact chlorophyll levels unless applied under specific conditions or during stress conditions. The T4 shows a strong positive correlation in Week 3 $r [7] = [0.91]$, $p = [.029]$, where a strong positive correlation is observed though it is not statistically significant (Table 3). This high positive correlation suggests a strong association between the T4 and chlorophyll concentration.

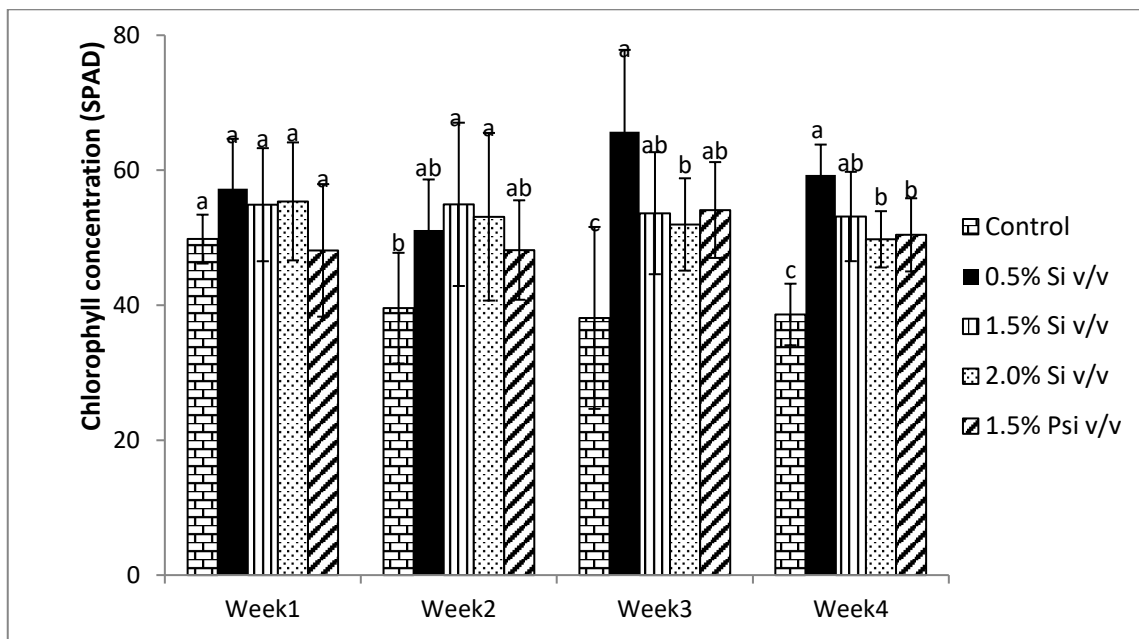


Figure 3. Chlorophyll concentration (SPAD) of pepper plant from week-1 until week-4 grown from stem cutting seedlings. Silicon was applied once a week by root applications. The treatments: T1 (0.5% Si v/v), T2 (1.5% Si v/v), T3 (2.0% Si v/v), T4 (1.5% potassium silicate) as positive control and T5 (control without silicon) as negative control

Table 3. Pearson correlation coefficients between treatments and pepper plant chlorophyll concentration

		W1	W2	W3	W4
Chlorophyll	Controls	-0.394	0.007	-0.627	0.735*
	0.5% Si	0.445	-0.432	-0.387	0.064
	1.5% Si	-0.200	-0.709*	0.442	-0.070
	2.0% Si	-0.232	0.290	-0.071	0.121
	1.5% PSi	-0.468	0.502	0.919	0.573

*Correlation is significant at the 0.05 level (2-tailed)

These results indicate that the 0.5% Si v/v concentration is most effective in maintaining a high chlorophyll concentration a four weeks period. The control group consistently showed a decrease in chlorophyll concentration, indicating the potential benefits of Si and Psi treatments in maintaining chlorophyll concentration.

It has been found that nutrient Si has a significant influence on the chlorophyll content and consequently on the photosynthetic activity of plants. Si has a significant influence on chlorophyll content. It also appears to improve various other plant growth parameters. Chlorophyll content is subject to the influence of various environmental factors such as light intensity, temperature and water content. In a

previous study, it was reported that salt-treated barley, enriched with Si, showed enhanced growth due to improved chlorophyll content and increased photosynthetic activity in the leaf cell organelles (Al-aghaby *et al.*, 2005). Productive changes in plants include improved leaf epidermal development, increased leaf chlorophyll content (Yao *et al.*, 2011;

Teixeira *et al.*, 2020) and increased photosynthetic rate (Asmar *et al.*, 2013; Lavinsky *et al.*, 2016). During a two-month observation period, it was observed that T1 [0.5% Si (v/v)] grew healthier and faster compared to T4 (positive control) and T5 (negative control) in the nursery (Figure 4).



Figure 4. Comparison of pepper plants treated with 0.5% Si (v/v) [T1], positive control (1.5% Potassium Silicate v/v) [T4] and negative control (without Si) [T5]

CONCLUSION

Si in the form of silicic acid has the potential to improve growth and increase the chlorophyll concentration of pepper plants cultivar Kuching. This is the first report on the application of Si to pepper plants in Malaysia and the results show that pepper plant could uptake Si and grow healthier. These results suggest that the 0.5% Si v/v concentration is the most effective in influencing plant growth over the course of four weeks. The control and other Si treatments had moderate effects, while the potassium silicate (1.5% Psi v/v) treatment was the least effective in plant growth. From this result, we suggest that Si could be applied gradually starting from the lowest concentration [0.5% Si (v/v)] to the highest concentration [1.5% Si (v/v)] by root application for pepper plant from stem cutting seedling. During early-stage application, it will strengthen the young plant before being transplanted to field. By strengthening the stem basis and promoting cell elongation, it reduces the risk of lodging, particularly during periods of increased peppercorn abundance. However, foliar spraying should be considered in the future since silicic acid absorption is quicker on leaves than via root.

Further research should investigate Si with other agronomic practices, such as fertilization, fertigation (fertilization by drip irrigation), irrigation management, and pest control, to develop integrated management strategies for optimizing pepper production while minimizing environmental impacts. We encourage further research on Si to investigate the mechanisms behind these observations and to determine the long-term effects of these treatments on overall plant health and productivity. By addressing this topic, could provide valuable insights into the sustainability and durability of silicon-based management practices in pepper plants production.

ACKNOWLEDGEMENT

The authors thank staff in the Soil Laboratory and Crop Science Laboratory, Faculty of Fisheries and Food Sciences, Universiti Malaysia Terengganu (UMT) and the Laboratory for Pest, Disease and Microbial Biotechnology (LAPDiM) for the facilities provided. This research was supported by Industrial Grant, UMT Research Management Centre Vot 53451.

REFERENCES

- Abdulla, I., Fatimah, M.A., Muhammad, T., Bach, N.L. & Sahra, M. (2015). A Systems Approach to Study the Malaysian Pepper Industry. *American Journal of Applied Sciences*, 12. DOI: 487-494. 10.3844/ajassp.2015.487.494.
- Adam, A., Kho, P.E., Sahari, N., Tida, A., Chen, Y.S., Tawie, & Mohamad, H. (2018). Dr.LADA: Diagnosing black pepper pests and diseases with decision tree. *International Journal on Advanced Science, Engineering and Information Technology*, 8(4-2):1584. DOI: 10.18517/ijaseit.8.4-2.6818.
- Al-aghaby, K., Zhu, Z. & Shi, Q. (2005). Influence of silicon supply on chlorophyll content, chlorophyll fluorescence, and antioxidative enzyme activities in tomato plants under salt stress. *Journal of Plant Nutrition*, 27(12): 2101-2115.
- Al-Wasfy, M.M. 2013. Response of Sakkoti date palms to foliar application of royal jelly, silicon and vitamins B. *Journal of American Science*, 9(5): 315-321.
- Asmar, S.A., Castro, E., Pasqual, M., Pereira, F., & Soares, J. (2013). Changes in leaf anatomy and photosynthesis of micro propagated banana plantlets under different silicon sources. *Scientia Horticulturae*, 161. DOI: 328-332. 10.1016/j.scienta.2013.07.021.
- Belanger, R.R., Benhamou, N. & Menzies, J.G. (2003). Cytological evidence of an active role of silicon in wheat resistance to powdery mildew (*Blumeria graminis* f. sp. *tritici*). *Phytopathology*, 93: 402-412.
- Chen, Y.S., Dayod, M., Tawan, C.S. & Science, F. (2010). Phenetic analysis of cultivated black pepper (*Piper nigrum* L.) in Malaysia. *International Journal of Agronomy*, 45(1):43-47.
- Damanhour, Z. & Ahmad, A. (2014). A Review on Therapeutic Potential of *Piper nigrum* L. (Black Pepper): The King of Spices. *Medicinal & Aromatic Plants*, 3: 161.
- Deshmukh, R.K., Ma, J.F. & Bélanger, R.R. (2017). Editorial: Role of silicon in plants. *Frontiers in Plant Science*, 8: 1858.
- Epstein, E. (1994). The anomaly of silicon in plant biology. *Proceedings of National Academy of Sciences, USA* 91 1994. 91(1): 11-17. DOI: 10.1073/Pnas.91.1.11.
- Fallah, A. (2012). Silicon effect on lodging parameters of rice plants under hydroponic culture. *International Journal of AgriScience*, 2(7): 630-634.
- Gong, H.J., Chen, K.M., Chen, G.C., Wang, S.M. & Zhang, C.L. (2003). Effects of silicon on growth of wheat under drought. *Journal of Plant Nutrition*, 26(5): 1055-1063.
- Joy, N., Abraham, Z. V. & Soniya, E. (2007). A preliminary assessment of genetic relationships among agronomically important cultivars of black pepper. *BMC Genetics.*, 8: 42.
- Jufri, A.F., Sudradjat. & Sulistyono, E. (2016). Studies on the Effects of Silicon an Antitranspirant on Chilli Pepper (*Capsicum annum* L.) Growth and Yield. *European Journal of Scientific Research*, Vol. 137: 5-10.
- Khan, M.A., Goyal, V. & Jain, N. (2017). Impact of ortho silicic acid formulation on yield and disease incidence of potatoes. In *Proceedings of the 7th International Conference on Silicon in Agriculture, Bengaluru, India* (pp. 137).
- Laane, H.M. (2017). The Effects of the Application of Foliar Sprays with Stabilized Silicic Acid: An Overview of the Results From 2003-2014. *Silicon*, 9: 803-807. DOI:10.1007/s12633-016-94660.
- Lavinsky, A., Detmann, K., Reis, J., Avila, R., Sanglard, M., Pereira, L., Sanglard, L., Rodrigues, F.,m Araujo, W. & DaMatta, F. (2016). Silicon improves rice grain yield and photosynthesis specifically when supplied during the reproductive growth stage. *Journal of Plant Physiology*, 206. DOI: 10.1016/j.jplph.2016.09.010.
- Liang, Y.C., Sun, W.C., Zhu, Y.G. & Christie, P. (2007). Mechanisms of silicon mediated alleviation of abiotic stresses in higher plants: a review. *Environment. Pollution.*, 147, 422-428.
- Liang, S.J., Li, Z.Q., Li, X.J., Xie, H.G., Zhu, R.S., Lin, J.X., Xie, H.A. & Wu, H. (2013). Effects of stem structural characters and silicon content on lodging resistance in rice (*Oryza sativa* L.). *Research on Crops*, 14: 621-636.
- Ma, J.F. & Yamaji, N. (2006). Silicon uptake and accumulation in higher plants. *Trends in Plant Science*, 11(8): 392-397.
- Malaysia's Open Data Portal, Department of Statistics Malaysia. (2022). Production of selected crops, Malaysia (2017-2021). Malaysian Pepper Board.
- Malaysia Pepper Board. (2022). Annual report 2022. Malaysia Pepper Board. <https://www.mpb.gov.my>.
- Martin, T.N, Nunes, U.R., Stecca, J.D.L. & Pahins, D.B. (2017). Foliar application of silicon on yield component of wheat crop. *Revista Caatinga*, 30, 578-585. DOI:10.1590/1983-21252017v30n305rc.
- Menzies, J., Bowen, P., Ehret, D. & Glass, A.D.M. (1992). Foliar applications of potassium silicate reduce severity of powdery mildew on cucumber, muskmelon, and zucchini squash. *Journal of the American Society for Horticultural Science*, 117: 902-905.

- Ouellette, S., Goyette, M.H., Labbé, C., Laur, J., Gaudreau, L., Gosselin, A., Dorais, M., Deshmukh, R.K. & Bélanger, R.R. (2017). Silicon Transporters and Effects of Silicon Amendments in Strawberry under High Tunnel and Field Conditions. *Frontiers in Plant Science*, 8: 949.
- Pasternak, T., Groot, E.P., Kazantsev, F.V., Teale, W., Omelyanchuk, N., Kovrizhnykh, V., Palme, K. & Mironova, V.V. (2019). Salicylic Acid Affects Root Meristem Patterning via Auxin Distribution in a Concentration-Dependent Manner. *Plant Physiology*, 180(3):1725-1739. DOI: 10.1104/pp.19.00130.
- Paulus, A.D. & Sim, S.L. (2005). A selection of Piper spp. for pepper breeding in Sarawak, Malaysia. In Tuen A.A. and I. Das (eds.) *Wallace in Sarawak-150 Years later*. Proceeding of the International Conference on Biogeography and Biodiversity, 13-15 July 2005, Kuching, Sarawak, UNIMAS, pp. 131-133.
- Paulus, A.D. (2011). Planting and maintenance. In Lai K.F. and Sim S.L. (eds.) *Malaysian Pepper Production Technology Manual*, pp. 48-65.
- Ravindran, P. N., Babu, K. N., Sasikumar, B. & Krishnamurthy, K. S. (2000). Botany and crop improvement of black pepper. In *Black pepper* (pp. 43-164). CRC Press.
- Sah, S.K., Reddy, K.R. & Li, J. (2022). Silicon Enhances Plant Vegetative Growth and Soil Water Retention of Soybean (*Glycine max*) Plants under Water-Limiting Conditions. *Plants* 11 (3), 1687.
- Samuels, A.L., Glass, A.D.M., Ehret, D.L. & Menzies, J.G. (1991). Mobility and deposition of silicon in cucumber plants. *Plant, Cell & Environment*, 14: 485-492.
- Sharma, Y.R. & Kalloo, G. (2004). Status of current research towards increased production and productivity in black pepper in India. *Focus on pepper*, 1:69-86.
- Silva, R.V., Oliveira, R.D.L., Nascimento, K.J.T. & Rodrigues, F.A. (2010). Biochemical responses of coffee resistance against *Meloidogyne exigua* mediated by silicon. *Plant Pathology*, 59: 586-593
- Shivaraj, S.M., Mandlik, R., Bhat, J.A., Raturi, G., Elbaum, R., Alexander, L., Tripathi, D.K., Deshmukh, R. and Sonah, H. (2022). Outstanding questions on the beneficial role of silicon in crop plants. *Plant and Cell Physiology*, 63(1), pp.4-18. DOI: 10.1093/pcp/pcab145
- Srinivasan, K. (2007). Black pepper and its pungent principle-piperine: a review of diverse physiological effects. *Critical Review in Food Science and Nutrition*, 47: 735-748.
- Suhaizan, L., Mohammad, N.M.A., Siti, N.M.S., Nurul, F.I. & Xiaolei, J. (2017). Growth development and natural infection incidence of tobacco mosaic virus (Tmv) on silicon-treated chilli (*Capsicum annuum* L.) cultivated in commercial soil. *Malaysian Applied Biology*, 46(3): 221-226.
- Suhaizan, L., Nur, S.S., Nurul, F.I., Norhidayah, C.S., Ramisah, M.S. & Muhammad, S.H.Z. (2023). Enhanced Growth of Chili (*Capsicum annuum* L.) by Silicon Nutrient Application in Fertigation System. *Malaysian Applied Biology*, 52(2): 13-20.
- Teixeira, G.C.M., de Mello Prado, R., Oliveira, K.S., D'Amico-Damião, V. & da Silveira Sousa Junior, G. (2020). Silicon increases leaf chlorophyll content and iron nutritional efficiency and reduces iron deficiency in sorghum plants. *Journal of Soil Science and Plant Nutrition*, 20(3): 1311-1320. DOI: 10.1007/s42729-020-00214-0
- Wakabayashi, K., Hossain, M.T., Mori, R., Soga, K., Kamisaka, S. & Fujii, S. (2002). Growth promotion and an increase in cell wall extensibility by silicon in rice and some other Poaceae seedling. *Journal Plant Research*, 115(1): 23-27. DOI: 10.1007/s102650200004.
- Wani S.H., Kumar V., Shriram V., Sah S.K. (2016). Phytohormones and their metabolic engineering for abiotic stress tolerance in crop plants. *The Crop Journal*, 4: 162-176. DOI: 10.1016/j.cj.2016.01.010
- Yang, W., Zhu, C., Ma, X., Li, G., Gan, L., Ng, D. & Xia, K. (2013) Hydrogen Peroxide Is a Second Messenger in the Salicylic Acid-Triggered Adventitious Rooting Process in Mung Bean Seedlings. *PLOS ONE*, 8(12): e84580. <https://doi.org/10.1371/journal.pone.0084580>.
- Yao, X., Chu, J., Cai, K., Liu, L., Shi, J. & Geng, W. (2011). Silicon improves the tolerance of wheat seedlings to ultraviolet-B stress. *Biological Trace Element Research*, 143(1), 507-517.
- Zellener, W., Tubana, B., Rodrigues, F. & Datnoff, L. (2021). Silicon's Role in Plant Stress Reduction and Why This Element Is Not Used Routinely for Managing Plant Health. *Plant Disease*, 105. DOI: 10.1094/PDIS-08-20-1797-FE.